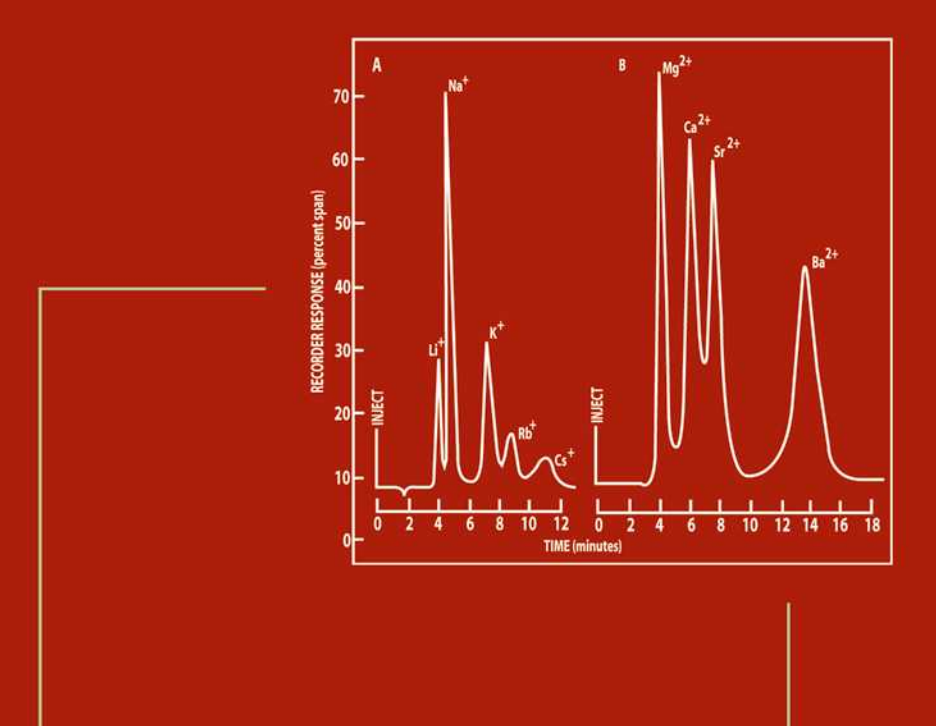


Soil and Environmental Analysis

Modern Instrumental Techniques

Third Edition

edited by

Keith A. Smith
Malcolm S. Cresser

Soil and Environmental Analysis
Modern Instrumental Techniques
Third Edition

edited by
Keith A. Smith
The University of Edinburgh
Edinburgh, Scotland

Malcolm S. Cresser
The University of York
York, England



MARCEL DEKKER, INC. NEW YORK • BASEL

The previous edition was *Soil Analysis: Modern Instrumental Techniques, Second Edition*, K. A. Smith, ed. (Marcel Dekker, Inc., 1991).

Library of Congress Cataloging-in-Publication Data
A catalog record for this book is available from the Library of Congress.

ISBN: 0-8247-0991-8

This book is printed on acid-free paper.

Headquarters
Marcel Dekker, Inc., 270 Madison Avenue, New York, NY 10016, U.S.A.
tel: 212-696-9000; fax: 212-685-4540

Distribution and Customer Service
Marcel Dekker, Inc., Cimarron Road, Monticello, New York 12701, U.S.A.
tel: 800-228-1160; fax: 845-796-1772

Eastern Hemisphere Distribution
Marcel Dekker AG, Hutgasse 4, Postfach 812, CH-4001 Basel, Switzerland
tel: 41-61-260-6300; fax: 41-61-260-6333

World Wide Web
http://www.dekker.com

The publisher offers discounts on this book when ordered in bulk quantities. For more information, write to Special Sales/Professional Marketing at the headquarters address above.

Current printing (last digit):

10 9 8 7 6 5 4 3 2 1

PRINTED IN THE UNITED STATES OF AMERICA

BOOKS IN SOILS, PLANTS, AND THE ENVIRONMENT

Soil Biochemistry, Volume 1, edited by A. D. McLaren and G. H. Peterson
Soil Biochemistry, Volume 2, edited by A. D. McLaren and J. Skujiņš
Soil Biochemistry, Volume 3, edited by E. A. Paul and A. D. McLaren
Soil Biochemistry, Volume 4, edited by E. A. Paul and A. D. McLaren
Soil Biochemistry, Volume 5, edited by E. A. Paul and J. N. Ladd
Soil Biochemistry, Volume 6, edited by Jean-Marc Bollag and G. Stotzky
Soil Biochemistry, Volume 7, edited by G. Stotzky and Jean-Marc Bollag
Soil Biochemistry, Volume 8, edited by Jean-Marc Bollag and G. Stotzky
Soil Biochemistry, Volume 9, edited by G. Stotzky and Jean-Marc Bollag
Soil Biochemistry, Volume 10, edited by Jean-Marc Bollag and G. Stotzky

Organic Chemicals in the Soil Environment, Volumes 1 and 2, edited by C. A. I. Goring and J. W. Hamaker
Humic Substances in the Environment, M. Schnitzer and S. U. Khan
Microbial Life in the Soil: An Introduction, T. Hattori
Principles of Soil Chemistry, Kim H. Tan
Soil Analysis: Instrumental Techniques and Related Procedures, edited by Keith A. Smith
Soil Reclamation Processes: Microbiological Analyses and Applications, edited by Robert L. Tate III and Donald A. Klein
Symbiotic Nitrogen Fixation Technology, edited by Gerald H. Elkan

MARCEL DEKKER, INC.
270 Madison Avenue, New York, New York 10016

Soil–Water Interactions: Mechanisms and Applications, Shingo Iwata and Toshio Tabuchi with Benno P. Warkentin
Soil Analysis: Modern Instrumental Techniques, Second Edition, edited by Keith A. Smith
Soil Analysis: Physical Methods, edited by Keith A. Smith and Chris E. Mullins
Growth and Mineral Nutrition of Field Crops, N. K. Fageria, V. C. Baligar, and Charles Allan Jones
Semiarid Lands and Deserts: Soil Resource and Reclamation, edited by J. Skujiņš
Plant Roots: The Hidden Half, edited by Yoav Waisel, Amram Eshel, and Uzi Kafkafi
Plant Biochemical Regulators, edited by Harold W. Gausman
Maximizing Crop Yields, N. K. Fageria
Transgenic Plants: Fundamentals and Applications, edited by Andrew Hiatt
Soil Microbial Ecology: Applications in Agricultural and Environmental Management, edited by F. Blaine Metting, Jr.
Principles of Soil Chemistry: Second Edition, Kim H. Tan
Water Flow in Soils, edited by Tsuyoshi Miyazaki
Handbook of Plant and Crop Stress, edited by Mohammad Pessarakli
Genetic Improvement of Field Crops, edited by Gustavo A. Slafer
Agricultural Field Experiments: Design and Analysis, Roger G. Petersen
Environmental Soil Science, Kim H. Tan
Mechanisms of Plant Growth and Improved Productivity: Modern Approaches, edited by Amarjit S. Basra
Selenium in the Environment, edited by W. T. Frankenberger, Jr., and Sally Benson
Plant–Environment Interactions, edited by Robert E. Wilkinson
Handbook of Plant and Crop Physiology, edited by Mohammad Pessarakli
Handbook of Phytoalexin Metabolism and Action, edited by M. Daniel and R. P. Purkayastha
Soil–Water Interactions: Mechanisms and Applications, Second Edition, Revised and Expanded, Shingo Iwata, Toshio Tabuchi, and Benno P. Warkentin
Stored-Grain Ecosystems, edited by Digvir S. Jayas, Noel D. G. White, and William E. Muir
Agrochemicals from Natural Products, edited by C. R. A. Godfrey
Seed Development and Germination, edited by Jaime Kigel and Gad Galili
Nitrogen Fertilization in the Environment, edited by Peter Edward Bacon
Phytohormones in Soils: Microbial Production and Function, William T. Frankenberger, Jr., and Muhammad Arshad
Handbook of Weed Management Systems, edited by Albert E. Smith
Soil Sampling, Preparation, and Analysis, Kim H. Tan
Soil Erosion, Conservation, and Rehabilitation, edited by Menachem Agassi
Plant Roots: The Hidden Half, Second Edition, Revised and Expanded, edited by Yoav Waisel, Amram Eshel, and Uzi Kafkafi
Photoassimilate Distribution in Plants and Crops: Source–Sink Relationships, edited by Eli Zamski and Arthur A. Schaffer

MARCEL DEKKER, INC.
270 Madison Avenue, New York, New York 10016

Mass Spectrometry of Soils, edited by Thomas W. Boutton and Shinichi Yamasaki
Handbook of Photosynthesis, edited by Mohammad Pessarakli
Chemical and Isotopic Groundwater Hydrology: The Applied Approach, Second Edition, Revised and Expanded, Emanuel Mazor
Fauna in Soil Ecosystems: Recycling Processes, Nutrient Fluxes, and Agricultural Production, edited by Gero Benckiser
Soil and Plant Analysis in Sustainable Agriculture and Environment, edited by Teresa Hood and J. Benton Jones, Jr.
Seeds Handbook: Biology, Production, Processing, and Storage, B. B. Desai, P. M. Kotecha, and D. K. Salunkhe
Modern Soil Microbiology, edited by J. D. van Elsas, J. T. Trevors, and E. M. H. Wellington
Growth and Mineral Nutrition of Field Crops: Second Edition, N. K. Fageria, V. C. Baligar, and Charles Allan Jones
Fungal Pathogenesis in Plants and Crops: Molecular Biology and Host Defense Mechanisms, P. Vidhyasekaran
Plant Pathogen Detection and Disease Diagnosis, P. Narayanasamy
Agricultural Systems Modeling and Simulation, edited by Robert M. Peart and R. Bruce Curry
Agricultural Biotechnology, edited by Arie Altman
Plant–Microbe Interactions and Biological Control, edited by Greg J. Boland and L. David Kuykendall
Handbook of Soil Conditioners: Substances That Enhance the Physical Properties of Soil, edited by Arthur Wallace and Richard E. Terry
Environmental Chemistry of Selenium, edited by William T. Frankenberger, Jr., and Richard A. Engberg
Principles of Soil Chemistry: Third Edition, Revised and Expanded, Kim H. Tan
Sulfur in the Environment, edited by Douglas G. Maynard
Soil–Machine Interactions: A Finite Element Perspective, edited by Jie Shen and Radhey Lal Kushwaha
Mycotoxins in Agriculture and Food Safety, edited by Kaushal K. Sinha and Deepak Bhatnagar
Plant Amino Acids: Biochemistry and Biotechnology, edited by Bijay K. Singh
Handbook of Functional Plant Ecology, edited by Francisco I. Pugnaire and Fernando Valladares
Handbook of Plant and Crop Stress: Second Edition, Revised and Expanded, edited by Mohammad Pessarakli
Plant Responses to Environmental Stresses: From Phytohormones to Genome Reorganization, edited by H. R. Lerner
Handbook of Pest Management, edited by John R. Ruberson
Environmental Soil Science: Second Edition, Revised and Expanded, Kim H. Tan
Microbial Endophytes, edited by Charles W. Bacon and James F. White, Jr.
Plant–Environment Interactions: Second Edition, edited by Robert E. Wilkinson
Microbial Pest Control, Sushil K. Khetan

Marcel Dekker, Inc.
270 Madison Avenue, New York, New York 10016

Soil and Environmental Analysis: Physical Methods, Second Edition, Revised and Expanded, edited by Keith A. Smith and Chris E. Mullins
The Rhizosphere: Biochemistry and Organic Substances at the Soil–Plant Interface, Roberto Pinton, Zeno Varanini, and Paolo Nannipieri
Woody Plants and Woody Plant Management: Ecology, Safety, and Environmental Impact, Rodney W. Bovey
Metals in the Environment: Analysis by Biodiversity, M. N. V. Prasad
Plant Pathogen Detection and Disease Diagnosis: Second Edition, Revised and Expanded, P. Narayanasamy
Handbook of Plant and Crop Physiology: Second Edition, Revised and Expanded, edited by Mohammad Pessarakli
Environmental Chemistry of Arsenic, edited by William T. Frankenberger, Jr.
Enzymes in the Environment: Activity, Ecology, and Applications, edited by Richard G. Burns and Richard P. Dick
Plant Roots: The Hidden Half, Third Edition, Revised and Expanded, edited by Yoav Waisel, Amram Eshel, and Uzi Kafkafi
Handbook of Plant Growth: pH as the Master Variable, edited by Zdenko Rengel
Biological Control of Crop Diseases, edited by Samuel S. Gnanamanickam
Pesticides in Agriculture and the Environment, edited by Willis B. Wheeler
Mathematical Models of Crop Growth and Yield, Allen R. Overman and Richard V. Scholtz III
Plant Biotechnology and Transgenic Plants, edited by Kirsi-Marja Oksman-Caldentey and Wolfgang H. Barz
Handbook of Postharvest Technology: Cereals, Fruits, Vegetables, Tea, and Spices, edited by Amalendu Chakraverty, Arun S. Mujumdar, G. S. Vijaya Raghavan, and Hosahalli S. Ramaswamy
Handbook of Soil Acidity, edited by Zdenko Rengel
Humic Matter in Soil and the Environment: Principles and Controversies, Kim H. Tan
Molecular Host Resistance to Pests, S. Sadasivam and B. Thayumanavan
Soil and Environmental Analysis: Modern Instrumental Techniques, Third Edition, edited by Keith A. Smith and Malcolm S. Cresser
Chemical and Isotopic Groundwater Hydrology: Third Edition, Emanuel Mazor

Additional Volumes in Preparation

Agricultural Systems Management: Optimizing Efficiency and Performance, Robert M. Peart and Dean W. David Shoup
Seeds Handbook: Biology, Production, Processing, and Storage, Second Edition, Revised and Expanded, Babasaheb B. Desai
Physiology and Biotechnology Integration for Plant Breeding, edited by Henry T. Nguyen and Abraham Blum

MARCEL DEKKER, INC.
270 Madison Avenue, New York, New York 10016

Preface

This third edition retains the range of analytical techniques and the structure of individual chapters of the second edition. However, there are some significant changes, with the introduction of new topics and some deletions, to take into account the changing priorities in environmental analysis.

The chapters on atomic absorption and flame emission spectrometry, inductively coupled plasma spectrometry, continuous-flow and flow-injection analysis, ion chromatography, combustion analyzers for carbon, nitrogen and sulfur, and x-ray fluorescence spectrometry have new or additional authors and their applications sections cover a wider range of environmental materials than before. This latter feature is one that generally applies to this edition, so that although the most important application is still the analysis of soils, much more attention is given to other materials. Thus, for example, the chapter on CNS analyzers has been extended to cover the important topic of the measurement of dissolved C and N in waters, which involves the use of different instruments from those used for soil analysis.

The coverage of ion-selective electrodes in the second edition has been included in an extended chapter on electroanalytical methods. Similarly, the previous chapter on isotope-ratio mass spectrometry has been extended to cover isotopes of hydrogen, carbon, and sulfur, as well as those of nitrogen, because of the importance of isotopic studies in current research into environmental and biospheric processes involving these elements. The previous chapters on nuclear and radiochemical analysis and instrumental neutron activation analysis have been replaced by a new chapter on the measurement of radioisotopes and ionizing radiation. The chapter on the measurement of gases in the soil atmosphere has been replaced by two chapters dealing with the measurement of gas fluxes between the land surface and the atmosphere, reflecting the current concentration of research effort on global warming. This expansion into a new interdisciplinary field, taken together with other changes already mentioned, means that the scientific coverage of the book extends to most of the techniques involved in

Marcel Dekker, Inc.
270 Madison Avenue, New York, New York 10016

studies of the biogeochemical cycles of carbon, nitrogen, and sulfur, in the context of improving our understanding of global change.

Contamination of soils, waters, and sediments with heavy metals continues to present problems of a more localized nature, and several chapters provide appropriate analytical techniques for investigating them. The concern over organic pollutants has changed over the last few years from a strong focus on persistent pesticides to worries about other categories of organic compounds, such as PCBs and aromatic hydrocarbons. The book reflects this change in that the chapter on pesticide analysis has been replaced by one concentrating on these other contaminants.

This third edition is aimed at researchers working in soil science, environmental chemistry, or ecological science, as well as scientists operating analytical service laboratories with substantial throughputs of soil, water, and other environmental samples. It provides information that should help in method selection by those who need to undertake a new determination as their projects develop. It will also guide those who are considering replacing outdated or worn out equipment used for a particular routine analytical task, either with a later model with new features (and probably more "bells and whistles"), or alternatively, with a new method of instrumental analysis. In regard to selection of a new method, the book should help in evaluating the techniques available, so that the optimal choice, in terms of speed, cost, or sensitivity, may be selected. It will also be useful to teachers and students of postgraduate courses in soil chemistry, environmental chemistry, and soil and environmental analysis.

We wish to thank the contributors for their efforts, Mary Lightbody for preparing the index, and Ann Pulido at Marcel Dekker, Inc., for managing the editing process. We acknowledge the tolerance of colleagues, families, and students who may have found us somewhat distracted from other tasks from time to time, as this volume passed through its various stages.

Keith A. Smith
Malcolm S. Cresser

Contents

Marcel Dekker, Inc.
270 Madison Avenue, New York, New York 10016

Marcel Dekker, Inc.
270 Madison Avenue, New York, New York 10016

Contributors

Nicholas T. Basta Department of Plant and Soil Sciences, Oklahoma State University, Stillwater, Oklahoma, U.S.A.

Mark Cave British Geological Survey, Nottingham, England

Franz Conen School of GeoSciences, The University of Edinburgh, Edinburgh, Scotland

Malcolm S. Cresser Environment Department, The University of York, York, England

Julian J. C. Dawson Department of Plant and Soil Science, The University of Aberdeen, Aberdeen, Scotland

Anthony C. Edwards The Macaulay Institute, Aberdeen, Scotland

Andrew Fisher Advanced Environmental Diagnostics, The University of Plymouth, Plymouth, England

Stephen J. Hill Advanced Environmental Diagnostics, The University of Plymouth, Plymouth, England

Shreekant V. Karmarkar Lachat Instruments, Milwaukee, Wisconsin, U.S.A.

Francis R. Livens Department of Chemistry, The University of Manchester, Manchester, England

Helena Maciel Department of Plant and Soil Science, The University of Aberdeen, Aberdeen, Scotland

Iain L. Marr Department of Chemistry, The University of Aberdeen, Aberdeen, Scotland

Olivia J. Marsden Department of Chemistry, The University of Manchester, Manchester, England

Marcel Dekker, Inc.
270 Madison Avenue, New York, New York 10016

John B. Moncrieff School of GeoSciences, The University of Edinburgh, Edinburgh, Scotland

Graeme I. Paton Department of Plant and Soil Science, The University of Aberdeen, Aberdeen, Scotland

Philip J. Potts Department of Earth Sciences, The Open University, Milton Keynes, England

David Robinson Department of Plant and Soil Science, The University of Aberdeen, Aberdeen, Scotland

Albert Scott Scottish Agricultural College, Edinburgh, Scotland

Charles M. Scrimgeour The Scottish Crop Research Institute, Dundee, Scotland

Kirk T. Semple Environmental Science Division, Lancaster University, Lancaster, England

Keith A. Smith School of GeoSciences, The University of Edinburgh, Edinburgh, Scotland

M. Ali Tabatabai Department of Agronomy, Iowa State University, Ames, Iowa, U.S.A.

1

Atomic Absorption and Flame Emission Spectrometry

Malcolm S. Cresser
The University of York, York, England

I. INTRODUCTION

A. Interaction of Light with Atoms

This chapter is concerned with atomic absorption spectrometry (AAS), which is a very widely used technique for the determination of over 20 elements in soils, plants, waters, and other environmental materials. It also briefly covers flame emission spectrometry (FES), which is also widely used, but for the determination of a smaller number of elements. For some elements at very high concentrations, absorption of visible light by atoms can be readily observed. Our sun's spectrum, for example, shows several dark absorption lines where the continuum emitted from the high-temperature solar surface is selectively absorbed by free atoms of elements such as sodium in the solar atmosphere. These dark lines, the Fraunhofer lines, are perhaps the oldest and best-known example of atomic absorption.

Any particular electronic transition in an atom requires photons with an appropriate amount of energy to induce a transition from a lower discrete (quantized) energy state to a higher quantized energy state. If the photons have insufficient energy (i.e., if the wavelength of the light is too long), the transition cannot occur. Nor can a transition occur if the wavelength is too short, because there is no mechanism by which the excess energy can be absorbed. Atomic absorption spectra therefore consist of isolated, very narrow bands, or lines, with one line for each possible electronic transition. This is why the atomic absorption bands of sodium in the sun's atmosphere are sharp lines.

Marcel Dekker, Inc.
270 Madison Avenue, New York, New York 10016

Atoms may also be excited thermally in a body of hot gas such as a flame or plasma. The thermally excited atoms may be subsequently deactivated by losing their electronic excitation energy via conversion to light energy, which is emitted in all directions. Measurement of the intensity of the light emitted constitutes the basis of FES. Over a moderate range of atom concentration, the intensity of the emitted light is proportional to the number of excited atoms present in the flame.

B. Quantitative AAS and FES—What Do We Need to Measure?

The wavelengths at which atomic absorption spectral lines occur are characteristics of the particular atoms that are giving rise to the lines and thus may be used for qualitative identification of the absorbing element(s). For quantitative analysis, we need to measure some property that varies, preferably linearly, with the concentration of the elements of interest. What parameter should we measure if we wish to exploit atomic absorption quantitatively?

Consider a narrow, monochromatic beam of photons (I_0) passing through a cloud of n atoms. If some photons are absorbed by the atoms in the cloud, the number of transmitted photons (I_t) will be less than I_0. Thus

$$I_t = xI_0$$

where $1 > x > 0$. Now suppose that the concentration of atoms in the cloud is doubled. If the probability of any particular photon being absorbed is independent of the number of photons and depends only upon the number of atoms intercepting the light beam, then $I_0 - I_t$ photons will still be absorbed by the first n atoms. For the second n atoms, once again a fraction x of these xI_0 photons will be absorbed. Thus when n is increased to $2n$, I_t is given by x^2I_0. Similarly, for $3n$, $4n$ . . . atoms, I_t would have the values x^3I_0, x^4I_0 . . . Thus the relationship between I_t, I_0, and the atom concentration, c, is of the form

$$I_t = x^c I_0$$
$$\log I_t = c \log x + \log I_0$$
$$\log I_t - \log I_0 = kc$$
$$\log(I_t/I_0) \text{ is proportional to } c$$

Since $I_t < I_0$, $I_t/I_0 < 1$, and $\log(I_t/I_0) < 0$, if we define a parameter A, the absorbance, as being equal to $-\log(I_t/I_0)$, then the parameter A will always

be positive and proportional to concentration. Thus absorbance is the parameter that should be measured if linear calibration plots are required in AAS. Note that if 90% of the light is absorbed, I_t/I_0 is equal to 10/100 or 0.1, and A is equal to 1. Similarly 99% absorption corresponds to an absorbance of 2, 99.9% to an absorbance of 3, and so on. Precisely measuring values of absorbance much greater than 2 will clearly be technically difficult.

In FES the parameter measured is simply the intensity of the light emitted by thermally excited atoms. As stated earlier, this will increase linearly with determinant element concentration. However, at high element concentrations, some of the emitted light will be reabsorbed. This decreases the light signal at the detector, so a calibration graph of emission intensity versus concentration will curve toward the concentration axis.

By the early 1950s, the concept of absorbance and the nature of atomic absorption spectra had been understood for many decades by spectro-physicists. However, the concept had not been applied quantitatively at that time, because of the limitation imposed by the narrowness of atomic absorption lines. Monochromators then commonly available could provide a "window" to isolate bands of the UV or visible spectrum about 0.1 nm wide, but atomic absorption occurred over a much narrower spectral interval, typically < 0.005 nm. Even if quite strong atomic absorbance occurred when light passed through a cell containing free atoms of an element, there would be no change in 95% of the light passing through the monochromator window. Therefore I_t would be only very slightly smaller than I_0, the ratio I_t/I_0 would be close to 1, and absorbance would be close to zero. In other words, sensitivity would always be very poor in AAS when absorption of light from a continuum source was measured.

Walsh (1955) made a major breakthrough when he realized that practical AAS instrumentation could be built around light sources that emitted atomic spectral lines at the same wavelengths as those at which atomic absorption occurred. By selecting appropriate sources, the emission line widths could be even narrower than the absorption line widths. Thus the potential sensitivity problem discussed above was solved at a stroke, and the concept of the modern atomic absorption spectrometer was born.

The technique of FES predated AAS, because the instrumental requirements of FES were conceptually simpler. In FES a monochromator is used to isolate the light emitted by the element of interest from light emitted by all other elements present in the sample. At the same time the isolation of a narrow wavelength interval by the monochromator increases the ratio of the intensity of the light emitted by the element of interest to the intensity of the background light emitted by the flame. This improves the detection capability of the technique.

C. Potential Selectivity of AAS

Walsh's conceptual breakthrough was of enormous significance. Not only had he suggested a potentially very sensitive analytical method to determine many elements in the periodic table but he had suggested also a method that, at least theoretically, should lead to virtually specific analysis. The very sharpness of the lines in atomic absorption spectra that hitherto had held back progress suddenly became the method's most powerful asset. Because the probability of spectral overlap of the absorption line of one element with the emission line of another was extremely small, atomic spectral interferences should be, and indeed are, extremely rare in AAS. In this respect AAS is vastly superior to FES, where the selectivity depends upon the complexity of the spectra of all elements present in the samples being analyzed. Thus FES is much more prone to spectral interferences.

II. INSTRUMENTATION FOR AAS AND FES

We are now in a position to consider the essential components of a typical atomic absorption spectrometer, as represented in Fig. 1. In this figure, a flame is used to convert the determinant species into a cloud of atoms, which absorb light from a hollow cathode lamp. The most sensitive absorption wavelength is isolated by a monochromator.

A. Hollow Cathode Lamps

As explained in Sec. I.B, to avoid the need for a very high resolution monochromator to isolate a very narrow (< ca. 0.005 nm) band of light from

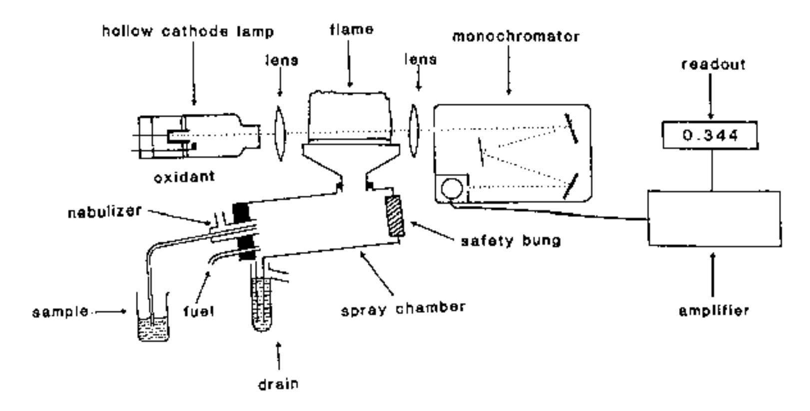


Figure 1 Schematic representation of the main components of a typical atomic absorption spectrometer.

Marcel Dekker, Inc.
270 Madison Avenue, New York, New York 10016

a continuum spectrum prior to absorbance measurement, lamps are used that emit sharp lines at the same wavelengths as those at which absorption occurs. The vast majority of applications use single-element line sources, and virtually all of these are hollow cathode lamps.

Figure 2 shows a typical hollow cathode lamp. The hollow cathode is constructed from the element of interest or one of its alloys. The lamp is filled with an inert gas, generally neon or argon, at low pressure. A high-voltage, low-current discharge is struck between the cathode and an anode. The latter, which commonly is made from tungsten, generally is a small cylinder or sometimes a small flag-shaped electrode. Sheets of insulator, often mica, confine the discharge to the central cathode region to obtain good stability at high intensity. The end window of the lamp is often quartz or optical silica, to transmit UV light. Ordinary glasses absorb increasingly strongly below about 320 nm.

For physical stability, traditionally hollow cathode lamps have an octal (eight-pin) base that attaches to an eight-hole socket. In simple instruments only two pins make any electrical connection, however, although in some more complex instruments additional pins may be connected to electrical components that serve to provide automated lamp identification. The lamp base itself invariably has a protruding plastic lip to make sure that the lamp can be fitted only in the correct position unless excessive brute force is applied (Fig. 2). The lamps are expensive to replace and therefore always should be handled gently. Always remember to budget for a range of lamps when purchasing an instrument for the first time, as they add significantly to the total package cost.

It is important to align correctly the lamp along the optical axis through the center of the flame or electrothermal atomizer to the monochromator entrance slit. Most AAS instruments can accommodate lamps from diverse manufacturers (check before changing manufacturers!), and such lamps often differ in size. The lamps fit inside some sort of

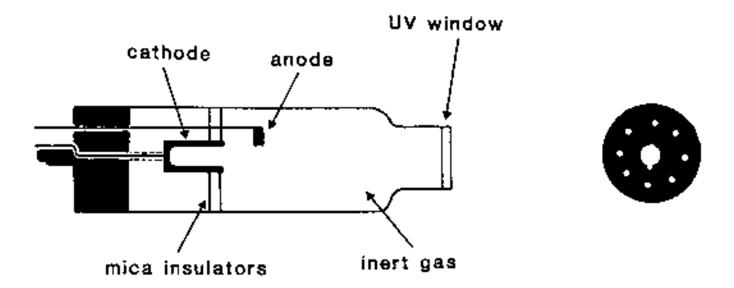


Figure 2 The essential components of a typical hollow cathode lamp.

Marcel Dekker, Inc.
270 Madison Avenue, New York, New York 10016

supporting cradle, so that their position is fully adjustable both horizontally and vertically. Optimal alignment generally is best found by maximizing the signal from the detector while the atomizer is off. It is tempting to use the image of the glowing cathode (usually red from the neon filler gas) at the entrance slit to align the lamp, but this is not advisable for final fine adjustment. This is because the focal point for UV light may be displaced by a few mm from that for red light if the instrument optics use lenses.

Most determinations by AAS are completed using single-element hollow cathode lamps, in spite of the high cost of having an additional lamp for each element to be determined. Single element lamps often give superior signal-to-noise ratios to those with multielement lamps and thus result in slightly better detection limits and improved precision. An exception in the author's experience is the calcium/magnesium dual-element lamp, which usually provides directly comparable performance to the corresponding single-element lamps. Multielement lamps containing up to six or more elements are commercially available but are not to be recommended generally if optimal performance is required.

B. Alternative Line Sources

Some very volatile elements such as arsenic and selenium have their main AAS wavelengths below 200 nm, at wavelengths where absorption by air becomes significant. The hollow cathode lamps for these elements invariably exhibit low intensity and poor stability. The search for more intense sources for such elements resulted in the development of microwave-powered electrodeless discharge lamps (EDLs) as line sources at the end of the 1960s. For volatile elements, these lamps were generally much more intense than the corresponding hollow cathode lamps, sometimes by two to three orders of magnitude. They were sometimes notoriously unstable, however, requiring too much operator skill to find favor for routine use in AAS.

Subsequently, however, radio-frequency-powered (r.f.) electrodeless discharge lamps became available commercially for many elements, including As, Bi, Cd, Cs, Ge, Hg, K, P, Pb, Rb, Sb, Se, Te, Tl, Sn, Ti, and Zn. Although dimmer than the earlier microwave EDLs, r.f. EDLs exhibit far superior stability and are still generally substantially brighter than the corresponding hollow cathode lamps. In the author's experience, they are well worth considering if arsenic or selenium is to be determined routinely, although considerable expense is incurred initially because the lamps require a separate r.f. power supply.

In flame atomic absorption spectrometry, the device used to detect the light signal will "see" the light emitted by the hollow cathode lamp but also the light emitted by the flame at the wavelength being used. Thus the

detector would "see" too much light, and absorbance would not be correctly measured. However, if the lamp power supply is modulated so that the lamp effectively flashes on and off at a frequency of, say, 180 Hz, and the instrument is designed so that it responds only to modulated light at this frequency, it is possible to discriminate between the modulated light emitted by the hollow cathode lamp and the unmodulated light emitted by the flame. Thus the true absorbance can be measured, even if the atomizer is emitting quite intensely. Therefore the power supplies to hollow cathode lamps in atomic absorption spectrometers invariably are modulated. The required lamp signal is isolated by synchronous demodulation, which further improves the signal-to-noise ratio.

C. The Flame as an Atomizer

In AAS and FES, the determinant species in a solid or solution sample must be converted into free atoms, because the techniques respectively involve the absorption of light by, or emission of light from, free atoms. This is most commonly achieved by dissolving the sample and spraying the resulting solution into a flame hot enough to convert the determinant to free atoms.

The function of the flame is threefold, in practice. It must dry, vaporize, and then atomize the sample in a reproducible manner with respect to both space and time. Unlike gravimetric or titrimetric analysis, AAS and FES are secondary methods of analysis. Concentrations of determinants are found by comparing the absorbance or emission values obtained for samples with those obtained for standards of known concentrations of the elements of interest. In both techniques it is therefore vital that samples and standards are always atomized with the same efficiency to produce an atomic vapor cloud with highly reproducible geometry. In FES, the extent of thermal excitation must also be similar for samples and standards. If samples and standards behave differently, errors must inevitably result.

1. The Air–Acetylene Flame

Air–propane and air–butane flames were used to atomize samples in the earliest days of flame AAS, as they had a reputation for being simple and safe enough for routine use. Unfortunately it was found soon that such flames were unsatisfactory for atomizing many thermally stable chemical compounds. Sometimes, therefore, samples and standards were not atomized to the same extent, so erroneous results were obtained. The most commonly used flame at the present time is the air–acetylene flame.

This is still safe, relatively inexpensive, and hot enough at ca. 2200°C to atomize molecules of most, though not all, common elements. It is not hot enough to break the element–oxygen bonds of some elements such as aluminum and silicon, the so-called refractory oxide-forming elements. Such determinants require a hotter flame. Another limitation of the air–acetylene flame is that atomization efficiency of some elements may be influenced by matrix elements and ions. For example, phosphate or aluminum suppress the atomic absorption signals of calcium in this flame.

Producing a stable flame on a burner head requires a gas mixture for which the upward flow velocity just exceeds the downward burning velocity. If the burning velocity becomes greater, there is a danger that the flame will burn back through the burner slot, resulting in a potentially dangerous explosion. This process is known as a flashback. Pre-mixed oxygen–acetylene flames, although substantially hotter than air–acetylene flames, are never used routinely because the burning velocity is too great, and the risk of flashback is too high.

If, on the other hand, the flow velocity exceeds the burning velocity by too much, the flame "lifts off" from the burner head. Chemistry students may have experienced this phenomenon when trying to ignite the flame of a Bunsen burner with the air hole fully open. The flame takes the form of an unstable fire ball a cm or two above the burner port for a few seconds, and then often is extinguished. In the case of the burner heads used in AAS, at a given total flow of fuel plus oxidant, the flow velocity is regulated by the dimensions of the burner slot; the narrower and/or shorter the slot, the faster the gas flow velocity.

2. The Nitrous Oxide–Acetylene Flame

For years it was thought that no flame appreciably hotter than the air–acetylene flame and also safe for routine use would be found, until John Willis (1965) investigated the use of the premixed nitrous oxide–acetylene flame (sometimes also known nowadays as the dinitrogen oxide–acetylene flame). This flame had a temperature of around 3000°C, and it provided a fuel-rich environment that was chemically very reducing. Thus it proved to be suitable for breaking refractory metal–oxide bonds. Its burning velocity exceeded that of the air–acetylene flame, so that a smaller burner slot was necessary but proved to be much less than that of oxygen–acetylene flames. Even so, the early days of its use were marred occasionally by very noisy flashbacks.

3. Safe Use of Acetylene Flames

The spray chamber containing the fuel–oxidant gas mixture in modern AAS instruments is always now fitted with a blowout membrane or safety bung. If

the explosive fuel–oxidant mixture inside the spray chamber is accidentally ignited via a flashback, the very rapid pressure buildup blows out the bung or ruptures the membrane, immediately releasing the pressure and minimizing the risk of damage to the mixing chamber, other instrumental components, and most importantly the operator. The drain that takes away surplus solution from the sample (see Fig. 1) also functions in this way to some extent, by emptying. It is imperative after a flashback to replace the bung or membrane, and to refill the drain, before attempting to relight the flame.

In the majority of modern instruments, especially the more expensive ones, a flashback automatically trips off the fuel supply to minimize the risk of fire. The trip switch must be reset before the flame can be relit. More sophisticated instruments incorporate a range of additional sensors to improve safety further. For example, instruments may be equipped with devices to detect the presence of the correct burner head prior to allowing the operator to light nitrous oxide–supported flames; gas pressure sensors may be fitted in the fuel and oxidant lines to ensure adequate operating pressures; flame detectors may be fitted that shut off the fuel automatically if the flame does not appear to be alight. It is useful to be aware of these devices, as they may cause delays in first lighting flames after gas cylinders have been replaced, or if, for example, air has been flushed inadvertently through the acetylene line.

It is important to check at intervals that all fuel and oxidant lines and their associated connectors within the instrument are in good condition, because as far as the author is aware, virtually no instrument automatically detects slow fuel leaks which could cause a buildup of an explosive gas mixture within an instrument casing. Obviously piping and connectors external to the instrument must also be checked to be in sound condition, but hidden tubing is more likely to be overlooked.

Acetylene should not be used routinely at pressures above 10 p.s.i. (70 kPa), because detonation becomes possible. Nor must it ever be allowed to come into contact with copper piping or fittings, because of the risk of formation of explosive copper acetylide. Acetylene cylinders contain the gas in solution in acetone on a porous ceramic support, so the cylinders always should be stored and handled in an upright position to avoid the risk of liquid acetone entering fuel lines. If, however, this does happen, it is best to get advice from the manufacturer of the instrument on the procedure to follow. Once the operating pressure of the cylinder falls to about 80 p.s.i. (0.6 MPa), it should be replaced, to prevent the passage of excessive acetone vapor into the flame.

The fumes from acetylene flames may be toxic, so an efficient extraction hood is required over the flame. The nitrous oxide–acetylene flame is hotter and taller than the air–acetylene flame, and manufacturers'

Marcel Dekker, Inc.
270 Madison Avenue, New York, New York 10016

advice should be sought on suitable extraction systems for the exhaust gases. It is important to use an appropriate rate of extraction and hood geometry.

4. Observations on Burner Heads

When flame AAS was first introduced, manufacturers opted for long-path flames (100–120 mm), because they wanted the technique to be sensitive and recognized that longer cells gave bigger signals in solution spectrophotometry. In flame AAS, the situation is rather different. Using a longer flame does not put more sample into the optical path. However, increasing the flame cross-sectional area increases the residence time of atoms in the hollow cathode lamp beam. The burner heads are designed to be mechanically robust and safe. However, flat-topped burner heads initially used rapidly got too hot to touch and were prone to clogging. Even ten minutes after the flame has been extinguished after a period of extended use, it is still possible to get a painful burn by touching the head of such a burner.

Boling (1966) described a novel burner head with three parallel slots rather than the normal single slot (Fig. 3A). His idea was to produce a flame-shielded flame that might have a higher central flame temperature by

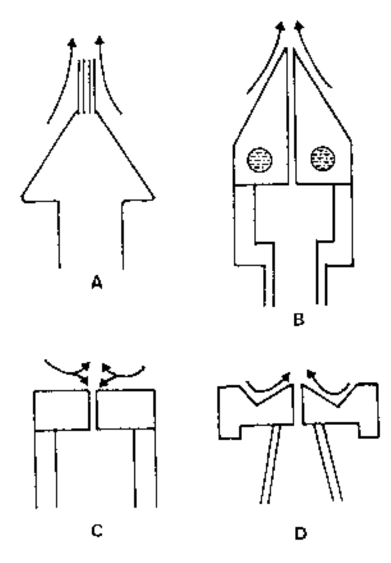


Figure 3 Examples of burner head designs. A, the Boling Triple Slot burner; B, a water-cooled burner head with a triangular cross section; C, a flat-topped burner head; D, a typical modern burner head design. In each case the arrows indicate the pattern of air entrainment.

minimization of cooling with entrained air. The design was operationally successful because sensitivities for elements such as chromium, which are not readily atomized, were improved. Almost 20 years later, Cresser (1993) was experimenting with water-cooling of burner heads to reduce clogging problems for solutions with high concentrations of dissolved solids frequently encountered in environmental analysis. With cooling water along either side of the slot in the head shown in Fig. 3B, the burner head became so cold that condensation in the slot rapidly extinguished the flame. Even with the cooling water disconnected, the head remained so cool that it was possible to touch the side of the head while the flame was alight without any risk of a burn. The explanation appears to be much smoother air entrainment when the burner head has a triangular cross section (Fig. 3B) compared to the very turbulent entrainment and associated heating effect with a flat-topped head (Fig. 3C). The head shown in Fig. 3B gave similar sensitivity enhancements and reduced chemical interferences to the Boling burner, suggesting that the benefits of the latter were possibly attributable to its cross section rather than the triple slot *per se*. Nowadays the majority of AAS instrument manufacturers use a head somewhere between a flat-topped head and a full triangular cross section, as shown in Fig. 3D.

5. The Flame as an Emission Source

It is to be expected that the hotter nitrous oxide–acetylene flame would excite more atoms and therefore provide greater emission intensity and better sensitivity than the cooler air–acetylene flame, and this is indeed the case. It is also capable of exciting refractory oxide-forming elements such as aluminum. However, elements that are not refractory, and that emit at wavelengths above about 350 nm, are excited to an appreciable extent in air–acetylene and can be measured by FES. Longer emission wavelengths are associated with lower excitation potentials (so atoms are more readily excited at a given flame temperature), and sensitivity at long wavelengths is therefore excellent. Thus elements such as sodium and potassium, which emit orange and red light respectively, can be determined with much better sensitivity by FES than by AAS, even in an air–acetylene flame.

Traditionally in FES, small, circular burner heads were the norm (Cresser, 1994). With the development of AAS, however, it was soon realized that excellent detection limits by FES could be obtained using a long-path burner head in an AA spectrometer. The only modification required was to make the detector respond to a signal that, unlike the hollow cathode lamp signal, was not modulated. This was often achieved by modulating the light signal emitted from the flame with a mechanical chopper. Now most AA spectrometers can be used in the emission mode.

The nitrous oxide–acetylene flame can give excellent detection limits by FES, but it is not that widely used in practice for emission measurements. Many analysts prefer AAS because of the greater freedom from risk of spectral interference with the absorption technique. It is useful, however, to be aware of the potential of FES if, for example, a hollow cathode lamp is unavailable for a particular determination that is required in a hurry.

D. Electrothermal Atomization

It will be seen in Sec. II.E that a major constraint in flame AAS is the limited efficiency of transport of sample from a beaker of solution to the flame. In the late 1960s, this prompted a number of distinguished researchers such as L'vov, West, Massmann, and others to look for alternative atomization systems that did not depend upon generation and transport of aerosol to flames (Potts, 1987; Slavin, 1991; Lajunen, 1992). Early systems used small discrete portions of sample solution (ca. 50 μL) injected by hand onto the center of a resistively heated graphite rod or into a graphite tube heated using an arc system. Graphite was chemically inert (provided it was sheathed in nitrogen or argon while being heated) and capable of withstanding high temperatures. Moreover the graphite surface provided reducing conditions well suited to the reduction of metal oxides to the free elements. What ultimately evolved commercially was the graphite furnace electrothermal atomization (ETA) system that is still widely in use today, based upon a resistively heated graphite tube furnace (illustrated schematically in Fig. 4). In the early days, samples were injected by hand, a process requiring great manual dexterity. Fortunately, nowadays, sample injection is invariably performed under computer control using a robotic arm/autosampler system, and the precision attainable is excellent provided the system has been properly optimized.

From the early days, ETA-AAS was plagued by interferences. This was because several processes had to occur sequentially to achieve atomization. The atomizer temperature was raised in stages, so that the

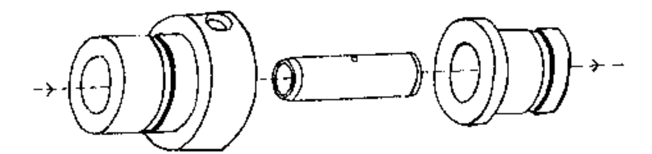


Figure 4 Exploded view of the main parts of a typical graphite furnace atomizer. When assembled, the sample is injected via the two holes shown. For simplicity, the water-cooled electrical connectors, lenses, and gas sheathing systems are not shown.

sample could first be dried by evaporating the solvent and then ashed at a few hundred degrees Celsius to remove any organic matrix, and finally atomized at a high temperature. A fourth and even hotter stage was then usually used to make sure every trace of determinant was removed from the atomizer. The problem was that the matrix had to be eliminated without any premature loss of determinant, and any chemical reactions between determinant and matrix components during heating could not be allowed to modify atomization efficiency. To make matters worse, atomic recombinations had to be prevented if they made samples and standards behave differently. As a consequence, although precision improved with automation, and some impressively low detection limits were eventually achieved (see, e.g., Slavin, 1991), attaining the necessary accuracy proved to be a real challenge.

From the outset, the light from the hollow cathode lamp was focused to a narrow beam passing along the furnace tube, parallel to the wall and passing just above the sample. The problem with this configuration was that the ends of the tube were, of necessity, much cooler than the tube center. Perkin-Elmer circumvented this problem by designing a transversely mounted tube, which was heated from the sides in such a way that the whole of the furnace containing the sample was at a more or less uniform temperature, as discussed by Lajunen (1992). This design minimized the condensation of determinant and matrix components at the furnace ends, but the tubes became rather expensive consumables because of the greater design complexity. This has led to some interesting studies of anything that might adversely affect the useful life of these tubes, such as corrosive acids in sample matrices (Rohr et al., 1999).

Three major developments were needed for ETA to become a reliable routine tool once automated sample introduction methodology had been developed. The first was the development of pyrolyic coatings on the inner graphite surface, which minimized penetration of sample solution into the porous graphite. Second came the development of matrix modifiers, which were chosen to delay atomization of determinant elements until high furnace temperatures had been attained, making atomic recombinations less likely to be a problem. Third came the ingenious idea from Boris L'vov of placing the sample not directly on the furnace tube wall but on a small boat or platform placed inside the tube (Fig. 5), and heating it primarily by conduction through the edges of the platform resting on the tube inner walls. This meant that by the time the sample was eventually atomized, the tube walls and the gas inside the tube were already at a much higher temperature than the volatilizing and atomizing determinant element. These developments dramatically reduced interference effects (Lajunen, 1992). They are discussed further in Sec. III.E.

Marcel Dekker, Inc.
270 Madison Avenue, New York, New York 10016



Figure 5 Vertical cross section (left) through a graphite furnace atomizer containing a L'vov platform. The end-on view (right) shows how the platform is positioned in premachined grooves to improve reproducibility between platforms.

E. Other Sample Introduction Systems in Flame AAS

1. Problems with the Pneumatic Nebulizer

We considered the use of flames as atomizers in AAS in some detail in Sec. II.C, but we have not yet considered how the sample is introduced into the flame. This is almost always achieved using a pneumatic nebulizer, which functions both as a pump for the sample solution and to break the sample up into a fine aerosol (Lopez-Garcia et al., 1987). The aerosol is then immediately and intimately mixed with the fuel and oxidant and then transported through a spray chamber to the base of the burner head. Figure 6 shows a typical pneumatic nebulizer. The oxidant doubles as the nebulizing gas, and issues at high velocity from a narrow jet that concentrically surrounds a central capillary through which the sample solution is sucked (aspirated).

Several other nebulizer designs have been suggested over recent years for various purposes (Cresser, 1990), and the complex operational theory underlying their design and manufacture has been extensively investigated (Sharp, 1988a,b). In spite of this, at the time of writing the simple concentric pneumatic nebulizer is still used in the vast majority of flame-based AAS instruments.

Once droplets of aerosol enter the flame, the solvent evaporates very rapidly, leaving minute solid particles. These must then be vaporized and then atomized. The bulk of the droplets never reach the flame, being lost by

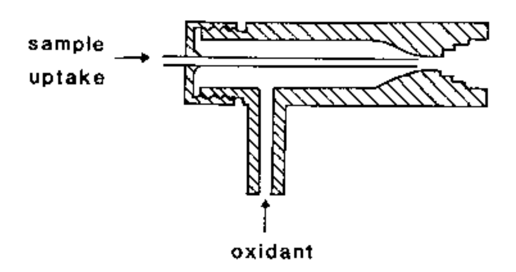


Figure 6 Cross section of a typical pneumatic nebulizer as used in AAS or FES.

Marcel Dekker, Inc.
270 Madison Avenue, New York, New York 10016

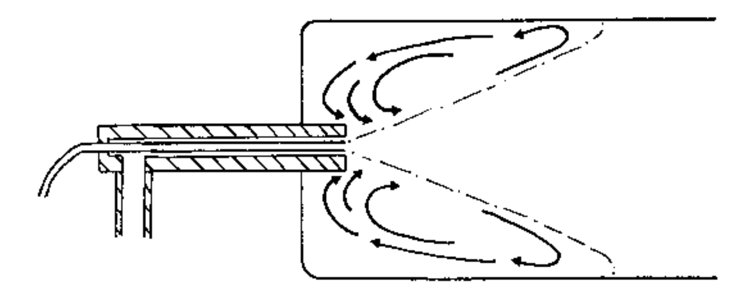


Figure 7 Schematic representation of the aerosol re-entrainment that occurs inside the end of a spray chamber.

deposition onto the spray chamber walls. It might be anticipated that most of this aerosol loss would occur on the end wall of the spray chamber opposite the nebulizer capillary tip, but in practice the exact opposite occurs. This was demonstrated very simply by O'Grady et al. (1985), by spraying colored dyes into chambers lined with absorbent paper and looking at the subsequent dye droplet distribution. Much of the loss was shown to occur close to, and even behind, the nebulizer capillary tip, as a consequence of turbulence and recirculation of aerosol into the expanding cone of spray. Further direct evidence for this turbulent entrainment pattern came from the use of cigarettes as smoke tracers, using progressively truncated spray chambers. Figure 7 illustrates schematically the aerosol recirculation pattern that occurs inside a normal chamber. Consequently at normal aspiration rates the transport efficiency (the ratio of the amount of determinant reaching the flame per second to the amount aspirated per second, expressed as a percentage) is generally only around 4–8%.

It appears that the only reliable way to improve transport efficiency with pneumatic nebulizers is to restrict significantly the aspiration rate (Cresser and Browner, 1980). Reducing the aspiration rate results in the nebulizer energy being distributed to less aerosol per unit time, resulting in a finer droplet size distribution; finer droplets (e.g., < 2000 nm in diameter) are more likely to be recirculated with the oxidant stream and transported through the spray chamber.

2. Cold Vapor Mercury Determination

An alternative approach to overcoming the transport efficiency limitation in flame AAS is to introduce the determinant to the flame in a gaseous form. Mercury exerts an appreciable vapor pressure of free mercury atoms even at room temperature. Therefore if mercury ions are reduced in solution to the

Marcel Dekker, Inc.
270 Madison Avenue, New York, New York 10016

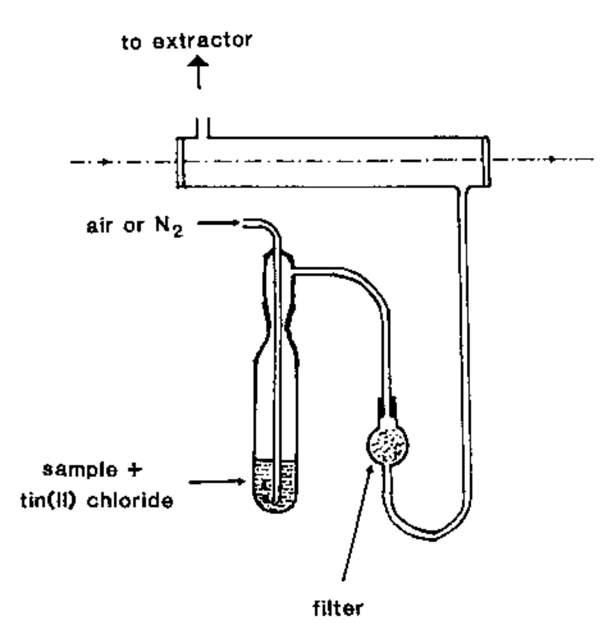


Figure 8 Sketch of apparatus that could be used for the determination of mercury by cold vapor AAS.

elemental state, and air or inert gas is bubbled through the solution, monatomic mercury vapor will be swept into the gas phase. This serves as a very sensitive basis for mercury determination. The very simple apparatus typically used is shown in Fig. 8. A glass tube atom cell with silica end windows replaces the flame or electrothermal atomizer. For convenience, the atom cell sometimes is simply clamped to the top of a conventional burner head. The apparatus is capable of yielding detection limits in the ng mL^{-1} range. Sensitivity may be further enhanced by trapping the mercury released from a large sample volume on fine gold wire as an amalgam; the mercury thus trapped is then liberated rapidly by heating. The transient signals are followed using a chart recorder or, more commonly, a suitably triggered integrator that measures the absorbance peak area.

When using the cold vapor method to enhance sensitivity, care must be taken to avoid interferences (Blankley et al., 1991). Ions such as sulfide and halides that complex mercury in solution interfere with the rate of reduction of ionic Hg to Hg^0. Any volatile organic compounds in the sample that happen to absorb at the wavelength used (253.6 nm) may also interfere. A water trap is built into the apparatus to avoid problems caused by condensation of water vapor in the atom cell.

3. Hydride Generation Techniques

The excellent sensitivity of cold vapor mercury determinations inspired a number of investigations of the possible conversion of other elements to simple molecular gases for sample introduction in AAS. Elements toward the right hand side of the periodic table tend to form covalent compounds such as hydrides, which are relevant here because they are volatile and generally readily decomposed to atoms. These hydrides are listed in Table 1, those that have been used in flame spectroscopic analysis being printed in italic type.

Of the elements with hydrides included in the table, carbon, nitrogen, oxygen, phosphorus, sulfur, and the halogens are not normally determined routinely by conventional AAS because their sensitive resonance lines are in the vacuum UV. Other elements, however, may all be determined with excellent sensitivity by flame AAS using hydride generation (Cresser, 1994). The hydride is generated in acidified sample solution, commonly by adding sodium borohydride, $NaBH_4$, and swept into the atomizer cell with a flow of inert gas such as argon or nitrogen. The cell is flame or electrically heated (Fig. 9). Peak height of the transient signal can be measured on a chart recorder, or integrated absorbance response can be measured over an appropriate time interval.

Sodium borohydride is a very strong reducing agent that can reduce several transition metals to free elements, which may interfere in the hydride generation technique. Interference may also occur as a consequence of consumption of reducing agent, the formation of metals that react with the hydride, the adsorption of hydrogen, and the disturbance of hydride transfer to the gas phase (Cresser, 1994). Techniques to eliminate interference include separation by solvent extraction, coprecipitation or ion exchange, and use of masking reagents. A helpful summary of these procedures can be found in a review of hydride generation techniques by Nakahara (1990).

Table 1 Volatile Hydride Compounds of Groups 4 to 7 of the Periodic Table. Italicized Compounds Have Been Employed in AAS or FES

Group 4	Group 5	Group 6	Group 7
CH_4	NH_3	H_2O	HF
SiH_4	PH_3	*H_2S*	HCl
GeH_4	*AsH_3*	*H_2Se*	HBr
SnH_4	*SbH_3*	*H_2Te*	HI
PbH_4	*BiH_3*		

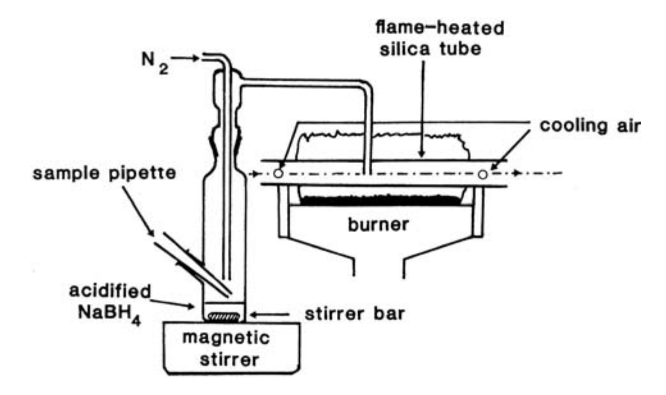


Figure 9 Sketch of apparatus that could be used for the determination by hydride generation AAS of the elements italicized in Table 1.

Hydride generation can also be used with ETA-AAS for the preconcentration of hydride-forming elements such as arsenic, antimony, and selenium. In this mode the hydride is passed into a furnace heated to a temperature just sufficient to decompose the hydride, and the determinant is trapped on a modifier coating (Niedzielski et al., 2002). High in-situ preconcentration factors are attainable using this approach.

A further element that usefully may be determined by vapor generation techniques is cadmium (Ebdon et al., 1993). Sodium tetraethylborate was used to produce a volatile cadmium species, and citrate was used to mask interferences from nickel and copper.

4. Sampling Cups and Boats

Several research groups around the world began to investigate alternatives to pneumatic nebulization for sample introduction from the late 1960s onwards, attempting to overcome transport efficiency limitations. The most successful approaches were those that involved heating small, discrete liquid or solid samples directly in a metal boat or cup that could reproducibly be positioned in a flame. The techniques were confined to the determination of relatively easily atomized elements such as arsenic, bismuth, cadmium, copper, mercury, lead, selenium, silver, tellurium, thallium, and zinc, because the temperature of the cup or boat would be less than that of the flame. For example, Schallis (1969) used a 50-mm long tantalum boat heated in an air–acetylene flame. The boat was preheated at the flame edge to volatilize the solvent and, if necessary, ash any organic matrix components, before being inserted into the center of the flame to achieve atomization. The transient absorption signals were recorded over ca. 1 s.

Marcel Dekker, Inc.
270 Madison Avenue, New York, New York 10016

The lower flame temperature tends to worsen the incidence and extent of matrix interferences when boat techniques are used, so precise matrix matching is necessary to achieve accurate results, or a standard additions method may be used (Kirkbright and Sargent, 1974). If in any doubt as to whether matrix matching alone is sufficient, the adequacy of the approach should be confirmed by analyzing certified reference materials and/or by applying the standard additions technique as well to a selection of samples. For bismuth, cadmium, lead, silver, and thallium, detection limits by AAS are a few $ng\,mL^{-1}$ or better (Kirkbright and Sargent, 1974). For arsenic, selenium, and tellurium they tend to lie in the range 10–30 $ng\,mL^{-1}$, depending upon the source used (Cresser, 1994).

Small tungsten filaments (often extracted carefully from small light-bulbs) have also attracted attention as atomizers, with the hope that they might be useful out at field sites. However, tungsten is readily attacked chemically at high temperatures, making it less than ideal. Recent studies have suggested that use of a permanent rhodium coating as a modifier may get around this problem (Zhou et al., 2002).

In 1970, Delves (1970) described the use of nickel foil micro crucibles 10 mm in diameter for the atomization of lead in blood samples, after a partial preoxidation with hydrogen peroxide at 140°C. The technique, widely known as the Delves' cup technique, was extensively used for more than a decade in many laboratories around the world and was also applied to environmental analyses such as the determination of lead in water.

A major advantage of cups and boats was their small sample requirement of 0.1 to 0.2 mg or less. Sample availability is not that often the major problem in environmental analysis, but some studies, for example of the heterogeneity of heavy metal distributions in leaves, are often only really viable if techniques with very small sample demands are available. However, for elemental analysis of small samples there is an increasing tendency to use electrothermal atomization if it is available.

F. Monochromators

It is necessary in AAS to isolate the desired line of the determinant element from any other background emitted light from the hollow cathode lamp. Not all lines of the determinant element give equal sensitivity, and it is therefore also necessary to isolate the determinant line at the wavelength that gives the most useful sensitivity. This is done with a grating monochromator. The typical optical layout in a monochromator used in AAS is the same as that used for sequential analysis in ICP-AES (see Chap. 2). The diffraction grating produces a spectrum in the plane of the exit slit, and the latter functions as a window to isolate the particular line (wavelength) of interest. When the

operator adjusts the wavelength setting of the monochromator, the grating slowly rotates and the spectrum moves laterally across the exit slit. This adjustment may be done manually, or, in more expensive automated instruments, under microprocessor control via a stepper motor.

G. Detector and Readout Systems

The light signal is invariably converted to an electrical signal by a photomultiplier tube (PMT). A description of the principle of the PMT may also be found in Chap. 2. The sensitivity (gain) of the PMT is regulated by altering the applied voltage. PMTs have a wide linear response range but do eventually become saturated. At high light levels, they often start to respond negatively to further increases in light intensity. This may cause confusion among novices in AAS when attempting to set up an instrument, so it is a good idea to have an idea of what the approximate gain setting should be on the instrument being employed.

The signal from the PMT is passed to a phase-sensitive and often frequency-tuned amplifier, which isolates the component attributable to light from the hollow cathode lamp from light emitted from the flame or stray daylight, as discussed in Sec. II.B. The absorbance is calculated electronically from stored values of I_0 and directly measured values of I_t, and the value is read from an analog or digital scale, or a computer, or fed to a chart recorder or printer.

On the simplest (or at least, the cheapest) instruments, absorbance is measured for a series of standards, and then for a series of samples. The values for the standards are used to draw a calibration graph, which is then used to estimate the concentrations of determinant in the samples from their measured absorbance values. On more expensive instruments, the calibration data is stored in a PC or microprocessor, which then calculates determinant concentrations directly. The calibration plot may be displayed on a monitor and/or printed if required. It is sensible to examine the calibration plot prior to accepting calculated results, to make sure that the standards are giving the anticipated calibration plot form. Some instruments take several readings of each sample and standard, and print out the standard deviation for the apparent concentration of each sample. This is a useful indicator of sudden drift problems. However, a low standard deviation does not necessarily indicate that the result is correct. It is important to discriminate between precision and accuracy!

H. Double-Beam Spectrometers in AAS

Source stability is very important in AAS, because the data processors in the instruments considered so far store values of I_0 to allow continuous

calculation of absorbance from the values of I_t monitored. If source intensity falls, the detector response will be equivalent to a positive absorbance signal. If the source intensity increases, the source drift will be detected as negative absorbance. One way around the problem of drift in source intensity is to rezero the spectrometer between each sample reading. A superior way is to employ a double-beam instrument. The light beam from the hollow cathode lamp in such an instrument is split into two parallel beams resolved in time, one passing to the detector through the flame as usual, the other by passing the flame. The latter beam can then provide a continuous value of I_0 in real time, the former a continuous value for I_t.

Double-beam instruments compensate for drift in source intensity (assuming the source line profile being used remains constant in shape) but not for fluctuations in flame background absorption. Thus it is still important to rezero instruments frequently. This is easily done between each reading while aspirating deionized water or an appropriate solvent blank. It is also important, however, to check periodically for drift in signal resulting from fluctuations in aspiration rate, by periodic aspiration of a standard of known concentration, typically after every 5–8 samples, and adjusting the instrument amplifier scale expansion as and when required. From this discussion it can be seen that double-beam instruments improve precision when precision is limited by source intensity fluctuations.

I. Making Atomic Emission Measurements

Generally a list of suitable wavelengths for making atomic emission measurements is provided with an AA spectrometer at time of purchase. Often more than one wavelength is suggested, each providing a different linear calibration range and detection limit. The monochromator wavelength setting should be carefully optimized while nebulizing a suitable concentrated solution of the element to be determined. It is important to establish that the determination is free from spectral interferences. Advice on how to do this is provided in Sec. III.F. The burner must be carefully aligned to maximize the signal-to-background-noise ratio and thus to optimize the detection limit.

III. INTERFERENCES AND THEIR ELIMINATION

To get accurate results in AAS, it is imperative that the determinant in samples and standards behaves in exactly the same way. Anything that stops this happening is an interference. Interferences fall into four classes, physical, chemical, ionization, and spectral. Each class needs to be considered, together with the methods used to combat the problems caused.

Differences may occur between the behavior of the determinant element in sample and standard solutions at a number of stages in flame AAS. These stages include aspiration, aerosol generation, transport of aerosol through the spray chamber, evaporation of solvent, volatilization of residual solid particulates in the flame, atomization, and the distribution and any subsequent recombination of atoms once formed. Interferences arising during the first four stages are termed ‘‘physical interferences.’’

A. Physical Interferences

Physical interferences occur during transport of determinant from the sample solution to the flame. The pneumatic nebulizer functions not only as a spray generator but also as a pump (Lopez-Garcia et al., 1987; Cresser, 1990). Anything that changes the pumping rate will alter the absorbance signal. The pumping rate is particularly sensitive to changes in viscosity of the sample solutions being aspirated. As aspiration rate is inversely proportional to viscosity, it is important that sample and standard solutions have the same viscosity. This is best achieved by reasonably precise matrix matching.

Viscosity is very much temperature dependent, so that samples or standards should not be aspirated straight after removal from a refrigerator (Cresser and Browner, 1980; O’Grady et al., 1984). The viscosity effect induced by change in temperature is not quite as great as simple theory predicts, for two reasons. As viscosity increases with decreasing temperature, the aspiration rate decreases, so that the energy of the nebulization gas is distributed to less solution per unit time. This produces a finer aerosol, that is transported with greater efficiency, partially offsetting the adverse effect of the increased viscosity (Cresser and Browner, 1980). Also the suction generated by a pneumatic nebulizer depends strongly upon the aspiration rate (O’Grady et al., 1984). If the rate of delivery of sample solution to the tip of the nebulizer capillary increases, the nebulizer suction falls, again having a compensatory effect.

The production of aerosol and its transport through the spray chamber are also important. The size distribution of the aerosol produced depends upon the surface tension, density, and viscosity of the sample solution. An empirical equation relating aerosol size distribution to these parameters and to nebulizer gas and solution flow rates was first worked out by Nukiyama and Tanasawa in 1939 (Cresser, 1994). Careful matrix matching is therefore essential not just for matching aspiration rates of samples and standards but also for matching the size distributions of their respective aerosols.

Marcel Dekker, Inc.
270 Madison Avenue, New York, New York 10016

Some organic solvents, for example 4-methylpentan-2-one (isobutyl methyl ketone, IBMK), produce a particularly fine aerosol and therefore exhibit a very high transport efficiency (Cresser, 1978). Such solvents are therefore useful for solvent extraction where very low detection limits are required. The enhancement in transport efficiency augments the benefit of preconcentration by solvent extraction.

For various reasons, the precise matrix composition may not be known, making exact matrix matching not feasible. The standard additions method should then be used. The sample is spiked with at least two additions of known amounts of determinant so that the matrix is not significantly altered, and the absorbance of spiked and unspiked samples measured and compared to that of aqueous standards, as shown in Fig. 10. The unknown concentration may be calculated by extrapolation back to the negative extension of the concentration axis. The standard additions method can only be used where the calibration graph is linear, and therefore it is best to make three or four standard additions in precise work. Small errors in slope from using too few additions may cause substantial errors.

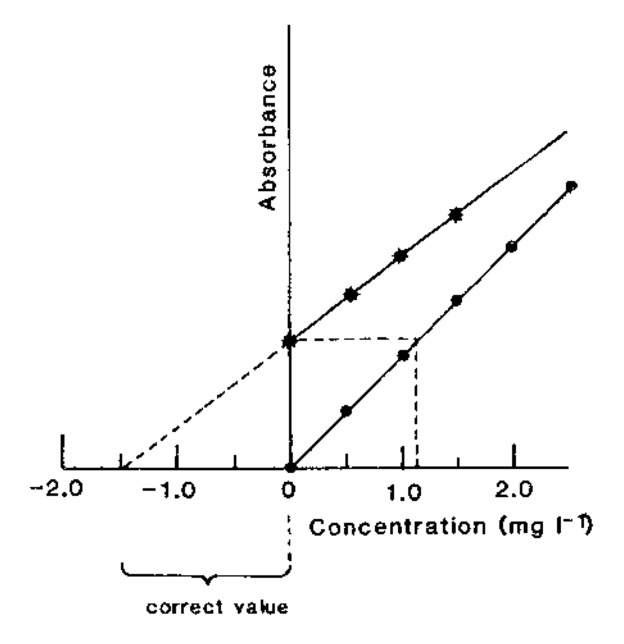


Figure 10 Typical results obtained by the standard additions method. The circles show the normal calibration graph, and the stars the calibration obtained using the sample and the sample after three incremental additions. Note that the slope of the calibration graph has changed.

B. Chemical Interferences

Chemical interference occurs if the determinant forms a thermally stable compound with one or more other ions or molecules in the sample solutions (Rubeška and Mosil, 1979). The best known examples in environmental analysis are the interferences of phosphate, silicate, and aluminum in the determination of calcium or magnesium in the air–acetylene flame.

Such effects can be overcome by using a hotter flame or adding a releasing agent. A releasing agent reacts preferentially with the interfering species, to form another thermally stable compound. Lanthanum or strontium is commonly used. The amount of interference that may be tolerated depends upon how much releasing agent is added. The same amount of releasing agent is always added to all samples and standards, not only for matrix matching purposes but also to compensate for the presence of trace amounts of determinant present as impurity in the releasing agent being used.

The extent of a chemical interference will be reduced if a hotter flame, such as nitrous oxide–acetylene, is employed because chemical interference depends upon the formation of thermally stable compounds. Sometimes, unless the interferent and determinant concentrations are both high, using a hotter flame may be sufficient to prevent interference from occurring at all, but this is not always the case. Chemical interferences are generally worse lower in the flame, and in cooler, fuel-rich flames (Cresser and MacLeod, 1976). Indeed, making analytical measurements at two different heights in a flame is useful for investigating whether chemical interferences are occurring (Gilbert et al., 1991). The same answer should be obtained at both heights if they are not.

The extent of chemical interferences is nearly always worse at higher determinant concentrations at any given interferent-to-determinant ratio (Cresser, 1977). This is because the small solid particles formed once the solvent evaporates will be larger and more difficult to vaporize and atomize at higher concentrations.

C. Ionization Interferences

Atoms of some elements are ionized relatively easily at high flame temperatures. This is especially true for the alkali and alkaline earth elements, and other elements on the left-hand side of the periodic table. The first ionization potentials also tend to be lower for heavier elements within a particular group. Thus for the Group 2A elements, ease of ionization follows the order Ba > Sr > Ca > Mg > Be. This would not matter in flame AAS, apart from a slight deterioration in sensitivity, if samples and standards were

ionized to the same extent. Suppose, however, that barium is to be determined in samples containing potassium. The potassium would be ionized:

$$K^0 \Leftrightarrow K^+ + e^-$$

This reaction would release many electrons into the flame, which would suppress the ionization of barium:

$$e^- + Ba^+ \Rightarrow Ba^0$$

Thus any potassium present in samples would increase the signal of barium, to an extent dependent upon the potassium concentration. This is an example of ionization interference, which is an enhancement in signal caused by depression of the determinant ionization by the presence of an easily ionizable concomitant element in a sample.

It is relatively straightforward to overcome ionization interferences. A constant and substantial excess of an easily ionizable element such as cesium or potassium is added to samples and standards, to maintain a constant flame electron concentration. The substance added is known as an ionization buffer. Ionization interferences are substantially worse in the hotter nitrous oxide–acetylene flame than in the air–acetylene flame. It is a common misconception that an ionization buffer totally suppresses determinant ionization, but this is not true. It buffers the degree of ionization at a constant and lower level.

D. Spectral Interferences in Flame AAS

It was explained earlier that very precise overlap of atomic absorption and emission profiles is required to obtain sensitive measurements in AAS. Absorption spectra of atoms at flame temperatures are much simpler than the emission spectra emitted by hollow cathode lamps. Many of the transitions observed in the emission spectrum do not have the unexcited state (the ground state) as their lower energy level. However, in flames, the vast majority of atoms exist in the ground state, and only transitions with the ground state as their lower energy state exhibit sensitive absorption (Cresser, 1971). The number of such transitions is small, so the probability of overlap of the atomic absorption line profile of one element with the emission line profile of another element is extremely small. The spectral selectivity of AAS is therefore excellent in this respect.

Examples of spectral line overlap are known. Europium at 324.7530 nm interferes in the determination of copper at 324.7540, but europium does not interfere in copper determination at 327.3962. As the interference occurs

only at one analytical wavelength, it must be spectral in nature, since the extent of physical, chemical, or ionization interferences would be similar at all wavelengths. Other pairs of overlapping lines include iron at 271.9025 and platinum at 271.9038 nm, aluminum at 308.2155 and vanadium at 308.2111 nm, and silicon at 250.6899 and vanadium at 250.6905 nm. Some further examples may be found in the useful monograph on spectrochemical analysis by Lajunen (1992). They are not problematic so long as the analyst is aware of their occurrence. They may be avoided by using an alternative atomic absorption wavelength. Most of the known examples do not in fact occur at the most sensitive absorption wavelength.

Several elements produce significant concentrations of polyatomic species in flames, particularly at high concentrations. Such species absorb, and they may cause spectral interference. Molecular absorption spectra are very wide compared with the atomic spectral lines. The formation of any solid particles in the flame causes scatter, which also causes an apparent broadband absorption, especially at lower wavelengths.

Molecular absorbance and scatter are overcome by the use of one of a number of background correction techniques. The simplest is to measure absorbance immediately adjacent to the determinant atomic absorption line. If light from a continuum source, such as a deuterium hollow cathode lamp, is passed through the flame at the analytical wavelength, the molecular absorbance is unchanged, but the atomic absorbance, as discussed earlier, becomes negligible. Thus subtracting the signal obtained with a continuum source from that obtained with the determinant line source provides a corrected absorbance. In several modern atomic absorption spectrometers, this correction is achieved automatically and simultaneously, time resolution of a few milliseconds being used to separate the two signals. Careful coalignment of the two source beams is very important to get good results, however. To overcome this need for precise beam matching, two other background correction systems have come into use over recent years.

In the Smith–Hieftje system, short pulses of high current are passed through the hollow cathode lamp (Smith et al., 1982). This in turn causes short pulses of high atom concentration in the hollow cathode lamp. The emission line profile is broadened as the atom cloud spreads beyond the hollow cathode itself, which causes absorption at the center of the emitted line profile. In effect, the single narrow emission line is split into a pair of lines immediately adjacent to the original line center. Thus the sum of atomic and molecular absorption is measured in the normal mode, but in the pulsed mode only molecular absorbance is monitored. The difference between the two signals yields a corrected atomic absorbance signal.

Background correction systems based upon the Zeeman effect also depend upon line splitting, but the absorption line profile (the π component) most commonly is split into two or more components (the σ components) by applying a strong magnetic field (Beaty, 1988). The σ and π components are resolved by exploiting the observation that the sigma components only absorb light with a particular plane of polarization. When the poles of an electromagnet are located around the atomizer, and measurements are made alternately with the magnetic field off and on, atomic plus molecular absorbance and molecular absorbance only may be measured in sequence. The difference gives the corrected atomic absorbance. Alternatively, it is possible to apply Zeeman splitting to the source atoms, which is more convenient in flame AAS, or to apply a constant intense magnetic field to the atom cell and to use a rotating polarizer to achieve separation of the σ and π components.

The advantages of Zeeman and Smith–Hieftje background correction systems over continuum source background correction is that they do not require precise alignment of two separate light beams (which is especially difficult in the UV) and they allow a high degree of correction to be applied. They may work well even if the molecular absorption is highly structured, which can cause problems with continuum source background correction.

E. Interferences in ETA-AAS

The origins and nature of interferences in ETA-AAS were briefly introduced in Sec. II.D. It might be anticipated that all determinations would now be conducted using the L'vov platform in a coated graphite furnace, and with a suitable matrix modifier. Unfortunately the situation is not quite that simple, as there may be loss in sensitivity for some elements when using platform rather than wall atomization. Moreover, although many researchers have sought a universally applicable matrix modifier, this has not yet been found. Palladium in particular has attracted much attention as a modifier in this context. It has been used, for example, to determine Ag, As, Cd, Cr, Hg, Ni, and Pb in seawater (Bermejo-Barrera et al., 1998). In this particular study, it was found that reducing the modifier to elemental palladium, rather than just using palladium nitrate, enhanced the performance, and multiple injections were used to enhance sensitivity. Sometimes palladium is used alone, sometimes in combination with other elements such as magnesium, strontium, or zirconium (Yang and Zhang, 2002). Rhenium has been evaluated as a semipermanent modifier, and with some success (Vale et al., 2001). Palladium and magnesium nitrates have been suggested for determination of cadmium and lead in coal slurries (Vale et al., 2001). For easily atomized elements like cadmium, ammonium

phosphate is also often used as a modifier, and the element can then again be determined directly in some slurried solid samples, such as seafoods (Bermejo-Barrera et al., 2000).

The optimum type and concentration of modifier depends to some extent on the type of graphite atomizer being employed and may differ between wall and platform atomization. Usually matrix modifiers are injected directly onto the sampling platform or furnace wall immediately prior to the sample solution injection. Sometimes a more permanent modifier coating is electroplated directly onto the furnace wall (Piascik and Bulska, 2001).

The extent of interferences in ETA-AAS may vary significantly with the height of observation in a graphite furnace. This has recently been demonstrated for the determination of tin, for which matrix effects depended both on the height of the light beam and on the nature of the modifier used (Ozcan et al., 2002).

In the early days of ETA especially, spectral interferences tended to be worse than when flames were used, because molecular absorption was more of a problem. This originated from matrix components, and as a consequence of atomic recombination to form molecular absorbing species. Smoke could be a problem, as well as inorganic molecular species from the matrix elements. The development of background correction systems played a major role therefore in turning ETA-AAS into an acceptable and reliable tool for routine analysis. However, the situation was also helped by the development of the L'vov platform and of matrix modifiers. Background correction is now regarded as essential if ETA is to be employed routinely.

F. Interferences in FES

Of the interferences described above for AAS, physical, chemical, and ionization interferences will be generally similar in incidence and extent in FES and AES. The methods used to overcome them are also similar and need not be discussed again here. In practice, the extent of ionization and chemical interferences may differ slightly because the optimized flame operating conditions may differ between the two techniques. In both AAS and FES, usually the fuel flow and burner height are optimized with respect to signal-to-background ratio, which may lead to slightly different flame temperature being used in the different techniques.

Spectral interferences are generally more severe in FES than in AAS. Unless emission wavelengths of two elements coincide exactly, it is usually possible to detect the presence of spectral interference by comparing scanned spectra obtained when nebulizing sample and standard solutions in turn. Alternatively, the determinant concentration should be measured at two

Marcel Dekker, Inc.
270 Madison Avenue, New York, New York 10016

different wavelengths. It is most unlikely that the extent of spectral interference would be identical at two different analytical wavelengths, so if the same concentration is found at two wavelengths, the analysis is usually free from spectral interference. Finally, analysis of certified reference materials is a valuable way to check that an analytical method is performing correctly.

IV. OPTIMIZATION OF PERFORMANCE IN AAS AND FES

If an adjustment is made to a spectrometer that doubles the signal value, but simultaneously doubles the noise on the baseline, the detection limit will not be improved. Thus to optimize detection limits, maximum signal-to-noise ratio is required and not the maximum signal. The factors that can be optimized in AAS include source-related parameters, atomizer-related parameters, and monochromator-related parameters. We should briefly consider each of these in turn. In FES, only flame- and monochromator-related parameters are important.

A. Source-Related Parameters in AAS

1. Effect of Lamp Current

Source operating power may substantially influence both absorbance and signal-to-noise ratio. For hollow cathode lamps, the maximum safe routine operating current is often printed on the lamp. To prolong operating lifetime, an appreciably lower current of around 4–7 mA is used routinely. If the lamp current is excessive, sputtered atoms escape from the immediate vicinity of the hollow cathode. The atoms thus liberated are cooler and in the ground state. They will therefore give very sharp absorption bands, absorbing most strongly at the centers of the resonance lines emitted by the lamp. The line profiles from the lamp thus become broader, eventually will exhibit self absorption, and ultimately display self reversal, giving the appearance of two lines close together immediately to either side of the original line. The effect closely resembles the Smith–Hieftje background correction effect discussed earlier.

As the absorption line profile in the atomizer still peaks at the initial emission line peak, absorbance is reduced as the emission line broadens, and even more if the emission line shows reversal. Thus atomic absorption signal decreases with increasing lamp current. The decline in sensitivity is greater for more volatile elements such as cadmium and zinc.

The biggest signal is obtained at very low current, but this will rarely give the best precision. At very low currents, the lamp discharge may be less stable, and a higher photomultiplier gain will be needed, so signal-to-noise ratio may become poorer. Thus it is important, but more time consuming, to find the operating current yielding the optimum signal-to-noise.

2. Effect of Warm-Up Time

Hollow cathode lamps take a few minutes (about 5) to stabilize. If the lamp gets brighter as it warms up, the baseline will tend to drift below zero. A double-beam AA spectrometer should compensate for this aspect of source intensity drift to a large extent. However, if as the lamp warms up, emission resonance line profiles broaden significantly, a small but significant decrease in signal over the first few minutes will be seen, even with a double-beam system.

3. Lamp Alignment

If the lamp is aligned properly, light from the most stable, central region of the hollow cathode is focused on the monochromator entrance slit. If it is not, light from the edge of the discharge (less stable) may be focused on the entrance slit. Moreover, much useful light may not reach the detector at all, resulting in a need for higher gain. Both effects may cause unstable signals.

Most hollow cathode discharges are red, because neon is the most common fill gas. Sometimes, to avoid unwanted neon emission lines, argon is used, and the discharge is then lilac. It is not advisable to use the red image of the cathode produced by a lens to align the lamp except to a first approximation, because UV and red light will focus through a lens at different points. Final fine alignment adjustments should be made using the meter or digital readout of the spectrometer to optimize light throughput.

4. Lamp Deterioration

Lamp performance deteriorates significantly after prolonged use (or after shorter periods of abuse). As the loss in precision is gradual, it may pass unnoticed for a long time. It is therefore sensible to keep a recorded trace of signal stability after a new lamp has been in use for a few hours for comparison purposes at a later date. To be useful, it is important to make a note of the slit width, photomultiplier gain setting, wavelength, and lamp current used, after ensuring that the lamp has been carefully aligned.

5. Choice of Lamp

In the author's experience, newish lamps from the same manufacturer, and even lamps from different manufacturers, tend to give rather similar

signal-to-noise ratios. Multielement hollow cathode lamps are available for some combinations of elements, but they tend to perform less well than single-element lamps. If microwave or electrodeless discharge lamps are employed, these too will have different performance characteristics. To compare sources, the absorbance signal size and stability for a suitable dilute standard solution should be compared, with all conditions, not just the lamp intensities and stabilities, carefully optimized.

B. Atomizer-Related Parameters

1. Choice of Atomizer

We saw when discussing instrumentation that the choice of atomizer may have a dramatic effect upon sensitivity and detection limits. The choice is not only between flames, electrothermal atomization (ETA), and cold-vapor and hydride generation techniques, but between different flames. Elements that form thermally stable oxides, such as Al, Ti, Si, Zr, may only be determined in the hotter, reducing nitrous oxide–acetylene flame. They cannot be determined with useful sensitivity in air–acetylene. Some elements, such as Ba and Cr, may be determined in air–acetylene but are more efficiently atomized by nitrous oxide–acetylene.

2. Effect of Fuel-to-Oxidant Ratio

For some elements, especially those that have a tendency to form thermally stable oxides, the fuel-to-oxidant ratio may have a dramatic effect upon the atomic absorbance signal. Precision will be much poorer for such determinations if the fuel flow is not carefully optimized. One point that is sometimes overlooked when optimizing the fuel-to-oxidant ratio is that the optimum conditions are sometimes highly matrix dependent. For example, the determination of calcium in water using an air–acetylene flame is more sensitive if a fuel-rich flame is used, whereas if the samples contain dilute sulfuric acid, a more fuel-lean flame usually gives much better sensitivity.

3. Optimization of Burner Position

Signal and signal-to-noise ratio both depend, sometimes quite dramatically, upon the position of the light beam from the lamp in the flame. In practice, burner position should be optimized in three respects:

1. Height
2. Sideways (lateral) position
3. Rotation

Marcel Dekker, Inc.
270 Madison Avenue, New York, New York 10016

Signal and signal-to-noise ratio often vary markedly with height of observation in the flame, but it should be remembered too that the precise optimal height often depends, sometimes critically, upon the matrix components in the sample. Passage of the light beam through the edge of the flame, rather than the flame center, results generally in reduced signals and poor signal stability. If the burner head is not properly aligned rotationally, the light beam may not pass through much of the atom population in the flame at all.

Burner rotation sometimes is recommended as a method of losing sensitivity deliberately in flame AAS, to extend the linear range of the calibration graph to higher concentrations to avoid the need for sample solution dilution. Such a practice is not really a good idea, because the flame edges will then make a greater relative contribution than the flame center to the total signal, so that precision is generally appreciably poorer. Moreover, as mentioned earlier, chemical matrix interferences tend to be more of a problem at higher determinant concentrations.

4. Burner Design, Warm-Up, and Cleanliness

Most often the analyst has no say in burner design; he or she has to use the burner heads provided. However, burner heads with a triangular cross section in the immediate vicinity of the slot are to be preferred, for reasons covered earlier. If the burner head is flat, severe turbulence at the point of air entrainment, where the inflowing air has to change direction very sharply, results in localized heating of the burner head, which adversely effects both warm up time and the tendency of the slot to clog. It is worth considering head design when buying a new spectrometer.

If the burner slot does become obstructed, it is easy to detect. The flame starts to appear uneven, and signal stability deteriorates. If this happens, it is necessary to extinguish the flame and clean the slot. After the burner head has cooled, use a razor blade or a cleaner provided by the manufacturer, preferably with air flowing through the slot, to eject deposits liberated. Sometimes thorough flushing with distilled water and then drying may be necessary for a longer lasting cure.

It takes from 5 to 10 minutes for a burner head to warm up thoroughly, depending upon the burner design. Significant changes in the appearance and flame geometry of the nitrous oxide–acetylene flame over this period are generally clearly visible. Results are much improved if the burner head, and the hollow cathode lamp, are both allowed to warm up for 10 minutes prior to the nebulization of any samples or standards.

5. Gas Flow Stability

Fuel and oxidant gas flow stabilities must be adequate to achieve good precision. Intermediate ballast tanks help to smooth out fluctuations caused by compressors and are often built into systems recommended by manufacturers. Nitrous oxide cools when it is subjected to a sharp pressure drop, which can result in substantial cooling of the cylinder head, and sometimes in instability. The effect is less of a problem if the nitrous oxide operating pressure is at around 45 p.s.i. (0.3 MPa) or above, as is generally the case with modern instruments, but the problem may be severe in older instruments operating at lower pressures. It may be reduced by using a ballast tank at an intermediate pressure, say 60 p.s.i. (0.4 MPa) (Cresser and Wilson, 1973), or by strapping heating tape to the cylinder head. Acetylene cylinders should be allowed to attain normal working temperature before use, especially after exposure to very cold weather.

C. Monochromator Parameters

The main monochromator variables are the slit width and the wavelength setting.

1. Choice of Slit Width

The slit width, or spectral band pass, chosen depends largely upon the complexity of the source spectrum being used. If the determinant element has a complex spectrum in the immediate vicinity of the resonance line to be used, a narrow slit must be employed to isolate the wavelength that gives the best sensitivity. A narrow slit also improves the line-to-flame background emission ratio, which may reduce noise associated with the detector. Modern lamps usually have sufficient light output for narrow monochromator slit widths to be used without the need for undesirably high electronic gain.

2. Choice of Wavelength

The optimum wavelength for a lamp with respect to sensitivity is normally provided by the manufacturer, and the values are now well known for all the elements. However, the line that gives the best sensitivity is not always employed, because it also gives the greatest curvature to the calibration graph. A line giving slightly poorer sensitivity may be selected deliberately to extend the linear working range of the calibration graph.

Care should be taken that the wavelength calibration of the monochromator is correct, or if it is not, what the magnitude of the error is so that correction can be applied. For elements that have complex

emission spectra, such as iron, a small wavelength calibration error may result in the wrong wavelength accidentally being employed, which can seriously adversely affect both sensitivity and precision. A lamp such as magnesium, with a very simple spectrum, makes it easier to check the wavelength calibration.

D. Optimization in ETA-AAS

Some aspects of optimization for ETA-AAS are identical to those for flame AAS, including all the source- and monochromator-related parameters discussed earlier. However, for the atomizer, there are several factors to consider. For some elements the choice of furnace tube type (e.g., normal graphite, pyrolytically coated graphite, totally pyrolytic graphite) can have a marked influence upon sensitivity, as can the decision about whether to use wall or platform atomization. Fortunately, nowadays the manufacturers' instrument manuals offer guidance on these decisions. As discussed in Sec. III.E, choice of matrix modifier can also be very important, not just to reduce or eliminate specific interferences but also because of the effect that modifier choice has upon sensitivity. Here too the manufacturer's guidelines should be closely followed. To obtain good sensitivity and precision, it is essential that the capillary that introduces the sample to the furnace is carefully trimmed, and aligned inside the furnace in accordance with the manufacturer's guidelines. The latter also provide data on optimum choice of gas to use for providing an inert atmosphere, gas flows, and the most appropriate temperature program to use for the drying, ashing, atomization, and cleanout stages of the determination.

Although many instruments can be operated without the operator examining the transient signal obtained during ETA-AAS, it is a good idea to study this carefully during the setting up of an analytical protocol, as the peak shape may provide useful information about possible problems such as erratic sample introduction or carryover effects between samples. It may also provide a good early warning if the capabilities of a particular background correction are being over-stretched.

E. Optimization in FES

The optimization procedure is simpler in FES than it is in AAS in some respects, because there is no hollow cathode lamp in FES, but it still requires thought and care. The monochromator slit width in FES may need to be selected based upon obtaining adequate spectral resolution to prevent spectral interferences, rather than to obtain the best signal-to-noise ratio. This requires knowledge of the approximate chemical composition of the

Marcel Dekker, Inc.
270 Madison Avenue, New York, New York 10016

sample matrix and of the emission spectra of elements present. Once an appropriate emission wavelength has been selected, the peak emission intensity at that wavelength may be precisely located by scanning slowly through the emission line while nebulizing a suitable standard solution. The burner position and the fuel-to-oxidant ratio of the flame then have to be adjusted to give the best possible signal-to-noise ratio.

V. APPLICATIONS IN ROUTINE ANALYSIS

A new atomic absorption spectrometer arrives with a full set of instructions on how to set the instrument up safely and the key parameters that should be used for every element that might be determined. The latter may be in a manual, or it may be stored on a computer CD to facilitate rapid access to information. Some more sophisticated instruments may even set the instrumental conditions automatically in default mode to those specified. The purpose of this section is to provide a concise guide to routine analysis for elements commonly regarded as being of environmental interest, to give readers a feel for what they need to know.

A. Commonly Determined Elements

1. Aluminum

Aluminum is often determined by flame AAS, and sometimes by FES, but a nitrous oxide–acetylene flame is essential. Ionization is significant, and potassium or cesium at a final concentration of 3–5 $mg\,mL^{-1}$ should be added as an ionization buffer. This is especially important at low determinant concentrations. Fuel flow is critical: a fuel-rich flame with a red-feather zone (a red zone above the bright and intensely emitting primary reaction zone in contact with the burner slot) of at least 5 mm is needed.

Flame AAS is useful for the determination of total aluminum in soils and rocks, and extractable (e.g. with 0.1 *M* potassium chloride) aluminum in soils. The extractants used for measuring amorphous aluminum in soils tend to cause severe burner obstruction (often termed clogging) problems, especially in the fuel-rich flames used. It may well be necessary to flick surface deposits off the burner head every five to ten samples, using a flat-ended metal spatula. This must be done rapidly, but with great care, both to avoid burns and to avoid melting the spatula. Deionized water should be nebulized between samples, not a reagent blank, to minimize clogging.

There is rarely enough aluminum in natural water samples to allow direct determination by flame AAS, except when the element is organically complexed in waters draining from very acid organic surface soils, for

Marcel Dekker, Inc.
270 Madison Avenue, New York, New York 10016

example during upland storm events. Aluminum may be preconcentrated by solvent extraction (Cresser, 1978), but ETA is more convenient and allows concentrations in freshwaters to be measured (e.g., Krivan et al., 1998). Silicic acid interferes, but magnesium nitrate will serve as a matrix modifier (Schneider and Exley, 2001).

2. Antimony

Because the concentration of antimony is usually very low, preconcentration of the element introduced as its hydride (stibine) in situ in a graphite furnace offers an interesting and viable approach to its determination by AAS (Niedzielski et al., 2002). Alternatively, the element in natural waters may be preconcentrated as the antimony (III)-pyrogallol complex on activated carbon prior to analysis of the latter by AAS after injecting its suspension into a graphite furnace (Kubota et al., 2001). Wojciechowski et al. (2001) showed that palladium or iridium was a better modifier than rhodium for antimony determination by ETA-AAS. Neither flame AAS nor FES has adequate sensitivity for most analytical applications.

3. Arsenic

Arsenic may be determined by flame AAS, but ETA-AAS or hydride generation are inevitably needed to obtain adequate sensitivity for environmental samples. An r.f. EDL will generally give a superior detection limit to a hollow cathode lamp. Hydride generation gives a detection limit of around 0.8 ng mL^{-1} by AAS under optimized conditions (Cresser and Marr, 1991). This has resulted in the development of automated, flow-injection-based hydride generation systems for the determination of arsenic in soil extracts (Welz and Schubert-Jacobs, 1991). Hydride generation has also been used in speciation studies for arsenic forms in waters (Van Elteren et al., 1991), and an automated flow-injection-based system for arsenic speciation has also been described (Tsalev et al., 2000a). If necessary, UV photo-oxidation may also be used on-line to facilitate in this determination (Tsalev et al., 2000b).

Some analysts prefer AAS with ETA to hydride generation for arsenic quantification, because of the interference problems when hydride generation is used (Lajunen, 1992), although Hershey and Keliher (1989) showed that ion exchange could be used to reduce these interferences. Chen et al. (2001) used ETA-AAS to quantify background arsenic concentrations in soils of Florida. Peramaki et al. (2000) used ETA and palladium–magnesium nitrate as modifier to determine arsenic in humus and moss samples after microwave-assisted acid/hydrogen peroxide digestion. Arsenic (III) and (V) have been separated as complexes of ammonium

tetramethylenecarbodithioate and Mo-malachite green, respectively, absorbed sequentially on C-18 silica gel, prior to elution with ethanol and determination by ETA-AAS using a palladium modifier (Hirano et al., 2001b). Arsenic in natural waters may be coprecipitated with the nickel tetramethylenecarbodithioate complex using APDC as a reagent, and the precipitate analyzed directly by graphite furnace AAS to quantify arsenic (Zhang et al., 2001).

4. Barium

Barium forms a thermally stable oxide, so it is only atomized to a useful extent in the nitrous oxide–acetylene flame, in which it may be determined at 553.6 nm by either FES or FAAS. An ionization buffer such as potassium at $5\,g\,L^{-1}$ must be added, as the element has a very low ionization potential. Fuel flow must be carefully optimized. Molecular band spectra of calcium species may be a problem when calcium is present at a large excess, as is generally the case in environmental samples. The problem can be minimized by adding an extra collimator to the instrument, to confine the field of view to the flame center, since the unwanted molecular absorption and emission are greater at the flame edges.

As barium is present at very low concentrations in most environmental samples, ETA is more commonly used for its determination. An exception is in the analysis of formation waters from offshore oil wells (Jerrow et al., 1991). In this matrix, interelement interferences were encountered from alkali and alkaline-earth elements, but these could be eliminated by the addition of $5\,g\,L^{-1}$ magnesium plus $3\,g\,L^{-1}$ sodium as a modifier.

5. Boron

Even in a fuel-rich nitrous oxide–acetylene flame, the atomization efficiency of boron is low because of the great strength of the B–O bond, so its determination in almost all environmental materials is not possible by flame AAS or FES. AAS with ETA is useful provided a suitable matrix modifier is employed (Szydlowski, 1979; Marr and Cresser, 1983). Determination by ETA-AAS can be difficult, but use of calcium and zirconium chlorides as modifiers avoids the problems associated with the very high atomization temperature of boron carbide and allows determination over the range $0.1–2.0\,mg\,L^{-1}$ (Nowka et al., 2000).

6. Cadmium

Cadmium is very easily atomized, and the determination by flame AAS is sensitive, with detection limits as low as $1\,ng\,mL^{-1}$ in air–acetylene (Cresser, 1978), and much lower than this by ETA-AAS. Many examples of its

determination in environmental samples using ETA-AAS have been listed by Dymott (1981). The determinations in acetylene flames are virtually free from chemical interference (Cresser, 1994). As mentioned earlier, a cold-vapor sample introduction technique has also been suggested for cadmium determination (Ebdon et al., 1993). Cadmium concentrations in most environmental samples are so low that the element is still often preconcentrated. For example, discrete nebulization flame AAS has been used to measure foliar cadmium after extraction of the APDC complex into chloroform (Welz et al., 1991). Many other solvent extraction procedures are well documented for cadmium (Cresser, 1978). The element is so easily atomized that its atoms can be trapped on a cooled tube above the flame (a slotted tube atom trap) and then atomized as a pulse by stopping the cooling of the tube. This approach has been applied to the determination of cadmium in fruits and soils, for example (Yaman and Dilgin, 2002).

The determination of cadmium by ETA-AAS is extremely sensitive with a suitable matrix modifier, and as the element is so readily atomized it may be determined directly in slurried solid samples for matrices such as clams and cockles (Bermejo-Barrera et al., 2000) or coal (Vale et al., 2001). Ammonium phosphate was used as modifier. For cadmium in seawater, hydrofluoric acid has been advocated as a matrix modifier, because it allows removal of chloride (as HCl) at a relatively low temperature (Cabon, 2002). A recent very comprehensive study of the determination of cadmium in a wide range of environmental samples concluded that recovery was between 93 and 106% by ETA-AAS (Rucandio and Petit-Dominguez, 2002), while another study using preconcentration on an iminodiacetate-type chelating resin, and AAS determination of cadmium in natural waters gave recoveries of 99–108% (Hirano et al., 2001a).

7. Calcium

Calcium has a simple atomic absorption spectrum, and the 422.7 nm line is used for its determination by AAS. The second most sensitive absorption wavelength gives sensitivity some 200 times poorer, so is of no practical interest. The element may also be determined readily by FES. Calcium is atomized in a fuel-rich air–acetylene flame, although its determination in this flame is prone to chemical interference from aluminum, phosphate, and silicate. A releasing agent, such as lanthanum at 5 mg mL^{-1}, is therefore mandatory in environmental analyses. Interferences are reduced, but not eliminated, high in a fuel-lean flame, and such conditions give poorer sensitivity anyway. Reagents present in the matrix, especially phosphoric and sulfuric acids, markedly effect both sensitivity and optimal flow conditions, and matrix matching is necessary. Some analysts prefer using

Marcel Dekker, Inc.
270 Madison Avenue, New York, New York 10016

nitrous oxide–acetylene to minimize risk of interferences, and this is a sound practice. Calcium, however, has a low ionization potential, so an ionization buffer such as 5 $mg\,mL^{-1}$ potassium must be added. Flame AAS is sufficiently sensitive to meet the needs of most environmental applications. ETA gives better sensitivity but this is not normally necessary.

8. Chromium

Although chromium is atomized in a fuel-rich air–acetylene flame, the determination is susceptible to interference from a range of elements likely to be present in environmental samples. Moreover, chromium in different oxidation states gives a different response in this flame, and for chromium (VI) the response tends to vary with solution pH (Cresser and Hargitt, 1976a). The determination is therefore best done in a fuel-rich nitrous oxide–acetylene flame, with careful optimization of the fuel flow for each sample matrix. The most sensitive resonance line at 357.9 nm is the one invariably employed. If necessary, Cr(III) and Cr(VI) may be measured individually, using an exchange resin to separate the cationic and anionic species (Cresser and Hargitt, 1976b). The speciation step may be coupled with a preconcentration step and the entire process automated using flow injection methodology (see Chap. 4) (Sperling et al., 1992).

The detection limit by conventional flame AAS is generally only around 10 $ng\,mL^{-1}$. Thus preconcentration is often necessary before applying flame AAS to determine chromium in environmental samples (Cresser, 1978). However, because of the low concentrations often present, many analysts favor ETA-AAS over flame techniques for this determination, to avoid the need for a time-consuming preconcentration step. Total chromium in soils has been determined using a soil slurry, with particles kept in suspension using ultrasonic agitation (Lilleengen and Wibetoe, 2002).

9. Cobalt

Flame AAS may be used for cobalt determination, usually with a lean air–acetylene flame and at a wavelength of 240.7 nm. However, even under carefully optimized conditions, the detection limit is only ca. 10 $ng\,mL^{-1}$, so ETA-AAS may be necessary to obtain adequate sensitivity. In air–acetylene, sulfate depresses the absorbance except at very low cobalt concentrations, so careful matrix matching is advisable, but generally few interferences have been documented (Cresser, 1994). For most environmental samples, preconcentration techniques such as solvent extraction are essential to achieve adequate sensitivity in flame AAS (Cresser, 1978). Total cobalt in soils has been determined, along with total chromium, by ETA-AAS using

a soil slurry, with particles kept in suspension by ultrasonic agitation (Lilleengen and Wibetoe, 2002).

10. Copper

Copper may be determined in a lean air–acetylene flame, using the most sensitive resonance line at 324.7 nm. The detection limit is around 10 ng mL^{-1}, which is adequate for many practical applications in environmental analysis, such as the measurement of plant copper concentrations or EDTA- or DTPA-extractable copper in soils. Matrix matching is advisable, although interferences are rare and unlikely to be a problem from other elements present in most environmental samples. The sensitivity of flame AAS is inadequate for the direct determination of copper in natural water samples, for which ETA must be used unless a suitable preconcentration technique is employed (Cresser, 1978). Copper could be determined directly in slurried coal samples by ETA-AAS, even without a modifier (Vale et al., 2001).

11. Iron

With a high natural abundance in the earth's crust, iron is present in many environmental samples at concentrations readily determinable by flame AAS without resort to preconcentration. The detection limit at 248.3 nm using a carefully optimized, lean air–acetylene flame, is around 10 ng mL^{-1}. Although silicate, nickel, and cobalt interfere in the air–acetylene flame, nickel and cobalt are rarely present in sufficient excess to pose a problem. Silicate interference may be eliminated by the use of lanthanum as a releasing agent or by using a nitrous oxide–acetylene flame. Careful optimization is necessary, especially in freshwater analyses when concentrations are often very low. Because the emission spectrum of an iron hollow cathode lamp is extremely complex, it is important to use a narrow spectral bandpass and to make sure that the correct wavelength is being used. Sensitivity at adjacent lines should be checked if anticipated sensitivity is not attained. For some samples it is best to exploit the superior sensitivity of ETA-AAS.

12. Lead

The determination of lead by flame AAS is not very sensitive, so for environmental samples the element is best determined using hydride generation, as plumbane, PbH_4, or by using ETA. In the latter case, modifiers such as palladium or magnesium nitrates are often used, in which case the element may sometimes even be determined in slurried solid

Marcel Dekker, Inc.
270 Madison Avenue, New York, New York 10016

samples. Coal, for example, may be analyzed in this way (Vale et al., 2001). For lead in seawater, hydrofluoric acid has been advocated as a matrix modifier, as it allows removal of chloride (as HCl) at a relatively low temperature (Cabon, 2002). Jorhem et al. (2000) used ETA-AAS to quantify lead in vegetation and associated contaminated soils in Sweden. The Delves' cup was originally developed to determine blood lead concentrations, but its use has been largely superseded by that of ETA-AAS.

13. Magnesium

Magnesium determination in a lean air–acetylene flame at 285.2 nm is remarkably sensitive, with a detection limit of around 0.1 ng mL^{-1} under properly optimized conditions. The normal working range unfortunately is only around 100–500 ng mL^{-1} in flame AAS, curvature of the calibration plot typically becoming severe at ca. 1500 ng mL^{-1}. At higher concentrations samples must be diluted, although some analysts use an impact cup to lower transport efficiency and extend the linear calibration range upwards (Cresser, 1979). An alternative line at 202.6 nm is sometimes used in flame AAS over the range 5–20 mg L^{-1}. Silicate, phosphate, and aluminum interfere in magnesium determination in air–acetylene, so a releasing agent, usually lanthanum at a final concentration of 5–10 mg mL^{-1}, is added. Above 2 mg magnesium L^{-1}, sulfate also starts to interfere in many instruments, although no such interference may be encountered at lower concentrations (Cresser and MacLeod, 1976).

The determination of magnesium is so sensitive that there is rarely any reason for attempting to determine the element by ETA-AAS unless sample availability is severely limited.

14. Manganese

The sensitivity of manganese determination by flame AAS is excellent, so the technique is widely used in environmental analysis. The detection limit at 279.5 nm in a lean air–acetylene flame is about 10 ng mL^{-1}, which is quite adequate for most samples. A narrow spectral bandpass should be used, and care taken to use the 279.5 nm line rather than adjacent lines at 279.8 or 280.1 nm. In natural water samples, concentrations of manganese may often be at or below the detection limit of flame AAS, and solvent extraction or some other technique must be used for preconcentration (Ganhdi and Khopkar, 1992; Yebra-Biurran et al., 1992), or, more conveniently, ETA-AAS should be used with a suitable matrix modifier. The element may also be determined by FES with good sensitivity, using one of a triplet of lines at around 403 nm.

15. Mercury

The detection limit using an air–acetylene flame is only about 500 ng mL^{-1}, which is far too high a concentration to be of any practical value in environmental analyses. By cold-vapor techniques, detection limits of around 1 ng mL^{-1} are generally attainable (see Sec. II.E.2). Lower detection limits are attainable by concentrating the mercury on a gold amalgamator (Liang and Bloom, 1993). Alternatively, the element may be determined using ETA-AAS, with a matrix modifier such as palladium plus zirconium to ensure that the element is not volatilized prematurely (Yang et al., 2002). Transfer of mercury from a solid sampling probe to the palladium-coated wall of a graphite furnace atomizer has been suggested for the determination of the element in solid coal samples (Maia et al., 2002).

16. Molybdenum

Molybdenum may be determined at 313.3 nm in a slightly reducing nitrous oxide–acetylene flame only down to ca. 30–50 ng mL^{-1}, which is inadequate for most environmental samples without preconcentration (Cresser, 1978). Solvent extraction procedures are time-consuming, and ETA-AAS is preferable for this determination. Care is then needed to ensure that the correct type of graphite furnace is used to obtain stable and sensitive calibration.

17. Nickel

The AAS detection limit for nickel at 232.0 nm under carefully optimized conditions in an oxidizing air–acetylene flame is about 10 ng mL^{-1}. This is only adequate for environmental applications where a low solution-to-sample weight ratio may be used. For example, if 1 g of plant material is digested with a mixture of nitric and perchloric acids, and the mixture diluted only to 10 mL, nickel can be determined directly by flame AAS. Similarly, the author has been able to analyze aqua regia digests of sludge-treated soils directly. The spectrum of nickel hollow cathode lamps around the main resonance line (232.0 nm) is complex, and it is important to use a narrow spectral bandpass and to make sure that the correct line has been selected. Passing light at adjacent wavelengths results in very pronounced curvature of calibration plots and decline in sensitivity. There are few interferences for environmental samples at low nickel concentrations (Cresser, 1994).

Sometimes, preconcentration by solvent extraction is essential. Often the nickel tetramethylenedithiocarbamate complex is extracted at pH 2–4 into 4-methylpentan-2-one (Cresser, 1978). This system has been applied extensively to water and other environmental samples. However,

determination by ETA-AAS may be more convenient and rapid. It has been used, for example, for speciation of nickel in airborne particulate matter (Fuchtjohann et al., 2001). Even using ETA, preconcentration was still required for determination of nickel in seawater (Zih-Perenyi et al., 2000).

18. Potassium

Potassium is readily determined by flame AAS or FES. Even in air–acetylene, potassium at low concentrations is significantly ionized unless an efficient ionization buffer is added. The element may be determined at 766.5 or 769.9 nm (the latter wavelength giving approximately three times poorer sensitivity) in an oxidizing air–acetylene flame. Absence of an ionization buffer results in concave curvature of the calibration graph at low concentrations. The superior sensitivity of ETA-AAS is not usually needed for potassium determination in environmental samples.

19. Selenium

Selenium may be determined at 196.0 nm by AAS, using a nitrous oxide–acetylene flame (which is more transparent than air–acetylene at this low wavelength). The detection limit at ca. $1\,mg\,L^{-1}$ is too low to be useful for environmental analyses. The element is therefore most commonly determined by hydride generation techniques, as discussed in Sec. II.E.3, or by ETA-AAS. If direct flame AAS is used for some reason, then preconcentration by solvent extraction is necessary (Cresser, 1978). However, this approach would be rare nowadays, as graphite furnace AAS can be used if a suitable modifier is employed, and the determination of the element in slurried soils has been described using PTFE, hydrofluoric acid, and nickel nitrate as modifiers (Dobrowolski, 2001). The method worked well when tested on certified reference materials.

20. Sodium

When determining sodium at very low concentrations by FES or by flame AAS, it is advisable to add $2–5\,mg\,mL^{-1}$ potassium or cesium as an ionization buffer. Some analysts believe it is unnecessary to invest in a sodium hollow cathode lamp, preferring instead to determine sodium by flame emission methods. The superior sensitivity of ETA-AAS compared with flame AAS is rarely required.

21. Strontium

Strontium may be determined at 460.7 nm by AAS or FES, using a nitrous oxide–acetylene flame and an ionization buffer to minimize the risk of

ionization interference, down to a few ng mL^{-1}. Chemical interference from phosphate, silicate, and aluminum is reduced dramatically in this flame compared with the air–acetylene flame. If better sensitivity is required, ETA-AAS should be used.

22. Sulfur

Sulfur is never determined routinely in environmental samples by flame AAS or FES techniques, because its lines lie in the vacuum UV.

23. Tellurium

Tellurium can be determined with moderate sensitivity by flame AAS, at 214.3 nm in an oxidizing air–acetylene flame. The detection limit is generally poor, at ca. 100 ng mL^{-1}, which is inadequate for environmental applications unless the element is preconcentrated by a substantial factor (Cresser, 1978). However, hydride generation AAS yields much more useful detection limits, as does ETA-AAS. Even so, preconcentration may be necessary if the element is to be determined in natural waters, for example by extraction as the tributylphosphate complex. Tellurium has attracted little interest from environmental scientists, probably because of its very low natural abundance.

24. Tin

Tin is best determined at 224.6 or 235.5 nm in a reducing nitrous oxide–acetylene flame. The use of hydrogen as a fuel may improve sensitivity, but only at the expense of serious interference problems, so it cannot be recommended. Fortunately hydride generation is applicable to tin, improving the detection limit to ca. 1 ng mL^{-1}. For natural water samples, the element is still sometimes preconcentrated prior to determination by hydride generation techniques (Nakashima, 1992). ETA-AAS may be used to determine alkyl tin compounds, but preconcentration by extraction into IBMK may be necessary for freshwater analysis, with multiple injection into zirconium-coated tubes used to enhance sensitivity (Bermejo-Barrera et al., 2002). Tin in natural waters may be coprecipitated with the nickel tetramethylenecarbodithioate complex using APDC as a reagent, and the precipitate analyzed directly to quantify tin (Zhang et al., 2001).

25. Titanium

Titanium has not been determined often in environmental samples, though it is of interest in pedogenesis and geology. A fuel-rich nitrous oxide–acetylene flame is essential for its determination, because it forms a very

Marcel Dekker, Inc.
270 Madison Avenue, New York, New York 10016

stable bond to oxygen. The detection limit at 364.3 nm is generally ca. 100 ng mL^{-1}. At low concentrations the determinations require addition of ca. 5 mg mL^{-1} cesium or potassium or as an ionization buffer, and usually excess aluminum, typically around 1 mg mL^{-1}, is also added to prevent interference from aluminum, iron, and fluoride. If necessary, the element may be preconcentrated by solvent extraction (Cresser, 1978).

26. Zinc

Zinc may be determined with excellent sensitivity by flame AAS because it is such a readily atomized element with a simple spectrum, the detection limit at 213.9 nm generally being ca. 1 ng mL^{-1} in air–acetylene. This is more than adequate for most environmental analyses. Interferences are rarely a problem, although matrix matching is still advisable. If, however, a lower detection limit is deemed necessary, ETA-AAS may yield a detection limit at least one order of magnitude lower, or alternatively solvent extraction can be used to further enhance sensitivity (Cresser, 1978).

B. Some Other Elements

The coverage of elements given above is selective rather than exhaustive. Other elements may be determined in environmental samples by flame and ETA-AAS or by FES from time to time for various reasons. An example is gallium. The detection limit for gallium in air–acetylene at 287.4 nm is only ca. 70 ng mL^{-1} (Cresser, 1994), which is too low to make the direct determinations useful for most environmental applications unless solvent extraction is used for substantial preconcentration (Cresser, 1978). The anionic keto-chloro complex of gallium may be extracted from strong hydrochloric acid solution (e.g., 5.5 *M*) into 4-methylpentan-2-one. For soil matrices, the coextraction of iron may be prevented by prior reduction to iron(II) with an excess of titanium(III) sulfate (Cresser and Torrent-Castellet, 1972). Flame AAS, even with solvent extraction, can only be used for samples with a high gallium content; for most environmental samples, ETA-AAS is necessary. Even then, preconcentration-separation may be required, together with an appropriate modifier (Bermejo-Barrera et al., 2001).

Platinum, palladium, and rhodium in the environment are attracting increasing attention because of their emissions from catalytic converters in vehicle exhausts. Both can be determined after preconcentration by ETA-AAS. The author has successfully used coprecipitation with tellurium for platinum determination in samples of roadside vegetation. Su et al. (2001) have described a flow-injection on-line cleanup system suitable for platinum,

palladium, and gold prior to their ETA-AAS determination. A system has been described for electrochemical preconcentration of palladium in road dust prior to final determination ETA-AAS (Godlewska-Zylkiewicz and Zaleska, 2002). Preconcentration of palladium in such samples is generally regarded as essential if they are to be determined by AAS (Tilch et al., 2000; Boch et al., 2002).

Germanium is not frequently determined in botanical samples. Such determination is possible using ETA-AAS, provided a suitable matrix modifier is chosen (Yang and Zhang, 2002). For bismuth in natural water samples, preconcentration is required prior to determination by ETA-AAS (Yamini et al., 2002), as it is for gold determination in ores, rocks, and other geological samples (Terashima and Taniguchi, 2000; Ramesh et al., 2001). In the latter instance extraction with IBMK was also used to separate gold from a very large excess of iron.

REFERENCES

Beaty, R.D. 1988. *Concepts, Instrumentation and Techniques in Atomic Absorption Spectrophotometry*, Perkin-Elmer, Washington D.C.

Bermejo-Barrera, P., Moreda-Pineiro, A., Moreda-Pineiro, J. and Bermejo-Barrera, A. 1998. Usefulness of the chemical modification and multi-injection technique approaches in the electrothermal atomic absorption spectrometric determination of silver, arsenic, cadmium, chromium, mercury, nickel and lead in sea water. *J. Anal. Atom. Spectrom.* 13:777–786.

Bermejo-Barrera, P., Moreda-Pineiro, A., Moreda-Pineiro, J., Kauppila, T. and Bermejo-Barrera, A. 2000. Slurry sampling for electrothermal AAS determination of cadmium in seafood products. *Atom. Spectrosc.* 21:5–9.

Bermejo-Barrera, P., Alfonso, N.C.M. and Bermejo-Barrera, A.B. 2001. ETAAS determination of gallium in environmental samples using chemical modifiers after separation with Amberlite XAD-2 coated with 1-(2-pyridylazo)-2-naphthol. *Atom. Spectrosc.* 22:379–385.

Bermejo-Barrera, P., Annlo-Sendin, R.M., Cantelar-Barbazan, M.J. and Bermejo-Barrera, A. 2002. Selective preconcentration and determination of tributyl tin in fresh water by electrothermal atomic absorption spectrometry. *Anal. Bioanal. Chem.* 372:837–839.

Blankley, M., Henson, A. and Thompson, K.C. 1991. Waters, sewage and effluent. In: *Atomic Absorption Spectrometry: Theory, Design and Applications* (Haswell, S.J., ed.). Elsevier, Amsterdam, pp. 79–123.

Boch, K., Schuster, M., Risse, G. and Schwarzer, M. 2002. Microwave-assisted digestion procedure for the determination of palladium in road dust. *Anal. Chim. Acta* 459:257–265.

Boling, E.A. 1966. A multiple slit burner for atomic absorption spectroscopy. *Spectrochim. Acta* 22:425.

Marcel Dekker, Inc.
270 Madison Avenue, New York, New York 10016

Cabon, J.Y. 2002. Determination of cadmium and lead in seawater by graphite furnace atomic absorption spectrometry with the use of hydrofluoric acid as a chemical modifier. *Spectrochim. Acta, Part B* 57:513–524.

Chen, M., Ma, L.Q., Hoogeweg, C.G. and Harris, W.G. 2001. Arsenic background concentrations in Florida surface soils: determination and interpretation. *Environ. Forensics* 2:117–126.

Cresser, M.S. 1971. The significance of thermally assisted processes in atomic absorption. *Spectrosc. Lett*. 4:275–283.

Cresser, M.S. 1977. Literature interpolation: a possible source of error in flame atomic absorption spectrometry. *Lab. Pract*., March, 171–172.

Cresser, M.S. 1978. *Solvent Extraction in Flame Spectroscopic Analysis*. Butterworths, London.

Cresser, M.S. 1979. The impact cup: a simple aid in flame spectrometric analysis at high analyte concentrations. *Analyst* 104:792–796.

Cresser, M.S. 1990. Pneumatic nebulization. In: *Sample Introduction in Atomic Spectroscopy* (Sneddon, J., ed.). Elsevier, Amsterdam, pp. 13–36.

Cresser, M.S. 1993. Atomic spectrometry in environmental analysis: jam today or jam tomorrow? *J. Anal. Atom. Spectrom*. 8:269–272.

Cresser, M.S. 1994. *Flame Spectrometry in Environmental Chemical Analysis: A Practical Guide*. Royal Society of Chemistry, Cambridge.

Cresser, M.S. and Browner, R.F. 1980. Sample temperature effects in analytical flame spectrometry. *Anal. Chim. Acta* 113:33–38.

Cresser, M.S. and. Hargitt, R. 1976a. The significance of the $CrO_4^{2-} \Leftrightarrow HCrO_4^-$ equilibrium in the determination of chromium (VI) by flame spectrometry. *Talanta* 23:153–154.

Cresser, M.S. and. Hargitt, R. 1976b. The determination of chromium (III) and chromium (VI) by total ion exchange and atomic absorption spectrometry. *Anal. Chim. Acta* 81:196–198.

Cresser, M.S. and MacLeod, D.A. 1976. Observations on the limitation imposed by interferences in flame atomic absorption spectrometry at high analyte concentrations. *Analyst* 101:86–90.

Cresser, M.S. and Marr, I.L. 1991. Optical spectrometry in the analysis of pollutants. In: *Instrumental Analysis of Pollutants* (Hewitt, C.N., ed.). Elsevier Applied Science, London, pp. 99–145.

Cresser, M.S. and Torrent-Castellet, J. 1972. Determination of gallium in an iron-aluminium matrix by solvent extraction and flame emission spectroscopy. *Talanta* 19:1478–1480.

Cresser, M.S. and Wilson, G. 1973. Stabilizer for nitrous oxide flow in analytical flame spectrometry. *Lab. Pract*., Feb., 117–118.

Delves, H.T. 1970. A micro sampling method for the rapid determination of lead in blood by atomic absorption spectrophotometry. *Analyst* 95:431–439.

Dobrowolski, R. 2001. Determination of selenium in soils by slurry-sampling graphite-furnace atomic-absorption spectrometry with polytetrafluoroethylene as silica modifier. *Fresenius' J. Anal. Chem*. 370:850–854.

Dymott, T.C. 1981. *Atomic Absorption with Electrothermal Atomisation*. Pye Unicam, Cambridge.

Ebdon, L., Goodall, P., Hill, S.J., Stockwell, P.B. and Thompson, K.C. 1993. Ultra-trace determination of cadmium by vapour generation atomic fluorescence spectrometry. *J. Anal. Atom. Spectrom*. 8:723–729.

Fuchtjohann, L., Jakubowski, N., Gladtke, D., Klockow, D. and Broekaert, J.A.C. 2001. Speciation of nickel in airborne particulate matter by means of sequential extraction in a micro flow system and determination by graphite furnace atomic absorption spectrometry and inductively coupled plasma mass spectrometry. *J. Environ. Monitor*. 3:681–687.

Ganhdi, M.N. and Khopkar, S.M. 1992. A rapid method for the extractive separation of trace level manganese (II) from an aquatic environment. *Anal. Sci*. 8:233–236.

Gilbert, A.A., Marr, I.L. and Cresser, M.S. 1991. Automated detection of chemical and incomplete volatilisation interferences in analytical flame spectrometry. *Microchem*. J. 44:117–121.

Godlewska-Zylkiewicz, B. and Zaleska, M. 2002. Preconcentration of palladium in a flow through electrochemical cell for determination by graphite furnace atomic absorption spectrometry. *Anal. Chim. Acta* 462:305–312.

Hershey, J.W. and Keliher, P.N. 1989. Some atomic-absorption hydride generation inter-element interference reduction studies utilizing ion-exchange resins. *Spectrochim. Acta* 44B:329–337.

Hirano, Y., Nakajima, J., Oguma, K. and Terui, Y. 2001a. Determination of traces of cadmium in natural water samples by flow injection on-line preconcentration-graphite furnace atomic absorption spectrometry. *Anal. Sci*. 17:1073–1077.

Hirano, Y., Sakurai, H., Endo, A., Oguma, K. and Terui, Y. 2001b. Differential determination of traces of arsenic (III) and arsenic (V) in water by flow injection on-line preconcentration graphite-furnace AAS. *Bunseki Kagaku* 50:885–891.

Jerrow, M., Marr, I.L. and Cresser, M.S. 1991. Magnesium as a modifier for the determination of barium by flame emission spectroscopy. *Anal. Proc*. 28:40–41.

Jorhem, L., Engman, J., Lindestrom, L. and Schroder, T. 2000. Uptake of lead by vegetables grown in contaminated soil. *Commun. Soil Sci. Plant Anal*. 31:2403–2411.

Kirkbright, G.F. and Sargent, M. 1974. *Atomic Absorption and Fluorescence Spectroscopy*. Academic Press, London.

Krivan, V., Barth, P. and Schnurer-Patschan, C. 1998. An electrothermal atomic absorption spectrometer using semi-conductor diode lasers and a tungsten coil atomizer: design and first applications. *Anal. Chem*. 70:3525–3532.

Kubota, T., Kawakami, A., Sagara, T., Ookubo, N. and Okutani, T. 2001. Determination of antimony content in natural water by graphite furnace atomic absorption spectrometry after collection as antimony (III)-pyrogallol complex on activated carbon. *Talanta* 53:1117–1126.

Lajunen, L.H.J. 1992. *Spectrochemical Analysis by Atomic Absorption and Emission*. Royal Society of Chemistry, Cambridge.

Liang, L. and Bloom, N.S. 1993. Determination of total mercury by single-stage gold amalgamation with cold vapor atomic spectrometric detection. *J. Anal. Atom. Spectrom*. 8:591–594.

Lilleengen, B. and Wibetoe, G. 2002. Graphite furnace atomic absorption spectrometry used for determination of total, EDTA- and acetic acid-extractable chromium and cobalt in soils. *Anal. BioAnal. Chem*. 372:187–195.

Lopez Garcia, I., O'Grady, C. and Cresser, M. 1987. Pneumatic nebulizers—poor pumps and inferior sub-samplers. *J. Anal. Atom. Spectrom*. 2:221–225.

Maia, S.M., Welz, B., Ganzarolli, E. and Curtius, A.J. 2002. Feasibility of eliminating interferences in graphite furnace atomic absorption spectrometry using analyte transfer to the permanently modifed graphite tube surface. *Spectrochim. Acta, Part B* 57:473–484.

Marr, I.L. and Cresser, M.S. 1983. *Environmental Chemical Analysis*. Blackie, Glasgow.

Nakahara, T. 1990. Hydride generation. In: *Sample Introduction in Atomic Spectroscopy* (Sneddon, J., ed.). Elsevier, Amsterdam, pp. 255–288.

Nakashima, S. 1992. Simultaneous separation of tin and bismuth from water and seawater by flotation with thionalide. *Fresenius' J. Anal. Chem*. 343:614–615.

Niedzielski, P., Siepak, M. and Siepak, J. 2002. Comparison of modifiers for determination of arsenic, antimony and selenium by atomic absorption spectrometry with atomization in graphite tube by hydride generation and in-situ preconcentration in graphite tube. 2002. *Microchem. J*. 72:137–145.

Nowka, R., Eichardt, K. and Welz, B. 2000. Investigation of chemical modifiers for the determination of boron by electrothermal atomic absorption spectrometry. *Spectrochim. Acta*, *Part B* 55:517–524.

O'Grady, C.E., Marr, I.L. and Cresser, M.S. 1984. Reappraisal of the effects of solution temperature on aspiration rates in analytical spectroscopy. *Analyst* 109:1183–1185.

O'Grady, C.E., Marr, I.L. and Cresser, M.S. 1985. Patterns and causes of deposition losses in a simple spray chamber. *Analyst* 110:729–731.

Ozcan, M., Akman, S., Schuetz, M., Murphy, J. and Harnly, J. 2002. The spatial distribution and photometric and analytical accuracy of Sn determined by graphite furnace atomic absorption spectrometry in the presence of sulphates and palladium. *J. Anal. Atom. Spectrom*. 17:515–523.

Peramaki, P., Pesonen, M. and Piispanen, J. 2000. Development of a microwave sample preparation method for the determination of arsenic in humus and moss samples by graphite furnace atomic absorption spectrometry. *Analusis* 28:830–834.

Piascik, M. and Bulska, E. 2001. Performance of permanent iridium modifier in the presence of corrosive matrix in graphite furnace atomic absorption spectrometry. *Fresenius' J. Anal. Chem*. 371:1079–1082.

Potts, P.J. 1987. *A Handbook of Silicate Rock Analysis*. Blackie, Glasgow.

Ramesh, S.L., Raju, P.V.S., Anjaiah, K.V., Mathur, R., Rao, T.G., Dasaram, B., Charan, S.N., Rao, D.V.S., Sarma, D.S., Mohan, M.R. and Balaram, V. 2001. *Atom. Spectrosc.* 22:263–269.

Rohr, U., Ortner, H.M., Schlemmer, G., Weinbruch, S. and Welz, B. 1999. Corrosion of transversely heated graphite tubes by mineral acids. *Spectrochim. Acta*, Part B 54:699–718.

Rubeška, I. and Musil, J. 1979. Interferences in flame spectrometry, their elimination and control. *Prog. Anal. Atom. Spectrosc.* 2:309–354.

Rucandio, M.I. and Petit-Dominguez, M.D. 2002. Study of the versatility of a graphite furnace atomic absorption spectrometric method for the determination of cadmium in the environmental field. *J. Assoc. Off. Anal. Chem. Int.* 85:219–224.

Schallis, J.E. 1969. Sampling boat modification. *Atom. Abs. Newslett.* 7:35–38.

Schneider, C. and Exley, C. 2001. Silicic acid (($Si(OH)_4$) is a significant influence on the atomic absorption signal of aluminium measured by graphite furnace atomic absorption spectrometry. *J. Inorg. Biochem.* 87:45–50.

Sharp, B.L. 1988a. Pneumatic nebulizers and spray chambers for ICP spectrometry. A Review. Part 1: Nebulizers. *J. Anal. Atom. Spectrom.* 3:613–652.

Sharp, B.L. 1988b. Pneumatic nebulizers and spray chambers for ICP spectrometry. A Review. Part 2: Spray chambers. *J. Anal. Atom. Spectrom.* 3:939–963.

Slavin, W. 1991. *Graphite Furnace AAS: A Source Book*. Perkin-Elmer Corp., Norwalk, Connecticut. 2d ed.

Smith, S., Schleicher, R.G. and Hieftje, G.M. 1982. New atomic absorption background correction technique. Paper 422, 33rd. Pittsburgh Conference on Analytical Chemistry and Applied Spectroscopy, Atlantic City.

Sperling, M., Xu, S. and Weltz, B. 1992. Determination of chromium (III) and chromium (VI) in water using flow-injection on-line preconcentration with selective adsorption on activated alumina and flame atomic-absorption spectrometric detection. *Anal. Chem.* 64:3101–3108.

Su, X.G., Wang, M.J., Zhang, Y.H., Zhang, J.H., Zhang, H.Q. and Jin, Q.H. 2001. Graphite furnace atomic absorption spectrometric determination of some noble metals using flow injection, on-line clean up. *J. Anal. Atom. Spectrom.* 16:1341–1343.

Szydlowski, F.J. 1979. B in natural waters by AAS with ETA. *Anal. Chim. Acta* 106:121–128.

Terashima, S. and Taniguchi, M. 2000. Fractional determination of gold in 26 geological reference materials by sequential extraction with graphite furnace atomic absorption spectrometry. *Geostandards Newslett. J. Geostand. Geoanal.* 24:7–17.

Tilch, J., Schuster, M. and Schwarzer, M. 2000. Determination of palladium in airborne particulate matter in a German city. *Fresenius' J. Anal. Chem.* 367:450–453.

Tsalev, D.L., Sperling, M. and Welz, B. 2000a. Flow-injection hydride generation atomic absorption spectrometric study of the automated on-line pre-reduction of arsenate, methylarsonate and dimethylarsinate and high performance liquid separation of their L-cysteine complexes. *Talanta* 51:1059–1068.

Tsalev, D.L., Sperling, M. and Welz, B. 2000b. On-line UV photooxidation with peroxodisulfate for automated flow injection and for high-performance liquid chromatography coupled to hydride generation atomic absorption spectrometry. *Spectrochim. Acta, Part B* 55:339–353.

Vale, M.G.R., Silva, M.M., Welz, B. and Lima, E.C. 2001. Determination of cadmium, copper and lead in mineral coal using solid sampling graphite furnace atomic absorption spectrometry. *Spectrochim. Acta, Part B* 56:1859–1873.

Van Elteren, J.T., Haselager, N.G., Das, H.A., De Ligny, C.L. and Agterdenbos, J. 1991. Determination of arsenate in aqueous samples by precipitation of the arsenic (V) molybdate complex with tetraphenylphosphonium chloride and neutron-activation analysis or hydride generation atomic-absorption spectrometry. *Anal. Chim. Acta* 252:89–95.

Walsh, A. 1955. The application of atomic absorption spectra to chemical analysis. *Spectrochim. Acta* 7:108–118.

Welz, B. and Schubert-Jacobs, M. 1991. Evaluation of a flow-injection system and optimisation of parameters for hydride generation atomic absorption spectrometry. *Atom. Spectrosc.* 12:91–104.

Welz, B., Xu, S. and Sperling, M. 1991. Flame atomic absorption spectrometric determination of cadmium, cobalt and nickel in biological samples using a flow-injection system with on-line pre-concentration by coprecipitation without filtration. *Appl. Spectrosc.* 45:1433–1443.

Willis, J.B. 1965. Nitrous oxide-acetylene flame in atomic absorption spectroscopy. *Nature* 207:715–718.

Wojciechowski, M., Piascik, M. and Bulska, E. 2001. Noble metal modifiers for determination by graphite furnace atomic absorption spectrometry in biological samples. *J. Anal. Atom. Spectrom.* 16:99–101.

Yaman, M. and Dilgin, Y. 2002. AAS determination of cadmium in fruits and soils. *Atom. Spectrom.* 23:59–64.

Yamini, Y., Chaloosi, M. and Ebrahimzadeh, H. 2002. Solid phase extraction and graphite furnace atomic absorption spectrometric determination of ultra trace amounts of bismuth in water samples. *Talanta* 56:797–803.

Yang, L.L. and Zhang, D.Q. 2002. Direct determination of germanium in botanical samples by graphite furnace atomic absorption spectrometry with palladium-zirconium as chemical modifier. *Talanta* 56:1123–1129.

Yang, L.L., Zhang, D.Q. and Zhou, Q.X. 2002. Determination of mercury in biological tissues by graphite furnace atomic absorption spectrometry with an in-situ concentration technique. *Anal. Sci.* 18:811–814.

Yebra-Biurran, M.C., Garcia-Dopazo, M.C., Bermejo-Barrera, A. and Bermejo-Barrera, M.P. 1992. Preconcentration of trace amounts of manganese from natural waters by means of a macroreticular poly(dithiocarbamate) resin. *Talanta* 39:671–677.

Zhang, Q., Minami, H., Inoue, S. and Atsuya, I. 2001. Preconcentration by coprecipitation of arsenic and tin in natural waters with Ni-pyrrolidine dithiocarbamate complex and their direct determination by solid-sampling atomic absorption spectrometry. *Fresenius' J. Anal. Chem.* 370:860–864.

Zhou, Y., Parsons, P.J., Aldous, K.M., Brockman, P. and Slavin, W. 2002. Rhodium as permanent modifier for atomization of lead from biological fluids using tungsten filament electrothermal atomic absorption spectrometry. *Spectrochim. Acta, Part B* 57:727–740.

Zih-Perenyi, K., Lasztity, A. and Kelko-Levai, A. 2000. On-line preconcentration and GFAAS determination of trace metals in waters. *Microchem. J.* 67:181–185.

2

Inductively Coupled Plasma Spectrometry

Stephen J. Hill and Andrew Fisher
The University of Plymouth, Plymouth, England

Mark Cave
British Geological Survey, Nottingham, England

I. INTRODUCTION

Environmental samples are often complex mixtures of organic and inorganic components that vary widely in their makeup depending on many factors, which include geological controls, geographical location, depth, climate, and anthropogenic inputs. Consequently, the chemical composition of environmental samples is very varied. For example, a major chemical component of one soil type can be a trace component of others. To provide a comprehensive elemental analysis of environmental samples it is therefore necessary to have an analytical method capable of determining most chemical elements over concentration ranges varying from percent to ultratrace.

The inductively coupled plasma (ICP) source used in conjunction with either atomic emission spectroscopy (AES) or mass spectrometric (MS) detection has a number of properties that make it ideally suited to the analysis of soils and other environmental materials.

1. In principle, around 75 of the chemical elements can be determined.
2. By judicious choice of emission lines, mass-to-charge range, and detectors, elements can be determined over 5 orders of magnitude in one sample solution.
3. With care, both the precision and the accuracy of the measurement is high.

Marcel Dekker, Inc.
270 Madison Avenue, New York, New York 10016

4. ICP spectrometric methods can provide fast multielement measurement of many elements in one sample. This is ideally suited to soil survey work, where a large number of samples must be analyzed.

A. Development of ICP as an Atomic Emission Source

The ICP source, as we know it today, was introduced by Reed (1961), who described an atmospheric argon (Ar) ICP sustained in a three-tube quartz torch using an RF induction coil. In this first application, the high temperature of the ICP was used for growing refractory crystals. Greenfield et al. (1964) were the first to realize the potential of the ICP as a source for multielement atomic emission. Almost simultaneously, but independently, in the U.S., Wendt and Fassel (1965) were also experimenting with an Ar ICP as an atomic emission source. From these early studies, during the late 1960s and the early 1970s, further work by Greenfield, Fassel, and other research groups established ICP-AES as a viable method for trace element analysis, producing published articles on a variety of analytical applications.

In 1975 Greenfield et al. (1975a, 1975b) described the analytical system that they had been using for routine analytical work for several years. This system had an ICP source coupled to a 30-channel direct reading spectrometer, allowing simultaneous multielement analysis with automated control of sample input and data readout. At a similar time Scott et al. (1974) described a "compact" design ICP torch in a system with a pneumatic nebulizer. The two systems generated much discussion on the most suitable torch design and operating conditions for ICP. Greenfield's group advocated the use of a robust ICP with a relatively large torch (29 mm o.d.) run at high powers of several kW, whereas Fassel's group used a smaller torch (20 mm o.d.) and lower power (1–2 kW). Despite these controversies, the early published work on ICP-AES was enough to convince the instrument manufacturers that the ICP was a marketable product, and the first commercial instruments were introduced in the mid-1970s.

During the 1970s and the 1980s a wide variety of commercial instruments were produced. In general these instruments fell into two categories: systems with polychromator spectrometers that were able to make simultaneous measurements of many emission lines and systems with monochromator spectrometers that measured each emission line sequentially. The former instruments had high sample throughput but were usually more costly, whereas the latter were less expensive but had more moving parts and a lower sample throughput. However, monochromator spectrometers also had the advantage of being able to address many more analytical lines than the fixed channel polychromator systems.

Some manufacturers opted to use a combination of both of these spectrometers in a single system. Although there were a number of spectrometer designs, by the end of the 1980s most commercial systems reflected the consensus of opinion over the best ICP operating conditions for routine analytical work. Torch dimensions and low power as originally advocated by Fassel's group (Scott et al., 1974) had become universally adopted, along with the use of generators operating at 27.12 MHz, although it was known that plasmas operating at 40–50 MHz provide a higher signal-to-background ratio (SBR) in the emission spectra (Capelle et al., 1982).

All of the early commercial systems relied on the photomultiplier tube in the spectrometer as a means of converting light intensity into an electrical signal that could be used to quantify concentration. Although very sensitive, the photomultiplier tube is quite bulky (a minimum packing cross sectional area of ca. 0.75–5 cm^2), which in many instances makes it difficult to fit the required number of lines necessary for a particular application into a polychromator system. At the end of the 1980s, however, developments in solid-state array optical detectors heralded a significant change in ICP-AES instrument design. These new detectors allowed many hundreds or thousands of detectors (referred to as pixels), each equivalent to a single photomultiplier tube, to be packed into the area occupied by a single photomultiplier tube. In one of the first applications of these new detectors to ICP, Pilon et al. (1990) described an ICP system that combined a charge injection device (CID) array detector with an echelle spectrometer. This system allowed simultaneous analysis with continuous spectral coverage from 185 to 511 nm, combining the advantages of the older polychromator and monochromator systems in a single, more compact instrument.

In conjunction with the advances in detector technology, the instrument manufacturers, under pressure to obtain very low detection limits to meet the needs of environmental legislation and keep pace with the advances in ICP-MS, have revisited the use of axial viewing of the ICP, originally described by Abdallah et al. (1976). This approach provided improvements in detection limits for some elements by factors varying from 2 to 20 (Brenner et al., 2000). Nearly all the major instrument manufacturers now offer solid-state detector instruments with axial ICP viewing. The implications of these current instrument design trends to environmental analysis will be discussed in more detail in later sections.

Despite some recent changes in instrument design since the early days, ICP-AES has been in everyday use for at least 25 years and can now be considered a mature analytical technique. In recent reviews of atomic spectrometry in environmental analysis (Cave et al., 2000; Cave et al., 2001; Hill et al., 2002), it has been concluded that multielement analyses of, for

example, plant and soil digests by ICP-AES are now so routine in many laboratories around the world that few reports of novel work, other than unusual applications, are to be expected.

II. FUNDAMENTAL PROPERTIES OF ICP-AES

The basic process of using emission spectroscopy for chemical analysis consists of introducing the sample to be analyzed, in an appropriate form, into an excitation source, where it is dissociated into atoms and ions by thermal decomposition. The atoms and ions are further excited from their ground state energy to an energized state from where they spontaneously revert to a lower energy state, accompanied by the emission of a photon of light. The energy of the photon (expressed as its wavelength) is specific to the element being excited, and the number of photons, or light intensity, is proportional to the concentration of the excited atoms or ions.

The instrumentation required for ICP-AES is shown in Fig. 1 and comprises three basic units: the source, a spectrometer, and a computer for control and data analysis.

The ICP source is ideally suited as an emission source because of two features.

1. The very high temperature of the source allows analyte material to be volatilized easily, and excitation of ions and atoms of most elements can occur.

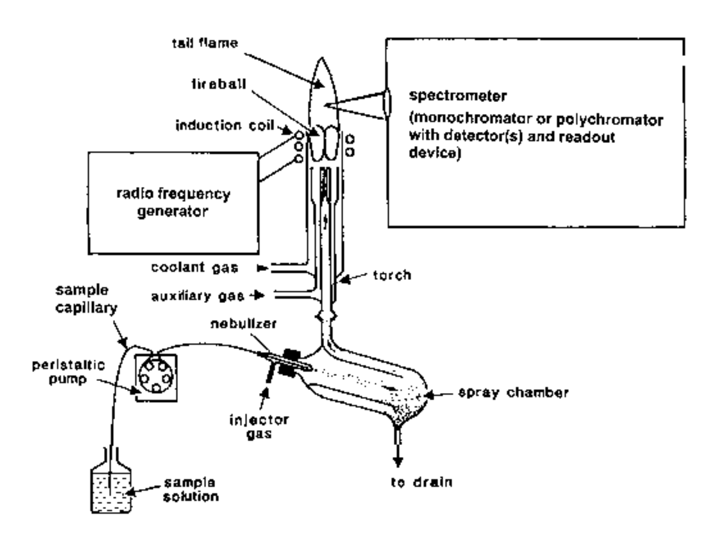


Figure 1 Schematic diagram of an ICP-AES instrument.

2. The unique geometry of the ICP allows the emission to be viewed in an "optically thin" region of the plasma. Here, degradation of the proportionality of the emission energy to the concentration of the determinant is not affected significantly by self-absorption of the photons by atoms or ions of the same element.

A. Plasma Formation

A three-turn water-cooled copper coil is used to couple the RF energy into a stream of flowing Ar within the plasma torch. When a RF current is applied to the coil, it sets up an oscillating magnetic field within the quartz tube. The argon flow through the torch is seeded with electrons from a spark discharge (usually produced by a Tesla coil). The electrons are accelerated by the oscillating magnetic field and collide with atoms of the gas, causing further ionization that leads to the formation of the hot ionized plasma. Rapidly, equilibrium is reached in which the rate of electron production is balanced by losses due to recombination and diffusion, and a stable plasma is formed. The plasma is effectively a conductor and is heated by the flow of current induced by the RF field. Electrically, the coil and plasma form a transformer with the plasma acting as a one-turn secondary coil of finite resistance.

Once formed, the ICP is constrained in a quartz torch made from three concentric tubes, as shown in Fig. 2. The coolant argon flow (typically in the range 10–20 $L\,min^{-1}$) is introduced tangentially through the outer annulus and performs a dual function of keeping the plasma from melting the outer quartz tube while providing the argon to sustain the plasma. The intermediate flow (typically 0–1 $L\,min^{-1}$) allows the plasma to be moved up or down in the torch and can be used to help prevent the buildup of salt on the injector tip. The injector flow (typically 0.5–1.5 $L\,min^{-1}$) punches a hole through the center of the plasma and is used to carry the sample (usually in the form of an aerosol) into the plasma for volatilization, atomization, ionization, and excitation.

B. Spectrochemical Emission Properties of an ICP

The temperature profile and the four main regions in a typical annular ICP that are important to the analyst are shown in Fig. 3. The preheating zone (PHZ) occurs at the base of the plasma just before the analyte reaches the central channel where desolvation of the sample aerosol takes place. The initial radiation zone (IRZ) is where the sample undergoes volatilization and atomization/ionization and excitation. Finally, there is the normal analytical zone (NAZ), which is a low background region just above the bright plasma fireball where the atomic emission measurements are made. There are two

Marcel Dekker, Inc.
270 Madison Avenue, New York, New York 10016

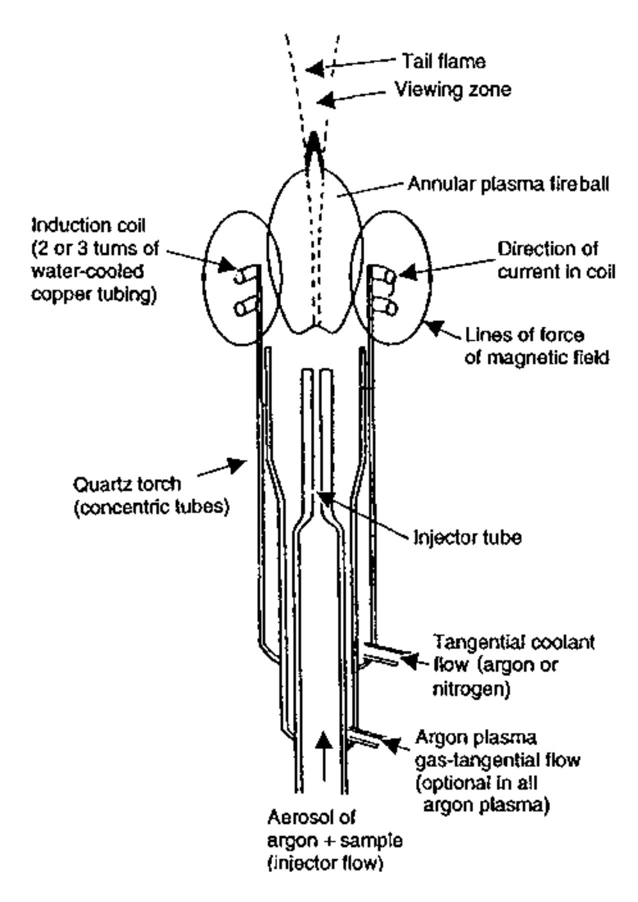


Figure 2 Schematic view of an inductively coupled plasma (ICP).

important parameters that control the relative positions of these zones in the plasma:

1. The injector flow rate, when increased, increases the diameter of the hole through the center of the plasma and shifts the IRZ and NAZ higher in the central channel. At higher injector flow rates the analyte residence time within the central channel is decreased, experiencing less heating from the plasma.
2. The RF power, when increased, tends to constrict the central channel for a given injector flow rate and push the IRZ and NAZ lower in the plasma. This increases the residence time of the analyte within the plasma channel.

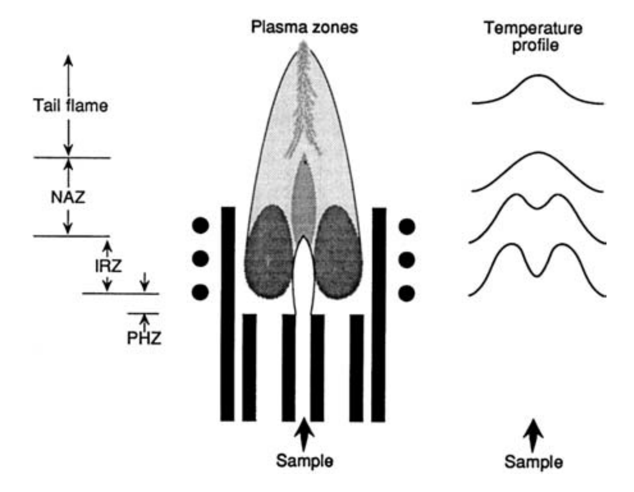


Figure 3 Axial channel emission zone of an ICP. PHZ: preheating zone; IRZ: initial radiation zone; NAZ: normal analytical zone. (Reproduced with permission from Sharp, B. in *Soil Analysis—Modern Instrumental Techniques*, 2d ed. [Smith, K.A., ed.]. New York: Marcel Dekker, 1991.)

The third parameter that is dependent on both the power and the injector flow rate is the viewing height at which the atomic emission is measured (when the ICP is viewed radially). This is measured as the distance above the load coil and is normally between 5 and 16 mm. As the relative positions of the IRZ and NAZ are moved through changes in RF power or injector flow rate, the relative viewing height within the NAZ also changes. These three parameters can therefore be varied to obtain optimum performance for any given emission line. Common optimization criteria are signal-to-background ratio and signal-to-noise ratio. In most instances, however, ICP-AES is used as a multielement tool, and therefore compromise operating conditions, usually set by the manufacturer, are supplied with commercial instrumentation.

In many instances, compromise operating conditions work extremely well for a wide range of sample types. Nevertheless, there may be instances where an unusual determinant or matrix requires some changes in operating conditions. In these instances it is useful to have a broad understanding of how plasma conditions affect particular line types. In general, emission lines can be divided into "hard" (excitation potential > 4.5 eV) and "soft" lines (excitation potential < 4.5 eV) as proposed by Boumans (1978). The behavior of the two types of line when changing ICP operating parameters can be summarized as follows.

Soft Lines

1. An increase in applied power enhances the emission and shifts the peak emission signal lower in the plasma.
2. An increase in sample carrier flow rate reduces the emission intensity and shifts the peak emission signal higher in the plasma.
3. The presence of an increasing concentration of an easily ionizable element (EIE) enhances the emission and shifts the peak emission signal lower in the plasma. Higher up in the vicinity of the NAZ, the enhancement is much less (Blades and Horlick, 1981).

Hard Lines

1. An increase in the applied power produces an increase in the emission intensity, but the position of the peak emission intensity signal changes very little.
2. An increase in sample carrier gas flow produces a small but significant upward shift of the peak emission intensity and a reduction in intensity.
3. An increasing concentration of an EIE causes depression in emission intensity in the vicinity of the peak emission intensity, but an enhancement lower in the plasma. This results in a crossover region where the effect of the interfering elements is minimized.

It is generally agreed that the excitation mechanism of soft lines is essentially thermal in nature, but for hard lines the excitation mechanism is nonthermal and involves interactions with metastable Ar ions (Blades, 1987).

The equation used to express the linear relationship between the spectral radiance B and the concentration of free atoms in the plasma, as used for calibration in analytical use, may be expressed as

$$B = \frac{1}{4\pi} h\nu_0 \frac{NL}{Z(t)} g_k A_{ki} \exp\left(\frac{-E_k}{kT}\right)$$

where

h = Planck's constant
ν_0 = the frequency of the emitted photons
N = the number of atoms per unit volume
$Z(t)$ = the partition function
g_k = the statistical weight of the kth state
A_{ki} = the Einstein transition probability for spontaneous emission
L = the optical depth of the source
E_k = the excitation energy of the kth state
k = the Boltzmann constant

Marcel Dekker, Inc.
270 Madison Avenue, New York, New York 10016

C. Axial/Radial Viewing of ICP

Atomic emission spectrometers may either be used to view the ICP in the radial position, i.e., the torch is vertical and the light emitted by the determinants is detected through the side of the plasma, or may be viewed in the axial position, in which case the torch is horizontal and the detected determinants' emissions have to pass through the tail flame (Fig. 4). For use

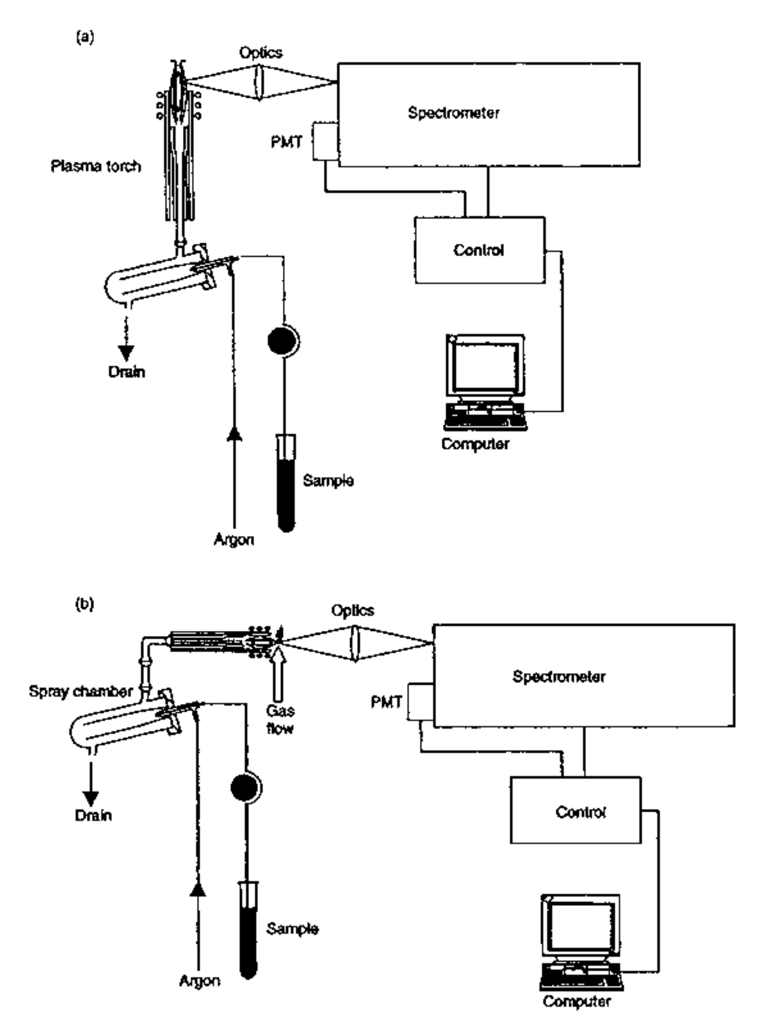


Figure 4 Typical configuration for ICP-AES instruments: (a) side-on radial viewing; (b) axial viewing, of the ICP.

in ICP-AES, the most common orientation to date has been the radial configuration (although in ICP-MS, the plasma is universally mounted horizontally). A comprehensive review of many aspects of axial viewing, including both instrumentation and analytical performance, has been published by Brenner and Zander (2000).

The first practical point regarding the use of axial viewing for ICP-AES is that the optical system is ''looking'' down the end of the plasma and therefore needs protection from the hot gases in the plasma tail flame and from the possibility of salt build up on the optical interface. There are two approaches to this: a shear gas is directed in a near-perpendicular stream at the tail flame of the plasma directing the tail flame away from the optics; the optical interface has a counter-current of purge gas flowing out from its input aperture directly against the plasma tail flame. The shear or purge gas can be air or an inert gas, the latter being a better choice if low UV wavelengths are to be measured. The gas has a dual function of protecting the optics and removing the cooler end of the tail flame, which could cause self-absorption or other interference effects.

By viewing the ICP end-on, an integrated emission from the whole length of the sample channel is obtained. This removes the spatial variable of viewing height, which is important in radial viewing. For axial viewing, therefore, there are only two important parameters governing the analytical properties of the plasma, RF power and injector gas flow rate. It is believed that both signal and background are increased when moving from radial to axial mode owing to the longer path length being viewed, but because the NAZ does not have to be viewed through the side of the high background plasma (as found in radial viewing), the signal increases more than the background, producing superior signal-to-background ratios (SBR).

While it is acknowledged that axial viewing improves detection limits, there is some debate as to whether there is reduction in the linear range and increase in interferences compared with viewing perpendicular to the central channel. In their review Brenner and Zander (2000) conclude that there are conflicting results with regard to linear dynamic range, but Bridger and Knowles (2000) suggest that curvature may be due to ionization suppression effects that can be alleviated by on-line addition of a CsCl buffer. It has also been suggested (Brenner and Zander, 2000) that when run under robust conditions (see Sec. II.D), axial viewing is as interference-free as radial viewing (Table 1).

D. Robust Operating Conditions for ICP-AES

In Sec. II.B, the use of compromise operating conditions for multielement analysis was discussed. One way of arriving at a set of operating conditions

Marcel Dekker, Inc.
270 Madison Avenue, New York, New York 10016

Table 1 Instrumental Detection Limits for ICP-AES and ICP-MS Using the Most Sensitive Lines and Most Abundant Isotopes

Determinant	ICP-AES ($ng\,mL^{-1}$)	ICP-MS ($ng\,mL^{-1}$)	Determinant	ICP-AES ($ng\,mL^{-1}$)	ICP-MS ($ng\,mL^{-1}$)
Ag	3	0.005	Nb	4	0.005
Al	2	0.05	Nd	2	0.001
As	12	0.005	Ni	6	0.005
Au	6	0.005	Os	5	0.005
B	2	0.05	P	18	0.5
Ba	0.1	0.001	Pb	14	0.001
Be	0.2	0.001	Pd	7	0.005
Bi	12	0.001	Pr	1	0.001
Ca	0.03	0.5	Pt	20	0.005
Cd	2	0.005	Rb	3	0.001
Ce	8	0.001	Re	11	0.005
Co	5	0.001	Rh	5	0.005
Cr	4	0.005	Ru	6	0.005
Cu	2	0.005	S	20	10
Dy	0.3	0.01	Sb	20	0.005
Er	1	0.001	Sc	0.4	0.05
Eu	0.3	0.001	Se	40	0.05
Fe	2	0.05	Si	5	0.5
Ga	7	0.001	Sm	7	0.001
Gd	3	0.001	Sn	15	0.005
Ge	13	0.05	Sr	0.02	0.001
Hf	4	0.005	Ta	10	0.005
Hg	10	0.001	Tb	5	0.001
Ho	0.5	0.001	Te	30	0.05
In	18	0.001	Th	20	0.001
Ir	4	0.005	Ti	1	0.05
K	10	0.5	Tl	16	0.001
La	0.02	0.05	Tm	2	0.001
Li	1	0.001	U	20	0.001
Lu	0.05	0.001	V	2	0.05
Mg	0.1	0.05	W	20	0.005
Mn	0.3	0.0004	Y	0.2	0.001
Mo	4	0.005	Yb	0.3	0.001
Na	1	0.05	Zn	1	0.005

that are practical for the relatively complex matrix obtained from environmental samples is to use “robust” operating conditions. Mermet (1989, 1991, 1998) used this term collectively to express energy transfer, residence time, and response of the plasma to changes in atomization and

excitation conditions and chemical composition of the aspirated solution. These workers determined that conditions that maximized the Mg II 280.270 nm/Mg I 285.213 nm emission line ratio should provide conditions that give minimum interference in routine analysis. A number of studies showed that such conditions were obtained when the internal diameter of the torch injector exceeds 2 mm i.d., when the injector flow rate is approximately 0.5–0.7 L min^{-1}, when the viewing height (in the case of radial viewing) is low (4–6 mm above the load coil), and when the forward power is high (typically > 1.4 kW). It is interesting to speculate that Greenfield et al. (1975a) were perhaps right when they suggested that operating at high powers had analytical advantages. These conditions are the same for both radial and axial viewing. Brenner and Zander (2000) have tabulated Mg ion/atom ratios for both radial and axial viewing and show that axial viewing ratios are usually lower. This may be additional evidence that axial viewing is less robust, but again, at present, the evidence is inconclusive. However, it is generally agreed that as long as the Mg atom-to-ion ratio is > 8, whatever the viewing geometry, robust conditions have been achieved.

III. INSTRUMENTATION

As stated above, a basic ICP instrument (Fig. 1) comprises an RF generator to supply the power to the plasma torch, a gas manifold and controller system, a sample introduction system, a detector, and a data readout system (Mermet, 1998).

A. Generators

A radio-frequency (RF) generator is the device used to provide the power for an ICP. It produces an alternating current at a desired frequency. There are two basic types of RF generator, free running and crystal controlled. The free running type is the more common in recent instruments. There are several versions of free running generators, including the Armstrong, the Hartley, the Colpitts and the tuned anode, tuned grid (TATG), but all have the same basic principles. The frequency of oscillation is fixed by the electrical components in the circuit. In the crystal controlled generators, the main component is a crystal oscillator that consists of a crystal (quartz or Rochelle salts) sandwiched between two metal plates. When a voltage is applied to the plates, the crystal expands and contracts with changing polarity. The frequency of expansion of the crystal is related to its thickness, but in most instruments this is constant at 13.56 MHz. Other components

include a frequency multiplier, a buffer circuit, a directional coupler, an impedance matching network, and a load coil.

Most generators in commercial instruments operate at either 27.12 MHz (a frequency doubler is used) or 40.68 MHz (where a frequency tripler is used), since manufacturers have to comply with strict regulations over emission of radiation and the generator should therefore not interfere with other equipment. Either generator is usually capable of producing a power of up to 2 kW, although operating powers are normally in the range of 900–1500 W. Generators and their associated matching networks are of varying quality. Some can accept the introduction of high solvent loading whereas others cannot. This capability is dependent upon the instrument manufacturer. A more detailed description of generators and their associated load coils and matching networks is given in the literature (Fisher and Hill, 1999).

B. Torch Design

Several variations in torch design have been produced over the years. Originally, the Greenfield style torch was used, but although this was very robust and tolerant of the introduction of other gases, it was much larger than the alternative Fassel type and required much higher gas flows. The running costs of the Greenfield torches were therefore higher, and so the Fassel style torch has become the norm in most modern instruments. There are, however, several different styles now available based on the basic Fassel torch. In general, the torches for ICP-AES and ICP-MS instrumentation are similar. In one ICP-AES torch design, there is a slot cut into the coolant tube so that the light emitted from the analyte can be transferred more efficiently, i.e., without diffraction, to the collection optics. As stated in Sec. II.A, the torch allows the flow of three gases through it, and it is these gases that sustain the plasma. All three gas flows are usually argon, but at very different flow rates. The coolant (also called plasma gas or outer gas) flow rate is typically 11–15 L min^{-1}, the auxiliary (also called the intermediate) is at approximately 1 L min^{-1}, and the nebulizer (also called the injector) gas flow is at between 0.7 and 1.2 L min^{-1}, depending on the nebulizer type and the determinant. It is the latter flow that forms the aerosol from the nebulizer and transports this through the spray chamber into the torch. The coolant and intermediate gases are introduced at right angles so that the gas flows out of the torch in a spiral fashion. It is this spiralling gas flow that keeps the walls of the torch cool and helps prevent it from melting.

A low-flow torch (also known as the minitorch) is also available that operates at about one-third of the gas consumption of the standard Fassel type torch using a forward power of 0.65 kW (Evans and Ebdon, 1991). The problem associated with the low-flow torch is that it is prone to blocking if

samples containing in excess of 1% m/v solids are aspirated. Thus although offering financial advantages in terms of gas consumption, these torches are not as widely used as the larger design. Demountable or semidemountable torches offer several advantages over one-piece torches, since various parts of the torch can be removed and replaced separately. In most designs, this includes the injector tube and the outer tubes, which erode more quickly than other parts of the torch, so that they can be replaced separately without having to replace the whole torch assembly. In some cases a different style or size of injector may be used for different sample types (Fig. 5). If a sample contains a relatively large concentration of dissolved or suspended solids, these may collect within the injector. After a while, the collected solid material accumulates until the injector becomes blocked. This will lead to signal drift until, when blocking is complete, no signal is observed. It therefore helps if a slightly wider injector is used (e.g., with a bore of 2 mm rather than 1.5 mm) or if a gently tapering injector is used. Operating with an injector tip of at least 2 mm in diameter also ensures that robust operating conditions can be achieved (see Sec. II.D). The capacity to change the injector is also of use when samples dissolved in HF are to be analyzed. Such samples would dissolve a standard quartz injector, and so it is useful to be able to change it to one made from alumina. The problem with demountable torches is that precision engineering is required to ensure perfect concentricity. If concentricity is not achieved, then the plasma will not be stable, leading to poor performance, and the torch may become quickly damaged.

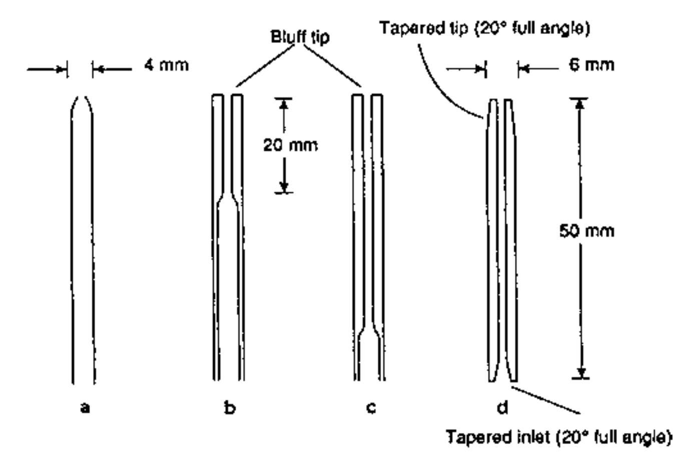


Figure 5 Injector tubes used in torches for ICP-AES. (a) Turbulent constricted injector tip; (b) intermediate laminar/turbulent capillary injector tip; (c) fully laminar capillary injector; (d) streamlined capillary injector for demountable torch.

C. Sample Introduction

Sample introduction plays a key part in any successful ICP-AES analysis. The ICP is very flexible in that it can accept samples in the form of solids, liquids, or gases. From the earliest work until the present day, the area of sample introduction has been a very fertile one for research. In a recent review of developments in atomic emission spectroscopy (Hill et al., 2000), the authors note the substantial literature concerning sample introduction that appears each year. A comprehensive review of this area has been produced by Montaser et al. (1998). However, despite this ongoing research, there are relatively few tried and tested sample introduction systems suitable for routine environmental analysis. These will be discussed in more detail in this section.

1. Nebulization

The vast majority of analyses are carried out using pneumatic nebulization. The three principal types used by commercial instruments, the concentric, the cross-flow, and the Babington V-groove, are shown in Fig. 6. The concentric and cross-flow nebulizers are self-priming, but the Babington nebulizer requires a pump to deliver the solution. The glass concentric nebulizer is probably still the most widely used, giving high stability and sensitivity. Its main drawbacks are that the sample solution has to pass through a narrow capillary (i.d. ca. 0.3 mm), which can become blocked by particulates, and that the narrow annular gas orifice (ca. 0.02 mm wide) can become clogged by the accumulation of salt crystals.

The instrumentation used for the sample introduction process can be identical for both ICP-AES and ICP-MS. Most samples are in liquid form, e.g., solutions of acid digests or leachates of soil, sediment, or rock samples. This liquid needs to be transported to the plasma, and this is normally achieved using a nebulizer to transform the liquid into an aerosol. There are numerous types of nebulizer available commercially. These include Meinhard, cross-flow, Ebdon, Burgener, Hildebrand grid, and assorted other pneumatic nebulizer types. The function of each is to shatter a stream of liquid into a cloud of droplets, which may be transported to the plasma in a stream of gas.

Depending on the application and the sample type, different nebulizers can be optimal. A standard Meinhard nebulizer is a good choice for filtered fresh waters, but if the sample contains a substantial amount of dissolved solids (e.g., saline waters) or suspended solids, it is very prone to blocking. Unblocking such nebulizers can be problematic, since they are made of glass and are very fragile. Immersion in a strong acid or ultrasonication may

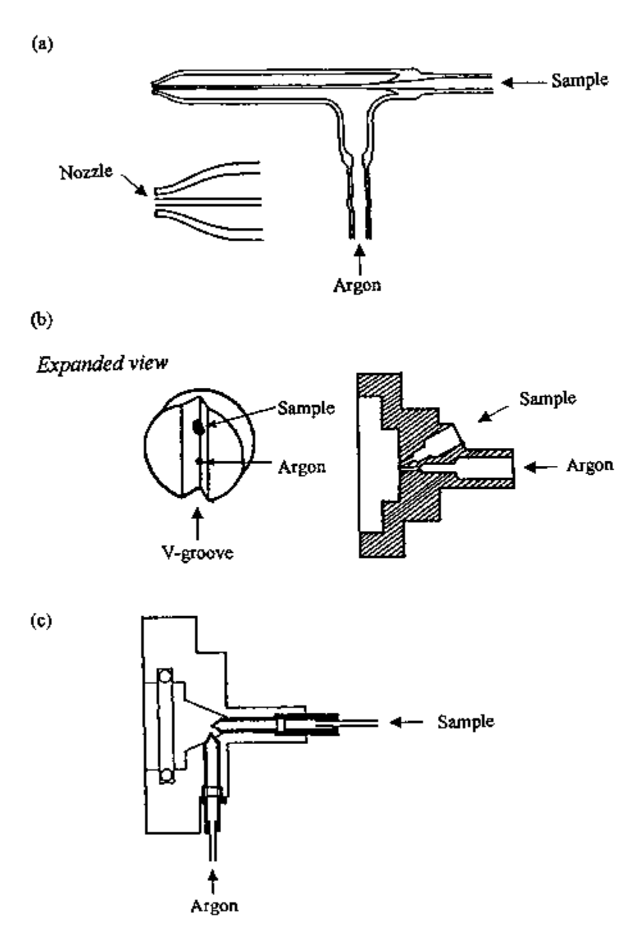


Figure 6 Common nebulizer designs: (a) pneumatic (Meinhard); (b) V-groove; (c) cross-flow.

unblock the nebulizers, but attempting to use thin wire usually leads to irreparable damage. Modified Meinhard style nebulizers have been produced that are more capable of aspirating more awkward samples. Other nebulizer types are much more tolerant, e.g., the Burgener, which can cope with a high concentration of dissolved salts, but which may still suffer from the problem of blockage when suspended solids are introduced. Various other types of nebulizer, e.g., Veespray and Sea Spray, are also available and are reputedly tolerant of both suspended and dissolved solids. The Ebdon V-groove nebulizer is also regarded as being generally unblockable and is useful with slurry samples.

Most of the nebulizers described above produce an aerosol, which then enters a spray chamber. The function of the spray chamber is to separate the larger droplets, which are passed to waste, from the smaller droplets, which are transported by the nebulizer gas to the plasma. A wide range of spray chamber designs is available. Scott double-pass chambers are common and can be made of glass or plastic (Fig. 7). Single-pass, cyclone, and impact-bead spray chambers are also available. The dimensions, surface area, and regions of dead volume of each are different, and so the washout period between samples is very variable. In general, the smaller the internal volume and surface area, the fewer the regions of dead volume, and hence the shorter the washout period. Unfortunately, a second function of the spray chamber is to act as a pulse dampener, i.e., to diminish noise originating from the peristaltic pump used to transport the sample to the nebulizer. The smaller spray chambers are often less efficient at reducing such pulses when compared with the larger Scott style designs, and consequently "noisier" signals may result.

Many spray chambers have a jacket of cooling liquid (e.g., water at 5–10°C) surrounding them so that a constant temperature within the spray chamber is obtained. This has the effect of keeping the solvent loading of the plasma at a constant level and hence makes the signals more stable. If an organic liquid, e.g., methanol, is introduced, then the spray chamber temperature should be decreased, ideally to −10°C, to prevent excess solvent entering the plasma and causing perturbation or possible extinction. The majority of combinations of nebulizer and spray chamber have an efficiency of 1–2%, i.e., of every 100 mL of sample that is introduced, only 1–2 mL reaches the plasma. Although this seems extremely inefficient, this represents the optimal sample loading for the plasma before severe perturbation or possible extinction occurs. The theory behind nebulization and spray

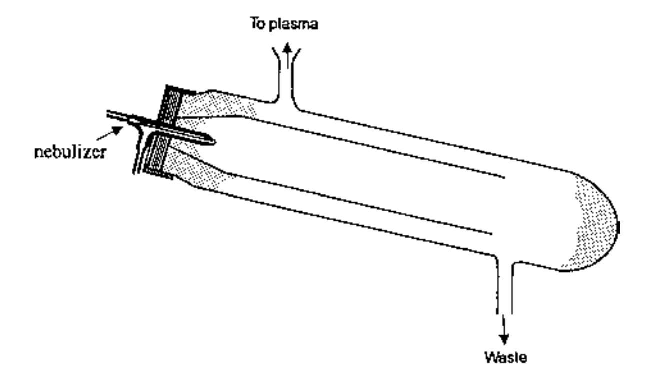


Figure 7 Scott double-pass spray chamber. Shaded areas represent "dead space" that may give rise to memory effects.

chamber design has been fully discussed in two papers by Sharp (1988a,b), and the theory of aerosol generation and sample transport in plasma spectrometry has been covered in detail elsewhere (Browner, 1999).

There are other types of nebulizer that do not require a spray chamber. One such device is the ultrasonic nebulizer (USN), where the sample is deposited onto a piezoelectric transducer that vibrates at ultrasonic speeds, thus shattering the liquid stream to form an aerosol (nebular). The aerosol is then transported via a desolvation device to the plasma. The desolvation device is required because the USN has a much higher sample transport efficiency, and hence excess liquid must be removed to prevent plasma perturbation. In general, the overall transport efficiency of the analyte is increased by an order of magnitude, and hence improved limits of detection are obtained. Since this type of nebulizer has the desolvation device as an integral part of its design, an external spray chamber is not required. Several examples of applications of this type of nebulizer have been published (Pandey et al., 1998; Poitrasson and Dundas, 1999).

The direct injection nebulizer (DIN) is capable of operating at exceptionally low sample flow rates (10–50 $\mu L\,min^{-1}$) and hence can be used if only a very limited sample volume is available. Since the flow rate is so small, the DIN may be plugged into the base of the torch and the sample nebulized directly into the plasma. Although 100% of the sample reaches the plasma, the absolute amount of material is approximately the same as for a typical pneumatic nebulizer (i.e., 100% at 20 $\mu L\,min^{-1}$ is the same as 2% of 1 $mL\,min^{-1}$), and hence there is no perturbation of the plasma. An example of the use of a direct injection nebulizer has been published elsewhere (Acon et al., 2001). Electrospray and thermospray sample introduction devices have also found use for environmental matrices (Zhang and Koropchak, 1999; Zheng et al., 2001), but these high-efficiency sample introduction devices have been used mainly in research laboratories, and few routine applications have been reported to date.

2. Alternative Sample Introduction Techniques

Although sample introduction is normally achieved via a nebulizer and spray chamber, several alternative methods are available, some of which facilitate the analysis of solid samples. These have an advantage in that the sample needs less manipulation, which reduces the possibility of contamination or determinant loss (e.g., loss by volatilization if an elevated temperature is used).

Laser ablation is one such technique that has become relatively popular in recent years, especially for geological samples. The analysis of rocks normally requires a complete acid digestion, usually using HF,

which is hazardous to handle and requires special fume extraction facilities. The use of laser ablation in which a laser is focused at or near the surface of the rock (or any solid sample) avoids the need for such sample preparation. The laser is used to volatilize the sample so that the ablated material can be transported by a flow of inert gas (usually argon) directly to the plasma. The disadvantage of laser ablation is that it is often difficult to find appropriate solid standards, since for accurate, fully quantitative results to be obtained, a standard of very closely matched matrix must be used. This is frequently difficult to achieve unless certified reference materials (CRMs) are used. The application of CRMs for environmental analysis will be discussed in more detail in Sec. IV. However, in general terms, if we assume that the CRM or other reference material is closely matrix-matched with the sample, then if the results obtained are in good agreement with the certified value, we can have some confidence in the results derived for the real sample. This approach will not correct for poor sample homogeneity, which can be problematic using laser ablation, since only a small area of sample is volatilized into the plasma. Clearly, if a sample is not homogenous, a representative portion of that sample may not be obtained.

Laser ablation is, however, a useful technique when there is only a very small mass of sample, because the laser can be focused onto a small area. One such application of laser ablation to environmental samples is the determination of platinum group metals in airborne particulate matter collected on filters (Rauch et al., 2001). Scanning laser ablation provides the resolution required to analyze individual particles. If a larger sample is available, then the laser can be used to "map" the sample, i.e., the laser can be used to ablate spots at regular intervals across the sample surface, building up a lattice of data points. This goes some way to overcoming problems associated with poor homogeneity. Depth profiling is another technique that can be achieved using laser ablation. If the laser is focused and fired onto the same spot repeatedly, the elemental composition at the surface, and then at successively lower levels, can be determined.

There are numerous types of laser available commercially, but the Nd-Y-Al garnet (Nd : YAG) operated at 1064 nm, at 532 nm (if frequency doubled), or at 266 nm (if frequency quadrupled) is the most commonly used type for laser ablation. Such a laser operated at a power of 1–1.3 mJ will produce a crater of approximately 15 μm in width. Other laser systems, e.g., infrared (IR) or ultraviolet (UV), have also found common usage.

Slurries are suspensions of solid materials in liquid matrices. They sometimes provide a convenient way of introducing solid samples, since their use may allow the sample to be aspirated through a nebulizer/spray chamber assembly as with liquid samples. Slurries also benefit from the

advantages of minimal sample manipulation and of not requiring strong acids for sample destruction. Another advantage is that slurry samples may frequently be analyzed against a calibration curve prepared using aqueous standards. There are, however, a few primary rules for slurry introduction. The most important of these is that the particle size of the sample must be extremely small. Grinding the sample so that the majority of particles are in the region of 2 μm in diameter is mandatory if reliable results are to be produced. The presence of larger particles will yield low recoveries, because such particles will be transported through the nebulizer/spray chamber assembly and into the plasma with lower efficiency than true solutions. Whether low recoveries are obtained will depend on the sample type. If the sample is composed of relatively volatile material, e.g., a powdered plant, then the particle in the plasma will become vaporized and atomized very rapidly, enabling all the atoms present to be detected. Other samples, e.g., a soil that has a relatively nonvolatile aluminosilicate matrix, may be only partially decomposed in the plasma, leaving smaller particles that will contain some determinant atoms that will not be available for detection. The theory behind using slurries for ICP analysis has been described in detail by Goodall et al. (1993).

Sample particle size may be reduced in several ways. The "bottle and bead method" may be used, in which sample is weighed into a plastic bottle to which ZrO_2 beads (2 mm diameter, typically 10 g) are added. A dispersant (about 5 mL) is added, and the bottle is sealed and placed on a mechanical shaker for several hours (depending on sample type). Several dispersants are available that are ideal for this purpose, including Aerosol OT and Triton X-100 for biological samples and sodium hexametaphosphate or sodium pyrophosphate for more refractory samples.

Applications papers on slurry introduction are numerous for environmental samples, including soils (Lu and Jiang, 2001), vegetation (Carrion et al., 2001), and dust particulates (Coedo et al., 2000). For some sample types, e.g., vegetation, where the levels of determinants are likely to be low, a preconcentration method can be used. The sample (5 g) is placed in a muffle furnace (typically 400–450°C) until it is thoroughly carbonized, and then the ash, which constitutes 5–10% of the sample mass, is slurried. This method is obviously not suitable if very volatile determinants, e.g., Hg, Cd, or Pb, are to be determined. Some workers have also used a combined acid leach/slurry technique (Persaud et al., 1999).

A micronizer is also a suitable method for preparing slurries. Once again, the sample is weighed into the container containing the grinding rods, and a small volume of dispersant is added. The method of choice for slurry preparation will often be governed by the nature of the determinants.

For example, if Hf and Zr are to be determined, then the bottle and bead method is inappropriate. If, however, the determinants of interest include Mg, the agate grinding rods of a micronizer will yield an enormous blank value. The hardness of the sample must also be taken into account. If the sample is harder than the grinding medium, then clearly the sample will not be ground, while damage will be done to the beads or rods. For rock samples, it is usual for a pregrinding to be undertaken in a tungsten carbide Tema mill. This exceptionally hard material breaks down the rocks into a powder that is then in a form ready to be ground further using ZrO_2 beads.

Electrothermal vaporization (ETV) is a method that has been adopted from atomic absorption spectrometry. An aliquot of the sample (typically 15–50 μL), usually in a liquid form, is placed on a rod or in a tube that is heated electrically in a stepwise manner. The temperatures used will depend on the sample type. Usually a drying step is required, in which the solvent is driven off at a temperature sufficient to vaporize the sample evenly, without frothing of the sample and potential loss due to excessive heating. Once dried, the sample may be charred or ashed. This step is required for organic samples to volatilize the matrix, leaving the determinant atoms on the heated surface. The temperature of this step will depend on the nature of the determinants and on the sample type, but it typically lies in the region of 300–1300°C. The overall effect of this process is to separate the potentially interfering matrix from the determinants, hopefully leading to fewer interference problems during the measurement step. The third step is to volatilize the determinants into a stream of inert gas so that they may be transported to the plasma for detection. Again, the temperature at which volatilization occurs will depend on the determinant, but it will typically be in the region of 1200–3000°C. The final step is usually a cleaning step to prevent determinant carryover to the next sample. This is usually achieved by heating at a temperature close to 3000°C.

It is possible to analyze solid materials directly using this technique, but weighing only a few mg of sample accurately onto the heating element can be problematical. The introduction of slurries into ETV is also possible (Li et al., 1998). Several workers have used chemical additives to modify the behavior of the determinant elements. Many elements, for example, have a very volatile fluoride and hence determinants that under normal circumstances are very refractory, e.g., Hf, Ti, W, or Zr may be volatilized as the fluoride into the plasma, which dissociates the compounds into atoms or ions. In cases such as this, the determinant may be volatilized in preference to the matrix. Alternatively, a silica-based material may be volatilized leaving the determinants on the atomizer. In any event, the matrix and determinant(s) are separated, facilitating interference-free determination.

Several fluorinating chemicals have been used, but the most common has been PTFE (Peng et al., 2000). Numerous other matrix modifiers have been reported in the literature. Further information on this area can be found in a review on ETV-ICP-MS prepared by Sturgeon and Lam (1999) or in a review of the relative merits of laser ablation, slurry nebulization, and electrothermal vaporization by Darke and Tyson (1994).

Some elements form compounds that are vapors at room temperature. Examples include the metalloids Sb, As, Se, and Te. If acidified samples are reacted with sodium tetrahydroborate, the gaseous hydrides of these elements will be formed. These hydrides may then be separated from the liquid matrix in a gas/liquid separator and transported as the gaseous form in a stream of inert gas to the plasma. The optimum concentrations of the acid and of the tetrahydroborate differ for each determinant, although if several of these hydride-forming elements are to be determined simultaneously, compromise conditions may be used. The advantage of this technique is that the determinants are transferred to the plasma at an efficiency close to 100%, hence increasing the sensitivity and improving the limits of detection significantly.

One potential disadvantage of the hydride technique is the risk of interference effects from the matrix. Transition metals such as Cu or Fe, or the Pt group metals, may alter the efficiency of formation of the hydrides. When calibrating against aqueous standards, very low recoveries may be obtained unless the chemistry of the method is optimized, e.g., by adding a sequestering or complexing agent to bind with the potential interfering species (Nakahara and Wasa, 1994). Another potential drawback is that not all species of the determinant elements form a hydride, and some species may form a hydride at a different rate or efficiency than others. For example, Se(IV) readily forms a volatile hydride, but Se(VI) does not form a hydride at all. In such a case, the sample is usually boiled with HCl, to reduce the Se(VI) to Se(IV) (Pitts et al., 1995). Another example is As, where both oxidation states, As(III) and As(V), form hydrides, but at different rates, whereas other As species, e.g., arsenobetaine (the main As species in many marine biological samples), do not form a hydride. In this case, either a powerful oxidant is required to destroy the arsenobetaine, e.g., alkaline persulfate (Cabon and Cabon, 2000) or photolytic decomposition may be used (Rubio et al., 1995). For certain other elements, other vapor-forming chemicals have been used. An example is sodium tetraethylborate, which has been used to form volatile ethyl compounds of Cd (Mota et al., 1999).

A modification of the above approach is used for Hg determinations. If the sample is mixed with a reducing agent, e.g., tetrahydroborate, or more commonly tin (II) chloride, elemental Hg vapor is formed. This may then be

transported directly to the plasma by a flow of inert gas. A more detailed coverage of the history, theory, and application of the extensive subject of vapor generation has been presented by Dedina and Tsalev (1995).

D. Line Isolation Devices and Detectors (ICP-AES)

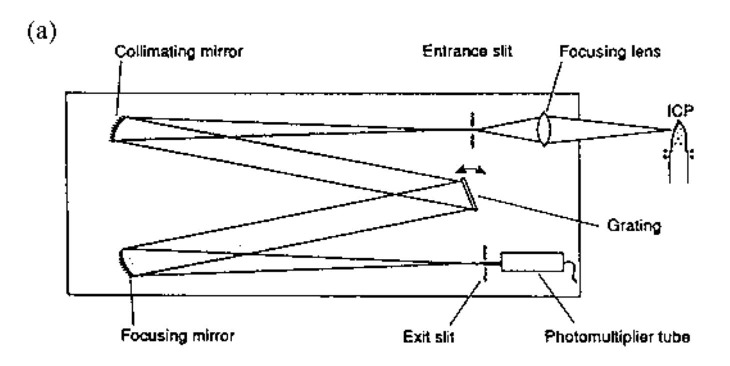
The spectral lines of interest emitted by the determinant species in the plasma need to be separated from all the other lines emitted, using some form of line isolation device. Nearly all of the useful analytical lines lie in the region 160–860 nm, although the majority occur below 450 nm. The ideal spectrometer should therefore be capable of detecting all lines within this region. At lower wavelengths, e.g., below 200 nm, the presence of molecular gases such as O_2 and N_2 in the atmosphere will severely limit the sensitivity because they will absorb much of the emitted light. For determinants such as As, which has analytical wavelengths of 188.979 and 193.696 nm, and Al, that has a wavelength of 167.017 nm, steps must be taken to ensure that molecular gases are excluded from the light path. This may involve flushing the spectrometer with an atomic inert gas, e.g., Ar, or using a vacuum pump to evacuate the potential light-absorbing species.

Several different types of instrument are available, but in general they may be split into two overall classes, sequential and simultaneous spectrometers. As the name implies, a sequential spectrometer may only interrogate one analytical line at a time. If a number of determinants are to be measured, the spectrometer must change wavelength for each element sequentially. In a modern instrument, this can be a relatively rapid process, but overall the measurement process is fundamentally slower than when using a simultaneous spectrometer.

In all sequential spectrometers, the line isolation device is a monochromator. Schematic diagrams of two types of line isolation device are shown in Fig. 8, although the Czerny–Turner mounting is the most widely used. The diffraction grating is the component that separates the light entering the monochromator into its constituent parts. There are several different types, e.g., ruled, holographic, and echelle gratings, but all have equidistant parallel grooves cut at an angle on the surface of a mirror. The density of these grooves on such ‘‘blazed’’ gratings differs between spectrometers but usually lies in the region of 600 to 4200 per mm. It is the angle and the density of the blaze that determines the separation of the wavelengths of the light. As the light, which is composed of multiple wavelengths, strikes the grating, it is diffracted at an angle that is dependent upon the wavelength. Light with longer wavelength will have a higher angle of diffraction. The angle of diffraction also increases as the number of grooves per unit area increases. The mirror focuses the light coming from

Marcel Dekker, Inc.
270 Madison Avenue, New York, New York 10016

(a)



(b)

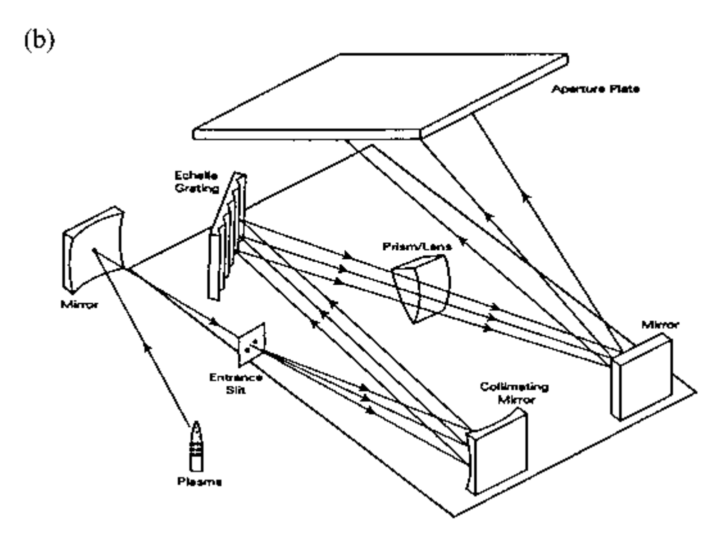


Figure 8 Line isolation devices used for ICP-AES. (a) Single-channel scanning spectrometer based on the Czerny–Turner optical configuration; (b) echelle polychromator.

the plasma through the entrance slit onto the grating, and then the diffracted light is focused onto the exit slit and detector. If more than one analytical line is to be interrogated, then the grating can be rotated so that a second wavelength is focused to the detector. This process may be repeated until all the wavelengths of interest have been examined.

Polychromators are line isolation devices that allow several analytical lines to be examined simultaneously. This not only saves time during an analysis but also offers the opportunity to obtain simultaneous background correction. In Paschen–Runge type polychromators, the grating is static,

Marcel Dekker, Inc.
270 Madison Avenue, New York, New York 10016

i.e., it does not rotate. This means that the instrument is relatively inflexible, because only a certain number of exit slits and detectors are available to the user. Most polychromators are programmed for between 20 and 30 analytical lines. Since changing to obtain another wavelength of interest is time-consuming, considerable thought should go into choosing the original set of wavelengths.

In both monochromator and polychromator spectrometers, the detector used has traditionally been a photomultiplier tube (PMT). Although it is not necessary here to describe in detail how these devices work, a brief overview may be useful. A PMT is basically a quartz vacuum tube containing a photosensitive cathode. When a photon exiting the spectrometer hits the cathode it emits electrons. These electrons are then accelerated down a series of between 9 and 16 ever more positive dynodes, emitting further electrons every time a dynode is hit. An avalanche effect is therefore created so that a 9-dynode PMT may yield 10^6 electrons per photon strike. The electrons are then collected by the anode and the current measured is proportional to the number of photons hitting the PMT, i.e., it is proportional to the amount of light emitted from the determinant, which in turn is proportional to the concentration of this element in the sample. Numerous types of PMT exist, and each has a slightly different wavelength operating range determined by the photosensitive material used to coat the cathode. Gallium arsenide is a common material for this purpose, since it has a fairly uniform response over a relatively wide wavelength range.

A more versatile version of the basic polychromator, the echelle-type polychromator (Fig. 8b), is now incorporated into many new instrument designs. This device uses both a prism and a grating to separate the polychromatic radiation. Individually, the prism and the grating produce poor resolution, with multiple overlapping wavelengths, but used in combination very high resolution may be achieved. A more comprehensive description of how the echelle-type polychromator works may be found elsewhere (Boss and Fredeen, 1997). One important feature of this dispersion system is that it makes possible the use of a completely different type of detector, the multichannel solid-state detector, which is now fitted to many new ICP-AES instruments. Each of these detectors contains many thousands of individual cells (pixels), usually arranged in a two-dimensional rectangle (Fig. 9). The number of pixels varies but can be between 512×512 and 4096×4096. There are several different types of such so-called charge-transfer devices (CTD), including charge-coupled (CCD), segmented charge-coupled (SCD), and charge-injection devices (CID). The SCD is slightly different from the others in that it contains individual collections of small subarrays (over 200 in total) of 20–80 pixels each, rather than a complete CCD, which contains hundreds of thousands of contiguous pixels.

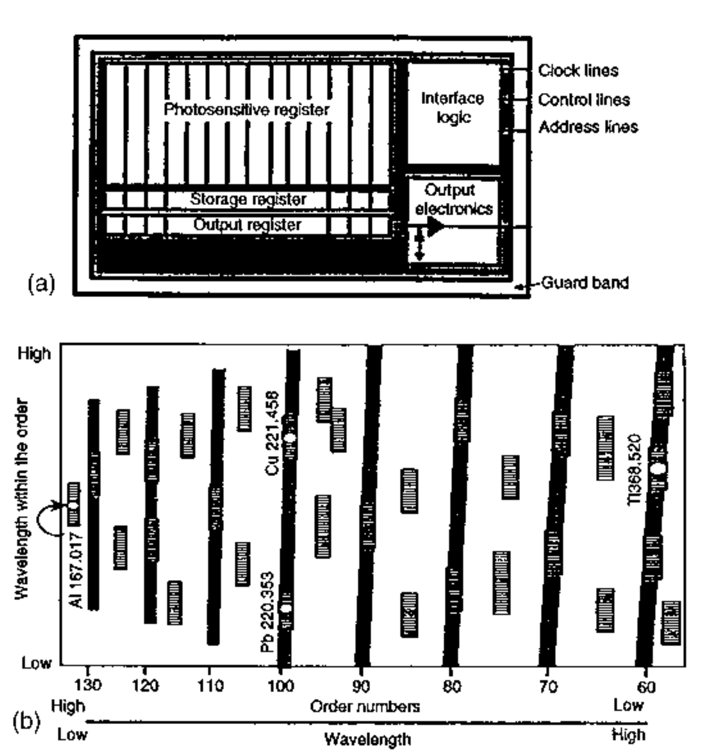


Figure 9 (a) Configuration of a SCD detector; (b) schematic diagram of the two-dimensional detector with respect to wavelength and order. (Reproduced with permission from the Perkin Elmer Corporation.)

Each pixel in a CTD is capable of storing a photon-generated charge. The different types of device are further characterized by the way in which the charge is obtained, interrogated, and stored. A comprehensive explanation of how these devices work is beyond the scope of this book, but many good accounts exist in the literature (e.g., Bilhorn et al., 1987). As may be expected, both advantages and disadvantages may be identified for these devices. Obviously, a very much greater number of analytical lines can be inspected simultaneously, yielding large savings of time and running cost when compared with sequential spectrometers. The number of lines that may be interrogated simultaneously is also far in excess of that achievable with a polychromator. In addition, the background signal may also be determined simultaneously. The overall cost of the instrumentation is substantially less than for a polychromator-based spectrometer. The disadvantages, however, include the risk of flooding of one pixel (if a

sufficiently large signal is obtained) and the subsequent spillage of the charge into neighboring pixels, thereby giving false high readings for other determinants. Since for the SCD only discrete sections of the spectrum are available, only 250–300 of the most commonly used lines for atomic spectrometry are actually available for use. This obviously leads to limitations in the flexibility of the instrument. A sequential spectrometer is capable of determining many thousands of lines (depending on the type and useful range of detector used), but it would take substantially longer to make the measurement. For routine analysis, the use of either echelle-based spectrometers with charge-transfer device detectors or rapid sequential spectrometers is adequate for the vast majority of applications.

E. Isotope Selection and Isolation (ICP-MS)

Inductively coupled plasma mass spectrometry (ICP-MS) is based on detecting ions using a mass-to-charge ratio rather than detecting photons. A schematic diagram of an ICP-MS instrument is shown in Fig. 10 and the interface between the ICP and the mass spectrometer in Fig. 11. In ICP-MS instruments the plasma must act as an ion source as well as an atom source. Rather than using a monochromator to disperse the light into relevant wavelengths, the mass spectrometer separates the determinants' isotopes according to their mass-to-charge ratio. For example, if Cu and Pb are to be

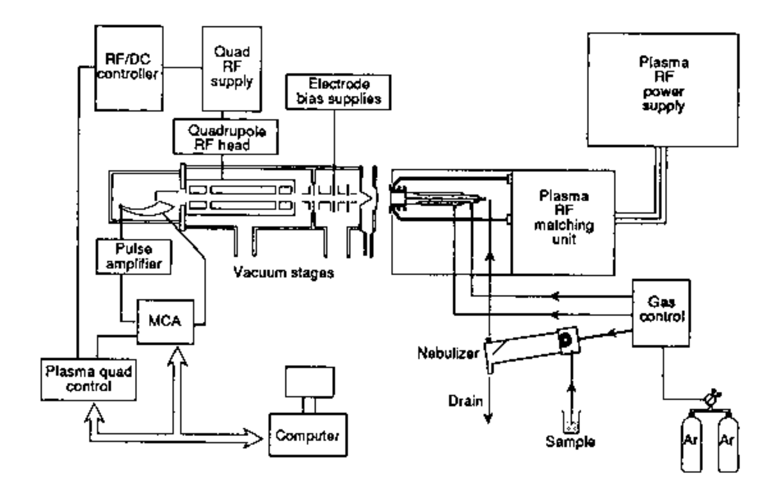


Figure 10 Schematic diagram of an ICP-MS instrument. (Reproduced with permission from Sharp, B., in *Soil Analysis—Modern Instrumental Techniques*, 2d ed. [Smith, K.A., ed.]. Marcel Dekker.)

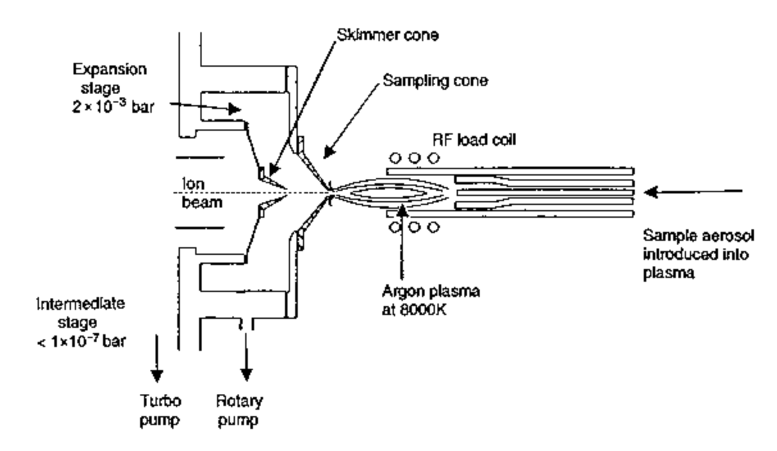


Figure 11 ICP-MS interface.

determined, then the mass spectrometer must be capable of separating the $^{63}Cu^{+}$ from the $^{65}Cu^{+}$ as well as the ^{206}Pb, ^{207}Pb, and ^{208}Pb isotopes from each other. In addition, it will also need to separate out all of the other isotopes of concomitant elements and interfering species. The large majority of ICP-MS instruments currently use a quadrupole mass spectrometer. This is a relatively low resolution device that may separate masses with a resolution of approximately 0.5 mass units. The quadrupole mass filter is composed of four electrically conducting rods that are oriented in a square configuration (O'Connor and Evans, 1999). In short, the device works by supplying the rods with dc voltage and a radio-frequency field, the amplitude of which varies very rapidly. As ions enter the mass filter, they begin to oscillate. At any one instant, ions of only one mass-to-charge ratio will be allowed to pass through the mass filter, while other ions will be deflected and impact onto the rods, causing them to be neutralized. An instant later, the amplitude of the rf and dc changes, and ions that were allowed to pass through now become deflected and hit the rods, while other ions of different m/z pass through to the detector. Although quadrupole mass analyzers are essentially sequential in their mode of operation, they are so rapid, with 200 m/z being scanned in less than 1 ms, as to become pseudosimultaneous. A more detailed description of the process may be found in the literature (Todd and Lawson, 1975).

The detector for a quadrupole ICP-MS instrument is most likely to be an electron multiplier. The ion beam exits the mass filter and impacts on a conversion plate that converts the ions into electrons. These electrons are then accelerated down either a continuous dynode (as in a horn-style

detector) or a series of discrete dynodes arranged in either a ''venetian blind'' or ''box and grid'' fashion, to a base plate, where the electron pulses are measured. The pulses last typically 10 ns and hence numerous determinants may be determined in rapid succession. The process is analogous to how a PMT works. An alternative type of detector is the Faraday cup collector, which consists of a collector electrode surrounded by a cage. These devices allow currents as low as 10^{-15} Å to be measured. A more extensive description of how all of these devices work has been presented by Fisher and Hill (1999).

As discussed above, the quadrupole mass filter offers relatively low resolution. Magnetic sector instruments provide better resolution (this advantage will be discussed in detail below) but are also far more expensive. In such an instrument, the ion beam enters the spectrometer, and the controllable magnetic field deflects the ions along curved paths. The extent to which they are deflected will depend upon their momentum, and therefore each ion will have a unique trajectory. By changing the magnitude of the magnetic field, only ions of one m/z will be focused onto the detector at any one instant.

Double focusing sector mass analyzers have the highest resolution. Whereas a quadrupole instrument has a resolution of 400 (unit mass), the double focusing instruments may reach a resolution of 10,000 and hence may resolve to below 0.01 mass unit. Examples of polyatomic ion interferences and the mass analyzer resolution necessary to resolve the interferences from the determinant of interest are shown in Table 2. Such instruments theoretically have numerous advantages when compared with other mass analyzers. These instruments use both an electrostatic and a magnetic field to disperse the ions according to their momentum. In the electrostatic field the trajectory of the ions is dependent upon their energy rather than their mass. The ions are therefore split using two different methods, and hence greater resolution is obtained. Another advantage of this type of instrument is that several (up to 10) detectors may be used.

Time-of-flight ICP-MS (TOF-ICP-MS) is the most recent development in commercial mass spectral analyzers (O'Connor and Evans, 1999). This too has advantages over the other methods, but as yet it is not really regarded as a routine tool. The advantages of TOF-ICP-MS include simultaneous determination of all masses, improved isotope ratio measurements, and good scope for the detection of transient signals such as those obtained from chromatography, laser ablation, or electrothermal vaporization. This is reflected in the number of environmental applications that have been reported using such equipment in recent publications (Mahoney et al., 1996; Mahoney et al., 1999; Haas et al., 2001).

Table 2 Examples of Polyatomic Ion Interferences When Using ICP-MS and the Mass Analyzer Resolution Necessary to Resolve the Interferences from the Determinant of Interest

Analyte ion		Interfering ion		
Nominal m/z	Accurate m/z	Nominal m/z	Accurate m/z	Resolution required
^{24}Mg	23.9850	$^{12}C_2$	24.0000	1599
^{28}Si	27.9769	$^{14}N_2$	28.0060	962
^{28}Si	27.9769	$^{12}C^{16}O$	27.9949	1555
^{31}P	30.9737	$^{14}N^{16}O^{1}H$	31.0057	968
^{31}P	30.9737	$^{15}N^{16}O$	30.9950	1455
^{32}S	31.9721	$^{16}O_2$	31.9898	1807
^{44}Ca	43.9555	$^{12}C^{16}O_2$	43.9898	1282
^{48}Ti	47.9479	$^{32}S^{16}O$	47.9670	2511
^{51}V	50.9440	$^{35}Cl^{16}O$	50.9637	2586
^{52}Cr	51.9405	$^{35}Cl^{16}O^{1}H$	51.9715	1676
^{52}Cr	51.9405	$^{40}Ar^{12}C$	51.9623	2383
^{54}Fe	53.9396	$^{40}Ar^{14}N$	53.9653	2099
^{56}Fe	55.9349	$^{40}Ar^{16}O$	55.9572	2509
^{63}Cu	62.9296	$^{40}Ar^{23}Na$	62.9521	2797
^{64}Zn	63.9291	$^{32}S^{16}O_2$	63.9619	1950
^{64}Zn	63.9291	$^{32}S_2$	63.9442	4234
^{75}As	74.9216	$^{40}Ar^{35}Cl$	74.9311	7887
^{80}Se	79.9165	$^{40}Ar_2$	79.9246	9867

IV. SAMPLE PREPARATION AND APPLICATIONS

ICP-AES and ICP-MS are now used routinely for the analysis of environmental samples in many laboratories worldwide. Despite this widespread use, there continues to be a lack of standardization in the methodologies used to prepare samples prior to analysis.

A. Digestion Procedures

1. Open-Vessel Digestions

For many commercial laboratories, the digestion step often involves the use of aqua regia, e.g., for soils as specified in the ISO Standard 11466. Although many laboratories refer to this as a ‘‘total digestion,’’ the method will not bring into solution those elements bound to silicate minerals. For many applications it is often believed that the silicate-bound

metals are not important, and that it is adequate to determine total-recoverable heavy metals in soils in order to estimate the maximum element availability to plants and their general mobility in the environment (Niskavaara et al., 1997; Vercoutere et al., 1999). In addition, many laboratories do not want to try and carry out a complete digestion because of the inevitable use of HF, which has a number of health and safety hazards associated with its use.

The conventional aqua regia digestion procedure consists of digesting samples such as soils on a hot plate with a 3 : 1 mixture of HCl and HNO_3 (Nieuwenhuize et al., 1991). The HNO_3 reacts with concentrated HCl to form aqua regia:

$$3HCl + HNO_3 \rightarrow 2H_2O + NOCl + Cl_2$$

This digestion procedure is widely used, and the European Bureau of Reference has certified several soil and sludge samples based on its use (Quevauviller et al., 1993; Vercoutere et al., 1995). In addition, in many countries (excluding the U.S.), this procedure is required by the statutory regulations when estimating the impact of soil amendments such as sewage sludge on the environment (Krause et al., 1995; Marr et al., 1995; Vercoutere et al., 1995). However, this procedure can be very tedious and time-consuming, and if open systems are used during digestion, there are risks of atmospheric contamination and volatilization losses during the oxidation of organic substances within the soils (Nieuwenhuize et al., 1991; Quevauviller et al., 1993).

Less well documented in the literature, but often favored by geological laboratories, is the use of programmable hot-block digestion systems as described by Thompson and Walsh (1989). In this type of system a small amount of sample (typically 0.1 g) is weighed into a Teflon tube (ca. 1.5 cm i.d. × 15 cm long) that is placed into a heating block that can accommodate 200–300 samples. A mixture of acids is added (usually a combination of HF, HNO_3, and $HClO_4$), and the hot block is taken through a heating cycle over a period of 8–12 h, during which the temperature is ramped up and held at a series of stages to allow the sample to digest and the acids to be boiled off. At the end of the cycle, the dried salts that are left in the bottom of the digestion tubes are brought into solution by warming in 50% HNO_3 and then finally made up to volume. By careful optimization of the amount of acid and the heating cycle program, a total digestion of the soil can be achieved, although Si and B are volatilized as fluorides and therefore cannot be determined (for details of the reactions see the following section on microwave digestion). The advantage of using such

a system is that large batches of samples can be digested simultaneously with only a minimum of operator supervision. The main disadvantage is the small size of sample used; in order to get a representative sample a number of grams of the material must be ground to $< 125\,\mu m$ before it is weighed into the tube.

2. Microwave Digestion

Since the 1980s, microwave-assisted sample digestion techniques have become increasingly popular and are now widely used (Quevauviller et al., 1993; Smith and Arsenault, 1996; Levine et al., 1999; Betinelli et al., 2000; Falciani et al., 2000; Chen and Ma, 2001; Ivanova et al., 2002; Sun et al., 2001). Microwave-assisted aqua regia digestion using a Teflon bomb provides a rapid, relatively safe, and efficient digestion and is not susceptible to losses of volatile metals (Rantala and Loring, 1989; Nieuwenhuize et al., 1991; Paudyn and Smith, 1992; Marr et al., 1995). However, microwave digestion has not always been found to be the best method for sample digestion. For example, aqua regia digestion methods have been shown to fail to quantify accurately more than 20 elements in some sediments (Krause et al., 1995), and it proved especially poor for K and Al, which form part of some clay mineral structures. Other reports have shown that aqua regia extracted less than 70% of Cd, Mn, and Ni from some sediments (Berrow and Stein, 1983) and that the typical elemental recovery in ashes and sediments using aqua regia digestion was ca. 80% (Paudyn and Smith, 1992). However, the recovery was higher for many elements (e.g., Al, Fe, Mg) using microwave rather than hot plate digestion.

Some reports in the literature have suggested that a mixture of aqua regia, HF, and H_3BO_3 provides satisfactory precision and accuracy for dissolving silica matrices using microwave digestion (Nadkarni, 1984). The following reactions are suggested to occur during digestion (Ryss, 1956; Wu et al., 1996):

$$6HF + SiO_2 \rightarrow H_2SIF_6 + 2H_2O$$
$$H_3BO_3 + 3HF \rightarrow HBF_3OH + 2H_2O$$
$$HBF_3OH + HF \rightarrow HBF_4 + H_2O$$

Adding boric acid in the second stage of the digestion not only complexes the free fluoride ions in the solution but also facilitates the dissolution of the precipitated fluorides (Wu et al., 1996). However, when ICP-AES is used for analysis, adding boric acid can create a matrix effect and was reported to result in a 20% decrease in sensitivity for Mo, Ni, Pb, Sb, Se, and Sn, and

50% and 70% decrease in sensitivity for P and S, respectively (Paudyn and Smith, 1992). This procedure has also been modified so that the HF is added to the solid 16 h before the aqua regia addition, and the mixture is then subjected to microwave heating (Ammons et al., 1995). This approach has been used to determine metals in soil with more than 45% sand.

B. Speciation Studies

Speciation analysis is a topic of research that has attracted a great deal of attention in recent years. This is because different chemical forms of an element may have different toxicity, mobility, and environmental fate, and thus knowing only the total concentration of an element is insufficient in many studies. There are several methods of achieving speciation analysis, but many use a chromatographic technique to separate the species of interest, coupled with an element-specific detector such as ICP-AES or ICP-MS. The methods of extraction used for speciation analysis frequently differ from those for "total" metal measurements. This is to ensure that there is no alteration of the speciation during the extraction process, since this would then result in an inaccurate estimate of, for example, the overall toxicity of the sample with respect to that particular element. To prevent such a situation arising, most of the extraction procedures used for speciation analysis are less aggressive than digestion using mineral acids. However, it is still necessary to test the extraction procedures on pure standards to ensure that no species alteration is occurring. In addition to the extraction procedure, it may also be necessary to test aqueous sample preservation techniques to ensure that the speciation is not altered during transit or storage of the sample.

Several comprehensive overviews of speciation have been published recently (Caruso et al., 2000; Ebdon and Fisher, 2000; TrAC, 2000). In addition to these, more specialized reviews detailing the design and application of interfaces for coupling chromatographic techniques with ICP-AES and ICP-MS instruments have been presented (Hill et al., 1993; Ellis and Roberts, 1997; Zoorob et al., 1998). In other cases, studies have focused on the speciation of a number of individual elements, e.g., antimony (Smichowski et al., 1998; Nash et al., 2000). The former paper discussed numerous methods of extraction, preconcentration, selective hydride generation, and chromatographic techniques (including those coupled with atomic spectrometric detection). The problems associated with species instability during sampling, storage, sample treatment, interferences, and lack of suitable CRMs with respect to arsenic speciation have also been discussed (Burguera and Burguera, 1997). Other studies have focused on the separation of species prior to detection, for example a review of the liquid chromatographic separations of As and Se compounds (Guerin et al., 1999).

There are many examples of the speciation of trace elements in waters, and so just a few will be highlighted to indicate what may be achieved. In-situ field sampling of Hg species in river waters has been undertaken using minicolumns of C-18 modified with sodium diethyldithiocarbamate (Blanco et al., 2000). On return to the laboratory, the species were eluted by 5% thiourea in 0.5% HCl (500 μL). Speciation was then achieved by liquid chromatography and ICP-MS detection of the inorganic and methyl mercury. Between-column precision was 12% at the $0.2\,ng\,mL^{-1}$ level, and the limit of detection was $5.2\,ng\,L^{-1}$. Stability of As, Sb, Se, and Te species in water, urine, fish, and soil extracts using HPLC-ICP-MS has been investigated, and it was concluded that for aqueous samples, storage at 3°C was better than that at −20°C, because at the lower temperature, species transformations occurred (Lindemann et al., 2000). Extraction methods from the solid samples were also investigated. Using spiking experiments and an extraction medium of water and H_2SO_4 (0.01 M), it was found that the recovery for many species was less than 20%. Organolead speciation in rainwater may be accomplished using a variety of detection methods including GC-ICP-TOF-MS (Baena et al., 2001). The GC-ICP-TOF-MS method yielded a limit of detection of 15 pg (as Pb). Speciation of vanadium(V) and vanadium(IV) has been achieved using flow injection (FI)-ICP-AES, using an ultrasonic nebulizer (Wuilloud et al., 2001). The flow injection chemistry facilitated a preconcentration factor of 15, and a further improvement of 15-fold in sensitivity was achieved using an ultrasonic nebulizer. Overall this system gave a limit of detection of $19\,ng\,L^{-1}$ and was successfully applied to the analysis of river water samples.

Inorganic and organic anionic As species have also been determined in river and ground water samples by HPLC-HG-ICP-AES (Gettar et al., 2000). The improvement in sensitivity arising from the sample introduction by hydride generation (HG) enabled limits of detection at the ng level to be reached. Unfortunately, in this example spiking experiments indicated that the recovery of the species may be dependent on the sample composition. Arsenic species have also been separated and determined by capillary electrophoresis (CE) coupled with ICP-MS (Van Holderbeke et al., 1999). To accommodate the very low flow rate of the CE system, a microconcentric nebulizer was used. Limits of detection of $1–2\,\mu g\,L^{-1}$ were achieved, and the method was applied to the analysis of mineral water, soil leachate, and urine.

C. Sampling for Air Analysis

Air analysis may involve the analysis of aerosols, metal vapors, airborne particulates, and sedimented dusts. A review of the collection and determination of metal contaminants in gases has been published (Telgheder

and Khvostikov, 1997). The first analytical problem to address is how to sample adequately. Frequently, metal vapors have been analyzed after cryotrapping. One such example was the determination of $Ni(CO)_4$, $Fe(CO)_5$, $Mo(CO)_6$, and $W(CO)_6$ in sewage gas (Feldmann, 1999). Here the air samples were collected in Tedlar bags and then analyzed by cryotrapping GC-ICP-MS. The Ni, Mo, and W compounds were found to be present at less than 1 ppb v/v, but the Fe compound was not detected. This was attributed to the instability of this compound in the presence of water vapor.

Methods have also been developed that determined tetra-alkyllead compounds, tetra-alkyltin compounds, organomercury compounds, and dimethylselenium (Pecheyran et al., 1998). In this case the samples were cryofocused in the field onto small glass wool-packed columns at $-175°C$. The columns were then returned to the laboratory and detection performed using low-temperature GC-ICP-MS. The limit of detection offered by the method was dependent upon the determinant but was typically sub-pg. This study also reported the successful qualitative determination of *tert*-butylarsenic, *tert*-butylphosphorus, and alkyl indium compounds.

On-line analysis of air samples is also possible, and air, together with particulate matter and metal vapors, has been introduced directly to the plasma (Seltzer, 1998). It was found that molecular emission bands, e.g., from CN, produced spectral interference for several metals, but that these interferences could be overcome. Improvements in the apparatus for continuous emission monitoring using ICP-AES have been reported in a study by Gomes et al. (1996). The method was reported to analyze a large volume of air without the need for sample storage, avoiding contamination, and offering low operating costs. The limits of detection for eight determinants were lower than the recommended threshold limit values, and the results were demonstrated to be comparable to those of other continuous emission monitoring methods.

Another approach to collecting airborne particulate matter is to use filters. Cellulose membrane filters may be used for this purpose; one example has been to collect and analyze particulates for V and Zn (Boix et al., 2001). Other studies have used PM_{10} filters to collect the particulate matter, for example prior to attempting to correlate the concentrations of the first-row transition metals with humic acid-like substances (Ghio et al., 1996). However, a plethora of other filters may be used, e.g., glass fiber (Wang et al., 1998) and PTFE (Chin et al., 1999). This latter example is interesting since the filter was used in conjunction with laser ablation (Nd : YAG laser at 1064 nm) to analyze the particulates, using the CRM NIST 1648 urban particulate matter for calibration. Electrostatic precipitation may also be used to collect airborne particulates. In one example,

smoke from cigarettes was collected by electrostatic precipitation using 17.5 kV on a tungsten electrode followed by two secondary acid traps (Rhoades and White, 1997). After collection, the precipitate was washed into a container with methanol, evaporated, and then acid-digested in a closed vessel microwave system.

Reference or certified reference materials, such as the example used above, are as applicable to these types of sample as they are to any other. One recently published account described the preparation and characterization of a set of reference air filters (Kucera et al., 2001). Several techniques, including ICP-AES and ICP-MS, were used to establish the reference values for 15 elements. In addition, the problems encountered during the preparation of these filters were also discussed. The International Standards Organization (ISO) has also been working on a standard method for analyzing such samples and has published the results of an interlaboratory comparison of several digestion methods (Butler and Howe, 1999). A total of five digestion procedures was tested, including an ultrasonic agitation procedure, two hot plate procedures (NIOSH 7300 and OSHA ID 125G), and two microwave-assisted digestions. It was concluded that the ultrasonic agitation and the hot plate methods may, depending on the sample type, be incapable of full extraction.

D. Water Analysis

Water analysis may appear to be very straightforward, since theoretically it requires the minimum of sample manipulation, and samples may be aspirated directly to the ICP. However, for seawater analysis, where the total dissolved salt loading may be 3.5%, matrix elimination or dilution is required to prevent blockage of nebulizers, torches, and cones if ICP-MS is used. Dilution of the sample to reduce the salt loading will frequently put the determinant of interest below the detection limit of the instrumentation, and so an assortment of methods has been developed that try to overcome the problem. Other issues involved in the analysis of water samples include sampling, analyte preservation, and the need for a preconcentration technique. Each of these subjects will be discussed below.

Sampling is often relatively straightforward because aqueous samples are normally homogeneous. Both the sampling and the analyte preservation stages must ensure that contamination and losses through adsorption to container walls are kept to a minimum. For relatively shallow waters, a suitable container may simply be immersed. Adsorption to container walls is more prevalent in glass containers than in plastic ones. A study comparing four different types of bottle, and the use of acid washing for the preservation, storage, and subsequent determination of 62 determinants,

concluded that new unwashed high-density polythene bottles were the best (Reimann et al., 1999). The use of Tedlar bags for the collection of waters has also been investigated (DeBruyn and Rasmussen, 1999). Under conditions of low pH, no appreciable adsorption occurred over a period of 24 hours.

Filtration may be necessary for some sample types. Very fine particulate matter may stay in suspension and, if small enough, these particles may pass through the sample introduction system and give rise to erroneously high results. The influence of filtration on the concentration of 62 elements from well waters has been investigated, and noticeable differences were found between the filtered and unfiltered samples, although most were relatively small (Reimann et al., 1999). It was noted, however, that filtration also leads to contamination from Sn. This example emphasises the necessity of method development and validation.

Sample preservation frequently involves the addition of an acid. This is sufficient to prevent the adsorption of most metals. In one study, unacidified samples were found to stay stable for less than two weeks, but once acidified to $pH < 2$, the metals could be remobilized and remained stable for over 180 days (Creed et al., 1995). The use of HNO_3 for this purpose is to be encouraged, especially for ICP-MS analyses, because H_2SO_4, H_3PO_4, and HCl are more likely to cause interference problems (although this depends on the determinant). H_2SO_4 and H_3PO_4 may also cause accelerated wear of the nickel cones on the interface region of the ICP-MS instrument. For some determinants, such as Hg, other preservative agents are necessary. A mixture of 5% HNO_3 and 0.01% w/w $K_2Cr_2O_7$ has been shown to stabilize the nominal Hg content in a sample for at least a month (Caroli et al., 1996). Other workers have reported the use of gold chloride to preserve Hg (Fatemian et al., 1999). However, it should be remembered that although helpful for the determination of Hg by ICP-MS, the gold would cause a problem if cold vapor or hydride generation were used in an attempt to improve sensitivity.

As described previously, preconcentration may be necessary for many determinants, and there have been many techniques reported. Preconcentration is frequently essential for the less sensitive ICP-AES technique but occasionally may also be required for ICP-MS determinations. The simplest form of preconcentration is to evaporate a large volume down to a smaller one. This technique can yield large preconcentration factors but may be inappropriate if volatile determinants, e.g., Hg, are to be determined, or if the sample is a saline water. Liquid–liquid extractions may also yield high preconcentration factors. If the determinants in a large volume of water are reacted with a complexing agent such as 8-hydroxyquinoline or sodium diethyldithiocarbamate, the complex so formed may be extracted into a

small volume of an organic solvent, e.g., 4-methylpentan-2-one or isobutyl methyl ketone (IBMK). Back extraction into acid may further increase the preconcentration.

Many more recent methods utilize the advantages associated with on-line preconcentration techniques, i.e. less risk from contamination and opportunities for matrix removal. A large number of commercial chelating resins has been used. These include Muromac A-1 (Hirata et al., 2001), Toyopearl AF 650M (Warnken et al., 2000), and Chelex-100 (Ebdon et al., 1993). All these resins are iminodiacetic acid-based chelating resins that operate under similar conditions. The resins are selective (but not specific) for transition metal ions and have very low affinity for alkali or alkaline earth metals. The determinants are retained at a pH that is buffered to a value that is dependent upon the determinant, and eluted with a small volume of dilute acid. In one of these applications (Warnken et al., 2000), method detection limits of 1.1, 0.08, 0.47, 0.06, and $0.16\,pg\,mL^{-1}$ were achieved for Mn, Ni, Cu, Cd, and Pb, respectively. Such limits of detection facilitate the analysis of open ocean seawaters, where the concentrations of trace elements are exceptionally low. If such a technique is used with ICP-AES, limits of detection rivalling those by direct ICP-MS analysis are frequently obtained. Matrix separation may be achieved and, if a switching valve is placed between the end of the column and the sample introduction system, the matrix may be directed to waste so that dissolved salts do not clog the sample introduction system.

Commercial resins may also be chemically modified. An example is the immobilization of Kelex-100 on a Bondapack C-18 column, which may be used to preconcentrate a range of determinants (Ferrarello et al., 2001). Polyurethane foam impregnated with piperidine dithiocarbamate packed into a 20 mL disposable syringe has been used to preconcentrate Cd, Co, Cr, Cu, Mn, Ni, Pb, and Zn from natural water samples (Ramesh et al., 2001). In this example, sorption recoveries were greater than 97% for all the determinants except Co and Cr. Other methods that have been used include columns of ZrO_2 (Vassileva and Furuta, 2001) and TiO_2 (Liang et al., 2001). Both techniques proved to be effective, with the latter resulting in a preconcentration factor of 50.

Several methods have been developed for in-situ preconcentration. Seawater may be filtered on-line, and the determinants Cd, Co, Cu, Mn, Ni, Pb, and Zn preconcentrated on a column of Metpac CC-1, for example (Nickson et al., 1999). The columns are then returned to the laboratory for elution and subsequent detection of the determinants. Such a method overcomes any problems associated with sample preservation and contamination. Other preconcentration methods include the use of

Marcel Dekker, Inc.
270 Madison Avenue, New York, New York 10016

electrochemical techniques (Ugo et al., 2001), flotation (Pavlovska et al., 2000), and coprecipitation (Yabutani et al., 2001).

E. Geological Materials

A large number of different methodologies have been used to determine trace metals in geological materials such as rocks, ores, coal, sediments, and soils. While appropriate sampling can in itself be problematic, once collected the samples usually require drying and sieving. This may be achieved in several ways, including oven drying, although care must be taken not to lose volatile elements and also to not use a temperature high enough to burn off volatile humic substances. Freeze-drying and desiccation are alternative methods. The soil may then need grinding so that it passes through a sieve of known mesh ($< 63\,\mu m$ is common). In general terms, the smaller the particle size of the sample, the smaller is the mass of subsample required to ensure that a representatively homogenous subsample is obtained.

Soil, sediment, and rock samples may be prepared for analysis by atomic spectrometry in a number of different ways (Thompson and Banerjee, 1991). Total metal concentrations usually require sample dissolution or another complete sample destruction technique. However, there are occasions when only bioavailable elements are required, i.e., the proportion of elements available for uptake by animals or plants. In such a case, a gentle leach using NH_4Cl, $CaCl_2$, or EDTA may be used. Alternatively, sequential leaches using different reagents may be used to determine the amount of determinant bound to different fractions of the soil or sediments (Cave and Wragg, 1997; Davidson and Delevoye, 2001; Santamaria-Fernandez et al., 2002). The use of sequential extractions is discussed in more detail below.

Numerous techniques have been utilized for "total" element concentrations. Rocks and other similar materials are often resistant to most acid attacks, and for many determinants, full recovery is only achieved when HF is used. This chemical is potentially hazardous and requires an appropriate laboratory with special fume extraction facilities. However, the use of HF remains popular, and there are very many accounts of its use prior to determinations using ICP-AES and ICP-MS. A number of studies have also compared its use with that of other acids, e.g., for determination of various elements in rocks by ICP-MS after a digestion using either 2 mL HF and 0.5 mL HNO_3 or 3 mL HF and 3 mL $HClO_4$ (Robinson et al., 1999). For other samples, e.g., many soils and sediments, total dissolution is frequently unnecessary since digestion with concentrated HNO_3 is sufficient to extract $> 90\%$ of many determinants. Some elements, e.g., Cr, will

however stay within the alumino-silicate matrix. Similarly, other determinants, e.g., Sb, are leached more efficiently using HCl.

Microwave digestion has proved to be an extremely popular method for soils and sediments, since sample preparation takes minutes rather than hours, and, because the digestion bombs are sealed, losses of volatile determinants and contamination from extraneous sources are kept to a minimum. Various studies have evaluated the effectiveness of microwave digestion, and the application of the technique to environmental samples has been reviewed by Lamble and Hill (1998).

Although both hot plate and microwave methods employing aqua regia, with or without HF, are commonly used as total or pseudototal soil digestion methods by researchers in many countries, especially Europe, these methods are not widely used in the USA for analyzing soils. This is partially due to the establishment of the USEPA methods (Chen and Ma, 1998). The accuracy and precision of these methods in determining elemental concentrations in soils can also vary with element, soil properties, and digestion method, as well as with the origin of the soils (anthropogenic vs. natural deposits). For example, aqua regia digestion might give good recoveries for the maximum levels of polluting metals such as Cd, Cu, Pb, and Zn in soils (Marr et al., 1995), while metals like Ba, Cr, and Ni can only be efficiently recovered using HF digestion (Sawhney and Stilwell, 1994).

There are several other types of sample preparation used for geological-type materials. Fusion is a commonly used method. In one example, sample (0.5 g) was fused with $LiBO_2$ (2.5 g) in a gold–platinum crucible, and the melt formed was dissolved in 150 mL of 5% HNO_3. The dissolved mixture was then diluted to 500 mL so that the overall concentration of dissolved solid material would not interfere excessively with the determination step (Brenner et al., 1999). A similar procedure has been compared with various acid decomposition methods prior to the determination of rare earth elements (REE) by ICP-MS (Bartha et al., 1989). Suitable isotopes for the determination of the rare earth elements by ICP-MS are shown in Table 3. Several other types of fusion may be used, including NaOH (Smith et al., 1995) and Na_2CO_3 (Crosland et al., 1995). In some cases, workers have not dissolved the fused mixture. Instead, they have cooled the mixture to obtain a glass and then used laser ablation. The fusion method ensures sample homogeneity, and hence one of the main problems associated with laser ablation, as described earlier, is overcome. An example of this type of analysis has been published by Kanicky and Mermet (1999). Here samples were fused with lithium tetraborate, Sc_2O_3 and Y_2O_3 were added as internal standards, and then the cooled pellet was subjected to laser ablation using a frequency tripled Nd:YAG laser. The use of laser ablation techniques for geological materials is common, and a review of LA-ICP-MS of

Table 3 Suitable Isotopes for the Quantification of the Rare Earth Elements by ICP-MS

Element	Mass	Comments
La	139	Almost monisotopic (99.9% abundant)
Ce	140	Major isotope
Pr	141	Monisotopic
Nd	146	17.2% abundant
Sm	147	15% abundant
Eu	151	Polyatomic interference by $^{135}Ba^{16}O^+$ provides use of ^{15}Eu
Tb	159	Polyatomic interference by $^{143}Nd^{16}O^+$, monitored using ^{146}Nd
Gd	160	Polyatomic interference by $^{144}Nd^{16}O^+$, monitored using ^{146}Nd, ^{160}Dy (2.34%)
Dy	163	24.94% abundant
Ho	165	Monoisotopic
Er	167	22.9% abundant
Tm	169	Monoisotopic
Yb	174	31.8% abundant
Lu	175	97.4% abundant

geological samples has been published recently (Gunther et al., 1999). As well as for bulk rock analysis, laser ablation has also been used to analyze pinpoint areas such as fluid inclusions (Gunther et al., 1998). In this study, a 193 nm excimer laser was used to ablate inclusions enabling the determination of 19 major, minor, and trace elements spanning a concentration range of five orders of magnitude. Detection limits were in the ng g^{-1} to μg g^{-1} range, depending on the determinant.

The direct analysis of rock samples has also been achieved using ETV as a sample introduction technique (Okamoto et al., 2001). Powdered rock and an aliquot of ammonium fluoride in a tungsten cuvette were heated on a hot plate for digestion. After decomposition was complete, the cuvette was placed in a furnace and the sample atomized into the ICP-MS instrument. The authors claimed that since the sample cuvette acted as a weighing dish, sample carrier, decomposition vessel, and electrothermal vaporizer, the problems normally associated with the direct analysis of small masses of powder were overcome. The method was validated by the successful analysis of several standard rock samples.

Sequential chemical extraction is a widely used method for characterizing the distribution of heavy metals in soils and sediments and is commonly used in conjunction with ICP analysis of the sequential extracts

(Ahnstrom and Parker, 1999; Brunori et al., 1999; Ariza et al., 2000a,b; Basta and Gradwohl, 2000; Krishnamurti and Naidu, 2000; Gleyzes et al., 2001; Shiowatana et al., 2001; Santamaria-Fernandez et al., 2002). A large proportion of these papers are based on the method of Tessier et al. (1979), which involves the selective extraction of elements through use of a specific reagent for each phase. However, these selective extraction methods have suffered from various limitations. The methodological definition of the distribution of the trace elements between the solid phases does not necessarily reflect those found in the test sample, and the individual extractions are not specific to a single mineral phase. Chemometric processing of data obtained from a Tessier-style extraction scheme shows that more than one phase was often being extracted by each reagent, and that the methodological definitions did not correctly identify the extracted components (Santamaria-Fernandez et al., 2002; Cave and Harmon, 1997). Further, it has been shown by a number of studies (Raksasataya et al., 1996; Hall, 1998; Gray et al., 1998; Lo and Yang, 1998; Bunzl et al., 1999; Gomez-Ariza et al., 1999, 2000; Ho and Evans, 2000) that during the leaching process liberated trace metals can be readsorbed onto the soil, again compromising the interpretation of the metal distribution within the sample.

Lack of comparability of data between laboratories has also caused difficulties. The literature contains many examples of slightly modified schemes that give different results (Ariza et al., 2000b; Krishnamurti and Naidu, 2000). In order to address this problem, the European Standard Measurement and Testing program has proposed a standardized leaching scheme commonly referred to as the BCR method. This consists of a methodologically defined extraction of exchangeable, reducible and oxidizable fractions, which, with some modifications, has been successfully used to produce reproducible interlaboratory data for a lake sediment reference material (Quevauviller et al., 1997; Lopez-Sanchez et al., 1998; Sahuquillo et al., 1999, 2000; Rauret et al., 1999). Although reproducible for this material, it is not clear that the procedure will be suitable for all soil and sediment types, and the method may still suffer from the lack of specificity and readsorption problems previously mentioned.

In exploration geochemistry, sequential extraction methodology can identify the presence of pathfinder elements in specific physicochemical phases and hence be used to locate deeply buried mineral deposits (Hall, 1998). Recent developments in this area have successfully used extraction protocols that specifically target those elements bound up in fine-grained Mn and Fe oxides. The mobile metal ion (MMI) extraction scheme uses extractants containing strong ligands to detach unbound or weakly attached metal ions from soils (Mann et al., 1998). The enzyme leach method (Clark, 1993) uses products of the enzyme reaction to leach preferentially part of the

Mn oxide coatings on mineral grains without attacking their matrix. Successful application of the use of these methods to locate ore bodies has been reported (Li et al., 1995; Bajc, 1998; Hall, 1998; Yeager et al., 1998; Gray et al., 1999; Turner and Olsen, 2000), but reproducibility of the data has been highlighted as a problem (Hall, 1998). Hence it is worth using caution when utilizing data from these methods without other confirmatory evidence (Bajc, 1998).

In addition to the methodological problems of sequential extraction, the chemical analysis of the extraction reagents can cause significant problems. The sequential extracts are normally analyzed by atomic spectrometric methods, most commonly ICP-AES and ICP-MS. The high concentration of salts in these extracts [molar concentrations of reagents are often used, e.g., 0.04 M $NH_2 \cdot OH \cdot HCl$ in 25% (v/v) CH_3CO_2H (Li et al., 1995)] can cause blockages to the sample introduction system and instability of the ICP, requiring the samples to be diluted or digested prior to analysis. Many of the extraction schemes are very time-consuming, with extraction steps lasting for many hours.

Cave and Wragg (1997) have addressed the problem of methodologically defined phases and of the reagents being difficult to analyze by using a simple nonspecific extraction reagent. Nitric acid was reacted for different periods of time and at different acid concentrations with the test sample. The resulting solutions were then analyzed, and chemometric data processing of the resulting trace element data was used to separate and identify the physicochemical phases present in the test sample. A subsequent study (Cave et al., 2002) combined the use of this nonspecific extraction method with chemometric data processing for a contaminated soil (NIST 2710). A rapid and simple extraction was then carried out using separate aliquots of HNO_3 of increasing concentration passed through the sample under centrifugal force. The proposed method is called chemometric identification of substrates and metal distributions (CISMeD).

Speciation in solid samples such as soils, sediments, and rocks poses many difficulties. The determinant species must be removed from the matrix without alteration of the speciation. Numerous methods have been used in an attempt to achieve this, and often a microwave-accelerated extraction is successful. One example is the use of acetic acid (5 mL) to quantitatively extract organotin species from a certified reference sediment. Measurement is made by HPLC-ICP-MS, and using 0.5 g of sample, limits of detection better than 0.1 $\mu g\ g^{-1}$ can be achieved (Yang and Lam, 2001). Another study has compared four different methods for extraction of Hg species from tissue samples and sediments (Rosenkranz et al., 2000). Again, a microwave extraction was found to be the best method, but this time, an in-situ ethylation was also performed. Measurement was achieved using a

GC coupled with a low pressure ICP-MS. The low pressure ICP-MS instrument has the advantage of being capable of operating in both atomic and molecular modes, i.e., providing molecular information on the species (as in conventional GC-MS) but also elemental information (as in conventional ICP-MS analysis). Such instruments are not, however, available commercially.

Overall there is still some debate (Falciani et al., 2000; Chen and Ma, 2001; Ivanova et al., 2001) as to the best methodologies for soil analysis. It seems clear that the term soil encompasses such a wide range of material types that there is no single best way to carry out sample preparation for such samples prior to determinations by ICP-AES or ICP-MS.

V. CONCLUSIONS: THE WAY FORWARD

Environmental analysis using ICP-AES or ICP-MS has reached the stage where, for routine applications, reliable results can be obtained for a large number of determinants and analytes. With judicious optimization of the operating parameters, many potential interferences may be readily overcome, yielding accurate and precise results. If the determinants are present at trace levels, then the use of ICP-AES is likely to be sufficient. If, however, a determinant is at ultratrace levels (e.g., if a soil contains $< 0.1\,mg\,kg^{-1}$ of a determinant, resulting in $< 1\,\mu g\,L^{-1}$ in the digest), an ICP-MS determination is likely to be required. For a difficult analysis such as iron in seawater, where the determinant is likely to be at extremely low levels and the matrix is likely to cause severe interference effects, more specialist instrumentation such as high-resolution ICP-MS will be required. In all cases, either the sample will have to be diluted to decrease the amount of salt entering the instrumentation (but this may dilute the determinant beyond the limit of detection of the technique), or a matrix separation stage may be required. This can be achieved either on- or off-line, e.g., using a chelating resin to preconcentrate the iron, while simultaneously allowing the matrix to pass to waste. The iron may then be eluted from the column into the plasma using a small volume of acid. The trouble with this sort of procedure is that the determination may be blank limited, i.e., there may be sufficient iron in one or more of the chemicals used to create problems with the analysis. However in most cases, by combining chemical pretreatment techniques and the most modern instrumentation, the vast majority of environmental applications are possible. In general, both ICP techniques have both advantages and disadvantages, but these may be related to individual elements. For some analyses, an ICP-AES determination will be far superior to that of a simple quadrupole ICP-MS, e.g., for S, P, Ca, K,

and Na, because ICP-AES suffers fewer interferences for these elements. However, if very high sensitivity is required, an ICP-AES instrument is unlikely to be fit for the purpose unless a preconcentration stage prior to the determination is performed. In such a case, ICP-MS is likely to be the measurement technique of choice. For routine analyses, a large number of certified reference materials (CRMs) is available to facilitate the validation of methods. It is unfortunate that many of these CRMs have data only for a small number of determinants.

In the future, the development of more CRMs is inevitable. Although a large number exist already, they do not cover the entire spectrum of environmental sample types. In addition, many laboratories require data on bioavailable metal concentrations. For example, at present, there are very few CRMs that give any data for sequential extraction experiments. Similarly, the number of speciation studies continues to grow, focusing on ever more complex sample matrices. The realization that "total" elemental concentrations yield little information on the environmental chemistry means that speciation studies on a wide range of sample types for numerous elements will be performed. Current state-of-the-art ICP-AES and ICP-MS instruments are well placed to meet this challenge, particularly if the range of CRMs is increased to aid method development and validation.

In addition to optimizing performance, chemometrics may also be used to process the experimental data so that much more information is obtained. One example from the literature is the analysis of tea leaves, where by applying chemometric methods to the trace element data obtained from ICP-MS analysis, it is possible to elucidate the country of origin of the tea (Marcos et al., 1998). Chemometrics may also be used in diagnostic work, i.e., to determine which part of an analytical procedure is the most prone to error. Sources of loss, contamination, interference, and drift can all be identified, and then steps can be taken to overcome the error (Moreda-Pineiro et al., 2001a,b). As computers become ever more powerful, and more advanced and versatile chemometrics packages become available, this area is likely to expand rapidly.

Finally, although many applications have been discussed in the sections above, it is worth noting that every year further advances are reported in the literature. The Atomic Spectrometry Update covering Environmental Analysis is published annually in the February edition of the Journal of Analytical Spectrometry (Cave et al., 2001; Hill et al., 2002) and is a rich source of such information. Similarly, the ASU reviews covering ICP-AES and ICP-MS in the June and August editions of the same journal describe recent advances in instrumental development (Hill et al., 2000; Evans et al., 2001).

Marcel Dekker, Inc.
270 Madison Avenue, New York, New York 10016

REFERENCES

Abdallah, M.H., Diemiaszonek, R., Jarosz, J., Mermet, J.M., Robin, J. and Trassy, C. 1976. Characterization of end-on-end plasma source atomic emission spectrometry with a new interface. *Anal. Chim. Acta* 84:271–282.

Acon, B.W., McLean, J.A. and Montaser, A. 2001. A direct injection high efficiency nebuliser interface for microbore high performance liquid chromatography inductively coupled plasma mass spectrometry. *J. Anal. At. Spectrom.* 16:852–857.

Ahnstrom, Z.S. and Parker, D.R. 1999. Development and assessment of a sequential extraction procedure for the fractionation of soil cadmium. *Soil Sci. Soc. Am. J.* 63:1650–1658.

Ammons, J.T., Essington, M.E., Lewis, R.J., Gallagher, A.O. and Lessman, G.M. 1995. An application of a modified microwave total dissolution technique for soils. *Comm. Soil Sci. Plant Anal.* 26:831–842.

Ariza, J.L.G., Giraldez, I., Sanchez-Rodas, D. and Morales, E. 2000. Selectivity assessment of a sequential extraction procedure for metal mobility characterization using model phases. *Talanta* 52:545–554.

Ariza, J.L.G., Giraldez, I., Sanchez-Rodas, D. and Morales, E. 2000. Metal sequential extraction procedure optimized for heavily polluted and iron oxide rich sediments. *Anal. Chim. Acta* 414:151–164.

Baena, J.R., Gallego, M., Valcarcel, M., Leenaers, J. and Adams, F.C. 2001. Comparison of three coupled gas chromatographic detectors (MS, MIP-AES, ICP-TOF-MS) for organolead speciation analysis. *Anal. Chem.* 73:3927–3934.

Bajc, A.F. 1998. A comparative analysis of enzyme leach and mobile metal ion selective extractions: case studies from glaciated terrain, northern Ontario. *J. Explor. Geochem.* 61:113–148.

Bartha, A., Bertalan, E., Fodor, P. and Ikrenyi, K. 1989. AAS and ICP spectrochemical methods of microelement analysis of standard rock samples. *Fresenius' Z. Anal. Chem.* 334:644–665.

Basta, N. and Gradwohl, R. 2000. Estimation of Cd, Pb and Zn bioavailability in smelter contaminated soils by a sequential extraction procedure. *J. Soil Contam.* 9:149–164.

Berrow, M.L. and Stein, W.M. 1983. Extraction of metals from soils and sewage sludges by refluxing with aqua regia. *Analyst* 108:277–285.

Bettinelli, M., Beone, G.M., Spezia, S. and Baffi, C. 2000. Determination of heavy metals in soils and sediments by microwave assisted digestion and inductively coupled plasma optical emission spectrometry analysis. *Anal. Chim. Acta* 424:289–296.

Bilhorn, R.B., Sweedler, J.V., Epperson, P.M. and Denton, M.B. 1987. Charge transfer device detectors for analytical optical spectroscopy—operation and characteristics. *Appl. Spectrosc.* 41:1114–1125.

Blades, M.W. and Horlick, G. 1981. Interference from easily ionisable element matrices in inductively coupled plasma emission spectrometry—a spatial study. *Spectrochim. Acta* 36B:881–900.

Blades, M.W. 1987. In: *Inductively Coupled Plasma Emission Spectrometry* (Boumans, P.W.J.M., ed.). Wiley, New York, pp. 353–386.

Blanco, R.M., Villanueva, M.T., Uria, J.E.S. and Sanz-Medel, A. 2000. Field sampling, preconcentration and determination of mercury species in river waters. *Anal. Chim. Acta* 419:137–144.

Boix, A., Jordan, M.M., Querol, X. and Sanfeliu, T. 2001. Characterisation of total suspended particles around a power station in an urban coastal area in eastern Spain. *Environ. Geol.* 40:891–896.

Boss, C.B. and Fredeen, K.J. 1997. *Concepts, Instrumentation and Techniques in Inductively Coupled Plasma Optical Emission Spectrometry*. Perkin Elmer.

Boumans, P.W.J.M. and De Boer, F.J. 1979. Experiences with a new 50 MHz 2 kW free-running RF generator and a pneumatic nebuliser for inductively coupled plasma emission spectrometry. *ICP Info. Newsl.* 3:228–233.

Brenner, I.B., Vats, S. and Zander, A.T. 1999. A new CCD axially viewed ICP atomic emission spectrometer for simultaneous multi-element geoanalysis. Determination of major and minor elements in silicate rocks. *J. Anal. At. Spectrom.* 14:1231–1237.

Brenner, I.B. and Zander, A.T. 2000. Axially and radially viewed plasmas—a critical review. *Spectrochim. Acta* 55B:1195–1240.

Bridger, S. and Knowles, M. 2000. A complete method for environmental samples by simultaneous axially viewed ICP-AES following USEPA guidelines. *Varian Application Note ICP–29*.

Browner, R.F. In: Inductively Coupled Plasma Spectrometry and its Applications (Hill, S.J., ed.). Sheffield Academic Press, Sheffield, UK, pp. 98–118.

Brunori, C., Balzamo, S. and Morabito, R. 1999. Comparison between different leaching/extraction tests for the evaluation of metal release from fly ash. *Int. J. Environ. Anal. Chem.* 75:19–31.

Bunzl, K., Trautmannsheimer, M. and Schramel, P. 1999. Partitioning of heavy metals in soils contaminated by slag: a redistribution study. *J. Environ. Qual.* 28:1168–1173.

Burguera, M. and Burguera, J.L. 1997. Analytical methodology for speciation of arsenic in environmental and biological samples. *Talanta* 44:1581–1604.

Butler, O.T. and Howe, A.M. 1999. Development of an international standard for the determination of metals and metalloids in workplace air using ICP-AES: evaluation of sample dissolution procedures through an inter-laboratory trial. *J. Environ. Monit.* 1:23–32.

Cabon, J.Y. and Cabon, N. 2000. Determination of arsenic species in seawater by flow injection hydride generation in-situ collection followed by graphite furnace atomic absorption spectrometry—stability of As(III). *Anal. Chim. Acta* 418:19–31.

Capelle, B., Mermet, J.M. and Robin, J. 1982. Influence of the generator frequency on the spectral characteristics of an inductively coupled plasma. *Appl. Spectrosc.* 36:102–106.

Caroli, S., Forte, G., Iamiceli, A.L. and Lusi, A. 1996. Stability of mercury in dilute aqueous systems: an open issue. *Microchem. J.* 54:418–428.

Carrion, N., Fernandez, A., Eljuri, E.J., Murillo, M. and Franceschetto, M. 1991. Trace metal analysis in plant tissue by inductively coupled plasma atomic emission spectrometry with slurry sample introduction. *At. Spectrosc.* 12:162–168.

Caruso J.A., Sutton K.L. and Ackley K.L. 2000. Elemental speciation. New approaches for elemental analysis. In: *Comprehensive Analytical Chemistry*, vol. 33 (Barcelo, D., series ed.). Elsevier, Amsterdam.

Cave, M.R., Butler, O., Cook, J.M., Cresser, M.S., Garden, L.M., Holden, A.J. and Miles, D.L. 2000. Atomic spectrometry update—environmental analysis. *J. Anal. At. Spectrom.* 15:181–235.

Cave, M.R., Butler, O., Cook, J.M., Cresser, M.S. and Miles, D.L. 2001. Atomic spectrometry update—environmental analysis. *J. Anal. At. Spectrom.* 16:194–235.

Cave, M.R. and Harmon, K. 1997. Determination of trace metal distributions in the iron oxide phases of red bed sandstones by chemometric analysis of whole rock and selective leachate data. *Analyst* 122:501–512.

Cave, M.R. and Wragg, J. 1997. Measurement of trace element distributions in soils and sediments using sequential leach data and a nonspecific extraction system with chemometric data processing. *Analyst* 122:1211–1221.

Cave, M.R., Milodowski, A.E. and Friel, H. 2002. *Geochem. Explor. Environ. Anal.* In press.

Chen, M. and Ma, L.Q. 1998. Comparison of four US EPA digestion methods for trace metal analysis using certified and Florida soils. *J. Environ. Qual.* 27:1294–1300.

Chen, M. and Ma, L.Q. 2001. Comparison of three aqua regia digestion methods for twenty Florida soils. *Soil. Sci. Soc. Am. J.* 65:491–499.

Chin, C.-J., Wang, C.-F. and Jeng, S.-L. 1999. Multi-element analysis of airborne particulate matter collected on PTFE membrane filters by laser ablation inductively coupled plasma mass spectrometry. *J. Anal. At. Spectrom.* 14:663–668.

Clark, J.R. 1993. Enzyme induced leaching of B-horizon soils for mineral exploration in areas of glacial overburden. *Trans. Inst. Mining Metal.* 102:B19–B29.

Coedo, A.G., Dorado, T., Padilla, I., Maibusch, R. and Kuss, H.M. 2000. Slurry sampling electrothermal vaporization inductively coupled plasma mass spectrometry for steel making flue dust analysis. *Spectrochim. Acta* 55B:185–196.

Creed, J.T., Martin, T.D. and Sivaganesan, M. 1995. Preservation of trace metals in water samples. *J. Am. Waterworks Assoc.* 87:104–114.

Crosland, A.R., Zhao, F.J., McGrath, S.P. and Lane, P.W. 1995. Comparison of aqua regia digestion with sodium carbonate fusion for the determination of total phosphorus in soils by inductively coupled plasma—atomic emission spectrometry. *Commun. Soil Sci. Plant Anal.* 26:1357–1368.

Darke, S.A. and Tyson, J.F. 1994. Review of solid sample introduction for plasma spectrometry and a comparison of results for laser ablation, electrothermal vaporization and slurry nebulization. *Microchem. J.* 50:310–336.

Davidson, C.M. and Delevoye, G. 2001. Effect of ultrasonic agitation on the release of copper, iron manganese and zinc from soil and sediment using the BCR three stage sequential extraction. *J. Environ. Monit.* 3:398–403.

DeBruyn, A.M.H. and Rasmussen, J.B. 1999. Applicability of Tedlar bags to aqueous sampling for ambient toxicity testing: adsorption of trace metals. *Environ. Toxicol. Chem.* 18:1932–1933.

Dedina J. and Tsalev D. 1995. *Hydride Generation and Atomic Absorption Spectroscopy*. John Wiley, Chichester, UK.

Dubuisson, C., Poussel, E. and Mermet, J.M. 1997. Comparison of axially and radially viewed inductively coupled plasma atomic emission spectrometry in terms of signal to background ratio and matrix effects—plenary lecture. *J. Anal. At. Spectrom.* 12:281–286.

Ebdon, L., Evans, E.H., Fisher, A. and Hill, S.J. 1998. *An Introduction to Analytical Atomic Spectrometry*. John Wiley, Chichester, UK.

Ebdon, L. and Fisher A. 2000. Organometallic compound analysis in environmental samples. In: *Encyclopedia of Analytical Chemistry* (R.A. Meyers, ed.). Wiley, Chichester, UK, pp. 3064–3084.

Ebdon, L., Fisher, A.S., Worsfold, P.J., Crews, H. and Baxter, M. 1993. On-line removal of interferences in the analysis of biological materials by flow injection inductively coupled plasma mass spectrometry. *J. Anal. At. Spectrom.* 8:691–695.

Ellis, L.A. and Roberts, D.J. 1997. Chromatographic and hyphenated methods for elemental speciation analysis in environmental media. *J. Chromatogr.* A 774:3–19.

Evans, E.H., Dawson, S.B., Fisher, A., Hill, S.J., Price, W.J., Smith, M.M., Sutton, K.L. and Tyson, J.F. 2001. Atomic spectrometry update: advances in atomic emission, absorption and fluorescence spectrometry and related techniques. *J. Anal. At. Spectrom.* 16:672–711.

Evans, E.H. and Ebdon, L. 1991. Comparison of normal and low-flow torches for inductively coupled plasma mass spectrometry using optimized operating conditions. *J. Anal. At. Spectrom.* 6:421–430.

Falciani, R., Novaro, E., Marchesini, M. and Gucciardi, M. 2000. Multi-element analysis of soil and sediment by ICP-MS after a microwave assisted digestion method. *J. Anal. At. Spectrom.* 15:561–565.

Fatemian, E., Allibone, J. and Walker, P.J. 1999. Use of gold as a routine and long term preservative for mercury in potable water, as determined by ICP-MS. *Analyst* 124:1233–1236.

Feldmann, J. 1999. Determination of $Ni(CO)_4$, $Fe(CO)_5$, $Mo(CO)_6$ and $W(CO)_6$ in sewage gas by using cryogenic trapping gas chromatography inductively coupled plasma mass spectrometry. *J. Environ. Monit.* 1:33–37.

Ferrarello, C.N., Bayon, M.M., Garcia-Alonso, J.I. and Sanz-Medel, A. 2001. Comparison of metal pre-concentration on immobilised Kelex-100 and quadrupole inductively coupled plasma mass spectrometric detection with direct double focusing inductively coupled plasma mass spectrometric measurements for ultra-trace multi-element determinations in seawater. *Anal. Chim. Acta* 429:227–235.

Fisher, A. and Hill, S.J. 1999. In: *Inductively Coupled Plasma Spectrometry and Its Applications* (Hill, S.J., ed.). Sheffield Academic Press, Sheffield, UK.

Gettar, R.T., Garavaglia, R.N., Gautier, E.A. and Batistoni, D.A. 2000. Determination of inorganic and organic anionic arsenic species in water by ion chromatography coupled to hydride generation inductively coupled plasma atomic emission spectrometry. *J. Chromatogr. A* 884:211–221.

Ghio, A.J., Stonehuerner, J., Pritchard, R.J., Piantadosi, C.A., Quigley, D.R., Dreher, K.L. and Costa, D.L. 1996. Humic like substances in air pollution particulates correlate with concentrations of transition metals oxidant generation. *Inhalation Technol.* 8:479–494.

Gleyzes, C., Tellier, S., Sabrier, R. and Astruc, M. 2001. Arsenic characterization in industrial soils by chemical extractions. *Environ. Technol.* 22:27–38.

Gomes, A.M., Sarrette, J.P., Madon, L. and Almi, A. 1996. Continuous emission monitoring of metal aerosol concentrations in atmospheric air. *Spectrochim. Acta* 51B:1695–1705.

Gomez-Ariza, J.L., Giraldez, I., Sanchez-Rodas, D. and Morales, E. 1999. Metal readsorption and redistribution during the analytical fractionation of trace elements in oxic estuarine sediments. *Anal. Chim. Acta* 399:295–307.

Gomez-Ariza, J.L., Giraldez, I., Sanchez-Rodas, D. and Morales, E. 2000. Comparison of the feasibility of three extraction procedures for trace metal partitioning in sediments from South West Spain. *Sci. Tot. Environ.* 246:271–283.

Goodall, P., Foulkes, M.E. and Ebdon, L. 1993. Slurry nebulisation inductively coupled plasma spectrometry—the fundamental parameters discussed. *Spectrochim. Acta* 48B:1563–1577.

Gray, D.J., Lintern, M.J. and Longman, G.D. 1998. Re-adsorption of gold during selective extraction—observations and potential solutions. *J. Geochem. Explor.* 61:21–37.

Gray, D.J., Wildman, J.E. and Longman, G.D. 1999. Selective and partial extraction of analyses of transported overburden for gold exploration in the Yilgam Craton, Western Australia. *J. Geochem. Explor.* 67:51–66.

Greenfield, S., Jones, I.L. and Berry, C.T. 1964. High pressure plasmas as spectroscopic sources. *Analyst* 89:713–720.

Greenfield, S., McGeachin, H. and Smith, P.B. 1975. Plasma emission sources in analytical spectroscopy—Part 1. *Talanta* 22:1–15.

Greenfield, S., McGeachin, H. and Smith, P.B. 1975. Plasma emission sources in analytical spectroscopy—Part 2. *Talanta* 22:553–561.

Guerin, T., Astruc, A. and Astruc, M. 1999. Speciation of arsenic and selenium compounds by HPLC hyphenated to specific detectors: a review of the main separation techniques. *Talanta* 50:1–24.

Gunther, D., Audetat, A., Frischknecht, R. and Heinrich, C.A. 1998. Quantitative analysis of major, minor and trace elements in fluid inclusions using laser ablation inductively coupled plasma mass spectrometry. *J. Anal. At. Spectrom.* 13:263–270.

Gunther, D., Jackson, S.E. and Longerich, H.P. 1999. Laser ablation and arc/spark solid sample introduction into inductively coupled plasma mass spectrometry. *Spectrochim. Acta* 54B:381–409.
Haas, K., Feldmann, J., Wennrich, R. and Stark, H.J. 2001. Species specific isotope ratio measurements of volatile tin and antimony compounds using capillary GC-ICP-time of flight-MS. *Fresenius' J. Anal. Chem.* 370:587–596.
Hall, G.E.M. 1998. Analytical perspective on trace element species of interest in exploration. *J. Geochem. Explor.* 61:1–19.
Hill, S.J., Arowolo, T.A., Butler, O.T., Chenery, S.R.N., Cook, J.M., Cresser, M.S. and Miles, D.L. 2002. Atomic spectrometry update—environmental analysis. *J. Anal. At. Spectrom.* 17:284–317.
Hill, S.J., Bloxham, M.J. and Worsfold, P.J. 1993. Chromatography coupled with inductively coupled plasma atomic emission spectrometry and inductively coupled plasma mass spectrometry—a review. *J. Anal. At. Spectrom.* 8:499–515.
Hill, S.J., Chenery, S., Dawson, J.B., Evans, J.B., Fisher, A., Price, W.J., Smith, C.M.M., Sutton, K.L. and Tyson, J.F. 2000. Advances in atomic emission, absorption and fluorescence spectrometry and related techniques. *J. Anal. At. Spectrom.* 15:763–805.
Hirata, S., Ishida, Y., Aihara, M., Honda, K. and Shikino, O. 2001. Determination of trace metals in seawater by on-line column preconcentration inductively coupled plasma mass spectrometry. *Anal. Chim. Acta* 438:205–214.
Ho, M.D. and Evans, G.J. 2000. Sequential extraction of metal contaminated soils with radiochemical assessment of readsorption effects. *Environ. Sci. Technol.* 34:1030–1035.
Ivanova, J., Djingova, R., Korhammer, S. and Markert, B. 2001. On the microwave digestion of soils and sediments for the determination of lanthanides and some toxic and essential elements by inductively coupled plasma source mass spectrometry. *Talanta* 54:567–574.
Kanicky, V. and Mermet, J.M. 1999. Use of a single calibration graph for the determination of major elements in geological materials by laser ablation inductively coupled plasma atomic emission spectrometry with added internal standards. *Fresenius' J. Anal. Chem.* 363:294–299.
Krause, P., Erbsloh, B., Niedergesass, R. and Pepelnik, R. 1995. Comparative study of different digestion procedures using supplementary analytical methods for multi-element screening of more than 50 elements of the River Elbe. *Fresenius' J. Anal. Chem.* 353:3–11.
Krishnamurti, G.S.R. and Naidu, R. 2000. Speciation and phyto-availability of cadmium in selected surface soils of south Australia. *Aust. J. Soil. Res.* 38:991–1004.
Kucera, J., Smodis, B., Burns, K., De Regge, P., Campbell, M., Havranek, V., Makarewicz, M., Toervenyi, A. and Zeiller, E. 2001. Preparation and characterisation of a set of IAEA reference air filters for quality control in air pollution studies. *Fresenius' J. Anal. Chem.* 370:229–233.
Lamble, K.J. and Hill, S.J. 1998. Microwave digestion procedures for environmental matrices. *Analyst* 123:103R–133R.

Levine, K.E., Batchelor, J.D., Rhoades, C.B. and Jones, B.T. 1999. Evaluation of a high pressure, high temperature microwave digestion system. *J. Anal. At. Spectrom.* 14:49–59.

Li, X.D., Coles, B.J., Ramsey, M.H. and Thornton, I. 1995. Chemical partitioning of the new National Institute of Standards and Technology standard reference materials (SRM 2709–2711) by sequential extraction using inductively coupled plasma atomic emission spectrometry. *Analyst* 120:1415–1419.

Li, Y.C., Jiang, S.J. and Chen, S.F. 1998. Determination Ge, As, Se, Cd and Pb in plant materials by slurry sampling electrothermal vaporization inductively coupled plasma mass spectrometry. *Anal. Chim. Acta* 372:365–372.

Liang, P., Qin, Y.C., Hu, B., Peng, T.Y. and Jiang, Z.C. 2001. Nanometer size titanium dioxide microcolumn on-line preconcentration of trace metals and their determination by inductively coupled plasma atomic emission spectrometry in water. *Anal. Chim. Acta* 440:207–213.

Lindemann, T., Prange, A., Dannecker, W. and Neidhart, B. 2000. Stability studies of arsenic, selenium antimony and tellurium species in water, urine, fish and soil extracts using HPLC-ICP-MS. *Fresenius' J. Anal. Chem.* 368:214–220.

Lo, I.M.C. and Yang, X.Y. 1998. Removal and redistribution of metals from contaminated soils by a sequential extraction method. *Waste Manage.* 18:1–7.

Lopez-Sanchez, J.F., Sahuquillo, A., Fiedler, H.D., Rubio, R., Rauret, G., Muntau, H. and Quevauviller, P. 1998. CRM 601, a stable material for its extractable content of heavy metals. *Analyst* 123:1675–1677.

Lu, H.H. and Jiang, S.J. 2001. Organic acids as the modifier to determine Zn, Cd, Tl and Pb in soil by slurry sampling electrothermal vaporization inductively coupled plasma mass spectrometry. *Anal. Chim. Acta* 429:247–255.

Mahoney, P.P., Li, G.Q. and Hieftje, G.M. 1996. Laser ablation inductively coupled plasma mass spectrometry with a time of flight mass analyser. *J. Anal. At. Spectrom.* 11:401–405.

Mahoney, P.P., Ray, S.J., Li, G.Q. and Hieftje, G.M. 1999. Preliminary investigation of electrothermal vaporization sample introduction for inductively coupled plasma time of flight mass spectrometry. *Anal. Chem.* 71:1378–1383.

Mann, A.W., Birrell, R.D., Mann, A.T., Humphreys, D.B. and Perdrix, J.L. 1998. Application of the mobile metal ion technique to routine geochemical exploration. *J. Geochem. Explor.* 61:87–102.

Marcos, A., Fisher, A., Rea, G. and Hill, S.J. 1998. Preliminary study using trace element concentrations and a chemometrics approach to determine the geographical origin of tea. *J. Anal. At. Spectrom.* 13:521–525.

Marr, I.L., Kluge, P., Main, L., Margerin, V. and Lescop, C. 1995. Digests or extracts—some interesting but conflicting results for 3 widely differing polluted sediment samples. *Mikrochim. Acta* 119:219–232.

Mermet, J.M. 1989. Ionic to atomic line intensity ratio and residence time in inductively coupled plasma atomic emission spectrometry. *Spectrochim. Acta*, 44B: 1109–1116.

Mermet, J.M. 1991. Use of magnesium as a test element for inductively coupled plasma atomic emission spectrometry diagnostics. *Anal. Chim. Acta* 250:85–94.

Mermet, J.M. 1998. Revisitation of the matrix effects in inductively coupled plasma atomic emission spectrometry, the key role of the spray chamber—invited lecture. *J. Anal. At. Spectrom.* 13:419–422.

Montaser, A., Minnich, M.G., Liu, H., Gustavsson, A.G.T. and Browner, R.F. 1998. Fundamental aspects of sample introduction in ICP spectrometry. In: *Inductively Coupled Plasma Mass Spectrometry* (Montaser, A., ed.). Wiley-VCH, New York, pp. 335–420.

Moreda-Pineiro, A., Marcos, A., Fisher, A. and Hill, S.J. 2001. Chemometrics approaches for the study of systematic error in inductively coupled plasma emission spectrometry and mass spectrometry. *J. Anal. At. Spectrom.* 16:350–359.

Moreda-Pineiro, A., Marcos, A., Fisher, A. and Hill, S.J. 2001. Parallel factor analysis for the study of systematic error in inductively coupled plasma emission spectrometry and mass spectrometry. *J. Anal. At. Spectrom.* 16:360–369.

Mota, J.P.V., de la Campa, M.R.F., Garcia-Alonso, J.I. and Sanz-Medel, A. 1999. Determination of cadmium in biological and environmental materials by isotope dilution inductively coupled plasma mass spectrometry: effect of flow sample introduction methods. *J. Anal. At. Spectrom.* 14:113–120.

Nadkarni, R.A. 1984. Applications of microwave oven sample dissolution in analysis. *Anal. Chem.* 56:2233–2237.

Nakahara, T. and Wasa, T. 1994. Hydride generation inductively coupled plasma atomic emission spectrometry for the determination of germanium in iron meteorites. *Microchem. J.* 49:202–212.

Nash, M.J., Maskall, J.E. and Hill, S.J. 2000. Methodologies for determination of antimony in terrestrial environmental samples. *J. Environ. Monitor.* 2:97–109.

Nickson, R.A., Hill, S.J. and Worsfold, P.J. 1999. Field preconcentration of trace metals from seawater and brines coupled with laboratory analysis using flow injection and ICP-AES detection. *Int. J. Environ. Anal. Chem.* 75:57–69.

Nieuwenhuize, J., Poleyvos, C.H., Vandenakker, A.H. and Vandelft, W. 1991. Comparison of microwave and conventional extraction techniques for the determination of metals in soil, sediment and sludge samples by atomic spectrometry. *Analyst* 116:347–351.

Niskavaara, H., Reimann, C., Chekushin, V. and Kashulina, G. 1997. Seasonal variability of total and easily leachable element contents in topsoils (0–5 cm) from eight catchments in the European Arctic (Finland, Norway and Russia). *Environ. Poll.* 96:261–274.

O'Connor, G. and Evans, E.H. 1999. Fundamental aspects of ICP-MS. In: Inductively Coupled Plasma Spectrometry and its Applications (Hill, S.J., ed.). Sheffield Academic Press, Sheffield, UK, pp. 119–144.

Okamoto, Y., Kikkawa, R., Kobayashi, Y. and Fujiwara, T. 2001. External furnace fusion digestion for the direct determination of lead in rock samples by inductively coupled plasma mass spectrometry (IPC-MS) using the tungsten boat furnace sample cuvette technique. *J. Anal. At. Spectrom.* 16:96–98.

Pandey, P.K., Patel, K.S. and Subrt, P. 1998. Trace elemental composition of atmospheric particulate at Bhilai in central–east India. *Sci. Total Environ.* 215:123–134.

Paudyn, A.M. and Smith, R.G. 1992. Microwave decomposition of dusts, ashes and sediments for the determination of elements by ICP-AES. *Can. J. App. Spec.* 37:94–99.

Pavlovska, G., Cundeva, K. and Stafilov, T. 2000. Flotation preconcentration of cobalt and nickel by lead (II) hexamethylenedithiocarbamate. *Sep. Sci. Technol.* 35:2663–2677.

Pecheyran, C., Quetel, C.R., Lecuyer, F.M.M. and Donard, O.F.X. 1998. Simultaneous determination of volatile metal (Pb, Ni, Sn, In, Ga) and non-metal species (Se, P, As) in different atmospheres by cryo-focusing and detection by ICP-MS. *Anal. Chem.* 70:2639–2645.

Peng, T.Y., Sheng, X.H., Hu, B. and Jiang, Z.C. 2000. Direct analysis of silicon carbide by fluorination assisted electrothermal vaporization inductively coupled plasma atomic emission spectrometry using a slurry sampling technique. *Analyst* 125:2089–2093.

Persaud, A.T., Beauchemin, D., Jamieson, N.E. and McLean, R.J.C. 1999. Partial leaching as an aid to slurry nebulisation for the analysis of soils by ICP-MS with flow injection and mixed gas plasmas. *Can. J. Chem.* 77:409–415.

Pilon, M.J., Denton, M.B., Schleicher, R.G., Moran, P.M. and Smith, S.B. 1990. Evaluation of a new array detector atomic emission spectrometer for inductively coupled plasma atomic emission spectrometry. *Appl. Spectrosc.* 44:1613–1620.

Pitts, L., Fisher, A., Worsfold, P. and Hill, S.J. 1995. Selenium speciation using high performance liquid chromatography–hydride generation atomic fluorescence with on-line microwave reduction. *J. Anal. At. Spectrom.* 10:519–520.

Poitrasson, F. and Dundas, S.H. 1999. Direct isotope ratio measurement of ultra-trace lead in waters by double focussing inductively coupled plasma mass spectrometry with an ultrasonic nebuliser and a desolvation unit. *J. Anal. At. Spectrom.* 14:1573–1577.

Quevauviller, P., Imbert, J.L. and Olle, M. 1993. Evaluation of the use of microwave oven systems for the digestion of environmental samples. *Mikrochim. Acta* 112:147–154.

Quevauviller, P., Rauret, G., Lopez-Sanchez, J.F., Rubio, R., Ure, A. and Muntau, H. 1997. Certification of trace metal extractable contents in a sediment reference material (CRM 601) following a three step sequential extraction procedure. *Sci. Tot. Environ.* 205:223–234.

Raksasataya, M., Langdon, A.G. and Kim, N.D. 1996. Assessment of the extent of lead redistribution during sequential extraction by two different methods. *Anal. Chim. Acta* 332:1–14.

Ramesh, A., Mohan, K.R., Seshaiah, K. and Jegakumar, N.D. 2001. Determination of trace elements by inductively coupled plasma atomic emission spectrometry (ICP-AES) after preconcentration on a support impregnated with piperidine dithiocarbamate. *Anal. Lett.* 34:219–229.

Rantala, R.T.T. and Loring, D.H. 1989. Teflon bomb decomposition of silicate materials in a microwave oven. *Anal. Chim. Acta* 220:263–267.

Rauch, S., Lu, M. and Morrison, G.M. 2001. Heterogeneity of platinum group metals in airborne particles. *Environ. Sci. Technol.* 35:595–599.
Rauret, G., Lopez-Sanchez, J.F., Sahuquillo, A., Rubio, R., Davidson, C., Ure, A. and Quevauviller, P. 1999. Improvement of the BCR three step sequential extraction procedure prior to the certification of new sediment and soil reference materials. *J. Environ. Monit.* 1:57–61.
Reimann, C., Siewers, U., Skarphagen, H. and Banks, D. 1999. Influence of filtration on concentrations of 62 elements analysed on crystalline bedrock groundwater samples by ICP-MS. *Sci. Total Environ.* 234:155–173.
Reimann, C., Siewers, U., Skarphagen, H. and Banks, D. 1999. Does bottle type and acid washing influence trace elemental analysis by ICP-MS on water samples? A test covering 62 elements and four bottle types: high density polyethene (HDPE), polypropylene (PP), fluorinated ethene propene copolymer (FEP) and perfluoroalkoxy polymer (PFA). *Sci. Total Environ.* 239:111–130.
Rhoades, C.B. and White, R.T. 1997. Mainstream smoke collection by electrostatic precipitation for acid dissolution in a microwave digestion system prior to trace metal determination. *J. Assoc. Off. Anal. Chem. Int.* 80:1320–1331.
Reed, T.B. 1961. The induction coupled plasma torch. *J. Appl. Phys.* 32:821–824.
Robinson, P., Townsend, A.T., Yu, Z.S. and Munker, C. 1999. Determination of scandium, yttrium and rare earth elements in rocks by high resolution inductively coupled plasma mass spectrometry. *Geostand. Newsl.* 23:31–46.
Rosenkranz, B., O'Connor, G. and Evans, E.H. 2000. Low pressure inductively coupled plasma ion source for atomic and molecular spectrometry: investigation of alternative reagent gases for organomercury speciation in tissue and sediment. *J. Anal. At. Spectrom.* 15:7–12.
Rubio, R., Alberti, J., Padro, A. and Rauret, G. 1995. On-line photolytic decomposition for the determination of organoarsenic compounds. *Trends Anal. Chem.* 14:274–279.
Ryss, L.G. 1956. US Atomic Energy Commission Translation Service Report No. AEC-tsn 3927.
Sahuquillo, A., Lopez-Sanchez, J.F., Rubio, R., Rauret, G., Thomas, R.P., Davidson, C.M. and Ure, A.M. 1999. Use of a certified reference material for extractable trace metals to assess sources of uncertainty in the BCR three stage sequential extraction procedure. *Anal. Chim. Acta* 382:317–327.
Sahuquillo, A., Pinna, D., Rauret, G. and Muntau, H. 2000. Modified three step sequential extraction scheme applied to metal determination in sediments from Lake Flumendosa (Sardinia, Italy). *Fresenius' Environ. Bull.* 9:360–372.
Santamaria-Fernandez, R., Moreda-Pineiro, A. and Hill, S.J. 2002. Optimisation of a multielement sequential extraction method employing an experimental design approach for metal partitioning in soils and sediments. *J. Environ. Monitor.* 4:330–336.
Sawhney, B.L. and Stilwell, D.E. 1994. Dissolution and Elemental Analysis of Minerals, Soils, and Environmental Samples. In: *Quantitative Methods in Soil*

Mineralogy (Amonette, J.E. and Zelazny, L.W., eds.). Soil Sci. Soc. Am., Madison, pp. 49–82.

Scott, R.H., Fassel, V.A., Kniseley, R.N. and Nixon, D.E. 1974. Inductively coupled plasma optical emission analytical spectrometry—a compact facility for trace analysis of solutions. *Anal. Chem.* 46:75–80.

Seltzer, M.D. 1998. Continuous air monitoring using inductively coupled plasma atomic emission spectrometry. Correction of spectral interferences arising from CN emission. *Appl. Spectrosc.* 52:195–199.

Sharp, B.L. 1988. Pneumatic nebulisers and spray chambers for inductively coupled plasma spectrometry—a review. 1. Nebulisers. *J. Anal. At. Spectrom.* 3:613–652.

Sharp, B.L. 1988. Pneumatic nebulisers and spray chambers for inductively coupled plasma spectrometry—a review. 2. Spray chambers. *J. Anal. At. Spectrom.* 3:939–963.

Shiowatana, J., Tantidanai, N., Nookabkaew, S. and Nacapricha, D. 2001. A novel continuous flow sequential extraction procedure for metal speciation in solids. *J. Environ. Qual.* 30:1195–1205.

Smichowski, P., Madrid, Y. and Camara, C. 1998. Analytical methods for antimony speciation in waters at trace and ultra-trace levels. A review. *Fresenius' J. Anal. Chem.* 360:623–629.

Smith, F.E. and Arsenault, E.A. 1996. Microwave assisted sample preparation in analytical chemistry. *Talanta* 43:1207–1268.

Smith, L.L., Crain, J.S., Yaeger, J.S., Horwitz, E.P., Diamond, H. and Chiarizia, R. 1995. Improved separation method for determining actinides in soil samples. *J. Radioanal. Nucl. Chem. Art.* 194:151–156.

Sturgeon, R.E. and Lam, J.W. 1999. The ETV as a thermochemical reactor for ICP-MS sample introduction. *J. Anal. At. Spectrom.* 14:785–791.

Sun, Y.C., Chi, P.H. and Shiue, M.Y. 2001. Comparison of different digestion methods for total decomposition of siliceous and organic environmental samples. *Anal. Sci.* 17:1395–1399.

Telgheder, U. and Khvostikov, V.A. 1997. Collection and determination of metal contaminants in gases—a review. *J. Anal. At. Spectrom.* 12:1–6.

Tessier, A., Campbell, P.G.C. and Bisson, M. 1979. Sequential extraction procedure for the speciation of particulate trace metals. *Anal. Chem.* 51:844–851.

Thompson M. and Banerjee, E.K. 1991. Atomic absorption methods in applied geochemistry. In: *Atomic Absorption Spectrometry, Theory, Design and Applications* (Haswell, S.J., ed.), Elsevier, Amsterdam, pp. 289–320.

Thompson, M. and Walsh, N. 1989. *Handbook of Inductively Coupled Plasma Atomic Emission Spectrometry*, 2d ed. Blackie, London.

Todd, J.F.J. and Lawson, G. 1975. In: *International Review of Science* (*Mass Spectrometry*). Physical Chemistry, Series 2, vol. 5 (Buckingham, A.D. and Maccol, A., eds.). Butterworth, London.

Trends in Analytical Chemistry. 2000. Special Edition on: Validation for Speciation Analysis. February/March.

Turner, A. and Olsen, Y.S. 2000. Chemical versus enzymatic digestion of contaminated estuarine sediment: relative importance of iron and manganese oxides in controlling trace metal bioavailability. *Est. Coast Shelf Sci.* 51:717–728.

Ugo, P., Zampieri, S., Moretto, L.M. and Paolucci, D. 2001. Determination of mercury in process and lagoon waters by inductively coupled plasma mass spectrometric analysis after electrochemical preconcentration: comparison with anodic stripping at gold and polymer coated electrodes. *Anal. Chim. Acta* 434:291–300.

Van Holderbeke, M., Zhao, Y.N., Vanhaecke, F., Dams, R. and Sandra, P. 1999. Speciation of six arsenic compounds using capillary electrophoresis inductively coupled plasma mass spectrometry. *J. Anal. At. Spectrom.* 14:229–234.

Vassileva, E. and Furuta, N. 2001. Application of high surface area ZrO_2 in preconcentration and determination of 18 elements by on-line flow injection with inductively coupled plasma atomic emission spectrometry. *Fresenius' J. Anal. Chem.* 370:52–59.

Vercoutere, K., Fortunati, V., Muntau, H., Griepink, B. and Maier, E.A. 1995. The certified reference materials CRM 142-R light sandy soil, CRM 143-R sewage sludge amended soil and CRM 145-R sewage sludge for quality control in monitoring environmental and soil pollution. *Fresenius' J. Anal. Chem.* 352:197–202.

Wang, C.F., Chin, C.J. and Chiang P.-C. 1998. Multi-element analysis of suspended particulates collected with a beta-gauge monitoring system by ICP-atomic emission spectrometry and mass spectrometry. *Anal. Sci.* 14:763–768.

Warnken, K.W., Tang, D.G., Gill, G.A. and Santschi, P.H. 2000. Performance optimisation of a commercially available iminodiacetate resin for the determination of Mn, Ni, Cu, Cd and Pb by on-line preconcentration inductively coupled plasma mass spectrometry. *Anal. Chim. Acta* 423:265–276.

Wendt, R.H. and Fassel, V.A. 1965. Induction coupled plasma spectrometric excitation source. *Anal. Chem.* 37:920–922.

Wu, S., Zhao, Y.H., Feng, X.B. and Wittmeier, A. 1996. Application of inductively coupled plasma mass spectrometry for total metal determination in silicon containing solid samples using the microwave assisted nitric acid hydrofluoric acid hydrogen peroxide boric acid digestion system. *J. Anal. At. Spectrom.* 11:287–296.

Wuilloud, R.G., Wuilloud, J.C., Olsina, R.A. and Martinez, L.D. 2001. Speciation and preconcentration of vanadium (V) and vanadium (IV) in water samples by flow injection inductively coupled plasma optical emission spectrometry and ultrasonic nebulization. *Analyst* 126:715–719.

Yabutani, T., Chiba, K. and Haraguchi, H. 2001. Multi-element determination of trace elements in seawater by inductively coupled plasma mass spectrometry after tandem preconcentration with cooperation of chelating resin adsorption and lanthanum coprecipitation. *Bull. Chem. Soc. Jpn.* 74:31–38.

Yang, L. and Lam., J.W.H. 2001. Microwave assisted extraction of butyltin compounds from PACS-2 sediment for quantitation by high performance

liquid chromatography inductively coupled plasma mass spectrometry. *J. Anal. At. Spectrom.* 16:724–731.

Yeager, J.R., Clark, J.R., Mitchell, W. and Renshaw, R. 1998. Enzyme leach anomalies associated with deep Mississippi Valley type zinc ore bodies at Elmwood Mine, Tennessee. *J. Geochem. Explor.* 61:103–112.

Zhang, X.H. and Koropchak, J.A. 1999. Thermospray methods for rapid, sensitive and nonchromatographic speciation of chromium oxidation states. *Anal. Chem.* 71:3046–3053.

Zheng, J., Iijima, A. and Furuta, N. 2001. Complexation effect of antimony compounds with citric acid and its application to the speciation of antimony (III) and antimony (V) using HPLC-ICP-MS. *J. Anal. At. Spectrom.* 16:812–818.

Zoorob, G.K., McKiernan, J.W. and Caruso, J.A. 1998. ICP-MS for elemental speciation studies. *Mikrochim. Acta* 128:145–168.

3

Electroanalytical Methods in Environmental Chemical Analysis

Iain L. Marr
The University of Aberdeen, Aberdeen, Scotland

I. BACKGROUND

Of the many electrical parameters that can be measured, only three need be considered here as of practical importance—potential, current, and conductivity—thus opening the way to three techniques that really have something to offer in the area of environmental analysis, where samples are always complex and determinants of interest usually are present at very low concentrations. Electrical charge, measured in the technique known as coulometry, does indeed have important analytical applications (especially in the Karl Fischer determination of water), but not often in the field of environmental analysis, and therefore will not be discussed further.

The *potential* of an electrode may be related to the concentration of a particular species if a number of conditions are met—the "clever" chemistry of electrode membrane manufacture makes it possible to construct probes with useful sensitivity and selectivity to individual species in solution. While the tendency for a chemical reaction to proceed is measured, no current is actually allowed to flow. *Potentiometry* using ion selective electrodes is the technique in question, and using the glass electrode for the measurement of pH is one special (and the best known) example.

A great deal more information can be obtained by electroanalytical methods if one parameter is varied and a second measured—so-called two-dimensional measurement. In this case a signal pattern rather than one measured value is used to identify, as well as quantify, one or more species in a solution. The *current* can be monitored as the potential across a cell is

Marcel Dekker, Inc.
270 Madison Avenue, New York, New York 10016

scanned: the approach is termed *amperometry*. When the current is controlled by diffusive processes in solution, the technique is termed *polarography*, and while few people will have any time for a dropping mercury electrode these days, the modern variants of anodic and cathodic *stripping voltammetry* have much to offer for the direct determination of very low concentrations of metal ions in natural waters, even in seawater.

Since the electrical *conductivity* of an aqueous solution depends on the concentration of ions dissolved in it, this parameter serves as a useful indicator of salinity, adequate for rough measurements in the field and for more precise determinations if care is taken with calibration and temperature compensation. While a current is allowed to flow in this technique, the potential is very small and is reversed at millisecond intervals so that there is no net chemical reaction on the electrode surface.

Finally, we should consider the factors that continue to make electroanalytical techniques attractive for routine measurements. They are generally simple, their limitations are well understood, and, above all, they provide an electrical signal that is very easy to transmit via telemetering systems, to store electronically, and to process in a computer. Thus they make possible a number of useful determinations at low concentrations in real samples.

II. POTENTIOMETRY

The Nernst law relates the potential of an electrochemical cell (E, in mV) to the activities (a_i, a_j) of a given species in the two halves of the cell, illustrated in Fig. 1.

$$E = \frac{R \cdot T}{n \cdot F} \ln \frac{a_1}{a_2} \tag{1}$$

This equation can be converted to use logarithms to the base 10, in which case the constant term is multiplied by 2.3 to become $0.059/n$ volts at room temperature, where n is the number of electrons involved in the electrochemical oxidation/reduction of the species. In dilute solutions, activities can be taken as equal to concentrations, so the equation takes on a simple practical significance. Instruments such as pH meters that have a temperature compensation circuit simply change the slope factor RT/nF and do not take into account any changes in potential due to the chemistry, such as changes in solubilities.

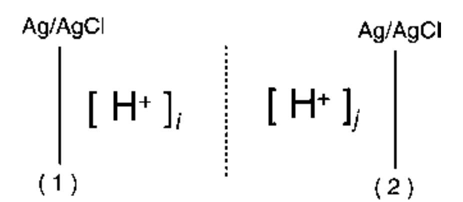


Figure 1 Schematic diagram of a Nernstian concentration cell with membrane.

Figure 1 indicates that we require a means of connecting our potential-measuring device, such as a digital voltmeter, to the two solutions. The two electrodes, shown as silver wires in Fig. 1, serve this purpose, and when coated with silver chloride and kept in a potassium chloride solution of constant concentration, they maintain constant potentials. Any difference in the two potentials is then taken up as a small constant included in Eq. (1).

There are a number of practical points which arise from this simple idea:

The membrane separating the two halves of the cell should be ideal and respond only to the ion of interest (here the hydrated proton, H^+_{aq}). The success of modern ion-selective electrodes derives from the ingenuity of chemists in developing a range of membrane systems that come close to meeting this requirement (Vesely et al., 1978).

No current should flow through this cell, as this would entail flow of the ions through the membrane. The digital voltmeter must therefore have a high input impedance, taking no more than a few pA of current from the cell.

Sufficient ions should be available in the two solutions to enable the membrane to respond to them. Measurements in very dilute waters are, for this reason, rather difficult and will certainly entail a longer equilibration time, say 1–2 minutes, till a stable potential is obtained.

Two electrodes are always required for potentiometry, even when it appears, at first sight, that the measurement can be made with only one, as is the case with combination pH electrodes (see below). The internal reference electrode is usually not accessible to the user, but the external one must be maintained by topping up with the electrolyte from time to time. A saturated calomel electrode (see below) is frequently used as a separate external reference electrode, and if the presence of traces of chloride is undesirable, then the sulfate version can be used instead.

A. The Glass Electrode—Measurement of pH

Much research has gone into the development of special glasses for the glass electrode, but the key to modern electrodes lies in the substitution of lithium in the glass for sodium, to avoid the electrode responding better to the sodium ions at high pH than to the very dilute hydrogen ions. Few users these days ever think of the ‘‘alkali error’’ associated with electrodes fabricated from Macinnes and Dole’s soda glass in 1930, and we can expect a working range from pH 1 to pH 13, with deviations becoming significant only outside this range, using the lithia–lime glass developed by Cary and Baxter in 1949. Everything you could possibly need to know about the glass electrode has been summarized excellently by Galster (1991).

A modern combination pH electrode is shown in Fig. 2, and a schematic diagram of the glass membrane in Fig. 3. The body may be glass or glass sheathed in plastic for greater robustness. The bulb is sometimes surrounded by a plastic protecting shield to minimize the chances of breaking it by rough contact against sample containers. However, this impairs the accessibility of the electrode surface to the ions in the solution and calls for either good stirring of the solution or longer waiting time until the reading is taken. Further, great care is then necessary to ensure that the electrode is thoroughly washed, e.g., with a jet of distilled water, between samples.

Glass electrodes will give excellent service for a working life of one to two years if looked after. A few important points should be remembered:

The glass membrane is thin (ca. 50 μm) and is easily scratched or broken, especially if used to stir crystals when making up solutions.

The membrane will change irreversibly if allowed to dry out, though if caught in time, an overnight soak in 1 *M* hydrochloric acid might rejuvenate the very thin hydrated gel coating.

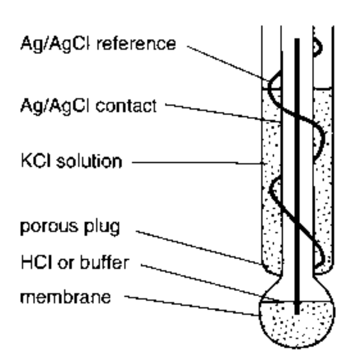


Figure 2 Combination glass electrode.

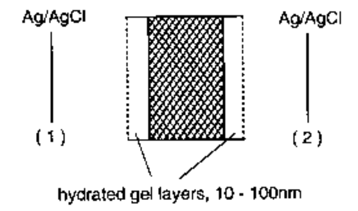


Figure 3 Schematic diagram of the glass membrane in a pH electrode. Shaded area: dry glass membrane electrode for fluoride.

The potential should stabilize in 15–30 seconds after immersion in a sample solution. Slower response may indicate that the electrode is nearing the end of its useful life. At the same time the Nernstian response is also beginning to be lost. For this reason, pH meters that permit the meter plus electrode to be checked and adjusted in two different buffers are always to be preferred. However, apparently slow response may be due to the behavior of the sample: outgassing of CO_2 from some water samples may cause the pH to drift upwards because the pH really is changing.

A pH electrode should always be checked against two buffers—even an electrode with a hole in it can be made to read pH 4, but will read that same value in all solutions.

The 0.05 *M* potassium hydrogen phthalate (10.2 $g\,L^{-1}$) buffer with pH = 4.00 and the 0.05 *M* sodium tetraborate buffer (19.1 $g\,L^{-1}$) buffer with pH = 9.20, both at 20°C, are reliable and easy to prepare one-component buffers. Make them up fresh each week, as they are likely to deteriorate owing to bacterial growth and to absorption of CO_2 from the air, respectively.

B. ISFET pH Sensors

Transistors are three-electrode electronic devices in which a small current flowing between two of the electrodes (emitter to collector) is controlled by a second, very small, current flowing between the emitter and a third, intermediate, electrode called the base. In a field-effect transistor (FET), the controlling electrode responds to potential, normally generated by the adjacent electronic circuitry, but sometimes by the external signal to be measured, for example a potential generated by a chemical electrode. Thus pH meters now use a metal oxide semiconductor FET (MOSFET) operational amplifier to measure the potential of the glass electrode without taking any current from it. The extension of the MOSFET concept has been to coat the metal oxide layer with a chemically selective coating – the "membrane" of a chemical electrode – and to allow a carefully

Marcel Dekker, Inc.
270 Madison Avenue, New York, New York 10016

chosen chemical system to control the transistor current. Such a device has been termed a CHEMFET, a chemically sensitive field-effect transistor, but now is more usually given the name ISFET, ion-selective field-effect transistor (Bergveld, 1972). A silicon nitride coating, for example, deposited on the metal oxide gate results in a device that has near ideal response to hydrogen ions, with a working range of pH 1–13, and that is a great deal tougher than any glass electrode. Mettler-Toledo and Thermo-Russell market ISFET pH electrodes for demanding environmental applications, but they can be used only with appropriate ISFET meters and not with conventional pH meters.

C. Single-Crystal Lanthanum Fluoride

Frant and Ross's announcement in 1966 that doping LaF_3 with a little EuF_2 resulted in a single crystal with sufficient electrical conductivity to be used as an electrode membrane, and one that would respond ideally to fluoride ions in solution, represented a major breakthrough in the area of ion-selective electrodes, much valued because of the difficulty at that time of determining this anion by any other route (Frant and Ross, 1966). The construction is shown in Fig. 4. One crucial practical problem was how to cement the LaF_3 single crystal to the plastic body and at the same time to guarantee perfect electrical insulation. Users should be warned that single crystals are brittle and will shatter if dropped on a hard surface.

The behavior of this electrode is worth discussing because it illustrates problems common to most other electrodes, and also ways of overcoming these problems.

Hydrofluoric acid, HF, is a weak acid, with $pK_a = 3.5$, and the electrode responds to the hydrated fluoride ion. Therefore all solutions must be adjusted to a pH of 5 or greater, where the acid is effectively fully dissociated. An acetate buffer is therefore added to all solutions, standards and samples alike.

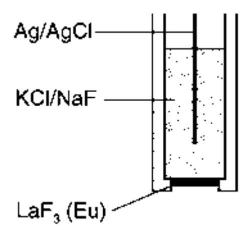


Figure 4 Single-crystal membrane electrode for fluoride.

As mentioned earlier, in high salt concentrations, ion activities deviate significantly from analytical concentrations and calibrations based on concentration, even for low fluoride concentration, and become inaccurate. The answer is to add a high concentration of sodium perchlorate to all solutions, to maintain a constant electrolyte strength for all measurements.

Certain metal ions, notably aluminum and iron(III), form very stable fluoride complexes and will effectively mask free fluoride in e.g. a river water sample, so that very low fluoride concentrations will be reported if the measured potential is converted to fluoride concentration. The answer here is to add a strong complexing agent, EDTA or CHDTA, to mask the metal ions.

The fluoride electrode is therefore used with TISAB (total ionic strength adjuster buffer) being added to all solutions, making possible a working range of 0.1–100 mg L^{-1} of fluoride (Frant and Ross, 1968). As the Nernst equation is operative, the potential, in mV, is plotted against the $\log_{10}$ of the concentration, either in mg L^{-1} or as molarity (Fig. 5).

D. Silver Halide in Silicone Rubber Membranes

The concept of using a sparingly soluble metal salt as the responsive component of a membrane lies behind the design of many types of electrode, and the silver halides are the obvious choices for making a halide ion selective electrode. The problem of making a "membrane" that was both mechanically strong and electrically conducting was solved by Pungor et al. (1966) by compressing finely powdered silver halide with a small amount of

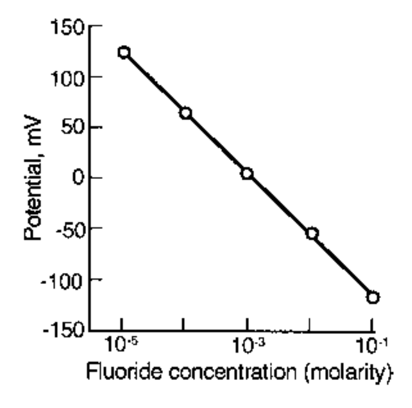


Figure 5 Typical calibration for determination of fluoride with a LaF_3 electrode.

silicone rubber as binder. Nernstian response was obtained over useful working ranges for chloride, bromide, and iodide, but there is a degree of response to other halides best described by the interion response factor:

$$E_{\text{cell}} = E_{\text{const}} + 2.3\frac{RT}{nF}\ln[a_i + K_{i,j}(a_j)]$$

For good performance and little interference, the K values should be small, ideally 0.001 or less. General problems with ISEs and how to characterize their performance have been discussed by Moody and Thomas (1972).

The sulfide electrode presents some difficulties in use, as free sulfide ion is obtained only at very high pH, where oxidation of the ion is facilitated. The standard procedure is to use a high pH buffer (1 *M* NaOH, ca. pH 14) with an oxygen scavenger such as cresol, but this usually is a messy solution that covers the electrode in oxidation products. It is also no solution to the problem of measuring sulfide directly in sediments, where depth profiles are of interest in investigations of the microbial mat and the pore water composition changes in composition with depth. However, as the main interference is a pH effect, it can be countered by measuring the pH and correcting the sulfide electrode potential directly, with a series of calibration graphs covering the pH range of interest (Fig. 6).

E. Liquid Ion Exchanger Membranes for Anions

Liquid ion exchangers can be held on porous glass or ceramic supports to serve as membranes for ion-selective electrodes but are nowadays more commonly mixed in with a polymer to give a solid plastic membrane, enabling a large variety of chemistries to be utilized. Long-chain quaternary amines are dissolved in a viscous solvent as their ion pairs, e.g., cetyltrimethylammonium cation with nitrate or perchlorate, offering good selectivity, especially for larger single-charged anions. Generally one makes the assumption that interfering ions will not be present in the test sample, as for example perchlorate when an electrode is being used to monitor nitrate

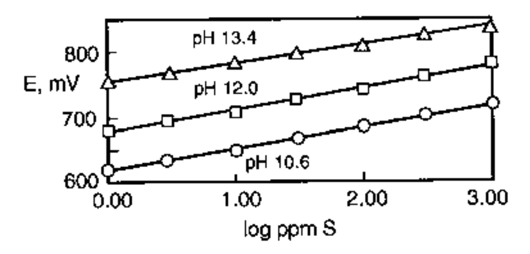


Figure 6 Sulfide calibrations recorded at different pH values.

Marcel Dekker, Inc.
270 Madison Avenue, New York, New York 10016

in river water. These electrodes require attention, with regular replacement of the liquid, but are nevertheless useful for environmental monitoring purposes, covering as they do the concentration range of interest.

F. Plastic Membranes for Cations

Early investigations in the 1960s showed that metal ions immobilized in a PVC (polyvinyl chloride) matrix, as sparingly soluble salts, could behave as selective membranes. These offer the advantage of simplicity of replacement compared with the liquid ion exchanger membranes. Successful calcium electrodes, for example, were made by incorporating the calcium salt of didecylphosphoric acid along with neutral dioctylphenylphosphonate as modifier, in PVC (Crags et al., 1974). Much research has subsequently gone into designing highly specific ligands for a range of metals, in which the dimensions of the chelate formed when the long-chain arms wrap around the metal ion approach the ideal for the particular metal ion.

G. Electrodes for the Alkali Metals

Glass electrodes were originally explored for determination of the alkali metals, especially sodium and potassium, particularly with medical applications in mind. However, though a glass electrode for sodium has long been marketed and is useful in that sodium is usually present, at least in physiological fluids, at one hundred times the concentration of potassium, so that potassium does not cause a significant interference, the complementary problem of the determination of potassium seemed insoluble. It was only when Simon and his team (1970) showed that complexes between certain antibiotics and potassium were so much more stable than the corresponding ones with sodium, that a really selective electrode could be manufactured. Valinomycin, a cyclic 6-membered peptide that displays a selectivity constant with a factor of three to four thousand in favor of potassium against sodium, has formed the basis of a range of successful commercial electrodes. The combination of reagents is formulated into a plastic membrane.

H. Gas-Sensing Electrodes

Electrodes are commercially available for a few gases—ammonia and carbon dioxide in particular. In fact, they do not respond in the way that the ion-selective electrodes do but are pH electrodes covered with special coatings, often of silicone rubber, that offer selective permeability to the gas in question. Thus ammonia arriving at the glass electrode surface causes a rise in pH, whereas carbon dioxide causes a lowering. The working ranges are much smaller than those of the true ion-selective electrodes.

Marcel Dekker, Inc.
270 Madison Avenue, New York, New York 10016

I. General Comments on ISEs

Because the response of an electrode to the determinant is logarithmic, establishing the limit of detection is a little more difficult than for linear response systems. Midgley (1984) has discussed this matter, showing how the intersection of the sloping line and the low-level constant potential can help. Technical data in Table 1 show that a wide range of electrodes is available, for many common ions, covering concentrations of interest in environmental work as well as in many medical applications. The advantages of such probes include

The simplicity of a direct reading device requiring little or no chemical sample treatment
A wide working range, typically three orders of magnitude
Reasonable tolerance to other ions in many environmental samples
Suitability for continuous monitoring using data loggers to collect measurements
The possibility of being made with very small dimensions for exploring concentration profiles, e.g., in tissue or in sediment

J. Redox Electrodes

Noble metal electrodes respond to the redox potential of their environment without actually dissolving or corroding, a fact frequently made use of for assessing the state of the chemistry in, e.g., sediment pore water. A 1-mm diameter platinum wire is sealed into an insulating sheath and can then be pushed into a wet sediment with little risk of breakage. Redox electrodes are

Table 1 Examples of Ion-Selective Electrodes

Species	Type	Range (*M*)	Species	Type	Range (*M*)
Ammonia	gas	5×10^{-7} to 1	Iodide	solid-state	5×10^{-8} to 1
Bromide	solid-state	5×10^{-6} to 1	Lead	solid-state	10^{-6} to 0.1
Cadmium	solid-state	10^{-7} to 0.1	Nitrate	plastic	7×10^{-6} to 1
Calcium	plastic	5×10^{-7} to 1	Nitrite	plastic	4×10^{-6} to 10^{-2}
Carbon dioxide	gas	10^{-4} to 10^{-2}	Perchlorate	plastic	7×10^{-6} to 1
Chloride	solid-state	5×10^{-5} to 1	Potassium	plastic	10^{-6} to 1
Copper	solid-state	10^{-8} to 0.1	Sulfide	solid-state	10^{-7} to 1
Cyanide	solid-state	8×10^{-6} to 10^{-2}	Sodium	glass	10^{-6} to 1
Fluoride	solid-state crystal	10^{-6} to 1	Thiocyanate	solid-state	5×10^{-6} to 1

Source: Data from Thermo-Orion (2001) and from Metrohm (1999).

Marcel Dekker, Inc.
270 Madison Avenue, New York, New York 10016

small, cheap, robust, and easily cleaned. Sediment cores for study in the laboratory can be filled into lengths of 6-cm plastic drainpipe, through the side of which, at regular intervals, are drilled holes just large enough for a micro redox electrode to be inserted and left for the duration of the experiment. The redox potential is a property of the solution, but it will be controlled by one chemical system (the predominating one) and be at the same time indicative of all others in the same solution. As iron is commonly present in sediment pore waters, has two readily acccessible oxidation states in solution, and does not show inhibiting kinetic effects, it is probably the indicating species, so that

$$E_{\text{measured}} = E^\circ + 2.3\frac{RT}{nF}\log\frac{[\mathrm{Fe}^{3+}_{\text{aquo}}]}{[\mathrm{Fe}^{2+}_{\text{aquo}}]}$$

As anaerobic bacterial activity increases and diffusion of oxygen into the pore water decreases, so the potential falls, controlled by the iron system and indicating the state of balance of other chemical couples. Interpretation of the measured E_h values is, however, complicated because the standard potentials of the different couples are all pH dependent. An idea of the values that may be expected in soils is given by the selected potential values in Table 2 (Cresser et al., 1993).

K. Reference Electrodes

Any measurement of potential is in fact one of *potential difference* between two electrodes, so an appropriate second electrode must always be selected,

Table 2 Eh Values for Important Redox Reactions in Soils and Sediments

Reaction	Eh (mV) at 25°C	
	pH 5	pH 7
O_2 to H_2O	930	820
NO_3^- to NO_2^-	530	420
MnO_2 to Mn^{2+}	640	410
$Fe(OH)_3$ to Fe^{2+}	170	−180
SO_4^{2-} to S^{2-}	−70	−220
CO_2 to CH_4	−120	−240
H_2O to H_2	−295	−413

Note: Potentials are with respect to the standard hydrogen electrode. *Source*: Cresser et al., 1993.

the potential of which must remain invariant, and preferably known, throughout the duration of the experiment. Reference electrodes make use of a single metal—usually silver or mercury—immersed in a solution of its ions. The form of the Nernst equation appears then slightly different from that for the concentration cell used to describe the behavior of ion-selective electrodes, as one of the oxidation states is now zero, that of the pure metal itself (which is not in solution):

$$E_{\text{measured}} = E^{\circ} + 2.3\frac{RT}{nF}\log[\text{Ag}^{+}_{\text{aquo}}]$$

It would in practice be difficult to ensure that the solution being measured always contained the same concentration of silver ions, so two steps are taken:

1. A separate chamber is constructed around the silver wire, containing the salt solution
2. A sparingly soluble silver salt is chosen—normally the chloride—and the electrolyte in the chamber, potassium chloride, is maintained at a constant, relatively high (say 0.1 *M* or 1 *M*) concentration.

The silver concentration is then governed by the chloride concentration, since

$$K_{sp} = [\text{Ag}^{+}_{\text{aquo}}] \cdot [\text{Cl}^{-}_{\text{aquo}}] = 10^{-9.5} \qquad \text{at ionic strength} = 1$$

The chamber surrounding the silver wire electrode is designed to have a small leak, such as a porous ceramic plug fused into the wall of the chamber, permitting electrical contact to be made with the sample solution. The more porous the plug, the faster the electrode cleans itself of any sample contamination, but the more often the electrolyte must be topped up to make good the loss. The silver electrode is the standard partner for all pH and ion-selective electrodes, and, as shown in Fig. 1 for glass pH electrodes, it is usually constructed as a concentric annular chamber surrounding the glass electrode itself. Clearly, for correct operation, both the glass bulb and the porous plug must be below the surface of the test solution.

The second common choice for a reference electrode is the calomel electrode, taking its title from the trivial name of mercury(I) chloride, Hg_2Cl_2, also a sparingly soluble salt. The commonly used "saturated calomel electrode" owes its name to the fact that the potassium chloride filling electrolyte is saturated, as should always be apparent from the crystals of that salt sitting inside the electrolyte chamber. The advantage of this system is that it is easy to check that the solution is indeed saturated and to know that the potential of the electrode will be that expected of it; the (small) disadvantage is that the solubility of potassium chloride in water

Table 3 Potentials of Some Common Reference Electrodes

Couple	3.5 *M* KCl	Saturated KCl	Saturated K_2SO_4
Ag^+/Ag	205	199	—
Hg_2^{2+}/Hg	250	244	658

Note: Potentials are in mV, with respect to the standard hydrogen electrode.

increases markedly with temperature, so that the mercury(I) concentration decreases correspondingly and the potential will decrease. For very precise work, therefore, the 3 *M* potassium chloride calomel electrode, which does not have the crystalline solid phase present, may be preferred.

Most reference electrodes are not designed to deliver much current—the resistance of the porous plug is quite high and the area of the metal is small—so reference electrodes for voltammetry must be designed differently from those for potentiometry. Potentials of the common reference electrodes, quoted with respect to the standard hydrogen electrode, are summarized in Table 3.

III. AMPEROMETRY

A. Dependence of Current on Concentration

When a current is allowed to flow through an electrochemical cell, it will be limited by one or more factors, primarily by the rate at which ions (or, indeed, molecules) can be transported to an electrode surface, there to undergo a redox reaction, but also by the electrical resistance of the system, composed of electrolyte, membrane, and electrode. If the current is to be taken as a measure of a concentration, then transport in the solution must be the limiting factor, so that Fick's laws of diffusion can be assumed to hold, i.e. that the flow of analyte to the electrode is proportional to a concentration gradient; and since the analyte is also assumed to react completely at the electrode on arrival, that the concentration at the electrode is therefore effectively zero, and the concentration gradient is dependent only on the bulk concentration. We may summarize as follows:

1. Current is proportional to rate of arrival of determinand molecules/ions
2. Rate of transport is dependent on the concentration gradient near the electrode
3. The concentration gradient is controlled by the bulk concentration
4. $i = k \cdot [A]$, where i is the current, usually in microamperes, and [A] is the concentration of the species being determined.

B. Dependence of Current on Potential—Polarography

There is, however, a second constraint, in that to effect oxidation or reduction of the determinand at the electrode it will usually be necessary to apply a potential, typically in the range up to ± 2 volts, determined by the oxidation–reduction potential of the analyte couple. Just as with potentiometry, also in amperometry, a second electrode is required, often acting as both counterelectrode (to carry the current) and reference electrode (to enable the potential of the working electrode to be precisely defined). The working electrode for polarography is the dropping mercury electrode (DME), first pioneered for this purpose by Heyrovsky in 1922. While it is bothersome to keep it in good working order, as the very fine glass capillary blocks readily, the DME does possess several important properties:

1. Most metals dissolve in it to form amalgams, and so behave ideally
2. Hydrogen ions are reduced with difficulty, creating an overvoltage and giving an enlarged potential window enabling more reactive metal ions, such as zinc, to be reduced
3. The dropping electrode always has a clean, new surface, uncontaminated by the products of electrolysis of the sample.

A polarographic procedure involves scanning a voltage range—say 0 to -2 volts—slowly, over a period of 2–3 minutes, while the electrode releases one drop every 3–5 seconds, and recording the current (of the order of microamps) flowing through the cell. The reference electrode is often a saturated calomel electrode, but with a larger working area and lower electrical resistance than the electrode used for potentiometry, so that it will not be affected by the flow of currents up to 10 μA. This may be seen in a classical polarogram, as shown in Fig. 7.

At low applied potentials, a very small current flows, due to unwanted processes such as, in the case of classical polarography, the carrying of charge by each mercury drop falling from the electrode capillary. As the electrode potential for the determinand in question is approached—here Pb^{2+}_{aq}—lead ions on the surface of the electrode are reduced to lead atoms, causing a flow of electrons between electrode and solution, and the lead atoms dissolve in the mercury drop electrode. The choice of this special electrode thus permits a clean and reproducible surface to be maintained throughout the experiment. As the potential E_{applied} is further increased, the concentration of lead ions at the electrode decreases (controlled by the Nernst equation) and the transport rate increases, so that the current, i, also increases.

$$E_{\text{applied}} = E_{1/2} + \frac{0.059}{n}\log_{10}\frac{(i_{\text{d}} - i)}{i}$$

Marcel Dekker, Inc.
270 Madison Avenue, New York, New York 10016

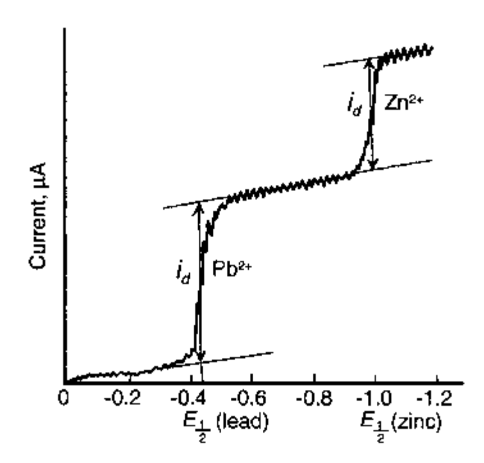


Figure 7 Classical polarogram for lead and zinc ions.

Eventually, the concentration at the surface of the electrode becomes nearly zero and the transport of determinand, and hence the current flowing, levels off, now controlled purely by the concentration gradient, obeying the laws of diffusion. Purely, that is, as long as the solution is not stirred. In classical polarography, the potential halfway up the "wave", $E_{1/2}$, where $[Pb^{2+}] = [Pb^0]$, approximates to the electrode potential for lead and hence serves to identify the element as lead (in this case), and the increase in current—the diffusion current i_d—serves to quantify its concentration in solution. Here, the information content of a two-dimensional plot is seen to be so much greater than that of a single potential measurement as in the case of potentiometry. Indeed, if there are other reducible ions in the solution, such as Cd^{2+}, Zn^{2+}, and others, they may be identified and quantified in the same analysis—truly a multicomponent analysis of solutions.

1. Limits of Detection of Polarography

While the capabilities of classical polarography—facilitating identification and quantification on multicomponent solutions—are clear from Fig. 8, so also is the principal drawback. The dropping mercury electrode, while guaranteeing a clean, reproducible surface, also guarantees a very noisy signal due to the aforementioned drop charging effect, as a result of which it is not practical to go below 10^{-5} *M* for reliable analyses, i.e., 2 mg L^{-1} for lead, hardly sensitive enough for modern environmental analysis. Atomic absorption spectrometry using a graphite furnace will go to one hundred times lower than this, so that even with the improvements offered by differential pulse polarography and some other variants, the technique has

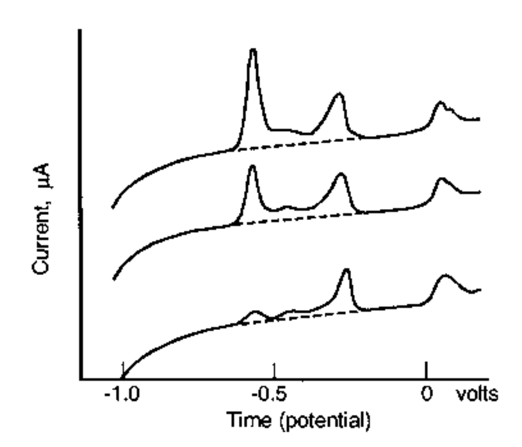


Figure 8 DC anodic stripping voltammograms for lead with standard additions of 20 μg L^{-1}; sample contained 5 μg Pb L^{-1}.

dropped out of use. But electroanalytical chemistry has another option, which is second to none for low-level trace analysis, stripping voltammetry.

C. Anodic Stripping Voltammetry (ASV)

If a single mercury drop, produced by extrusion from a micrometer burette, is held at a negative potential on the upper plateau of the polarographic "wave," the metal, such as lead, will be deposited and dissolved into the mercury, being thus accumulated: the longer the period of electrolysis, the greater will be the amount of metal collected. This amount is still proportional to the bulk concentration, as well as to the deposition time. After, say, ten minutes, the potential is scanned back towards zero, and at around the half-wave potential the lead atoms will be "stripped" out of the mercury drop, being oxidized back to soluble hydrated Pb^{2+} ions in solution, and a current will flow. The current will be short-lived (say 10 seconds), but the peak current will be, in this case, sixty or more times greater than during the deposition step, and it will not be superimposed on a noisy background of the electrode drop charging current. Moreover, while stirring is undesirable in classical polarography, it can greatly help the transport of ions to the single drop electrode and give a corresponding further increase in sensitivity. This is the principle of stripping voltammetry (Neeb, 1969, 1989).

The single drop mercury electrode was originally proposed for this technique by Kemula and Kublik (1958)—the hanging drop, and by Neeb (1961)—the sitting or "sessile" mercury drop. However, there

Marcel Dekker, Inc.
270 Madison Avenue, New York, New York 10016

is a drawback to using the mercury drop—that of controlling its size and of keeping it still. Large drops lead to wide stripping peaks, as it takes time for the atoms to diffuse through the mercury back to the surface for oxidation in the stripping process. The alternative is to use some other, solid, electrode, but to prevent the effect of one metal "trapping" another on the solid surface, it is coated with a thin film of mercury by simultaneous electrodeposition during the preconcentration step, allowing each deposited metal to behave independently during the stripping process. The glassy carbon electrode is the solid material of choice, as it does not suffer from the problems of adsorption of other chemically active species, especially oxygen, into pores, such as occurs with ordinary graphite electrodes (Neeb, 1969). Unfortunately, easy though the glassy carbon electrode is to use, the limits of detection obtained using it (in the mercury film mode) are typically ten times higher than those obtained with the hanging mercury drop extrusion electrode. Typical stripping voltammograms, showing the sharpness of the peaks, are shown in Fig. 8. Another variant, instead of stirring the solution, is to rotate the electrode—using the so-called rotating disk electrode, which may also be amalgamated during the deposition step.

Of course, several metals can be determined in one analysis, just as with classical polarography; Cd, Cu, and Pb are the most important, from dilute acid solution, and Zn from a buffered alkaline solution; so this technique, getting down to 5–10 $\mu g\,L^{-1}$, competes with GF-AAS as far as sensitivity goes and wins as far as speed of analysis is concerned. A number of interferences are known that arise due to the formation of sparingly soluble intermetallic compounds in the mercury drop. Some are of little importance, as they involve a noble metal such as gold, but a troublesome combination is that of copper (or nickel) and zinc. Copper can be determined from acid solution, leaving zinc in solution, but zinc must be determined from an alkaline solution containing a little cyanide (the amount is critical) to mask the copper and permit deposition of the zinc (Marques and Chierice, 1991).

Finally, while some electrolyte must be present, to render the solution electrolytically conductive, high salt concentrations are actually welcome, as they guarantee diffusion control of transport and eliminate any charge-dependent transport effects. But at higher salt concentrations the diffusion coefficients of the determinand ions will become less, resulting in a variable calibration factor. The answer is to use the standard addition technique—recording first the voltammogram for the sample itself, then again, after one and two additions of known amounts of the element(s) in question. Such in situ calibration (Fig. 8) overcomes many uncertainties and is to be strongly recommended for environmental analysis.

Limits of detection depend on the one hand on contamination—so great attention must be paid to acid cleaning of all apparatus including the sample bottles, as well as to choice of any reagents added—and on the other hand to sloping baselines due to other species in solution. This problem can be overcome by using differential pulse measurement during the scan, rather than simple DC measurement, taking limits of detection for lead, for example, down from around 1 μg/L with DC scanning, to one hundred times less with DP scanning voltammetry. So now we have a clear winner, $\mu g\,L^{-1}$ or even $ng\,L^{-1}$ concentrations can be determined directly in seawater, eliminating the need for any sample pretreatment and the associated risks of introducing contamination. The determination of several metals in seawater by several approved polarographic methods has been reviewed (Standing Committee of Analysts, 1987a). Details of determinations of Cd and Pb using ASV are summarized in Table 4.

D. Cathodic Stripping Voltammetry (CSV)

Not all metals are easily reduced onto a mercury electrode, but the two-step approach can be modified to cope with a number of other metals, by making use of adsorption of the desired metals species, as sparingly soluble compounds, often as organic chelates. These are then reduced during a potential sweep step, allowing the metals to be transferred to the mercury drop. This is particularly important for metals which are not normally readily reduced at a mercury electrode, such as aluminum, vanadium, and uranium. Accumulation is still diffusion-controlled (and assisted by controlled stirring), so that the resulting peaks are proportional to the initial concentration in the sample solution. Details of some determinations using CSV are also summarized in Table 4.

1. Sample Preparation—UV Photolysis

While it has been mentioned that ASV and CSV offer the attraction of being directly applicable to the analysis of very dilute aqueous samples, with little or no sample pretreatment, the problem of interference from high-molecular-weight organic materials should be mentioned. Surface-active subtances collecting on the surface of the electrode will significantly affect the stripping voltammograms—sloping baselines and broadened peaks result, making reliable quantitation difficult. Irradiation of the sample solutions, in quartz test tubes set around a high-power mercury vapor UV lamp (typically 500 W, e.g., the Metrohm model 705 UV Digester) for 30 minutes will usually solve this problem. UV irradiation will also break down any organic complexing ligands, releasing the metals into the (acidified)

Marcel Dekker, Inc.
270 Madison Avenue, New York, New York 10016

Table 4 Determination of Some Trace Metals in Seawater by Stripping Voltammetry

Element	Technique	Reagent	Peak potential, V	Limit of detection	Upper working limit
Al	DP-CSV	Alizarin Red S, pH 7.1	−1.13	30 ng L^{-1}	10 µg L^{-1}
Cd + Pb	DP-ASV	pH 2.8 with HCl	−0.7	10 ng L^{-1}	50 µg L^{-1}
Co + Ni	CSV	Dimethylglyoxime, pH 8.3	−1.13	10 ng L^{-1}	60 µg L^{-1}
Cu	DP-CSV	Catechol, pH 7.5	−0.27	5 ng L^{-1}	10 µg L^{-1}
Fe	CSV	1-Nitroso-2-naphthol, pH 6.9	−0.53	60 ng L^{-1}	2 µg L^{-1}
Ni	CSV	Dimethylglyoxime, pH 8.3	−1.01	10 ng L^{-1}	60 µg L^{-1}
Pb	DP-ASV	pH 2.8 with HCl	−0.5	30 ng L^{-1}	50 µg L^{-1}
U	CSV	8-Hydroxyquinoline, pH 6.9	−0.68	50 ng L^{-1}	10 µg L^{-1}
V	DP-CSV	Catechol, pH 6.9	−0.69	15 ng L^{-1}	50 µg L^{-1}
Zn	DP-CSV	Ammonium pyrrolidone dithio-carbamate, pH 7.3	−1.15	10 ng L^{-1}	10 µg L^{-1}

Note: All determinations done using a dropping mercury electrode. *Source*: Standing Committee of Analysts, 1987a.

solution (Standing Committee of Analysts, 1987a). The initial volume of solution in the tube should be noted, and the loss of water occurring during this pretreatment made good after cooling.

Finally, one special advantage of ASV should be mentioned: its unique role in speciation. While filtration is normally used, e.g., with 0.45 μm membrane filters, to separate suspended solids from "soluble" forms of an element in a natural water sample, the question of colloidal material is conveniently overlooked. This would pass through such a filter, and be determined by flame or plasma spectroscopic methods, but would not be detected by stripping voltammetry, which "sees" only genuinely soluble forms of the element being determined.

E. Voltammetry of Nonmetals

A very exciting development in environmental electroanalytical chemistry has been the new voltammetric methods enabling speciation of sulfur compounds in sediments to be studied. Luther and coworkers (2001) have used solid gold amalgams to probe bacterial mats on sediments, and from the very fast (1,000 mV s^{-1}) cyclic voltammograms they have been able to distinguish not only ionic forms such as sulfide and thiosulfate but also elemental sulfur, with 0.5 mm resolution in depth. One of these electrode systems has been fitted to a deep ocean lander to investigate the sulfur speciation around deep-sea hydrothermal vents. A cyclic voltammogram showing peaks for several sulfur species is shown in Fig. 9.

F. Determination of Dissolved Oxygen

In the realm of classical polarography, dissolved oxygen was the omnipresent problem. The well understood reduction first to peroxide and then to water, giving two polarographic waves, necessitated removal of the

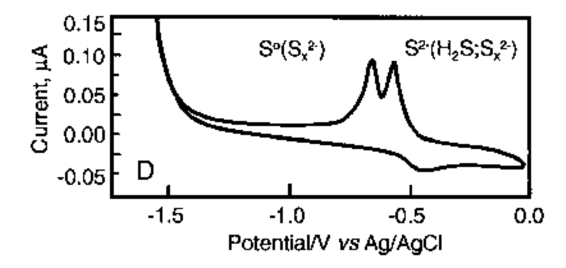


Figure 9 Cyclic voltammetry trace for sulfur species in a salt marsh microbial mat. (From Luther et al., 2001.)

oxygen by bubbling an inert gas through the solution to displace the oxygen, according to Henry's law—if there is no oxygen in the gas phase over the solution, then there should be none in the solution. On the other hand, portable polarographs with polished mahogany cases to contain the apparatus and the dropping mercury electrode were used in the field and proved the point that samples that could not be transported back to the laboratory could nevertheless be analyzed.

Measurement of dissolved oxygen (DO) in natural surface waters is important, as it is a key indicator of water quality, and is included, for example, in arriving at the Solway Water Quality Index for an environmental sample (Bolton et al., 1978). What is often forgotten by chemists is that in any but the cleanest waters, the dissolved oxygen level does not remain steady but increases during the day, owing to photosynthesis by algae and plants; and it decreases at night, owing to the respiration of bacteria and algae. A third factor contributing to the changes is the transfer between the water and the air, which works in either direction depending on the concentration in the water in relation to the DO saturation level, and which depends mainly on the perturbation of the surface by wind action (Ansa-Asari et al., 1999). There are two approaches to dealing with this difficulty—sample at the same time each day, and measure in the field. It is best to measure directly in the water body itself, to avoid disturbing the oxygen, particularly when the water is supersaturated, as will be the case in the late afternoon, or to monitor round the clock and analyze the changing signal to give a measure of the three different activities mentioned above. In either case, a small portable measuring device is required.

The development by Mackereth (1964) of an alternative electrochemical cell (to the dropping mercury electrode) solved the practical problems and gave the analyst a valuable tool for environmental analysis. Oxygen diffuses from the test solution through a polymer membrane (often PTFE) into a small volume of electrolyte (such as potassium carbonate) in which are immersed two electrodes—a silver–lead pair or a gold–silver pair (Fig. 10).

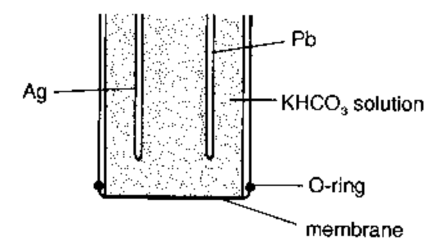


Figure 10 Mackereth cell for determination of dissolved oxygen (DO).

The overall reaction of $Pb + O_2 \rightarrow PbO_2$ takes place in two steps, made possible by a flow of current through the external circuit: Reduction of oxygen takes place at the silver electrode:

$$O_2 + 4e^- + 2H_2O \rightarrow 4OH^-$$

and oxidation of the lead takes place at the other electrode:

$$Pb + 4OH^- \rightarrow PbO_2 + 2H_2O + 4e^-$$

The current depends on the rate of diffusion of oxygen into the cell, which in turn is dependent on the concentration in the sample solution, or, more strictly, on the concentration in the water at the surface of the membrane. If there is no movement of the water, the DO concentration at the membrane surface becomes depleted and the current falls. In the laboratory, a small stirrer is incorporated to ensure a steady and reproducible movement of the water and hence a reproducible response from the device. In a river, the motion of the water may suffice, but in a lake or pond the response will be low and the calibration will not be reliable.

Calibration is often achieved simply by setting the response to 100% of saturation by holding the probe in air, on the assumption that the DO level in solution will equate to that partial pressure in equilibrium with air. In practice, while this is very convenient, it should not be trusted too far, and all oxygen probes should be checked on a series of test solutions from which differing amounts of oxygen have been displaced by bubbling nitrogen for some minutes. The actual DO levels should be determined by the Winkler titration method, and calibrations constructed for each probe. Experience has shown that response factors for probes do vary from probe to probe and that such calibration is necessary. Some commercial DO probes and meters (e.g., the Russell RL series) incorporate not only temperature correction but also a salinity correction.

To sum up, whatever be the difficulties with lifetimes of membranes and probe capsules, and of calibration, the modern DO probe is an invaluable tool for use not only in the laboratory but also in the field, for the direct measurement of true dissolved oxygen concentration from the surface down to depths of several meters, even in highly supersaturated waters (Standing Committee of Analysts, 1987b).

DO Measurements in Sediments. There has been increasing interest over the last twenty years in the study of marine sediments at great depths — in principle an ideal application for electrochemical probes. The problem of trying to measure DO gradients through short distances, as in microbial mats on the surface of sediments, and to do so without the possibility of

stirring, led to the development of microelectrodes (Revsbech et al., 1980), but they tended to be delicate and easily broken. A new idea employs quenching of a dyestuff fluorescence by dissolved oxygen, realized by a ‘‘micro-optrode’’ in which exciting and emitted light is transmitted through fiber optics in a very rugged miniaturized construction. Such a device has been shown to work well at depths of over 10 m, and still with a depth resolution in the sediment of 0.1 mm (Glud et al., 1999).

IV. CONDUCTIVITY

Measurement of electrical conductivity of a water sample serves simply to give an indication of the levels of dissolved salts present and does not of itself contribute any chemical information about the sample. The specific conductance of a solution, κ, is the electrical conductivity of a 1-cm cube with 1-cm^2 electrodes on opposite faces. Hence, for a practical measurement using a conductivity cell, with plates (electrodes) of area A and separated by a distance d, the measured conductance σ (reciprocal of the resistance in ohms) is

$$\sigma = \kappa \cdot \frac{A}{d}$$

The old term mho for reciprocal ohm is now superseded by the siemen, S, so that the specific conductivity κ of a solution has the units of $\mathrm{S\,cm^{-}1}$. Conductivity cells have dimensions close to, but not the same as, those referred to in the definition. Accordingly, each cell will have its ‘‘cell constant’’ $\theta = d/A$ stamped on it. Hence $\kappa = \sigma \cdot \theta$. The two electrodes, enclosed in a small chamber with openings at either end permitting rapid flushing of the cell, but minimizing the contribution of a ‘‘round the back’’ conductivity, may be platinum sheet supported on the glass, but in some cases they are coated with finely electrodeposited platinum black. Measurement makes use of a traditional Wheatstone bridge circuit, but one which is supplied with a small AC voltage to minimize buildup of products of electrolysis of the sample solution. Frequencies may be 50 Hz (for low conductivities) or, preferably, 1 kHz (for higher conductivities where the greater capacitance contribution will be less important).

The conductance of a salt solution varies with temperature, increasing by about 2–3% per degree. For good results, therefore, temperature control must be employed, especially where the conductivities of different solutions are to be compared. Good practice will therefore include a check on the conductivity of a potassium chloride solution: a 0.005 M solution (0.373 $\mathrm{g\,L^{-1}}$) will have a specific conductivity of 654 $\mu\mathrm{S\,cm^{-1}}$ at 20°C (Standing Committee of Analysts, 1978).

Marcel Dekker, Inc.
270 Madison Avenue, New York, New York 10016

An interesting application of conductivity measurement is to estuarine waters, where the boundary between the upper (river water) and lower (seawater) layers can often be sharply defined. A very special application, calling for great precision and demanding great care in experimental measurement, is the determination of the slight variations in salinity of different seawater samples, discussed in some detail by Grasshoff et al. (1999).

V. CONCLUSIONS

It will have become clear to the reader that the techniques described in this chapter have been in routine use for many years and are well established and well documented. While many older electroanalytical procedures described in textbooks have fallen out of use, a small number of new approaches are now making possible automated remote measurements in inaccessible locations such as the ocean floor, thus helping to retain an important role for electroanalytical techniques in environmental analysis.

REFERENCES

Ansa-Asari, O., Marr, I.L. and Cresser, M.S. 1999. Evaluation of cycling patterns of dissolved oxygen in a tropical lake as an indicator of biodegradable organic pollution. *Sci. Total Environ.* 231:145–158.

Bergveld, P. 1972. Development, operation and application of the ion-selective field-effect transistor as a tool for electrophysiology. *IEEE Trans. Biomed. Eng.* 19:340–354.

Bolton, P.W., Currie, J.C. and Tervet, D.J. 1978. An index to improve water quality classification. *Water Pollut. Control* 271–284.

Crags, A., Moody, G.J. and Thomas, J.D.R., 1974. PVC matrix membrane ion-selective electrodes. *J. Chem. Ed.* 51:541–544.

Cresser, M.S., Killham, K. and Edwards, T. 1993. *Soil Chemistry and Its Applications*. Cambridge University Press, Cambridge.

Frant, M.S. and Ross, J. W. 1966. Electrode for sensing fluoride ion activity in solution. *Science* 154:1553–1555.

Frant, M.S. and Ross, J. W. 1968. Use of a total ionic strength adjustment buffer for electrode determination of fluoride in water supplies. *Anal. Chem.* 40:1169–1171.

Galster, H. 1991. *pH Measurement*. Verlag Chemie, Weinheim.

Glud, R.N., Klimant, I., Holst, G., Kohls, O., Meyer, V., Kühl, M. and Gundersen, J.-K. 1999. Adaptation, test and in situ measurements with O_2 microoptrodes on benthic landers. *Deep-Sea Research* I 46:171–183.

Grasshoff, K., Kremling, K. and Ehrhardt, M. 1999. *Methods of Seawater Analysis*. 3d ed. Wiley-VCH, Weinheim.

Marcel Dekker, Inc.
270 Madison Avenue, New York, New York 10016

Kemula, W. and Kublik, Z. 1958. Application de la goute pendante de mercure à la détermination de minimes quantités de differents ions. *Anal. Chim. Acta* 18:104–111.
Luther, G.W., Glazer, B.T., Hohmann, L., Popp, J.I., Taillefert, M., Rozan, T.F., Brendel, P.J., Theberge, S.M. and Nuzzio, D.B. 2001. Sulfur speciation monitored in situ with solid state gold amalgam voltammetric microelectrodes: polysulfides as a special case in sediments, microbial mats and hydrothermal vent waters. *J. Environ. Monit.* 3:61–66.
Mackereth, F.J.H. 1964. Improved galvanic cell for determination of oxygen concentration in fluids. *J. Sci. Instrum.* 41:38–41.
Marques, A.L.B. and Chierice, G.O. 1991. Elimination of copper–zinc interference in ASV by addition of a complexing agent. *Talanta* 38:735–739.
Metrohm Ltd. 1999. Metrosensor Electrodes Catalogue. Metrohm Ltd., CH-9101 Herisau, Switzerland.
Midgley, D. 1984. Limits of detection of ion-selective electrodes. *Anal. Proc.* 21:284–287.
Moody, G.J. and Thomas, J.D.R. 1972. Development and publication of work with selective ion-sensitive electrodes. *Talanta* 19:623–639.
Neeb, R. 1961. Anodische amalgamvoltammetrie: III. Comparison of amalgamated platinum and stationary mercury electrodes. *Z. Anal. Chem.* 180:161–168.
Neeb, R. 1969. *Inverse Polarographie und Voltammetrie*. Verlag Chemie, Weinheim.
Neeb, R. 1989. *Stripping Voltammetry*. Metrohm Ltd., CH 9101 Herisau, Switzerland.
Pungor, E., Tóth, K. and Havas, J. 1966. Theorie und Anwendung der heterogen Gummimembranelektroden für die Bestimmung einiger Ionen. *Mikrochim. Acta* 689–698.
Revsbech, N.P., Jørgensen, B.B. and Blackburn, T.H. 1980. Oxygen in the sea bottom measured with a microelectrode. *Science* 207:1355–1356.
Simon, W., Wuhrmann, H.-R., Vasak, M., Pioda, A.R. and Stefanac, Z. 1970. Ion-selective sensors. *Angew. Chem. Int. Ed. Eng.* 9:445–455.
Standing Committee of Analysts. 1978. *Measurement of Electrical Conductivity and Laboratory Determination of the pH Value of Natural, Treated and Waste Waters*. HMSO, London.
Standing Committee of Analysts. 1987a. *Determination of Twelve Trace Metals in Marine and Other Waters by Voltammetry or AAS*. HMSO, London.
Standing Committee of Analysts. 1987b. *Dissolved Oxygen in Natural and Waste-waters*. HMSO, London.
Thermo-Orion. 2001. Laboratory Products Catalogue. Thermo-Orion, Beverly, MA, U.S.A.
Vesely, J., Weiss, D. and Stulik, K. 1978. *Analysis with Ion-Selective Electrodes*. Ellis Horwood, Chichester, England.

Marcel Dekker, Inc.
270 Madison Avenue, New York, New York 10016

4

Continuous-Flow, Flow-Injection, and Discrete Analysis

Anthony C. Edwards
The Macaulay Institute, Aberdeen, Scotland

Malcolm S. Cresser
The University of York, York, England

Keith A. Smith
The University of Edinburgh, Edinburgh, Scotland

Albert Scott
Scottish Agricultural College, Edinburgh, Scotland

I. INTRODUCTION

Automation of one or more steps in the analysis of environmental samples, whether it be the sample preparation/dissolution stage, the determination stage, or simply the collation/reporting of results, is accepted as essential in many modern laboratories. Long-term comparisons of manual and automated methods for nutrient analysis show that both give similar results (Nausch, 1997). Automated analytical procedures, however, offer numerous advantages. These include the reduced possibility of procedural errors (perhaps through a momentary lapse in concentration), capability for multielement or multispecies analysis, small sample volume requirement, and the possibility of inclusion within a laboratory information management system (LIMS), whereby samples are identified automatically throughout the analytical procedure. Automated instruments used in seawater surveys, for example, may produce vast quantities of data, and

Marcel Dekker, Inc.
270 Madison Avenue, New York, New York 10016

in such cases fully automated data handling may be deemed essential (Whitehouse and Preston, 1997).

Since the previous edition of this book was written, the choice of commercially available automated analyzers has widened, with improvements being made in the sample throughput, detector systems, and data handling aspects. There is an increasing requirement for equipment that can be sited remotely, and a variety of automated systems capable of unattended operation have been developed. The increased access to affordable computing capacity has meant that many new systems are totally reliant upon a computer for data capture, subsequent processing, and control of the analytical console. Computer technology has increased the sample throughput and lowered analytical detection limits, with particular benefits for laboratories with a large throughput of similar samples. However, the increased reliance on computers has reduced the direct contact an operator has with the "wet end" of the automated analytical process. As a consequence, the operator's understanding of basic analytical principles that underpin automated analysis can suffer. The importance of fluid dynamics in constrained systems is just as relevant today as when the first continuous-flow analysis (CFA) systems were described by Skeggs (1957). Much of the information originally presented that relates to the principles of CFA systems therefore has been retained in this edition. While CFA is still popular, flow-injection analysis (FIA) (Růžička and Hansen, 1975) has become a very widely accepted alternative in environmentally related analysis (Ferreira et al., 1998). Discrete or batch analysis remains an alternative approach to full automation.

Automated systems based on colorimetric detection remain an established requirement for many analytical laboratories dealing with environmental samples, despite the apparent potential direct competition from multielement techniques such as ICP-AES or ICP-MS (see Chap. 2). This is due to a combination of factors. Several determinants of interest, such as nitrogen, phosphorus, and carbon, are determined most cost-effectively and with excellent sensitivity and precision by automated colorimetry or other automated molecular techniques. The lower detection limit of automated colorimetric analysis for elements such as phosphorus, compared with alternative methods of determination, may be an important consideration. There is a continued need to distinguish between chemical species of elements, for example between inorganic and organically complexed aluminum, or between the individual contributions to total dissolved nitrogen of nitrate, ammonium, and organic N. The value of automated colorimetry has been highlighted recently through the increasing significance that is being placed upon the analysis of organically associated forms of N (Yesmin et al., 1995) and P (Ron Vaz et al., 1992, 1993) in soil

Marcel Dekker, Inc.
270 Madison Avenue, New York, New York 10016

extracts and natural water samples. In this chapter, the principles underlying the systems of continuous-flow and discrete analysis are discussed, and examples of applications of these techniques to the analysis of soils, waters, and other environmental materials are described.

II. PRINCIPLES

A. Continuous-Flow (Segmented-Flow) Analysis

In a basic system for colorimetric analysis, sample and reagent solutions are pumped through narrow-bore flexible tubes of various diameters. The relative quantities of reagents and sample are regulated by controlling the flow rate of each individually by choice of its pump tube diameter. Sample throughput is usually between 30 and 100 or more determinations per hour. Interaction and carryover between successive samples is minimized by segmentation of the liquid streams by air bubbles (hence the alternative name of segmented-flow analysis, SFA). Streams are merged via T or Y pieces, and thorough mixing within each liquid segment is promoted via passage through a coil (usually made of glass with 1–2 mm internal diameter), and the color reaction takes place. The typical combined flow rate of sample and reagents is around 2 mL min^{-1}. It may take upwards of 10 min for the sample to undergo reaction and finally reach the detector system.

While analysis by colorimetry remains most common in routine laboratories, many other detection techniques, including ICP-MS, ICP-AES, AAS, flame photometry, and ion-selective electrodes, have been employed in automated systems. This is reflected in a recent review by Ferreira et al. (1998) of publications involving flow-injection analysis (FIA). They counted the numbers of papers published using different detector systems in FIA. Of the total number, 35% used u.v.-visible spectrophotometry, 33% AAS, 14% potentiometry, 11% FES, and 4% ICP-MS. "Others" accounted for only 3%. However, to some extent the distribution shown reflects novelty (and therefore how publishable a work is), rather than the distribution of routine usage of methods.

1. Dispersion and Interaction Between Samples

The flow of a segmented liquid stream through a tube that is wetted by the liquid is illustrated in Fig. 1. The thin film of liquid, thickness *df*, remaining on the tube wall from the passage of the first segment (#0) will be overtaken by, and mixed into, segment #1, and so on. Thus solute present in segment #0 will be transferred to segment #1. The process is repeated between segments 1 and 2, 2 and 3, and so on over many following segments.

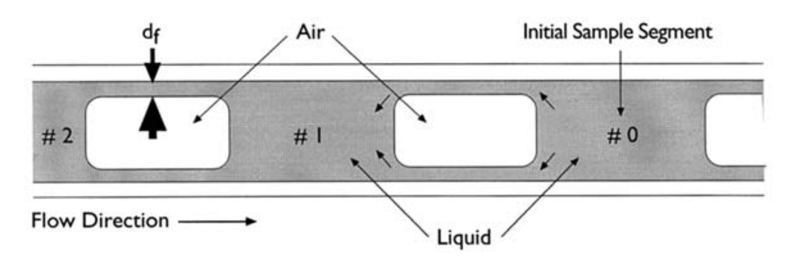


Figure 1 Segmented flow through an open tube. (Redrawn with permission from L. R. Snyder and H. J. Alder, Dispersion in segmented flow through glass tubing in continuous-flow analysis: the ideal model. *Anal. Chem.* 48:1017 (1976). Copyright © American Chemical Society, Washington, D.C.)

Consider now what happens when a series of liquid segments containing no determinant (a wash solution) is followed by a series with determinant, and then a further series without determinant. The initially sharp transitions in concentration (Fig. 2a) between the series of sample segments containing the determinant and preceding and following series (wash solution) become transformed into more gradual ones (Fig. 2b). The relationship between concentrations in successive segments and sample–sample interactions has been investigated experimentally, modeled, and used as a basis for computer programs to correct analytical data for memory effects (Snyder and Adler, 1976a,b). In practice most analysts still prefer

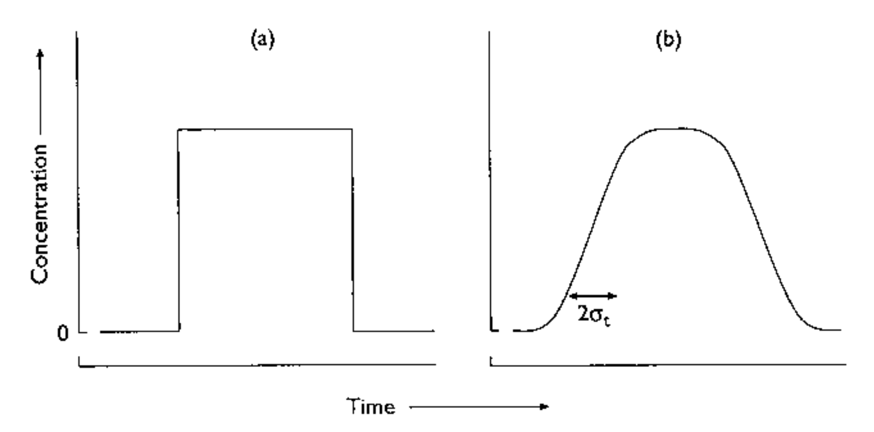


Figure 2 Solute concentration profiles in segmented CFA, (a) at injection and (b) at the detector. (After Snyder, 1980.)

to rely on direct experimental measurement of possible carryover effects to make sure errors are within acceptable limits.

The dispersion process limits the spacing of samples and the resulting throughput rate. In Fig. 2b the increasing and decreasing parts of the curve are integrated Gaussian curves (Snyder and Adler, 1976a,b; Snyder, 1980), and the extent of sample dispersion is given by σ_t, which is the standard deviation of the Gaussian curve and is measured in seconds. The throughput rate F depends on the spacing of sample bands in units of σ_t. Snyder (1980) has derived a value of $8\sigma_t$ for curves with flat plateaux as shown in Fig. 2b. For the latter, the throughput rate F (in samples per hour) is given by Eq. (1):

$$F = \frac{3600}{8\sigma_t} = \frac{450}{\sigma_t} \tag{1}$$

According to Snyder and Adler (1976a,b), the variance σ^2 of the dispersion occurring during segmented flow through a length of tubing is given by Eq. (2):

$$\sigma^2 = \left[\frac{(\pi^2/72)d_t^4 u^{5/3}\eta^{2/3}}{\gamma^{2/3}V_s D_m} + 1\right]\left[\frac{0.5\pi L d_t^2 (u\eta/\gamma)^{2/3}}{V_s}\right] \tag{2}$$

where d_t is the internal diameter and L is the length of the tube, u is the linear velocity of the liquid with viscosity η and surface tension γ, V_s is the liquid-segment volume, and D_m is a mass transfer coefficient that varies with the nature of the sample (solute) molecules and the viscosity of the liquid. For other liquids and/or temperatures, D_m is related to the value of D_m for water at 25°C ($D_{w,25}$) and to liquid viscosity by the relationship in Eq. (3):

$$D_m = D_{w,25}\left(\frac{\eta}{0.0089}\right)^{-5/3} \tag{3}$$

The dispersion σ in Eq. (2) can be expressed in terms of σ_t [Eq. (1)]:

$$\sigma_t = \frac{\sigma}{n} \tag{4}$$

where n is the air-bubble rate. A number of other variables in Eq. (2) can be replaced by easily measured parameters such as the flow rate F_l. Equation (2) has been tested over a wide range of values of the various parameters, and general agreement within ±10% has been found (Snyder, 1980). However, continuous-flow systems are generally run at lower throughput rates than those indicated by Eqs. (1) and (2). This is because

of the additional contribution to dispersion resulting either from debubbling or, for systems in which bubbles pass through the detector, from the requirement that each liquid segment be more than large enough to fill the detector flow cell (Snyder, 1980).

2. Mixing of Sample and Reagents

Mixing is required whenever a reagent or a diluent is added, and several such mixing steps may be required in the course of one analysis. Complete mixing must occur in each liquid segment, or an irregular (noisy) detector output will result. The natural fluid motions that occur within a short moving segment of liquid bounded at each end by a gas–liquid interface bring about mixing. These motions, known as *bolus* flow, result in rapid longitudinal mixing along the segment and in slow radial mixing (Snyder and Adler, 1976b). In straight lengths of tubing, radial mass transfer occurs mainly by molecular diffusion, which is slow in liquids, but this can be overcome by inducing convective mixing simply by substituting a helical coil for the straight tube. Both the physical properties of the liquid and tube geometry are important in determining the rate of mixing. Viscosity, density, and flow rate all affect the process, with viscosity the most significant factor. Tube internal diameter, helix coil diameter, and segment length are also important.

3. Flow Stability

To achieve a stable detector output, the relative proportions of sample to reagents mixed must be constant for all segments derived from the same sample. This requires constant flow rates and a very regular bubble pattern. Second- and third-generation peristaltic pumps of the Bran & Luebbe (Technicon) type run at a lower speed and with a higher roller frequency than in the original (Technicon) versions, and air injection is under electronic control. Both of these developments contribute significantly to improved stability.

B. Flow Injection Analysis

In the mid-1970s, Růžička and Hansen (1975) in Denmark and Stewart et al. (1976) in the United States independently introduced a new concept of CFA called flow-injection analysis (FIA). The flow-injection method is based, in its simplest form, on the rapid injection of the sample solution (as a "plug") into a nonsegmented carrier stream of reagent. The technique has many of the features of HPLC.

The initial shape of the sample distribution (bolus shape) is controlled predominantly by convection, with diffusion becoming increasingly dominant over distance. Taylor (1953, 1954) derived the theory describing these two limiting situations over 20 years before the advent of flow-injection analysis. Taylor showed that when solute is introduced into a liquid stream moving by laminar flow with a mean velocity u and disperses by convection alone, the shape of the solute plug becomes distorted in time into a paraboloid (as shown in Fig. 3). He also showed that the effect of molecular diffusion gave rise eventually to dispersion with an apparent diffusion coefficient k given by Eq. (5):

$$k = \frac{a^2u^2}{48D} \tag{5}$$

where D is the molecular diffusion coefficient and a the radius of the tube. The distribution tends to normality, and the effective distribution coefficient K is the sum of the molecular diffusion coefficient and Taylor's apparent diffusion coefficient, as in Eq. (6):

$$K = D + k = D + \frac{a^2u^2}{48D} \tag{6}$$

In practice, the dispersion in FIA systems is of the intermediate type in which both convection and diffusion play significant parts (Fig. 4c), and to

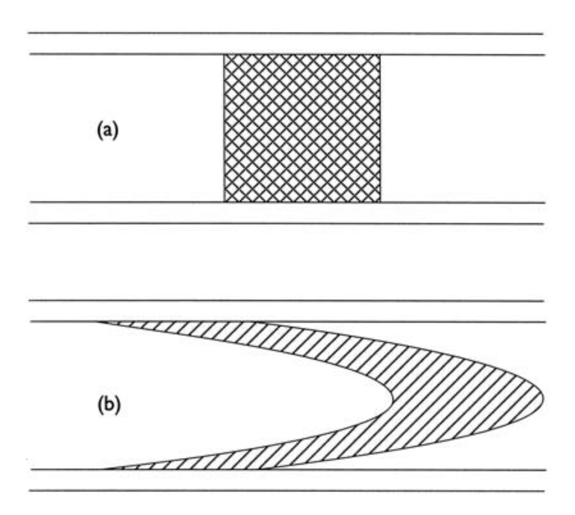


Figure 3 Bolus shapes (a) at injection and (b) after injection. (After Vanderslice et al., 1986.)

MARCEL DEKKER, INC.
270 Madison Avenue, New York, New York 10016

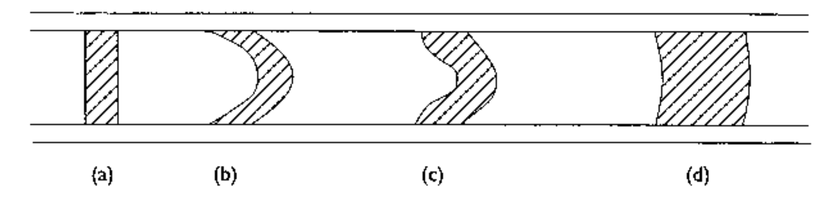


Figure 4 Shapes of an injected bolus under different conditions: (a) zero time, (b) convection-controlled region, (c) diffusion–convection region, (d) diffusion-controlled. (After Vanderslice et al., 1981.)

which Taylor's solutions are therefore not applicable (Vanderslice et al., 1981). For example, studies with a typical FIA system showed that the volume dispersion increased rapidly with a flow rate up to 0.6 mL min^{-1} but then leveled off (Vanderslice et al., 1981). Such results cannot be explained by Taylor's equations, which predict a steadily increasing dispersion when flow rate is increased. Numerical methods for solution of the equations governing the diffusion–convection process in the regions of interest in FIA have been applied by Vanderslice et al. (1981) to obtain the expressions in Eqs. (7) and (8) for the initial appearance of a peak at the detector (travel time t_a), and the total time of observation of the peak (i.e., baseline to baseline, Δt_B):

$$t_\text{a} = \frac{[109a^2 D^{0.025} (L/q)^{1.025}]}{f} \tag{7}$$

$$\Delta t_\text{B} = \frac{[35.4a^2 f (L/q)^{0.64}]}{D^{0.36}} \tag{8}$$

where q is the flow rate, L the tube length, D the diffusion coefficient, a the radius of the tube, and f an empirical factor that varies with experimental conditions between 0.5 and 1.0. Equations for relating peak width to injection concentrations for single-line and merging-stream manifolds can be found in Tyson (1986).

The magnitude of the dispersion in a practical system is dependent on the operating parameters, including sample volume, tubing bore size and length, and flow rate. By varying these parameters, the dispersion may be controlled, and this allows optimization of individual flow-injection systems (Ranger, 1981). Limited dispersion is appropriate when FIA systems are used with detectors such as ion-selective electrodes or atomic absorption spectrometers at high sample rates. Medium dispersion is often appropriate for color development in colorimetric applications. Finally, large dispersion

can be utilized to give a substantial degree of mixing between sample and carrier stream to form a well-developed concentration gradient, e.g., for performing continuous-flow titrations (Ranger, 1981).

Sample dispersion decreases with decreasing flow rate, and when the latter is zero, dispersion virtually ceases. This is exploited in so-called stopped flow measurements, which increase reaction times and thus may improve the sensitivity of the determination.

C. Discrete Analysis

Discrete or batch analyzers are designed to simulate the operations commonly used in manual procedures and can be complex in design. In contrast to CFA, in which each sample in turn traverses a common pathway of tubes to a detector, in discrete analysis each sample usually is contained in its own particular test tube or reaction vessel until it reaches the detector. In a typical integrated system, disposable plastic cups containing the samples are loaded, together with reaction tubes, into racks on a conveyor. A predetermined aliquot of sample is transferred by means of a pneumatic or motor-driven syringe into the tube. One or more reagents are dispensed in a similar manner, and the mixture is stirred mechanically. The time interval between additions may be programmed to allow the necessary reactions to take place. During this sequence of operations the tubes may be immersed in a constant-temperature water bath to standardize reaction conditions, if necessary. The solution is finally pumped into the flow cell of a spectrophotometer for absorbance measurement, and then to waste.

In many applications of the discrete analysis principle, only one or two of these operations may be employed. For example, automatic dispensing and dilution of samples may be all that is required prior to determination of metal ions by flame photometry or atomic absorption spectrometry. For pH determinations, the automated steps could include the addition of water or calcium chloride solution to the soil, stirring, and insertion of the pH electrode into the suspension. In general, the large integrated analyzers are intended mainly for clinical chemical applications, although they can be adapted readily to a variety of other uses, whereas the simpler dispensers, diluters, and samplers are the instruments that have become more readily adopted for agricultural and environmental analysis.

It is worth mentioning briefly here that, for the processing of relatively small numbers of samples, programmable microprocessor-controlled dispenser/diluters may be used inexpensively for semiautomatic direct colorimetric analysis. For example, a 5 mL teflon tube may be used to suck up, in sequence, 0.5 mL of sample, 0.5 mL of reagent, and 1 mL of buffer, each segregated by a small uptake of air. These may then be dispensed

directly into disposable plastic spectrophotometer cells along with, say, 0.5 mL of deionized water, and the absorbance measured. The authors have used such an approach successfully for the determination of phosphate and boron in water samples. Mixing conditions differ appreciably from those associated with manual mixing in volumetric flasks, so the standards should be prepared using the same procedure. A time delay may be necessary prior to absorbance measurement.

III. PRACTICAL SYSTEMS: CONTINUOUS-FLOW ANALYSIS

A. General Aspects

Initially the only commercially available CFA equipment was the AutoAnalyzer produced by the Technicon Instruments Corporation, Tarrytown, New York. This evolved over the years into the system currently marketed by Bran & Luebbe (Norderstedt, Germany/Buffalo Grove, IL, USA). Several conceptually similar systems are now available from different manufacturers. Most continuous-flow systems can be separated into four distinct but linked modules (Fig. 5). These include an automatic sampler, a peristaltic pump, an analytical unit (otherwise known as a ‘‘cartridge’’ or ‘‘manifold’’), in which reagents and sample are mixed in glass coils and reactions take place, and finally a detector and a data-recording system, usually nowadays a PC (Figs. 5 and 6).

Because of the modular nature of CFA apparatus, it is perfectly feasible to assemble a system, or part of it, utilizing existing laboratory apparatus such as a conventional spectrophotometer. Accessories that perform specific functions such as heating baths, dialysis blocks, and

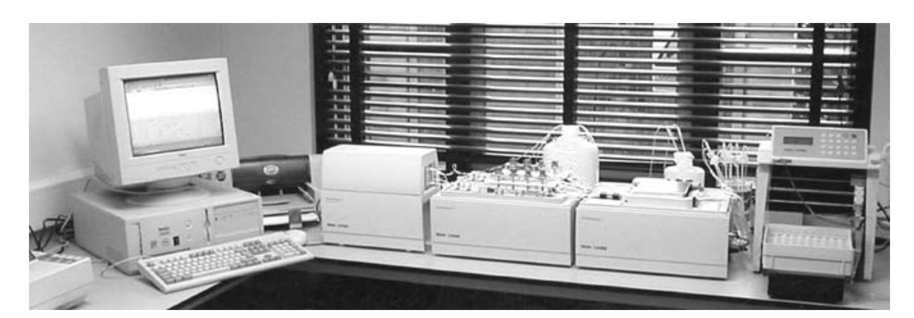


Figure 5 A typical modern segmented continuous-flow analysis system in the laboratory of one of the authors. From right to left: autosampler, 2-speed peristaltic pump, analytical unit or manifold, colorimeter, and PC/data processing and control station.

Marcel Dekker, Inc.
270 Madison Avenue, New York, New York 10016

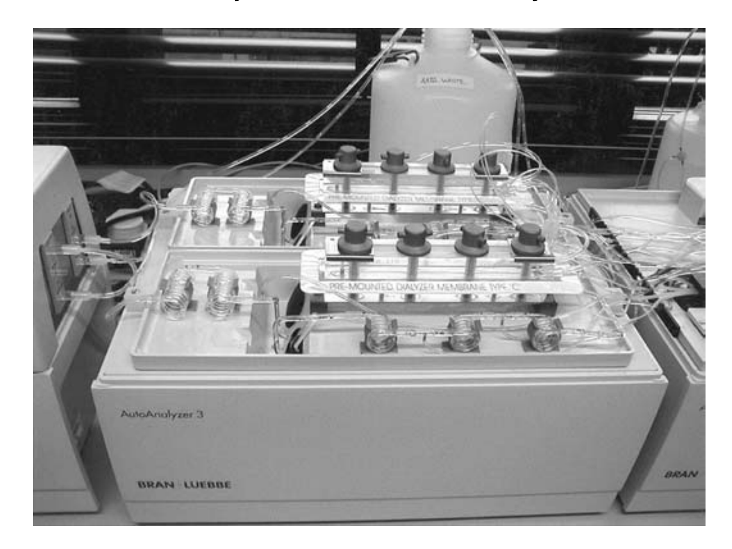


Figure 6 Close-up of a typical modern segmented continuous-flow analysis system analytical unit or manifold, including dialyzers (perspex blocks to front and rear), and a heating coil out of sight below the front dialysis block.

oxidation chambers are available separately. However, it is important to understand that considerable attention to detail is necessary if stable output is to be obtained, particularly in the context of the manifold components and how they are connected together. It should not be forgotten that manufacturers have a wealth of experience in this respect. The less experienced often find that assembling their own manifold, and getting it to function adequately, takes appreciably longer than anticipated!

B. Pumps and Tubing

The regular flow of samples and reagents through a continuous-flow system is most commonly achieved using a single-speed peristaltic pump (Fig. 7) in combination with tubes of various diameters. However, a two-speed pump such as that in the Bran & Luebbe AutoAnalyzer 3, with a higher rate for system flushing, is advantageous. The need for a regular flow rate, to achieve a stable detector signal, is generally more important than the absolute value of the flow rate achieved. The accurate proportioning of sample and reagents is achieved using tubing differing in internal diameter. Standard pump tubing is made from extrusions of polyvinyl chloride manufactured to very fine tolerance limits and also treated to relieve mechanical stress. Two grades of this tubing are commonly available: the normal grade, with

Marcel Dekker, Inc.
270 Madison Avenue, New York, New York 10016

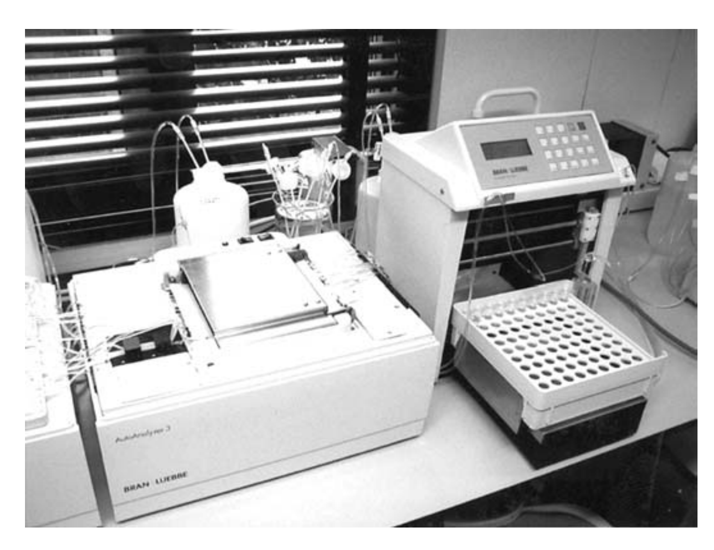


Figure 7 Closer view of the 2-speed peristaltic pump and the autosampler shown in Fig. 5. The steel plate compresses the pump tubes (flow from right to left) at a factory-set pressure against a set of moving and revolving steel rollers, thus trapping and pumping slugs of liquid between each adjacent pair or rollers.

internal diameters ranging from 0.13 mm (0.005 in.) to 2.79 mm (0.110 in.) (Table 1), which is usually quoted with approximate flow rates, and the more expensive flow-rated grade, in which the tubes have precise flow rates varying from 0.015 to 3.90 mL min^{-1} at the normal AutoAnalyzer pump rate. Colored identification tags, usually 152 mm apart (or in the case of the Bran & Luebbe Traacs system, 65 mm apart), indicate the internal diameter (Table 1). A range of chemically resistant pump tubes is available. Those recommended for use in the Technicon AutoAnalyzer 2 and 3 systems are shown in Table 2.

If a pump tube is incompatible with a given liquid, it may swell, crack, or snake, or may become cloudy or brittle, or turbidity may develop in the liquid as constituents leach from the tube. Invariably the tube life will be much reduced. The compatibility of tubing for a given solvent may be tested by immersing a short length in the solvent for about 30 min. If there is no sign of swelling or softening, the next step is to proceed with a dynamic test, by fitting a pump tube of the same material and pumping the solvent through it for 20–30 min. Then the flow rate should be measured by pumping into a graduated cylinder for 5–10 min. After pumping with the same tube for an hour or more, the flow rate should be checked again. If the two values are similar, rapid degradation of the tube has not occurred

Table 1 Internal Diameters and Colors of Identification Tags on Pump Tubes Used in Continuous-Flow Analysis

Tube no.			
Acid resistant/ solvent resistant	Silicone	Internal diameter (mm)	Tag colors
−01	—	0.13	Orange and black
−02	—	0.19	Orange and red
−03	—	0.25	Orange and blue
−04	—	0.38	Orange and green
−05	—	0.51	Orange and yellow
−06	−07	0.64	Orange and white
−07	−08	0.76	Black and black
−08	−09	0.89	Orange and orange
−09	−10	1.02	White and white
−10	−11	1.14	Red and red
−11	−12	1.30	Gray and gray
−12	−13	1.42	Yellow and yellow
—	−01	1.47	Clear and clear
−19	−14	1.52	Yellow and blue
−13	−15	1.65	Blue and blue
−14	−16	1.85	Green and green
−15	−17	2.06	Purple and purple
−16	−18	2.29	Purple and black
−17	−19	2.54	Purple and orange
−18	−20	2.79	Purple and white

(Technicon Instruments Corp., 1972). An alternative approach for pumping chemically aggressive solvents is to use physical displacement. In this approach the problem solution is introduced by pumping an immiscible liquid with much higher or lower density, and which does not degrade the tubing, into a stoppered flask containing the solution. The displaced solution then passes on to the manifold in the normal way.

Temperature affects chemical resistance; the recommendations given in Table 2 apply at room temperatures only. By diluting a solvent with a relatively inert diluent, it is possible to decrease chemical effects on the tube. Tubes may have a life of up to 500 h, but this is not precise and depends upon the quality of tubing and the working conditions imposed on the tubing. It is sensible to keep a log showing tube replacement dates and amount of operating time, as a basis for a routine replacement schedule. On occasion, some environmental samples may result in microbial growth in manifold

Table 2 Tubing Types Recommended for Specified Solvents

Tubing type	Solvent/solution
Clear standard (polyvinyl chloride)	acetaldehyde (dilute) dilute mineral acids (to 50%) except HF aqueous solutions formaldehyde glycerine glycol sodium hydroxide water
Silicone	acetic acid (95%) acetone alcohols (low molecular mass) dioxane pyridine
Acid-resistant	acids (> 50%) benzene chloroform ethylene dichloride styrene toluene trichloroacetic acid xylene
Solvent-resistant	carbon tetrachloride hexane MIBK-ethanol (50%–50%) methanol, ethanol, propan-2-ol

pump tubes. Flushing with an appropriate biocidal agent may then be necessary prior to periods of prolonged instrumental inactivity.

In the Technicon Monitor 650 system, developed for industrial process control and monitoring pollutants in effluents, pump tubes are replaced as a unit by means of a "Tech-Fit" quick-disconnect device. For each new determination, the entire pump harness is removed and replaced by a new preassembled one.

Transmission tubing is available for connecting individual parts of the system, and similar considerations of solvent tolerance should be applied as for pump tubes. Glass transmission tubing is recommended, and the internal diameter of tubing, coils, and fittings should be the same, or at least within ± 0.2 mm. Plastic transmission tubing or sleeving should not be used for

pump tubes because of the greater dimensional tolerances and lack of stress relief.

A wide variety of single and multiple way connectors is available for use in manifolds. Some examples are shown in Fig. 8. Connectors are available with a metal capillary side arm or with small or wider bore glass side arms. The precise connector used depends on the flow rate of the reagent being introduced. Use of an inappropriate connector adversely affects the smoothness of the air segment (bubble) pattern and hence the output stability. Many multiple connectors with four or more connection points are available. Minimizing the number of tubing connectors promotes a smoother bubble pattern. Debubblers are specially designed T connectors that remove air plus a small fraction of the total liquid flow, to produce the nonsegmented flow required by some manifold devices such as cadmium reductor columns.

C. Analytical Unit

The analytical unit (or manifold) is where the sample and reagent streams are combined and mixed, any specific treatment stages being included. Individual analytical units vary in their complexity, the simplest form containing only mixing coils to facilitate mixing and allow sufficient time of color development. Mixing coils are usually made of glass, except when alkaline solutions are being pumped at elevated temperatures, for which application Teflon or Kel-F coils are available. Increasing complexity of

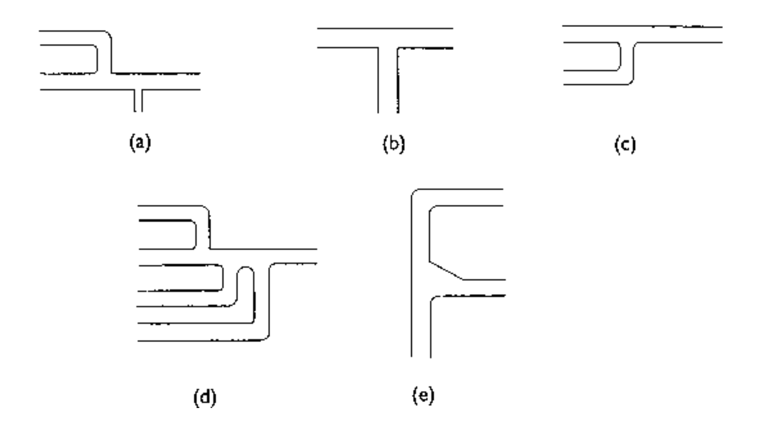


Figure 8 Some typical examples from the very wide range of available connectors, and a debubbler. (a) Connector with metal capillary side arm; (b) and (c) standard-bore connectors; (d) multiple connector with standard bore side arms; (e) debubbler.

units may result from a requirement for temperature control via a heating bath, or sample pretreatment, such as dialysis (Fig. 6) or photochemical oxidation of organic species in a quartz (u.v.-transparent) coil positioned around a tubular mercury discharge lamp. In multichannel analyzer systems the times of arrival of different streams at the detectors can be adjusted using phasing or delay coils. Ready-made analytical units for particular applications are commercially available or can with care and experience be self-assembled to meet particular needs. Obtaining suitable rates of flow and proper mixing are essential when doing any self-assembling.

A useful development by Bran and Luebbe over recent years for cost-conscious laboratories with modest sample throughput requirements has been the design of manifolds suitable for sequential determination of several components of a sample, or indeed of different samples. For example, ammonium, nitrate, and several other ions may be determined on a single manifold simply by changing reagents and colorimeter filters.

D. Samplers

An automatic sampler normally consists of a motor-driven carousel with space for somewhere between 20 and 160 cups, each typically of 2- or 4-mL capacity. Sample and standard solutions are removed in sequence and aspirated into the continuous-flow system. The sample probe then returns to a reservoir wash solution for a period, so that successive samples are separated in the flow system by the wash solution. Programming the movement of the sampling tube and the sample cups ensures that solutions are sampled in the desired sequence.

The sample probe, which is usually made from stainless steel (unless strong acids are present in the samples), is connected to the sample pump tube via a short length of polyethylene tubing. This is used in preference to other materials because of its nonwetting properties and should be the same diameter as the sample tube or of smaller diameter.

The sample-to-wash ratio is an important analytical variable and should be adjusted according to the requirements of the method being employed. For optimum results, the minimum sampling time is that taken for the recorder or computer trace of the most concentrated standard to reach a plateau and remain there for 5 s. The time taken for the recorder to return to the baseline gives the maximum wash time. For most analyses, it is not necessary to have complete resolution of the individual peaks, and the wash time can be reduced progressively to the point where significant interference between a sample of high concentration and a following one of low concentration is just avoided. A typical recorder trace of adequately resolved peaks is illustrated in Fig. 9.

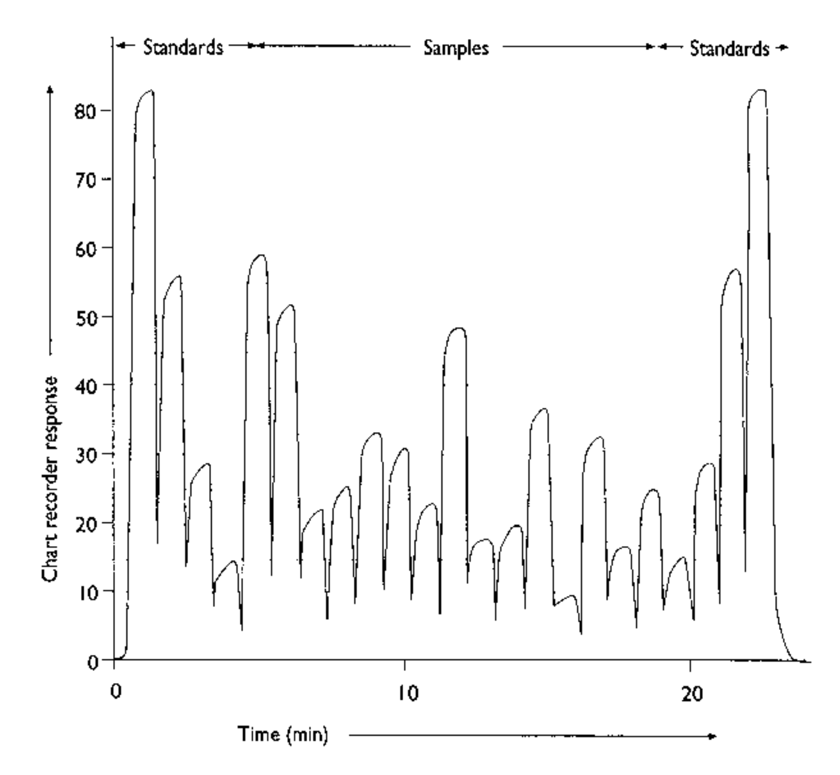


Figure 9 Recorder trace of adequately resolved peaks in segmented continuous-flow analysis (of ammonium in water samples). Standards are 0.5, 1.0, 1.5, and 2.0 μg N mL^{-1}. Analysis rate was ca. 40 samples per hour.

E. Other Modules

Several items of equipment developed to perform specific functions for CFA are available, and three of the most commonly used ones are discussed.

1. Dialyzer

Dialysis provides a convenient method of separating the determinant in the analyte solution from interfering materials such as strongly colored humic substances or suspended matter. It is also useful in reactions where colloids or precipitates are formed and can be used as an alternative to a dilution/recycling stage when sample concentrations are too high. A dialyzer is usually constructed from thick acrylic blocks (see Fig. 6) containing matching grooves up to 60 cm in length, with a membrane, usually made of

Marcel Dekker, Inc.
270 Madison Avenue, New York, New York 10016

cellulose acetate for solutes and PTFE for gas exchange, sandwiched between the blocks. The segmented stream containing the sample is pumped through the groove above the membrane, while a segmented receiver stream (of similar composition, except for the determinant) flows at a similar rate below. The determinant passes through the membrane and reaches a concentration in the receiver stream proportional to the concentration in the original sample. The rate of dialysis for a particular determinant is a function of the membrane and flow properties and path length.

2. Reductor

A common method for determining low concentrations of nitrate in water and soil extracts involves its reduction to nitrite, which is then determined colorimetrically. A method using copperized cadmium for this reduction was first applied to soil extracts by Henriksen and Selmer-Olsen (1970). The reductor is included in many of the standard analytical cartridges for nitrate determinations. It can also be constructed in the laboratory by packing a small glass tube with 40–60 mesh (250–420 μm) cadmium that has been stirred briefly in copper sulfate solution. The solution enters the bottom of the reductor tube after passing through a debubbler (Fig. 8e). Gas bubbles may form in the column after prolonged use. When this occurs, they can be removed by locating a debubbler after the reductor column (Henriksen and Selmer-Olsen, 1970). Air is then reinjected into the stream in the normal controlled manner to create a segmented sample once again.

A minor drawback to the use of the cadmium reductor column in segmented flow analysis is that it increases dispersion and thus slows the permissible sample throughput rate unless correction is made carefully for any carryover between subsequent samples. For this reason some analysts prefer to use hydrazine at carefully optimized concentration as a reductant for nitrate.

3. U-V Digestor

Soluble organic matter is a common constituent of natural water samples and soil extracts. It can be distinguished from inorganic forms of carbon (carbonates and bicarbonates) by acidification and purging the resulting carbon dioxide derived from alkalinity. Subsequent oxidation of organic carbon can be achieved by passing the extract through a U-V digestor unit. Usually the oxidation module consists of a long helical silica coil surrounding an axially mounted U-V lamp, and an oxidant such as persulfate.

Recent interest in quantifying N (Agren and Bosatta, 1988; Yesmin et al., 1995) and P (Broberg and Persson, 1988; Ron Vaz et al., 1993) budgets for terrestrial and aquatic ecosystems has led to a requirement for the determination of the N and P present in soluble organic forms. This is achieved usually by running samples with and without a U-V oxidation step (Ron Vaz et al., 1992; Yesmin et al., 1995). The organic forms are calculated by the difference between the total N or P determined after digestion and the sum of inorganic forms of the elements. For nitrogen the equation is

$$\text{Organic N} = \text{total N} - (\text{nitrate N} + \text{ammonium N})$$

F. Measuring Instruments

The liquid stream emerging from the manifold must enter a measuring instrument to allow the parameter proportional to the determinant concentration to be measured and recorded. For multiple analysis on the same sample, the sample stream is split, and two or more manifolds and/or detector systems are operated in parallel. Colorimetry remains the most commonly used detection system in routine analysis, although a wide range of other techniques has also been employed in practice. Some of these are discussed briefly below.

1. Colorimeter or Spectrophotometer

A colorimeter of spectrophotometer measures the transmission of monochromatic light through a solution or colored species that absorbs at the wavelength of the light. The relationship between transmission and concentration is given by the Beer–Lambert law:

$$I_{\mathrm{t}} = I_0\, e^{-kcd} \qquad (9)$$

where I_{t} and I_0 are the intensities of the transmitted light and the incident light, respectively, c is the concentration of the absorbing species (moles per liter), k is its molar extinction coefficient for the particular wavelength, and d is the path length of the light through the solution. Rearranging Eq. (9) and taking logarithms, we obtain

$$-kcd = 2.303 \log\left(\frac{I_{\mathrm{t}}}{I_0}\right) \qquad (10)$$

The value of $-\log(I_t/I_0)$ is termed the absorbance, A, or the optical density of the solution. Absorbance is thus directly proportional to concentration. Thus

$$A = -\log\left(\frac{I_t}{I_0}\right) = Kc \tag{11}$$

The Beer–Lambert law applies to monochromatic radiation and to low concentrations at which there is no interaction between absorbing species. In practice, using filters, prisms, or gratings, it is impossible to obtain perfect monochromatic radiation. However, the narrower the band that can be obtained, the more closely experimental data conform to the law (Prince, 1965). Departures from a linear relationship may occur in systems involving ionization or dissociation equilibria that may be affected by such factors as pH and dilution, or when high concentrations cause changes in the refractive index of the solution (Prince, 1965; Allen et al., 1974). Absorbance is calculated electronically from the measured transmitted light intensities for blank and sample solutions. Where curvature of the calibration curve does occur, the graph is usually deflected toward the concentration axis at higher concentrations.

Continuous-flow analyzers are equipped either with a photomultiplier and a monochromator adjustable to any wavelength in the 300–800 nm range or, more commonly, with a colorimeter containing a filter of the desired wavelength for a particular determination and a simpler, less expensive detector. Multichannel colorimeters make it possible to carry out up to six or even eight determinations in parallel. Fiber optics may be used to ensure efficient light transfer from the flow cells to the phototube detectors. Standard laboratory spectrophotometers equipped with flow cells also may be used as detector systems.

a. Flow Cells. These are usually about 1.5 mm in internal diameter, with a path length of 15–50 mm. These dimensions are considerably smaller than those of the cells used with the original AutoAnalyzer systems, and consequently much smaller flow rates are needed to wash them out.

The segmented sample stream may be debubbled before entering the flow cell (Fig. 10). Alternatively, the bubbles may be allowed to pass through, using an electronic control to prevent the recorder response from oscillating in response to the intermittent signal. This approach has been adopted successfully in several commercially available systems such as the Traacs. It works very satisfactorily provided flow conditions are stable and the bubble pattern is regular.

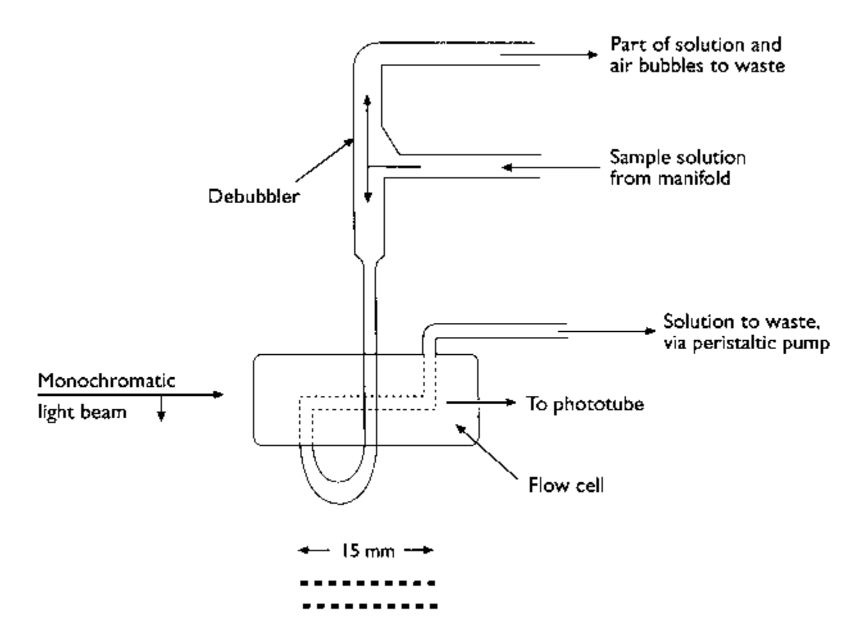


Figure 10 A flow cell with an external debubbler.

b. Turbidimetric Methods. Colorimeters or spectrophotometers may be used for turbidimetric determinations such as that of sulfate as barium sulfate (Sinclair, 1973). Barium chloride solution containing a suspension-stabilizing agent such as gelatine or polyvinyl alcohol is added to the sample, and the apparent absorbance caused by the barium sulfate suspension is measured in the flow cell. The technique requires precautions to minimize adsorption of barium sulfate on the flow cell wall, which causes recorder baseline drift.

2. Flame Photometers and Atomic Absorption Spectrometers

Flame photometers are used in conjunction with continuous-flow systems principally for the determination of sodium and potassium, while atomic absorption spectrometers provide the most satisfactory, relatively inexpensive way of determining calcium and magnesium.

Both atomic emission and absorption spectrometry measure the total amount of an element in the sample as presented. The purpose of the continuous-flow system here is to allow automation of sampling, dilution, and transfer to the nebulizer–burner assembly. A major advantage of the continuous-flow system is that it is capable of making large-order dilutions with a high degree of accuracy and consistency. The air-segmented stream

must be debubbled before being aspirated to maintain a stable output. The final solution delivery rate to the spectrometer should be close to its normal aspiration rate. If it is too slow, the solution may become disrupted in the nebulizer capillary, leading to noisy signals. Starvation feeding of nebulizers is however sometimes used to reduce interferences or to improve linearity of calibration graphs. The extent of interference is reduced because the nebulizer energy is distributed over less solution per unit time. This produces a finer aerosol, which in turn produces smaller residual solid particles, which are more readily atomized.

3. Nephelometry

The determination of sulfate may be carried out by nephelometric (light scattering) methods instead of the turbidimetric method referred to above (Ogner and Haugen, 1977). A nephelometer is essentially a modified fluorescence spectrophotometer (or fluorimeter) in which a square glass or quartz flow cell is used to reduce the background scattering to an acceptable level. A light beam that falls on the flowing stream is scattered by the suspended particles of barium sulfate, and some of the scattered light passes to the detector.

4. Applications of Chemiluminescence Detection

A review by Bowie et al. (1996) of the analytical applications of chemiluminescence in the liquid phase cited 160 references from the early 1990s, indicating the increasing acceptance of chemiluminescence as an analytical tool. Continuous-flow methodology lends itself very readily to chemiluminescence systems, because of the high reproducibility of both timing and mixing conditions of reactants. Combining the tools can result in some impressively low detection limits, some of which have been exploited in environmental analysis. For example, Cannizzaro et al. (1999) have described the use of the pyrogallol–hydrogen peroxide–sodium hydroxide reaction in the presence of methanol and a surfactant for the determination of Co and Fe in coastal and estuarine waters. Detection limits were 5 and 40 pM, respectively, for Co(II) and Fe(II+III). The equipment was evaluated in surveys of the Tamar Estuary in S.W. England. Carretero et al. (2000) described the use of a spectrometer incorporating a two-dimensional CCD and fiber optic probes along with a continuous-flow system to measure Co(II) and Fe(II). The linear ranges were 50–700 and 150–600 $\mu g\,L^{-1}$ for the two species, respectively. A particularly interesting application of chemiluminescence detection/flow injection was the ship-board determination of hydrogen peroxide in the western Mediterranean

Sea (Price et al., 1998). Analysis time for a 12-sample depth profile (including standard additions) was only 45 min.

5. Ion-Selective Electrodes and Electrochemical Sensors

A wide range of ion-selective electrodes or probes is available, and these are finding increasing application in continuous-flow systems. Precision is often better with continuous-flow than with manual methods, because of the greater standardization of the conditions.

To incorporate the ion-selective electrode into a continuous-flow system, it is normally fitted into a flow-through cap or cell. When a separate reference electrode is required, this can be located in a reservoir downstream from the indicator electrode, so that the cell dead volume can be kept as small as 5–10 μL (Hansen et al., 1977). It is sometimes necessary to debubble a segmented stream before it enters the detector cell to avoid an erratic response. However, the ammonia probe has no external reference electrode, and the partial pressure of ammonia in the air bubbles is in equilibrium with the solution, so a steady response can be achieved without debubbling. Ion-selective electrodes are useful for the automated determination of Ca and F in freshwaters and have been used for routine monitoring of these determinants in borehole waters (van Staden and Stefan, 1999). Liu et al. (1992) described a potentiometric detection system for FIA that did not involve the use of a conventional reference electrode. Instead they used two ion-selective electrodes in parallel, and the sample was injected into two carrier streams alternately. The approach was applied to the determinations of potassium and nitrate in soil extracts, fluoride and nitrate in natural waters, and sodium and potassium in natural waters.

Anodic stripping voltammetry (ASV) can also be used as a sensor in CFA. Van Staden and Matoetoe (2000) have used a glassy carbon electrode for the simultaneous determination of Cd, Cu, Pb, and Zn by differential pulse ASV (DPASV), using pyrophosphate solution at pH 4 as a supporting electrolyte. Working ranges were in the tens to hundreds of $\mu g\,L^{-1}$ range. DPASV in a flow configuration has also been used for speciation of Fe(II) and Fe(III) (van Staden and Matoetoe, 1998). Adsorptive cathodic stripping voltammetry (AdCSV) has been employed for the automated determination of Ni in estuarine waters, in a manifold incorporating on-line filtration and U-V digestion (Whitworth et al., 1998); 37 measurements could be made over 13 h.

An amperometric detector has been advocated for the determination of cyanide down to $2\,\mu g\,L^{-1}$ in water and wastewater samples (Solujic et al., 1999); the system was based on segmented flow with injection and photochemical digestion on line. The RSD was 1.5% and mean spike recovery was 101.0%.

G. Optimization of Analytical Conditions

1. Sensitivity

To improve the sensitivity of an analytical system, a number of conditions may be altered:

1. Sample uptake rate may be increased by increasing the diameter of the sample pump tube, and reagent concentration can be increased to counteract the resulting dilution of the final reaction mixture. However, care must be taken to check that changes in amounts of sample components other than the determinant do not adversely affect the manifold chemistry. This is best confirmed by the analysis of certified reference materials.
2. The path length of the flow cell may be increased, because according to the Beer–Lambert law the absorbance is directly proportional to path length. This is not always possible with some commercially available systems.
3. When a reaction is dependent on elevated temperatures or takes a considerable time, the temperature of the heating bath can be raised, a larger volume heating coil can be used, or a time-delay coil can be added to allow the reaction to progress further. Again checks should be made to ensure that the changes made do not adversely affect selectivity.
4. When dialysis is involved, the path length can be increased, the temperature increased, or a more permeable membrane substituted for the one normally used.

2. Accuracy and Precision

a. Absorbance. For greatest accuracy, it is desirable that absorbance should be about 0.4 unit, because this is near the point at which photometric error is minimized (Technicon Instruments Corp., 1972). This is obviously much easier to accomplish for samples that are of similar concentration than for those for which the concentration varies widely, and repeated analyses after dilution may be desirable for samples that give rise to very high absorbance.

b. Drift and Noise. Calibration drift may occur due to changes in baseline and/or changes in method sensitivity. Changes in ambient, module, or reagent temperatures may cause changes in mass flow rates and hence in mixing ratios. Stray light becomes a problem if it changes. Manifold tube stretching with aging, coating of the flow cell with precipitate or adsorbed reagent, and reagent degradation may also be problems. Instrumental drift

Marcel Dekker, Inc.
270 Madison Avenue, New York, New York 10016

should not be a problem in a well-designed instrument. Attempts should be made to eliminate the cause of drift, e.g., when coating occurs, wetting agents can be employed to overcome the problem.

When drift cannot be eradicated, mid-range standards and water blanks should be inserted at intervals to monitor it, so that appropriate compensation may be made. The compensation can be applied automatically on modern PC-controlled systems, although it is still up to the analyst to make sure that an appropriate number of drift correction standards is applied. At very low concentrations these drift correction standards should not be applied, because the lower precision of measurement may then result in over compensation or even totally spurious corrections in extreme cases.

If recorded signals or the baseline are noisy, all fittings and connections should be checked to ensure that joints have been made properly. Uniformity of air-bubble injection should also be checked, transmission tubing made as short as practicable, and wetting agents used when appropriate. With care, manifold glass/metal components rarely need replacing. However, if they do, it is important to use precisely manufactured components, even if this proves a little more expensive in the short term. Inferior components can result in increased gaps in joints, which may be a source of bubble nucleation or intermittent bubble trapping, and hence a source of instability.

c. Sample and Wash Times. The sampling time needs to be long enough to allow a response plateau to be sustained for at least 5 s. If a digital printer is to be used, then a few more seconds should be added. Interaction between samples (carryover) may be checked experimentally by analyzing several high-concentration samples and then several low-concentration samples, alternately. If the second low sample produces a lower peak than the first, or if the second successive high sample is higher than the first, the wash time should be extended until all peaks from replicate samples agree within the limits required. Alternatively, the percentage carryover can be measured and a carryover correction factor applied. This works adequately unless the range of determinant concentrations is very large.

IV. PRACTICAL SYSTEMS: FLOW-INJECTION ANALYSIS

A. General Aspects

The basic components of an FIA system are an autosampler, a pump, a sample injection valve, an analytical manifold, and a detector/readout system. Autosamplers, several types of flow-through detectors (e.g., spectrophotometers, ion-selective electrodes, atomic absorption spectrometers), and units such as dialyzers are similar to those used in CFA systems and are not

considered further here. The major differences from CFA apparatus are the presence of an injection valve for the introduction of the sample into the liquid stream, and the use of tubing with much smaller bore. A very simple example of a FIA assembly is shown diagrammatically in Fig. 11.

In comparison with air-segmented continuous-flow analysis, FIA has a number of desirable characteristics (Riley and Rocks, 1983):

1. FIA has shorter solution retention times in the analytical manifold, which means that the speed at which results are produced is fast (Fig. 12) compared to that in most segmented flow systems. This is primarily because in FIA there is no need for chemical equilibrium and full color development to be attained to obtain a reliable analytical result. According to Ranger (1981), timing is the most important parameter to control in FIA to ensure precision. This requires a high-precision injection valve and reproducible and stable slow rates of pumping.
2. FIA has a smaller demand for reagents and, normally, sample, particularly when the merging zone technique is used (Bergamin et al., 1978). Sample and reagent for this system are injected into separate carrier streams that meet at a confluence where they mix partially. They then pass through a coil to promote further mixing and reaction. Thus only sufficient reagent is introduced to meet the needs of the sample, whereas the washout is achieved by the inexpensive carrier-stream solution.
3. FIA is ready for use almost immediately after startup, whereas CFA systems require several minutes of operation for the baseline to stabilize.

Some of the most important practical aspects of FIA are outlined in the following sections. A more detailed discussion of FIA theory and

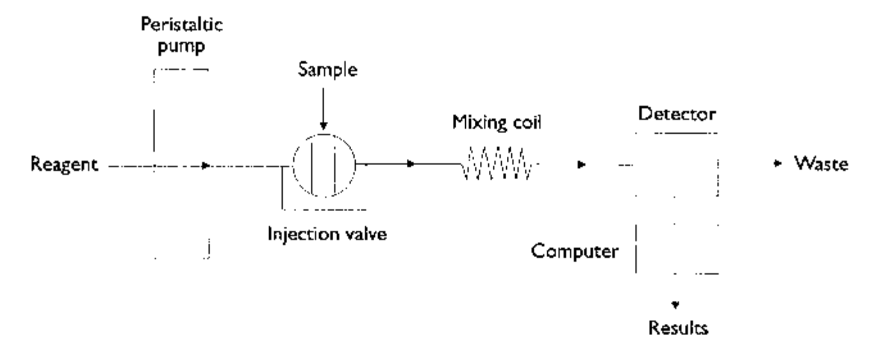


Figure 11 An example of the simplest type of single-channel FIA system.

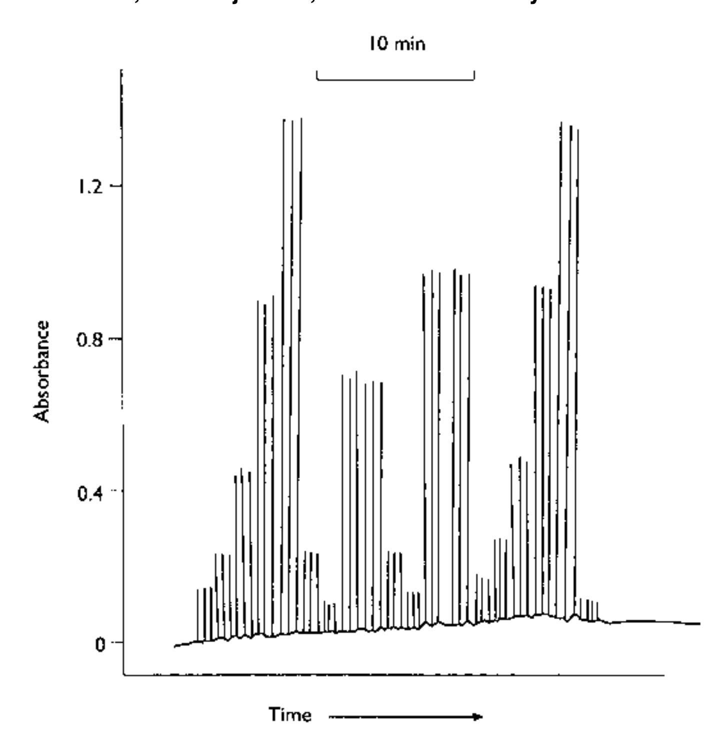


Figure 12 A typical FIA detector output trace if a chart recorder is used. The run here starts with 5 standards run in triplicate, followed by 8 samples also run in triplicate, and a repeat of the standards. More often now a PC is used, and the shape of individual peaks may be examined in detail if desired before the concentration is printed out directly for each sample. Single standards are analyzed periodically in a large batch of samples to check/compensate for sensitivity drift.

practice may be found in the book by Růžička and Hansen (1981) and the proceedings of an international conference (Macdonald et al., 1986).

B. Pumps, Tubes, and Coils

The maintenance of a reproducible and regular flow rate is equally as important in FIA as it is in CFA, and a variety of pump systems have been tried. In general, peristaltic pumps are most commonly used, together with the same types of vinyl or silicone flow-rated tubing as are used for CFA (see Table 2). The use of pumps originally intended for working against much higher back pressures (such as those used in HPLC) is also satisfactory in some situations (Wolf and Stewart, 1979). Some caution is required under

conditions of low or even negative back pressures encountered when the FIA system is coupled to an atomic absorption spectrometer (i.e., when there are sometimes no mixing coils to create a resistance to flow). In such circumstances, back pressure may be created artificially by including a length of fine-bore tubing between pump and injector (Yoza et al., 1979).

All connecting tubes, manifolds, and mixing coils are of narrow bore (commonly 0.4–1.0 mm). Mixing coils are usually made from rigid polyethylene, tygon (vinyl), or teflon. If elevated temperatures are required, the coils (and reagent reservoirs) may be immersed in a constant-temperature vessel.

C. Injection Valves

Sample injection into the moving stream of reagent is by means of a rotary or sliding switching valve, which is actuated pneumatically or electrically. The sampling loop of a six-port, two-position valve is filled by pumping sample from a cup on the autosampler while the preceding sample is passing through the manifold. The valve is then switched to the alternate position, diverting the carrier stream through the loop and pushing the sample as a "plug" into the manifold. Usually, the parts of valves coming into contact with the solutions are made from inert fluorocarbon (Tyson, 1985).

Sherwood et al. (1985) and Riley et al. (1983) have described the use of a valveless injection technique to introduce very small sample volumes into the FIA manifold. The technique, called controlled dispersion analysis, uses a computer-controlled peristaltic pump and aspiration probe. To introduce a sample, the pump is stopped, the probe transferred from carrier to sample, the pump activated to draw up the desired volume, and then it is stopped again; the probe is returned to the carrier, and finally the pump is restarted. This avoids the loss of sample that occurs with valves, as a certain volume is needed to fill the connecting lines and flush out the preceding sample (Tyson, 1985).

D. FIA/Atomic Absorption Spectrometer Systems

Flow-injection analysis equipment can be used for the supply of sample solutions directly to a detector such as an atomic absorption spectrometer. Tyson (1985) and Fang et al. (1986) have reviewed this topic, and their conclusions about the positive attributes of speed and convenience of this powerful combination of methodologies are still valid today.

With a single-line manifold, simply choosing appropriate injection volumes and tube dimensions can achieve a suitable dilution of samples. Addition of an interference suppressant, such as lanthanum, is simply

Marcel Dekker, Inc.
270 Madison Avenue, New York, New York 10016

achieved by including it in the carrier stream with a substantial saving on the amount required compared with that for the manual method. The alternative way of adding reagents is to merge a reagent stream with the carrier stream at a confluence point. A more economical approach, in terms of reagent consumption, is to use the merging zones method (Tyson, 1985). More complex manifolds have also been devised, including systems with phase separators to allow the determination of elements such as Hg and Bi in gaseous form, Hg as the cold vapor (De Andrade et al., 1983; Murphy et al., 1996; Sakuma et al., 1999) and Bi as the hydride (Aström, 1982). For Hg, lower detection limits can be obtained by atomic fluorescence spectrometry (AFS) than by AAS. Bloxham et al. (1996) described a FIA system for determination of Hg in filtered sea water that used on-line bromide-bromate oxidation in a heated reaction coil to convert organic Hg to Hg(II), AFS as a detector. The system was used to measure Hg concentrations in samples from Sutton Harbour, Plymouth in the 20–60 ng L^{-1} concentration range.

The use of FIA as a system for feeding sample solutions directly to atomic absorption spectrometers (or other detectors such as ion-selective electrodes; see, e.g., Couto and Montenegro, 2000) undoubtedly can give satisfactory results. However, it is sometimes an expensive and somewhat inflexible approach compared with the use of programmable discrete analysis systems discussed in Sec. V. The relatively low cost of colorimeters compared with AAS for detection in FIA means that some workers even determine elements such as calcium and magnesium in natural waters and soil extracts by colorimetric FIA systems rather than by AAS (Nogueira et al., 1996).

V. PRACTICAL SYSTEMS: DISCRETE ANALYSIS

A. General Aspects

Discrete or batch analyzers have continued to improve over the past decade, and instruments designed to carry out a number of routine functions, such as pipetting, diluting, adding reagents, stirring, and transferring solutions to a flow cell or flame photometer, are available commercially. Many others have been purpose-built in laboratory workshops and described in the scientific literature. The functions of single pieces of apparatus vary much more widely than in the case of continuous-flow systems, which are essentially modular in construction. It is convenient to consider separately here the multistage analyzers that carry out a complete sequence of operations and those that are intended to perform one or two functions only.

B. Automation of Individual Processes

1. Sample Processors, Diluters, and Dispensers

Robotic sampling systems, coupled to increasingly powerful microprocessors, and diluters/dispensers with high-resolution stepper motors have made discrete analysis a very fast and accurate tool in analysis. The use of dual-syringe diluters, in which the relationship between sample and diluent syringe volumes can be optimized over a wide range, also enhances the precision and variety of tasks that can be undertaken with the modern discrete analyzer.

Two kinds of sampler are currently available, the robot arm type and the XYZ type with single or dual sampling heads. Of the two, the XYZ type is generally favored because of its simplicity and speed of operation, and because it is less prone to software problems and mechanical breakdown.

Systems utilizing integral microprocessors or stand-alone microcomputers demonstrate a high degree of flexibility in their programming and can have random access capabilities as well, i.e., the ability to repeat analysis of "dubious" samples or to dilute and rerun samples whose concentrations lie outside the calibration range. The introduction of a dual sampling head or even the use of multiple sampling probes can extend the analytical throughput to more than 1000 samples per hour, without reduction in analytical performance.

A range of sophisticated accessories is also available from a number of manufacturers, e.g., conductive liquid sensors to minimize contamination of the sampling probes, or bar-code readers to assist with the large numbers of samples being processed.

As well as being used for sample preparation, these instruments can also be coupled directly to analytical instruments such as colorimeters, atomic absorption and emission spectrometers, and inductively coupled plasma emission spectrometers. In this mode, one considerable advantage that discrete processes have, when compared with continuous-flow systems, is that results can be obtained virtually instantaneously at throughputs of up to 400 samples per hour.

Current techniques used for data capture in CFA involve recording electronically all the data relating to a particular analysis that have been recorded traditionally by a chart recorder. From this electronic record, the sample peaks are identified and results calculated, with corrections being made for any acceptable baseline drift. Discrete processors, by their very nature, produce near–square wave outputs (see Fig. 2a). When the system is interfaced to an external computer, two-way communication between the sample processor and the computer is possible. This simplifies both peak

identification and the end of data collection, with results being calculated and verified for quality-control tests during the rinse cycle.

2. Systems for the Determination of pH

The determination of soil pH is one of the most common tasks in soil analytical laboratories, and it is the type of repetitive operation that is admirably suited to automation. Commercial instruments dedicated to the determination of soil pH are few, but modifications can easily be made to linear or rotary multisamplers designed for automatic titrators.

Several laboratory-made systems have been described (Adamchuk et al., 1999). In one system (Baker, 1970), 500 polystyrene containers were mounted in rows of 10 on aluminum plates, which were joined to form an endless conveyor belt. A fixed volume of each soil for analysis was introduced into each of the containers in the ''loading area,'' together with a small plastic-covered bar magnet. As each row of containers moved forward stepwise, a fixed volume of distilled water was added automatically to each, and the suspensions were mixed by a row of magnetic stirrers under the belt, stirring continually for 12 min. Ten pH electrodes mounted on a Perspex plate were lowered automatically into the suspensions. Each electrode was switched in sequence to a pH meter interfaced to a digital voltmeter and printer. After the readings had been made, the containers were inverted and washed with distilled water, and the bar magnets collected in an aluminum mesh tray and recovered for reuse. The system was used to analyze 20,000 samples per year.

Goodman (1976) developed a system that could handle batches of 6 to 60 samples and used motor-driven glass paddles for stirring and a single electrode. The apparatus could be fitted not only with a pH electrode but also with an ion-selective electrode and was applied to nitrate determinations. The paddles were necessary to disrupt lumps of fresh soil that were used when nitrate was to be measured.

Grigg et al. (1980) described a system in which an LKB Radirac fraction collector rotator was fitted with a 60-position aluminum turntable carrying PVC sample cups. To $12\,cm^3$ soil samples 30 mL of water was added from a dispenser, 10 cups at a time. The cups were stored at constant temperature overnight and then loaded onto the turntable, together with cups of buffer solutions. Stirrers and a combination glass-calomel electrode, attached to a single beam, were lowered into each cup in turn by means of a motor-driven cam. After 40 s, a series of 12 measurements was made at 1 s intervals. A programmable calculator rejected the highest and lowest values, worked out the mean of the other 10, and adjusted the result for any instrument drift during a run of samples. After the measurements, the electrode was withdrawn and automatically washed by a water jet.

Marcel Dekker, Inc.
270 Madison Avenue, New York, New York 10016

The methodology described in the above paragraphs, though developed some time ago, is still applicable at the present time, and some laboratories still develop systems to meet their own specific needs when analyzing large numbers of samples. Nowadays automation of pH measurement is more likely to involve continuous monitoring of pH in the field, using pH electrodes connected to data loggers. For laboratory experiments with environmental systems, Hanna Instruments (Woonsocket, RI, USA) produce electrodes which can be very simply interfaced to a PC.

VI. APPLICATIONS

A. Nitrogen

1. Total Nitrogen and Ammonium in Environmental Materials

Wet chemical methods for the determination of total nitrogen in soils and plant material are commonly based on the conversion of nitrogen to ammonium ion, followed by measurement of the ammonium. The conversion to ammonium is achieved by Kjeldahl digestion, either manually using a block digester or in an automatic wet digestion device. The ammonium in the digests may then be analyzed by any of the alternative automated systems: CFA (Schuman et al., 1973; Searle, 1975; Markus et al., 1985; Tel et al., 1992), FIA (Krug et al., 1979), or discrete analysis. Many of the automated colorimetric systems employed have been in successful use for many years. On-line microdistillation units are available for use with both continuous and flow-injection systems. Ferreira et al. (1996b) described a gas diffusion unit for the measurement of ammonia in soil digests for total N determination by FIA. A purpose-built tubular ion-selective electrode was used as detector.

A commonly used colorimetric method for ammonium in soil digests and extracts is the indophenol method, in which the ammonium present produces a blue color with alkaline phenol and sodium hypochlorite (Schuman et al., 1973; Searle, 1975; Markus et al., 1985). The quality of agreement possible between this continuous-flow method (modified by complexing interfering metals, e.g., iron and manganese, with citrate and tartrate) and the manual Kjeldahl distillation and titration method were explored by Searle (1975). Table 3 shows his results for 50 soils, both for total nitrogen and the measurement of cation exchange capacity, in which the soils were first saturated with ammonium ions and then leached with sodium chloride. The values obtained by the two methods were highly correlated ($p < 0.001$), and the slope of the regression line was close to unity, indicating no significant bias between the methods. Alves et al. (1993) used

Marcel Dekker, Inc.
270 Madison Avenue, New York, New York 10016

Table 3 Results of Regression Analysis of AutoAnalyzer Data Values (A) Against Distillation/titration Data Values (D) in the Determination of Cation Exchange Capacity (CEC) and Total Nitrogen

	CEC, $mmol_c\,kg^{-1}$	Total N %
Range	0–300	0–0.50
Regression	$A = 0.9932D + 0.0947$	$A = 0.9907D + 0.0005$
r	0.9987***	0.9991***

Source: From Searle (1975).
*** is where $p < 0.001$.

a reaction temperature of 70°C to speed up the salicylate/hypochlorite colorimetric reaction for FIA in the determination of ammonium in tropical pasture soils.

Sources of interference in colorimetric determination of ammonium in soil extracts are colored humic substances or suspended matter, and the presence of labile organo-nitrogen compounds, e.g., amino acids (Selmer-Olsen, 1971; Adamsen et al., 1985). The former may be overcome by incorporating a dialyzer into the manifold (Selmer-Olsen, 1971). Wang et al. (2000) have described a FIA system for the determination of ammonia in the presence of surfactants. Ammonia is transferred in the gaseous phase from an alkaline sample solution to an indicator acceptor stream.

Tel and Jansen (1992) used a Traacs-800 analyzer at 100 samples per hour for the determination of total N in soil digests in a process that involved pretreatment with potassium permanganate, sulfuric acid, and reduced iron. Nascent hydrogen functioned as a reductant.

A flow-injection method for ammonium in soil extracts and natural waters has been described by Krug et al. (1979). This method uses Nessler's reagent (mercury (II) chloride and potassium iodide in alkaline solution), with the colored turbidity produced measured colorimetrically at 410 nm. An analysis rate of 120 samples per hour was achieved with the method. Carneiro et al. (2000) described the spectrophotometric determination of total nitrogen in plant materials using a flow-injection system with a solid silver chloride reactor. Ammonia released Ag from the mini AgCl column, and the $[Ag(NH_3)_2]^+$ ions were then reacted with bromopyrogallol red and *o*-phenanthroline to form a colored ternary complex. Kjeldahl digests of plant samples could be precisely analyzed at 100 per hour.

2. Nitrate and Nitrite

Continuous-flow methods for the determination of nitrate in soil extracts are based usually on its reduction to nitrite, with subsequent colorimetric

Marcel Dekker, Inc.
270 Madison Avenue, New York, New York 10016

determination of the nitrite formed plus any nitrite originally present in the sample. The latter may be determined separately by leaving out the reduction step, and the nitrate obtained by difference. The reducing agent may be copperized cadmium (Li and Smith, 1984), or hydrazine and copper (Rowland et al., 1984; Ananth and Moraghan, 1987). A manifold for nitrate and/or nitrite determination is shown in Fig. 13. The nitrite formed is usually determined by diazotizing sulfanilamide and coupling with *N*-1-naphthylethylenediamine to form an azo-dye, which is measured at 520–540 nm. As in the case of ammonium determinations, when colored or turbid samples are being analyzed, a dialyzer can be incorporated into the manifold. These azo-dye colorimetric procedures are used in both conventional and discrete analysis. Van Staden and van der Merwe (1998) have described a sequential injection analysis system for the determination of nitrite in natural and wastewater effluents, at 49 samples per hour with an RSD of $< 2.7\%$. Care is also required in the Cu plus hydrazine methods when samples contain significant amounts of organic matter, as free copper can be complexed and there may be insufficient remaining to allow full color development. This too requires a dialyzer in the manifold. Tebault and Poziomek (2000) have

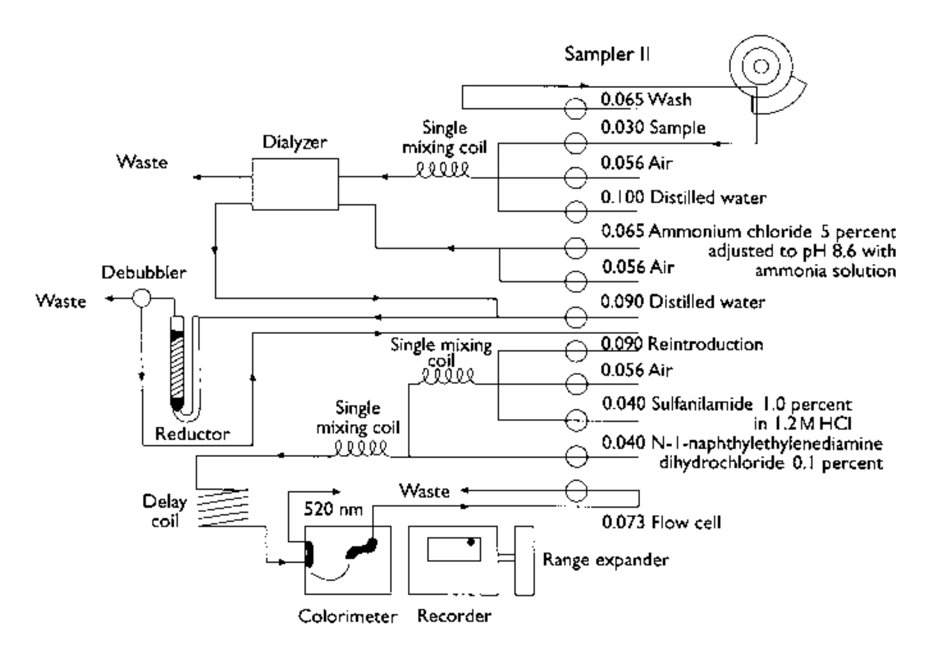


Figure 13 A manifold for segmented continuous-flow analysis determine nitrate and/or nitrite in soil extracts. (After Henriksen and Selmer-Olsen, 1970.)

discussed problems with humic acid interference in the determination of nitrite in water when the Griess reaction is employed. The interference is caused by association of the reaction dye with the humic acid. Tel and Heseltine (1990a) have described the use of a Traacs 800 analyzer for the determination of nitrate, nitrite, and ammonium in KCl extracts of soil.

Nitrate absorbs strongly in the U-V. This has been exploited in a low-power U-V spectrophotometer which could be used for very rapid shipboard determination of nitrate in sea water (Finch et al., 1998). By working at several wavelengths, absorbance due to sea salts and dissolved organic matter could be taken into account. The system gave results that compared favorably with those obtained by a standard AutoAnalyzer method for nitrate.

Nitrate ion-selective electrodes with a FIA system have been used to determine nitrate in soil extracts and fertilizer solutions (Hansen et al., 1977) and have also been applied in discrete analysis (Goodman, 1976). Adsett et al. (1999) have reported the development of an automated method for in-the-field soil nitrate measurement using a nitrate ion-selective electrode and soil water extracts.

3. Organic Nitrogen

The significance of soluble organic forms of nitrogen is becoming apparent for both terrestrial and aquatic N cycles (Yesmin et al., 1995). Digestion of organic nitrogen in natural waters and soil extracts is achieved through oxidation to inorganic forms, either in-line using commercially available U-V digester systems (Yesmin et al., 1995) or after a preoxidation stage such as the one described by Williams et al. (1995). In both cases organic nitrogen is calculated as the difference between total nitrogen and inorganic nitrogen.

B. Phosphorus

1. Orthophosphate

Phosphorus is one of the most common elements determined on a wide range of environmental samples, including filtered or unfiltered natural water samples and soil extracts. The normal procedure usually involves colorimetric detection of the phosphate anion by the reduction of a molybdophosphate complex to "molybdenum blue." Continuous-flow methods are very widely employed. Van Staden and Taljaard (1998) have described a sequential injection FIA system for on-line monitoring of phosphate in natural water and effluent streams. Phosphate could be monitored in the

Table 4 Some Applications of Automated Methods for the Determination of Phosphorus in Soil Extracts

Extractant	References
0.001 M H_2SO_4/0.002 M $(NH_4)_2SO_4$ at pH 3 (Truog)	Allen et al. (1974) Grigg (1975)
0.5 M Na_2CO_3/NaOH at pH 8.5 (Olsen)	Salt (1968) Grigg (1975) Brown (1984)
0.3 M NH_4F/0.025 M HCl (Bray and Kurtz No. 1)	Grigg (1975)
0.3 M NH_4F/0.1 M HCl (Bray and Kurtz No. 2)	Grigg (1975)
0.4 M acetic acid	Allen et al. (1974)
0.01 M $CaCl_2$	Brown (1984)
0.05 M Na_2SO_4, after sorption on an anion exchange resin	Hislop and Cooke (1968)
1 M NH_4Cl, 0.5 M NH_4F, 0.1 M NaOH, 0.3 M Na citrate/$Na_2S_2O_4$ (Chang and Jackson's solutions)	Grigg (1975)

range 0–70 mg L^{-1} with a standard deviation of 0.9%. Determinations of the total phosphorus content of plant samples in acid digests often utilize the less sensitive molybdovanadate phosphate yellow colorimetric method, which is readily automated (Varley, 1966; Basson et al., 1968).

In addition to being applied to phosphorus in the extractants listed in Table 4, automated methods are also suitable for solutions resulting from wet digestion procedures or fusion (Allen et al., 1974). The molybdate method is prone to a number of well-documented chemical interferences. Iron (III) is a common interfering species, but its effect can be reduced by reduction to iron (II) by hydrazine (Allen et al., 1974) or hydroxylammonium chloride (McLeod and Clarke, 1978). Organic matter can also interfere and, as in the determination of ammonium or nitrate, may be removed by dialysis (Grigg, 1975). Carbon dioxide liberation from alkaline bicarbonate (Olsen) soil extracts can cause problems in CFA (Zandstra, 1968; Allen et al., 1974), but the problem may be overcome satisfactorily by passing the liquid stream through a debubbler to remove CO_2 after acidification (Salt, 1968; Grigg, 1975). Another problem in the determination of very low concentrations of phosphorus in estuarine and seawater samples using continuous-flow systems is due to a refractive index effect at the high salinity. McKelvie et al. (1997) have shown that this can be eliminated using FIA methodology; the sample is simply injected into a NaCl solution carrier stream of similar refractive index.

2. Organically Associated Phosphorus

Soil solution and soil extracts contain a range of inorganic and organic phosphorus-containing compounds, including phosphorus contained in ternary complexes. On-line photo-oxidation procedures have been developed for CFA (Ron Vaz et al., 1992) and FIA (McKelvie and Hart 1989; Peat et al., 1997) that enable the distinction to be made between dissolved organic phosphorus, phosphate, and condensed phosphorus. In both systems an oxidant is added to the reagent stream prior to passing through a U-V digester, and phosphorus is determined using the molybdenum blue procedure. Recoveries of a range of phosphorus-containing organic and inorganic model compounds were tested for each procedure. The procedure was shown to be selective for phosphorus-containing organic compounds, while condensed polyphosphates remained unaffected. The technique was prone to various chemical interferences, especially when samples contained high concentrations of Al and Fe that tended to precipitate and then adsorb phosphate after the oxidation stage. Ron Vaz et al. (1992) used a high background concentration of added fluoride to complex with the Al, while Peat et al. (1997) employed an ion-exchange column for sample pretreatment. The continuous flow technique was capable of 20 determinations an hour compared to 40 for the flow-injection method.

C. Potassium, Calcium, Magnesium, and Sodium

In routine advisory soil analysis, some or all of the elements K, Ca, and Mg, and occasionally Na can be determined by continuous-flow methods, in parallel with the colorimetric determination of phosphorus (and sometimes ammonium or nitrate). A simultaneous flame spectrophotometric determinations of Ca, Li, K, and Na in 1 mol L^{-1} ammonium acetate extracts of soils were reported by Fang et al. (1985). Calcium and Mg in waters have been determined sequentially using a FIA system, the Ca by a flow-through tubular electrode, and the Mg by flame AAS (Alonso et al., 1986). Ferreira et al. (1995) have described a FIA system for soil analysis in which Na and K were determined by flame emission spectrometry and Ca and Mg by AAS, at 60–150 samples per hour, with relative standard deviations better than 4%.

For Ca in natural fresh water samples, an ion-selective electrode may be used as a sensor. Van Staden and Stefan (1999) used membrane ISEs in series to monitor Ca and F concentrations in borehole waters.

D. Aluminum, Silicon, and Iron

Hawke and Powell (1994) used a three-line flow injection system with short reaction times for the spectrophotometric determination of kinetically labile

Marcel Dekker, Inc.
270 Madison Avenue, New York, New York 10016

Al^{3+}. Allen et al. (1974) recommended for Al a method using the complex formed with eriochrome cyanine R. The results of a thorough comparison of five analytical methods for the fractionation and subsequent determination of Al in natural water samples have been published by Wickstrom et al. (2000). They showed that two different continuous flow methods gave similar results for the labile Al fraction in soil water and lake water samples in Norway and Finland. Downard et al. (1992) have described an indirect FIA method for the determination in soil extracts of Al^{3+}. The procedure involved the formation of a complex with 1,2-dihydroxyanthraquinone-3-sulphonic acid at pH 9.0 and amperometric determination of the excess reagent.

For silicon, Allen et al. (1974) advocated a method based on the reduction of molybdosilicic acid to a molybdenum blue complex, i.e., a reaction analogous to that used for phosphate. Though old, this method still works well today. A similar FIA method has been developed for silicon in soil extracts (Fig. 14; Borggaard and Jorgensen, 1985). Rabenlange et al. (1994) have described a procedure for minimization of phosphate interference in the determination of Si by FIA. They used ascorbic acid as a reductant in the molybdenum blue method.

Iron is a major component of most soils, and total iron or the fractions that are extractable with reagents such as oxalic acid and pyrophosphate are determined frequently in pedological investigations. For the determination of plant-available iron, 2.5% acetic acid is used commonly. Allen et al. (1974) adapted the manual colorimetric method for iron, based upon

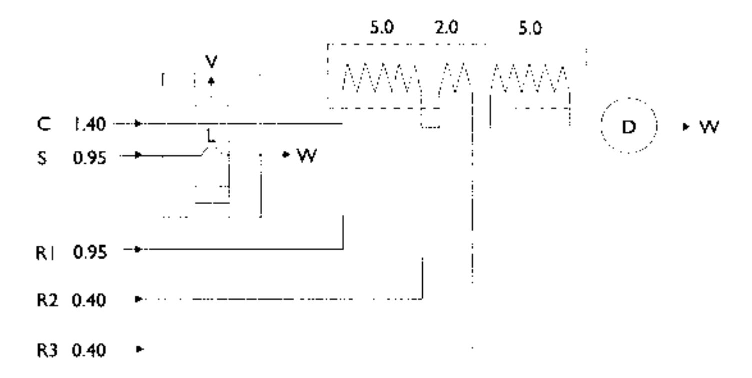


Figure 14 Flow-injection manifold for determination of silicon in soil extracts. V, sliding injection valve (moves in direction of arrow); L, sampling loop (300 μL); D, detector; W, waste; C, carrier stream (water); S, sample; R1, ammonium molybdate reagent; R2, oxalic acid 9%; R3, ascorbic acid 2%. Numbers are flow rates in $mL\,min^{-1}$. (From Borggaard and Jorgensen, 1985.)

sulfonated 4,7-diphenyl-1,10-phenanthroline, to CFA so that it could be used for both 3% oxalic acid and 2.5% acetic acid extracts. Ferreira et al. (1996a) reported a colorimetric FIA method for the determination of available Fe in soil extracts, and later a single-line flow-injection system linked to AAS (Ferreira et al., 1998). Van Staden and Matoetoe (1998) have used differential pulse ASV at a glassy carbon electrode in a flow-through configuration for the determination of iron (II) and iron (III). Herzsprung et al. (1998) used a segmented flow system for Fe speciation in acidic mining lakes.

E. Sulfur

Published methods for sulfur (as sulfate) in soil and plant extracts and natural waters have involved turbidimetric (Sinclair, 1973; Coutinho, 1996), nephelometric (Ogner and Haugen, 1977), and colorimetric (Cronan, 1979) methods of measurement. An alternative development for the determination of sulfate in water samples is the use of a lead-sensitive ion-selective electrode to measure the free lead (II) after mixing a reagent stream containing lead with the sample stream. Both FIA (Coetzee and Gardner, 1986) and CFA (Hare et al., 1988) methods have been developed.

F. Trace Elements

Many environmental laboratories interested in trace element analysis have a requirement for the determination of a substantial number of elements, often 10 or more. Where this is the case, and sample throughput is high, it becomes much more cost effective to use an analytical technique such as ICP-AES or ICP-MS, which has multielement analytical capability. Even for determination of a limited number of elements, simplicity of operation may dictate that AAS is the method of choice for trace element analysis. Nevertheless, there are laboratories that, for various reasons, use automated colorimetric or fluorimetric methods even for some trace analyses.

Several automated methods have been developed for boron in plant material, including colorimetric methods based on reactions with azomethine-H (Porter et al., 1981; Carrero et al., 1993; Sah and Brown, 1997) and quinalizarin (Willis, 1970). The former was adapted with only slight modification to the analysis of hot water extracts of soils (Allen et al., 1974). Also, a manual spectrofluorimetric method for boron using carminic acid was adapted to CFA by Ogner (1980). Several of these older methods are still in use today, in part because of the very poor sensitivity of the determination of boron by flame AAS.

Automated procedures for chlorine, bromine, and iodine have long been available. Chloride can be determined colorimetrically by a reaction involving iron and thiocyanate (Allen et al., 1974). Tel and Heseltine (1990b) have evaluated the Traacs 800 analyzer for determination of chloride in soil leachates. Bromide can be determined by a CFA method involving oxidation of iodine to iodate (Pyen et al., 1980), or by FIA using a tubular bromide-selective electrode (van Standen, 1987). Iodine in plant tissue and sodium hydroxide extracts of soil may be determined by a CFA procedure based on the catalytic action of iodine on the oxidation of arsenic (III) (van Vliet et al., 1975). Provided the halide ions are present at sufficient concentrations, however, and the matrix is suitable, many analysts are more likely nowadays to employ ion-selective electrodes or ion chromatography for anion analysis.

Trace metals in soil extracts and plant tissues have been determined by automated wet chemical procedures, although usually there are more suitable alternatives. A comprehensive review of FIA techniques has been published by Ferreira et al. (1998). Molybdenum has been determined in plants by CFA (Bradfield and Strickland, 1975), and chromium (VI) in soil extracts and natural waters has been determined by FIA (Jorgensen and Regitano, 1980). Automated colorimetry may be attractive for these elements at the low concentrations typically present in many environmental samples, unless one of the more sensitive atomic spectrometry techniques such as ICP-AES or ICP-MS is available. The measurement of As, Sb, and Se in natural waters (Goulden and Brooksbank, 1974) is another example. Van Staden and Matoetoe (2000) have described a sensitive CFA system for the determination of Cd, Cu, Pb, and Zn in water samples using differential pulse anodic stripping voltammetry (DPASV) for detection.

Flow-injection methodology lends itself readily to the exploitation of catalytic methods of analysis, because of the high reproducibility of timing between reaction and measurement. Feng et al. (1999) have described a FI spectrophotometric method for the determination of Hg(II) in water samples, based upon the catalytic decomposition of ferrocyanide.

Flow injection is also finding application for preconcentration procedures in ultratrace analysis. For example, Hollenbach et al. (1994) used flow-injection methodology for on-line preconcentration of ^{99}Tc, ^{230}Th, and ^{234}U in soils prior to their determination by ICP-mass spectrometry. On-line exchange has also been used to remove interferences in the determination of thallium in soils by FIA with differential pulse ASV detection (Lukaszewski and Zembrzuski, 1992).

G. pH

Reference has already been made (Sec. V.B) to several purpose-built systems for the automated measurement of soil pH. Bellerby et al. (1995) developed a shipboard flow-injection method for the determination of seawater pH, based upon spectrophotometric detection. The methodology was based upon the acid/base absorption characteristics of phenol red injected into a seawater stream. The pH was accurate to ± 0.005 pH units at a sampling frequency of 25 determinations per hour.

H. Carbon

Various different approaches have been used to determine carbon in natural water samples. For example, the carbon dioxide produced by U-V oxidation (either with or without an oxidant such as persulfate) of organic C in seawater may be measured via the change in electrical conductivity of dilute sodium hydroxide solution as the CO_2 is adsorbed (Ehrhardt, 1969). More recently, O'Sullivan and Millero (1998) have used infrared detection of evolved CO_2 in an automated shipboard system for monitoring total inorganic C in surface seawater. Their system allowed them to detect changes over small temporal and spatial scales. If samples are acidified and purged (often with nitrogen) prior to oxidation, a distinction can be made between the total carbon and the organic carbon present in the sample as presented (Small et al., 1986). Roche and Millero (1998) used an automated shipboard system to monitor surface seawater alkalinity in the Indian Ocean. Their procedure involved a single-step addition of hydrochloric acid followed by rapid spectrophotometric (using a diode array detector) measurement of pH. Direct determination of soluble organic matter can be performed using an automated fluorimetric system (Brun and Milburn, 1977) once the system is calibrated.

I. Miscellaneous

The bulk of this review has concentrated on applications of CFA and FIA methodologies in elemental analysis and elemental speciation studies. However, over recent years these methodologies have been applied also to the determination of a wide range of compounds or groups of compounds in environmental samples. For example, Tel and Covert (1992) have investigated methods for the determination of phenolic acids and tannins in soil water extracts using a Technicon AutoAnalyzer 2 system. They used the method developed to study the rates of disappearance of individual

phenolic compounds added to soils. Such applications are too specialized to be considered fully in a general text such as this one.

VII. CONCLUSIONS

Automated methods for wet chemical analysis have now been adopted widely in agricultural and environmental laboratories. The most widespread applications have been in the routine analysis of soil extracts and plant materials in connection with advisory and extension services, and for determination of nitrate, ammonium, low concentrations of phosphate, and organic N and P in water samples, particularly in environmental monitoring work. The potential of automated colorimetric methods to include elemental speciation steps ensures that they will continue to retain their place in busy environmental laboratories. The first phase of the switch to automated methods concentrated on the use of segmented continuous-flow systems, but more recently, the greater speed of flow-injection analysis and the improved speed and greater flexibility possible with discrete systems have made them popular alternatives. Whichever automated system has been adopted in soil and plant testing or water monitoring/research laboratories, the experience has invariably been that both sample throughput and the quality and reproducibility of the data obtained are generally superior to that which could be obtained normally by traditional manual methods.

Automation is not confined to chemical procedures; data capture by computer (whether a dedicated personal computer or a larger system, via a link) has both reduced the need for manual computation and increased the reliability of analytical data.

To the factors of speed and reliability must be added that of cost. The cost, in real terms, of microprocessor-based instrumentation has fallen considerably in the last few years relative to that of manual operations. This trend may be expected to continue and lead to the ever more widespread use of automated systems for chemical analysis.

From time to time in the applications section of this chapter, examples were discussed of the use of CFA systems for in-situ analysis (Andrew et al., 1994). Monitoring directly in the field obviously is advantageous where data are needed in real time, but it has the additional advantage of minimizing some of the errors that may arise during preservation and storage of environmental samples (Kotlash and Chessman, 1998). Losses of nutrient elements in stored samples were particularly severe at low determinant concentrations. David et al. (1998, 1999) reported the development and performance of a remotely deployed submersible flow-injection system for the determination of nitrate in estuarine and coastal waters. Such systems

may allow three-dimensional mapping of pollutant concentrations in natural waters at reasonably good resolution. This is an example where sample collection and analysis off-line would be far less useful. Various FI systems have been designed for use on board marine research vessels. O'Sullivan and Millero (1998) found that the variability in the total inorganic carbon concentration in surface seawater was completely missed unless an on-line system was employed. In recent years, global variations in surface seawater alkalinity have been attracting considerable attention (Millero et al., 1998). For monitoring open ocean waters, much time may be wasted if data are not obtained sufficiently rapidly for the monitoring strategy to be modified in response to current findings.

Remote monitoring of borehole waters (van Staden and Stefan, 1999) and of determinants such as ammonia in landfill leachate (Bloxham et al., 1997) are other areas in which automated systems have a crucial role to play. For pollutant monitoring at remote stations, data may be transferred periodically to a central laboratory for interpretation. Alternatively the analyzer may be configured to trigger automatically a warning should a determinant of interest fall outside acceptable preset safe limits.

REFERENCES

Adamchuk, V.I., M.T. Morgan, and D.R. Ess. 1999. An automated sampling system for measuring soil pH. *Trans. Am. Soc. Agric. Eng.* 42:885–891.

Adamsen, F.J., D.S. Bigelow, and G.R. Scott. 1985. Automated methods for ammonium, nitrate and nitrite in 2M KCl–phenylmercuric acetate extracts of soil. *Commun. Soil Sci. Plant Anal.* 16:883–898.

Adsett, J.F., J.A. Thottan, and K.J. Sibley. 1999. Development of an automated on-the-go soil nitrate monitoring system. *Appl. Eng. Agric.* 15:351–356.

Agren, G.I. and E. Bosatta. 1988. Nitrogen saturation of terrestrial ecosystems. *Environ. Pollut.* 54:185–197.

Allen, S.E., H.M. Grimshaw, J.A. Parkinson, and C. Quarmby. 1974. *Chemical Analysis of Ecological Materials.* Blackwell, Oxford.

Alonso, J., J. Bartroli, J.L.F.C. Lima, and A.A.S.C. Machado. 1986. Sequential flow-injection determinations of calcium and magnesium in waters. *Anal. Chim. Acta* 179:503–508.

Alves, B.J.R., R.M. Boddey, and S.S. Urquiaga. 1993. A rapid and sensitive flow-injection technique for the analysis of ammonium in soil extracts. *Commun. Soil Sci. Plant Anal.* 24:277–284.

Ananth, S. and J.T. Moraghan. 1987. The effects of calcium and magnesium on soil nitrate determination by automated segmented-flow methods. *Soil Sci. Soc. Am. J.* 51:664–667.

Andrew, K.N., N.J. Blundell, D. Price, and P.J. Worsfold. 1994. On-site automated FI monitors provide near-continuous, reliable, and low-cost data for assessing water quality. *Anal. Chem.* 66:916A–922A.

Aström, O. 1982. Flow-injection analysis for the determination of bismuth by atomic absorption spectrometry with hydride generation. *Anal. Chem.* 54:190–193.

Baker, K.F. 1970. An automated method for the detection of the pH of soil. *Analyst* 95:885–889.

Basson, W.D., D.A. Stanton, and R.G. Böhmer. 1968. Automated procedure for the simultaneous determination of phosphorus and nitrogen in plant tissue. *Analyst* 93:166–172.

Bellerby, R.G.J., D.R. Turner, G.E. Millward, and P.J. Worsfold. 1995. Shipboard flow-injection determination of seawater pH with spectrophotometric detection. *Anal. Chim. Acta* 309:259–270.

Bergamin, H., E.A.G. Zagatto, F.J. Krug, and B.F. Rels. 1978. Merging zones in flow injection analysis. Part 1. Double proportional injector and reagent consumption. *Anal. Chim. Acta* 101:17–23.

Bloxham, M.J., S.J. Hill, and P.J. Worsfold. 1996. Determination of mercury in filtered sea water by flow injection with on-line oxidation and atomic fluorescence detection. *J. Anal. Atom. Spectrom.* 11:511–514.

Bloxham, M.J., M.H. Depledge, and P.J. Worsfold. 1997. In-situ flow injection monitoring of ammonia in landfill leachate. *Lab. Robotics Automation* 9:175–183.

Borggaard, O.K. and S.S. Jorgensen. 1985. Determination of silicon in soil extracts by flow-injection analysis. *Analyst*, 110:177–180.

Bowie, A.R., M.G. Sanders, and P.J. Worsfold. 1996. Analytical applications of liquid phase chemiluminescence reactions—a review. *J. Biolum. Chemilum.* 11:61–90.

Bradfield, E.G. and J.F. Strickland. 1975. The determination of molybdenum in plants by an automated catalytic method. *Analyst* 100:1–6.

Broberg, O. and G. Persson. 1998. Particulate and dissolved phosphorus forms in freshwater: composition and analysis. In: *Phosphorus in Freshwater Ecosystems* (G. Persson and M. Jansson, eds.). Kluwer Academic Publishers, Dordrecht, The Netherlands, pp. 61–90.

Brown, M.W. 1984. Application of automation and computerisation to a soil testing laboratory. *Analyst* 109:469–471.

Brun, G.L. and D.L.D. Milburn. 1977. Automated fluorimetric determination of humic substances in natural water. *Anal. Lett.* 10:1209–1219.

Cannizzaro, V., A.R. Bowie, A. Sax, B.P. Achterberg, and P.J. Worsfold. 1999. Determination of cobalt and iron in estuarine and coastal waters using flow injection with chemiluminescence detection. *Analyst* 125:51–57.

Carneiro, J.M.T., R.P. Sartini, and E.A.G. Zagatto. 2000. Spectrophotometric determination of total nitrogen in plant materials using a flow-injection system with an AgCl(s) reactor. *Anal. Chim. Acta* 416:185–190.

Carrero, P., J.L. Burguera, M. Burguera, and C. Rivas. 1993. A time-based injector applied to the flow injection spectrophotometric determination of boron in plant materials and soils. *Talanta* 40:1967–1974.

Carretero, A.S., J.R. Fernandez, A.R. Bowie, and P.J. Worsfold. 2000. Acquisition of chemiluminescence spectral profiles using a continuous flow manifold with two dimensional CCD detection. *Analyst* 125:387–390.

Coetzee, J.F. and C.W. Gardner. 1986. Determination of sulfate, ortho-phosphate, and triphosphate ions by flow-injection analysis with the lead ion-selective electrode as detector. *Anal. Chem.* 58:608–611.

Coutinho, J. 1996. Automated method for sulphate determination in soil-plant extracts and waters. *Commun. Soil Sci. Plant Anal.* 27:727–740.

Couto, C.M.C.M. and M.C.B.S.M. Montenegro. 2000. Potentiometric detectors for flow injection analysis systems, evolution and application. *Quimica Nova* 23:774–784.

Cronan, C.S. 1979. Measurement of sulfate in organically colored water samples. *Anal. Chem.* 51:1333–1335.

David, A.R.J., T. McCormack, A.W. Morris, and P.J. Worsfold, 1998. A submersible flow injection-based sensor for the determination of total oxidised nitrogen in coastal waters. *Anal. Chim. Acta* 361:63–72.

David, A.R.J., T. McCormack, and P.J. Worsfold. 1999. A submersible battery-powered flow injection (FI) sensor for the determination of nitrate in estuarine and coastal waters. *J. Automat. Meth. Manage. Chem.* 21:1–9.

De Andrade, J.C., C. Pasquini, N. Ballan, and J.C. Van Loon. 1983. Cold vapour atomic-absorption determination of mercury by flow-injection analysis using a teflon membrane phase separator coupled to the absorption cell. *Spectrochim. Acta, Part B* 38:1329–1338.

Downard, A.J., H.K.L. Powell, and S.H. Xu. 1992. Flow-injection analysis for aluminium with indirect amperometric detection. *Anal. Chim. Acta* 256:117–123.

Erhardt, M. 1969. A new method for the automated measurement of dissolved organic carbon in sea water. *Deep-Sea Res.* 16:393–397.

Fang, Z., J.M. Harris, J. Růžička, and E.H. Hansen. 1985. Simultaneous flame photometric determination of lithium, sodium, potassium, and calcium by flow injection analysis with gradient scanning standard addition. *Anal. Chem.* 57:1457–1461.

Fang, Z., S. Xu, X. Wang, and S. Zhang. 1986. Combination of flow-injection techniques with atomic spectrometry in agricultural and environmental analysis. *Anal. Chim. Acta* 179:325–340.

Feng, Y.L., H. Narasaki, L.C. Tian, S.M. Wu, and H.Y. Chen. 1999. Flow-injection spectrophotometric determination of mercury(II) in water by the catalytic decomposition of ferrocyanide. *Anal. Sci.* 15:915–918.

Ferreira, A.M.R., J.L.F.C. Lima, and A.O.S.S. Rangel. 1996a. Colorimetric determination of available iron in soils by flow injection analysis. *Analusis* 24:343–346.

Ferreira, A.M.R., J.L.F.C. Lima, and A.O.S.S. Rangel. 1996b. Potentiometric determination of total nitrogen in soils by flow injection analysis with a gas diffusion unit. *Aust. J. Soil Res.* 34:503–510.

Ferreira, A.M.R., A.O.S.S. Rangel, and J.L.F.C. Lima. 1995. Flow-injection systems with stream splitting and a dialysis unit for the soil analysis of sodium and

potassium by flame emission spectrometry and calcium and magnesium by atomic absorption spectrometry. *Commun. Soil Sci. Plant Anal.* 26:183–195.

Ferreira, A.M.R., A.O.S.S. Rangel, and J.L.F.C. Lima. 1998. Flow injection systems for elemental soil analysis determinations. *Commun. Soil Sci. Plant Anal.* 29:327–360.

Finch, M.S., D.J. Hydes, C.H. Clayson, B. Weigl, J. Dakin, and P. Gwilliam. 1998. A low power ultra violet spectrophotometer for measurement of nitrate in seawater: introduction, calibration and initial sea trials. *Anal. Chim. Acta* 377:167–177.

Goodman, D. 1976. Automatic apparatus for the determination of pH and nitrate in soils. *Analyst* 101:943–948.

Goulden, P.D. and P. Brooksbank. 1974. Automated atomic absorption determination of arsenic, antimony and selenium in natural waters. *Anal. Chem.* 38:1431–1436.

Grigg, J.L. 1975. Determination of phosphate in soil extracts by automatic colorimetric analysis. *Commun. Soil Sci. Plant Anal.* 6:95–112.

Grigg, J.L., H.J. Flewitt, G.A. Baird, R.B. Jordan, and K.V. Vo. 1980. Automatic soil pH measuring and recording apparatus. *Analyst* 105:1–10.

Hansen, E.H., H.K. Ghose, and J. Růžička. 1977. Flow injection analysis of environmental samples for nitrate using ion-selective electrode. *Analyst* 102:705–713.

Hare, H., G. Horval, and E. Pungor. 1988. Continuous-flow determination of sulfate with a lead-sensitive electrode. *Analyst* 113:1817–1820.

Hawke, D.J. and H.K.J. Powell. 1994. Flow injection analysis applied to the kinetic determination of reactive (toxic) aluminium—comparison of chromophores. *Anal. Chim. Acta* 299:257–268.

Henriksen, A. and A.R. Selmer-Olsen. 1970. Automatic methods for determining nitrate and nitrite in water and soil extracts. *Analyst* 95:514–518.

Herzsprung, P., K. Friese, G. Packroff, M. Schimmele, K. Wendt-Potthoff, and M. Winkler. 1998. Vertical and annual distribution of ferric and ferrous iron in acid mining lakes. *Acta Hydrochim. Hydrobiol.* 26:253–262.

Hislop, J. and I.J. Cooke. 1968. Anion exchange resin as a means of assessing soil phosphate status: a laboratory technique. *Soil Sci.* 105:8–11.

Hollenbach, M., J. Grohs, S. Mamich, M. Kroft, and E.R. Denoyer. 1994. Determination of ^{99}Tc, ^{230}Th and ^{234}U in soils by inductively coupled plasma-mass spectrometry using flow injection preconcentration. *J. Anal. Atom. Spectrosc.* 9:927–933.

Jorgensen, S.S. and M.A.B. Regitano. 1980. Rapid determination of chromium (VI) by flow injection analysis. *Analyst* 105:292–295.

Kotlash, A.R. and B.C. Chessman. 1998. Effects of water sample preservation and storage on nitrogen and phosphorus determinations: implications for the use of automated sampling equipment. *Wat. Res.* 32:3731–3737.

Krug, F.J., J. Růžička, and E.H. Hansen. 1979. Determination of ammonia in low concentrations with Nessler's reagent by flow injection analysis. *Analyst* 104:47–54.

Li, S. and K.A. Smith. 1984. The rapid determination of nitrate at low concentrations in soil extracts: comparison of ion-selective electrode with continuous-flow analysis. *Commun. Soil Sci. Plant Anal.* 15:1437–1451.

Liu, R.M., D.J. Liu, and A.L. Sun. 1992. Potentiometric detection in flow-injection without the use of a conventional reference electrode. *Analyst* 117:1335–1337.

Lukaszewski, Z. and W. Zembrzuski. 1992. Determination of thallium in soils by flow-injection differential pulse anodic-stripping voltammetry. *Talanta* 39:221–227.

Macdonald, A.M.G., H.L. Pardue, A. Townshend, and J.T. Clere, eds. 1986. *Flow Analysis III*. Proc. Int. Conf., Birmingham, U.K., 1985, *Anal. Chim. Acta* 179 (special issue).

Markus, O.K., J.P. McKinnon, and A.F. Buccafuri. 1985. Automated-analysis of nitrite, nitrate and ammonium nitrogen in soils. *Soil Sci. Soc. Am. J.* 49:1208–1215.

McKelvie, I. and B.T. Hart. 1989. Spectrophotometric determination of dissolved organic P in natural waters using on-line photo-oxidation and flow injection. *Analyst* 114:1459–1463.

McKelvie, I.D., D.M.W. Peat, G.P. Matthews, and P.J. Worsfold. 1997. Elimination of the Schlieren effect in the determination of reactive phosphorus in estuarine waters by flow injection analysis. *Anal. Chim. Acta* 351:265–271.

McLeod, S. and A.R.P. Clarke. 1978. Determination of phosphorus in the presence of iron (III) and iron (II). *Analyst* 103:238–245.

Millero, F.J., K. Lee, and M. Roche. 1998. Distribution of alkalinity in the surface waters of the major oceans. *Marine Chem.* 60:111–130.

Murphy, J., P. Jones, and S.J. Hill. 1996. Determination of total mercury in environmental and biological samples by flow injection cold vapour atomic absorption spectrometry. *Spectrochim. Acta, Part B* 51:1867–1873.

Nausch, G. 1997. Nutrient analysis: manual methods and autoanalyser and vice versa. *Marine Pollut. Bull.* 35:171–173.

Nogueira, A.R.A., S.M.B. Brienza, E.A.G. Zagatto, J.L.F.C. Lima, and A.J. Araulo. 1996. Flow injection system with multi-site detection for spectrophotometric determination of calcium and magnesium in soil extracts and natural waters. *J. Agric. Food Chem.* 44:165–169.

Ogner, G. 1980. Automatic determination of boron in plants. *Analyst* 105:916–919.

Ogner, G.O. and A. Haugen. 1977. Automatic determination of sulphate in water samples and soil extracts containing large amounts of humic compounds. *Analyst* 102:453–457.

O'Sullivan, D.W. and F.J. Millero. 1998. Continual measurement of the total inorganic carbon in surface seawater. *Marine Chem.* 60:75–83.

Peat, D.M.W., I.D. McKelvie, G.P. Mathhews, P.M. Haygarth, and P.J. Worsfold. 1997. Rapid determination of dissolved organic phosphorus in soil leachates and runoff waters by flow injection analysis with on-line photo-oxidation. *Talanta* 45:47–55.

Porter, S.R., S.C. Spindler, and A.E. Widdowson. 1981. An improved automated colorimetric method for the determination of boron in extracts of soils,

soil-less peat based composts, plant materials and hydroponic solutions with azomethine-H. *Commun. Soil Sci. Plant Anal.* 12:461–467.

Price, D., R. Fauzi, C. Mantoura, and P.J. Worsfold. 1998. Shipboard determination of hydrogen peroxide in the western Mediterranean sea using flow injection with chemiluminescence detection. *Anal. Chim. Acta* 377:145–155.

Prince, A.B. 1965. Absorption spectrophotometry. In: *Methods of Soil Analysis* (C.A. Black, ed.). Am. Soc. Agron., Madison, WI, pp. 866–878.

Pyen, G.S., M.J. Fishman, and A.G. Hedley. 1980. Automated spectrophotometric determination of trace amounts of bromide in water. *Analyst* 105:657–662.

Rabenlange, B., A.B. Bendtsen, and S.S. Jorgensen. 1994. Spectrophotometric determination of silicon in soil solutions by flow-injection analysis—reduction of phosphate interference. *Commun. Soil Sci. Plant Anal.* 25:3241–3256.

Ranger, C.B. 1981. Flow-injection analysis—principles, techniques, application, design. *Anal. Chem.* 53:20A–28A.

Riley, C. and B.F. Rocks. 1983. Flow-injection analysis—the end of the beginning—segmented-flow analysis—the beginning of the end. *J. Automat. Chem.* 5:1–2.

Riley, C., L.H. Aslett, B.F. Rocks, R.A. Sherwood, J.D.M. Watson, and J. Morgan. 1983. Controlled dispersion analysis—flow-injection analysis without injection. *Clin. Chem.* 29:332–335.

Roche, M.P. and F.J. Millero. 1998. Measurement of total alkalinity of surface waters using continuous flowing spectrophotometric technique. *Marine Chem.* 60:85–94.

Ron Vaz, M.D., A.C. Edwards, C.A. Shand, and M.S. Cresser. 1992. Determination of dissolved organic phosphorus in soil solutions by an improved automated photo-oxidation procedure. *Talanta* 39:1479–1487.

Ron Vaz, M.D., A.C. Edwards, C.A. Shand, and M.S. Cresser. 1993. Phosphorus fractions in soil solution: influence of soil acidity and fertiliser additions. *Plant Soil* 148:175–183.

Rowland, A.P., H.M. Grimshaw, and O.M.H. Rigaba. 1984. Control of soil solution interferences in an automated nitrate method. *Commun. Soil Sci. Plant Anal.* 15:337–351.

Růžička, J. and E.H. Hansen. 1975. Flow injection analysis. Part 1. A new concept of fast continuous flow analysis. *Anal. Chim. Acta* 78:145–157.

Růžička, J. and E.H. Hansen. 1981. *Flow Injection Analysis*. New York: John Wiley.

Sah, R.N. and P.H. Brown. 1997. Techniques for boron determination and their application to the analysis of plant and soil samples. *Plant Soil* 193:15–33.

Sakuma, A.M., F.D. de Maio, R.Q. Utishiro, C.S. Kira, M.D.H. Carvalho, and J. Lichtig. 1999. Optimization of parameters for trace inorganic mercury determination in urine by flow injection cold vapor AAS. *Atom. Spectrosc.* 20:186–190.

Salt, P.D. 1968. The automatic determination of phosphorus in extracts of soils made with 0.5 M sodium bicarbonate and 0.01 M calcium chloride. *Chem. Ind.* 18:584–586.

Schuman, G.E., M.A. Stanley, and D. Knudsen. 1973. Automated total nitrogen analysis of soils and plant samples. *Soil Sci. Soc. Am. Proc.* 37:480–481.

Searle, P.L. 1975. Automated colorimetric determination of ammonium ions in soil extracts with 'Technicon AutoAnalyser II' equipment. *N.Z. J. Agric. Res.* 18:183–187.

Selmer-Olsen, A.R. 1971. Determination of ammonium in soil extracts by an automated indophenol method. *Analyst* 96:565–568.

Sherwood, R.A., B.F. Rocks, and C. Riley. 1985. Controlled-dispersion flow-analysis with atomic-absorption detection for the determination of clinically relevant elements. *Analyst* 110:493–496.

Sinclair, A.G. 1973. An 'AutoAnalyser' method for determination of extractable sulphate in soil. *N.Z. J. Agric. Res.* 16:287–292.

Skeggs, L.T. 1957. Application for determination of crystalloid constituents of a liquid that contains also a noncrystalloid substance. *Am. J. Clin. Pathol.* 28:311–312.

Small, R.A., T.W. Lowry, and E.M. Ejzak. 1986. Oxidation and detection techniques in TOC analysis. *Inter. Lab.* May, 56–67.

Snyder, L.R. 1980. Continuous-flow analysis: present and future. *Anal. Chim. Acta* 114:3–18.

Snyder, L.R. and H.J. Adler. 1976a. Dispersion in segmented flow through glass tubing in continuous flow for analysis: the ideal model. *Anal. Chem.* 48: 1017–1022.

Snyder, L.R. and H.J. Adler. 1976b. Dispersion in segmented flow through glass tubing in continuous flow for analysis: the non-ideal model. *Anal. Chem.* 48:1022–1027.

Solujic, L., E.B. Milosavljevic, and M.R. Straka. 1999. Total cyanide determination by a segmented flow injection-on-line UV digestion-amperometric method. *Analyst* 124:1255–1260.

Stewart, K.K., G.R. Beecher, and P.E. Hare. 1976. Rapid analysis of discrete samples: the use of non-segmented, continuous flow. *Anal. Biochem.* 70:167–173.

Taylor, G. 1953. Dispersion of sol. matter in solvent flowing slowly through a tube. *Proc. Roy. Soc. Lond., Ser. A* 219:186–203.

Taylor, G. 1954. The dispersion of matter in turbulent flow through a pipe. *Proc. Roy. Soc., Lond. Ser. A* 223:446–468.

Tebault, S.A. and E.J. Poziomek. 2000. Humic substances as interferences in the analysis of nitrite in water. *Field Anal. Chem. Technol.* 4:134–146.

Technicon Instruments Corp. 1972. Manual TN1 0170-01, Technicon Instruments, Tarrytown, N.Y.

Tel, D.A. and J.A. Covert. 1992. Determination of phenolic-acids and tannins in soil-water extracts using a Technicon AutoAnalyzer II system. *Commun. Soil Sci. Plant Anal.* 23:2737–2747.

Tel, D.A. and C. Heseltine. 1990a. The analysis of KCl soil extracts for nitrate, nitrite and ammonium using the TRAACS 800 analyser. *Commun. Soil Sci. Plant Anal.* 21:1681–1688.

Tel, D.A. and C. Heseltine. 1990b. Chloride analysis of soil leachate using the TRAACS 800 analyser. *Commun. Soil Sci. Plant Anal.* 21:1689–1693.

Tel, D.A. and J. Jansen. 1992. Determination of total nitrogen in soil digest using a TRAACS-800 Autoanalyzer. *Commun. Soil Sci. Plant Anal.* 23:2729–2736.

Tel, D.A., L. Liu, and B.J. Shelp. 1992. Determination of total nitrogen in plant digests using a Traacs-800 AutoAnalyzer. *Commun. Soil Sci. Plant Anal.* 23:2771–2779.

Tyson, J.F. 1985. Flow injection analysis techniques for atomic-absorption spectrometry. *Analyst* 110:419–429.

Tyson, J.F. 1986. Peak width and reagent dispersion in flow injection analysis. *Anal. Chim. Acta* 179:131–148.

van Staden, J.F. 1987. Flow injection determination of inorganic bromide in soils with a coated tubular solid-state bromide-selective electrode. *Analyst* 112:595–599.

van Staden, J.F. and M.C. Matoetoe. 1998. Simultaneous determination of traces of iron (II) and iron (III) using differential pulse anodic stripping voltammetry in a flow-through configuration on a glassy carbon electrode. *Anal. Chim. Acta* 376:325–330.

van Staden, J.F. and M.C. Matoetoe. 2000. Simultaneous determination of copper, lead, cadmium and zinc using differential pulse anodic stripping voltammetry in a flow system. *Anal. Chim. Acta* 411:201–207.

van Staden, J.F. and R.I. Stefan. 1999. Simultaneous flow injection determination of calcium and fluoride in natural and borehole water with conventional ion selective electrodes in series. *Talanta* 49:1017–1022.

van Staden, J.F. and R.E. Taljaard. 1998. On-line monitoring of phosphate in natural water and effluent streams using sequential injection analysis. *Mikrochim Acta* 128:223–228.

van Staden, J.F. and T.A. van der Merwe. 1998. On-line monitoring of nitrite in fertilizer process streams, natural and waste water effluents with sequential injection analysis. *Microchim. Acta* 129:33–39.

van Vliet, H., W.D. Basson, and R.G. Böhmer. 1975. A semi-automated procedure for the determination of iodine in plant tissue and soil extracts. *Analyst* 100:405–407.

Vanderslice, J.T., A.G. Rosenfeld, and G.R. Beecher. 1986. Laminar-flow bolus shapes in flow-injection analysis. *Anal. Chim. Acta* 179:119–129.

Vanderslice, J.T., K.K. Stewart, A.G. Rosenfeld, and D.G. Higgs. 1981. Laminar dispersion in flow-injection analysis. *Talanta* 28:11–18.

Varley, J.A. 1966. Automatic methods for the determination of nitrogen and phosphorus and potassium in plant material. *Analyst* 91:119–126.

Wang, L.J., T.J. Cardwell, R.W. Cattrell, M.D.L. de Castro, and S.P. Kolev. 2000. Pervaporation-flow injection determination of ammonia in the presence of surfactants. *Anal. Chim. Acta* 416:177–184.

Whitehouse, M.J. and M. Preston, 1997. A flexible computer-based technique for the analysis of data from a sea-going nutrient autoanalyser. *Anal. Chim. Acta* 345:197–202.

Whitworth, D.J., E.P. Achterberg, M. Nimmo, and P.J. Worsfold. 1998. Validation and in-situ application of an automated dissolved nickel monitor for estuarine studies. *Anal. Chim. Acta* 377:217–228.

Wickstrom, T., N. Clarke, K. Derome, J. Derome, and E. Rogeberg. 2000. Comparison study of five analytical methods for the fractionation and subsequent determination of aluminium in natural water samples. *J. Environ. Monitoring* 2:171–181.

Williams, B.L., C.A. Shand, M. Hill, C. O'Hara, S. Smith, and M.E. Young. 1995. A procedure for the simultaneous oxidation of total soluble nitrogen and phosphorus in extracts of fresh and fumigated soils and litters. *Commun. Soil Sci. Plant Anal.* 26:91–106.

Willis, A.L. 1970. An automated procedure for the analysis of boron in plant tissue. *Commun. Soil Sci. Plant Anal.* 1:205–211.

Wolf, W.R. and K.K. Stewart. 1979. Automated multiple flow injection analysis for flame atomic absorption spectrometry. *Anal. Chem.* 51:1201–1205.

Yesmin, L., S.M. Gammack, L.J. Sanger, and M.S. Cresser. 1995. Impact of atmospheric N deposition on inorganic- and organic-N outputs in water draining from peat. *Sci. Total Environ.* 166:201–209.

Yoza, N., Y. Aoyogi, and S. Ohashi. 1979. Flow injection system for atomic absorption spectrometry. *Anal. Chim. Acta* 111:163–167.

Zandstra, H.G. 1968. Automated determination of phosphorus in sodium bicarbonate extracts. *Can. J. Soil Sci.* 48:219–220.

Marcel Dekker, Inc.
270 Madison Avenue, New York, New York 10016

5
Ion Chromatography

M. Ali Tabatabai
Iowa State University, Ames, Iowa, U.S.A.

Nicholas T. Basta
Oklahoma State University, Stillwater, Oklahoma, U.S.A.

Shreekant V. Karmarkar
Lachat Instruments, Milwaukee, Wisconsin, U.S.A.

I. INTRODUCTION

Ion chromatography (IC) is a term that describes the advances made in the determination of ions. It has become a field of its own since its introduction by Small et al. (1975). Within the past 20 years, research in the area of IC has made significant advances in separation and determination of ionic species, and IC has become a rapid and sensitive technique for analyzing complex mixtures of ions. Now, ion chromatographs are available that feature high-speed separation, continuous monitoring by detector systems, and the instantaneous readout of analytical data. The IC technique, a type of high-performance liquid chromatography (HPLC), has gained popularity for accurate and precise determination of anions and cations in soils, plants, water, and other environmental materials, as well as samples from clinical, metal plating, power generation, semiconductor fabrication, and other industrial sources. Several books have been published on IC, including the development and use of its components, and the potential of the technique as an analytical tool (Sawicki et al., 1978; Mulik and Sawicki, 1979a; Fritz et al., 1982; Smith and Chang, 1983; Weiss, 1986; Tarter, 1987; Small, 1989).

Marcel Dekker, Inc.
270 Madison Avenue, New York, New York 10016

This is a revised version of the corresponding chapter in the previous edition (Tabatabai and Basta, 1991). It covers the basic principles of IC, the instruments and methods that have been developed, and the application of these methods to the analysis of soil, plant, water, and environmental samples. New approaches for application of IC to chemical speciation are described. Application of IC to soil and environmental analysis has been previously reviewed by Frankenberger et al. (1990), Tabatabai and Basta (1991), Tabatabai and Frankenberger (1996), and Karmarkar (1998). Several IC methods are available for the determination of ions other than those discussed in this chapter, but these methods have not been evaluated for soil analysis (Sawicki et al., 1978; Mulik and Sawicki, 1979a, b; Johnson, 1987).

II. BASIC PRINCIPLES

Ion chromatography has its roots in pioneering work in the area of ion exchange, including the development of synthetic ion-exchange resins. This technique falls under the broad category of liquid chromatography. A review of the work published on these topics is beyond the scope of this chapter, but information on the basic principles involved in the operation of ion chromatographs is presented. Typical components of an IC system (Fig. 1) include an optional autosampler, a high-pressure pump, and an injection valve with a sample loop of suitable size (typically 10–250 μL), a guard column (also called a precolumn), an analytical column, a postcolumn reaction system, a flow-through detector, and a data station ranging in complexity from a chart recorder to a computerized data system. A suitable

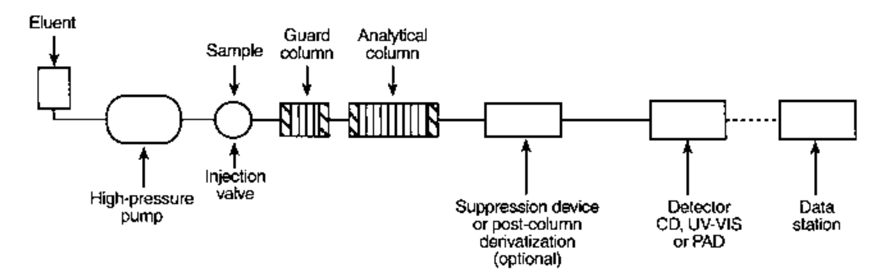


Figure 1 Schematic diagram of components of a typical IC system. CD, conductivity detector; PAD, pulse amperometric detector.

mobile phase, the eluent, flows continuously through the columns and detector. Typically, all the components in contact with the eluent and sample are made from inert materials, such as polyetheretherketone (PEEK), Teflon, or other polymers that are stable under acidic or basic solutions. After sample preparation, usually the sample is filtered through a 0.45 μm filter and diluted, and then a fixed volume is injected onto the guard column. It then passes on to the analytical column. The ions in the sample are separated as a result of differing affinities for the column packing material as the ions are swept along in the flowing eluent (Karmarkar, 1998). The packing material is selected on the basis of its ion selectivity and ion exchange capacity.

Ion chromatographic separation takes place by one of three separation modes: (1) ion exchange, examples of which include determination of common anions (e.g., Br^-, Cl^-, F^-, NO_3^-, NO_2^-, SO_4^{2-}, and PO_4^{3-}, and alkali and alkaline-earth cations (e.g., Na^+, Li^+, K^+, Ca^{2+}, and Mg^{2+}) and NH_4^+; (2) ion exclusion, which is used for the separation of low-molecular-weight organic acids (e.g., adipic, acetic, formic, malic, malonic, oxalic, succinic, and tartaric acids); and (3) ion pair separation, including separation of heavy metals and transition metal ions (e.g., Cd^{2+}, Co^{2+}, Cu^{2+}, Fe^{2+}, Fe^{3+}, Pb^{2+}, Mn^{2+}, Ni^{2+}, and Zn^{2+}). Details of each of these separation modes are described by Haddad and Jackson (1990).

The first IC system developed in the early 1970s used conductimetric detection, but recent IC equipment features colorimetric (UV-VIS), pulse amperometric or spectroscopic detection systems, including inductively coupled plasma (ICP) spectrometry or hydride generation and atomic absorption spectrometry. The development of new detection modes has increased the capability of IC to measure a great number of analytes with improved detection limits.

Depending on the analytical accuracy and precision required, ion chromatographs can be divided into two major groups: those that operate on the principle of eluent suppression (dual-column system) and those with no suppressor column (single-column system). Detailed comparisons between eluent-suppressed and nonsuppressed ion chromatography have been presented by Pohl and Johnson (1980) and Tarter et al. (1987).

Both types employ conductimetric detection systems, based on the variation in electrical conductivity of a solution with the concentration of ions present. These detectors are used for the determination of all ionic species (inorganic anions and cations, and organic acids) in solution. Calibration graphs of specific conductance vs. ion concentration used in IC are usually linear at low concentrations of each ion ($< 100\,mg\,L^{-1}$).

A. Systems with Conductimetric Detectors

1. Eluent-Suppressed Ion Chromatography

Until the late 1980s, the suppressed-type IC was only marketed by Dionex Corporation (Sunnyvale, CA). Figure 2 shows its basic components. For simplicity, the reservoirs of the eluent and water used for regeneration of the suppressor column and the valving system involved in the IC are not shown. The instrument employs the following components:

1. An eluent pump and reservoir
2. A sample injection valve (the sample loop can be adjusted from about 50 μL to several hundred μL)
3. An ion-exchange separation column
4. A suppressor column coupled to a conductivity detector, meter, and output device
5. A regenerating pump with electronic timer and controls

Several types of column are commercially available for the ion-exchange separation of the common inorganic and organic anions via eluent-suppressed IC. The resin material used and the available columns were described by Weiss (1995).

In the eluent-suppressed IC, the ion species are resolved by conventional elution chromatography followed by passage through an eluent stripper, or "suppressor," column, wherein the eluent coming from the separating column is stripped or neutralized. Thus only the ion species of interest leave the bottom of the suppressor column; anions emerge in a background of H_2CO_3, which exhibits a low conductivity, while cations emerge in water. These ions are monitored subsequently in the conductivity

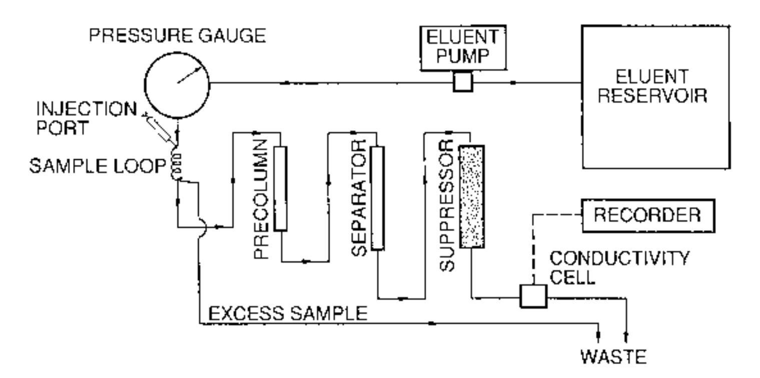


Figure 2 Simplified schematic diagram of suppressed-type IC.

cell/meter/recorder (integrator) combination. The eluent flow rate can be varied by adjusting the pump pressure, but normally it is about 2–3 mL min^{-1}. An aliquot (~2 mL) of, for example, a suspension-free soil extract is injected by a plastic syringe into the injection valve of the IC. The sample loop on the injection valve can be adjusted, but normally a volume of 100 μL is used. The 2-mL volume is convenient to ensure proper flushing of the injection valve loop and lines.

The first suppression device introduced by Small et al. (1975) consisted of a column (dimensions ranging from 9 × 250 mm to 9 × 110 mm, or 2.8 × 300 mm) packed with a high-capacity resin material. The resin of the suppressor column had to be regenerated after about 50 analyses (8–10 h) by flushing the suppressor column with 0.5 *M* H_2SO_4 (15 min) to remove anions or 1 *M* NaOH (15 min) to remove cations, followed by deionized water (25 min). In some early Dionex models (e.g., the Model 10) this could be accomplished without attending the instrument after each working day. This device had two disadvantages: (1) a relatively large volume of the suppressor column resulted in band broadening, which resulted in loss in chromatographic efficiency; and (2) the detector response to the ions of strong acids or bases decreased, whereas the response to ions of weak acids or bases increased as the active sites of the suppressor column were steadily depleted. The lack of a steady state resulted in poor precision. Despite these disadvantages, the packed-bed suppressor provided the foundation on which the suppressed IC was developed. The background suppression (eluent, $NaHCO_3 + Na_2CO_3$) was achieved according to

$$R^- {-} H^+ + Na^+HCO_3^- \rightarrow R^- {-} Na^+ + H_2CO_3^0$$

$$2R^- {-} H^+ + 2Na^+CO_3^{2-} \rightarrow 2R^- {-} Na^+ + H_2CO_3^0$$

The signal enhancement was achieved according to

$$R^- {-} H^+ + Na^+A^- \rightarrow R^- {-} Na^+ + H^+A^-$$

where R^- is a functional group attached to the resin within the suppressor and A^- is an anionic species in the sample. The batch-type or packed-bed column device was in used until 1975, when a continually operated fiber-based device was developed (Henshall et al., 1992). Presently, the following five suppression devices are commercially available:

1. A hollow-fiber membrane suppressor (Steven et al., 1981) and micro-membrane suppressor (Franklin, 1985; Stillian, 1985) that is generated

Marcel Dekker, Inc.
270 Madison Avenue, New York, New York 10016

electrochemically (Henshall et al., 1992); commercially available with IC systems from Dionex.
2. The QuikChem small suppressor that is regenerated after every sample using chemicals (Karmarkar, 1996); commercially available with an IC system from Zellweger Analytics, Inc., Lachat Instruments Div. (Milwaukee, WI).
3. A set of two parallel small suppressor columns: one is regenerated electrochemically while the other is being used (Saari-Nordhaus and Anderson, 1996); commercially available with an IC system from Alltech Associates, Inc. (Deerfield, IL).
4. A device with postcolumn addition of a colloidal suspension of a high-capacity ion exchange material, also called solid phase reagent (Gjerde and Benson, 1992); available commercially from Sarasep, Inc. (San Jose, CA).
5. A self-regenerating suppressor (SRS), which utilizes autosuppression to enhance analyte conductivity while decreasing eluent conductivity, thus resulting in a significant improvement in analyte detection limits, is marketed by Dionex. The ions required for eluent suppression are generated in the SRS by the electrolysis of water. The SRS combines the best features of micromembrane suppressor—high suppression capacity, minimal peak dispersion, solvent compatibility, and continuous use—with the added advantage of effortless operation and no maintenance.

With the use of a hollow-fiber membrane suppressor or micromembrane suppressor, the problems associated with the original packed-bed suppressor technique, such as band broadening, ion exclusion, and oxidation of NO_2^-, are eliminated. The disposable solid-phase chemical suppressor (SPCS) simplifies the instrumentation required to perform suppressed-based IC by eliminating the regeneration system and the complex postcolumn reaction system needed with other suppression techniques (Saari-Nordhaus et al., 1994). The lifetime of the SPCS cartridge is dependent on the ionic strength and flow rates of the eluent, varying from 7 to 12 h.

In a variant of the suppressor column system, the resin in the suppressor column is replaced by an ion-exchange membrane in tubular form to condition the eluent continuously (Stevens et al., 1981). This membrane (sulfonated polyethylene hollow fiber) acts exactly like the suppressor resin in that ions are exchanged from the membrane for ions in the eluent system. The innovation is that for the analysis of anions the membrane is regenerated continuously by a gravity-fed (or low-pressure) flow of low-concentration H_2SO_4 that continuously replaces the ions that

are exchanged onto the fiber with ions from the regenerant. Thus, separate regeneration steps are eliminated. The replacement of the conventional ion-exchange resin bed suppressor column with the hollow fiber suppressor allows continuous operation of an IC without varying interference from baseline dips, ion-exclusion effects, or chemical reaction. Stevens et al. (1981) concluded that conventional suppressor column systems had less band spreading than those using hollow-fiber suppressor, and this resulted in slightly poorer resolution of early eluting ions with the latter type of eluent suppression technique. However, our experience is different. Furthermore, work by Weiss (1986) showed that because of the low dead volume of a membrane suppressor, mixing and band broadening effects are minimized and the sensitivity is generally enhanced compared with the more traditional packed bed suppressor. Details of the theory of operation of the hollow-fiber suppressor were discussed by Stevens et al. (1981), Hanaoka et al. (1982), Small (1983), Weiss (1986), and Dasgupta (1992).

The reactions involved in the separator column and suppressor column (or one of the devices listed above) in the determination of anions, alkali metals, and alkaline earth metals are shown in Table 1. In the determination of anions, the IC is equipped with a separator column packed with a low-capacity anion-exchange agglomerated resin in the HCO_3^- form, and the suppressor column contains a strong acid high-capacity cation-exchange resin in the H^+ form or one of the other suppression devices listed above. The eluent used normally is a mixture of dilute $NaHCO_3$ and Na_2CO_3, although other dilute mixtures (e.g., $Na_2CO_3 + NaOH$) are also used (Johnson, 1987). The anions are separated and converted to their strong acids in a background of $H_2CO_3^0$, which has no charge and low conductivity. The presence of strong acids in H_2CO_3 is measured by a conductivity cell and reported as peaks on a stripchart recorder or integrator. The peak height is directly proportional to the concentration of ions in solution. From calibration graphs prepared for peak height versus concentration of ions in standard solutions containing the ions of interest, the concentrations of the ionic species in the sample are calculated. Because of the excellent signal-to-noise ratios, when equipped with a suppressed conductivity detector the IC system can achieve detection limits two orders of magnitude lower than those obtained in a nonsuppressed IC system. The mixture of the standards can be prepared from reagent-grade chemicals. Figure 3 shows a typical chromatogram of a standard solution containing $2\,mg\,L^{-1}$ each of F^-, Cl^-, PO_4^{3-}-P, NO_3^--N, SO_4^{2-}-S. The separation of PO_4^{3-} from several other oxyanions is shown in Fig. 4.

Recent developments by Dionex involve the use of an autosuppression with the anion self-regenerating suppressor, which uses water as a regenerant. In this system, water undergoes electrolysis to form oxygen

Table 1 Reactions in Separator and Suppressor Columns in Determination of Anions and Alkali/Alkaline Earth Metal Cations by Ion Chromatography

	Reaction		
Component	Anion[a]	Alkali metal cation[b]	Alkaline earth metal cation[c]
Eluent	3 m*M* $NaHCO_3$ + 1.8 m*M* Na_2CO_3	5 m*M* HCI	2.5 m*M* HCI + 2.5 m*M* *m*-PDA.2HC1[d]
Displacing ion	HCO_3^-	H^+	*m*-PDH_2^{2+}
Separator column			
Eluent	$R\text{-}HCO_3 + NaHCO_3 \Leftrightarrow R\text{-}HCO_3 + NaHCO_3$	$R\text{-}H + HCl \Leftrightarrow R\text{-}H + HCl$	$R\text{-}PDAH_2 + PADH_2^{2+} + 2Cl^- \Leftrightarrow R\text{-}PDAH_2 + PDAH_2^{2+} + 2C1^-$
Sample	$R\text{-}HCO_3 + MA \rightarrow R\text{-}A + MHCO_3$	$R\text{-}H + MA \rightarrow R\text{-}H + MA$	$R\text{-}PDAH_2 + MA + 2C1^- \rightarrow R\text{-}M + PDAH_2^{2+} + 2C1^- + A$
	$R\text{-}A + NaHCO_3 \rightarrow R\text{-}HCO_3 + NaA$	$R\text{-}M + HCl \rightarrow R\text{-}H + MC1$	$R\text{-}M + PDAH_2^{2+} + 2C1^- \rightarrow R\text{-}PDAH_2 + MC1_2$
Suppressor column			
Eluent	$R\text{-}H + MHCO_3 \rightarrow R\text{-}M + H_2CO_3$	$R\text{-}OH + HCl \rightarrow R\text{-}Cl + H_2O$	$2R\text{-}OH + PDAH_2^{2+} + 2C1^- \rightarrow 2R\text{-}C1 + PDA + 2H_2O$
Sample	$R\text{-}H + NaA \rightarrow R\text{-}Na + HA$	$R\text{-}OH + MCl \rightarrow R\text{-}C1 + MOH$	$2R\text{-}OH + MC1_2 \rightarrow R\text{-}C1 + M(OH)_2$

[a]M = Na, A = anion.
[b]M = alkali metal, A = associated anion.
[c]M = alkaline earth metal, A = associated anion.
[d]*m*-PDA.2HCI = *m*-phenylenediamine dihydrochloride.

Marcel Dekker, Inc.
270 Madison Avenue, New York, New York 10016

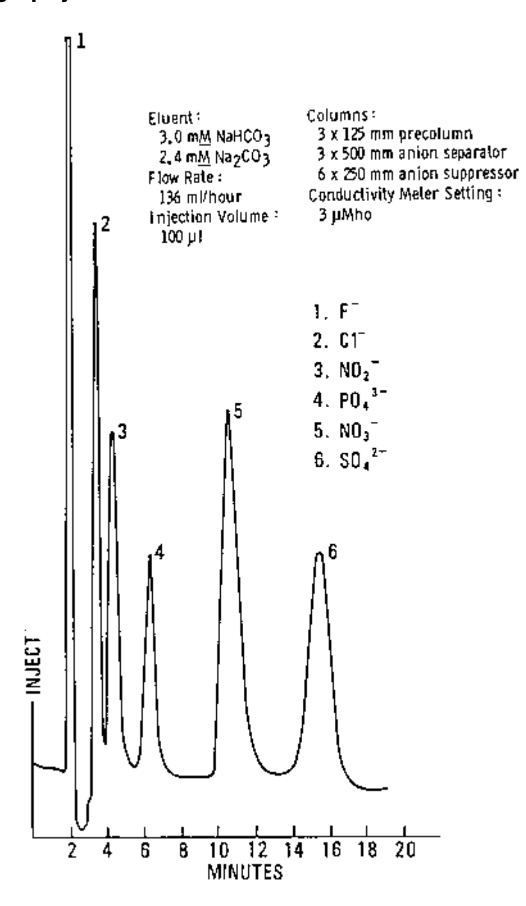


Figure 3 Typical chromatogram of anions separated in a suppressed-type IC system.

gas and hydronium ions in the anode chamber, and hydrogen gas and hydroxide ions in the cathode chamber. The hydroxide ions generated at the cathode are excluded from the eluent chamber by Donnan exclusion. Cation exchange membranes allow hydronium ions to move from the anode chamber into the eluent chamber to neutralize hydroxide eluent, while Na^+ ions in the eluent move across the membrane into the cathode chamber, maintaining the charge balance. In this process, the eluent (e.g., NaOH, Na_2CO_3/$NaHCO_3$, or boric acid/Na tetraborate) is converted to water. The result is a dramatic improvement in signal-to-noise ratio due to three factors: (1) eluent background conductivity decreases as the eluent is suppressed to a less conductive medium, water, (2) analyte conductivity

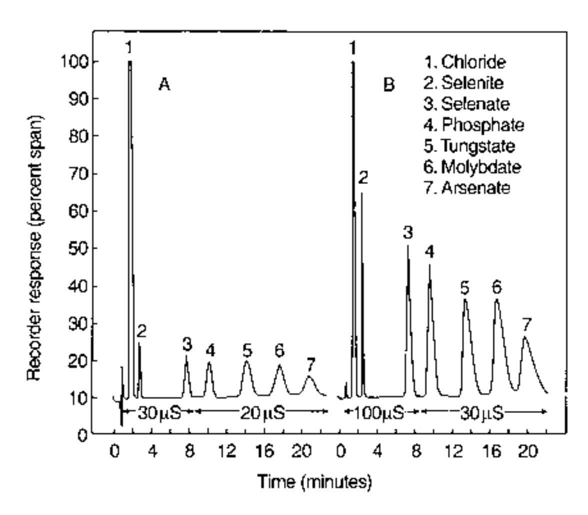


Figure 4 Typical chromatogram of oxyanions separated in a suppressed-type IC system. (A) 0.05 m*M*; (B) 0.5 m*M* with respect to each of the oxyanions. (Karmarkar and Tabatabai, 1992.)

increases because the analyte anions associate with the more conductive hydronium ions, and (3) sample counter ion peaks typical of nonsuppressed IC are eliminated.

In the determination of the alkali metal ions (Li^+, Na^+, K^+, Rb^+, and Cs^+), the separator column is a low-capacity cation-exchange agglomerated polystyrene divinylbenzene copolymer cation resin in the H^+ form, and the suppressor column contains a strong base high-capacity anion-exchange resin in the OH^- form. The alkali metals are separated and converted to their hydroxides in a background of H_2O, which has a very low conductivity. The conductivity of the metal hydroxides is measured by a conductivity cell and reported as peaks on a stripchart recorder or integrator. The reactions involved in the separator and suppressor columns are shown in Table 1. The separation and detection of the alkaline-earth metal ions (Mg^{2+}, Ca^{2+}, Sr^{2+}, and Ba^{2+}) are similar to the procedures for the alkali metals, except that a mixture of 2.5 m*M* HCl + 2.5 m*M* *m*-phenylenediamine (PDA) dihydrochloride is used as the eluent (Table 1). Suppression of the 5 m*M* HCl eluent used for measuring monovalent cations, or of PDA dihydrochloride eluent used for determining divalent cations, is achieved according to

$$R^+OH^- + HCl \rightarrow R^+Cl^- + H_2O$$
$$2R^+OH^- + PDA(2HCl) \rightarrow 2R^+Cl^- + PDA + 2H_2O.$$

Marcel Dekker, Inc.
270 Madison Avenue, New York, New York 10016

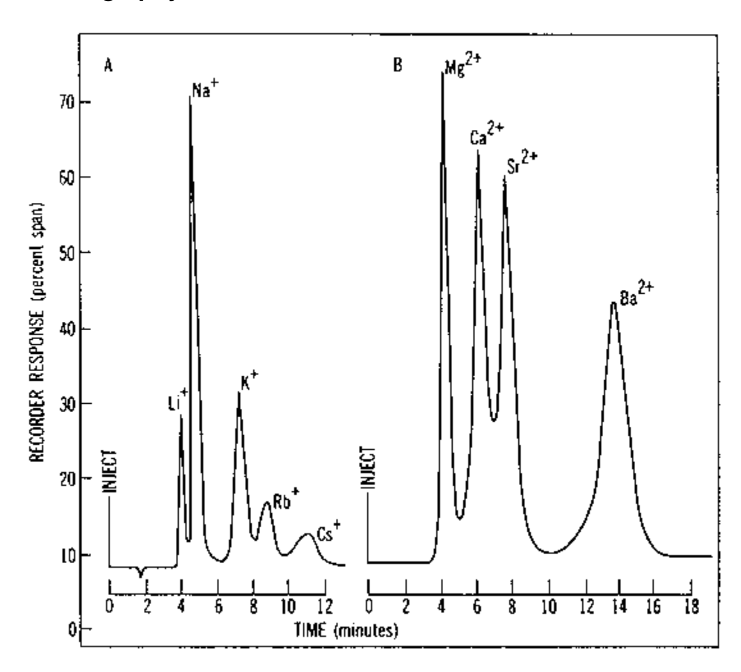


Figure 5 Typical chromatograms of (A) alkali; (B) alkaline earth metal cations. (Tabatabai and Basta, 1991.)

Typical chromatograms of standard solutions containing mixtures of Li^+, Na^+, K^+, Rb^+, and Cs^+, and Mg^{2+}, Ca^{2+}, Sr^{2+}, and Ba^{2+}, respectively, are shown in Fig. 5.

Another recent development by Dionex involves the use of an autosuppression with the cation self-generating suppressor (CRSR). This system also uses hydrolysis of water as described above for ARSR. Anion exchange membranes allow the hydroxide ions to move from the cathode chamber into the eluent chamber to neutralize hydronium ions in the eluent, while eluent counterions (e.g., methanesulfonic acid, MSA) moves across the membrane into the anode chamber, maintaining the charge balance. Response is maximized by association of the analyte cations with the more conductive hydroxide ions. As with the ARSR, the result is a significant improvement in signal-to-noise ratio.

2. Single-Column Ion Chromatography

Two alternative methods to that described above are now available for ion separation and determination. In both methods, no suppressor column is needed (single-column systems). Instead, moderately conducting eluents are

Marcel Dekker, Inc.
270 Madison Avenue, New York, New York 10016

used to elute a variety of ions, which then flow directly into a conductivity detector. The typical eluents used in nonsuppressed IC are phthalic acid and *p*-hydroxybenzoic acid for determination of anions and methanesulfonic acid for determination of cations. The equivalent conductance values of Cl^-, SO_4^{2-}, and other common anions are appreciably greater than the conductance of the eluent anion, so a positive peak is detected as the ions are carried through the detector. Conversely, the equivalent conductance values of Na^+, K^+, and other common cations are appreciably smaller than the conductance of the eluent cation, so a negative peak is detected as the cations are carried through the detector.

One technique is a variation of conventional HPLC, in which silica-based column packings provide ion separations. In a second similar approach, specially synthesized macroporous polystyrene-divinylbenzene resins with low capacities are coupled with moderate-conductivity mono- or polyvalent eluting ions (Smith and Chang, 1983). In the early 1980s, dedicated systems for single-column IC were introduced by Wescan (Santa Clara, CA), Hewlett-Packard (now Agilent) (Palo Alto, CA), and Brinkman (Westbury, NY). The instrument distributed by Brinkman was manufactured by Metrohm in Switzerland.

Compared with suppressed IC, nonsuppressed IC is easy to operate. It is also a useful technique for determining ions of weak acids, such as cyanide and sulfide, that do not conduct in chemically suppressed systems. However, for several reasons, nonsuppressed IC has not gained as much acceptance as suppressed IC, especially in environmental analysis. One reason is that regulatory methods, such as the USEPA method 300.0, are based on suppressed IC. The other is that the signal-to-noise ratio is much greater with suppressed IC than that with nonsuppressed IC. Lastly, the suppression devices developed since 1981 eliminate the drawbacks of the original packed-bed suppressor.

The basic components of a nonsuppressed-type (single-column system) ion chromatograph (SCIC) are shown in Fig. 6. The technique employs the following main components:

1. An eluent pump and eluent reservoir
2. A sample injection valve (a sample loop of $\sim$500 μL is normally used
3. An ion-exchange separator column
4. A conductivity detector coupled to an output device

In this system, a low-capacity exchange column and low-conductivity eluent are used without the need for a suppressor column (Gjerde and Fritz, 1979, 1981; Gjerde et al., 1979, 1980). Eliminating the suppressor column reduces the postcolumn dead volume, resulting in faster analyses, but the SCIC system is about two orders of magnitude less sensitive than the

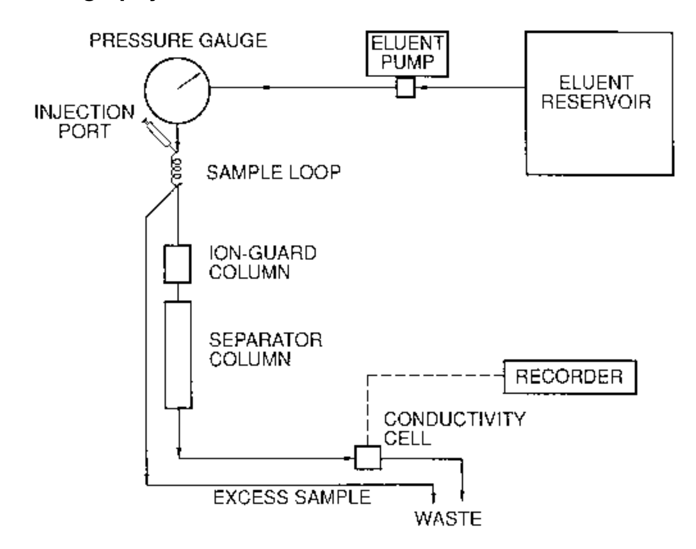


Figure 6 Simplified schematic diagram of single-column-type IC. (Tabatabai and Basta, 1991.)

eluent-suppressed system. Appropriate low-capacity exchange columns used in the SCIC systems include a macroporous polystyrene divinylbenzene resin (Gjerde and Fritz, 1979, 1981) or a surface-quaternized silica (Girard and Glatz, 1981). Organic acids (phthalate, benzoate, or citrate) are often used in the mobile phase of SCIC (Gjerde and Fritz, 1981; Jupille, 1987), with phthalic acid being the most common because of its wide range of retention control (via pH adjustment) and equivalent conductance (Jupille et al., 1983). Anions of interest elute in the hydrogen form (e.g., HCl, HNO_3, H_2SO_4) against a background of ionized phthalate ions. A number of equilibria affect SCIC. Buffer ions (usually weak acid ions) equilibrate with the free acid in solution. Both of these species, in turn, equilibrate with their bound forms at the surface of the stationary phase (Jupille, 1987). Details of the reactions involved and factors affecting ion-exchange separations in the SCIC system, information on other types of separations, and column technology were presented by Jupille (1987). Most of these systems, however, have not been used for soil analysis.

For the determination of NH_4^+ and alkali metals, the mobile phase used in the SCIC system must have a strong affinity for the ion-exchange resin in order to displace separated ions from the analytical column. Maximum sensitivity is achieved when the equivalent conductance of the ionic species gives a detection signal well above the eluent background (Gjerde et al., 1979). Dilute HNO_3 is used for the determination of

NH_4^+ and the alkali metals (Fritz et al., 1980). Use of 10 mM HNO_3 (pH 2.1) has been shown to give excellent resolution of monovalent cations, with elution complete in < 6 min when a Vydac 401 TP cation-exchange column (Separation Group, Hesperia, Calif.) is used (Nieto and Frankenberger, 1985). Ethylenediammonium dinitrate (5 mM, pH 6.1) competes more strongly with divalent cations in solution than does HNO_3, thus providing better resolution and peak symmetry for the divalent cations. Fritz et al. (1980) recommended a solution pH of 6.1 so that all carbonic acid species would elute as bicarbonate and cause no interference with the analysis.

Background conductance and minimum detection limits of both alkali and alkaline earth metals increase with increasing concentration of the electrolyte mobile phase (Iskandaranl and Pletrzyk, 1982), whereas retention times decrease with increasing eluent concentration and decreasing resin capacity (k') (Gjerde et al., 1980). The commercially available columns (e.g., Vydac 401 TP cation-exchange column) have relatively low k' [0.10 mol(-) kg^{-1}], although resins of even lower k' have been synthesized for chromatographic separation of ions (Boyd et al., 1954; Fritz and Story, 1974a,b; Gjerde and Fritz, 1979; Gjerde et al., 1979).

B. Systems with Spectroscopic Detectors

Many inorganic ions display strong absorbance in the lower range of UV. At first, these wavelengths were not readily accessible to IC photometers, but when UV detectors that could reach down to ≤ 200 nm became available, inorganic anions such as $NO_3^-, NO_2^-, Br^-, I^-, BrO_3^-, IO_3^-$, and $S_2O_3^{2-}$ could be determined (Small, 1983). Nitrate, NO_2^-, and Br^- have been determined in such diverse environments as river and waste treatment waters, rain, eutectic salt mixtures, and saliva, although little information is available on the use of UV detectors for the determination of these or other inorganic ions in soils. Also, ions such as SCN^-. $S_2O_3^{2-}$ and several polythionate species have been measured successfully by using low-capacity resins and $NaClO_4$ as an eluent. Cortes (1982) used silica-based columns with amino functional groups for the effective separation of both organic and inorganic anions that are UV-absorbing. Another approach involves "postcolumn derivatization", whereby the separated ions are converted into complexes that absorb ultraviolet and visible (UV-VIS) light (Fig. 7). This is accomplished by merging separator column effluent with a stream of complexing agent to form absorbing complexes prior to a UV-VIS detector (Figs. 8, 9). Postcolumn derivatization detection has extended the use of IC to measure trace levels of transition and other heavy

Marcel Dekker, Inc.
270 Madison Avenue, New York, New York 10016

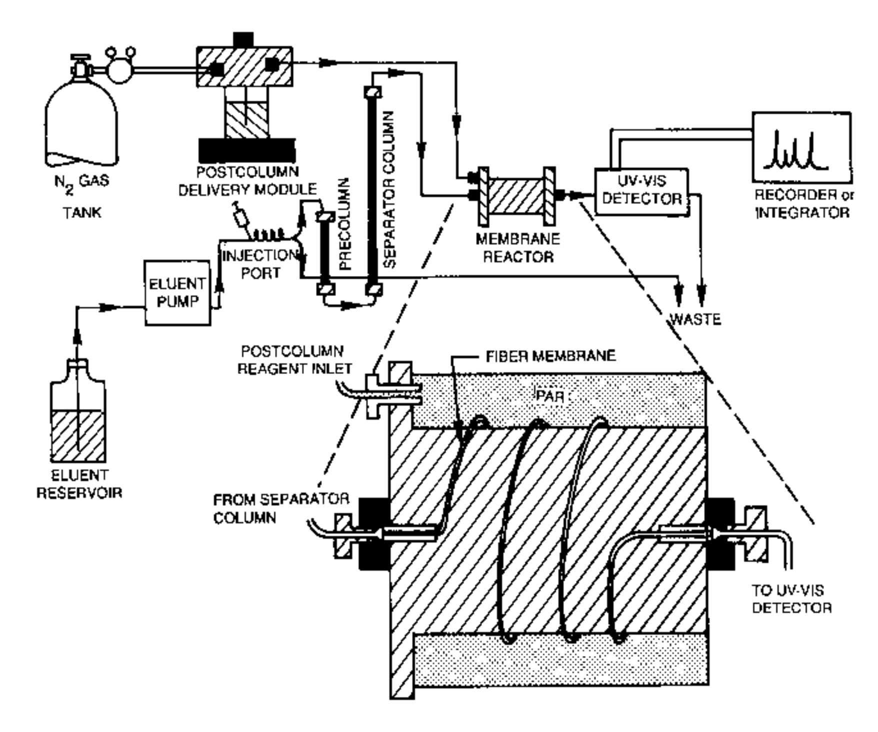


Figure 7 Schematic diagram of Dionex Model 2002I ion chromatograph equipped with membrane reactor and UV-VIS detector. (Basta and Tabatabai, 1990.)

metals (Fig. 10) in soil and sewage sludge digests (Basta and Tabatabai, 1990, 1991).

C. Systems with Pulse Amperometric Detectors

Pulse amperometric detection (PAD) is useful for IC analysis of anion or weak acids with $pK_a > 7$. These anions cannot be measured by IC based on suppressed conductivity because they form poorly conducting weak acids after chemical suppression. Anions in this category include S^{2-} and CN^-. Ion chromatography based on amperometric detection has been reviewed by Weiss (1986). Applications of HPIC-PAD to the determination of such organic species as saccharides, aminosaccharides, and aminoacids are described in Sec. III.A.3 below.

D. Design and Operational Features

The two crucial milestones in the IC system developed by scientists at Dow Chemicals in the early 70s (Small et al., 1975) were the development of

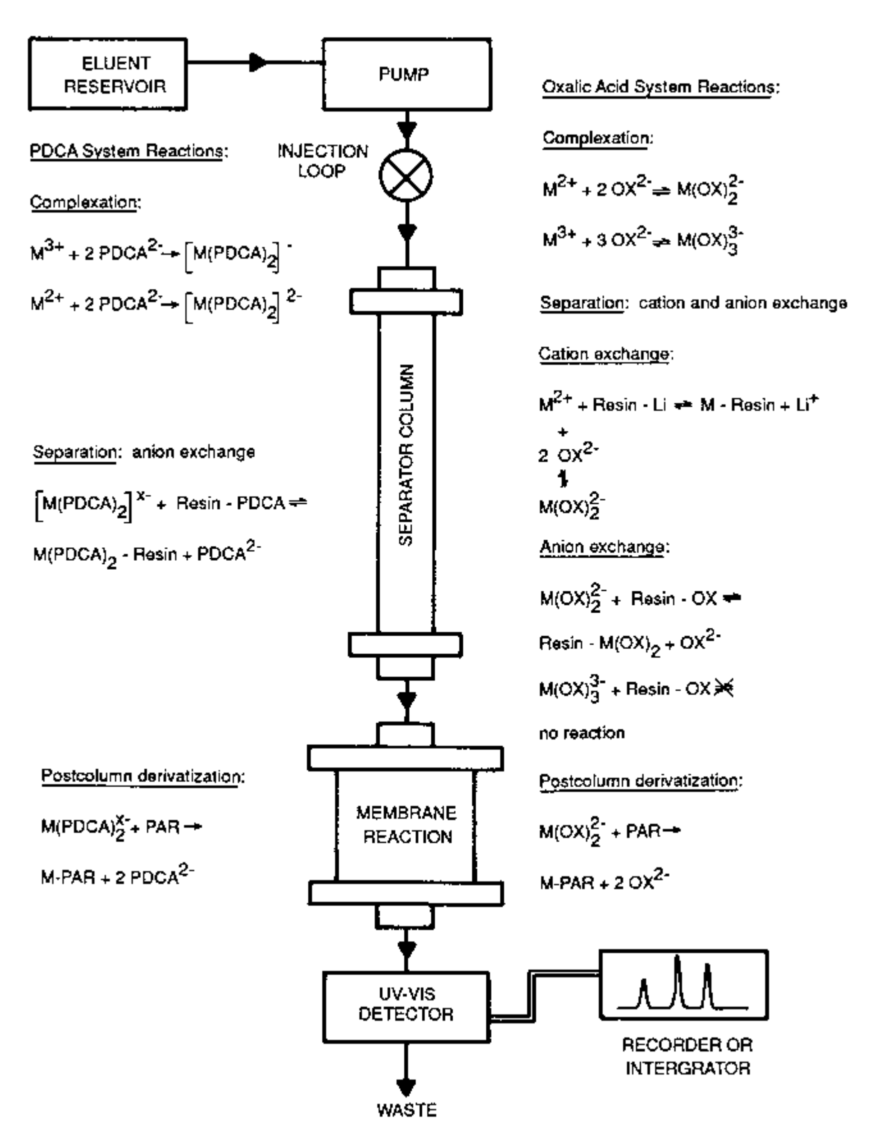


Figure 8 Chemical reactions in the Dionex Model 2002I system shown in Fig. 7. (Basta and Tabatabai, 1991.)

low-capacity ion-exchange resins for efficient chromatographic separation and chemical suppression for enhanced S/N ratio. As mentioned before, chemical suppression lowers the background conductance and enhances the signal by converting the ions to their highly conducting forms. The chemical

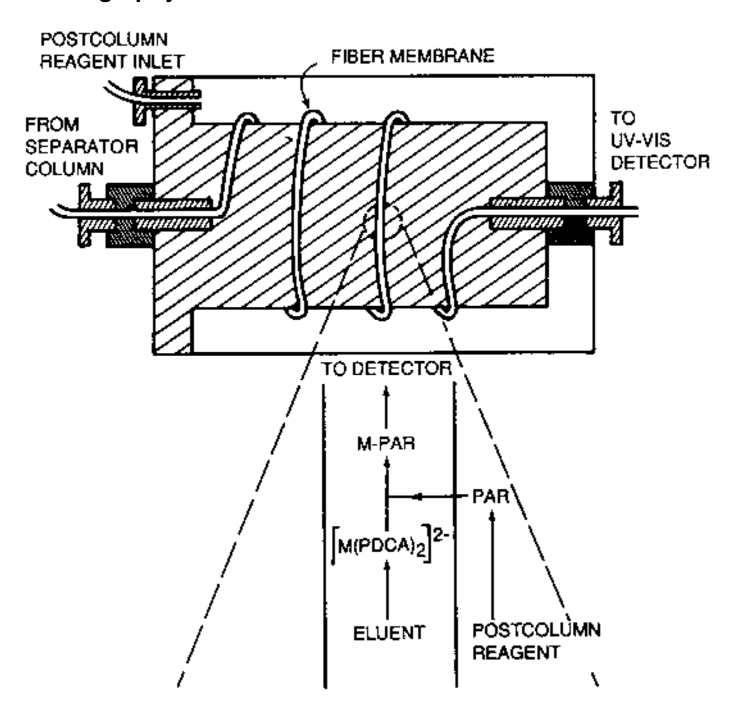


Figure 9 Schematic of postcolumn reaction with PAR in the postcolumn reactor membrane. (Basta and Tabatabai, 1991.)

suppression devices available now essentially fall into three broad categories. In the first type, the suppression reactions occur in a packed bed of high-exchange-capacity resin material (Karmarkar, 1996; Saari-Nordhaus and Anderson, 1996). In the second type, the suppression reactions occur as the eluent stream mixes with the flowing stream of high-capacity resin material (Gjerde and Benson, 1992). In the third type, the reactions occur across an ion exchange membrane (Stevens et al., 1981; Stillian, 1985; Henshall et al., 1992).

There are at least three types of commercially available packed bed suppressors; in each case the geometry of the suppressor is significantly smaller than that of the pioneering invention of Small et al. (1975). In the first type, a 4.6×20 mm cartridge is regenerated after every sample by pushing through it about 1 mL of 0.25 M H_2SO_4 followed by about 2 mL of deionized water (Karmarkar, 1996). In the second type, there are two small cartridges, one being used while the second one is regenerated electrochemically. The suppression system toggles between these two

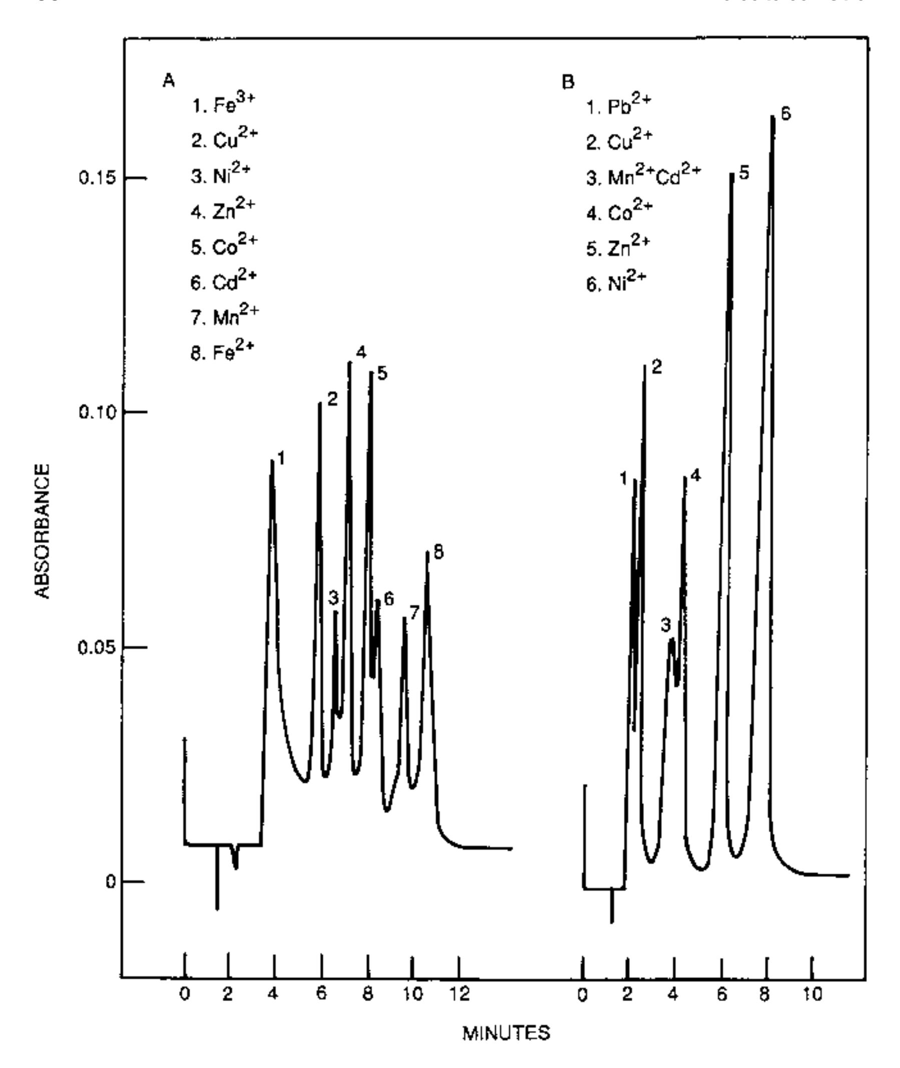


Figure 10 Typical chromatogram of transition and heavy metals obtained by ion chromatography with (A) 2,6-pyridinedicarboxylic acid and (B) oxalic acid as eluent. (Basta and Tabatabai, 1990.)

cartridges (Saari-Nordhaus and Anderson, 1996). In the third type, commercially available on IC systems from Metrohm, three suppressor cartridges are used. While one of the three is being used for IC analysis, the second one is being regenerated with H_2SO_4, and the third one receives a deionized water wash. The IC systems employing these cartridges have been

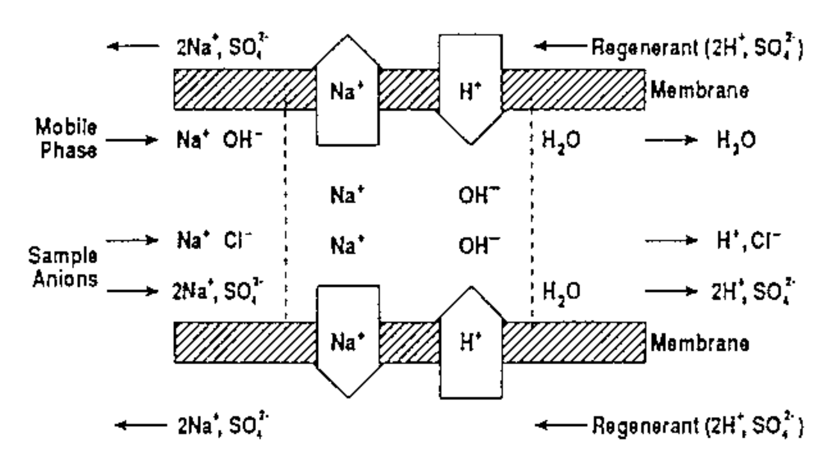


Figure 11 Schematic of chemical suppression using anion exchange membrane. (Stevens et al., 1981.)

found useful for the analysis of waters and soil and plant extracts. The second type of suppression, with flowing stream resin material, has not found many commercial applications (Gjerde and Benson, 1992).

The third type of suppression, using membranes for transport of eluent and suppressing ions, has been an evolutionary process driven by Dionex Corp. At the beginning of the 1980s the fiber-based suppressor was developed (Stevens et al., 1981), followed by the micromembrane-based suppressor (Stillian, 1985). The reactions involved in the micromembrane device are shown in Fig. 11. The IC systems employing these two types of suppressors were evaluated for the analysis of soil and plant extracts (Karmarkar and Tabatabai, 1991, 1992). Further improvements to the micromembrane suppressor were then made in which, instead of regenerating the ion exchange membranes with a chemical, the regenerating ions were formed in situ by electrolysis of deionized water (Henshall et al., 1992). The reactions involved in the autosuppression with the anion and cation self-generating suppressor are shown in Figs. 12 and 13, respectively. The IC system using this improved micromembrane suppressor has not yet been evaluated for the analysis of soil and plant extracts.

The columns used in eluent-suppressed-type IC were initially made of glass, but present versions are made of plastic, with a performance equivalent to or better than that of glass columns and no breakage. Typical diameters are from 4 to 9 mm; the lengths vary from 50 to 250 mm. Dionex Corp. is the sole distributor.

The columns in single-column-type (nonsuppressed) IC can be glass, plastic, or (most commonly nowadays) stainless steel. The phthalate and

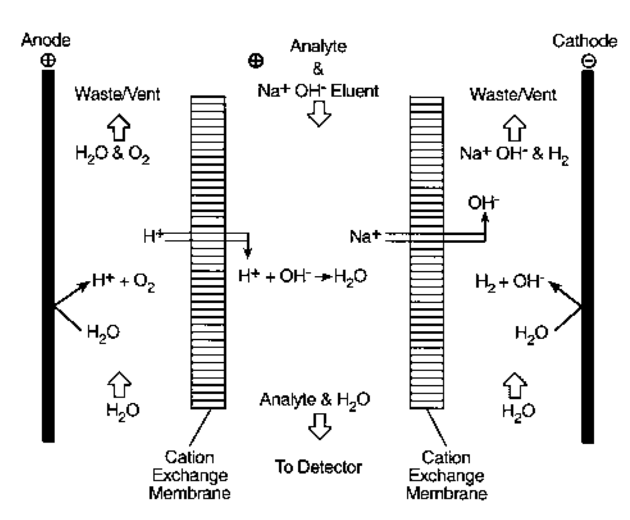


Figure 12 Reactions involved in Dionex autosuppression device for anion self-regenerating suppressor.

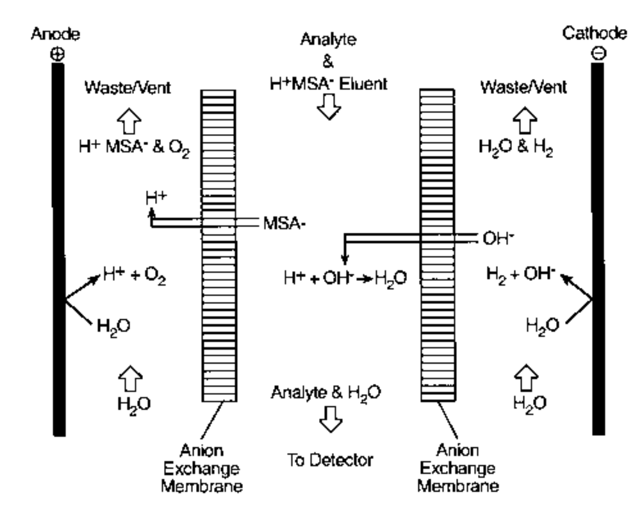


Figure 13 Reactions involved in Dionex autosuppression device for cation self-regenerating suppressor.

benzoate eluents used in SCIC have pH values ranging from 3 to 7, so little corrosion is expected. The injection of samples with pH values higher than 7 is not advisable because the silica packing will degrade severely. Samples with pH values > 7 are normally treated with eluent until the proper pH balance is achieved.

The commonly used detector is a high-sensitivity flow cell conductivity meter. The cell body is constructed of Kel-F plastic with an internal volume ranging from 2 to 6 μL. The electrodes are made of 316 stainless steel. The conductivity meter setting ranges from 0.1 to 1000 μS (Dionex Model 10) or up to 10,000 pS (Dionex Model 2002i). The conductivity meter setting commonly used, however, is 3, 10, or 30 μS. The signal is displayed either on a meter or on a digital readout. Conductivity measurements are quite sensitive to temperature fluctuations, so adequate temperature control is desirable. Some of the early eluent-suppressed IC instruments manufactured by Dionex (e.g., the Model 10) did not have this temperature control, but his has been remedied in later models. To facilitate temperature compensation a thermistor is placed in the liquid line just after the electrode of the conductivity detector module (e.g. Dionex Model 2002i). The cell is driven by a high-frequency oscillator from the main circuit board. The cell output drives an amplifier, and changes in the ionic composition in the cell result in signal changes to the amplifier. The signal caused by the presence of conductive ions in the cell, after temperature compensation, results in meter and recorder-pen deflection.

The SCIC instruments have many of the components of eluent-suppressed–type instruments. The main difference between these two types of instruments lies in the column packing, and the lack of a regeneration pump and timer in the SCIC systems.

E. Commercial IC Systems

Current ion chromatographic systems are available from Dionex (Sunnyvale, CA), Lachat (Milwaukee, WI), Brinkman (Westbury, NY), Wescan/Alltech (Deerfield, IL), Waters (Milford, MA), and Agilent (Hewlett-Packard)(Palo Alto, CA), or their associate/subsidiary companies in other countries. All IC systems feature ion separation and detection modes.

Other instruments are available from most manufacturers that involve postcolumn reaction systems for the determination of polyphosphates and the transition metals in aqueous solutions. No information is available, however, on the use of these instruments for soil or plant analysis.

Several advanced eluent-suppressed IC models manufactured by various companies have not been evaluated for soil analysis, but it should not be difficult to adapt most of the methods available for this purpose to make them compatible with those IC systems. In using any IC instrument, the operator must be familiar with the principle of operation and the reactions involved. Knowledge of the sample composition is also very useful. Cleanup procedures for most IC instruments are provided by the manufacturers. Although most of these procedures are not difficult to

perform, experience with the IC system and familiarity with the functions of its components are helpful.

F. Sample Preparation and IC Conditions

One of the most important requirements of the IC technique is that the sample injected for analysis should be free of particulates. Loss of resolution can result from a contaminated precolumn or analytical column. Reproducibility may be affected by a contaminated column, an insufficiently conditioned column, or microbial growth in the eluents when stored at room temperature for several days, especially those used with single-column systems. Therefore, the eluent used with the single-column system should be prepared freshly on a daily basis. The precolumn, analytical column, and suppressor column can be used for many months. Degradation of the columns' resins can be detected easily from inconsistent peak heights and lack of peak resolution. The relative retention time for the eluent-suppressed IC system is affected by the eluent composition, and for the single-column system is affected by the pH and ionic strength of the mobile phase. An increase in the ionic strength and pH of the eluent causes the solute retention time to decrease. In general, retention of ionic species is directly proportional to column length and inversely related to eluent flow rate. Increasing the column length generally results in greater resolution of the solute; however, the time required for analysis is increased (Dick and Tabatabai, 1979; Tabatabai and Dick, 1983). Analysis time is decreased at high flow rates, but this can lead to poor resolution with overlapping peaks. Analyte retention time is also indirectly proportional to the concentration of the sample injected, but this effect is minor at low analyte concentrations (Small et al., 1975; Iskandaranl and Pietrzyk, 1982). Another factor that significantly affects peak height, peak resolution, and reproducibility of results is temperature (approximately 2% $^{\circ}C^{-1}$ for peak height). Temperature variations may also cause changes in retention time and produce baseline drift. Waterbaths, jackets, or column heaters may be used to eliminate fluctuations in laboratory temperature, but these are costly and difficult to operate at room temperature with small columns. In most situations, the fluctuation in laboratory temperature can be overcome easily by running standard samples more often during the workday or placing the instrument in an air-conditioned room to eliminate severe fluctuations in daily temperature. The sensitivity of the IC system can be adjusted by changing the range of the conductivity detector and/or sample size (sample loop). Sample pretreatment is often required before analysis by IC systems. Some of the techniques used in sample preparation are summarized in Table 2.

Table 2 Summary of Off-Line and On-Line Techniques for Sample Preparation in IC

Sample preparation objective	Recommended technique	Reference
Off-line techniques		
Removal of particulates	Filtering through 0.45 μm membrane	Karmarkar (1995)
Removal of high concentration of chloride	Solid-phase extraction using a cartridge packed with Ag^{+}-saturated cation exchange resin.	Saari-Nordhaus et al. (1994)
Removal of high concentration of sulfate	Solid-phase extraction using a cartridge packed with Ba^{2+} -saturated resin.	Slingsby and Pohl (1996)
	Sulfate precipitation as lead sulfate by treating the sample with lead perchlorate solution.	Medina et al. (1996)
	Sulfate removal from the sample onto a liquid resin, Amberlite LA-2 consisting of a secondary amine.	Mattusch and Wennrich (1996)
Removal of high-molecular-weight organic compounds	Solid-phase extraction using a cartridge packed with C18 silica treated with cetyltrimethylammonium *p*-hydroxybenzoate	Zerbinati (1995)
Adjusting pH	Solid-phase extraction using a cartridge packed with H^{+}- or OH^{-}-saturated resin for basic or acidic samples, respectively	Saari-Nordhaus et al. (1994)
Ion collection and dissolution for airborne samples.	Collection of airborne samples with an impinger followed by liquid extraction or sparging the gas through a collection solvent	Frankenberger et al. (1990) NIOSH (1994) OSHA (1991)
In-line techniques		
Elimination of matrix	Heart-cut column switching to eliminate matrix. Examples: (1) elimination of organic matrix in an analgesic formulation for sulfite determination, and (2) elimination of phosphate matrix in determination of sulfate in sodium phosphate	Kilgore and Villasenor (1996)

(*continued*)

Table 2 Continued

Sample preparation objective	Recommended technique	Reference
Neutralization of strongly alkaline samples	On-line electrodialysis	Haddad and Laksana (1994); Novic et al. (1995)
Sample dilution	Dilution using a dialysis block	Msada et al. (1996)
Removal of Na^+, Mg^{2+}, and Ca^{2+} from marine, estuarine, and fresh waters	Flow injection with gas diffusion to remove neutral volatile amines and ammonia at high pH	Gibb et al. (1995)
Removal of particulates	Two-stage automated filtration: through a 10 μm filter prior to the injection valve and through a 0.8 μm guard disc prior to the guard column. During IC analysis, the 10 μm filter gets backflushed with 12 mL of deionized water	Karmarkar (1999b)

III. APPLICATIONS

Application of IC to soil analysis was pioneered by the senior author and his associates at Iowa State University in the late 1970s (Dick and Tabatabai, 1979). Since then, many papers have appeared in the soil science literature on the use of suppressed and nonsuppressed IC systems for the determination of anions and cations in soil solutions and exchangeable bases in soils. Some of these methods have been applied successfully to plant and water analysis. The IC system should be useful for a variety of methods used in soil, plant, and environmental analyses, provided that the reagents used in the procedures are compatible with the basic principles of operation of the IC. As such, many of the current methods used in soil and plant analysis produce ionic species in a background of either highly acidic media or high salt concentrations. Consequently, new approaches or modifications of current methods are essential before using the IC system for the determination of the ionic species produced. In this section, the IC systems that have been evaluated for the analysis of soils are discussed, and the application of the method to analysis of plant material, waters and other substrates is integrated into this discussion.

A. Soil and Plant Analysis

1. Anions

The first report on the application of IC for the determination of anions (NO_3^- and SO_4^{2-}) in soils was that by Dick and Tabatabai (1979). In this work, these anions were extracted with water or salt solutions and determined by using a Dionex Model 10, which basically is a low-pressure dual-column (suppressed-type IC system) ion chromatograph, and the results obtained by IC were compared with those obtained by the steam distillation method for NO_3^- and by the methylene blue method for SO_4^{2-}. The system involved a separator column (3×250 mm) packed with a Dionex low-capacity anion-agglomerated resin (in addition to this column, a precolumn, 3×125 mm, containing the same resin was used to protect the separator column by removing particulates and other potentially poisonous substances from the eluent stream) and a suppressor column (6×250 mm). The eluent was $3.0\,\mathrm{m}M\,\mathrm{NaHCO_3} + 1.8\,\mathrm{m}M\,\mathrm{Na_2CO_3}$ at a flow rate of $3\,\mathrm{mL\,min^{-1}}$ and pump pressure of 3.1 MPa (450 psi). The sample loop on the injection valve contained a volume of 100 μL. The NO_3^--N values obtained by the IC method were in close agreement with those obtained by the steam distillation method, and the IC procedure gave quantitative recovery of NO_3^--N added to soils (Dick and Tabatabai, 1979).

Marcel Dekker, Inc.
270 Madison Avenue, New York, New York 10016

The SO_4^{2-}-S values obtained by the IC method were in close agreement with those obtained by the methylene blue method. Water, 10 m*M* LiCl, 10 m*M* KCl, 0.15% $CaCl_2$, 10 m*M* $Ca(C_2H_3O_2)_2$, and a solution containing $100\,mg\,L^{-1}$ P as $Ca(H_2PO_4)_2$ extracted almost identical amounts of SO_4^{2-}-S from soils, and the recovery of added SO_4^{2-} was quantitative (Dick and Tabatabai, 1979). Rapid methods (< 4 min) for determination of SO_4^{2-} in soils extracted with 20 m*M* phosphate salt have been reported (Watkinson and Kear, 1994; Karmarkar, 1996). The effect of eluent composition on determination of oxyanions equilibrated with soils has also been reported, by Karmarkar and Tabatabai (1991, 1992).

Wet digestion or fusion procedures, used for elemental analysis of soil or plant materials, produce digests that are strongly acidic and contain high concentrations of dissolved salts that make the analysis incompatible with the IC system. Chemical methods, however, that do not employ strong acids or use solvent extraction to remove the analytes from the acid matrix could be analyzed by the IC system. Busman et al. (1983) developed a method for the simultaneous determination of total S and Cl in plant samples after combustion of the sample in a Schöniger-type oxygen flask (Fig. 14) containing deionized water (the S and Cl gases produced were absorbed in water, producing SO_4^{2-} and Cl^-). The IC was equipped with a precolumn and separator column (each 4×50 mm, Dionex concentrator columns), and a suppressor column (9×100 mm). The eluent was 3.0 m*M* $NaHCO_3$ + 1.8 m*M* Na_2CO_3 pumped at a flow rate of $2.5\,mL\,min^{-1}$ and a

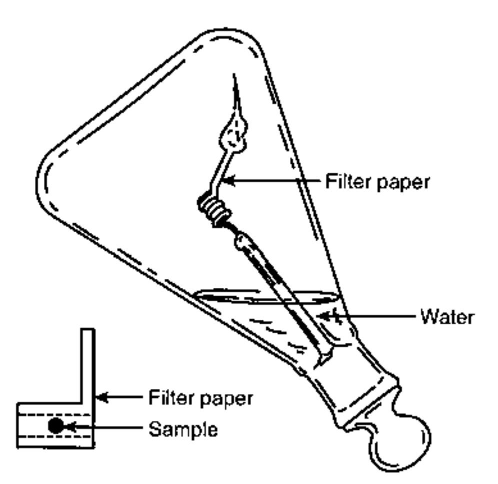


Figure 14 Diagram of oxygen combustion flask and filter paper used for enclosing plant sample. (Busman et al., 1983.)

pump pressure of 3.1 MPa (450 psi). The average total S values of 15 plant samples by the IC method and by the methylene blue method after digestion with NaOBr were 0.255 and 0.259%, respectively. Comparison of the results obtained for Cl by the IC method and by a colorimetric method involving the use of mercuric thiocyanate and ferric ammonium sulfate showed that the average Cl values for the plant samples were in close agreement: 0.380 and 0.377%, respectively. Busman et al. (1983) reported, however, that the recovery of total N and P by the IC method after combustion in an oxygen flask was not quantitative. This is to be expected, because combustion of organic N compounds results in the production of dinitrogen (N_2) and nitrogen oxides (NO, NO_2, and N_2O). The N_2 and N_2O gases produced are inert and relatively insoluble in water. Therefore quantitative recovery is not expected for total N by the ignition and IC procedure. However, the NO and NO_2 are highly soluble in water, producing HNO_2 and HNO_3, respectively, and the anions of these acids can be determined by the IC instrument described.

Busman et al. (1983) reported that the total P values obtained by the ignition of plant samples and subsequent analysis by the IC procedure were very low as compared with those obtained by the molybdenum blue method after oxidation with NaOBr. They examined the fate of the unrecovered P by this IC procedure and concluded that either the plant P was oxidized to polyphosphate(s), which are not detectable by the IC method (being retained by the IC analytical column), or that insoluble metal phosphates (in the ash) were produced on the ignition of the plant material.

A method for the determination of total S in soils and plant materials by IC was described by Tabatabai et al. (1988). In this method, the sample was ignited with $NaHCO_3$ and Ag_2O at 550°C for 3 h. The ignition mixture was dissolved in acetic acid, and an aliquot was injected into the IC instrument after filtration through a 0.45 μm Metrical GA-8 membrane filter. The IC employed was a Dionex 2002i high-pressure liquid chromatograph, equipped with a precolumn (AG-3, 3×50 mm) and a separator column (AS-3, 3×250 mm), both packed with a low-capacity anion-exchange resin, and a suppressor column (9×100 mm) packed with a high-capacity cation-exchange resin in the H^+ form. The injection valve was attached to a 50-μL sample loop, and the eluent was 3.0 mM $NaHCO_3 + 2.4$ mM Na_2CO_3 at a flow rate of 2.3 mL min^{-1} and pump pressure of 4.8 MPa (700 psi). The detector consisted of a conductivity cell fitted with a thermistor and microprocessor-based system that allowed temperature compensation; the output was measured with a Perkin-Elmer integrator (LCI-100). Tabatabai et al. (1988) reported that the total S values in soils and plant materials agreed closely with those obtained by a methylene blue method after alkaline oxidation with NaOBr.

Kalbasi and Tabatabai (1985) developed a method for the determination of NO_3^-, Cl^-, SO_4^{2-}, and PO_4^{3-} in water extracts of plant material by eluent-suppressed IC. They used a Dionex Model 10 IC instrument equipped with a precolumn (3×40 mm, No. 022596), a separator column (3×240 mm, HPLC-AS-3, P/N 030985), a suppressor column (9×80 mm, No. 025670), and a dual pen recorder (Honeywell) for the independent recording of peaks at a conductivity setting of 30 μS full scale. The eluent was 3.0 m*M* $NaHCO_3$ + 1.8 m*M* Na_2CO_3, with a flow rate of 2.1 mL min^{-1} and a pump pressure of 3.4 MPa (500 psi). The average concentrations for 10 plant samples determined by this IC method agreed closely with those obtained by the steam-distillation method for NO_3^--N (0.158 versus 0.164%), with the titrimetric method using $AgNO_3$ and K_2CrO_4 for Cl^- (1.22 vs. 1.19%), and with the colorimetric heteropoly blue method for PO_4^{3-}-P (0.335 vs. 0.330%). The average SO_4^{2-}-S value of the 10 plant samples by the IC method (0.0679%) was somewhat lower than the corresponding value (0.075%) obtained by the reduction to H_2S and colorimetric determination as methylene blue. This disagreement between the average values of SO_4^{2-}-S is expected because the reagent used for its reduction to H_2S in the methylene blue method is not specific for SO_4^{2-}; it reduces a variety of inorganic and organic S compounds. In addition to these anions, Kalbasi and Tabatabai (1985) reported the separation and determination of malic acid by the same IC system. They also showed that F^- was eluted together with an unidentified organic acid. Therefore the amount of water-soluble F^- in plant materials could not be determined accurately. Water extraction of plant tissues for determination of anions by IC was described by Russo and Karmarkar (1998).

Nieto and Frankenberger (1985) evaluated a single-column ion chromatograph (SCIC) for the determination of Cl^-, NO_2^-, NO_3^-, and ${SO_4}^{2-}$ in soil extracts obtained with water or salt solutions containing LiCl, KCl, $Ca(C_2H_3O_2)_2$, or $CaCl_2$. They showed that these anions, and also SO_3^{2-}, Br^-, I^-, and ClO_4^-, could be separated within 10 min. This latter group, however, were not detected in soils. The SCIC system that they used was based on a commercially available HPLC instrument and an eluent containing 4 m*M* phthalic acid (pH 4.5). The inorganic anions were quantified by using a conductivity detector. The elution times for the anions were in the order: $Cl^- < NO_2^- < Br^- < NO_3^- < I^- < ClO_4^- < SO_4^{2-} < SO_3^{2-}$. These SCIC conditions, however, did not detect PO_4^{3-}. The results by this IC system were close to those obtained by conventional methods (Nieto and Frankenberger, 1985). When a 500-μL injection loop was used, this single-column technique had detection limits, expressed in mg L^{-1} of soil extract, as follows: Cl^-, Br^-, NO_3^--N, and SO_4^{2-}-S: 0.025; ClO_4^- and I^-: 0.5; and NO_2^--N and SO_3^{2-}-S: 1.0. This technique proved reproducible for determination of

anions in soil extracts, as is evident from the low coefficient of variation values reported (3.6 to 8.4%).

Because the SCIC conditions described above did not detect PO_4^{3-}, Karlson and Frankenberger (1987) modified these conditions for the determination of this form of P in aqueous extracts of soils. The SCIC system that they used consisted of a Beckman model 332 HPLC equipped with a Model 110A pump and a Model 210 sample injector. This system was connected to a Vydac 3021C4.6 anion-exchange column (4.6×250 mm), a Wescan 269-003 ion-guard column (4.6×40 mm), an Eldex Model III thermostat column heater, a Wescan Model 213 conductivity detector, and a Hewlett-Packard Model 3390A integrator with variable input voltage. The column was maintained at 27°C throughout the analysis. The eluent stream consisted of 1.5 mM phthalic acid adjusted to pH 2.7 with formic acid. The method allowed precise measurements of trace amounts of orthophosphate in the presence of high background levels of Cl^- and NO_3^- (relative standard deviation = 1.1–3.3%). Karlson and Frankenberger (1987) showed that orthophosphate values obtained by the SCIC system agreed closely with those by an Autoanalyzer based on the Mo blue chromophore reaction. Under these SCIC conditions, the elution of orthophosphate occurred after 6 min, whereas Cl^- and NO_3^- had respective retention times of 11 and 20 min.

Barak and Chen (1987) used a SCIC system for the determination of Cl^-, NO_3^-, and SO_4^{2-} in 3 min by using 15 mM phthalic acid (pH = 2.5) as an eluent and a guard column as an analytical column. The equipment configuration that they used consisted of a Perkin-Elmer Series 10 Liquid Chromatograph pump, a 50 μL sample injection loop, a Wescan ion-guard anion cartridge (269-003, 4.6×30 mm), a Wescan ion-guard holder (269-002), a Jasca Uvidec 100-V UV spectrophotometer with a flowthrough cell (10-mm optical path), and an LDC/Milton Roy CI-10 computing integrator. The eluent flow rate was 5 mL min^{-1}, producing a back pressure of 7×10^5 kg m^{-2} or less. The detection was based on UV absorbance at 300 nm.

Although no results for soils were presented, Barak and Chen (1987) claimed that they used the above system for the analysis of soil extracts prepared from saturated pastes. Concentration ranges that can be determined by this IC system are to a large extent a function of sample injection loop size, which thereby determines the amount of analyte injected. In addition to the 50-μL loop, Barak and Chen (1987) used loop sizes ranging from 6 μL for an extremely saline soil extract to 200 μL for rainwater analysis. They recommended the routine measurement of electrical conductivity in order to estimate total anion concentration and thereby ensure that the sample falls within the range of the calibration graph. They reported that hundreds of

analyses were performed on a single column over periods of up to 3 months, and they attributed the relative longevity of the guard column used to the fact that, at pH 2.5, the organic contaminants, including humic substances, are almost uncharged, resulting in much less adsorption on the resin.

Karmarkar (1999a) developed a sequential IC-flow injection analysis (FIA) method using Lachat's QC8000 IC system, which allows determination of NO_3^-, PO_4^{3-}, and NH_4^+ in a single injection. In this system, a QuikChem Small Suppressor cartridge is regenerated in between the samples. A sample is injected while leaving the suppressor off-line. The cationic NH_4^+ elutes in the void volume of an anion-exchange column. The unsuppressed column effluent, exiting the conductivity flow cell, up to this point is used for the FIA determination of NH_4^+. When NH_4^+ exits the conductivity flow cell, a fully regenerated suppressor is brought on-line for conductometric detection of the anions. Analog data is simultaneously acquired from colorimetric and conductometric detectors, for the cationic and anionic nutrients, respectively. The method is accurate, with spike recoveries in wastewater samples ranging from 91% for NO_3^- to 114% for Cl^-, and also has a good precision, with RSD values, for replicate analyses ($n = 7$) of a mid-range standard, ranging from 0.4% for PO_4^{3-} to 1% for NO_3^-.

2. Cations

The IC technique can be used for the simultaneous determination of NH_4^+ and alkali and alkaline earth metals in soil and plant extracts and water samples, provided that the aliquot analyzed is free from interfering substances such as organic materials, high concentrations of soluble salts, and extreme pH values. Both the eluent-suppressed and single-column IC systems have been evaluated for the determination of these metals in soils, plant materials, and natural waters.

Basta and Tabatabai (1985a) developed a method of determination of exchangeable bases in soils by an eluent-suppressed IC system equipped with a precolumn, a separator column, and a suppressor column. Separate precolumns and separator columns were employed for the determination of alkali (monovalent) and alkaline earth (divalent) metals. A 3 × 150 mm precolumn and a 6 × 250 mm separator column were used for the determination of the alkali metals, and a 4 × 50 mm precolumn together with a 3 × 250 mm separator column for the alkaline earth metals. A separate suppressor column (9 × 100 mm) was used for the determination of each of the monovalent and divalent metals. The injection valve contained a 100 μL sample loop. The eluent for the determination of the monovalent bases was 5 m*M* HCl at a flow rate of 3 mL min^{-1} and pump pressure of 2.8 MPa (400 psi). The eluent for the determination of the divalent

bases was 2.5 mM HCl + 2.5 mM *m*-phenylenediamine dihydrochloride [$C_6H_4(NH_2)_2 2HCl$] at a flow rate of 2 mL min^{-1} and pump pressure of 3.4 MPa (500 psi).

This method (Basta and Tabatabai, 1985a) involved extraction of the exchangeable bases with neutral 1 M NH_4OAc, followed by ignition of the soil extract at 400°C for 30 min, dissolution of the residue in 5 mM HCl, and determination of the exchangeable bases by using a Dionex Model 10 IC equipped as described above. Results obtained for Na and K by this IC method were in close agreement with those obtained by both atomic emission spectrometry (AES) and atomic absorption spectrometry (AAS). Equally good agreement was obtained for Ca and Mg with results by AAS. The eluent-suppressed IC method has the same degree of precision as those of AAS and AES, and an excellent sensitivity, with detection limits of 0.1, 0.05, 0.1, and 0.03 mg L^{-1} for K, Na, Ca, and Mg, respectively. With this method, K and Na can be determined simultaneously in 6 min, and Ca and Mg in 7 min.

Basta and Tabatabai (1985b) applied the eluent-suppressed IC system described above to the determination of total K, Na, Ca, and Mg in plant materials. This method involved dry ashing approximately 0.1 g of plant material, followed by the dissolution of the residue in 5 mM HCl and the determination of K, Na, Ca, and Mg in the digest by using a Dionex Model 10 IC under the same conditions described for the determination of exchangeable bases in soils (Basta and Tabatabai, 1985a). They showed that the average total concentrations of base cations in 25 plant materials by this IC method, atomic absorption spectrometry (AAS), and atomic emission spectrometry (AES) were in very good agreement, as shown in Table 3. Other work by Basta and Tabatabai (1985c) showed that the eluent-suppressed IC system described above was also readily applicable to the determination of K, Na, Ca, and Mg in natural waters.

Table 3 Comparison of Mean Concentration of Base Cations in 25 Samples of Plant Material, Determined by IC, AAS, and AES

	Concentration (%)		
Ion	IC	AAS	AES
K	3.08	3.08	3.07
Na	0.258	0.264	0.256
Ca	1.20	1.19	—
Mg	0.327	0.331	—

Source: Basta and Tabatabai, 1985a.

Although Basta and Tabatabai (1985a) showed that all alkali and alkaline earth metals could be separated and determined by the suppressed-type IC system, Li, Rb, Cs, Sr, and Ba were not detected in the soil, plant materials, or water samples that they analyzed (Basta and Tabatabai, 1985a, b,c). However, the use of cation concentration columns that are now commercially available makes possible the detection of cations at the part-per-billion level, which may be useful for the determination of these metals when present in very low concentrations.

Nieto and Frankenberger (1985) evaluated a single-column IC for the determination of NH_4^+, alkali metals, and alkaline earth metals in soil extracts by using 10 m*M* HNO_3 (pH 2.1) and 5 m*M* ethylenediammonium dinitrate (pH 6.1) for the mono- and divalent cations, respectively. The metal ions were separated on a commercially available low-capacity cation-exchange column, with conductimetric detection. Simultaneous determination of Li^+, Na^+, NH_4^+, and K^+, or Mg^{2+}, Ca^{2+}, Sr^{2+}, and Ba^{2+} was performed on standards in < 7 min with a precison ranging from 3 to 8%. The monovalent cation elution sequence was $Li^+ > Na^+ > NH_4^+ > K^+$, whereas that for the divalent cations was $Mg^{2+} > Ca^{2+} > Sr^{2+} > Ba^{2+}$.

Minimum detectable concentrations of the selected cations by using a 500-μL loop were Na^+, Ca^{2+}, and Mg^{2+}: 0.05 mg L^{-1}; Li^+ and Ba^{2+}: 0.1 mg L^{-1}; NH_4^+: 0.5 mg L^{-1}; K^+ and Sr^{2+}: 1 mg L^{-1}. Results obtained by this single-column IC system agreed closely with those obtained by other methods: steam distillation for NH_4^+ ($r = 0.996$***), AES for Na^+ ($r = 0.992$***), AES for K^+ ($r = 0.999$***), AAS for Ca^{2+} ($r = 0.996$**), and AAS for Mg^{2+} ($r = 0.995$***) (Nieto and Frankenberger, 1985).

3. Organic Compounds

Saccharides. Application of HPIC-PAD for determination of the saccharides inositol, ribitol, fucose, arabinose, rhamnose, galactose, glucose, xylose and mannose, extracted from soils with 0.25 *M* H_2SO_4, was reported by Martens and Frankenberger (1990a). Lactose was used as an internal standard. High performance anion-exchange chromatography (HPAEC) coupled with PAD under alkaline conditions (pH 13) has been used to separate neutral saccharides based upon their molecular size, saccharide composition and glycosidic linkages (Martens and Frankenberger, 1990b). The compounds were detected by oxidation with a gold working electrode. Comparison of HPAEC-PAD with high-performance liquid chromatography (HPLC) with refractive index (RI) detection indicated that the former was more precise, two orders of magnitude more sensitive (pmol range), and gave better resolution of saccharides than HPLC-RI. It also required less

sample preparation and was not subjected to matrix interferences. This use of HPAEC-PAD was applied to the analysis of organic materials (plant residues, animal wastes and sewage sludge) and soil.

Glycuronic Acids. Acid hydrolysis (0.25 *M* H_2SO_4) coupled with enzyme catalysis (pectolyase and β-D-glucuronidase) was employed by Martens and Frankenberger (1990c) to extract galacturonic and glucuronic acids from microbial polysaccharides, plant residues, animal wastes, sewage sludge, and soil. The glycuronic acids were separated by HPAEC on a strong anion-exchange column using 0.1 *M* NaOH with 0.25 *M* NaOAc as the mobile phase and determined by PAD. HPAEC-PAD was found to be superior to HPLC with UV detection for analysis of glycuronic acids, in terms of resolution and sensitivity. It was not subject to interferences present with low UV detection (210 nm) and was highly selective for glycuronic acids. Enzymatic hydrolysis after treatment with mild acid (0.25 *M* H_2SO_4) released galacturonic acids from orange peel and pectin, while glucuronic acid was released from acacia leaf powder. Large amounts of glycuronic acids were also extracted from plant materials. Low levels of uronic acids were detected in poultry manure, sewage sludge, and organic-amended soils.

Aminosaccharides. Martens and Frankenberger (1991) used HPAEC for the determination of aminosaccharides in microbial polymers, chitin, animal waste, sewage sludge, plant residues, and soil. Galactosamine, mannosamine, and glucosamine were separated on a strong anion-exchange column with 10 m*M* NaOH as the eluent, and determined by PAD. HPAEC-PAD was highly selective for aminosaccharides and not subject to matrix interferences; it required less sample preparation, was more precise, and was nearly two orders of magnitude more sensitive than HPLC-RI. More than 3% of the total nitrogen in alfalfa, and 20% of that in straw, was found to be present in this form.

Amino Acids. Direct determination of both primary and secondary amino acids with PAD was achieved under alkaline conditions by oxidation of the amino and hydroxyl functional groups with a gold working electrode (Martens and Frankenberger, 1992). PAD was found to be more sensitive (0.01 to 1.2 n*M* mL^{-1}) than ninhydrin derivatization (4.5 to 55.0 n*M* mL^{-1}) with UV-VIS detection. Detection of 18 amino acids by PAD was in good agreement with previous published work on the amino acid composition for the enzyme ribonuclease A. Amino acid analysis by HPAEC-PAD required little to no sample preparation and was not subject to matrix interferences previously noted with reverse phase separation and OPA or ninhydrin detection. Application of the developed methodology indicated that several

wheat (*Triticum aestivum* L.) varieties grown in sterile nutrient–sand media had a wide range of amino acid composition in their respective root mass and root exudates.

B. Water Analysis

Ion chromatography is routinely used to measure anions and basic cations in drinking water, wastewater, rainwater, and groundwater. However, routine analysis of heavy metals is usually conducted by a spectroscopic method such as AAS or inductively coupled plasma emission (ICPAES), and not IC, except where chemical speciation is important (see Sec. III.C below). The spectroscopic methods measure the total dissolved element and are not capable of chemical speciation. U.S. standard methods for IC analysis of anions commonly found in water samples were summarized by Karmarkar (1998) and are presented in Table 4. Other applications of IC for chemical speciation of ions in water samples have also been reviewed (Karmarkar, 1998). The suppressed IC gives accurate and precise results in the determination of NO_3^-, Cl^-, SO_4^{2-} and PO_4^{3-} in natural waters (Tabatabai and Dick, 1983; Krupa and Tabatabai, 1984).

C. Chemical Speciation

Some heavy metals and metalloids have several ions with different oxidation states that are stable in soil and aqueous systems, and which often have different mobility, bioavailability, and/or toxicity in soil and aqueous environments. For example, Cr(VI) is much more toxic than Cr(III), and arsenate $As(V)O_4^{3-}$ is generally less soluble, mobile, and toxic than arsenite, $As(III)O_3^{3-}$. IC is capable of differentiating between these forms. USEPA Method 218.6 is a standard method that describes the determination of Cr(VI) in drinking water and wastewater by IC (Table 4); anionic Cr(VI) is separated from Cr(III) in the IC column, followed by postcolumn reaction of Cr(VI) with diphenylcarbazide and colorimetric determination at 530 nm.

Application of IC to speciate chromium, arsenic, selenium, and aluminum in soil and aqueous solutions has been reviewed (Karmarkar, 1998) and is outlined below.

McGeehan and Naylor (1992) used suppressed IC with electrochemical and conductivity detectors in series for simultaneous determination of arsenite, arsenate, selenite, and selenate in soil solution. Ions were separated on a Dionex OmniPac PAX-500 column using $NaHCO_3 + Na_2CO_3$ eluent. Arsenic (III) was measured by an electrochemical detector (Pt working electrode) and As(V), Se(IV) and Se(VI) were passed through a Dionex AMMS-MPIC anion fiber suppressor and measured by a conductivity

Marcel Dekker, Inc.
270 Madison Avenue, New York, New York 10016

Table 4 U.S. Regulatory Methods Using IC for Environmental Analysis of Water and Air

Method no.	Publisher	Ions determined	Application/comments	Ref.[a]
Water Analysis				
D4327–91	ASTM	Bromide, chloride, fluoride, nitrate, nitrite, phosphate, and sulfate	Anions in waters	A
4110	(Standard methods)	Bromide, chloride, nitrate, nitrite, phosphate, and sulfate	Anions in waters	B
300.0, part A	USEPA	Bromide, chloride, fluoride, nitrate, nitrite, phosphate, and sulfate	Anions in waters to comply with NPDWR and NPDES	C
300.0, part B	USEPA	Bromate, bromide, chlorate, and chlorite	Disinfection by-products in drinking waters to comply with ICR	C
300.1	USEPA	Bromide, bromate, chlorate, chloride, chlorite, fluoride, nitrate, nitrite, phosphate, and sulfate	Common anions and disinfection by-products in drinking waters	D
300.6	USEPA	Chloride, nitrate, phosphate, and sulfate	Anions in wet deposition	E
300.7	USEPA	Ammonium, calcium, lithium, magnesium, potassium, and sodium	Cations in wet deposition	F
218.6	USEPA	Dissolved chromium (VI)	Chromate in drinking water, groundwater, and industrial wastewater effluents.	G
9056	USEPA Office of Solid Waste	Bromide, chloride, fluoride, nitrate, nitrite, phosphate, and sulfate.	Anions in collection solutions from bomb combustion of solid waste samples	H
Air Analysis				
2008	NIOSH	Chloroacetic acid	Sample desorbed in water, suppressed conductivity detection	I

(*continued*)

Table 4 Continued

Method no.	Publisher	Ions determined	Application/comments	Ref.[a]
3509	NIOSH	Monoethanolamine, diethanolamine, triethanolamine	Sample desorbed in hexane-sulfonic acid, ion pair separation followed by suppressed conductivity detection.	I
5022	NIOSH	Methylarsenic acid, dimethylarsenic acid, *p*-aminophenyl arsonic acid	Sample desorbed in borate-carbonate buffer, hydride generation AAS	I
6004	NIOSH	Sulfur dioxide analyzed as sulfite and sulfate	Sample desorbed in sodium bicarbonate/carbonate, suppressed conductivity detection	I
6005	NIOSH	Iodine	Sample desorbed in sodium carbonate, suppressed conductivity detection	I
6011	NIOSH	Chlorine and bromine	Sample desorbed in sodium thiosulfate, suppressed conductivity detection	I
6012	NIOSH	Sulfuryl fluoride analyzed as fluoride	Sample desorbed in sodium hydroxide, suppressed conductivity detection	I
6013	NIOSH	Hydrogen sulfide	Sample desorbed in ammonium hydroxide and hydrogen peroxide, suppressed conductivity detection	I

7903	NIOSH	Fluoride, chloride, bromide, nitrate, phosphate, and sulfate	Sample desorbed in water, suppressed conductivity detection	I
7604	NIOSH	Hexavalent chromium	Sample desorbed in sodium hydroxide, suppressed conductivity detection.	I
7906	NIOSH	Fluorides: aerosol and gas	Sample desorbed in sodium hydroxide, suppressed conductivity detection	I
ID-104	OSHA	Sulfur dioxide	Sample collected in H_2O_2, suppressed conductivity detection	J
ID-182	OSHA	Nitrogen dioxide	Sample desorbed in triethanolamine, suppressed conductivity detection	J
ID-190	OSHA	Nitric oxide	Sample desorbed in triethanolamine, suppressed conductivity detection	J
ID-211	OSHA	Sodium azide and hydrazoic acid	Sample desorbed in a buffer made of sodium carbonate and sodium bicarbonate, UV detection.	J
ID-212	OSHA	Iodine	Sample desorbed in a buffer made of sodium carbonate and sodium bicarbonate, pulsed amperometric detection	J

[a]A, ASTM (1994); B, APHA/AWWA/WEF(1995); C, Pfaff et al. (1993); D, Pfaff et al. (1997); E, Bachman et al. (1986a); F, Bachman et al. (1986b); G, Arar et al. (1994); H, USEPA (1994); I, NIOSH (1994); J, OSHA (1991).

detector. Ion chromatography results were in good agreement with those obtained by ICPAES with hydride generation (ICP-HG) and by ICP with mass spectroscopic detection (ICP-MS). Detection limits in mg L^{-1} were 0.026 for Se(IV), 0.029 for Se(VI), 0.114 for As(III), and 0.120 for As(V).

Ion chromatography methods based on amperometric or conductivity detection of chemical contaminants have limited application to drinking water because detection of chemical species is not possible at μg L^{-1} levels. Manning and Martens (1997) used IC coupled with hydride generation atomic absorption spectrometry (HGAAS) to speciate sub μg L^{-1} levels of As(V) and As(III) in water and sediment extracts. Arsenate and arsenite were separated using a Dionex OmniPac PAX-500 column and a mobile phase containing 30 m*M* NaOH/1% methanol. The column effluent was linked to a continuous hydride generator. The HPLC-HGAAS method allows determination of As(III) and As(V) in < 5 min, with detection limits of 200 pg of arsenic (0.8 μL^{-1} of arsenic). Jackson and Miller (1998) have reported the simultaneous determination of As(III), As(V), Se(IV), and Se(VI) in aqueous extracts of coal fly-ash using IC coupled with ICP mass spectroscopic detection (ICP-MS). Simultaneous determination of these chemical species was achieved in < 7 min. Absolute detection limits of 7.2, 87, 117, and 28 pg for As(III), Se(IV), Se(VI), and As(V), respectively, were obtained, corresponding to 0.07, 0.87, 1.17, and 0.28 μg L^{-1}.

Willett (1989) developed an IC method for the chemical speciation of monomeric aluminum (Al^{3+}, and hydroxo-, sulfato-, oxalato-, and fluorocomplexes) in solution and applied it to the analysis of monomeric Al species in soil solutions. This IC method featured cation exchange separator columns and postcolumn derivatization with pyrocatechol, followed by UV-VIS detection. Aluminum speciation by IC agreed with results from a geochemical speciation model. Anderson and Bertsch (1988) used IC to study the rates of formation of Al complexes in the presence of multiple complexing ligands. Sloan et al. (1995) used IC to determine reduction of phytotoxic forms of dissolved Al (e.g. Al^{3+}) following phosphate fertilizer additions to acid soils.

D. Air Quality Analysis

Standard methods are available to measure a wide range of air pollutants by IC methods (Table 4). Contaminants are collected and preconcentrated from air using solid phase sorbents and then are desorbed by using aqueous solutions (Table 4), followed by subsequent analysis by IC.

E. Heavy Metals in Soils and Sewage Sludges

A method was developed for the ion chromatographic determination of total Cu, Ni, and Zn in soils by Basta and Tabatabai (1990). The method involved four steps: (1) sample digestion using HNO_3, $HClO_4$, and HF, (2) extraction of Cu, Ni, and Zn from the acid digest using dithizone in $CHCl_3$, (3) destruction of the metal–dithizone complex using HNO_3, and (4) use of IC to measure Cu, Ni, and Zn in the diluted HNO_3 sample digest. Metal ions (Cd, Cu, Mn, and Zn) were separated on a HPIC-CS5 column using 4 m*M* 2,6-pyridinecarboxylic acid and 50 m*M* HOAc-NaOAc buffer (pH 4.8), or Cu, Ni, Pb, and Zn were separated using 40 m*M* oxalic acid and 50 m*M* HOAc-LiOAc buffer (pH 4.8). Determination of metals involved postcolumn derivatization using 4-(2-pyridylazo) resorcinol (PAR) and measuring absorbance of metal–PAR complexes at 520 nm using a UV-VIS detector (Figs. 7–9). Basta and Tabatabai (1991) reported that a similar IC method allowed accurate and precise determination of Cu, Ni, Pb, and Zn in sewage sludge, with results in good agreement with those obtained by AAS (Fig. 15). However, the results also showed that this proposed IC method was inadequate for the determination of total Cd or Mn.

IV. SUMMARY AND CONCLUSIONS

Several IC instruments and separator columns and other accessories are commercially available. The principles of IC methods and studies to evaluate these instruments for soil, plant, and water analysis have been reviewed and applications described. It has been shown that IC gives very satisfactory results for the determination of inorganic anions, alkali metal and alkaline earth metal cations, and some major groups of organic compounds in these materials.

The IC is well suited to the analysis of complex mixtures of ions, but care must be taken to obtain the samples in a suitable solution. This is because many of the procedures employed in soil analysis result in matrices that are not compatible with the chemistry of the IC systems. Therefore such procedures have to be modified before using them in conjunction with any IC system. Although this field of analytical chemistry has matured, and IC now enjoys a wide use and distribution, it will take several years before analytical techniques are fully developed for use in soil and environmental analysis. Some currently available IC instruments and methods that have not so far been used for soil and environmental analysis should, with appropriate care, be capable of being adaptable to it.

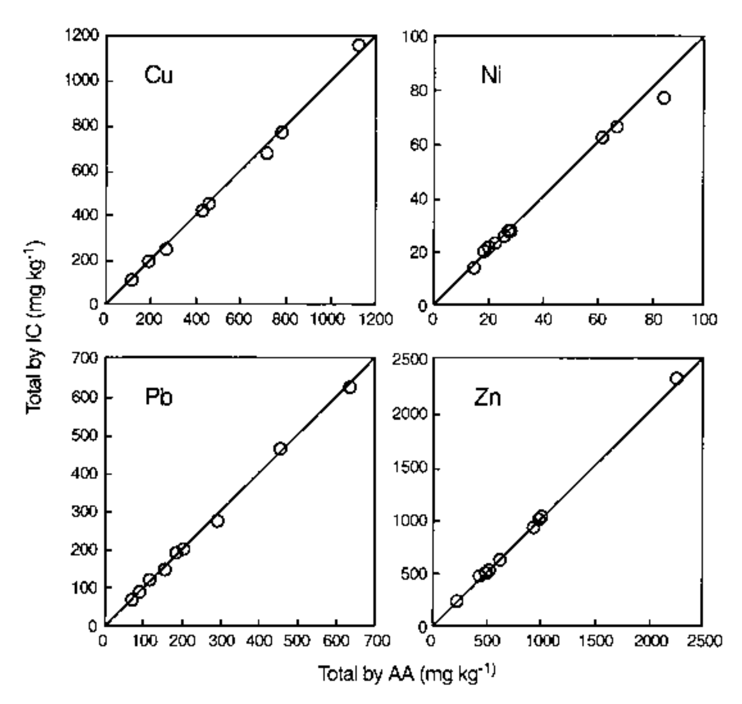


Figure 15 Comparison of total metal concentrations in sewage sludges obtained by IC with oxalic acid as eluent and by flame atomic absorption spectrometric (AA) methods for Cu, Ni, Pb, and Zn. (Basta and Tabatabai, 1991.)

Because of the potential that IC offers, particularly for the simultaneous analysis of several anions (for which there is no alternative instrumental method, unlike the situation for metal cations), widespread future use in this field can be safely predicted.

REFERENCES

American Public Health Association (APHA)/American Water Works Association (AWWA)/Water Environment Federation (WEF). 1995. Determination of anions by ion chromatography. In: *Standard Methods for the Examination of Water and Wastewater*. 19th ed. Washington, DC: APHA.

American Society for Testing and Materials (ASTM). 1994. Standard test method for anions in waters by chemically suppressed ion chromatography method. D4327-91. In: *Annual Book of Standards*, Vol. 11.01, ASTM, Philadelphia.

Anderson, M. A. and P. M. Bertsch. 1988. Dynamics of aluminum complexation in multiple ligand systems. *Soil Sci. Soc. Am. J.* 52:1597–1602.

Arar, E., J. Pfaff and T. Martin. 1994. Determination of dissolved hexavalent chromium in drinking water, groundwater, and industrial wastewater effluents by ion chromatography, method 218.6. Environ. Monitoring and Systems Lab., Office of Res. and Dev., USEPA, Cincinnati.

Bachman, S., C. Brennan, J. Rothert and M. Peden. 1986a. Chloride, orthophosphate, nitrate, and sulfate in wet deposition by chemically suppressed ion chromatography, method 300.6. Environ. Monitoring and Systems Lab., Office of Res. and Dev., USEPA, Cincinnati.

Bachman, S., J. Rothert, B. Kaiser, C. Brennan and M. Peden. 1986b. Dissolved sodium, ammonium, potassium, magnesium, and calcium in wet deposition by chemically suppressed ion chromatography, method 300.7. Environ. Monitoring and Systems Lab., Office of Res. and Dev., USEPA, Cincinnati.

Barak, P. and Y. Chen. 1987. Three-minute analysis of chloride, nitrate, and sulfate by single column anion chromatography. *Soil Sci. Soc. Am. J.* 51:257–258.

Basta, N. T. and M. A. Tabatabai. 1985a. Determination of exchangeable bases in soils by ion chromatography. *Soil Sci. Soc. Am. J.* 49:84–89.

Basta, N. T. and M. A. Tabatabai. 1985b. Determination of potassium, sodium, calcium, and magnesium in plant materials by ion chromatography. *Soil Sci. Soc. Am. J.* 49:76–81.

Basta, N. T. and M. A. Tabatabai. 1985c. Determination of potassium, sodium, calcium, and magnesium in natural waters by ion chromatography. *J. Environ. Qual.* 14:450–455.

Basta, N. T. and M. A. Tabatabai. 1990. Ion chromatographic determination of total metals in soils. *Soil Sci. Soc. Am. J.* 54:1289–1297.

Basta, N. T. and M. A. Tabatabai. 1991. Determination of total metals in sewage sludge by ion chromatography. *J. Environ. Qual.* 20:79–88.

Boyd, G. E., B. A. Soldano and O. D. Bonner. 1954. Ionic equilibria and self-diffusion rates in desulfonated cation exchangers. *J. Phys. Chem.* 58: 456–460.

Busman, L. M., R. P. Dick and M. A. Tabatabai. 1983. Determination of total sulfur and chlorine in plant materials by ion chromatography. *Soil Sci. Soc. Am. J.* 47:1167–1170.

Cortes, H. J. 1982. High-performance liquid chromatography of inorganic and organic anions using ultraviolet detection and an amino column. *J. Chromatog.* 234:517–520.

Dasgupta, P. K. 1992. Ion chromatography: the state of the art. *Anal. Chem.* 64:775–783A.

Dick, W. A. and M. A. Tabatabai. 1979. Ion chromatographic determination of sulfate and nitrate in soils. *Soil Sci. Soc. Am. J.* 43:899–904.

Frankenberger, W. T., Jr., H. C. Mehra and D. T. Gjerde. 1990. Environmental applications of ion chromatography. *J. Chromatog.* 504:211–245.

Franklin, G. O. 1985. Development and applications of ion chromatography. *Am. Lab.* 17(6):65–80.

Fritz, J. S., D. T. Gjerde and R. M. Becker. 1980. Cation chromatography with a conductivity detector. *Anal. Chem.* 52:1519–1522.

Fritz, J. S., D. T. Gjerde and C. Pohlandt. 1982. *Ion Chromatography*. Huthig, New York.

Fritz, J. S. and J. N. Story. 1974a. Selectivity behavior of low-capacity, partially sulfonated, macroporous resin beads. *J. Chromatog*. 90:267–274.

Fritz, J. S. and J. N. Story. 1974b. Chromatographic separation of metal ions on low capacity, macroreticular resins. *Anal. Chem*. 46:825–829.

Gibb, S., R. Mantoura and P. Liss. 1995. Analysis of ammonia and methylamines in natural waters by flow injection gas diffusion coupled to ion chromatography. *Anal. Chim. Acta* 316:291–304.

Girad, J. E. and J. A. Glatz. 1981. Ion chromatography with conventional HPLC instrumentation. *Am. Lab*. 13(1):26–35.

Gjerde, D. T. and J. V. Benson. 1992. Fluid analysis with particulate reagent suspension. US patent 5,149,661.

Gjerde, D. T. and J. S. Fritz. 1979. Effect of capacity on the behavior of anion exchange resin. *J. Chromatog*. 176:199–206.

Gjerde, D. T. and J. S. Fritz. 1981. Sodium and potassium benzoate and benzoic acid as eluents for ion chromatography. *Anal. Chem*. 53:2324–2327.

Gjerde, D. T., J. S. Fritz and G. Schmuckler. 1979. Anion chromatography with low-conductivity eluents. *J. Chromatog*. 186:509–519.

Gjerde, D. T., G. Schmuckler and J. S. Fritz. 1980. Anion chromatography with low-conductivity eluents. II. *J. Chromatog*. 187:35–45.

Haddad, P. R. and P. E. Jackson. 1990. *Ion Chromatography: Principles and Practices*. Elsevier, New York.

Haddad, P. and S. Laksana. 1994. On-line analysis of alkaline samples with a flow through electrodialysis device coupled to an ion chromatograph. *J. Chromatog*. 671:131–139.

Hanaoka, Y., T. Murayama, S. Muramoto, T. Matsuura and A. Nanba. 1982. Ion chromatography with ion-exchange membrane suppressor. *J. Chromatog*. 239:537–548.

Henshall, A., S. Rabin, J. Statler and J. Stillian. 1992. A recent development in ion chromatography: the self-regenerating suppressor. *Am. Lab*., Nov. issue: 20R–20Z.

Iskandaranl, Z. and D. J. Pietrzyk. 1982. Ion interaction chromatography of inorganic anions on a poly(styrene-divinylbenzene) adsorbent in the presence of tetraalkyl-ammonium salts. *Anal. Chem*. 54:2427–2431.

Jackson, B. P. and W. P. Miller. 1998. Arsenic and selenium speciation in coal fly-ash extracts by ion chromatography-inductively coupled plasma-mass spectrometry. *J. Anal. At. Spec*. 13:1107–1112.

Johnson, E. L. 1987. Eluent suppressed ion chromatography. In: *Ion Chromatography* (J. G. Tarter, ed.). Marcel Dekker, New York, p. 1–22.

Jepille, T. 1987. Single-column ion chromatography. In: *Ion Chromatography* (J. G. Tarter, ed.). Marcel Dekker, New York, pp. 23–82.

Jupille, T. H., D. W. Togami and D. E. Burge. 1983. A single-column ion chromatography aids rapid analysis. Wescan Instruments, Inc., Santa Clara, CA.

Kalbasi, M. and M. A. Tabatabai. 1985. Simultaneous determination of nitrate, sulfate, and phosphate in plant materials by ion chromatography. *Commun. Soil. Sci. Plant Anal.* 16:787–800.

Karlson, W. and W. T. Frankenberger, Jr. 1987. Single column ion chromatography. III. Determination of orthophosphate in soils. *Soil Sci. Soc. Am. J.* 51:72–74.

Karmarkar, S. 1995. Environmental IC analysis: operation and problem solving. *Water Environ. Lab. Solutions* 2:6–8.

Karmarkar, S. V. 1996. System and a method for using a small suppressor column in performing liquid chromatography. US patent 5,567,307.

Karmarkar, S. V. 1998. Ion chromatography. In: *Encyclopedia of Environmental Analysis and Remediation* (R. A. Meyers, ed.). John Wiley, New York, pp. 2391–2404.

Karmarkar, S. V. 1999a. Analysis of wastewater for anionic and cationic nutrients by ion chromatography in a single run with sequential flow-injection analysis. *J. Chromatog.* 850:303–309.

Karmarkar, S. V. 1999b. Ion chromatography with in-line filtration of samples and automated column switching. Proc. Internat. IC Symposium, San Jose, CA, September 12–15, 1999, p. 75.

Karmarkar, S. V. and M. A. Tabatabai. 1991. Ion chromatographic method for determination of oxyanions in solutions equilibrated with soils. *Common. Soil Sci. Plant Anal.* 22:1383–1395.

Karmarkar, S. V. and M. A. Tabatabai. 1992. Eluent composition effect on ion chromatographic determination of oxyanions in solutions equilibrated with soils. *Chromatographia* 34:643–647.

Killgore, J. and S. Villasenor. 1996. Systematic approach to generic matrix elimination via ‘‘heart cut’’ column switching techniques. *J. Chromatog.* 739:43–48.

Krupa, S. V. and M. A. Tabatabai. 1984. Measurement of sulfur in the atmosphere and in natural water. In: *Sulfur in Agriculture* (M. A. Tabatabai, ed.) Am. Soc. Agron., Madison, WI, pp. 491–548.

Manning, B. A. and D. A. Martens. 1997. Speciation of arsenic (III) and arsenic (V) in sediment extracts by high-performance liquid chromatography-hydride generation atomic absorption spectrophotometry. *Environ. Sci. Technol.* 31:171–177.

Martens, D. A. and W. T. Frankenberger, Jr. 1990a. Quantification of soil saccharides by spectrophotometric methods. *Soil Biol. Biochem.* 22:1173–1175.

Martens, D. A. and W. T. Frankenberger, Jr. 1990b. Determination of saccharides by high performance anion-exchange chromatography with pulsed amperometric detection. *Chromatographia* 29:7–12.

Martens, D. A. and W. T. Frankenberger, Jr. 1990c. Determination of glycuronic acids by high-performance anion chromatography with pulsed amperometric detection. *Chromatographia* 29:651–656.

Martens, D. A. and W. T. Frankenberger, Jr. 1991. Determination of aminosaccharides by high-performance anion-exchange chromatography with pulsed amperometric detection. *Talanta* 38:245–251.

Martens, D. A. and W. T. Frankenberger, Jr. 1992. Pulsed amperometric detection of amino acids separated by anion exchange chromatography. *J. Liquid Chromatog*. 15:423–439.

Mattusch, J. and R. Wennrich. 1996. Elimination of sulfate interference in the chromatographic determination of *o*-phosphate using liquid-liquid extraction. *Fresenius J. Anal. Chem*. 356:335–338.

McGeehan, S. L. and D. V. Naylor. 1992. Simultaneous determination of arsenite, arsenate, selenite, selenate by suppressed ion chromatography. *J. Environ. Qual*. 21:68–73.

Medina, H., E. Gutierrez, M. Vargas, G. Gonzalez, J. Marin and E. Andueza. 1996. Determination of phosphate and sulfite in natural waters in the presence of high sulfate concentration by ion chromatrography under isocratic conditions. *J. Chromatog*. 739:207–215.

Msada, S., E. Jones-Watson and H. Farrer. 1996. Automation of sample dilution and injection for the determination of anions by ion chromatography. *Water SA* 22:85–89.

Mulik, J. D. and E. Sawicki. 1979a. *Ion Chromatographic Analysis of Environmental Pollutants*, Vol. 2, Ann Arbor Science, Ann Arbor, MI.

Mulik, J. D., and E. Sawicki. 1979b. Ion chromatography. *Environ. Sci. Technol*. 13:804–809.

National Institute for Occupational Safety and Health (NIOSH). 1994. *Manual of Analytical Methods*. 4th ed. U. S. Govt. Printing Office, Washington DC.

Nieto, K. F. and W. T. Frankenberger, Jr. 1985. Single column ion chromatography: II. Analysis of ammonium, alkali metals, and alkaline earth cations in soils. *Soil Sci. Soc. Am. J*. 49:592–596.

Novic, M., A. Dovzan, B. Pihlar and V. Hudnik. 1995. Determination of chlorine, sulfur, and phosphorus in organic materials by ion chromatography using electrodialytic sample pretreatment. *J. Chromatog*. 704:530–534.

Occupational Safety, and Health Administration, US Dept. of Labor (OSHA). 1991. *Analytical Methods Manual*. Parts 1 and 2. 2nd ed. OSHA Technical Center, Salt Lake City, UT.

Pfaff, J., C. Brockhoff and J. O'Dell. 1993. The determination of inorganic anions in water by ion chromatography, Method 300.0, Environ. Monitoring and Systems Lab., Office of Res. and Dev. USEPA, Cincinnati, OH.

Pfaff, J., D. P. Hautman and D. J. Munch. 1997. Determination of inorganic anions in drinking water by ion chromatography, method 300.1, Nat. Exposure Res. Lab., Office of Res. and Dev. USEPA, Cincinnati, OH.

Pohl, C. A. and E. L. Johnson. 1980. Ion chromatography: the state-of-the-art. *J. Chromatog. Sci*. 18:442–452.

Russo, V. M. and S. V. Karmarkar. 1998. Water extraction of plant tissues for analysis by ion chromatography. *Commun. Soil Sci. Plant Anal*. 29: 245–253.

Saari-Nordhaus, R. and J. Anderson, Jr. 1996. Electrochemically regenerated solid-phase suppressor for ion chromatography. *Am. Lab*. Feb. issue, 33N–33U.

Saari-Nordhaus, R., L. Nair and J. Anderson Jr. 1994. Elimination of matrix interference in ion chromatography by the use of solid-phase extraction disks. *J. Chromatog*. 67:159–163.

Sawicki, E., J. D. Mulik and E. Wittgenstein, eds. 1978. *Ion Chromatographic Analysis of Environmental Pollutants*. Ann Arbor Science, Ann Arbor, MI.

Slingsby, R. and C. Pohl. 1996. Approaches to sample preparation for ion chromatography: sulfate precipitation on barium-form ion exchangers. *J. Chromatog*. 739:49–55.

Sloan, J. J., N. T. Basta and R. L. Westerman. 1995. Aluminum transformations and solution equilibria induced by banded P fertilizer in acid soil. *Soil Sci. Soc. Am. J*. 59:357–364.

Small, H. 1983. Modern inorganic chromatography. *Anal. Chem*. 55:235A–242A.

Small, H. 1989. *Ion Chromatography*. Plenum Press, New York.

Small, H., T. S. Stevens and W. C. Baumann. 1975. Novel ion exchange chromatographic method using conductimetric detection. *Anal. Chem*. 47:1801–1809.

Smith, F. C., Jr. and R. C. Chang. 1983. *The Practice of Ion Chromatography*. John Wiley, New York.

Stevens, T. S., J. C. Davis and H. Small. 1981. Hollow fiber ion-exchange suppressor ion chromatography. *Anal. Chem*. 53:1488–1492.

Stillian, J. 1985. An improved suppressor for ion chromatography. *LC Magazine* 3:802–805.

Tabatabai, M. A. and W. A. Dick. 1983. Simultaneous determination of nitrate, chloride, sulfate, and phosphate in natural waters by ion chromatography. *J. Environ. Qual*. 12:209–213.

Tabatabai, M. A. and N. T. Basta. 1991. Ion chromatography. In: Soil Analysis: Instrumental Techniques and Related Procedures. (K. A. Smith, ed.). 2nd ed. Marcel Dekker, New York, pp. 229–259.

Tabatabai, M. A. and W. T. Frankenberger, Jr. 1996. Liquid chromatography. In: *Methods of Soil Analysis*, *Part 3 – Chemical Methods* (D. L. Sparks, ed.). *Soil Sci. Soc. Am*., Madison, WI, pp. 225–245.

Tabatabai, M. A., N. T. Basta and H. J. Pirela. 1988. Determination of total sulfur in soils and plant materials by ion chromatography. *Commun. Soil Sci. Plant Anal*. 19:1701–1714.

Tarter, J. G. ed. 1987. *Ion Chromatography*. Marcel Dekker, New York.

Tarter, J. G., E. L. Johnson and T. Jupille. 1987. Comparison of eluent-suppressed and single-column ion chromatography. In: *Ion Chromatography* (J. G. Tarter, ed.). Marcel Dekker, New York, pp. 83–86.

U.S. Environmental Protection Agency (USEPA). 1994. Determination of inorganic anions by ion chromatography, method 9056. In: *Test Methods for Evaluating Solid Waste*, Vol. 1C. USEPA, Office of Solid Waste and Emergency Response, Washington D.C.

Watkinson, J., and M. Kear. 1994. High performance ion chromatography measurement of sulfate in 20 mM phosphate extracts of soils. *Commun. Soil Sci. Plant Anal*. 25:1015–1033.

Weiss, J. 1986. *Handbook of Ion Chromatography*, Dionex Corp., Sunnyvale, CA.
Weiss, J. 1995. *Ion Chromatography*. 2nd ed. VCH, New York.
Willett, I. R. 1989. Direct determination of aluminum and its cationic fluorocomplexes by ion chromatography. *Soil Sci. Soc. Am. J.* 53:1385–1391.
Zerbinati, O. 1995. Clean-up procedure for the determination of inorganic anions by ion chromatography. *J. Chromatog.* 706:137–140.

6

Automated Instruments for the Determination of Total Carbon, Hydrogen, Nitrogen, Sulfur, and Oxygen

Keith A. Smith
The University of Edinburgh, Edinburgh, Scotland

M. Ali Tabatabai
Iowa State University, Ames, Iowa, U.S.A.

I. INTRODUCTION

The use of automated laboratory instruments for the determination of total carbon, C, and nitrogen, N, by dry combustion has become well established in recent years. This has become possible through the development of simple and rapid combustion procedures and by coupling them with modern high-sensitivity gas analysis systems in single integrated instruments. As instruments have become more sophisticated, the capability of simultaneous measurement of sulfur, S, and/or hydrogen, H, along with the C and N determinations, has been added to some commercially available systems. Yet another optional add-on is the capacity to determine oxygen, O, in the same samples. Prior to such developments, the techniques available for dry combustion systems were complicated and time-consuming, and manual wet oxidation methods were generally preferred for analysis of soils, plants, and other environmental materials. However, the balance now lies in the opposite direction.

This chapter describes the principles on which automated dry combustion instruments and automated analyzers dedicated to the

Marcel Dekker, Inc.
270 Madison Avenue, New York, New York 10016

determination of dissolved organic C are based. It examines the particular features available with a selection of different commercial systems and reviews recent information from the scientific literature concerning the application of these instruments to the analysis of soils, plants, waters, and other environmental materials.

This chapter is an updated and extended version of that on dry combustion analyzers in the previous edition (Tabatabai and Bremner, 1991), to which reference should be made for information on evaluations of earlier commercial instruments for soil analysis.

II. DRY COMBUSTION SYSTEMS

A. Dumas Systems for C, H, N Analysis

The various automated dry combustion systems for the analysis of C, H, and N in soils, plant materials, and other agricultural and environmental samples generally have several important features in common. They all employ high-temperature combustion (oxidation) of the sample, the determination of C and H as CO_2 and H_2O vapor, respectively, and the determination of N as N_2. The historical developments, the principles involved, and a description of the mode of operation of this type of analytical system can be found in Pella (1990a,b), and further material relating particularly to C analysis is also contained in Nelson and Sommers (1996).

The essential components of a CHN analyzer operating on the dry combustion principle are:

1. An automated sample introduction system
2. A high-temperature oxidation zone in which the sample is combusted to CO_2, H_2O vapor, N_2 and NO_x, and other gases
3. A carrier gas system, to sweep the products of combustion through the remaining stages of the analyzer
4. A gas purification/reduction train in which the oxides of N produced in the combustion are reduced to N_2, and unwanted gases (e.g., halogen compounds and S oxides) removed
5. A gas separation stage, e.g., a gas chromatographic system or a series of selective traps for individual gases
6. A single, or multiple, gas detector(s)
7. A signal recording/readout system

The major developments between the first appearance of commercial C, N, CN, and CHN analyzers and the present generation of instruments are in

Marcel Dekker, Inc.
270 Madison Avenue, New York, New York 10016

the incorporated computer control and data analysis systems, and in the employment of new types of gas detectors in some products. The essential oxidation, reduction, and gas separation operations carried out within the analyzers are usually much as they were in earlier-generation instruments, as can be seen in the next section.

B. Examples of Commercial Instrument Systems

The intention of this section is to present the main features and operating principles of some of the available commercial CHN analyzer systems in a generic way, and to give the reader an overall understanding of the capabilities of this type of analyzer and of its potential application to future analytical requirements. It must be pointed out, however, that instrument models come and go from the market, as new developments occur and as companies merge (Table 1). Within any one product range, modifications are frequently made, and new accessories become available from time to time. Thus any precise details presented on current instrumentation will inevitably become out of date in due course. A potential user should always check with the supplier to confirm the detailed specifications of any particular instrument and to identify new features that may have become available.

1. CE Instruments Systems

The CE Instruments range (Table 1) includes the EA 1110 Elemental Analyzer, applicable to C, H, and N analysis, and the NA 2500 N and CN systems, applicable to N only, and to C and N, respectively. These instruments have many common features; they are also direct descendants of well-known models such as the NA 1500 based on similar principles (see Table 1), many of which are still in use and continuing to yield valuable analytical data (see Sec. IV).

The typical CE sample introduction system consists of an autosampler containing one or more sample carousels, each of which may hold up to 50 samples. Solid samples (e.g., dried soils or plant materials), ranging in weight from a few mg to 500 mg, are contained in crimped tin capsules. Standards are introduced in the same manner. For normal operation, at the start of the analytical cycle the carousel is rotated to the inlet position, allowing the first sample capsule to drop into the oxidation zone. On the completion of the analysis, which is normally controlled by a computer program, the carousel moves to the next position, the next sample is introduced, and the whole cycle is repeated until the preset number of analyses has been completed. Although the system is primarily intended for

Table 1 Some Current/Recent Automated Dry Combustion CNS Analyzer Systems, Related Earlier Models, Operating Principles, and Applications

Manufacturer	Address/website	Model(s)	Related earlier makes/models	Operating principle/detection system(s)	Typical applications
Antek Instruments Inc.	300 Bammel Westfield Rd, Houston, Texas 77090, USA www.antekhou.com	9000 Series N, S, NS Analyzers		Combustion at selected temperatures up to 1100°C. N detection by chemiluminescence, S by fluorescence method	N and/or S in soils, waters, feces & urine, foods & beverages, plant materials, pesticides
CE Instruments (formerly Carlo Erba, then Fisons, now part of ThermoQuest Corp.)	Strada Rivoltana 20090 Rodano, Milan, Italy www.ceinstruments.it	EA-1110 Elemental Analyser; NA-2100 N & Protein Analyser; NA-2500	Carlo Erba NA-1400 & NA-1500; Fisons NA-1500; Carlo Erba 1102, 1104, 1106, 1108; CE NA-2000	Tin capsules/flash combustion with O_2/reduction on hot Cu. O determination by pyrolysis. GC separation. Injector for liquid samples. Detection by TCD or MS	C, H, N, (O) or C, H, N, S (O) or N only in soils, sediments, waste waters, liquid fertilizers, plant materials
LECO Corp.	3000 Lakeview Ave., St. Joseph, Michigan 49085-2396, USA www.leco.com	CN-2000, CHN-2000, CNS-2000, FP-2000; 144 Series; 400 Series	70-sec C Analyzer; CR-412; CHN-600, -800 & -1000; FP-228N; IR-12; DC-12; CS-46; TN-15; FP-228N; TC-36; UO 14SP; Sulfur Analyzer; SC-32; SC-132	Combustion with accelerator & O_2/reduction on hot Cu. O determination by adding external pyrolysis furnace. Detection by IR for C, H, S, O; by TCD for N	Various combinations of C, N, and/or S in soils, plant tissue, fertilizers

Exeter Analytical Inc.	7 Doris Drive, Unit 1, N. Chelmsford, MA 01863, USA www.eail.com	CE-440		Combustion in tin or Al cups in pure O_2/reduction on hot Cu. O by pyrolysis. S determined as SO_2. Detection by TCD	C, H, N (and O/S) in agric. materials, foodstuffs, air and water filters, oil residues, etc.
PDZ Europa Ltd.	Hill St, Elsworth, Sandbach, Cheshire CW11 3JE, UK www.europa-uk.com	ANCA-GSL and ANCA-SL, with 20-20 or GEO-Series mass spectrometer	Europa Scientific SL CN Analyzer; Europa ANCA-NT	Tin capsules/flash combustion with O_2/reduction on hot Cu. O by pyrolysis. GC separation. Detection by isotope ratio MS, giving total element concn. & stable isotope composition	C, H, N, S, (O) in soils, plant material, plus ^{13}C, ^{2}H, ^{15}N, ^{34}S, ^{18}O content
Perkin-Elmer Analytical Instruments (including former Coleman Instruments)	761 Main Avenue Norwalk, Connecticut 06859-0001, USA www.perkinelmer.com	2400 Series II CHNS/O Analyzer; 2410 Series II Nitrogen Analyzer.	Coleman Models 29 & 29A	Combustion with O_2 in Pt boat/reduction on hot Cu. Detection by TCD	C, H, N, S (O) in soils, sediments, fertilizers, plant materials
Skalar Analytical BV	PO Box 3237, 4800 DE Breda, The Netherlands; www.skalar.com	Primacs SC, Primacs SN		Dual oven system: total C combustion with O_2, catalyst at 950–1100°C; inorg C reaction with acid at 20–150°C; TOC by difference. Detection by nondispersive IR	Total org C, total N in sludges, sediments, soils

the analysis of solid samples, liquid samples may be introduced in special sealed tin capsules, or by fully automated syringe sampling from small vials, followed by injection into the combustion chamber.

The oxidation zone is composed of a quartz tube packed with an oxidizing agent (CrO_2), within an induction furnace maintained at $1000 \pm 50°C$. The sample combustion process is aided by a pulse of O_2 gas, introduced at the same time as the sample. The strongly exothermic combustion of the tin capsule and its contents raises the temperature to ca. 1700–1800°C, ensuring the complete combustion of organic compounds present to CO_2, water vapor, N_2, and oxides of N (NO and NO_2). The gaseous products are swept in a stream of carrier gas (helium) through the CrO_2 packing, where any pyrolysis products such as hydrocarbons are completely oxidized to CO_2 and H_2O. Carbon monoxide is commonly oxidized to CO_2 by passage over copper oxide as a catalyst.

The gas stream then passes through a purification zone, over reagents such as silver vanadate on silver wool or silver-coated Co_3O_4, to remove halogens and sulfur oxides. The gases then pass through a reduction column packed with copper granules at 650°C to remove excess O_2 and reduce NO_x to N_2 (the Dumas reaction). In instruments configured for C and N determinations, the water vapor is then removed by absorption in a trap filled with a drying agent, e.g., magnesium perchlorate (Fig. 1). The gas stream then passes through a gas chromatographic (GC) column packed

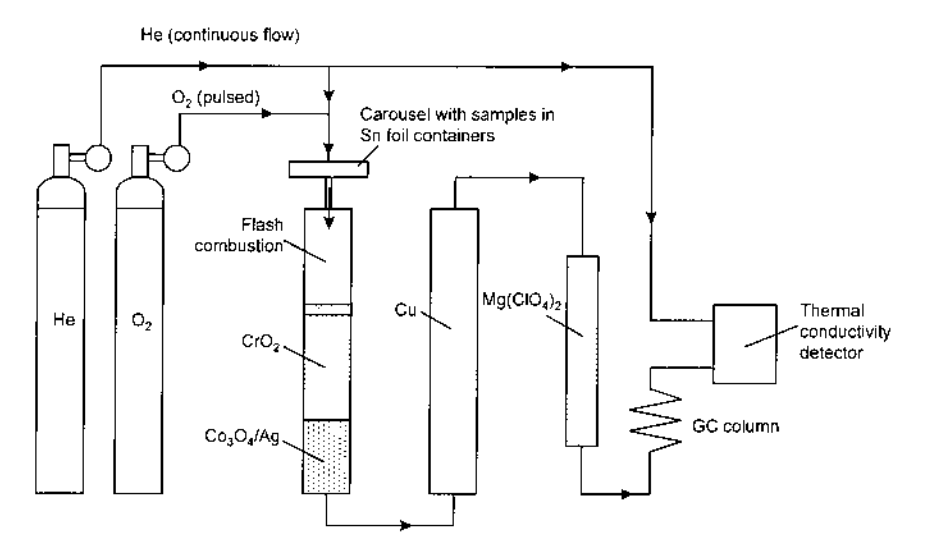


Figure 1 Schematic diagram of the CE-Instruments CN analyzer system.

with a material such as Porapak Q, where N_2 and CO_2 are separated, and then through a thermal conductivity detector (TCD). The output signal of the detector is converted to give a final result in terms of units of C and N in the original sample.

In CE Instruments analyzers configured to include the determination of H, as well as the C and N content of the sample, the water vapor is not trapped out but instead passes to the GC column. Here it is separated from the N_2 and CO_2 and measured by the TCD.

2. The Leco Range

Another widely used range of instruments is that produced by Leco (Laboratory Equipment Corporation, St. Joseph, MI, USA) (Table 1). Several early applications in soil analysis featured Leco models that are now superseded but may still be in use in some laboratories (see Tabatabai and Bremner, 1991, and Table 1). Second-generation automated elemental analyzers such as the Leco CHN-600 and CHN-800 Series have been used widely in soil and environmental investigations through the 1990s (see Sec. VI). These particular models permit the simultaneous determination of total C, H, and N in solid or liquid organic materials. The CHN-600 Analyzer, shown schematically in Fig. 2, is a macrosample instrument capable of analyzing samples ranging in weight from 100 to 200 mg and is thus well suited to soil and plant samples, whereas the CHN-800 Analyzer is a microsample instrument capable of analyzing samples ranging in weight from 3 to 15 mg and is aimed more at the analysis of organic compounds.

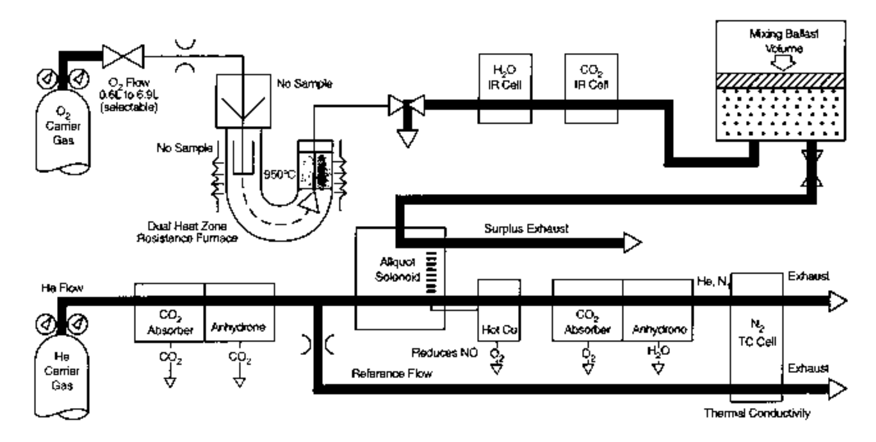


Figure 2 Schematic diagram of the Leco CHN-600 analyzer system.

Marcel Dekker, Inc.
270 Madison Avenue, New York, New York 10016

In total N analysis by these instruments, a weighed sample is encapsulated in tin or copper and dropped into a reusable ceramic crucible centered in the primary hot zone of a U-shaped combustion tube located in a resistance furnace, and the sample is burned in O_2 at 950°C. The potential combustion products are CO_2, water vapor, oxides of N or N_2, and oxides of S. Oxides of S are removed with a reagent in the secondary hot zone to prevent the formation of H_2SO_4. The secondary hot zone also ensures the complete combustion of all volatile gases. The remaining products of combustion (CO_2, H_2O, O_2, N_2, and NO_X) are collected and mixed thoroughly in a glass tube under a sliding PVC piston. The CO_2 and H_2O levels are constantly monitored during combustion by two independent selective IR detectors, and when they drop to predetermined levels, combustion is terminated. At this stage, an aliquot of the combustion products is removed automatically and carried by H_2 gas through a reagent train containing hot Cu for the reduction of NO_X to N_2, ascarite for the removal of CO_2, and anhydrone for the removal of H_2O. The N_2 thus obtained is then collected and measured by a thermal conductivity detector. The measurements are weight-compensated and displayed digitally as percent C, H, and N. Total analysis time for all three elements is 4–5 min with the CHN-600 Analyzer and less than 2.5 min with the CHN-800 Analyzer.

The successors to the CHN-600 have been the CHN-1000, and most recently the 2000 Series (Table 1). These latter instruments are micro-computer-based, use nondispersive infrared detection systems, and are designed to measure the C, H, and N content in a wide variety of organic compounds and environmental materials. The CN-2000/CNS-2000 models can accommodate samples weighing up to 2 g, and these are introduced in sample boats into a horizontal combustion system. This makes it possible to remove the sample ash, along with the boat, after each analysis, thus reducing the problem of ash accumulation. However, the standard operating procedures for CN, or CNS, analysis in soils and plant materials recommend sample weights of 0.15–0.8 g, depending on the sample. For soils, the furnace temperature is set at 1350–1450°C, while for CN analysis of plant material, 1050°C is sufficient. Use of the lower temperature extends the life of the combustion tube. The procedure for noncarbonate C (total organic C) in soils involves manual treatment of the sample with HCl in nickel-lined combustion boats, until all reaction with carbonate has ceased, followed by evaporation on a hotplate, before introduction into the analyzer. The FP-2000 variant can determine N in 1–2 g soil samples in reusable ceramic crucibles, in plant samples up to 4 g, and in 0.25 g samples of fertilizer materials.

3. Other Systems

The Perkin-Elmer Corp. have developed a model CHN-2400 analyzer that simultaneously measures C, H, and N using the principle employed in the traditional Pregl and Dumas procedures (Nelson and Sommers, 1996). A sample contained in a platinum boat is oxidized with O_2 at about 1000°C in a combustion tube in the absence of carrier gas (He) flow. After combustion, He flow is initiated, and the CO_2, H_2O, and N_2 gases produced are passed over CuO to convert CO to CO_2 and silver mesh (silver vanadate on silver wool) to remove S and halogen gases. The gases then pass into a tube packed with copper granules between end plugs of silver wool and maintained at 650°C to reduce the N oxides to N_2. The gases are brought to constant pressure and volume in a gas-mixing chamber and then allowed to expand into the analyzer portion of the instrument. The analyzer consists of three thermal conductivity detectors (TC) connected in series and separated by two traps. The sequence of the TC detectors and traps enabling quantification of H, C, and N is as follows (Nelson and Sommers, 1996): (1) TC detector 1 (output equals total gas composition), (2) $Mg(ClO_4)_2$ traps to remove H_2O, (3) TC detector 2 (decrease in output from detector 1 is proportional to H content), (4) soda asbestos plus $Mg(ClO_4)_2$ trap to remove CO_2, (5) TC detector 3 (decrease in output from detector 2 is proportional to C content), and (6) the remaining gases in the sample are N_2.

The RoboPrep-CN Analyzer marketed by Europa Scientific Ltd., Crewe, England (now PDZ Europa) and its successor models, the ANCA-GSL and GL, are essentially CN analyzers of the CE (Carlo Erba) type. Their special feature is that they can be linked via a capillary interface to a mass spectrometer for the ^{15}N analysis of the N_2 produced by Dumas combustion, and ^{13}C analysis of the CO_2 (Fig. 3). These instruments also give total C and N contents of the samples and can be used routinely for such measurements even where isotopic data are not required. The ANCA-GSL system can be fitted with either a 66- or a 130-position autosampler, with alternative versions available for small or large samples.

C. Modifications for S and O Analysis

1. Sulfur

Some automated analyzers are available with either a CHN or a CHNS capability. In the latter versions, generally the SO_2 formed by reduction of the SO_3 in the gas stream leaving the oxidation furnace is not trapped out but instead is quantitatively determined, along with the gaseous forms of the other target elements: H_2O vapor, CO_2, and N_2. In the CE Instruments

Marcel Dekker, Inc.
270 Madison Avenue, New York, New York 10016

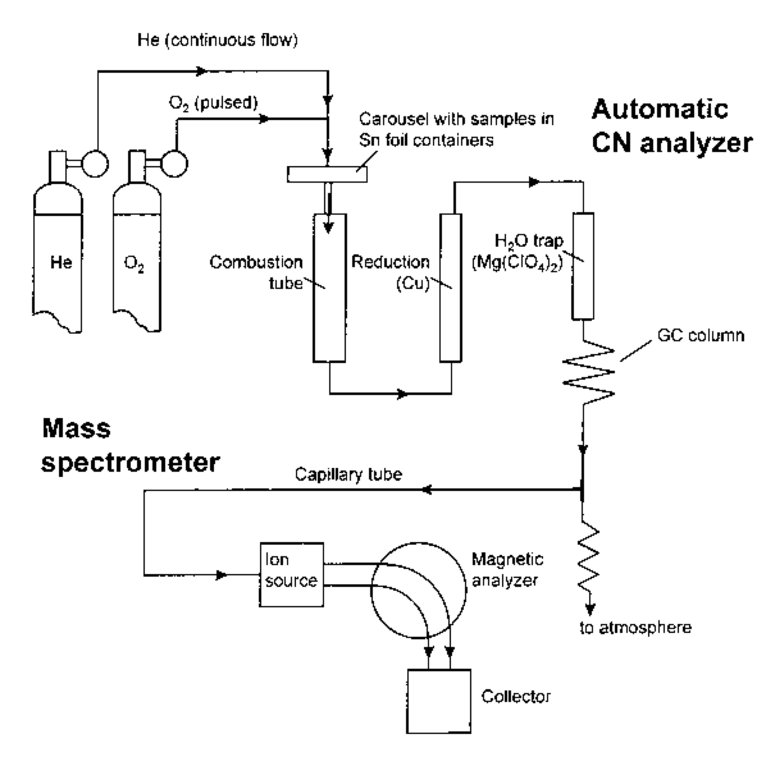


Figure 3 Schematic diagram of an automatic CN analyzer interfaced with an isotope ratio mass spectrometer.

EA-1110 instrument, for example, the SO_2 is separated from these other gases chromatographically and determined by the TCD. Alternatively, analysis of trace sulfur contents down to a few mg kg^{-1} in the original sample can be performed with this particular analyzer by connecting it to an optional electron capture detector (ECD), which has a much greater sensitivity than the TCD to SO_2. There seems no reason in principle why a similar adaptation could not be made with various other analyzer systems.

In the Leco family of instruments a different approach is used. The sample is combusted in a stream of oxygen, and the SO_2 produced, like CO_2 and H_2O, is determined by IR absorption. For example, in the Leco model SC-132 automated total S analyzer (an instrument dedicated to S analysis), the sample is mixed with combustion accelerators in a ceramic boat and combusted in a resistance furnace at 1370°C in an O_2 atmosphere. The SO_2 thus produced is passed through an infrared (IR) cell which is used as both a reference and a measurement chamber. It detects total S, as SO_2,

Marcel Dekker, Inc.
270 Madison Avenue, New York, New York 10016

continuously, and includes an IR source, a chopper motor, a precise wavelength filter, a condensing cone, and an IR energy detector.

2. Oxygen

In instruments designed for the purpose, conversion of a CHN or CHNS system to permit determination of oxygen is fairly straightforward. In the Perkin-Elmer 2400 Series II instrument, for example, the sample is pyrolyzed in a H_2/He mixture at 1000°C. The resulting gaseous products containing oxygen are passed over platinized carbon, where they are converted to CO. After passage through scrubbers to remove interfering species, the CO is separated and determined. The CE EA-1110 is comparable in its mode of operation. The samples are dropped into a pyrolysis chamber maintained at 1060°C and containing nickel-coated carbon. The oxygen in the sample reacts with the C to form CO, which is then chromatographically separated from other combustion products and determined quantitatively by the GC/TCD system.

D. Precision and Accuracy

Several of the first generation of automated analyzers were evaluated for their precision and accuracy in the measurement of total C, N, or S in soils. Details relating to such instruments as the Leco 70-Second Carbon Analyzer and the Coleman Models 29 and 29A Nitrogen Analyzers (all of which were reasonably satisfactory for this purpose), and the Leco Sulfur Analyzer (which was not) can be found in Tabatabai and Bremner (1991). Data that have become available on several of the second- and third-generation instruments have shown that, in general, they are capable of producing results that are both precise and accurate, not only for soils but also for such diverse materials as sediments, plant materials, processed foods, feedstuffs, sludges, manures, and fertilizers. Some of the available information on these instruments comes from academic studies in the late 1980s and early 1990s, but increasingly since then the focus of research involving these analyzers has been on applications rather than on performance evaluation, and the user community is therefore becoming more and more dependent on manufacturers' own information. Consequently, as indicated above, potential users are well advised to organize their own cross-checks on the suitability of a system for their particular intended application. On the other hand, some reassurance is provided by the fact that the development of the newer instruments has drawn heavily on the experience gained with earlier types, particularly in relation to dealing with the more intractable sample matrices. Also, the overall reliability of the electronic systems and sensitivity

of detectors has much improved, and the software-controlled routines for calibration following analysis of standards and blanks provide an automatic check on performance. These trends have led, generally, to better and more reliable analyses.

Yeomans and Bremner (1991) showed that the performance of two Leco instruments, the CHN-600 analyzer and the CR-12 carbon analyzer, was satisfactory for routine analysis of soils for total organic C content. Their comparison of C measurements on 20 soils made with these two instruments, with those obtained by the Allison (1960) wet oxidation method, is shown in Fig. 4. The sample combustion in the CHN-600 was carried out at 950°C, a much lower temperature than that used in the CR-12 (1372°C). In both systems, an atmosphere of pure oxygen was used. The performance of the two analyzers was almost identical, giving correlation coefficients of better than 0.999 with the wet oxidation method, and only very slightly higher absolute values—by about 4% (Fig. 4).

A similar comparison was also made by Yeomans and Bremner (1991) between nitrogen measurements with the CHN-600 (using the same conditions as for C analysis) and those obtained by the Kjeldahl method. The results are shown in Fig. 5. Here, too, the correlation coefficient was greater than 0.99, with the instrumental results averaging about 5% higher than the Kjeldahl values. McGeehan and Naylor (1988) also showed that the results obtained with the CHN-600 for plant materials were satisfactorily correlated with those obtained by Kjeldahl analysis ($r^2 = 0.92$) and were on average 7% higher.

There have been other reported studies of the performance of the CHN-600 for the measurement of total organic C in soils. A comparison of results obtained by this instrument with those obtained by a Leco induction furnace and a wet-oxidation method indicated that the CHN-600 gave the most precise results and allowed an operator to perform 90 to 100 analyses in 8 h (Sheldrick, 1986).

Although work by McGeehan and Naylor (1988) showed that the CHN-600 gave organic C values that were greater for four samples out of five than those obtained by the wet oxidation method of Walkley and Black (1934), this is not surprising and does not indicate a failure of the instrumental method. The traditional Walkley and Black method relies on the heat of reaction when dichromate and sulfuric acid are added to a soil, to convert the C to CO_2, and the originators estimated that, on average, 76% of the C in a soil was liberated by the procedure, and therefore that results should be multiplied by 1.32 to give the total C content. Allison (1960) found that the necessary correction factor ranged from 1.16 to 1.59. More recent variants of the wet oxidation technique, in which the mixture is vigorously heated, give much better recoveries of C and good absolute

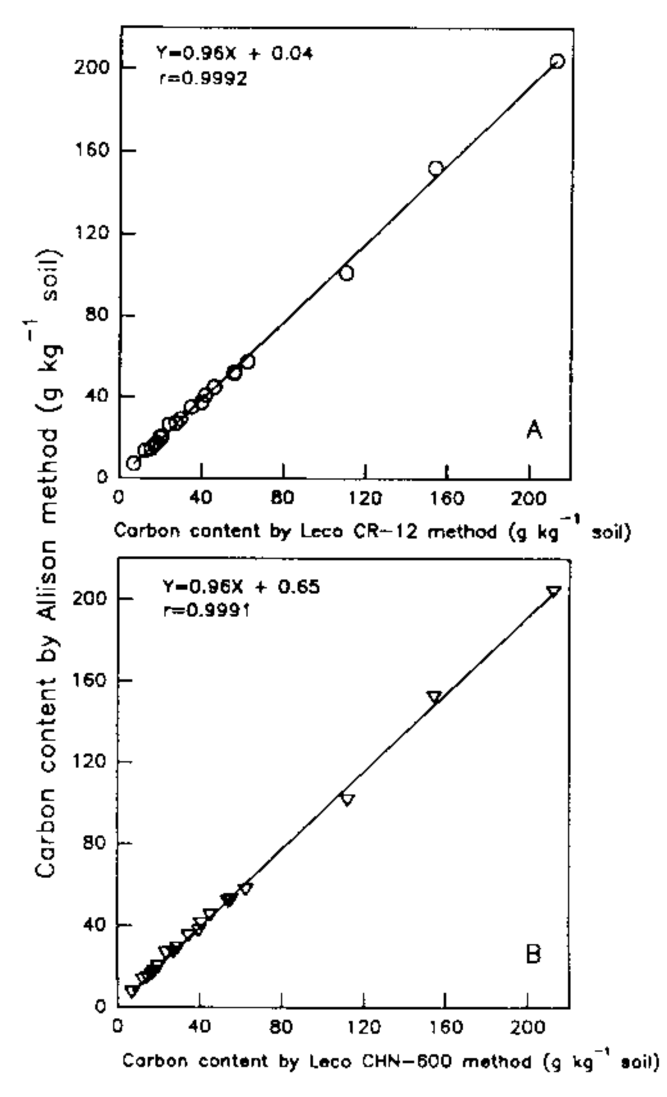


Figure 4 Total C content of 20 soil samples determined with (A) Leco CR-12 and (B) Leco CHN-600 analyzers, versus total C content by Allison method. (From Yeomans and Bremner, 1991.)

agreement with results obtained with a CHN analyzer (e.g., Ciavatta et al., 1989, who made the comparison using a Carlo Erba 1102).

Schepers et al (1989) evaluated the Carlo-Erba NA-1500 coupled with a mass spectrometer (the arrangement shown in Fig. 3) for simultaneous

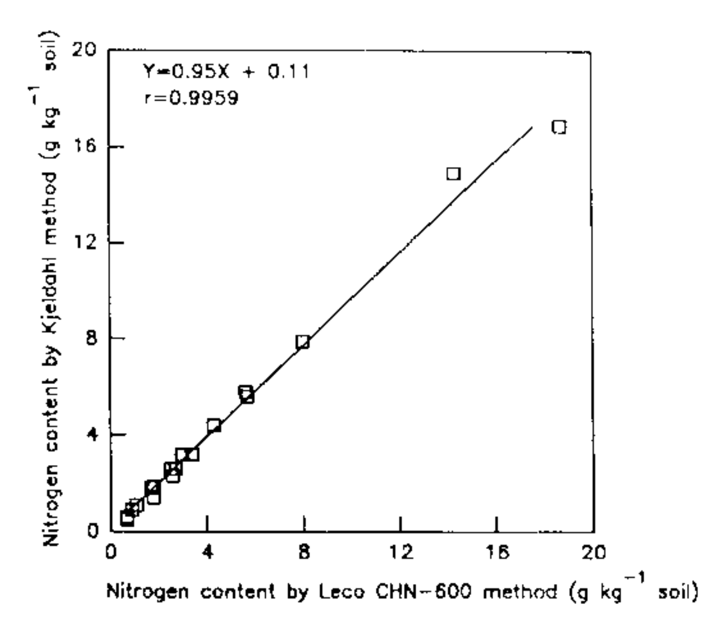


Figure 5 Total N content of 20 soil samples determined with the Leco CHN-600 analyzer, versus total N content by Kjeldahl method. (From Yeomans and Bremner, 1991.)

determination of total C, total N, and ^{15}N in soils and plant materials. They showed that this system gave results comparable to those obtained with conventional manual methods. Coefficients of variation for C were 1.03–1.41% for plant materials, and 1.46–1.62% for soils; the corresponding values for total N were 1.44–2.70% and 1.96–2.45%. Verardo et al. (1990) have described procedures for using the Carlo Erba NA-1500 for determination of total C and N in marine sediments. They used aluminum sample containers rather than tin ones, and prior to combustion removed carbonate-C from calcium carbonate in the sediments by treatment with sulfurous acid. This practice was adopted instead of the more conventional HCl treatment to avoid the creation of deliquescent $CaCl_2$. The precision of their measurements is given in Table 2.

The newer Leco 2000 series instruments are capable of achieving a satisfactory level of precision in analysis of soils and plant materials, judging from the information available from the manufacturer. Table 3 shows, for example, the results of six replicate analyses of soil and grass samples, for C, N, and S, determined with the CNS-2000 instrument, and Table 4 shows those for N only in two contrasting soils, determined with the FP-2000 instrument. It would appear that the precision is somewhat better when N

Table 2 Precision of Organic Carbon and Nitrogen Determinations in a Marine Sediment, Using the Carlo Erba NA-1500 Analyzer

Replicate	Organic C (wt %)	Nitrogen (wt %)
1	0.918	0.185
2	0.920	0.183
3	0.923	0.184
4	0.923	0.188
5	0.917	0.190
Mean	0.920	0.186
Std. dev.	0.003	0.003

Source: Verardo et al., 1990.

Table 3 Precision of Replicate C, N, S Determinations on a Soil and a Grass Sample, Using a Leco CNS-2000 Analyzer

Soil				Grass			
Wt (g)	% C	% N	% S	Wt (g)	% C	% N	% S
0.8245	2.67	0.175	0.033	0.2358	39.27	3.67	0.300
0.8407	2.67	0.175	0.034	0.2214	39.37	3.69	0.289
0.8387	2.56	0.160	0.030	0.2183	39.21	3.7	0.289
0.8568	2.57	0.169	0.033	0.2341	38.91	3.67	0.289
0.9493	2.55	0.167	0.032	0.2330	39.16	3.71	0.296
0.8587	2.68	0.176	0.035	0.2267	38.96	3.68	0.286
$\bar{\chi}$	2.62	0.170	0.033	$\bar{\chi}$	39.15	3.69	0.292
Std. dev.	0.06	0.006	0.002	Std. dev.	0.16	0.01	0.005
CV (%)	2.18	3.35	4.79	CV (%)	0.42	0.40	1.67

Source: Leco CNSP-2000 Organic Application Note, 1999.

only is being determined. Wright and Bailey (2001) reported more accurate and more precise measurements of organic C with the CN-2000 instrument than with the CNS-2000. They attributed this difference to the finer control of the combustion cycle of the CN-2000, which was not possible with the other instrument because of its built-in flow conditions required for S analysis.

The data in Tables 3 and 4 do not include comparisons with other accepted methods of analysis. However, Kowalenko (2000) compared the values for plant S content in fertilizer response trials obtained with the Leco CNS-2000 instrument with those obtained by five other methods, and

Marcel Dekker, Inc.
270 Madison Avenue, New York, New York 10016

Table 4 Precision of N Determination in Two Soil Samples, Using a Leco FP-2000 Analyzer

Sample A		Sample B	
Weight (g)	% N	Weight (g)	% N
1.3843	0.094	1.4220	0.495
1.5243	0.094	1.4714	0.492
1.4706	0.093	1.5416	0.500
1.4425	0.090	1.4822	0.497
1.3961	0.093	1.5316	0.503
1.5012	0.092	1.4528	0.499
$\bar{\chi}$	0.093	$\bar{\chi}$	0.498
Std. dev.	0.001	Std. dev.	0.004
CV (%)	1.48	CV (%)	0.71

Source: Leco FP-2000 Organic Application Note, 1997.

Table 5 Comparison of Analytical Results by CE Instruments NA 2100 and by Kjeldahl Analysis

	Total N (%)	
Sample type	by NA 2100	by Kjeldahl
Maize	1.22	1.2
Rice	1.10	1.1
Soya	6.99	6.8
Yeast	7.87	7.8
Fodder plant	1.44	1.4
Cheese	3.45	3.3
Cocoa	4.35	4.3
Tobacco	2.79	2.6
Fishmeal	10.48	10.43
Soil	0.038	0.04
Beer	0.0634	0.0633

Source: http://www.ceinstruments.it/OEA_Dir/na2100.htm (2000).

concluded that the Leco instrument gave the best results. Kowalenko (2001) also concluded that this instrument provided good to excellent results for total C and S in soils, and reasonably acceptable values for total N, which were slightly lower than, but proportional to, those by Kjeldahl analysis. Table 5 and Fig. 6 show manufacturer's data for total N analysis of soils,

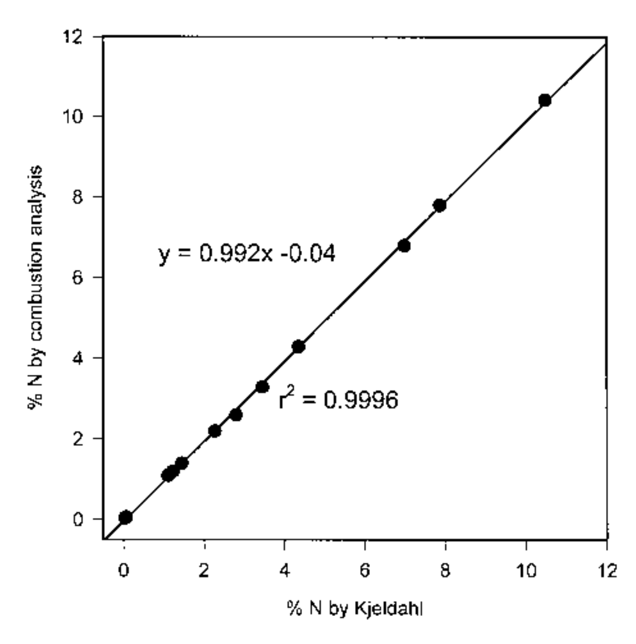


Figure 6 Total N content of soil, plant materials, foods and feedstuffs determined by CE NA-2100 combustion analysis, versus N content by Kjeldahl method. (From http://www.ceinstruments.it/OEA_Dir/na2100.htm, 2000.)

plants, foods, and feedstuffs by the CE NA-2100 instrument and by Kjeldahl analysis. Here, there is excellent agreement between the two methods right across the concentration range.

Leitao et al. (2001) have compared the performance of a CE instrument for total S analysis of soils and plants with a method involving dry ashing and ion chromatographic detection of sulfate. Close agreement was found between the two methods, but the automated dry combustion method was superior in accuracy, precision, and detection limits.

David et al. (1989) investigated the suitability of the Leco SC-132 total S analyzer for the analysis of sediment, soil, and wood samples. They compared the results obtained with the analyzer with those by the Johnson-Nishita alkaline oxidation method (Tabatabai and Chae, 1982), for 146 sediment samples from lakes and reservoirs, which had S contents ranging from 2 to 232 mmol S kg^{-1}. A regression of these results (Fig. 7) gave an R^2 value of 0.97 and a slope of 1.018, i.e., an average value by the S analyzer only 1.8% different from that by the wet oxidation method. Results for wood and soil samples agreed to within one standard deviation with those by the Johnson-Nishita method, and total S in an NBS

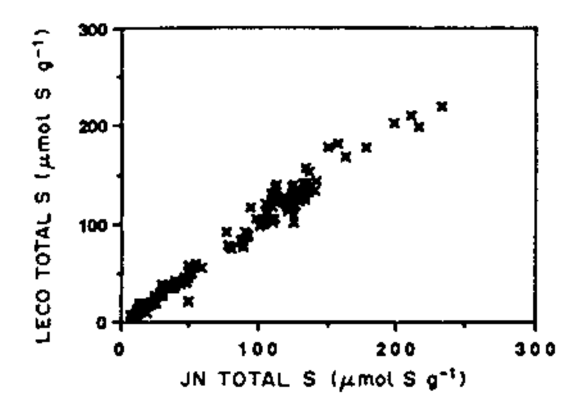


Figure 7 Total S content of lake and reservoir sediment samples determined by Leco SC-132 analyzer, versus S content by Johnson-Nishita alkaline oxidation method. (From David et al., 1989.)

standard orchard leaf sample gave a value within 2% of the recognized concentration.

In the absence of such evidence on the accuracy of a given determination by any particular new system, it is strongly recommended that the would-be user have a batch of samples with known elemental values determined by both the new system and an established one, before making a commitment to purchase. Such precautions should be applied to any of the instruments identified in Table 1 for which an evaluation of performance for the element and matrix of interest is not available. Nonetheless, it should be pointed out that in most studies of soil- and environmentally-related processes, problems arising from, for example, spatial variability in the concentration of the element of interest may be much greater than those caused by any modest bias attributable to the analyzer. In such circumstances the ability to undertake the analysis of larger numbers of replicate samples, and to get better statistical data on how concentrations vary in response to controlling variables, may be a more important consideration.

1. Sample/Matrix Problems

Homogeneous soil and plant samples are essential to provide a satisfactory degree of precision in the analytical results obtained with a combustion analyzer. The larger the sample that can be analyzed, the less the problem of particle size is likely to be, and in analyzers accommodating samples of the order of 1 g, a 420 μm maximum size should be adequate (see, for example,

Keeney and Bremner, 1967). However, grinding or ball-milling to a fine powder is necessary to ensure that a representative sample is taken for analysis in the CE range of instruments, where the typical sample size is 5–10 mg (e.g., Schepers et al., 1989; Verardo et al., 1990).

Earlier, Tabatabai and Bremner (1970) examined the effect of grinding on results with the Leco 70-Second Carbon Analyzer. The precision increased substantially with a decrease in maximum particle size from 2000 μm to 420 μm but showed relatively little improvement with further grinding to smaller sizes (Table 6).

Indigenous fixed ammonium N in clay soils may be fully recovered by the Kjeldahl method only when the samples are treated with HF before analysis (Stewart and Porter, 1963). Keeney and Bremner (1967) showed that automated combustion analyzers may give higher values than the Kjeldahl method with such soils but still not give a quantitative recovery of the fixed ammonium N. Apart from this early study, conducted with a Coleman 29A analyzer, there is no other information, and in any investigation in which data were required on fixed ammonium N, currently available systems would need to be evaluated to determine their performance in such a determination. Likewise, if it is desired to determine

Table 6 Effect of Sample Mesh Size on Total Carbon Analysis of Soils by Leco 70-Second Carbon Analyzer

	Max. particle size		Total C content (%)[a]		
Soil	Mesh	μm	Range	Mean	SD
Lindley	10	2000	1.16–1.41	1.29	0.11
	40	420	1.31–1.38	1.33	0.03
	100	150	1.35–1.38	1.36	0.01
Sharpsburg	10	2000	2.30–2.45	2.36	0.06
	40	420	2.28–2.34	2.31	0.02
	100	150	2.28–2.32	2.29	0.02
	300	50	2.26–2.29	2.28	0.01
Grundy	10	2000	2.60–2.69	2.63	0.04
	40	420	2.63–2.75	2.68	0.04
	100	150	2.62–2.69	2.66	0.03
	300	50	2.60–2.68	2.64	0.03
Glencoe	10	2000	5.65–6.05	5.81	0.15
	40	420	5.68–5.86	5.78	0.07
	100	150	5.77–5.84	5.80	0.03

[a]Five analyses. SD, standard deviation.
Source: Tabatabai and Bremner (1970).

soil mineral N (nitrate, nitrite and nonfixed ammonium) along with the organic N, there should be a comparable evaluation of the performance of the analyzer employed.

The total C content of a soil can include the element in the form of calcium and magnesium carbonate and bicarbonate, as well as in organic form. To determine organic C in soils where these inorganic forms are present, it is usual first to remove the carbonate/bicarbonate by treatment with acid before subjecting the sample to Dumas combustion (Nelson and Sommers, 1996; Kerven et al., 2000). If the inorganic C content is also to be determined, then samples may be analyzed with and without the acid treatment, and the result obtained by difference.

In the absence of acid treatment, Matejovic (1997) found that carbonate C was increasingly liberated as the furnace temperature of a Leco CNS-2000 analyzer was increased from 700 to 1100°C—a result quite similar to that of Merry and Spouncer (1988), using a Leco CR-12 instrument. However, Wright and Bailey (2001) obtained very good agreement with the values of certified standard soils, for organic C at 1040°C ("Combustion Profile 1") and total C at 1300°C ("Combustion Profile 2"), respectively, using a Leco CN-2000 analyzer (Table 7 and Fig. 8). The organic C content was overestimated at the higher temperature and the total C correspondingly underestimated at the lower one (the 1300°C setting was essential for total N).

Table 7 "Combustion Profiles" Established for Leco CN-2000 Analyzer for Determination of (a) Organic C and (b) Total C, in Soils

(a) Profile 1 (organic C)				(b) Profile 2 (total C)			
Furnace temperature			1040°C	Furnace temperature			1300°C
Lance O_2 flow			1.5 L min^{-1}	Lance O_2 flow			1.5 L min^{-1}
Purge O_2 flow			4.5 L min^{-1}	Purge O_2 flow			4.5 L min^{-1}
Instrument settings				*Instrument settings*			
Burn cycle	Lance flow	Purge flow	Flow time (s)	Burn cycle	Lance flow	Purge flow	Flow time (s)
1	Off	On	5	1	Off	On	5
2	On	On	15	2	On	On	5
3	On	On	15	3	On	On	5
4	On	Off	25	4	On	Off	95
5	On	On	End	5	On	Off	End

Source: Wright and Bailey, 2001.

Marcel Dekker, Inc.
270 Madison Avenue, New York, New York 10016

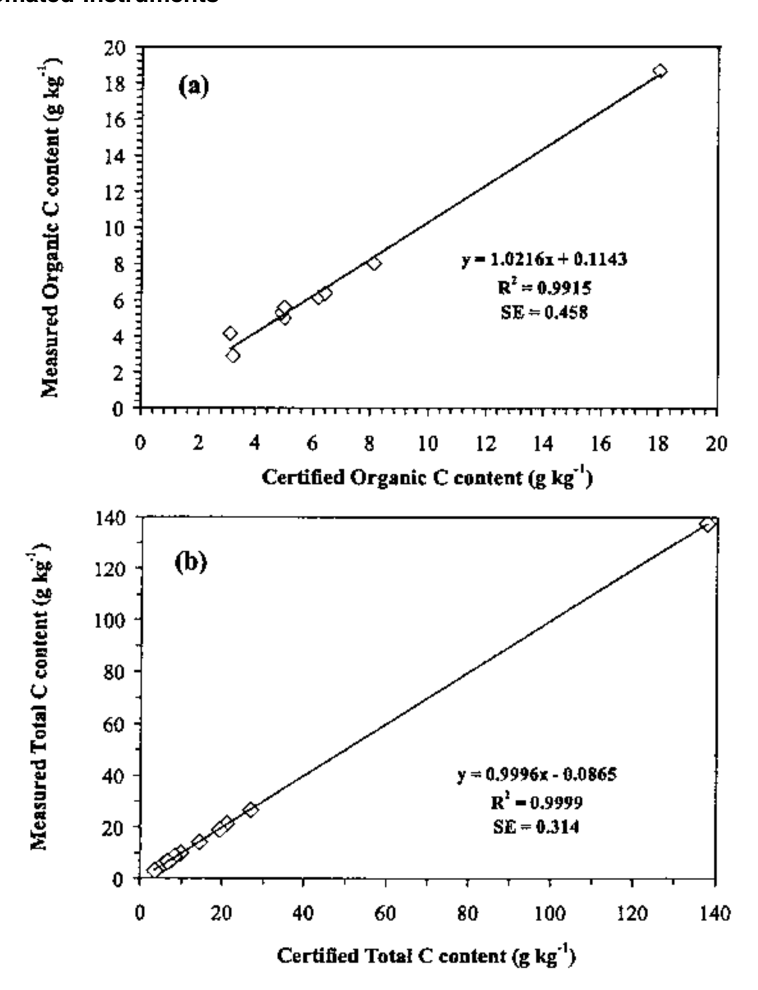


Figure 8 Values of (a) organic C (obtained using combustion profile 1) and (b) total C (obtained using combustion profile 2) in reference soils, measured with a Leco CN-2000 analyzer, versus the certified values. Combustion profiles as in Table 7. (From Wright and Bailey, 2001.)

III. SYSTEMS FOR DISSOLVED ORGANIC C AND N

The widespread need to determine concentrations of dissolved organic C in drinking water supplies and in natural water bodies—lakes, rivers, aquifers, and oceans—has led to the development of a substantial range of automated analyzers dedicated to this task. These provide

an alternative to the continuous-flow methods for dissolved C covered in Chap. 4. Some well-established analyzer makes and models are listed in Table 8. Some of these instruments are also capable of measuring the total N content of the water samples, by the addition of a second detector.

Generally these analyzers are capable of measuring the *total organic carbon* (TOC) present in a sample, and also the *total inorganic carbon* (TIC). The analytical process is shown schematically in Fig. 9. Release of the TIC by acidification leaves only the TOC, which is then oxidized to CO_2 and measured quantitatively with a suitable detection system. The *total carbon* (TC) in the sample, if required, is then given by the sum of the TOC and TIC.

The total organic C in an aqueous sample includes particulate material (suspended solids) as well as the *dissolved organic carbon* (DOC). The most common means of separating dissolved and particulate matter is filtration. Material that passes through a membrane filter, usually with a pore size of 0.45 μm, is regarded as being "dissolved," but other size limits (e.g., 0.22 μm) have been chosen by some investigators (Urbansky, 2001).

TOC/DOC analyzers may be characterized according to the method of sample oxidation employed. There are essentially two methods available: high-temperature combustion, and low-temperature wet oxidation involving peroxydisulfate ions, with or without irradiation by UV light. These systems are described separately in the following sections.

A. Analyzers Based on High-Temperature Combustion (HTC)

The essential components of a TOC/DOC analyzer using an HTC procedure have much in common with those of dry combustion CN analyzers described in Sec. II above, as they include

1. An automated sample introduction system
2. A combustion tube in which the organic matter in the sample is oxidized to CO_2, water vapor, NO_x, and sulfur oxides
3. A carrier gas system to sweep the products of the combustion through the remaining stages of the analyzer
4. A drying system to remove water vapor, and a scrubber to remove other unwanted gases
5. A CO_2-specific NDIR detector (plus a nitrogen-specific detector if N is included in the analysis)
6. A signal recording/readout system

Marcel Dekker, Inc.
270 Madison Avenue, New York, New York 10016

Table 8 Some Current/Recent Automated Analyzer Systems for DOC/TOC and N in Waters, Related Earlier Models, Operating Principles, and Applications

Manufacturer	Address/website	Model(s)	Related earlier makes/models	Operating principle/detection system(s)	Typical applications
Analytik Jena GmbH	Konrad-Zuse-Strasse 1 07745 Jena, Germany www.analytik-jena.de	TOC Analyzer micro C, multi N/C 3000		High-temp. combustion; detection by NDIR	TOC, TN in drinking, ground, surface, waste waters
Ionics Instruments	65 Grove St. Watertown, MA 02472-2882, USA www.ionics.com	Model 555		High-temp. combustion; detection by IR	TOC in waters (various)
Metrohm UK	Unit 2, Buckingham Industrial Park Buckingham, MK18 1TH, UK www.metrohm.co.uk	Thermalox TOC/TN Analyser		High-temp. combustion; detection by NDIR	TOC, TN in drinking, ground, surface, landfill seepage waters
Monitor Sensors	7-9 Industrial Drive Caboolture Queensland 4510 Australia	1500 Series		High-temp. combustion; detection by CO_2-specific IR detector	TOC in waters (various)
OI Analytical	PO Box 9010, College Station, Texas 77842-9010, USA www.oico.com	Models 1010, 1020 TOC Analyzers	Model 700	UV-persulfate oxidation (1010), combustion (1020). Detection by NDIR	TOC in waters (various); 2 ppb–125 ppm C content

(continued)

Marcel Dekker, Inc.
270 Madison Avenue, New York, New York 10016

Table 8 Continued

Manufacturer	Address/website	Model(s)	Related earlier makes/models	Operating principle/detection system(s)	Typical applications
Pollution & Process Monitoring Ltd.	Bourne Enterprise Centre, Borough Green, Sevenoaks, Kent TN15 8DG, UK	LABTOC		UV-persulfate oxidation. detection by IR	TOC in waters (various); 0–10 ppm and 0–4000 ppm C
SGE International Pty Ltd	7 Argent Place Ringwood, Victoria Australia www.sge.com.au www.anatoc.com	ANATOC Series II		Photo-catalytic oxidation (UV/TiO_2); detection by dual wavelength NDIR	TOC in waters (various); 0.05–50,000 ppm C
Shimadzu Corp. and Shimadzu Scientific Instruments	3, Kanda-Nishikicho 1-chome, Chiyoda-ku Tokyo 101, Japan; 7102 Riverwood Drive Columbia, Maryland 21046, USA; www.sel.shimadzu.com	TOC-4100, -5000A & 5050A; TOCN-4100; TN-4100.		High-temp. combustion at 680°C. Detection of C by NDIR, of N by chemiluminescence. Optional nonautomated solid sample module	TOC, or C & N, in waters; on-line analysis of aqueous waste streams, cooling waters, river and lake water
Skalar Analytical BV	PO Box 3237, 4800 DE Breda, The Netherlands www.skalar.com	Formacs HT, Formacs TN, Formacs LT		High-temp. combustion (Model HT); low-temp. UV/persulfate digestion (LT), detection of C by NDIR, N by added chemiluminescence detector	TOC and/or total N in drinking, ground, surface, sea waters

Tekmar-Dohrmann Co.	PO Box 429576, Cincinnati, Ohio 45242-9576, USA www.tekmar.com www.dohrmann.com	Apollo 9000		Combustion at 680–1000°C with Pt catalyst. Detection by NDIR	TOC in sludges, sediments, particulated waste waters & effluents, drinking, surface, sea waters
Tekmar-Dohrmann Co.	PO Box 429576 Cincinnati, Ohio 45242-9576, USA www.tekmar.com www.dohrmann.com	Phoenix 8000	Dohrmann DC-80, DC-190	Low-temp. UV/persulfate digestion (LT), detection by NDIR	TOC in sludges, sediments, particulated waste waters & effluents, drinking, surface, sea waters

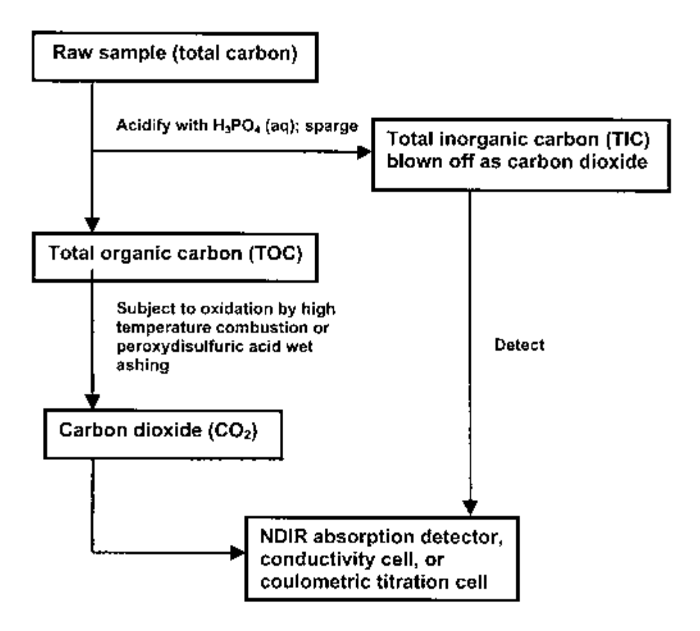


Figure 9 Sequence of operations in the automated analysis of dissolved total organic C and inorganic C in water samples. (From Urbansky, 2001.)

1. Examples of Commercial Systems

The layout of a typical DOC analyzer (the Tekmar-Dohrmann Apollo 9000HS) is shown schematically in Fig. 10, which also illustrates the system for the measurement of inorganic C, i.e., carbonate and bicarbonate C. The sample is injected into a reaction vessel in which carrier gas is bubbled through a dilute acid solution (usually phosphoric acid). The carbonate and bicarbonate are converted to CO_2, which is then purged (sparged) from the solution. The CO_2 is dried and scrubbed and passes to the NDIR detector.

Generally, as an alternative, the throughput of samples for organic C can be maximized by pretreatment to remove inorganic C rather than by carrying out the successive analyses of TOC and TIC. In this mode, a sample is acidified and the released CO_2 purged by a carrier gas stream and vented to the atmosphere, instead of passing through the gas detector.

In the Tekmar-Dohrmann Apollo 9000HS analyzer (Fig. 10), samples are withdrawn from sample vials in an autosampler module (not shown) by a 2.5 mL automatic syringe and then introduced into the analyzer via the multiport valve. The sample is transferred to the combustion furnace, which contains a platinum catalyst and can be operated at temperatures

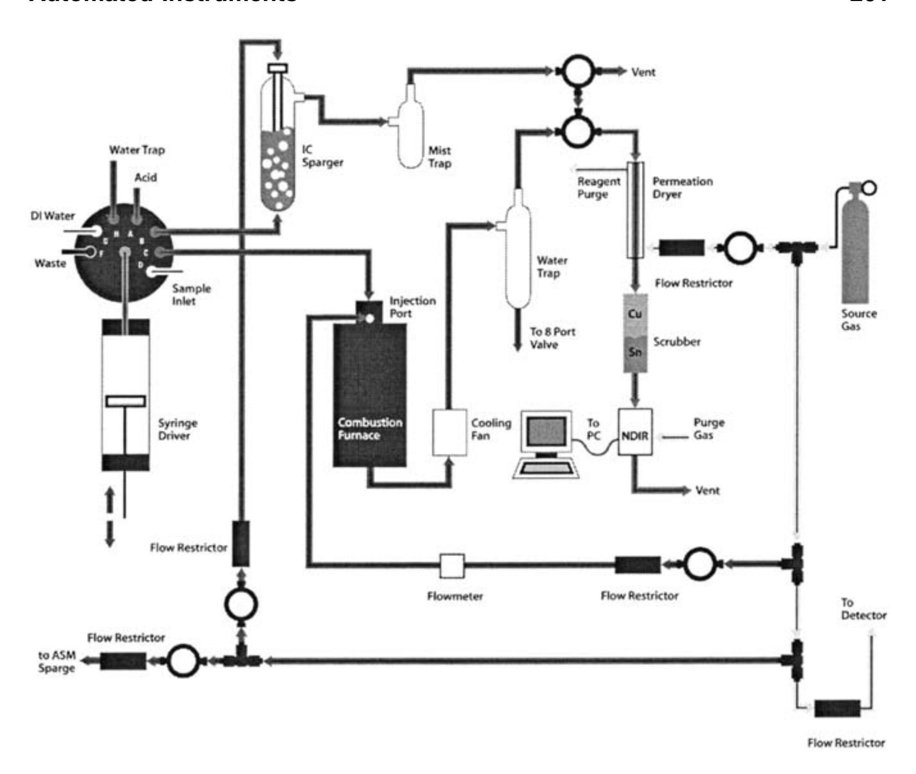


Figure 10 Schematic diagram of the Tekmar-Dohrmann Apollo 9000HS TOC analyzer, based on sample oxidation by high-temperature combustion. (From Wallace et al., 2002.)

between 680 and 1000°C. The gas stream leaving the furnace is cooled and then passed through a water trap, followed by a permeation dryer to remove water vapor. Unwanted gases (e.g., oxides of N and S) are removed in the Cu/Sn scrubber, leaving only the CO_2 from the organic C; this is measured with an NDIR detector and the data recorded with a PC.

The Shimadzu TOC-5000 has a similar operating system. Water samples (4–250 μL or 50–2000 μL) from 5-mL vials in an autosampler are automatically injected via a syringe. The oxidation takes place at 680°C. The normal oxidation catalyst in the Shimadzu combustion tube is alumina impregnated with 0.5% platinum (Alvarez-Salgado and Miller, 1998), although a variety of different catalysts is used in HTC instruments, including copper (II) oxide, cobalt oxide, and platinum on quartz wool or titanium dioxide (Fukushima et al., 1996; Wallace et al., 2002). High-purity air or oxygen is used as carrier gas at a flow rate of 150 mL min^{-1}.

The analog output signal of the NDIR detector is displayed as peaks, the areas of which are measured and processed by the data processing unit. The peak areas are proportional to the total C concentrations, so the total C in a sample may be readily determined from a calibration graph prepared using standard solutions of known C content.

2. Nondispersive Infrared (NDIR) Detectors

These detectors are so-called because the infrared beam has not passed through a monochromator (e.g., a grating or a prism). For them to function successfully as CO_2 detectors, the gas stream must be purified by the removal of water vapor and compounds such as SO_2 and SO_3, all of which absorb strongly in the IR region. The water vapor comes mainly from the evaporation of the sample. It can be removed in permeation tubes, by freezing out in cold fingers at ca. $-20°C$, or by passing the gas stream through a drying agent. The Shimadzu TOC-5000A instrument uses a thermoelectric (Peltier) dehumidifier, which cools and dries the gas stream leaving the combustion tube. Two NDIRs used in DOC analyzers are illustrated in Fig. 11.

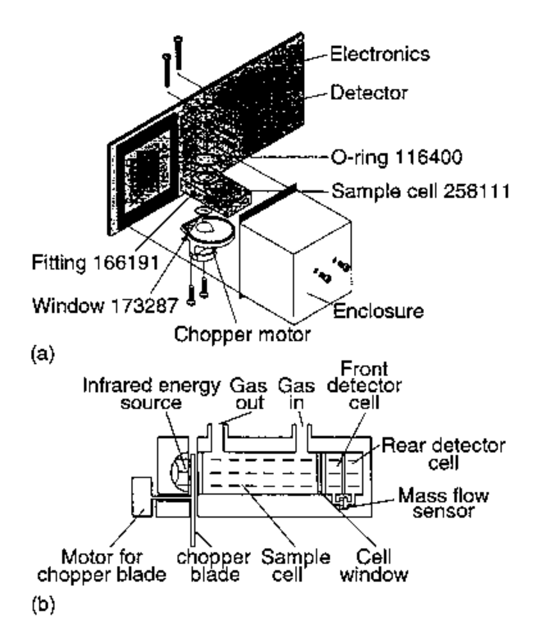


Figure 11 Schematic diagrams of nondispersive infrared detectors used in (a) OI Analytical and (b) Tekmar-Dohrmann TOC analyzers. (From Urbansky, 2001.)

B. Analyzers Based on Wet Oxidation

The second common type of TOC/DOC analyzer is based on the conversion of C to CO_2 by a wet oxidation procedure, with peroxydisulfate ion, $O_3SOOSO_3^{2-}$ (more usually known as "persulfate"), as the most common oxidizing agent. Analyzers of this type differ essentially from the HTC type by having a reactor vessel for the wet oxidation instead of a combustion tube and furnace. In the reactor, the sample is mixed with acidified sodium persulfate solution and either heated to ca. 100°C or irradiated at ambient temperature with UV radiation from a mercury vapor lamp. The layout of a UV-type analyzer, and its reactor vessel, are shown schematically in Figs. 12 and 13(b), respectively, while Fig. 13a shows the layout of a reactor that relies on heat rather than UV to catalyze the reaction. Either method induces the release of OH radicals, which attack the organic matter in the sample and oxidize it to CO_2 (Urbansky, 2001). The CO_2 formed during the oxidation is purged from the solution by the carrier gas stream, dried

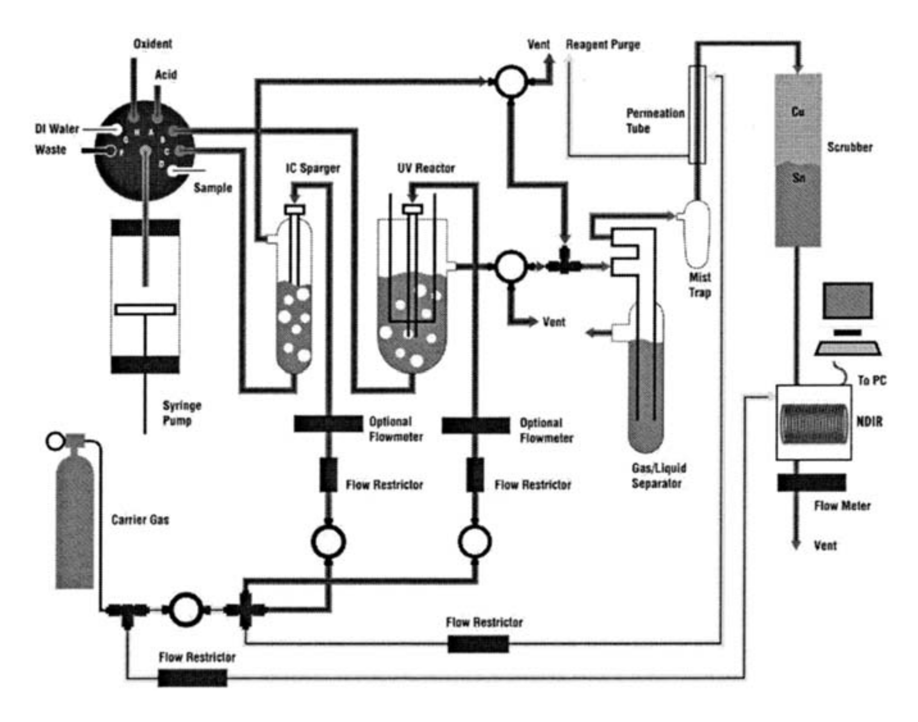


Figure 12 Schematic diagram of the Tekmar-Dohrmann Phoenix 8000 TOC analyzer, based on sample oxidation by the UV-persulfate method. (From Wallace et al., 2002.)

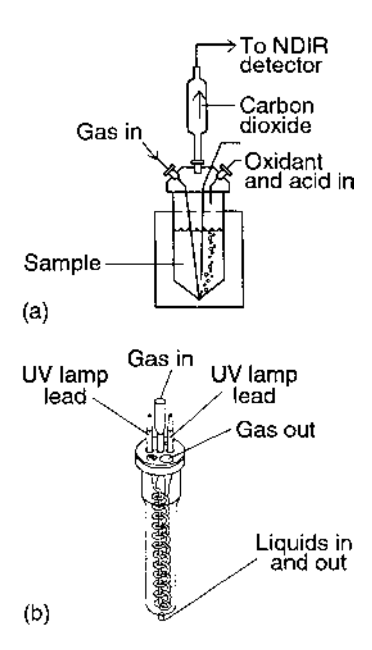


Figure 13 Diagrams of the reaction chambers used for persulfate wet oxidation in (a) OI Analytical 1010 (thermal) and (b) Tekmar-Dohrmann Phoenix 8000 (UV) TOC analyzers. (From Urbansky, 2001.)

and scrubbed, and then measured in the usual way with an NDIR detector. Figure 14 is a photograph of the reactor and other major components of the wet chemistry section of the Tekmar-Dohrmann Phoenix 8000 UV-type analyzer.

The ANATOC Series II analyzer, made by CGE in Australia, has an oxidation system based on a slurry of titanium dioxide and UV irradiation. The sample is introduced directly into the reactor containing the slurry. Air is circulated continuously in a closed loop and provides the necessary oxygen for the oxidation of bound C to CO_2, which is circulated through the closed loop until equilibrium is reached and determined with a dual-wavelength NDIR detector. The system is then vented and the CO_2 concentration returns to ambient baseline level, ready for the next analysis. The analyzer is shown schematically in Fig. 15.

C. Choice and Performance of Methods

The absolute and relative performances of peroxydisulfuric oxidation systems and those based on HT combustion have been assessed

Marcel Dekker, Inc.
270 Madison Avenue, New York, New York 10016

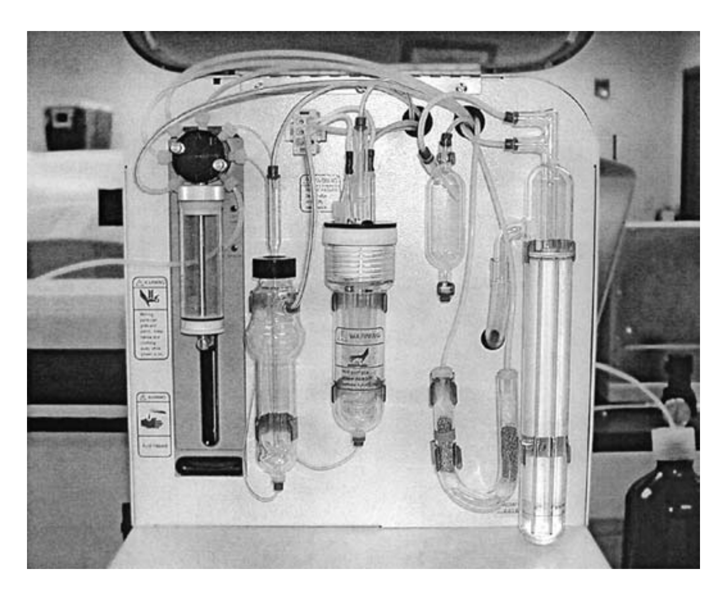


Figure 14 Photograph of wet chemistry section of the Phoenix 8000 TOC analyser. Far left: automated syringe and 8-port valve; 2d from left: IC chamber where sample is acidified, and the CO_2 released is removed by sparging; 3d from left: chamber for oxidation of organic C by UV/persulfate; far right: gas–liquid separator. (Courtesy of Tekmar-Dohrmann.)

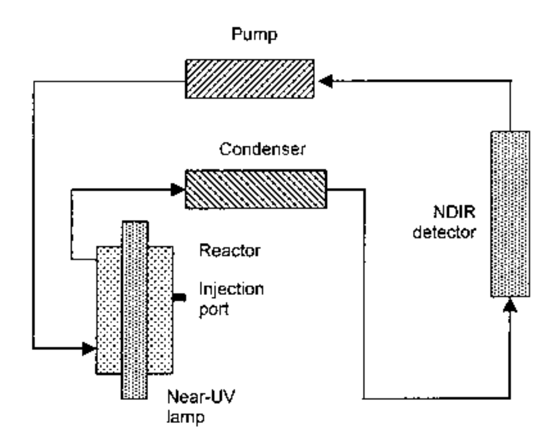


Figure 15 Schematic diagram of the CGE ANATOC Series II DOC analyzer, based on sample oxidation by UV/titanium dioxide.

by Urbansky (2001) as part of a comprehensive examination of DOC systems. Urbansky concluded, “there is continual concern over the efficacy of different digestion methods, because (1) the composition of organic matter is variable both geographically and temporally; (2) the frequency with which recalcitrant compounds may be found is unknown; and (3) the characteristics of such compounds are not well defined.”

Dissolved organic materials such as polycyclic compounds, and suspended particulate matter, are not completely oxidized by wet-oxidation procedures such as the UV-persulfate process. According to Wallace et al. (2002), the water industry regards the HTC system as being more effective for oxidizing TOC in samples with particulate matter. Wallace et al. commented that this may be so for particles > 0.2 mm in size, but that evidence for other samples is conflicting. They obtained very good correlations between the two oxidation methods for both DOC and TOC in drinking water, with very slightly higher values for HTC (Fig. 16).

Tests carried out with suspended cellulose particles have shown an increasing standard deviation between replicate measurements, with increasing particle size and heterogeneity, even when C recoveries are essentially quantitative (Lee-Alvarez, 1999).

The following examples illustrate the different experiences relating to oxidation efficiency reported for contrasting sample sources. Sharp (1973) found that natural organic matter from deep sea water was partly resistant to wet oxidation, but Benner and Hedges (1993) found no significant difference between HTC and UV-persulfate digestion methods applied to Amazon river water samples (Table 9). These workers also found a good 1 : 1 relationship between the results obtained with a Shimadzu TOC-500 HTC analyzer and a Carlo-Erba 1106 elemental analyzer (Fig. 17). Peltzer et al. (1996) compared the HTC and wet oxidation methods against a reference method involving combustion in a sealed tube, described by Fry et al. (1993). They concluded that their commercial HTC analyzer (a Shimadzu TOC-5000) performed well with marine samples but showed a small loss of oxidation efficiency for freshwater samples high in DOC (> 800 μ*M* C). Their commercial persulfate-based analyzer (an OI Model 700) also performed very well with low- to moderate-DOC marine and estuarine samples but showed a slightly greater loss of oxidation efficiency with the high-DOC freshwater samples. Peltzer et al. (1996) recommended that analysts should:

1. Calibrate their method and instruments daily.
2. Make the appropriate blank corrections using carbon-free distilled water.

Marcel Dekker, Inc.
270 Madison Avenue, New York, New York 10016



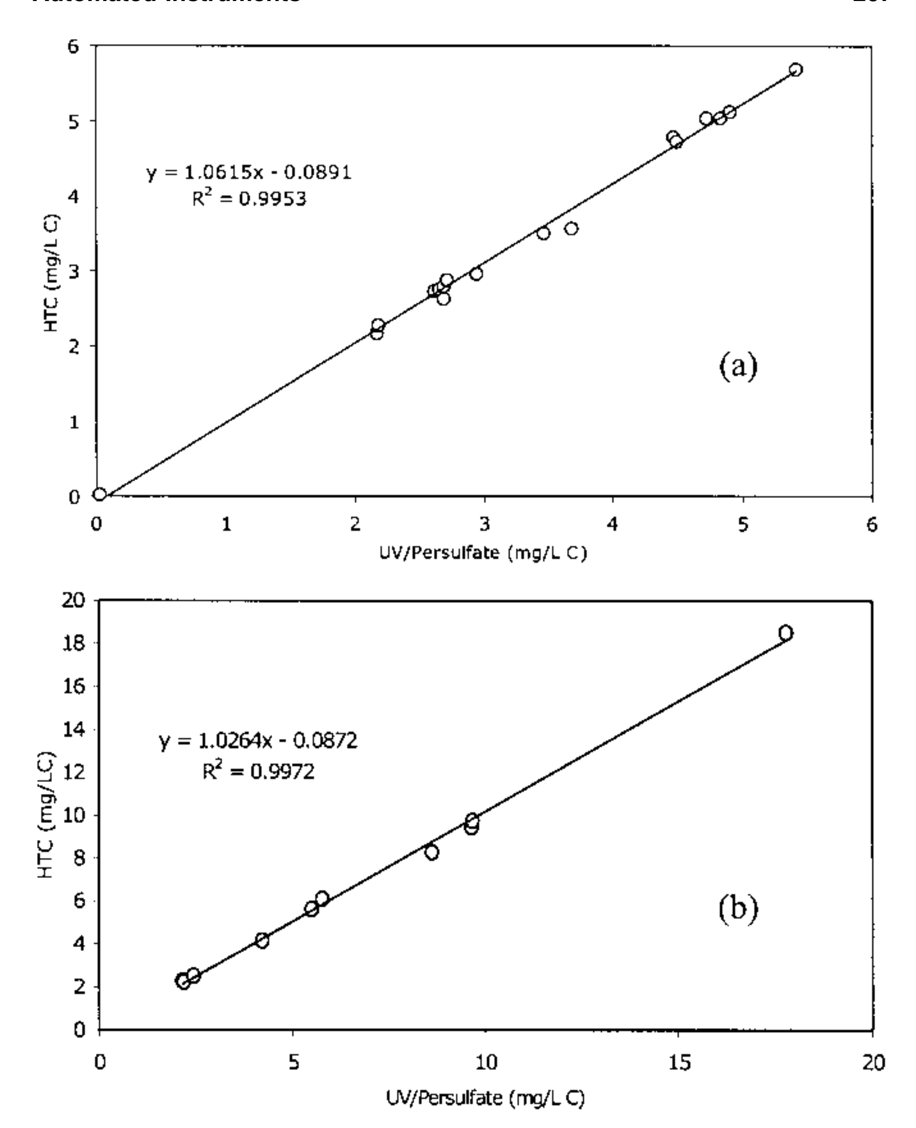


Figure 16 (a) DOC and (b) TOC content of drinking water samples determined by HTC method, versus content determined by UV-persulfate method. (Adapted from Wallace et al., 2002.)

Table 9 Comparison of a Shimadzu TOC-500 (HTC-type) Analyzer with a Dohrmann DC-80 (Wet Oxidation Type) Analyzer for the Measurement of DOC in Amazonian Freshwater Samples

Sample source	DOC by Shimadzu DOC-500 (mg L^{-1} ± SD)	DOC by Dohrmann DC-80 (mg L^{-1} ± SD)
Obidos	2.39 ± 0.06	2.44 ± 0.06
Rio Ica	2.62 ± 0.07	2.74 ± 0.11
Rio Negro	8.06 ± 0.31	7.98 ± 0.29
Salmon Pond	2.73 ± 0.16	2.77 ± 0.10
Portage Bay	2.67 ± 0.04	2.84 ± 0.16
KPA standard[a]	10.11 ± 0.20	9.87 ± 0.20

[a]KPA: 10 mg C L^{-1} as potassium hydrogen phthalate.
Source: Benner and Hedges, 1993.

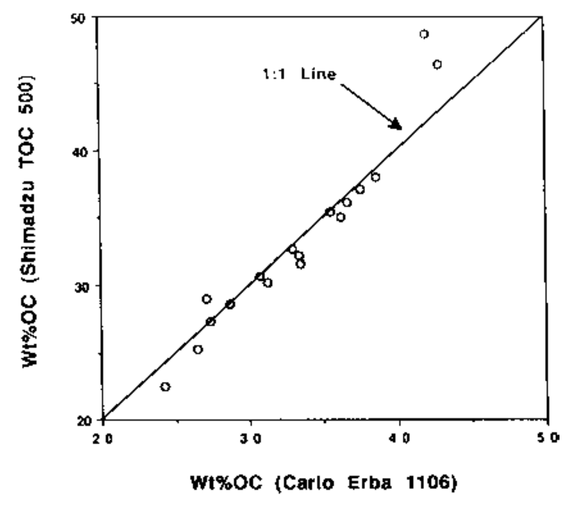


Figure 17 TOC in Amazon river water samples determined by Shimadzu TOC 500 analyzer, versus corresponding measurements using a CE 1106 elemental analyzer. (Benner and Hedges, 1993.)

3. Determine the combustion efficiency for their method at least once, either by direct comparison with a referee technique or by oxidation tests performed on recalcitrant compounds.
4. "Certify" the accuracy of their method by the regular measurement of reference samples.

Sharp et al. (1995) compared the results from five HTC analyzers, including one laboratory-made system, and a persulfate oxidation method, for DOC in seawater. Agreement was obtained between all the systems, within ±7.5%, but only after some instruments had been modified by, for example, reconditioning the combustion tube and in one case replacing the CO_2 detector.

1. Differential vs. Purging Method

Fukushima et al. (1996) compared the *differential method*, in which both dissolved total C and dissolved inorganic C (DIC) are measured, and the DOC is estimated by difference, with the *purging method*, in which DIC is removed from acidified filtrates by purging with CO_2-free gas before DOC measurement. They did this for waters collected from lakes, rivers, and pollution sources that included a septic tank, a sewage treatment plant, and domestic "gray" water. Their results (Table 10) show an underestimation by the purging method, compared with the differential method. The difference was attributed primarily to the precipitation of dissolved OM at low pH, followed by deposition on the vessel wall, rather than to the removal of

Table 10 Comparison of DOC Concentrations Determined by (a) Differential Method, and (b) Purging Method (at ca. pH 2)

	DOC (mg C L^{-1} ± SD)		
Sample source	Differential	Purging	(A−B)/B (%)
Lake water:			
Station 1	3.86 ± 1.12	3.31 ± 1.16	17
Station 2	4.49 ± 0.44	4.05 ± 0.58	11
Station 3	4.48 ± 0.38	4.19 ± 0.32	7
Influent rivers:			
Agric. catchments (*n*=5)	3.35 ± 0.81	2.88 ± 0.80	16
Forest catchments (*n*=2)	2.76 ± 1.14	2.33 ± 0.99	18
Urban catchments (*n*=3)	4.22 ± 0.52	3.39 ± 0.56	24
Pollution sources:			
Gray water	29.4 ± 1.46	16.8 ± 0.62	75
Effluent, septic tank	8.15 ± 0.28	7.53 ± 0.37	8
Effluent, sewage treat.	4.93 ± 0.82	4.97 ± 0.99	−1
Effluent, paddy field	10.09 ± 2.98	9.10 ± 4.52	11
Effluent, plowed field	0.37 ± 0.03	0.22 ± 0.06	68
Effluent, forest	0.83 ± 0.07	0.50 ± 0.01	66

Source: Fukushima et al., 1996.

volatile organic compounds. These observations suggest that for any new sample source, such comparisons should be made before adopting the purging method.

2. Problems with New Catalyst

The introduction of a new filling of catalyst into the combustion tube of an HTC analyzer can result in a very high blank value. Skoog et al. (1997) reported that the Pt/alumina catalyst used in the Shimadzu TOC-5000 analyzer gave blank values of $> 1000\,\mu M$, which were reduced to $< 50\ \mu M$ by preheating the catalyst particles in a muffle oven at 500°C for 6 h. Subsequent injections of low-C water then reduced the blank to acceptable concentrations (10–20 μM).

3. Detectors for Shipboard Operation

Much of the study of TOC/DOC in ocean waters takes place on ships during research cruises. This causes a problem because of the distortions to the analyzer output signals caused by the vibrations usually experienced on a research ship. Alvarez-Salgado and Miller (1998) overcame the problem by fitting a Li-Cor 6252 NDIR detector to their Shimadzu TOC-5000 analyzer. This detector (one of a family of instruments also covered in Chaps. 10 and 11) incorporates a lead selenide solid-state photometric detection device that is insensitive to such movements, whereas the Shimadzu gas detector, which has a membrane-based pressure differential detection mechanism, is prone to interference from both low- (ship's roll) and high-frequency vibrations (Peltzer and Brewer, 1993).

4. Total N Determinations

Commercial analyzers configured for the analysis of total nitrogen in water samples have a generally similar operating system to the TOC/DOC analyzers but with some distinctive features. The Analytik Jena TN analyzer (Table 8), for instance, uses a combustion tube packed with copper oxide, CuO, as catalyst, operating at 950°C. Pure oxygen (> 99.9%) is used as carrier gas. The N in the sample is converted to NO, which is then detected with a chemiluminescence detector. In this detector, the NO reacts with ozone to form NO_2 in an excited state; the de-excitation to a lower energy state is accompanied by emission of light, with an intensity proportional to the amount of NO released from the sample. This emission is quantified by the detector. (Detectors of this type are also discussed in Chap. 10.) Sample sizes are in the range 0.1–1 mL, and the manufacturers claim upper and lower detection limits of 200 and 0.02 mg L^{-1}, respectively, with

a reproducibility (at 1 mL sample volume) of 5% at 0.5 mg N L^{-1}, and 2% at 10 mg L^{-1}.

The Skalar Formacs TN analyzer (Table 8) also uses a catalytic combustion procedure but operates at 850°C. Essentially it comprises a Formacs HT DOC analyzer with an added chemiluminescence detector.

Ammann et al. (2000) investigated the simultaneous determination of total bound nitrogen (TN_B) by high-temperature combustion analyzers. To do this they coupled an Ecophysics 700AL chemiluminescence detector to Shimadzu TOC-500 and TOC-5000 analyzer systems. When using the instruments without further modification (i.e., employing the usual direct injection of wastewater components onto the hot Pt-coated catalyst), N recoveries ranged from 40 to 90%, although the C recoveries were consistently quantitative. These low recovery rates were transformed into quantitative recoveries by simply inserting quartz wool into the top of the combustion tube, to improve sample evaporation before entry into the combustion zone.

5. Handling of Samples

Whatever instrumental technique is used to measure the DOC, TOC, and/or N content of water samples, the procedures used in collection, filtration, preservation, and storage prior to analysis play a vital part in determining the accuracy of the overall process. A valuable discussion of this issue, which is particularly focused on DOC in freshwater samples but is also of more general relevance, is provided by Kaplan (1994) and the references he cites.

IV. APPLICATIONS

The following examples are meant to provide an illustrative, rather than a comprehensive, coverage of applications of automated CNS analyzers, in fields such as soil science, agronomy, ecological studies, and environmental sciences. The intention is to indicate to researchers who have hitherto used alternative methods for the determination of C, N, and/or S where and how this capacity for automated measurement might be applied.

A. C and N in Soils and Plants

A major focus for soil C measurements in recent years has been provided by concerns about global warming. In particular, there is a need to assess the size of C stocks in soils, to be able to predict how these stocks will change

Marcel Dekker, Inc.
270 Madison Avenue, New York, New York 10016

if temperatures rise, and to estimate the potential for C sequestration in soils to offset global warming. Measurements of C and N concentrations in soils have been made for many other purposes, often as part of basic pedological and ecological investigations and in studies of the effects of land use and land use change on soil fertility. The automated instruments described in the sections above are proving very useful in all these areas, and some illustrative examples are given below.

Potter et al. (1999) used a Leco CR-12 instrument to determine organic C in 1 g soil samples (the method of Chichester and Chaison, 1991) to measure the C sequestration rate in clay soils in Texas returned to grass from arable cultivation 6–60 years earlier. Soils that had been cultivated for > 100 years contained 1.53–1.88% C, native prairie soils contained 4.44–5.95%, while those returned to grass showed a linear accumulation of C with time. It was estimated that another 100 years or so would be needed to reach the original C level. The total N in the soils was measured with another automated instrument, a Fisons NA-1500 CN system. De Camargo et al. (1999) studied the recuperation of soil C stocks under secondary forest growing on abandoned degraded pastures in Amazonia, also using an NA-1500 analyzer. Soil organic C and N were determined both in bulk soil samples and in OM separated on the basis of density into $> 2\ g\ cm^{-3}$ and $< 2\ g\,cm^{-3}$ fractions, using sodium polytungstate solution. Because of the rapid C cycling rate, the soil C concentrations differed little from those of primary forest after 7 years of secondary forest following 23 years of pasture.

Domisch et al. (1998) used a Leco CHN-600 analyzer (together with ^{14}C studies) to investigate if a drained peat soil in Finland was gaining or losing C under afforestation. Measurements were made both in the litter layer (pine needles and fine roots) and in the underlying peat. Garten and Wullschleger (1999) used a CE NA-1500 analyzer to measure soil C inventories in soils growing a bioenergy crop (switchgrass). The soil C contents were not significantly different from those under other plant covers, but a particularly useful outcome of the work was the assessment of how many samples are needed to assess changes in soil C. A difference of 5 Mg SOC ha^{-1} (10–15% of existing SOC) could be detected by analyzing 16 samples, but differences of 2–3% (1 Mg SOC ha^{-1}) could only be established with > 100 samples. Bashkin and Binckley (1998) used a Leco 1000 analyzer in studies of changes in soil C after afforestation of former sugar cane fields in Hawaii with *Eucalyptus*. Soil samples had to be acidified to remove residual $CaCO_3$ (from liming during cane production), before drying, grinding, and analysis. No net change in soil C was found in this study: an increase in the top 10 cm was offset by a loss in the 10–55 cm layers.

Increases in soil N (and C) in an agricultural soil converted from a conventionally tilled to a no-till system were studied by McCarty et al. (1998) using a Leco CNS-2000 analyzer. The sample size was 500–750 mg. Over 3 years, the profile composition was significantly transformed toward that found under long-term no-till systems, with a substantial increase in total N and C in the uppermost 2.5 cm. A CE-Fisons NA-1500 system was used by Zarin and Johnson (1995) to measure total N and C accumulation in a montane tropical forest soil in Puerto Rico during a primary succession phase on bare soil created by landslides. Nitrogen accumulation in soil microcosms growing a C_3 grass under elevated CO_2 concentrations was determined by Lutze and Gifford (2000) in Canberra, Australia, with the aid of a Europa ANCA-NT 20-20 Stable Isotope Analyser, which gave both total N data and values for the ^{15}N natural abundance.

Giardina et al. (2000) investigated changes in soil N and P during slash-and-burn clearing of a Mexican dry tropical forest. They measured total N in the ash and total C and N in the topsoil using a Leco 1000 CHN analyzer (and P with a flow-injection analyzer), and showed that there was a large transformation of previously unavailable nutrients into readily available mineral forms. The same type of instrument was employed by Halverson et al. (1999) to study the effect of 11 years' N fertilization on soil C and N in a dryland cropping system. The results showed a steady increase in both elements with increasing N input. The recovery of N from *Leucaena* and *Dactyladenia* leaf residues by maize and cowpeas in an alley cropping system in Nigeria was measured by Vanlauwe et al. (1998) with the aid of ^{15}N labeling and total $N/^{15}N$ measurement using a Roboprep CN analyzer interfaced to a Micromass 622 mass spectrometer. Applications in greenhouse-based crop studies include measuring N accumulation in flooding-stressed soybeans (Bacanamwo and Purcell, 1999, using a Leco FP-228 instrument), and in wheat cultivars (Oscarson, 2000, using a CE NA-1500). Johnson et al. (2000) applied a Perkin-Elmer 2400 CHN analyzer to the investigation of biotic and abiotic processes responsible for N retention in a forest soil. Examples of automated C and N analysis in ecosystem studies include the work of Bridgham et al. (1998) on the mineralization of C and N in wetlands in Minnesota, and that of Frank and Groffman (1998) on the impact of grazing by large herbivores on mineralization in grasslands of Yellowstone National Park (using, respectively, Leco and CE 1500 instruments).

B. C, N, and S in Peats and Sediments

Automated dry combustion analyzers have found a place in the last few years in environmental, ecological, and geochemical studies of C, N, and S

in peats and sediments from a diversity of wetland, estuarine, and ocean systems. Analysis for C and N content appears to be straightforward, and dried samples can be handled in a similar way to soils and plant material. However, if freeze-drying is used prior to S analysis, whatever analytical method is then employed, cross-checks on losses of S against other drying procedures may need to be made. Amaral et al. (1989) reported S losses from lacustrine sediments dried in this way, though Wieder et al. (1996) found no such problem with sphagnum peat samples.

Freeze-drying was in fact used in most of the following examples of studies with automated combustion analyzers. Bates et al. (1998) measured C, N, S (and O) in peat cores from the Florida Everglades by using a CE 1106 analyzer after first treating the dried samples with 1 *M* HCl to remove carbonates. They found that the total S contents increased in the uppermost 25–45 cm, suggesting that more S had entered the sediments in recent times, and that more S may have been retained in the peat because of the diminished oxidation/mobilization of reduced S following water conservation measures in the study area. Craft and Richardson (1998) used a Perkin-Elmer 2400 instrument for similar analyses in peats from the same region. Rates of C, N, and S accumulation were correlated with nutrient enrichment over the previous 30 years by agricultural drainage water. Zimmerman and Canuel (2000) used a CE 1108 analyzer for total C and total N measurement to investigate the impact of increased use of inorganic fertilizers and population growth on organic matter deposition in Chesapeake Bay, North America's largest estuary. The dried sediments were acidified with HCl to remove carbonate, prior to combustion analysis. A marked increase in organic C (and total S) was found in layers corresponding to deposition in 1934–1948, coincident with the first signs of eutrophication and anoxia in the bay. Dissolved organic C and N in sediment pore water from the same bay were measured by Burdige and Zheng (1998) with a Shimadzu TOC-5000 and a modified Dohrmann DN-1900 analyzer, respectively, in a study of the biogeochemical cycling of dissolved organic N (DON) and the proportion escaping to the ocean. Ammonia was first removed from the samples, and then, for the determination of total dissolved N (TDN), samples of up to 40 μL (from low DON waters) were injected into the combustion tube. Nitrate- plus nitrite-N were also determined by the Dohrmann instrument by directly injecting water samples of up to 200 μL downstream of the combustion tube, so that only these inorganic forms of N were converted to NO and therefore detected by the chemiluminescence detector. Subtraction of the (nitrate + nitrite)-N value from the TDN then gave the DON content.

Other applications include analysis of ocean sediments from many parts of the world. Böttcher and Lepland (2000) measured total S with

a Leco CNS analyzer and total organic C with a CE CHN analyzer (after removing carbonate with HCl) in sediments from the Baltic Sea. There was a general correlation between C and S contents, but some samples were enriched in S, attributed to pyrite formation within an anoxic water column or near the sediment–water interface. In sediments from the continental slope in the Arabian Sea, total C and N were determined by Cowie et al. (1999) with a CE CNS analyzer, and stable C isotope ratios with a Fisons CHN analyzer (an instrument from the same ''family'') coupled to a VG PRISM mass spectrometer. The isotopic measurements indicated that the OM was of predominantly marine origin, rather than terrestrial soil carried by rivers entering the sea. Cowie et al. (1995) had earlier investigated the organic geochemistry of deep sediments from 5400 m depth in the Atlantic, measuring total C and N, and the C : N ratio, with a CE 1106 analyzer.

C. Dissolved Organic C in Soils, Freshwaters, and Marine Environments

The impacts of climate change on dissolved organic C in soils have also been explored with the aid of DOC analyzers. For example, Briones et al. (1998) used a Skalar UV/persulfate system to show that temperature had a marked effect on the vertical distribution of soil fauna, which in turn affected the leaching of DOC from a humic gley soil in northern England. Moore and Dalva (2001) used a Shimadzu TOC-5050 analyzer to investigate the effect of temperature on the release of DOC from a peat in Quebec, Canada. The system was calibrated with standards prepared from potassium biphthalate in the range 0–1000 mg L^{-1}.

Gregorich et al. (1998) examined the relationship between soil CO_2 emissions and soluble organic C in maize soils in Canada receiving dairy manure. Soils were extracted with 0.5 *M* K_2SO_4 solution, and the SOC in the extracts was determined in a Shimadzu TOC-5050 analyzer equipped with an autosampler.

An important part of the global C cycle involves transport of organic matter in rivers to the ocean. McClain et al. (1997) used a Shimadzu TOC-5000 instrument to investigate the relationship between DOM concentrations in rivers of the Amazon basin and soil type. They found that within the more oxide- and clay-rich oxisols underlying *terra firme* forest, groundwater DOM concentrations were much lower (120 μ*M* C) than in the groundwater under oxide- and clay-deficient spodosols (3000 μ*M* C). Total C and N in the soils were measured with a Carlo Erba analyzer, which showed that the corresponding C/N ratios for these soils were also very different: 10 and about 60, respectively. In a comparable temperate region study, Cronan et al. (1999) investigated the effect of land use on DOC in streams in

Marcel Dekker, Inc.
270 Madison Avenue, New York, New York 10016

northern Maine, using an O.I. Model 700 TOC analyzer calibrated with potassium biphthalate standards prepared with carbon-free glass-distilled water. Brooks et al. (1999) investigated the controls on soil-derived DOC entering streams during snowmelt in Colorado. With the aid of a Dohrmann DOC analyzer (and a CE CHN analyzer for soil S and N determinations), they found that less DOC was leached from soils with lower pH, brought about by pyrite weathering. All samples were filtered through glass fiber filters and stored at 4°C in precombusted amber glass bottles prior to DOC analysis. Samples from the River Elbe and groundwater from an adjacent aquifer were analyzed for DOC by Grischek et al. (1998) by using a Dohrmann DC 190 analyzer, in a study of factors affecting denitrification, because of its importance in keeping nitrate concentrations low in the aquifer. Samples were stored at 4°C after acidification to $pH < 2$. They found that oxidizable organic C required for denitrification was derived both from the river water and from solid OM in the river bed sediments and aquifer material.

Chromophoric dissolved organic matter is the fraction of the DOC that absorbs visible light and thus affects the growth of photosynthetic plankton. This fraction was measured in seas around the European coasts by Ferrari (2000) with a Carlo Erba 480 analyzer with high-temperature catalytic combustion. In river plume areas, 40–60% of the DOC was nonabsorbing in the visible region, whereas in areas not affected by continental inputs, the entire DOC belonged to the chromophoric DOM. Marine mesocosms from off the Norwegian coast were manipulated with inorganic nutrients by Søndergaard et al. (2000) to investigate organic C partitioning between particulate OC and DOC, the timing of production of DOC and DON, and the C:N ratios of the DOM. DOC and DON were measured with an integrated on-line system including a Shimadzu TOC-5000 and a Sievers NO analyzer. Wiebinga and de Baar (1998) measured the distribution of TOC and DOC in the Southern Ocean by using a modified Ionics Model 555 carbon analyzer with a pure platinum gauze catalyst at 775°C for oxidation of DOC to CO_2. They found that the concentrations of C in deep water were fairly constant, and similar to those found in equatorial ocean regions.

D. Dissolved Organic C in Polluted Waters and Wastewater

A Shimadzu TOC 600 analyzer was used by Wiessner et al. (1999) to evaluate the removal efficiency of organic components of large molecular weight, when developing a pilot-scale subsurface-flow constructed wetland to treat wastewater remaining after lignite pyrolysis in eastern Germany. Servais et al. (1999) investigated the impact on the River Seine of wastewater

Marcel Dekker, Inc.
270 Madison Avenue, New York, New York 10016

effluents from Paris and its suburbs, measuring DOC, particulate OC, and their biodegradable fractions. The DOC was measured with a Dohrmann DC 180 analyzer; for POC analysis, 1–5 mL samples were filtered through a precombusted glass fiber filter. The organic matter retained on the filter was oxidized by catalytic combustion, and the CO_2 produced was determined with the same detector as for the DOC analysis. Drewes and Jekel (1998) investigated the fate of DOC in wastewater intended for recharge of an aquifer in the Berlin area of Germany. Water was passed through columns containing aquifer material, and the DOC was measured with a Foss-Heraus TOC analyzer. The work showed that 65% of the DOC was not biodegraded by this process, but the proportion increased after ozone treatment. Oil pollutants in seawater can cause problems in desalination plants, and in a study of the weathering of contaminating oil by Wen et al. (1999), DOC in the seawater was measured using a Shimadzu TOC-5000 analyzer. They found that the soluble components from the weathering process were resistant to biodegradation but could be easily adsorbed by granular activated carbon.

REFERENCES

Allison, L. E. 1960. Wet-combustion apparatus and procedure for organic and inorganic carbon in soil. *Soil Sci. Soc. Am. Proc.* 24:36–40.

Alvarez-Salgado, X.A. and A.J. Miller. 1998. Simultaneous determination of dissolved nitrogen in seawater by high temperature catalytic oxidation: conditions for precise shipboard measurements. *Mar. Chem.* 62:325–333.

Amaral, J.A., R.H. Hesslein, J.V.M. Rudd and D.E. Fox. 1989. Loss of total sulfur and changes in sulfur isotopic ratios due to drying of lacustrine sediments. *Limnol. Oceanogr.* 34:1351–1358.

Ammann, A.A., T.B. Rüttimann and F. Bürgi. 2000. Simultaneous determination of TOC and TN_B in surface and wastewater by optimised high temperature catalytic combustion. *Wat. Res.* 34:3573–3579.

Bashkin, M.A. and D. Binckley. 1998. Changes in soil carbon following afforestation in Hawaii. *Ecology* 79:828–833.

Bacanamwo, M. and L.C. Purcell. 1999. Soybean dry matter and N accumulation responses to flooding stress, N sources and hypoxia. *J. Exp. Bot.* 50:689-696.

Bates, A.L., E.C. Spiker and C.W. Holmes. 1998. Speciation and isotopic composition of sedimentary sulfur in the Everglades, Florida, USA. *Chem. Geol.* 146:155–170.

Benner, R. and J.I. Hedges. 1993. A test of the accuracy of freshwater DOC measurements by high-temperature catalytic oxidation and UV-promoted persulfate oxidation. *Mar. Chem.* 41:161–165.

Böttcher, M. and A. Lepland. 2000. Biogeochemistry of sulfur in a sediment core from the west-central Baltic Sea: evidence from stable isotopes and pyrite textures. *J. Mar. Sys.* 25:299–312.
Bridgham, S.D., K. Updegraff and J. Pastor. 1998. Carbon, nitrogen, and phosphorus mineralization in northern wetlands. *Ecology* 79:1545–1561.
Briones, M.J.I., P. Ineson and J. Poskitt. 1998. Climate change and *Cognettia sphagnetorum*: effects on carbon dynamics in soils. *Funct. Ecol.* 12:528–535.
Brooks, P.D., D.M. McKnight and K.E. Bencala. 1999. The relationship between soil heterotrophic activity, soil dissolved carbon (DOC) leachate, and catchment-scale DOC export in headwater catchments. *Wat. Resour. Res.* 35:1895–1902.
Burdige, D.J. and S. Zheng. 1998. The biogeochemical cycling of dissolved organic nitrogen in estuarine sediments. *Limnol. Oceanogr.* 43:1796–1813.
Chichester, F.W. and R.F. Chaison. 1991. Analysis of carbon in calcareous soils using a two temperature dry combustion infrared instrumental procedure. *Soil Sci.* 153:237–241.
Ciavatta, C., L.V. Antisari and P. Sequi. 1989. Determination of organic carbon in soils and fertilizers. *Commun. Soil Sci. Plant Anal.* 20:759–773.
Cowie, G.L., J.I. Hedges, F.G. Prahl and G.J. de Lange. 1995. Elemental and major biochemical changes across an oxidation front in a relict turbidite: an oxygen effect. *Geochim. Cosmochim. Acta* 59:33–46.
Cowie, G.L., S. Calvert, T.F. Pedersen, H. Schulz and U. von Rad. 1999. *Mar. Geol.* 161:23–38.
Craft, C.B. and C.J. Richardson. 1998. Recent and long-term organic soil accretion and nutrient accumulation in the Everglades. *Soil Sci. Soc. Am. J.* 62:834–843.
Cronan, C.S., J.T. Piampiano and H.H. Patterson. 1999. Influence of land use and hydrology on exports of carbon and nitrogen in a Maine river basin. *J. Environ. Qual.* 28:953–961.
David, M.B., M.J. Mitchell, D. Aldcorn, and R.B. Harrison. 1989. Analysis of sulfur in soil, plant and sediment materials: sample handling and use of an automated analyzer. *Soil Biol. Biochem.* 21:119–123.
De Camargo, P.B., S.E. Trumbore, L.A. Martinelli, et al. 1999. Soil carbon dynamics in regrowing forest of eastern Amazonia. *Glob. Change Biol.* 5:693–702.
Domisch, T, L. Finer, M. Karsisto, R. Laiho and J. Laine. 1998. Relocation of carbon from decaying litter in drained peat soils. *Soil Biol. Biochem.* 30:1529–1536.
Drewes, J.E. and M. Jekel. 1998. Behavior of DOC and AOX using advanced treated wastewater for groundwater recharge. *Wat. Res.* 32:3125–3133.
Ferrari, G.M. 2000. The relationship between chromophoric dissolved organic matter and dissolved organic carbon in the European Atlantic coastal area and in the West Mediterranean Sea (Gulf of Lions). *Mar. Chem.* 70:339–357
Frank, D.A. and P.M. Groffman. 1998. Ungulate vs. landscape control of soil C and N processes in grasslands of Yellowstone National Park. *Ecology* 79:2229–2241.

Fry, B., S. Saupe, M. Hullar and B.J. Peterson. 1993. Platinum-catalyzed combustion of DOC in sealed tubes for stable isotopic analysis. *Mar. Chem.* 41:187–193.

Fukushima, T., A. Imai, K. Matsushige, M. Aizaki and A. Otsuki. 1996. Freshwater DOC measurements by high-temperature combustion comparison of differential (DTC-DIC) and DIC purging methods. *Wat. Res.* 30:2717–2722.

Garten, C.T. and S.D. Wullschleger. 1999. Soil carbon inventories under a bioenergy crop (switchgrass): measurement limitations. *J. Environ. Qual.* 28:1359–1365.

Giardina, C.P., R.L. Sanford and I.C. Døckersmith. 2000. Changes in soil phosphorus and nitrogen during slash-and-burn clearing of a tropical forest. *Soil Sci. Soc. Am. J.* 64:399–405.

Gregorich, E.G., P. Rochette, S. McGuire, B.C. Liang, and R. Lessard. 1998. Soluble organic carbon and carbon dioxide fluxes in maize fields receiving spring-applied manure. *J. Environ. Qual.* 27:209–214.

Grischek, T., K.M. Hiscock, T. Metchies, P.F. Dennis and W. Nestler. 1998. Factors affecting denitrification during infiltration of river water into a sand and gravel aquifer in Saxony, Germany. *Wat. Res.* 32:450–460.

Halverson, A.D., C.A. Reule, and R.F. Follett. 1999. Nitrogen fertilization effects on soil carbon and nitrogen in a dryland cropping system. *Soil Sci. Soc. Am. J.* 63:912–917.

Johnson, D.W., W. Cheng and I.C. Burke. 2000. Biotic and abiotic nitrogen retention in a variety of forest soils. *Soil Sci. Soc. Am. J.* 64:1503–1514.

Kaplan, L.A. 1994. A field and laboratory procedure to collect, process and preserve freshwater samples for dissolved organic carbon analysis. *Limnol. Oceanogr.* 39:1470–1476.

Keeney, D. R. and J. M. Bremner. 1967. Use of the Coleman Model 129A Analyzer for total nitrogen analysis of soils. *Soil Sci.* 104:358–363.

Kerven, G.L., N.W. Menzies and M.D. Meyer. 2000. Soil carbon determination by high temperature combustion: a comparison with dichromate oxidation procedures and the influence of charcoal and carbonate carbon on the measured value. *Commun. Soil Sci. Plant Anal.* 31:1935–1939.

Kowalenko, C.G. 2000. Influence of sulphur and nitrogen fertilizer applications and within-season sampling time on measurement of total sulphur in orchardgrass by six different methods. *Commun. Soil Sci. Plant Anal.* 31:345–354.

Kowalenko, C.G. 2001. Assessment of Leco CNS-2000 analyzer from simultaneously measuring total carbon, nitrogen, and sulphur in soil. *Commun. Soil Sci. Plant Anal.* 32:2065–2078.

Lee-Alvarez, M.T. 1999. *Total organic carbon analysis of particulated samples.* Applic. Note, Vol. 9.22, Tekmar-Dohrmann, Cincinnati, OH.

Leitao, J.M.M., F.S. Costa and F.M.G. Tack. 2001. Determination of total sulfur in soils and plants by an automated dry combustion method. *Int. J. Environ. Anal. Chem.* 80:219–226.

Lutze, J. and R.M. Gifford. 2000. Nitrogen accumulation and distribution in *Danthonia richardsonii* swards in response to CO_2 and nitrogen supply over four years of growth. *Glob. Change Biol.* 6:1–12.

Matejovic, I. 1997. Determination of carbon and nitrogen in samples of various soils by dry combustion. *Commun. Soil Sci. Plant Anal.* 28:1499–1511.
McCarty, G.W., N.N. Lyssenko and J.L. Starr. 1998. Short-term changes in soil carbon and nitrogen pools during tillage management transition. *Soil Sci. Soc. Am. J.* 62:1564–1571.
McClain, M.E., J.E. Richey and J.A. Brandes. 1997. Dissolved organic matter and terrestrial-lotic linkages in the central Amazon basin of Brazil. *Glob. Biogeochem. Cycl.* 11:295–311.
McGeehan, S.L. and D.V. Naylor. 1988. Automated instrumental analysis of carbon and nitrogen in plant and soil samples. *Commun. Soil Sci. Plant Anal.* 19:493–505.
Merry, R.H. and L.R. Spouncer. 1988. The measurements of carbon in soils using a microprocessor-controlled resistance furnace. *Commun. Soil Sci. Plant Anal.* 19:707–720.
Moore, T.R. and M. Dalva. 2001. Some controls on the release of dissolved organic carbon by plant tissues and soils. *Soil Sci.* 166:38–47.
Nelson, D.W. and L.E. Sommers. 1996. Total carbon, organic carbon, and organic matter. In *Methods of Soil Analysis. Part 3. Chemical Methods* (Sparks, D.L., ed.). Soil Sci. Soc. Am., Madison, WI, pp. 961–1010.
Oscarson, P. 2000. The strategy of the wheat plant in acclimating growth and grain production to nitrogen availability. *J. Exp. Bot.* 51:1921–1929.
Pella, E. 1990a. Elemental organic analysis. Part 1. Historical developments. *Am. Lab.* 22:116–125.
Pella, E. 1990b. Elemental organic analysis. Part 2. State of the art. *Am. Lab.* 22:28–32.
Peltzer, E.T. and P.G. Brewer. 1993. Some practical aspects of measuring DOC—sampling artifacts and analytical problems with marine samples. *Mar. Chem.* 41:243–252.
Peltzer, E.T., B. Fry, P.H. Doering, J.H. McKenna, B. Norrman and U.L. Zweifel. 1996. A comparison of methods for the measurement of dissolved organic carbon in natural waters. *Mar. Chem.* 54:85–96.
Potter, K.N., H.A. Torbert, H.B. Johnson and C.R. Tischler. 1999. Carbon storage after long-term grass establishment on degraded soils. *Soil Sci.* 164:718–725.
Schepers, J.S., D.D. Francis and M.T. Thompson. 1989. Simultaneous determinaton of total carbon, total N, and ^{15}N in soils and plant material. *Commun. Soil Sci. Plant Anal.* 20:949–959.
Servais, P., J. Garnier, N. Demarteau, N. Brion and G. Billen. 1999. Supply of organic matter and bacteria to aquatic ecosystems through waste water effluents. *Wat. Res.* 33:3521–3531.
Sharp, J.H. 1973. Total carbon in seawater—comparison of measurements using persulfate oxidation and high temperature combustion. *Mar. Chem.* 1:211–229.
Sharp, J.H., B. Benner, L. Bennett, C.A. Carlson, S.E. Fitzwater, E.T. Peltzer and L.M. Tupas. 1995. Analyses of dissolved organic carbon in seawater: the JGOFS EqPac methods comparison. *Mar. Chem.* 48:91–108.

Sheldrick, B.H. 1986. Test of the Leco CHN-600 determinator for soil carbon and nitrogen analysis. *Can. J. Soil Sci.* 66:542–545.
Skoog, A., D. Thomas, R. Lara and K.-U. Richter. 1997. Methodological investigations on DOC determinations by the HTCO method. *Mar. Chem.* 56:39–44.
Søndegaard, M., J. le B. Williams, G. Cauwet, B. Riemann, C. Robinson, S. Terzic, E.M.S. Woodward and J. Worm. 2000. Net accumulation and flux of dissolved organic carbon and dissolved organic nitrogen in marine plankton communities. *Limnol. Oceanogr.* 45:1097–1111.
Stewart, B.A. and L.K. Porter. 1963. Inability of the Kjeldahl method to fully measure indigenous fixed ammonium in some soils. *Soil Sci. Soc. Am. Proc.* 27:41–43.
Tabatabai, M.A. and J.M. Bremner. 1970. Use of the Leco Automatic 70-Second Carbon Analyzer for total carbon analysis of soils. *Soil Sci. Soc. Am. Proc.* 34:608–610.
Tabatabai, M.A. and J. M. Bremner. 1991. Automated instruments for determination of total carbon, nitrogen, and sulfur in soils by combustion techniques. In: *Soil Analysis*: *Modern Instrumental Methods,* 2d ed. (Smith, K.A., ed.). Marcel Dekker, New York, pp. 261–286.
Tabatabai, M.A. and Y.M. Chae. 1982. Alkaline oxidation method for determination of total sulfur in plant materials. *Agron. J.* 74:404–406.
Urbansky, E.T. 2001. Total organic carbon analysers as tools for measuring carbonaceous matter in natural waters. *J. Environ. Monitoring* 3: 102–112.
Vanlauwe, B., N. Sanginga and R. Merckx. 1998. Recovery of leucaena and dactyladenia residue nitrogen-15 in alley cropping systems. *Soil Sci. Soc. Am. J.* 62:454–460.
Verardo, D.J., P.N. Froelich, and A. McIntyre. 1990. Determination of organic carbon and nitrogen in marine sediments using the Carlo Erba NA-1500 analyzer. *Deep Sea Res.* 37:157–165.
Walkley, A. and I.A. Black. 1934. An examination of the Degtjareff method for determining soil organic matter and a proposed modification of the chromic acid titration method. *Soil Sci.* 37:29–38.
Wallace, B., M. Purcell and J. Furlong. 2002. Total organic carbon analysis as a precursor to disinfection byproducts in potable water: oxidation technique considerations. *J. Environ. Monitoring* 4:35–42.
Wen, J., A. Kitanaka, W. Nishijima, A.U. Baes and M. Okada 1999. Removal of oil pollutants in seawater as pretreatment of reverse osmosis desalination process. *Wat. Res.* 33:1857–1863.
Wiebinga, C.J. and H.J.W. de Baar. 1998. Determination of the distribution of dissolved organic carbon in the Indian sector of the Southern Ocean. *Mar. Chem.* 61:185–201.
Wieder, R.K., M. Novák and D. Rodríguez. 1996. Sample drying, total sulfur and stable isotopic ratio determination in freshwater wetland peat. *Soil Sci. Soc. Am. J.* 60:949–952.

Wiessner, A., P. Kuschk, U. Stottmeister, D. Struckmann and M. Jank. 1999. Treating a lignite pyrolysis wastewater in a constructed subsurface flow wetland. *Wat. Res.* 33:1296–1302.

Wright, A.F. and J.S. Bailey. 2001. Organic carbon, total carbon, and total nitrogen determinations in soils of variable calcium carbonate contents using a Leco CN-2000 dry combustion analyzer. *Commun. Soil Sci. Plant Anal.* 32:3243–3258.

Yeomans, J. C., and J. M. Bremner. 1991. Carbon and nitrogen analysis of soils by automated combustion techniques. *Commun. Soil Sci. Plant Anal.* 22:843–850.

Zarin, D.J. and A.H. Johnson. 1995. Nutrient accumulation during primary succession in a montane tropical forest, Puerto Rico. *Soil Sci. Soc. Am. J.* 59:1444–1452.

Zimmerman, A.R. and E.A. Canuel. 2000. A geochemical record of eutrophication and anoxia in Chesapeake Bay sediments: anthropogenic influence on organic matter composition. *Mar. Chem.* 69:117–137.

7

X-Ray Fluorescence Analysis

Philip J. Potts
The Open University, Milton Keynes, England

I. INTRODUCTION

X-ray fluorescence spectrometry (XRFS) is a technique for the determination of elemental abundances in samples that are normally presented for analysis in solid form (liquids can be analyzed directly as well, although such applications are not as common). The sample surface is excited by a primary beam of x-ray radiation. Provided they are sufficiently energetic, x-ray photons from this primary beam are capable of ionizing inner shell electrons from atoms in the sample, resulting in the emission of secondary x-ray fluorescence radiation of energy characteristic of the excited atoms. The intensity of this fluorescence radiation is measured with a suitable x-ray spectrometer and, after correction for matrix effects, can be quantified as the elemental abundance. The technique is notionally claimed to have the potential of determining all the elements in the periodic table from sodium to uranium to detection limits that vary down to the $\mu g\, g^{-1}$ level. However, using specialized forms of instrumentation, this range may be extended for same sample types down to at least carbon, although with reduced sensitivity and with some care required in the interpretation of results, owing to the very small depth within the sample from which the analytical signal originates for this element. The technique is very well established and, in contrast to other common atomic spectrometry techniques, it is not usual to take the sample into solution before analysis. The preferred forms of sample preparation

Marcel Dekker, Inc.
270 Madison Avenue, New York, New York 10016

for quantitative analysis include a solid disk prepared by compressing powdered material, a glass disk prepared after fusion of a powdered sample with a suitable flux, loose powder placed in an appropriate sample cup, and dust analyzed in situ on the collection filter.

A number of categories of instrumentation have been developed, the standard laboratory technique being based on wavelength dispersive (WD) x-ray spectrometers. However, alternative instrumentation using energy dispersive (ED) x-ray detectors offers particular advantages, and there is growing interest in the use of portable instrumentation, which permits x-ray fluorescence measurements to be made in the field, offering exciting possibilities in the direct measurement of heavy metal contamination in soils or in the assessment of workplace hazards from dust settling on surfaces at industrial sites.

One advantage of XRFS is its capability of determining a range of "difficult" elements, such as S, Cl, and Br that cannot always be detected satisfactorily by other atomic spectrometry techniques. One disadvantage is that the technique does not have adequate sensitivity for the direct determination of other key elements (Cd, Hg, Se, for example) at the low concentrations of interest in environmental studies. Furthermore, for quantitative analysis, the technique is most successfully applied to sample types that benefit from the availability of well characterized "matrix-matched" reference materials, although "standardless" analysis is also possible, and ED-XRF has unrivalled capabilities in the rapid and comprehensive qualitative analysis of samples from a visual display of spectra in the course of data acquisition.

Being such a well-established technique, there are a wide range of standard texts available on XRFS, including Bertin (1975), Jenkins (1976), Tertian and Claisse (1982), Van Grieken and Markowicz (1993), Jenkins et al. (1995), Lachance and Claisse (1995), and reviews specifically covering the analysis of silicate materials, such as Potts (1987), Ahmedali (1989), and Potts and Webb (1992). Recent developments in the field are reviewed annually in the Atomic Spectrometry Update section of the *Journal of Analytical Atomic Spectrometry* [the latest available reviews being Hill et al. (2003) and Potts et al. (2002)] and biennially in *Analytical Chemistry* (e.g., Szaloki et al., 2000). In this chapter the principles and practice of XRFS are reviewed as applicable to the analysis of soils and other environmental samples. Topics covered include theoretical aspects, instrumentation, correction procedures, analytical performance, and typical applications. Consideration is given to wavelength dispersive, energy dispersive, and portable instrumentation as well as more specialized forms of the technique, including total reflection XRFS and the use of synchrotron excitation sources.

II. X-RAY FLUORESCENCE—THEORETICAL ASPECTS

X-rays are a form of electromagnetic radiation lying between the ultraviolet and gamma ray regions of the spectrum. Most XRF measurements are made between 1 and 20 keV, although low atomic number elements can be determined from the spectrum < 1 keV and there are some applications for the determination of the heavy elements from the higher energy region of the spectrum (> 20 keV). The energy of an x-ray photon (E) is related to its wavelength (λ) by the equation

$$E = h\nu = \frac{hc}{\lambda} \tag{1}$$

where h = Planck's constant = 6.626×10^{-34} J s, c is the velocity of light in vacuum = 2.998×10^{8} m s^{-1}, and ν is the frequency of the radiation (s^{-1}). If E is expressed in kiloelectron volts (keV) and λ in nm (where 1 nm = 10^{-9} m), this expression simplifies to

$$E = \frac{1.24}{\lambda} \tag{2}$$

The energy range 1 to 20 keV corresponds, therefore, to a wavelength range of 1.24 to 0.062 nm.

The aspect that distinguishes x-rays from gamma rays (which can overlap in energy range) is that x-rays originate from the transition of electrons between the orbitals of an atom, whereas gamma rays are emitted by decay of an activated nucleus. In terms of a characteristic fluorescence x-ray, E in Eqs. (1) and (2) corresponds to the energy difference between the two electron orbital levels involved in the transition from which the fluorescence x-ray originated.

A. Production of X-Rays

1. Characteristic Fluorescence X-Rays

A fluorescence x-ray is emitted when an inner shell orbital electron in an atom is displaced by some excitation process such that the atom is excited to an unstable ionized state. In the case of x-ray fluorescence, excitation is achieved by irradiating the sample with energetic x-ray photons from a suitable source. If the irradiating x-ray photon exceeds the ionization energy of the orbital electron, there is a certain probability that the energy of the photon will be absorbed, leading to the ionization loss of the electron from

the atom. This process is called the photoelectric effect and is shown diagrammatically in Fig. 1. Because of the vacancy in the inner electron orbital, the atom is left in a highly unstable state. Electron transitions occur immediately, whereby the inner shell vacancy is filled by an outer shell electron so that the atom can achieve a more stable energy state. Because this transition involves the electron moving from an orbital of higher potential energy to one of lower, this process is accompanied by a loss in energy equal to the difference in energy of the two orbital states. Usually, this energy is lost by the emission of a characteristic x-ray photon. The orbitals that are able to participate in these transitions are restricted by selection rules, and where a transition is permitted, the intensity of emission depends on the transition probability. The displacement by ionization of particular inner shell orbital electrons can lead to a number of fluorescence lines of characteristic energy,

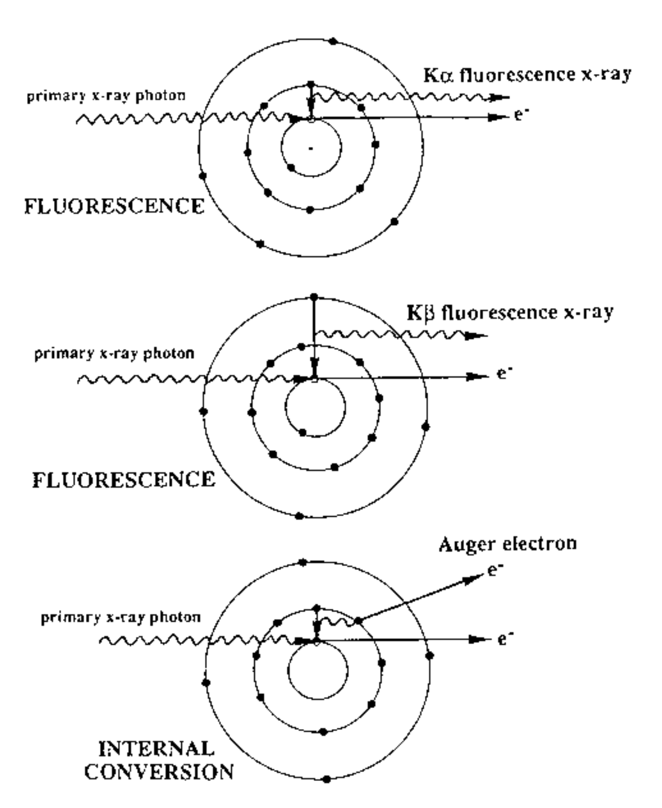


Figure 1 Schematic diagram of the electron transitions that lead to the emission of Kα and Kβ fluorescence x-ray photons and an Auger electron. (Reprinted from Potts, 1993, Fig. 2, p. 140. Copyright ©1993, Marcel Dekker.)

the relative intensity of each depending on the relevant transition probability. Each emission line can be described using the traditional Siegbahn notation, which is based on a symbol representing the electron orbital from which the electron has been ionized (K, L, M ...), supplemented by a symbol approximating to the relative intensity of the emission (α, β, γ). Thus the K series of lines originates from ionization of a K-shell electron, and the most intense lines in this series originate from transitions between L and K orbitals (Kα line) and M and K orbitals (Kβ line). An L-shell ionization event leads to the emission of the L series lines of which Lα, Lβ, Lγ are the most prominent, and an M-shell ionization leads to the emission of Mα and Mβ lines. The notation is further extended to account for small differences in the energy of the L^{I}, L^{II} and L^{III} orbitals, leading to the Kα emission being split in energy into the $K\alpha_1$ (L^{III} to K transition) and $K\alpha_2$ (L^{II} to K transition) with other line series being subclassified in a similar way.

It should be noted that although the Siegbahn notation is still almost universally used by practising XRF analysts, this is no longer the approved designation for fluorescence lines. The official IUPAC notation (Jenkins et al., 1991) identifies a fluorescence line by the orbitals involved in the transition; thus the $K\alpha_1$ line is designated KL_{III}, $K\alpha_2$: KL_{II}, $K\beta_{1,3}$: $KM_{II,III}$, $L\alpha_{1,2}$: $L_{III}M_{IV,V}$ and so on. Reflecting current widespread usage, the older notation is used in this chapter.

Although x-ray photons are employed to excite spectra in XRF analysis, similar fluorescence spectra can be excited by electrons (as in electron probe microanalysis) or protons (as in particle induced x-ray emission, PIXE), although in these cases, excitation probabilities and some spectral characteristics (e.g., background continuum intensities) differ.

One of the important properties of x-ray fluorescence spectra is that they are simple to interpret in comparison with, for example, optical emission spectra. This arises because the difference in energy between electronic orbitals depends on the potential energy field generated by the nucleus of an atom. This field varies systematically with the atomic number of the element, an observation first reported by Moseley (1913, 1914), who presented the relationship

$$\frac{1}{\lambda} = k(Z - \sigma)^2 \tag{3}$$

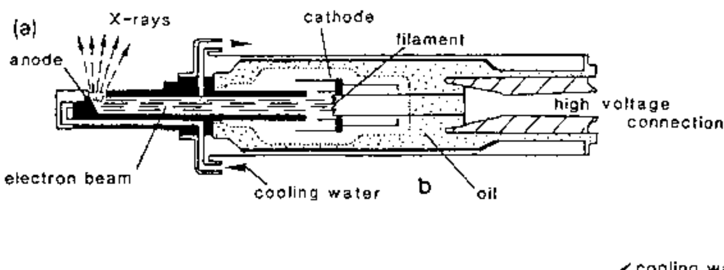
where k is a constant for a line series, σ is a "shielding" constant, and Z the atomic number of the element. Thus the energy of the K lines of successive elements in the periodic table increases in a progressive and predictable manner. This observation means that not only are spectra relatively simple to interpret but also the presence of overlap interferences is relatively easy to

predict. In the earlier decades of the 20th century, the systematic variation of emission line intensity with atomic number was used to predict the existence of the then unknown elements scandium and hafnium. This systematic relationship is followed by K, L, and M line series. However, because differences in energy between the orbitals involved in L line emissions are systematically smaller than those involved in K-lines, the energy of the L line series of fluorescence x-ray lines for an element is about 5 to 10 times lower than that of the corresponding K line for a particular element. The M-lines are correspondingly lower in energy than the L-lines and are rarely used in XRFS (except to account for overlap interferences), although this is not the case in electron microprobe analysis, where, for example, the heavier elements such as Th and U would normally be determined from their M-lines. Because of the greater intensity, the Kα line is normally selected for the determination of an element to maximize sensitivity. However, account must be taken of the fact that optimum measurements using conventional WD-XRF instrumentation are normally made in the region between 1 keV and 20 keV (below 1 keV, attenuation of x-ray radiation in the windows of x-ray tubes and counters becomes significant; above 20 keV, the excitation capabilities of the most commonly used x-ray tubes and the resolution of WD spectrometers begin to fall off). This restricted range places some constraints on line selection and means that the elements from Na to about Mo in the periodic table may be determined from the K lines (which fall within the range 1 to 17.5 keV) and that higher atomic number elements are normally determined from the corresponding Lα lines. Some excitation sources are suitable for the determination of the higher atomic number trace elements (e.g., Ba Kα at about 32 keV), but only very specialized instrumentation is capable of exciting the Kα of highest atomic number elements such as U at about 98 keV (noting, however, that such instrumentation has been developed for the determination of Au for the mining industry).

2. Continuum Radiation—the X-Ray Tube

Continuum x-ray radiation is generated when electrons (or protons or other charged particles) interact with matter. The phenomenon is most conveniently considered in conjunction with the mode of operation of the x-ray tube (Fig. 2), the most widely used excitation source in XRF analyzers. The x-ray tube consists of a filament, which when incandescent serves as a source of electrons, which are accelerated through a large potential difference and focused onto a metal target (the anode). When the filament is heated to incandescence by an electric current, thermionic emission of electrons occurs. By applying a large potential difference between filament

Marcel Dekker, Inc.
270 Madison Avenue, New York, New York 10016



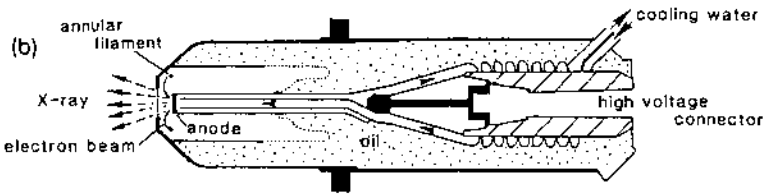


Figure 2 Schematic diagrams of (a) side window design of x-ray tube, (b) end window x-ray tube. (Reprinted from *Journal of Geochemical Exploration*, Potts and Webb, 1992, after Philips Scientific Ltd., Fig. 6, p. 258, with permission from Elsevier Science.)

and anode (typically 10–100 kV), the electrons are accelerated and bombard the anode with a corresponding energy (in keV). Interactions between energetic primary electrons and atoms of the sample result in the following phenomena.

Characteristic Fluorescence Radiation. Incident electrons are capable of displacing inner shell electrons of atoms of the anode causing the emission of fluorescence x-rays characteristic of the anode material (Fig. 3). Choice of anode is an important consideration in exciting groups of elements of analytical interest. Commonly used tubes include those having anodes of Rh, Mo, Cr, Sc, W, Au, or Ag.

Continuum Radiation. Incident electrons also lose energy by a repulsive interaction with the orbital electrons of target atoms. As a result of this deceleration effect, x-ray photons are emitted (from considerations of conservation of energy), and these photons form a continuum or *bremsstrahlung* component to the tube spectrum. Unlike fluorescence x-rays, which have discrete energies characteristic of the emitting atom, these *bremsstrahlung* photons are emitted with a continuum of energies ranging from 0 up to the incident energy of the electron beam. The continuum spectrum has a characteristic shape with a maximum at an energy equivalent to about one-third of the operating potential of the tube (Fig. 3). The x-ray spectrum emitted from an x-ray tube comprises, therefore, intense

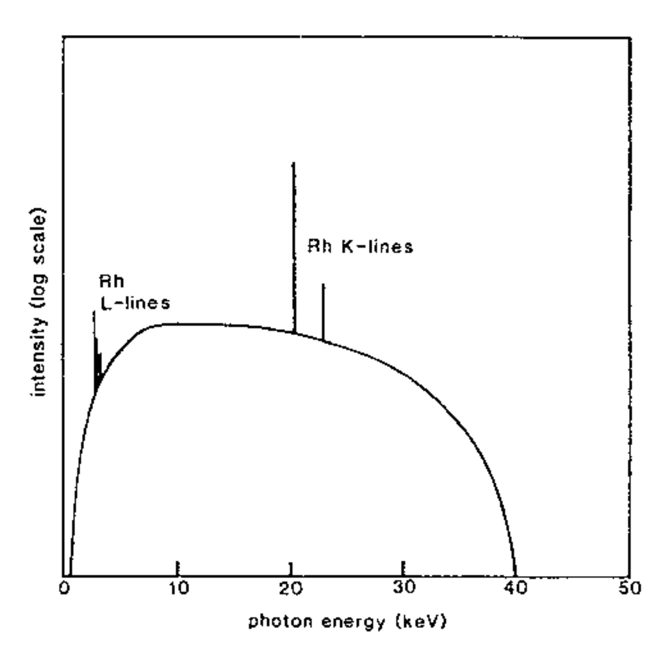


Figure 3 Spectrum emitted by a rhodium anode x-ray tube showing the Rh Kα/Kβ and L lines characteristic of the anode material and continuum radiation. The high-energy continuum cutoff corresponds to the 40 kV operating potential of the tube. Attenuation of the low-energy continuum is mainly caused by absorption in the beryllium window fitted to the tube. (Reprinted from *Journal of Geochemical Exploration*, Potts and Webb, 1992, Fig. 3, p. 255, with permission from Elsevier Science.)

characteristic lines of the anode material accompanied by a continuum background.

Heat. A considerable amount of heat is dissipated when the electron beam from the filament interacts with the anode (the production of x-rays is a relatively inefficient process). A high-powered tube fitted to a modern WD-XRF analyzer is likely to operate with a maximum power dissipation of 3 to 4 kW so that the anode must be designed with an efficient cooling system, normally based on the circulation of water or oil, to prevent its destruction. In certain forms of instrumentation (for example, some ED-XRF configurations), low power x-ray tubes with a power capacity of up to 50 W are adequate, and air-cooling of the tube (sometimes using an oil reservoir to transmit heat away from the anode) is then adequate.

Backscattered Electrons. A small proportion of the electrons from the primary beam are scattered back out of the surface of the anode.

These electrons can still carry a significant amount of energy and are an important consideration in the design of the tube. In particular, the tube must operate under conditions of very high vacuum (to prevent the absorption and scatter of the primary beam of electrons), and a window must be provided adjacent to the anode through which the usable x-ray beam emerges. In order to minimize the attenuation of x-rays, the window is normally made from beryllium foil. In the traditional ''side-window'' design of tube (Fig. 2a), the anode is held at ground potential (with a large negative potential being applied to the filament). Electrons that are scattered out of the anode can then impinge on the beryllium window, causing a heating effect. To resist thermal degradation and mechanical failure, the window must be made sufficiently thick (perhaps 200–300 μm) and, in consequence, the low-energy x-ray output of the tube is attenuated and the potential for exciting low-atomic-number elements impaired. In an alternative design, the ''end-window'' tube (Fig. 2b), a reverse bias is applied: that is, the filament is held at earth potential and the anode at high positive potential, to maintain the necessary potential difference. Electrons scattered out of the anode then tend to be attracted back towards the anode by this high positive potential and the window can in consequence be made of thinner beryllium foil. Excitation of the lower atomic number elements is then improved in comparison with that for a side-window design, although there may be some restrictions on the maximum potential that can be applied to the tube.

3. Radioisotope X-Ray Sources

In some forms of compact or portable instrumentation, the x-ray tube can be replaced by a radionuclide excitation source. Unless the instrument is dedicated in application to a restricted range of elements, several sources are required to excite effectively the full spectral range of analytical interest. There are only a limited number of sources with suitable decay characteristics for this application, including ^{55}Fe, ^{109}Cd, and ^{241}Am. The sources ^{55}Fe and ^{109}Cd both decay by electron capture, which involves a transformation in which the nucleus captures a K-shell orbital electron. In so doing, a nuclear transformation occurs in which a proton is converted into a neutron. The progeny atoms are therefore manganese and silver, respectively. The electron transitions that follow this capture event cause the emission of Mn K lines (5.9–6.5 keV) and silver K lines (22.2–25.0 keV), respectively. The nuclide ^{241}Am has an alternative decay scheme involving the emission of alpha particles of several energies, producing ^{237}Np as the progeny. One of these decay routes results in the ^{237}Np nucleus being

Marcel Dekker, Inc.
270 Madison Avenue, New York, New York 10016

formed in a nuclear excited state, and its immediate decay to the ground state results in the emission of a 59.5 keV gamma ray.

In combination, therefore, ^{55}Fe, ^{109}Cd, and ^{241}Am sources are capable of exciting the full x-ray spectrum. A specific difference between radionuclide excitation as compared with that from an x-ray tube is that whereas the spectral output from the latter comprises both characteristic and continuum radiation, the former emits characteristic x-ray lines, only. This offers an advantage in that scattered backgrounds detected in fluorescence spectra from radionuclide excitation are reduced (so favoring lower detection limits), but at the same time restricting the range of elements that can be excited simultaneously because of the absence of supplementary continuum excitation.

4. Synchrotron Radiation Sources

Synchrotron radiation represents a rather specialized excitation source, normally used for specialized applications. A synchrotron is a large (high-energy physics) facility in which "bunches" of electrons are accelerated through a very large potential difference and then constrained to travel at velocities approaching the speed of light round a near-circular flight tube, usually tens of meters in diameter (Fig. 4). The electron bunches are deflected into the circular orbit by forces associated with typically 20 to 30 electromagnets spaced round the flight tube. The magnetic field generated by each bending magnet imparts an accelerating (centripetal) force on each bunch of electrons which not only deflects these electrons along a near circular flight path but also causes them to emit continuum radiation. This continuum radiation is caused by an effect that is analogous to the *bremsstrahlung* effect described above, the difference being that the continuum emission arises from acceleration rather than a deceleration effect. Various wave-mechanical interferences occur in this continuum x-ray radiation, and the net effect is that a very intense x-ray beam is emitted in a direction tangential to the flight path as it passes through the bending magnet. This beam has some unusual properties including (1) very high intensity, (2) very low divergence (typically a few milliradians) and (3) polarization in the plane of the storage ring. By arranging for this x-ray beam to be directed onto a sample, it is possible to undertake x-ray fluorescence measurements. If the x-ray beam is focused down to a small diameter (sub-μm for the latest third-generation synchrotrons), it can be used as an "x-ray fluorescence" microprobe. Furthermore, x-ray fluorescence measurements can be combined with x-ray absorption measurements. This is achieved by scanning the spectrum transmitted by a sample through the region of the x-ray absorption edge of a selected element. Small

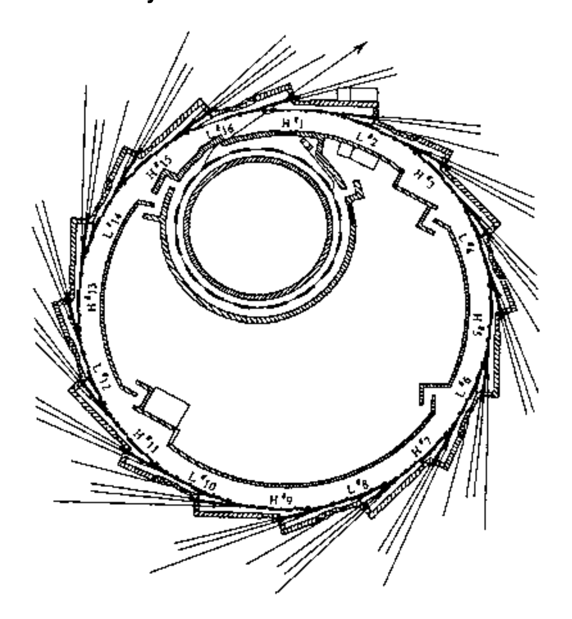


Figure 4 Overview of a synchrotron radiation facility, in this case based on the third-generation BESSY II facility in Berlin, Germany. The large outer ring represents the main sychrotron flight tube, with the tangential lines emanating from bending magnets representing the x-ray beam lines available for experimentation. (Reprinted with permission from World Scientific from Winick, 1994, p. 20.)

differences in absorption pattern can be detected in the x-ray absorption spectrum of some samples. Two techniques are used, involving either measuring variations in the absorption spectrum near the absorption edge (x-ray absorption near-edge spectroscopy, XANES) or further away from it (extended x-ray absorption fine structure, EXAFS). These techniques provide information about the chemical environment of the atom such as oxidation state and/or nearest neighbor coordination. Further details may be found in the review of Smith and Rivers (1995).

There are only a limited number of synchrotron facilities available worldwide (examples of the most powerful third-generation facilities being the European Synchrotron Radiation Facility in Grenoble and the Advanced Photon Source at the Argonne National Laboratory, USA), and access is normally by competitive evaluation. Such facilities are therefore available for measurements when a case of scientific merit can be made, normally taking advantage of the fact that the brightness of synchrotron sources is several orders of magnitude higher than that offered by an x-ray tube.

B. Excitation, Attenuation, and Scatter Characteristics of X-Rays

When a sample is excited by a beam of x-ray photons, several interactions can occur, each having important analytical consequences. The analytical signal in XRF results from the photoelectron effect, described above, whereby x-ray photons from the source cause the displacement of an inner shell electron from atoms of the sample, resulting in the emission of a characteristic fluorescence x-ray. An important aspect of this process is that the energy of the exciting photon must exceed the ionization energy of the orbital electron in question. This concept may be illustrated by considering the behavior of an x-ray beam, transmitted through a thin foil of an element. Low energy x-rays are heavily attenuated by the foil, but as the energy of the x-ray beam is increased, the intensity of the transmitted beam will progressively increase (because higher energy x-rays have a greater penetrating power) until a point is reached where the beam just has sufficient energy to excite atoms of the foil by the ionization of orbital electrons. At this point, a step decrease occurs in the intensity of x-rays transmitted through the foil as a function of increased x-ray energy, corresponding to this x-ray fluorescence process in the foil (Fig. 5). This step is called an absorption edge. K-shell electrons produce a single absorption edge; L-shell electrons produce three absorption edges in close proximity, caused by the small differences in the ionization energies of L_{I}, L_{II}, and L_{III} orbitals. A monochromatic beam of x-rays is capable of exciting elements, providing its energy exceeds the absorption edge of the corresponding x-ray line; the lines that are most efficiently excited are those having absorption edges *just below* the energy of the incident x-ray beam rather than at much lower energies.

Matrix correction procedures must be applied to almost all XRF measurements. One basic concept in applying such corrections is the need to calculate the attenuation of a polychromatic x-ray beam by samples of varying composition. In the simplest case (for monochromatic x-rays), the intensity of x-rays (I_x) passing through a sample of thickness x is related to the incident intensity (I_0) by Beer's law:

$$I_x = I_o\, e^{-\mu x} \tag{4}$$

where μ is the linear absorption coefficient. To make this equation more generally applicable, it is more convenient to replace μ in the exponential term by $(\mu/\rho)\rho$, where ρ is the density and μ/ρ is known as the mass attenuation coefficient. The modified expression becomes

$$I_x = I_o\, e^{-(\mu/\rho)\rho x} \tag{5}$$

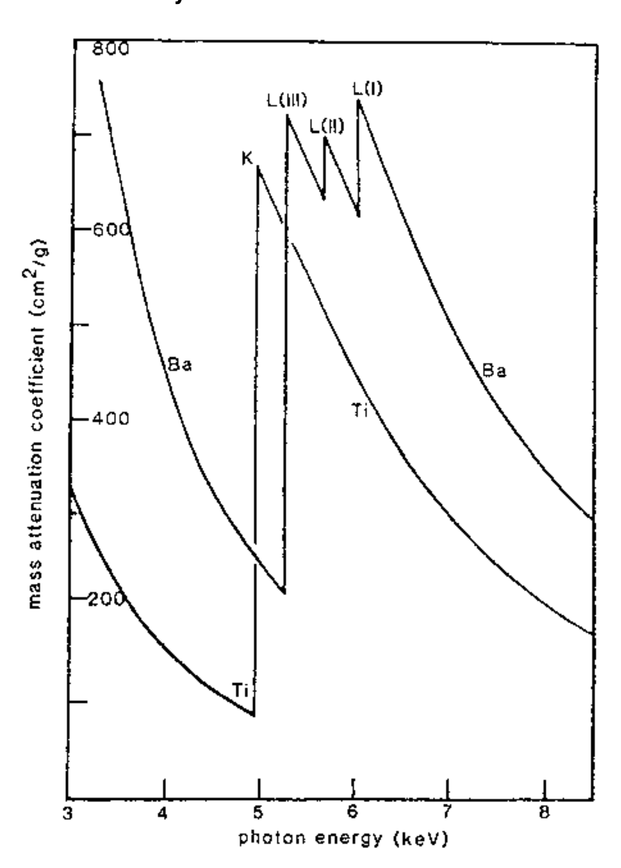


Figure 5 Intensity of the x-ray beam transmitted through a foil shown here as the mass attenuation coefficient plotted as a function of x-ray energy. Data are plotted for Ti, showing the Ti K absorption edge at 4.97 keV, and for Ba, showing the L_I, L_{II}, and L_{III} absorption edges at 2.07, 2.20, and 2.36 keV, respectively. (Reprinted from *Journal of Geochemical Exploration*, Potts and Webb, 1992, Fig. 3, p. 255, with permission from Elsevier Science.)

The value of μ/ρ is tabulated for designated elements at specified x-ray energies and is important in the derivation of correction procedures (Sec. III).

When considering the properties of absorption edges, it should be reemphasized that (1) only x-ray photons that exceed the energy of the absorption edge are capable of exciting an atom, resulting in the emission of characteristic fluorescence x-rays and (2) the photons that are most efficient at exciting characteristic fluorescence radiation are those with energies

immediately above the absorption edge (the excitation efficiency of higher energy photons progressively decreases). These observations have important analytical consequences in the selection of an x-ray tube (or radionuclide source) capable of exciting the range of elements of interest. Thus, the widely used Rh tube emits K-line radiation at about 22 keV, which is very efficient at exciting the K lines of Rb, Sr, Y, Zr, Nb, and Mo with absorption edges in the 15.2 to 19.0 keV range. However, the excitation efficiency of the tube is much reduced for the trace elements Sc, V, and Cr (for example), which have absorption edges in the 4.5 to 6.0 keV region. Excitation of lighter elements (e.g., P with an absorption edge at 2.1 keV) is enhanced by the Rh L lines of energy 2.7 to 3.1 keV. To maximize the excitation of elements such as Sc, Cr, and V, an alternative x-ray tube must be chosen, if justified by the application.

The emission of characteristic x-rays is not the only phenomenon observed in spectra from samples excited by an x-ray beam. A fraction of x-ray photons from the source is scattered by atoms of the sample. Detected spectra will then comprise fluorescence radiation from atoms of the sample superimposed on a scattered component of the spectrum emitted by the excitation source. As explained below, this effect has some important analytical consequences. There are two scatter phenomena relevant to x-ray spectroscopy. The first is Rayleigh or coherent scatter. A simplified model to understand this scatter mechanism is to consider that the energy of a photon from the excitation source is absorbed by an atom and then reirradiated with its energy unchanged. The second phenomenon is Compton or incoherent scatter. Part of the energy of an absorbed photon is transferred to the atom. The remainder is reirradiated as a Compton scatter photon of lower energy. In this case, because of the requirement to conserve momentum, the energy of the scattered photon (E') is related to the incident photon energy (E) according to the angle of scatter (Θ) by the relationship

$$E' = \frac{E}{1 + 0.001957(1 - \cos\Theta)} \tag{6}$$

where energy is expressed in units of keV, or

$$\Delta\lambda = 0.00243(1 - \cos\Theta) \tag{7}$$

where $\Delta\lambda$ is the wavelength shift in nm.

As a result of these scatter phenomena, detected fluorescence spectra will contain a fraction of the spectrum emitted by the excitation source with its energy both unchanged (Rayleigh scatter) or shifted to lower energy (Compton scatter). The scatter components will include a contribution from

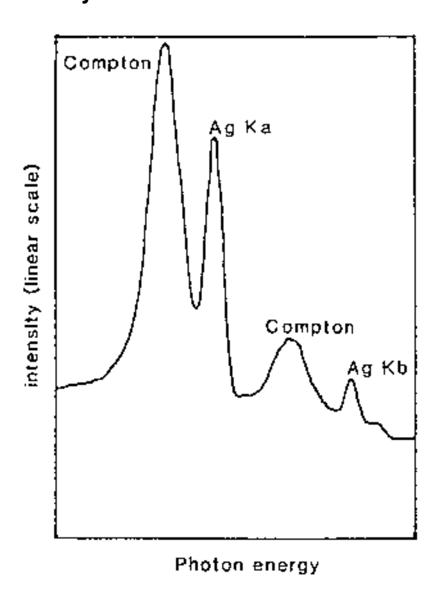


Figure 6 Rayleigh and Compton peaks observed by scatter of the Ag K and Kβ lines, when a sample is excited with a silver anode x-ray tube. (Reprinted from *Journal of Geochemical Exploration*, Potts and Webb, 1992, Fig. 2, p. 256, with permission from Elsevier Science.)

both the characteristic tube lines (which will be observed as discrete peaks in the detected spectrum) and a scattered contribution from continuum photons (Fig. 6). This scattered continuum component will generally increase background intensities in the measured fluorescence spectra, and the magnitude of this background is one of the fundamental limitations to the detection limit capability of the technique. The larger the background, the poorer is the detection limit performance. There is considerable advantage, therefore, to optimizing instrument design to minimize scattered backgrounds and so to enhance the performance of the technique. In the case of laboratory instruments, one way in which this can be done is by design of the instrument so that the angle between x-ray source—sample—detector is about 100°, at which the scatter intensity is minimized. Alternatively, in some applications where an x-ray tube is used as an excitation source, a thin metal foil may be placed between source and sample to modify the energy distribution of the spectrum available to excite the sample. The aim is to attenuate the continuum component of the spectrum (which would otherwise contribute to the background under the fluorescence lines of interest), and at the same time to minimize the attenuation of the characteristic tube lines. This arrangement is used in ED-XRF instruments

using direct tube excitation by selecting a primary beam filter made of the same metal as the tube anode. Such foils (sometimes referred to as regenerative monochromatic filters) minimize the attenuation of the tube lines which lie just on the low-energy (and, therefore, the high-transmission) side of the foil's absorption edge. This technique can also be used in WD-XRF, but in many applications, the benefit of reducing the intensity of scattered continuum radiation is negated by a significant attenuation of characteristic tube lines, so reducing sensitivities.

C. Polarized Excitation Geometries

A more fundamental way of minimizing scattered backgrounds is to use a polarized excitation source. The principle behind this arrangement is that if a sample is excited by a polarized beam of x-rays, there is a low probability that this radiation will be scattered at an angle of 90° to the plane of polarization. If, therefore, the fluorescence spectrum is detected at 90° to the plane of polarization of the exciting beam, the intensity of background radiation originating from scatter will be significantly reduced. As a consequence, detection limit capabilities will be correspondingly improved. The scattered radiation is only reduced, not eliminated, because in any practical arrangement, the x-ray optical path will always be represented by a finite cone of x-rays covering a small range of angles about the ideal 90°, and because the scatter suppression does not apply to the small proportion of photons scattered more than once within the sample.

One versatile way of achieving this aim is to use so-called Barkla scatter radiation as an excitation source (Fig. 7). Low atomic materials such as boron carbide, boron nitride, and corundum (Al_2O_3) are efficient scatterers of x-ray radiation. Radiation from an x-ray tube is polarized by scattering off a boron carbide substrate, and the sample is excited by the beam that has been scattered through 90° with respect to the source. If the fluorescence spectrum is measured at 90° to this polarized beam (that is, using an orthogonal source—scatterer—sample—detector excitation and detection geometry), significant reduction in scattered background intensities will be observed.

A more specialized form of polarization arises from the fortuitous situation where the characteristic lines from an x-ray tube can be diffracted from an appropriate diffraction crystal at a 2Θ angle of 90°. This combination of circumstances is satisfied for the diffraction of Rh Lα tube radiation from the 002 planes of a highly orientated pyrolytic graphite crystal at a 2Θ angle of 86.3°. Although not perfectly polarized, the Na to S K lines can be effectively excited with a suppression in background caused by scatter, since the tube-diffracting crystal-sample detector can then be

Marcel Dekker, Inc.
270 Madison Avenue, New York, New York 10016

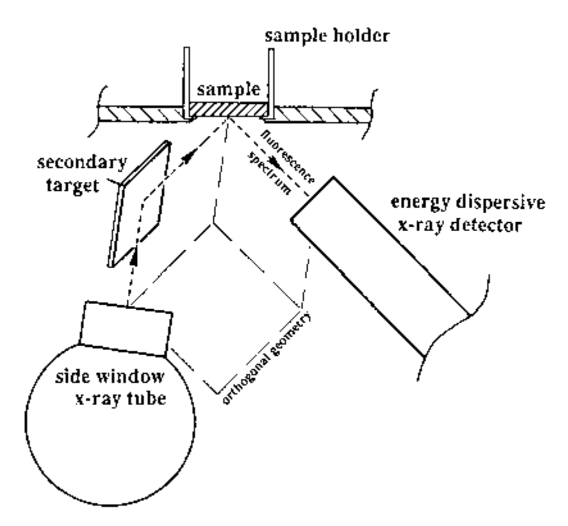


Figure 7 Barkla scatter polarized excitation geometry in which the x-ray path from tube to scatter target to sample to detector is arranged in an orthogonal geometry. In this configuration, the target would be a low atomic number material such as boron carbide. In secondary target XRFS, a similar excitation/detection geometry is used, but the target would be a metal such as Mo that emitted characteristic x-rays of appropriate energy to excite the elements of interest. (Reprinted from Potts, 1993, Fig. 5, p. 145, Copyright © 1993, Marcel Dekker.)

arranged in an almost orthogonal geometry. One disadvantage is the relative narrow range of elements that can be effectively excited using this arrangement. Other Barkla scatter (or secondary target) excitation devices must be provided to excite other spectral regions.

D. Secondary Target Geometries

Partial polarization can also be achieved using secondary target excitation geometry. The x-ray output from an x-ray tube is used to excite a "secondary target," normally a metal (for example, Co, Zn, Ge, Zr, Pd, Sm) having characteristic lines of energy suitable to excite the range of elements of interest. The optical arrangement of x-ray tube—secondary target—sample—detector is the same orthogonal geometry as for the Barkla scattering arrangement. The sample is then excited by characteristic secondary target radiation (which is not polarized and can be scattered into the detector) and tube radiation scattered off the secondary target (which is polarized, leading to some suppression of the scattered background in detected spectra).

E. Total Reflection XRF

Quite another approach to the suppression of scattered backgrounds is followed in the design of total reflection XRF (TXRF) instruments (Fig. 8). When a beam of x-rays is directed at a quartz glass reflector plate, the quartz will normally become excited (emitting characteristic fluorescence x-rays) as well as scattering the x-ray beam, as discussed above. However, if the angle of incidence of the x-ray beam is progressively reduced to a near-grazing incidence with respect to the reflector plate, a point will be reached (at the "critical angle") where the entire beam is reflected off the glass surface. The critical angle decreases with an increase in x-ray energy and varies according to the materials that form the air/substrate boundary, but a typical value would be around 0.005 radians. In a TXRF instrument, the sample is deposited on the quartz glass plate, normally by evaporation from solution. The evaporated sample is then excited by the x-ray beam using this total reflection excitation geometry, and the fluorescence spectrum is detected using an ED detector positioned normal to, and in close proximity with, the sample plate (but not close enough to obstruct the primary beam). Very low detection limits can be achieved because (1) the sample is efficiently excited by the primary beam before and after reflection, (2) the scattered background is considerably suppressed because primary x-ray photons that do not contribute to x-ray fluorescence in the sample are reflected from the quartz plate rather than contributing to the detected spectrum by scatter. To avoid significant matrix effects, the deposited sample must be formed as a very thin layer. Although normally this is achieved by evaporation from

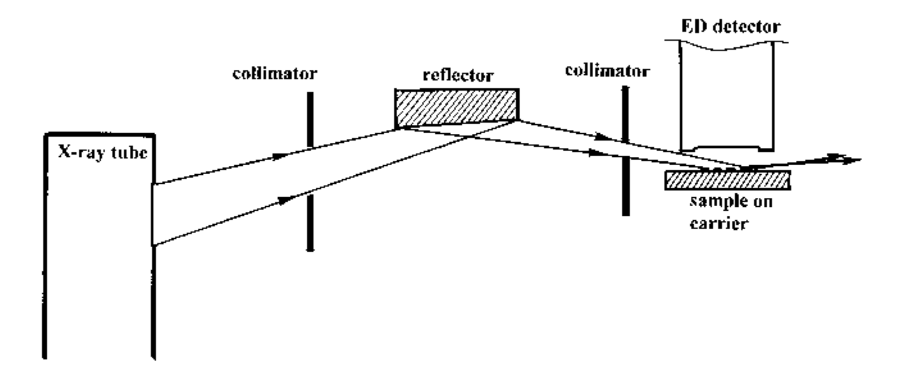


Figure 8 Total reflection XRF instrumentation—general arrangement of excitation geometry. The two reflector elements serve to collimate and monochromatize the excitation beam, which is then directed at grazing incidence onto the sample mounted on a quartz reflector plate. (Based on Schwenke and Knoth, 1993.)

solution, there are also possibilities for exciting particulate samples. There are advantages if the primary beam has a restricted angle of dispersion and is partially monochromatized. This can be achieved by reflecting it off a preliminary plate at an angle of incidence below the critical angle (i.e., total reflection) before directing this beam at the sample (again using a total reflection geometry).

F. Synchrotron XRF

Because synchrotron beams offer a high degree of polarization and have very low divergence with high intensity, they represent an almost ideal excitation source for applications that can justify access to this facility, as described in Sec. II.A.4.

III. MATRIX CORRECTION PROCEDURES

Matrix corrections take on a different meaning when considering XRF in comparison with other atomic spectrometry techniques. In XRF, this term refers specifically to the attenuation of x-rays within a sample. When the exciting x-ray beam penetrates into a sample, it suffers attenuation so that the primary beam intensity is progressively reduced and its energy spectrum progressively modified. Similarly, fluorescence radiation emitted from atoms in a sample must pass through a certain distance within the sample before emerging for detection, and this radiation too will suffer attenuation (and sometimes enhancement) effects. The net result is that the intensity of the x-ray fluorescence signal is not usually linearly related to the determinant concentration but is affected by the presence of matrix elements in the sample. A correction must be applied to compensate for these composition-dependent effects. However, application of the correction is complicated by the fact that prior to analysis, the composition is not known.

There are several methods used for applying matrix corrections, the principal techniques being fundamental parameter and empirical matrix correction methods, corrections based on normalization to the Compton scatter peak intensity, and the elimination (or minimization) of matrix, effects by dilution of the sample or presentation for analysis as a thin film.

A. Mathematical Matrix Correction Procedures

Starting first with mathematical matrix corrections, although the derivation of some of these correction procedures can involve detailed mathematical

Marcel Dekker, Inc.
270 Madison Avenue, New York, New York 10016

expressions (for which the reader is referred to the texts cited in the introduction), the principles and concepts are relatively simple.

1. Fundamental Parameter Matrix Correction Procedures

Fundamental parameter matrix correction procedures are derived from physical models that describe the excitation and attenuation processes. The term "fundamental parameter" refers to the fact that the mathematical equations that describe these physical processes incorporate various parameters that must normally be quantified by experimental measurement (the determination of mass attenuation coefficients by measuring the degree of attenuation through an elemental foil of known thickness being one example). The physical processes that must be modeled are as follows:

1. The intensity of x-ray radiation emitted from the excitation source as a function of photon energy, taking into account factors such as attenuation in the beryllium window of an x-ray tube.
2. The degree of attenuation suffered by the primary beam as it penetrates into the sample.
3. The probability that photons from the primary beam will excite atoms of the determinant, resulting in the emission of the x-ray fluorescence line selected for measurement.
4. The probability that fluorescence photons will excite atoms of a second element, so producing an enhancement effect (for example, Fe Kα fluorescence radiation can efficiently excite Cr, resulting in an enhanced emission of Cr Kα).
5. The degree of attenuation of fluorescence x-rays within the sample.
6. The detection efficiency of the instrument on which measurements are made, taking into account the size of collimators, the size and reflectivity of diffraction crystals, the attenuation within counter windows, and the photon efficiency of the counting device.

If all these physical processes can be modeled accurately, then it is possible to predict the intensity of selected x-ray lines in samples of known composition. When applied to the correction of fluorescence x-ray intensities measured from an unknown sample, therefore, an initial estimate of composition can be made (ignoring matrix effects). This estimated composition is used to calculate first estimates of matrix correction factors using the fundamental parameter model. These correction factors may then be applied to the initial estimates of composition and the revised concentrations used to calculate improved estimates of the correction factors, and so on. This procedure is iterated until the difference in corrected

compositions between successive cycles is insignificant. This correction procedure can be applied in a "standardless" manner (that is, without any preliminary measurements on reference samples contributing to a calibration procedure or prior knowledge of the composition of the sample). However, in practice it is preferable to undertake preliminary measurements on a range of calibration samples matched to the composition of samples to be analyzed, as this reduces uncertainties in the correction procedure. Intensities calculated from the known composition of the reference materials can then be compared with measured fluorescence intensities and a linear fit determined from all data for each element. This proportionality factor is then applied to the correction procedure during the analysis of unknown samples. The main benefits of incorporating measurements from reference samples in fundamental parameter correction procedures are that (1) instrument detection efficiency factors are normalized out of the calculation, since they apply to both calibration and unknown sample measurements, and (2) some of the uncertainties in the physical constants used in the fundamental parameter equations cancel out. Well-known algorithms based on these procedures were first introduced by Criss and Birks (1968) and Shiraiwa and Fujino (1966, 1974), developed from the so-called Sherman (1955, 1958) equations, but have since been widely adapted by other workers.

2. Empirical Correction Procedures

Quite a different approach to the correction of matrix effects was developed by a number of workers culminating in the widely used proposals of Traill and Lachance (1965) and Lachance and Traill (1966). In these models, the effect of any particular element on the determinant is solved by assuming that the magnitude of that effect can be described by a constant (α) known as an influence coefficient. Thus, if α_{AB}, $\alpha_{AC}, \ldots$ represent the influence coefficients of elements B, C, ... on A, respectively, the weight fraction of element A (W_A) can be calculated from

$$W_A = R_A(1 + \alpha_{AB} W_B + \alpha_{AC} W_C + \cdots) \qquad (8)$$

where W_B, W_C are the weight fractions of the respective elements and R_A is the intensity of element A, relative to the intensity from a pure elemental standard (measured under identical conditions). The assumption is made that the influence coefficients are independent of elemental concentrations. Furthermore, the influence of the determinant on itself is taken into account because influence coefficients represent the effect of another element on the determinant *relative* to the determinant. Correction procedures of this kind

are normally only applied to the major elements (not the trace elements). If there are n elements (or oxides) in a sample, there are $n-1$ terms in the Lachance–Traill summation, so defining the minimum number $(n-1)$ of reference materials from which measurements must be made to solve the equations.

The Lachance–Traill model attracted considerable interest, not least because the accuracy with which the correction procedure could be applied did not depend on uncertainties in fundamental parameters. Furthermore, corrections could be solved using early computers which had relatively restricted computational power. However, although enhancement effects can be accommodated as negative absorptions, the assumption that alpha coefficients are independent of concentration is not strictly valid over a wide range of concentrations. Several related approaches have found widespread use, including the approach of De Jongh (1973, 1979), which allows one element to be eliminated from consideration in an influence-type coefficient approach (e.g., Fe in steels or loss-on-ignition in the analysis of rocks and soils).

Following further consideration of the derivation of influence coefficients, it has been shown that influence coefficients associated with the Lachance–Traill, De Jongh, and some other models can be calculated from fundamental parameters and therefore calculated from first principles, rather than measured using an empirical method based on the excitation of reference samples. This approach was promoted by Rousseau (1984a,b), who showed that the fundamental parameter equation could be rewritten in the same form as the Lachance–Traill influence coefficient equation, allowing alpha coefficients to be calculated directly from fundamental parameters.

The outcome of all these developments is that there is a choice of mathematical correction models available to XRF analysts. One of the more flexible approaches derived from the work of Rousseau and others is the possibility of a combined approach in which influence coefficients determined from physical measurements on suitable reference samples are used to account for matrix effects originating from the major elements, whereas the contribution of minor (and if necessary trace) elements is accounted for using influence coefficients calculated from fundamental parameter data. In this way, physical measurements are used to evaluate the largest matrix effects, but at the same time additional reference samples are not required to characterize the much smaller matrix effects associated with trace elements.

B. Compton Scatter Correction Procedures

During the discussion of scatter phenomena in Sec. II.A.2, it was shown that the spectrum from an x-ray tube is scattered from a sample by two

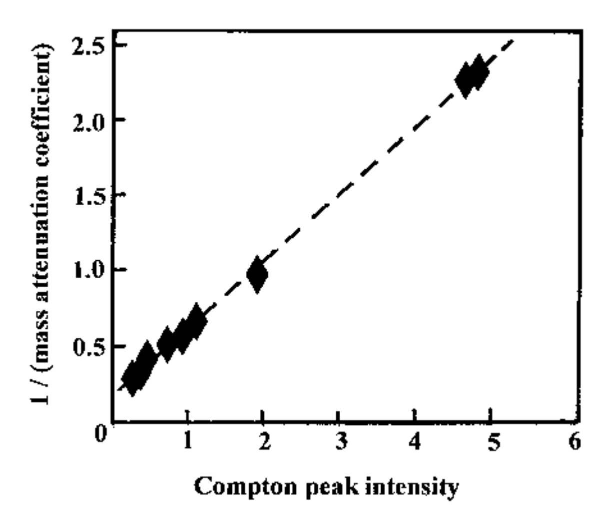


Figure 9 Graph showing the linear relationship between the reciprocal of the mass absorption coefficient and the Compton scatter peak intensity for the WLβ_1 line from a tungsten anode x-ray tube. (Based on Willis, 1989.)

mechanisms, Compton scatter and Raleigh scatter. Work by Andermann and Kemp (1958), Hower (1959) and Reynolds (1963, 1967) showed that variations in composition of the sample matrix have the same effect on the intensity of Compton scattered radiation (normally measured from one of the x-ray tube scatter lines) as on x-ray fluorescence intensities from atoms in the sample. An important limitation is that there must be no significant absorption edge between the energy at which scatter measurements are made and the energy of the fluorescence line. The implication of these observations is that the intensity of the Compton scatter peak can be used as a measure of the bulk mass absorption coefficient of the sample to correct for matrix effects on fluorescence lines of interest (Fig. 9). In the analysis of silicate materials, including soils, this correction procedure can be used for the higher atomic number elements that give fluorescence lines above the absorption edge of iron (7.1 keV), iron normally being the element having the highest energy absorption edge that is usually present at sufficiently high concentration to give a step in the mass absorption coefficient of such samples. In the application of this procedure to contaminated soil samples, care needs to be taken to ensure that elements such as Cu, Ni, or Zn, normally present at trace levels, are not present at sufficiently large concentrations that they too influence the mass absorption of the sample. In practical application, measurements are usually made of the intensity of the Compton scatter peak from one of the characteristic tube lines (I_s) as well as

the fluorescence line of element i of interest (I_i). The correction factor to compensate for matrix effects is then proportional to $(I_i)/(I_s)$.

C. Dilution and Heavy Absorber Fluxes

Matrix effects in solid samples may be reduced by dilution and/or by the addition of a heavy absorber. These considerations are most relevant to the commonly used sample preparation procedure based on fusing the sample with a suitable flux and quenching the glass as a solid disk prior to XRF analysis. The main reason for following this scheme is to eliminate mineralogical effects that cause discrepancies that would occur in the determination of the lower atomic number elements (Na–Si) if determinations were made on compressed powder pellets. However, at the same time, matrix attenuation differences between unknown and calibration samples are reduced, so reducing the magnitude of, and therefore the uncertainty associated with, the matrix correction. Residual matrix effects can be reduced even further by using a flux containing a heavy absorber such as lanthanum. The presence of lanthanum in the glass disk then makes a significant (but constant) contribution to the total mass absorption coefficient of the sample. In this way, *differences* between samples are reduced, with the same effect of reducing the magnitude of the matrix correction and its associated uncertainty.

One disadvantage of dilution is that element sensitivities are reduced and detection limits are increased (owing to the additional scatter from the flux), and in the case of heavier absorbers, a few additional spectral interferences may be observed (e.g., the La M lines on Na Kα). There is also an increased possibility that the presence of unsuspected contaminants will influence analytical measurements. However, because of an increase in confidence in matrix correction procedures, heavy absorber fluxes are not now used as frequently, and the main consideration in preparing glass disks is to select a flux and the lowest flux-to-sample ratio that can be used to prepare reliably the range of sample types of interest. In most cases, this is satisfied by a flux-to-sample dilution of 5 or 6 to 1 (2 to 1 dilutions have also been used), with higher dilutions reserved for samples that do not readily dissolve during fusion. A full discussion of fusion procedure with particular emphasis on industrial minerals is given by Bennett and Oliver (1992).

D. Thin Films

Special considerations apply to samples that can be presented for analysis as thin films. Of particular interest in this category is the environmental monitoring of airborne dust using filters for sample collection. It is possible

Table 1 Maximum Thin Film Thickness (μm) of Relevance to the Analysis of Dusts by XRF

Element	Kα energy (keV)	Maximum film thickness (μm)
Na Kα	1.0	0.07
Mg Kα	1.3	0.06–0.07
Al Kα	1.5	0.10–0.16
Si Kα	1.7	0.19–0.15
K Kα	3.3	0.52–0.54
Ca Kα	3.7	0.60–0.70
Ti Kα	4.5	0.9–1.0
Fe Kα	6.4	1.8–3.1

Data are taken from Cohen and Smith (1989) and represent the range for various silicate mineral particles.

to analyze such dust samples directly on the collection filter substrate without the necessity of applying matrix corrections, providing the dust layer is sufficiently thin that significant attenuation of fluorescence x-rays within the sample does not take place. By convention, this thickness is normally taken as the value for which attenuation of the fluorescence line of an element is no more than 1%. Since lower energy x-ray lines are attenuated more severely than higher energy lines, the critical thickness for a thin film will vary with x-ray energy. Typical values of thin film thickness for silicate dusts are shown in Table 1. In the analysis of dust filters by XRF, these values can be converted into limiting concentrations on the filter, usually expressed in $mg\,cm^{-2}$. There are clearly advantages in maintaining the sample loading below that of the critical figure, but this is likely to be very restrictive for the low atomic number elements. Corrections for samples that lie between the thin and infinitely thick criteria have been developed but are complex and not widely used. Practical considerations in the analysis of dust filters are considered in Sec. V.B.

IV. INSTRUMENTATION

Although all XRFS instruments comprise an x-ray source, a sample presentation device, and a detector to measure the fluorescence spectrum, there is considerable variation in the form and design of the two main categories of instrumentation, one based on wavelength dispersive spectrometers and the other on energy dispersive detectors. The main characteristics of these categories of instrument are considered next.

A. Wavelength Dispersive XRF

A typical WD-XRF instrument comprises an X-ray tube, a sample changing device, which is often coupled to an external sample carousel, and a monochromator based on Bragg diffraction from certain crystalline (or pseudocrystalline) lattices (Fig. 10).

1. X-Ray Tube

WD-XRF instruments are normally fitted with an x-ray tube of 3 or 4 kW (maximum power dissipation) and with a maximum operating potential of 60, 75, or 100 kV. Side-window and end-window tubes are available

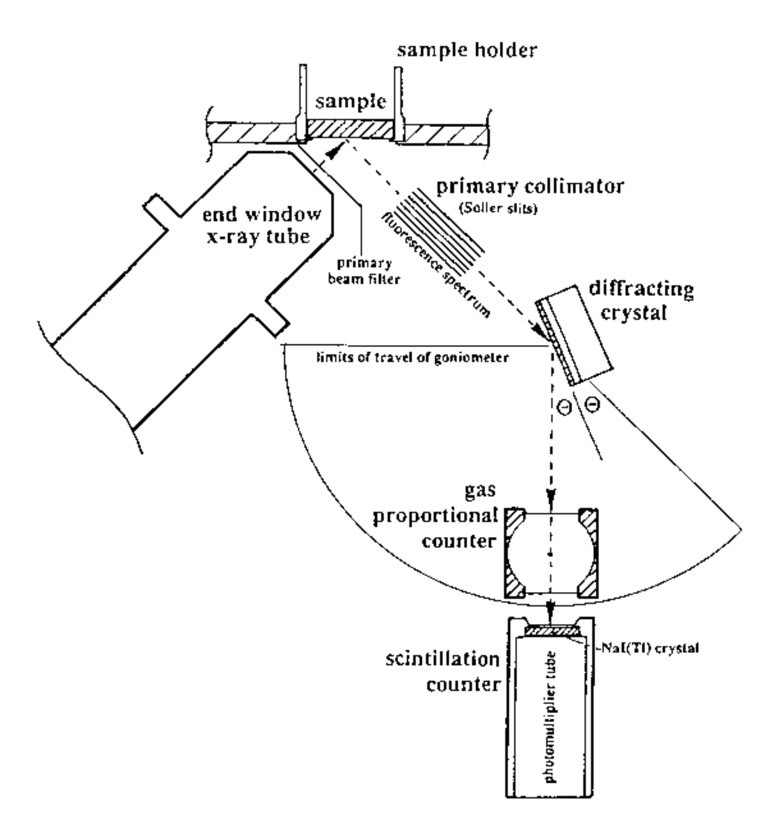


Figure 10 Schematic diagram of WD-XRF instrumentation, showing an end-window x-ray tube exciting a sample and the fluorescence spectrum, collimated by a Soller slit arrangement, diffracted from an appropriate crystal and detected by a gas proportional counter and/or a scintillation counter electron. (Reprinted from Potts, 1993, Fig. 3, p. 142, Copyright © 1993, Marcel Dekker.)

(see Fig. 3), but a recent trend has been for instruments to be fitted with end-window tubes, because of the enhanced lower energy photon output. Recent emphasis has also been placed on close coupling of the anode of the tube to the sample surface to maximize the x-ray flux available to excite the sample, although adequate collimation is then important to minimize extraneous x-ray photons (i.e., those scattered off instrument surfaces or which penetrate shielding) entering the monochromator. A metal foil can normally be placed in the primary x-ray beam to act as a filter to modify the energy spectrum reaching the sample. It is also usually possible to insert a mask in the primary beam to reduce its size, which is of benefit in the analysis of small samples that do not completely fill the standard sample holder.

2. Sample Changer

The sample is normally mounted in a cup in a sample exchange mechanism designed to transport the sample from an external sample carousel into an air lock, which can be evacuated before transferring the sample into the spectrometer vacuum chamber. The spectrometer must normally be kept under vacuum to avoid the attenuation of low-energy fluorescence photons in air. As an alternative, liquid samples may be analyzed with the spectrometer chamber flushed with helium, a gas with low x-ray attenuation properties. Very precise mechanical alignment is required when the sample is moved to the analysis position to avoid discrepancies that would occur if the sample surface were misaligned with respect to the x-ray optical path of the instrument. The sample cup will normally accept a disk 25 or 32.5 mm in diameter, XRF measurements being normally made on the lower surface.

3. WD Monochromator

WD spectrometers can be designed with either a fixed geometry (optimized for the determination of a single element), or more commonly with a mechanism to scan from one element line to the next. Fixed geometries are used on simultaneous instruments, which would typically be fitted with 10 or more fixed channels for the routine determination of a preselected range of elements. Sequential instruments are normally fitted with one (sometimes two) scanning monochromators, which operate on the same principles as fixed channels but with the provision of an elaborate mechanism to scan the spectrum so that a programmable series of x-ray lines can be measured in sequence. In both cases, the principal components (see Fig. 10) are as follows:

Entrance slits normally in the form of closely spaced parallel plates of metal (Soller slits) designed to limit the divergence of the beam accepted by

the monochromator. A choice of blade settings is normally provided (e.g., fine, medium, and coarse) to match the dispersion characteristics of the diffracting crystal.

The Diffracting crystal is normally a crystalline material mounted on a flat (sometimes curved) substrate selected so that x-rays that satisfy the Bragg equation will be strongly diffracted. When the polychromatic spectrum originating from the sample interacts with the diffracting crystal at an angle of incidence Θ, strong diffraction (at an angle of diffraction Θ) will occur for x-ray photons that comply with the Bragg equation:

$$n\lambda = 2d \sin \Theta \tag{9}$$

where n is an integer ($n = 1, 2, 3 \ldots$), λ is the wavelength of the diffracted x-ray photon, d is the spacing between successive layers of atoms in the diffracting crystal, and Θ is the angle of incidence (and diffraction) of the x-ray beam (Fig. 11). The spectrometer is normally adjusted to measure the first-order diffractions (i.e., $n = 1$ in Equation 9); higher orders are of substantially lower intensity and regarded as a potential source of spectral interferences.

The two principal properties of a diffracting crystal are the reflectivity (the higher the reflectivity, the higher the intensity of the diffracted beam) and the dispersion (the higher the dispersion, the greater the separation between lines in the diffracted spectrum). In order to maximize performance over the full spectrum range, a number of different diffracting crystals are

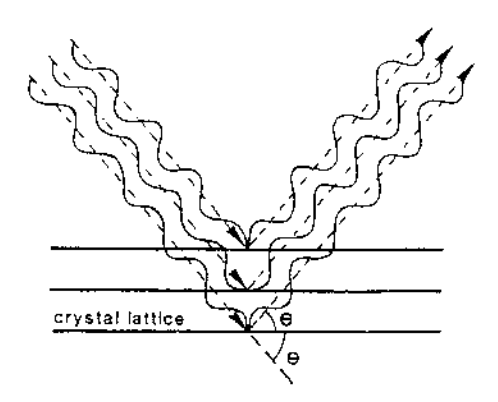


Figure 11 Schematic diagram of Bragg diffraction showing that when the Bragg equation ($n\lambda = 2d \sin \Theta$) is satisfied, constructive interference causes a strong reflection of x-ray wavelength λ. (Reprinted from *Journal of Geochemical Exploration*, Potts and Webb, 1992, Fig. 7, p. 260, with permission from Elsevier Science.)

Table 2 Diffracting Crystals Most Commonly Encountered and Their Analytical Ranges

Diffraction crystal		2d spacing (nm)	Application
LiF(220)	Lithium fluoride	0.2848	Higher resolution alternative to LiF(200)
LiF(200)	Lithium fluoride	0.4028	*K lines* of Ca to Mo, *L-lines of* Ba, La, Ce, Pb, U, Th
Ge(111)	Germanium	0.6532	*K lines of* P, S, Cl
InSb	Indium antimonide	0.748	*K line of* Si (offering higher diffracted intensities than PET)
PET	Pentaerythritol	0.8742	*K lines of* Al, Si and K
TAP	Thallium hydrogen phthalate	2.575	*K lines of* F, Na, Mg
Usually for use in electron microprobe applications:			
Lead stearate (or lead octadecanoate)		10.04	B to O *K lines*
Multilayer		6.0	O, F *K lines*
Multilayer		10.0	C, O *K lines*
Multilayer		16.0	B, C *K lines*

required having different 2*d* spacings. The diffracting crystals most commonly encountered and their analytical ranges are listed in Table 2. They can be divided into three categories:

LiF, PET, TAP, InSb, and Ge are all *crystalline materials*, which are cut along specific crystallographic orientations to produce the desired 2*d* spacing. Three orientations of the LiF crystal, offering different 2*d* and resolution characteristics, are available, although the LiF (200) orientation is the most widely used.

Stearate crystals represent a class of pseudo crystals originating from the work of Langmuir and Blodgett. These ‘‘crystals’’ are in fact made by coating a suitable substrate with successive layers of lead salts of soap molecules. The lead atoms serve as the diffracting layers, and this technology used to be the only way of extending the range of diffracting media to 2*d* spacings greater than could be grown in natural crystals. However, this technology has now been largely replaced by so-called layered synthetic microstructure devices, more commonly known as multilayers.

Multilayers are devices fabricated by depositing alternate layers of a low and a high atomic number material on a suitable substrate normally using vapor deposition techniques. Conditions can be set to control the thickness of

layers, and the aim is to produce a device with a specified 2*d* spacing between the high atomic number layers (which reflect the fluorescence x-rays of interest) and the low atomic number layers (which must be essentially transparent to the fluorescence x-rays of interest). The principal use of multilayers is in the diffraction of low-energy fluorescence x-rays. Diffracted intensities from multilayers are often higher than those from alternative crystals (e.g., lead stearate, TAP), but their resolving power is inferior. Furthermore, multilayers must normally be selected with a specified 2*d* spacing suitable for only a relatively narrow range of fluorescence lines, so that several of these devices are required if the detection of all the elements from B to F is required. In fact this is a region of the spectrum that is more of interest in electron microprobe analysis, and although the potential also exists for XRF measurements, there are few applications relevant to the analysis of soil or environmental samples.

X-Ray Counter. The intensity of the diffracted beam is measured with an x-ray counter, but since no one counter design has a uniformly high detection for the full spectral range of interest, WD spectrometers are normally provided with two.

For the detection of the lower energy x-ray region, a *gas flow counter* is normally used (Fig. 12). This comprises a chamber filled with argon-10% methane (sometimes argon-10% carbon dioxide) gas and with a thin wire electrode passing longitudinally along the axis. X-rays enter through an entrance window (made, for example, of polypropylene foil, 2 to 6 μm thick). Individual x-ray photons cause ionization of the counter gas, and the resulting electrons drift towards the wire electrode, to which a positive potential of 0.5 to 2 kV is applied. In the vicinity of the wire, the large potential fields cause the electrons to accelerate, causing considerable further ionization (“gas multiplication”). The single photon event is detected by the charge of electrons deposited on the wire. Complementary ions drift in the opposite direction to earth at the body of the counter. The methane (or carbon dioxide) “quench” gas is designed to suppress further ionization that could result from this earthing process. A flow of gas through the counter is necessary to compensate for the gradual loss of gas by diffusion through the counter window into the spectrometer vacuum system.

An important aspect of the operation of gas-proportional counters is that the electronic charge associated with the detection of each photon and the derived amplified signal is proportional in magnitude to the energy of the detected photon. This property permits the detected signal to be filtered electronically to eliminate some interference effects. Filtering is undertaken by “pulse height discrimination.” The analyst has the option of

Marcel Dekker, Inc.
270 Madison Avenue, New York, New York 10016

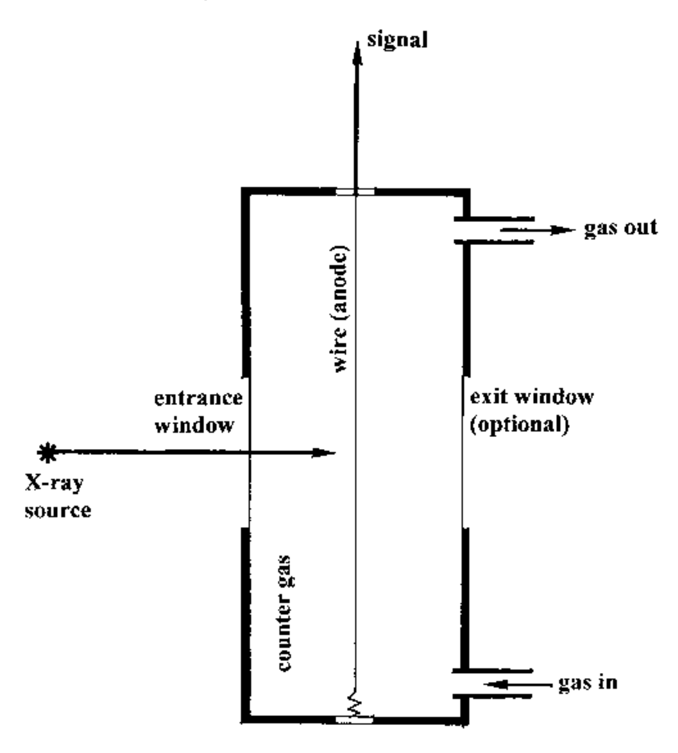


Figure 12 Gas flow proportional counter.

setting a lower level discriminator setting (which causes the counting system to ignore low-level pulses including electronic noise) and an upper level discriminator (which causes the counting system to ignore higher level pulses caused, for example, by unwanted multiple-order diffractions and scattered continuum photons).

The argon gas flow proportional counter has a decreasing detection efficiency for x-rays above about 6 to 8 keV. For higher energy photons, a *sealed gas proportional counter* containing krypton or xenon as the counter gas can be used. Because of the greater x-ray absorbing properties of these gases, these counters have a greater detection efficiency for higher energy photons. However, a more common alternative for the higher x-ray energy region is the scintillation counter.

The *scintillation counter* comprises a wafer of sodium iodide (doped with thallium), which is coupled optically to a photomultiplier tube (see Fig. 10). When an x-ray photon interacts with the NaI(Tl) wafer, it causes the crystal to emit light (scintillate) in the optical region of the spectrum.

This light is detected and amplified by the photomultiplier, which serves as a high-gain amplifier. Again, proportionality between the photon energy and the output signal is maintained so that pulse height discrimination can be used.

In some instruments, there is an option to use the signals from both argon gas flow and scintillation counters in tandem to detect the x-rays in the intermediate region of the spectrum (6 to 8 keV). In this case, the proportional counter must be fitted with both entrance and exit windows to allow the fraction of photons that is not detected in the counter gas to pass through to the scintillation detector.

Goniometer. The final aspect of the WD spectrometer considered here is the goniometer mechanism. Based on the Bragg equation, a precise geometric relationship must be maintained between the position of the diffraction crystal and the counter(s) in relation to the entrance collimator. The goniometer mechanism is designed to maintain a total angle of diffraction of 2Θ for any angle of incidence of Θ at the diffracting crystal, by controlling the rotation of the diffracting crystal and the movement of the counter assemblies. The 2Θ range of movement of a goniometer is normally about 15° to 165°. Lower angles imply grazing incidence; higher angles would cause the counter assembly to obstruct the entrance slits. To ensure reproducible operation, very precise repositioning of the mechanism is necessary. Whether 2-to-1 gearing or some form of optical position encoder is used, careful consideration must be given to avoid mechanical backlash that would otherwise cause small discrepancies in the rest position of the device.

4. Overall Configuration of WD-XRF Instruments

There is considerable uniformity in the design of modern WD-XRF instruments (see Fig. 10). A typical instrument comprises a 3 to 4 kW end-window x-ray tube directly exciting a sample, with a single scanning goniometer fitted with selectable entrance (Soller) slits, up to eight selectable diffraction crystals, and selectable flow proportional and scintillation counters. The majority of instruments are interfaced to an external large-capacity sample carousel. Variations of this basic design include (1) the installation of two scanning goniometers, (2) fixed-channel instruments designed for the simultaneous detection of specified element lines, (3) hybrid instruments that also incorporate an energy dispersive instrument as a multielement channel, and (4) hybrid instruments that also include an XRD channel capable of quantifying particular mineral species (e.g., lime in cement) in the course of an XRF determination.

B. Energy-Dispersive XRF

An ED detector is a device used to detect x-ray spectra in a manner that differentiates x-ray photons on the basis of their energy. Because the mode of operation of ED detectors is different from WD spectrometers, some of their analytical characteristics are also different. The most common type of energy dispersive detector is the lithium-drifted silicon detector, but other semiconductor materials can be used, including germanium and mercury (II) iodide. Even the proportional counter can be used as an energy dispersive detector, as in some forms of portable XRF instrumentation where low resolution is acceptable. To illustrate the general characteristics of ED devices, the design and operation of the Si(Li) detector are considered further here.

1. Si(Li) Detectors

The Si(Li) x-ray detector system comprises a crystal of high-purity silicon, which is coupled to a high sensitivity field effect transistor (FET) as amplifier (Fig. 13). The silicon crystal has lithium atoms drifted into it to compensate for impurity atoms that would interfere with the semiconductor properties of the device. The detector is often machined in a "top-hat" shape, although other configurations are used. An x-ray photon entering the detector crystal loses its energy by interacting with silicon atoms, mainly causing electrons to be excited from the valence band of the semiconductor crystal to the conduction band. Electrons in the conduction band are mobile, and by applying an electrical bias between front and rear faces of the crystal, these electrons can be caused to drift to an electrode attached to the rear face.

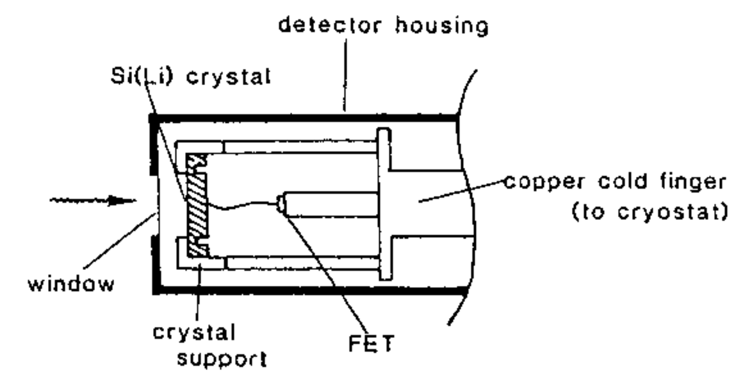


Figure 13 Si(Li) detector. (Reprinted from *Journal of Geochemical Exploration*, Potts and Webb, 1992, Fig. 9, p. 265, with permission from Elsevier Science.)

Marcel Dekker, Inc.
270 Madison Avenue, New York, New York 10016

This electronic charge is collected and then amplified by the FET before being passed on for further stages of amplification, shaping, and filtering. The detector system is designed so that the total charge deposited in the detector (and amplified by the associated pulse processing circuits) is proportional to the energy of the detected x-ray photon. There is no mechanical monochromator incorporated in this device, but output pulses are sorted and displayed using the multichannel analyzer. This device is designed with typically 4096 channels. Detected pulses are sorted according to magnitude, and one "event" for each detected photon is stored in the appropriate channel. The contents of the multichannel analyzer can be displayed as the detected x-ray spectrum both during and after data acquisition, permitting rapid and effective qualitative interpretation of the composition of the sample.

The two important characteristics used to describe the quality of the ED detection systems (i.e., detector and pulse processing electronics) are (1) energy resolution and (2) maximum count rate capability. In fact, these are the two characteristics in which the performance of energy dispersive detectors is often considered to be inferior to that of WD spectrometers.

Energy Resolution. By convention, the energy resolution of an ED detector is specified as the full width at half the maximum peak intensity (FWHM) of the peak detected from the Mn Kα line at 5.9 keV. This line is selected because it can readily be measured from a ^{55}Fe source. Since the resolution characteristics of an ED detector normally degrade with the input count rate, FWHM data are normally specified under low count rate conditions. There are two factors that affect detector resolution. The most fundamental is the average energy required to create an electron–hole pair in the semiconductor device (the process by which electrons are promoted from valence to conduction bands). This parameter depends on the energy gap between conduction and valence bands in the semiconductor device and can only be changed by selecting a different semiconductor material as detector. The component of resolution associated with this phenomenon can be calculated from

$$\text{FWHM} = 2.344\,(FE\varepsilon) \tag{10}$$

where F is the Fano factor ($=0.10$ to 0.13), which accounts for the fact that, from a statistical point of view, the creation of electron–hole pairs cannot be considered to be entirely independent events in a semiconductor detector, E is the x-ray photon energy, and ε is the energy corresponding to the band gap ($\varepsilon = 3.8$ eV for Si).

The second factor that contributes to the resolution of detected signals is the magnitude of electronic noise within the detector. This noise arises mainly from thermal effects, which cause vibration of the atoms of the semiconductor crystal lattice. This source of electronic noise can be minimized by cooling the detector and the associated FET amplifier, usually with liquid nitrogen, but sometimes by electronic Peltier cooling devices. Taking into account these factors, the best Si(Li) detectors used in EDXRF offer practical resolutions of about 135 eV FWHM at 5.9 keV (better resolutions can be achieved). A typical spectrum from an ^{55}Fe source, showing various spectral artifacts, is shown in Fig. 14.

When comparing resolution performance of an ED detector with that of a WD spectrometer, account must be taken of the way in which the resolution of these devices varies with x-ray energy. Very broadly, a WD spectrometer offers an advantage in resolution at x-ray energies below about 14 keV (i.e., for K lines of Rb and below), and indeed a substantial advantage below about 8 keV (i.e., the K lines of Cu and below). Between 15

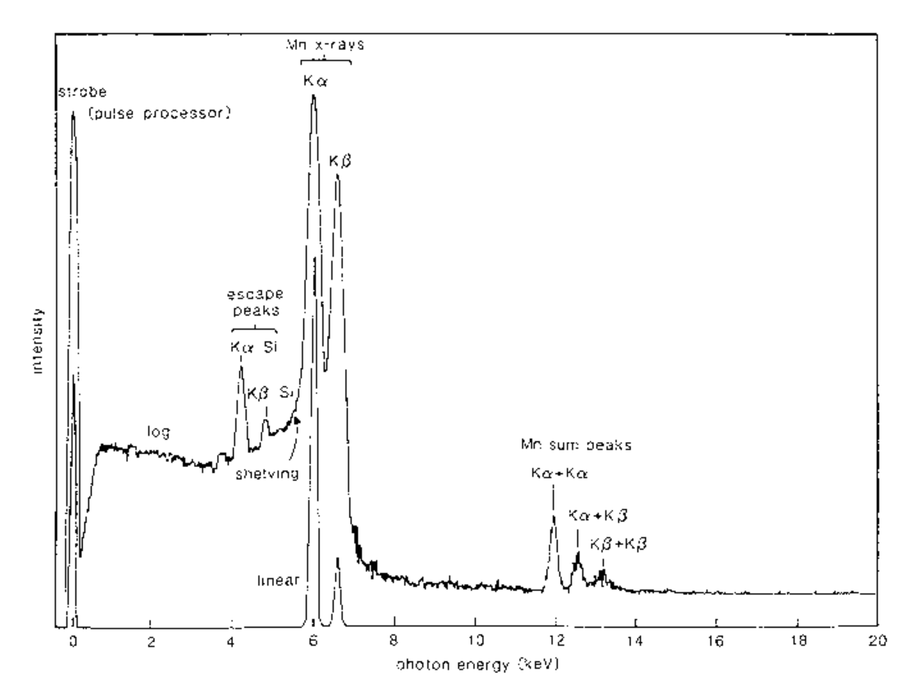


Figure 14 Si(Li) spectrum from a ^{55}Fe source showing the Mn, Kα, and Kβ lines and various spectrum artifacts, including sum peaks and escape peaks. (Reprinted from Potts, 1987, p. 304, Fig. 9.25, with permission from Kluwer Academic Publishers.)

and 18 keV (Rb-Mo K lines), resolution performance of these detection systems is about equivalent. Above about 20 keV, Si(Li) detectors offer superior performance.

Count Rate Capability. Whereas most modern WD spectrometers can operate at count rates in excess of 10^6 cps, few ED counting systems can cope with an input count rate of more than about 50,000 cps. The reason is related to the need to minimize statistical fluctuations in the detection of the ED signal referred to above. Noise is a significant issue, especially in the detection of the low-energy x-ray photons, because each photon creates only a relatively small electronic charge during the detection process. In order to minimize the effect of statistical fluctuations on this small electronic signal, a relatively long time constant must be selected on the pulse-processing amplifier. Values of 6 to 20 μs are typical, the larger values being appropriate for the detection of the lower energy spectrum (< 5 keV), where electronic noise makes the largest contribution to the detector signal. By contrast, an amplifier coupled to a WD proportional counter would normally operate at a time constant of less than 1 μs. Counting systems encounter problems when the input count rate approaches the reciprocal of the time constant. The problem is associated with amplifier circuits not being able to measure satisfactorily the current signal, before being disturbed by the next one. To prevent signal distortion that would occur in these circumstances, ED amplifier circuits are designed to switch off the acceptance of new pulses until the current one has been measured. For this period, the counting system is effectively dead as far as the detection of further x-ray events is concerned, giving rise to the phenomenon of *dead time*. Dead time is mainly a function of the input count rate (and the selected time constant), which, in a simplified form, are related by the equation

$$R_\mathrm{t} = \frac{R_\mathrm{m}}{1 - R_\mathrm{m}\tau} \tag{11}$$

where R_t is the true (input) count rate, R_m is the measured (output) count rate, and τ is the dead time constant of the counting system. The output count rate can be increased by selecting a smaller amplifier time constant (so reducing τ), if the corresponding degradation in spectral resolution is acceptable.

Pulse Pile-Up. Energy dispersive counting systems are often operated at up to 50% dead time, but higher values are usually avoided. One reason is the problem of pulse pile-up interferences in detected spectra. ED detector amplifier circuits are designed to detect and reject pulse pile-up events. These events arise when two photon events are detected almost simultaneously. The probability of such an occurrence increases significantly at very high

count rates (which are associated with high dead times). Pulse pile-up peaks appear in detected spectra at the sum of the energies of the coincident events. For example, at very high count rates, pulse pile-up peaks will be observed in the K line spectrum of Mn at energies corresponding to $K\alpha+K\alpha$, $K\alpha+K\beta$, and $K\beta+K\beta$ (Fig. 14). Another reason for avoiding very high count rates is that detected peak shapes become distorted and shift in position, causing difficulties in quantifying spectral data.

Escape Peaks. The other principal spectrum artifact observed in ED spectra is escape peaks. Detected photons not only cause ionization in the silicon crystal but can also cause the fluorescence of silicon atoms. Most of the resultant Si $K\alpha$ x-rays are internally absorbed within the detector crystal, but a small proportion can escape and so avoid contributing to the detected signal. When this happens, the total charge deposited in the detector crystal corresponds to that of the incident x-ray photon, less the energy of the escaped Si $K\alpha$ photon. This phenomenon is observed in spectra as an artifact peak lying at 1.74 keV (the energy of the Si $K\alpha$ escape photon) below the energy of the host peak (Fig. 14). Phosphorus $K\alpha$ x-rays are most effective in exciting escape peaks, since this photon has an energy just above the Si K absorption edge. Higher energy x-rays become progressively less effective in contributing to the escape peak phenomenon.

2. Spectral Interpretation and Analysis

Because ED detectors are capable of "viewing" the full x-ray spectrum, they have an unrivaled capability in qualitative analysis and in fingerprinting samples. Most instruments have the capability of displaying fluorescence spectra during acquisition so that the interpretation of the major constituents of a sample need only take a few seconds. However, the majority of ED-XRF systems are used for quantitative analysis. Although procedures for matrix correction are identical to those from WD-XRF instruments, the determination of intensities from recorded spectra requires more consideration. In the case of WD spectrometers, intensities are measured as the count rate observed with the spectrometer set on the peak maximum of the fluorescence line of interest, from which must be subtracted a background count rate. In the case of ED detectors, the spectrum is recorded in digital form (usually in 4096 channels); and because the detector resolution is significantly worse than that of a WD spectrometer, particularly in the lower spectrum region, account must be taken of spectrum overlap interferences. The three main approaches used for ED spectral analysis are as follows:

Region-of-Interest Integration. Peak intensities are measured by summing the contents of a selected number of channels on either side of

Marcel Dekker, Inc.
270 Madison Avenue, New York, New York 10016

the peak maximum. This simple approach works well providing there is negligible drift in the energy calibration of the spectrum and there is a facility to apply precalibrated spectrum overlap corrections.

Peak Fitting. The spectrum is analyzed by fitting gaussian or modified gaussian functions to peaks in the spectrum. In this approach, it is normally necessary to fit the background, and use may be made of the known ratio in intensity between $K\alpha$ and $K\beta$ lines to remove $K\beta$ line overlap interferences.

Library Spectra. A series of x-ray "library" spectra are recorded for all the lines occurring in a region of the spectrum to be analyzed by exciting samples prepared from spectroscopically pure reagents. These spectral profiles are then fitted to the sample spectrum using a least squares minimization routine, normally after subtraction of the background continuum component. In one widely used approach, a digital filter is first applied to the spectral data to remove the background.

3. Other ED Detector Devices

Silicon PIN Detectors. The conventional Si(Li) detector comprises a relatively large crystal that requires liquid nitrogen cooling to operate satisfactorily. However, recent advances in semiconductor technology have led to the development of silicon photodiode devices in which a small 300 μm layer of silicon acts as the detecting device. Currently, these devices offer a resolution of about 200 eV at 5.9 keV and are cooled to about $-30\,^{\circ}C$ using an integral Peltier device.

Germanium. Germanium crystals are routinely used as detectors in gamma ray spectrometers, where advantage can be taken of the greater stopping power of Ge than of Si. However, Ge detectors can also be used for x-ray spectra. One advantage is that germanium has a slightly smaller semiconductor band gap, so that the theoretical resolution of a Ge x-ray detector is slightly better than that of a Si(Li) device. One disadvantage is that Ge escape peaks can cause more troublesome spectrum overlap interferences; but these can be reduced in intensity if x-ray detection is restricted by collimation to the center of the detector crystal.

Mercury (II) Iodide. This material is relatively new to x-ray detector technology but has found an application in portable XRF instrumentation. The advantage of mercury (II) iodide is that the crystal only requires a small degree of cooling to reduce electronic noise and offers an extended efficiency to the detection of x-rays of higher energy (>30 keV). Typical resolution is about 280 eV at 5.9 keV. Because of the way detector resolutions vary with

energy, mercury (II) iodide detectors offer inferior resolution to Si(Li) devices for the detection of lower energy x-ray spectra (< 10 keV), but performance is not markedly different at higher energies.

Proportional Counter Detectors. Although normally used as x-ray counters in a WD spectrometer, gas proportional counters can also be used as stand-alone energy dispersive detectors. The advantage is that these devices are simple, light, and rugged, all of value in portable XRF instrumentation. The major disadvantage is resolution, typically 900 eV at 5.9 keV, a significantly inferior figure to that of semiconductor detectors. As a consequence, these devices are normally used in applications involving the analysis of samples that give simple spectra, where results are not seriously affected by spectrum overlap interferences or where simplification in the detected spectrum can be achieved by selective filtering.

4. Overall Configuration of ED-XRF Instrumentation

One of the characteristics of ED-XRF instruments is that they can be designed so that the detector accepts a much larger solid angle of radiation than in WD spectrometers (which require careful collimation using Soller slits to restrict the angular divergence of the beam accepted for diffraction). As a consequence, ED-XRF instruments tend to be much more compact, the alignment geometry is not as critical, and ED detector devices can be used in applications where the fluorescence spectral intensities are too low to justify the efficient use of a WD spectrometer.

The main categories of ED-XRF instrumentation are

Direct Tube Excitation. This excitation geometry (Fig. 15) is similar to that used in WD-XRF instruments. In view of the greater detection efficiency of ED devices, a 50 W tube is adequate, but careful optimization of excitation conditions is required by the appropriate choice of tube kV, often by using metal foil filters in the primary x-ray beam. The aim here is to maximize excitation of the elements in the spectral range of interest while minimizing the degree of scatter from the tube continuum into the detector by attenuating this part of the x-ray tube output, if appropriate. Using a general purpose Ag tube, the major and trace elements in silicate materials can be determined to a performance approaching that expected from a conventional WD-XRF instrument (Potts et al., 1984).

Secondary Target Geometry. The x-ray tube is used to excite a secondary target, radiation from which excites the sample (see Fig. 7). Using an orthogonal, x-ray optical path, some suppression of scattered continuum can be achieved (see Sec. II.D). However, because secondary targets are only capable of exciting a relatively restricted range of elements having

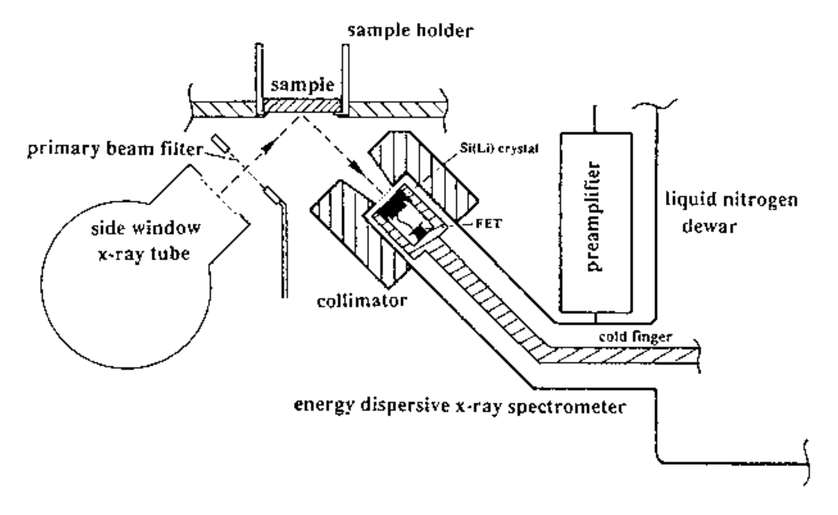


Figure 15 Energy dispersive XRF system with direct tube excitation. (Reprinted from Potts, 1993, Fig. 4, p. 144, Copyright© 1993, Marcel Dekker.)

absorption edges below the energy of the characteristic secondary target fluorescence radiation, several secondary targets are required (e.g., Co, Zn, Ge, Zr, Pd, Sm) if the full range of elements is to be determined. Instruments must normally revert to direct tube excitation for the low atomic number elements ($< \text{K K}\alpha$), owing to the increasingly narrow range of elements for which secondary target excitation is effective in this low-energy x-ray region.

Barkla Scatter Geometry. As discussed in Sec. II.C, significant advantages arise from orthogonal excitation geometries in which the sample is excited by x-ray tube radiation scattered from a suitable target (see Fig. 7). Because of the reduction in background intensities observed in detected spectra, detection limits are significantly lower than for instruments using conventional excitation geometries. To optimize scatter efficiencies, different materials are required to scatter radiation in different regions of the spectrum. In one instrument, boron carbide and corundum were selected as complementary scatter devices for the 6–30 and 17–40 keV regions of the spectrum, respectively. As with secondary target excitation, an ED detector is required to compensate for the reduction in excitation efficiency associated with the scatter process, compared with direct tube excitation.

Portable Instrumentation. XRFS is one of the few techniques suited to the direct in situ analysis of samples. However, if such instrumentation is to be truly field portable, there are significant design constraints in terms of compactness, maximum allowable weight, and battery power consumption.

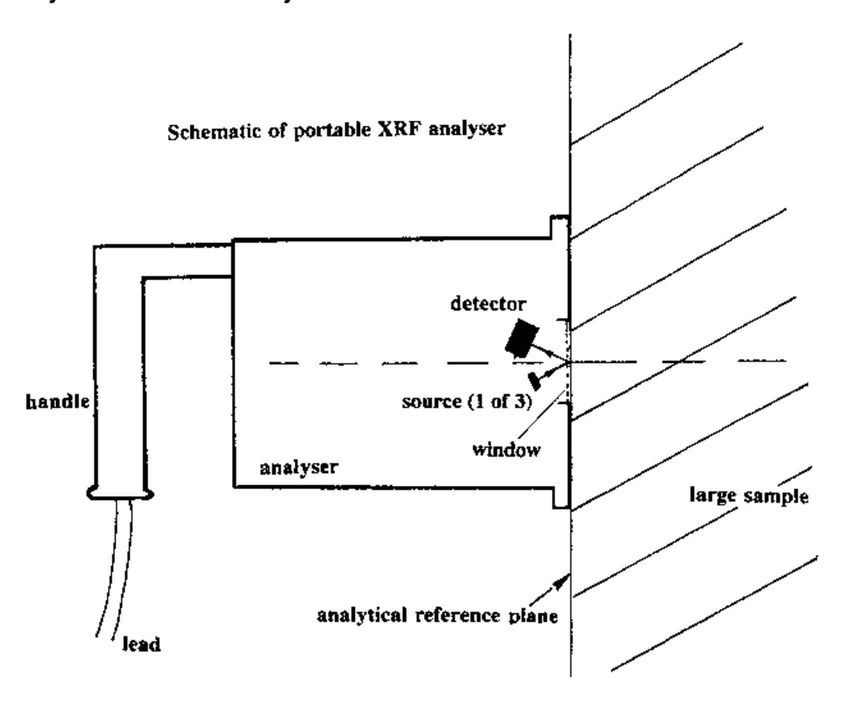


Figure 16 Handheld portable XRF analyzer. (Reproduced from Potts et al., 1997, with permission from The Royal Society of Chemistry.)

Weight and compactness are particularly significant aspects if the analyzer unit is to be held against a sample for the duration of a field analysis. These design constraints are normally met by using up to three radioactive sources (generally ^{55}Fe, ^{109}Cd, and ^{241}Am) to excite the full spectrum range of interest (miniature x-ray tubes are also available). The energy dispersive detector can be based on a proportional counter detector (for applications involving simple spectra) or higher resolution mercury (II) iodide or Si-PIN diode detectors. A hand-held analyzer unit incorporating these features is shown in Fig. 16.

V. APPLICATIONS

The different forms of XRFS instrumentation have been used in a wide range of applications for the analysis of soils and other environmental samples. In this section, some examples are described to illustrate a number of representative applications and demonstrate the performance characteristics that may be expected.

A. Analysis of Bulk Soil Samples

1. Major Elements by WD-XRF

To achieve the highest accuracy in the determination of the major elements, it is necessary to analyze samples as glass disks using methods primarily developed for silicate rock analysis. A typical procedure would be as follows.

A glass disk is prepared by fusing the powdered sample with a suitable flux, over an open gas burner or in a muffle furnace. In the analysis of silicate rocks, a variety of fluxes have been developed, most based on either lithium tetraborate on its own or in combination with lithium metaborate. One common "universal" flux is a mixture of 4 parts of lithium metaborate and 1 of lithium tetraborate. Samples may be prepared by mixing 7.500 ± 0.001 g of flux with 1.500 ± 0.0005 g of ignited sample to prepare a 35 mm glass disk (see Bennett and Oliver, 1992), giving a sample-to-flux ratio of 1 : 5. After intimately mixing sample and flux, the mixture is heated in a platinum-5% gold crucible. In the procedure recommended by Bennett and Oliver, the crucible (almost covered by a lid) is first progressively heated from low to full heat over a period of 10 min using a Meker burner and then transferred to a muffle furnace at 1200°C for final fusion, the crucible now being completely covered. The crucible must be swirled throughout fusion to ensure complete mixing. After about 5 min in the muffle furnace, the melt is poured into a preheated casting mold, which is then cooled with an air jet to solidify the glass. If glass disks are prepared from unignited samples, the sample weight should be increased by taking into account the loss-on-ignition figure so that an equivalent of 1.5 g of ignited sample will be present in the glass disk. In this latter case, the initial stages of heating should be extended to ensure that carbonaceous material is removed and that iron has an opportunity to oxidize to the ferric state.

Samples prepared in this way are then analyzed by WD-XRF, often using a Rh anode tube operated at 40 kV, 60 mA. The major element oxides normally reported include Na_2O, MgO, Al_2O_3, SiO_2, P_2O_5, K_2O, CaO, TiO_2, MnO, and Fe_2O_3 using the appropriate diffracting crystals (Table 2). Calibration is preferably undertaken against matrix matched calibration samples prepared from high-purity chemical reagents and fused as glass disks in the same way as the samples. As an alternative, glass disks prepared from reference materials may be used, although it is advisable to use a range of reference materials to avoid errors caused by bias in individual values. Whichever method is chosen, the calibration samples should have a composition range that covers that of the samples to be analyzed. Matrix corrections can be undertaken by any of the standard procedures (except the

Compton scatter method), a typical method for this application being based on influence coefficients (see Sec. III.A).

Although this procedure (sometimes with minor variations) is widely used in the analysis of silicates, particular attention needs to be paid to the distinctive composition of soils—in particular the possible high concentrations of moisture, carbonate minerals, and organic matter. A standard procedure for silicate rocks would involve drying the sample before fusion with flux, but samples containing clay minerals emit moisture over a range of temperatures, and samples with high volatile contents may cause difficulties during fusion owing to the formation of bubbles in the melt. In order to overcome these difficulties, drying should, therefore, be carried out at $110 \pm 5°C$ for a specified time (e.g., 2 h) to avoid discrepancies in the residual moisture content caused by variations in drying conditions. The same care is required to standardize conditions for loss-on-ignition determinations, in particular, to ensure that the temperature is raised slowly to remove carbon and oxidize iron to the Fe(III) state as completely as possible. Typical ignition conditions using a muffle furnace would be to increase the temperature to $1025 \pm 25°C$ over a period of 20 min and to maintain this temperature for 30 min with an oxidizing environment in the furnace.

Caution must also be expressed concerning soils contaminated with heavy metals. Some metals (Cu, for example) and other elements (As and S, for example) react with platinum crucibles, causing the alloy to become pitted and brittle and eventually to fail (see, for example, Lupton et al., 1997). If samples are not preignited, an oxidizing agent, such as ammonium nitrate, can be added to the flux to promote the oxidation of sulfide sulfur to sulfate to mitigate the problem for samples with high contents of this element.

In order to indicate the analytical performance of WD-XRF in the determination of the major elements in soils, representative data are listed in Table 3 taken from the work of Hallett and Kyle (1993). Data in this table show the precision (in terms of coefficient of variation) that can be achieved over a concentration range representative of soils, using count times of 20 to 200 s (as appropriate to elemental sensitivity). These data show that providing the elemental concentration is significantly above the detection limit, precisions of better than 0.5% (coefficient of variation) can readily be achieved.

2. Trace Elements

The standard method for the quantitative analysis of the trace elements in silicate samples is to dry, sieve, and powder the sample, mix 8 to 10 g

Marcel Dekker, Inc.
270 Madison Avenue, New York, New York 10016

Table 3 WD-XRF Analysis of Igneous and Sedimentary Rocks for the Major Elements

Element oxide	Count time (s)	Analyzing crystal	Precision at high concentration		Precision at low concentration	
			g/100 g	cv (%)	g/100 g	cv (%)[a]
SiO_2	80	PET	75.6	0.7	42.6	1.0
TiO_2	20	LiF(200)	1.6	0.4	0.04	15.3
Al_2O_3	100	PET	18.4	0.2	0.6	17.7
Fe_2O_3T	40	LiF(200)	14.8	0.3	0.1	14.9
MnO	20	LiF(200)	0.2	1.1	0.03	20.2
MgO	100	TAP	44.1	0.4	0.2	92.3
CaO	20	LiF(200)	11.8	0.2	0.5	1.8
Na_2O	200	TAP	4.0	1.3	0.2	22.9
K_2O	20	LiF(200)	9.8	0.6	0.2	0.9
P_2O_5	40	Ge	0.3	0.6	0.02	16.1

[a]cv = coefficient of variation. Samples were prepared as glass disks and excited at 35 kV, 75 mA, with a Rh anode tube using the indicated crystal and a gas flow proportional counter as the detector.
Source: Hallett and Kyle (1993).

of powder with a binder, and compress the mixture in a cylindrical mold at pressures of 2.3×10^7 kg m^{-2} (15 tonne in^2) to form a powder pellet. The binder serves to stick the particles together to make a strong and nonfriable pellet. This is one of the few examples in analytical chemistry where it is not necessary to weigh accurately the sample powder, since the aim is to prepare a sample of sufficient thickness to exceed the critical penetration depth (ca. 4 mm) of the most energetic fluorescence x-ray (otherwise the x-ray signal will vary with sample thickness as well as determinant concentration). One procedure for undertaking this form of sample preparation has been described by Watson (1996). Powder pellets can then be excited by an x-ray tube operated at typically 60 to 75 kV, 35 to 40 mA. Choice can be made from a variety of x-ray tubes. The Rh anode tube is a general purpose tube capable of exciting the standard suit of trace elements routinely determined by XRF (Ba, Cr, Cu, Ga, Nb, Ni, Pb, Sr, Th, V, Y, Zn, Zr). However, excitation (and, therefore, detection limits) can be improved for smaller groups of elements by choice of a Mo, Cr, Au, or W tube (see, for example, Chappell, 1991). The elements that can be advantageously excited in this way are those with absorption

edges at energies immediately below the characteristic tube lines, although it is not then possible to determine the full suit of elements. Typical element ranges are as follows:

Mo anode tube: Y, Sr, Rb, As, Ga (K lines); U, Th, Pb (L lines).
W or Au anode tube: Sn, Mo, Nb, Zr, Co, Mn, Cr, V (K lines); Pr, Ce, La, Ba, Cs (L lines).
Cr anode tube: Sc, Cl, S (K lines); Ba, Cs (L lines).

The preferred form of calibration is to use matrix matched blank samples and to add appropriate amounts of standard solutions of the elements of interest to prepare a range of calibration samples covering the full range of compositions of interest (see, for example, Wilson et al., 1995). The spike powders are dried, recrushed to disaggregate the dried cake, and prepared as powder pellets. Alternatively, reference materials may be used, although it may still be necessary to supplement available reference materials with spiked samples to extend the calibration range, particularly if contaminated soils are to be analyzed.

Matrix correction is commonly undertaken by the Compton scatter normalization procedure for the trace elements with fluorescence lines at energies higher than the Fe absorption edge. A supplementary correction must be applied to any trace element data with lines at lower energy than the Fe absorption edge. However, in the analysis of contaminated soils, the Compton scatter procedure will break down if any heavy metal is present at a sufficiently large concentration to cause a significant absorption edge in the bulk mass absorption of the sample. In these circumstances a fundamental parameter correction may be adequate, or an influence correction procedure using a range of matrix matched calibration samples.

In contrast to silicate rock analysis, it may be necessary to modify the sample preparation procedure to take into account the nature of the sample. In particular, soils need to be dried and crushed to a fine powder so that a strong (nonfriable) powder pellet can be prepared. Samples containing a high proportion of clay minerals are more suitable than samples with a high sand content. In the latter case, it may be necessary to increase the proportion of binder. As an alternative, samples may be analyzed as loose powders. The crushed sample is poured into a cup with a thin polymer film (transparent to x-rays) covering the base. After consolidating the powder by tapping gently, the sample powder is analyzed directly. Because small differences may occur in duplicate samples prepared in this way because of particle size effects in relation to small variations in the packing density, analytical results are expected to show slightly larger variability than data derived from compressed powder pellets. However, this variability is likely to be small in comparison with typical sampling errors, particularly in the

Marcel Dekker, Inc.
270 Madison Avenue, New York, New York 10016

analysis of contaminated soils, and so have a negligible effect on the interpretation of results. A greater problem is likely to be the resistance of many XRF operators to put powdered samples inside the spectrometer vacuum chamber for fear of contaminating the instrument. A similar sample presentation procedure can be used in the analysis of liquids, by use of a sample cup with a thin polymer film base that is transparent to X-rays. Indeed, XRFS is one of the favored methods for the direct analysis of brines (and other aqueous samples of high salt content) and some hazardous liquids. However, in such applications, the spectrometer cannot be evacuated and must be flushed with helium to minimize x-ray absorption.

In some schemes of analysis, low atomic number elements such as F, Na, Cl, and S are determined on compressed powder pellets to avoid diluting samples by fusion with a flux and to compensate for the reduced excitation available from older designs of x-ray tube, fitted with relatively thick beryllium windows.

As described in Sec. II.C, polarized excitation geometries offer the advantage of a significant reduction in background in detected spectra, resulting from the fact that the characteristic and continuum radiation from the x-ray tube cannot be detected if an orthogonal geometry is used for the x-ray tube-scatter target-sample-energy dispersive detector optical path. The main analytical benefit arises in improved detection limits, illustrated by the work of Heckel et al. (1991) as listed in Table 4. One set of data in this table shows detection limit results for a quartz sample excited with radiation from a Rh tube operated at 38 kV and scattered off a B_4C target, using a 30 µm Pd filter and a 750 s count time. The second set of results was again obtained using Rh tube radiation, this time operated at 58 kV and using an Al_2O_3 target, a 125 µm Ta filter, and a 250 s count time. Comparison of results in Table 4 with detection limit data reported by conventional WD-XRF (Table 5) shows that detection limits are often more than 10 times smaller and that, in consequence, the range of elements for which routine determinations are possible is extended.

3. Direct Analysis of Soils by Portable XRF

One of the aspects of XRF that few other techniques can match is the possibility of using portable instrumentation for the direct analysis of samples in the field. An overview of portable instrumentation has already been considered in Sec. IV.B.4. Portable XRFS instruments are normally provided with sample cups that allow samples to be prepared and analyzed using the conventional techniques described in the previous sections in a mobile field laboratory. However, for in situ analysis, little sample preparation is necessary (or possible). The main requirement is to expose a

Table 4 Detection Limits Using Polarized Excitation Geometries Based on Barkla Scatterers

Operating conditions	Element	Detection limit ($\mu g\, g^{-1}$)[a]	Element	Detection limit ($\mu g\, g^{-1}$)
Rh tube operated at 38 kV, B_4C target, 30 μm Pd filter, 750 s count time	As	1.8	Pb	1.3
	Bi	1.2	Rb	0.3
	Br	0.3	Se	0.4
	Cr	5	Sr	0.3
	Cu	0.7	Th	0.9
	Ga	0.6	Ti	15
	Hg	1.8	U	0.8
	Mn	2.8	Y	0.4
	Nb	0.7	Zn	0.6
	Ni	0.8	Zr	0.5
Rh tube operated at 58 kV, Al_2O_3 target, 125 μm Ta filter, 250 s count time	Ag	0.3	I	1.2
	Ba	2.0	La	3.2
	Cd	0.3	Sb	0.6
	Ce	3.4	Sn	0.6
	Cs	2.0		

[a]Detection limits are calculated as the concentration equivalent to three standard deviations on the background count rate measured from a quartz glass sample.
Source: Data abstracted from Heckel et al. (1991).

representative sample surface (by removing vegetation and unrepresentative rocky material in the analysis of soils) and to ensure that the sample locality is as flat as possible. The portable XRF analyzer unit is then placed in position and the analysis sequence commenced. Although the count time of measurements may be extended to improve detection limits, performance equivalent to laboratory WD-XRF is unlikely to be achieved, for several reasons. One is that practical considerations limit the activity of radioactive sources that may be used in portable instrumentation, thus restricting the sensitivity of determinations (in terms of counts per second per unit concentration). Another is that the instrumentation is most effectively used in the determination of heavy metal contamination for selected elements at concentrations substantially above the detection limit of instrumentation, when detection limit performance is not a significant limitation. Finally, in contaminated soil studies, the precision of measurements is likely to be limited by sampling precision (that is, differences in measurements at duplicate sample positions caused by local heterogeneity effects), not by analytical precision. In these circumstances, it is likely to be more beneficial to record a larger number of measurements of different sample localities at

Table 5 WD-XRF Analysis of Igneous and Sedimentary Rocks for the Trace Elements[a]

Element	Count time: Peak (s)	Count time: Background (s)	Precision at high concentration: $\mu g\,g^{-1}$	Precision at high concentration: cv (%)	Precision at low concentration: $\mu g\,g^{-1}$	Precision at low concentration: cv (%)	Detection limit $\mu g\,g^{-1}$
Ba	200	200	1730	0.8	25	14.7	8.2
Cr	200	200	3000	0.7	6.3	30.7	6.8
Cu	100	160	1040	0.2	13.9	2.0	7.0
Ga	100	80	22.1	8.1	11.1	8.7	2.8
Nb	200	160	29.4	1.0	2.6	10.1	1.5
Ni	100	160	2390	0.3	7.7	6.8	8.0
Pb	200	100	148	0.6	4.5	35.2	4.3
Rb	100	140	298	0.2	5.5	8.2	2.2
Sr	100	80	449	0.3	3.9	7.9	2.3
Th	200	100	35.8	2.3	3.5	9.2	2.5
V	200	200	655	0.4	3.9	25.6	2.3
Y	100	120	85	0.7	2.0	16.5	2.0
Zn	100	160	1960	0.3	12.0	3.7	5.8
Zr	100	160	194	0.2	7.2	3.0	2.2

[a]Samples were prepared as compressed powder pellets and excited at 60 kV, 45 mA, using a Rh anode tube. Fluorescence lines were measured using a LiF(200) crystal and either scintillation or gas flow proportional counters as appropriate.
Source: Hallett and Kyle (1993).

adequate precision (i.e., using shorter count times) rather than a smaller number of high-precision measurements (using longer count times). Taking these factors into account and applying other pragmatic constraints, count times of 2 to 3 min per sample are often appropriate.

There are a number of further important considerations in the use and interpretation of data from portable XRF measurements.

(1) Determinations cannot be made of the low atomic number elements, because their low-energy characteristic x-rays are attenuated in air. Although fluorescence lines down to the Cl Kα line can be detected, sensitivity is relatively poor below K Kα.

(2) The mass of sample analyzed is an important constraint on the interpretation of results. The mass may be evaluated from the area of the analyzer window (typically 25 mm in diameter), the critical penetration depth of the fluorescence x-ray, and the density of the soil. The critical penetration depth is normally defined as the depth from which 99% of the

fluorescence signal originates. Deeper than this, the fluorescence x-ray is attenuated within the sample and so cannot make a significant contribution to the detected signal. The critical penetration depth is affected to a significant extent by x-ray energy as well as sample composition. Some values estimated for a typical soil are listed in Table 6. Data are listed for both the depth from which 99% of the signal originates and 90% and 50% of the signal. These data indicate that measurements are limited to surface layers. Care is then required if data are compared with soil results obtained by conventional sampling using an auger, followed by conventional laboratory analysis. Portable XRF data represent a ''spot'' analysis of the surface layers, whereas results from auger samples represent the average composition integrated over, say, the top 100 mm. Account must also be taken of the fact that portable XRF data are clearly susceptible to larger uncertainties from sampling precision in view of the much smaller mass from which the analytical signal originates.

(3) When results from in situ portable XRF analyses are compared with results obtained by augering followed by conventional laboratory techniques, account must also be taken of the moisture content. The moisture content of samples in the field is likely to be large and perhaps variable depending on recent weather and drainage conditions, whereas

Table 6 Critical Penetration Depths of Characteristic Fluorescence X-rays in a Typical Soil

Element	Kα energy (keV)	99% of signal (μm)	90% of signal (μm)	50% of signal (μm)
Na	1.0	4.7	2.3	0.7
Si	1.7	12	6	1.9
K	3.3	29	14	4.3
Ti	4.5	48	24	7
Fe	6.4	160	81	24
Cu	8.0	230	120	35
Rb	13.4	850	430	130
Nb	16.6	1370	690	210
Sn	25.3	5390	2700	810
Ba	32.2	8870	4440	1340

Results show the estimated depth (μm) into a soil sample from which 99%, 90%, and 50% of the analytical signal originates for the Kα lines Na (1.0 keV) to Ba (32.2 keV). Calculations were undertaken using the composition data for the soil reference material. SOIL-5 using concentration values abstracted from Potts et al., 1992.

samples for laboratory analysis are conventionally dried before any measurements are made. In temperate climates, soils could contain up to 30% moisture (w/w), less than 10% w/w being unusual. Unless this component is taken into account, significant bias will be observed when field measurements are compared with laboratory results.

(4) Portable XRF instruments are calibrated to offer fully quantitative data for ideal samples that are perfectly flat so that the surface lies exactly in the reference plane of the analyzer unit. Practical considerations mean that this requirement is unlikely to be met with in situ measurements. However, in terms of data quality that meets fitness-for-purpose criteria, small discrepancies caused by surface irregularities may be acceptable, particularly if the overall precision of measurements is limited by sampling precision. If data of the highest accuracy is required, a correction is required. Work by Potts et al. (1997) directed at the quantitative analysis of irregular rock surfaces has shown that analytical bias caused by surface irregularity effects can be compensated by normalizing fluorescence intensities to that of the scatter peak originating from the scatter in the sample of an emission line from the excitation. This correction is based on the observation that sample surface irregularities change the intensity of this scatter peak to the same degree as fluorescence lines of interest, provided surface irregularities are not excessive. Hence by multiplying the measured fluorescence intensity by the ratio of the scatter peak intensities from a flat sample to that from the sample being measured, the equivalent fluorescence intensity from a flat sample can be estimated. In practical application, some care is required in selecting the sample from which the scatter peak intensity of an ideal flat surface can be measured. One possibility is to prepare a sample surface in the field by tamping the soil with a suitable tamping tool. Another possibility is to make preliminary measurements on a suitable reference material prepared as a compressed powder pellet, accepting that some differences will arise owing to a mismatch in moisture content.

To illustrate the potential of portable XRF instrumentation, detection limits obtained using a radionuclide instrument are listed in Table 7. These data were in fact obtained in the laboratory by exciting a series of silicate rock reference materials prepared as compressed powder pellets using a count time of 200 s per source, but should be representative of the field analysis of soils. In circumstances where instrumentation can be applied to the analysis of contaminated soils, higher detection limits can often be tolerated with the benefit of shorter count times. As a guide, using normal statistical criteria, halving the count time causes the detection limit to increase by a factor of approximately 2. As an example, if a detection limit for Pb of about 80 $\mu g\,g^{-1}$ is acceptable for an application, the ^{109}Cd spectrum count time can be reduced to 50 s.

Table 7 Guide to the Detection Limits That Can be Obtained in the Analysis of Soils Using Portable XRF Instrumentation

		Detection limits ($\mu g\, g^{-1}$)		
Source	Element	"Instrumental"[a] (siliceous matrix) (manufacturer's data)	"Working"[b] (silicate rock) (portable XRF)	Laboratory[c] ED-XRF (tube-excited) (silicate rock)
Fe-55	K	150	360	—
	Ca	70	225	—
	Ti	55	120	—
	V	50	49	—
	Cr	90	1080	—
Cd-109	Mn	200	354	—
	Fe	110	424	—
	Co	100	354	—
	Ni	65	116	12
	Cu	50	80	8
	Zn	40	63	7
	Ga	35	58	6
	Rb	5	13	3
	Sr	4	14	3
	Y	4	9	3
	Zr	3	9	3
	Nb	4	6	3
	Pb-L	15	39	7
Am-241	Ba-K	9	21	—
	La-K	8	—	—
	Ce-K	8	14	—

[a]Instrumental: 200 s count time per source on a siliceous matrix. (Spectrace TN9000 Manufacturer's data.)
[b]Working: 200 s count time per source on silicate rock powder pellets. (Data abstracted from Potts et al., 1995.)
[c]Laboratory ED-XRF: 800 s count time, Si(Li) detector, Ag tube excited. (From Potts and Webb, 1992.)

Although PXRF has a multielement capability, its application in the analysis of contaminated land depends on the detection limit of the technique in comparison with the trigger level, down to which concentrations of contaminants must be monitored. As a rule of thumb, the detection limit should be less than the trigger level by a factor of

MARCEL DEKKER, INC.
270 Madison Avenue, New York, New York 10016

Table 8 P-XRF Detection Limits ($\mu g\ g^{-1}$) for Various Toxic Elements of Environmental Interest Compared with UK Soil Guideline Values for the Specified Categories of Land Use

		UK soil guideline value			
Element	P-XRF detection limits	Residential with plant uptake	Residential without plant uptake	Allotments	Commercial and Industrial
As	60*	20	20	20	500
Cd	250*	1,2,8(*)	30	1,2,8(*)	1400
Cr(VI)	1080	130	200	130	5000
Hg (total)	80*	8	8	15	480
Ni	116	50	75	50	5000
Pb	39	450	450	450	750
Se	45*	35	460	35	8000

P-XRF detection limits: 200 s count time (* = estimated).
Cd(*): Cadminum values represent data for pH6, 7 and 8.
Cr: Assumes all Cr is Cr(VI).
Soil guideline values taken from the UK Government Department of the Environment, Foods and Rural Affairs (2002).

between 5 and 10. In Table 8, the most recent UK Government "soil guide line values" for the elements As, Cd, Cr(VI), Hg, Ni, Ph, and Se are listed, together with estimated detection limits by PXRF using a spectrum acquisition time of 200 s. The soil guideline values are listed from different forms of land use and indicate that in the monitoring of land used for residential purposes, PXRF has adequate sensitivity for the determination of Pb. In terms of land used for commercial and industrial purposes, PXRF has the potential to monitor all the elements in this table.

These data (Table 8) explain why one of the most popular applications of PXRF is in the analysis of Pb in contaminated soil, particularly associated with the remediation of soil at disused industrial sites or related to mining operations. As an example, Argyraki et al. (1997) undertook a comparison of field measurements of Pb by PXRF with laboratory analyses of soil samples recovered by auger at a medieval lead smelter site. After correcting the PXRF results for moisture content and surface irregularity effects, no significant bias was observed between the two techniques. In fact, in this application, the precision of results was dominated by sampling effects caused by the heterogeneous distribution of the analyte.

B. Analysis of Dust

The collection and analysis of airborne dust is becoming an increasingly important aspect of environmental monitoring, particularly in relation to concerns about air quality. Samples of interest include dust in the workplace (see, for example, Dost, 1996) and in urban environments, including fog and seaspray. One widely used method of collecting samples is to suck a calibrated volume of air through a filter and then to analyze the filter directly by XRF. From an analytical point of view, the two principal considerations are the nature of the sample deposited on the filter and the most appropriate method of preparing calibration samples.

The thickness of a sample that complies with thin film criteria varies significantly with the energy of fluorescence radiation (as well as the composition of the sample), as can be seen from data listed in Table 1. These data show that the maximum thickness varies from about 0.07 μm for Na Kα to 0.6–0.7 μm for Ca Kα, 2 to 3 μm for Fe, and > 15 μm for Rb Kα and above. Considering that the maximum size of a particle in suspension in air is generally regarded to be in the 6 to 10 μm range (with a continuum of lower sizes), it is unsafe to assume that thin film criteria will apply in the XRF determination of the lower atomic number elements.

Filters used for sampling dust are normally classified as membranous (usually made of PTFE or polycarbonate) or fibrous (usually made of quartz fibers). Fiber filters offer the advantage of a higher loading capacity, so that they can be used for sampling over extended periods with nearly constant air flow. Conversely, because their mass per unit area is higher, so is the XRF background. Furthermore, it is important that calibration samples should match the form and composition of filter samples, in particular for fiber filters in which the aerosol particles are deposited as a layer approximately 100 μm deep.

Turning now to the preparation of calibration samples, one simple method that has been widely used is to spot the filter material with standard solutions to represent the range of determinant loading expected in the samples to be analyzed. There are some limitations to this technique, since calibration samples prepared in this way will not match the mineralogy, particle size distribution, or filter loading of real samples. To overcome these difficulties, some effort has been put into the preparation of filter reference materials. As an example, Haupt et al. (1995) compared standard filter materials prepared by dropping multielement solutions onto quartz fiber filters and air drying with a sample prepared using an aerosol generator in which the dried aerosol was deposited onto the filter. Results indicated that the dropping technique was not applicable for fiber filters and achieved a lower accuracy in the calibration of light elements

[$Z < 30$ (Zn)]. The particular advantages of the aerosol deposition method were considered to be the provision of small particles and a homogeneous coating of the multielement filter sample. With careful matching of calibration samples, reliable data for the elements from Al to Zn could readily be determined.

C. Total Reflection XRF (TXRF) in Environmental Analysis

Although TXRF can achieve much lower detection limits than conventional XRF, the TXRF technique requires careful consideration of the form of sample preparation. Samples must be deposited onto a quartz glass (or Plexiglas) reflector and excited by a primary beam that is directed at the reflector at a grazing angle of incidence of $<0.1°$ (Sec. II.E). Fluorescence spectra are measured by an ED detector positioned above the reflector, which views a circular area of 6 to 8 mm diameter (Fig. 8). Provided the sample is sufficiently thin, matrix effects caused by attenuation of fluorescence within the sample can be ignored. As a consequence, the technique can be used most effectively to analyze either liquid samples, where typically 10 μL of solution is pipetted onto the reflector and evaporated to dryness, or alternatively pulverized material, where a few μg is placed on the reflector. Examples, based on the useful review of Klockenkämper and von Bohlen (1996) of three areas where the technique can be applied to the analysis of environmental samples, are as follows:

1. Water

Rainwater can be analyzed by TXRF by collecting about 100 mL of sample, spiking a 1 to 3 mL aliquot with a nitric acid-based standard solution containing a suitable internal standard spike (Co, Ga, or Y are often selected), and pipetting 50 to 100 μL onto the reflector, which must normally be covered with a hydrophobic film to prevent the liquid ‘‘bleeding’’ across the reflector surface. The liquid sample is allowed to dry using a hot plate or infrared lamp, leaving a solid residue of a few micrograms, which may be analyzed using count times of 100 to 200 s for up to 16 elements, with detection limits in the 1 to 2300 $ng\,mL^{-1}$ range. Lower detection limits, down to the $pg\,mL^{-1}$ level, can be achieved by freeze-drying a volume of, say, 10 mL of water. In the analysis of river and sea water, additional consideration must be given to the effect of high salt content, suspended material, and, in some cases, high organic content. Relevant schemes of analysis usually incorporate some form of separation procedure to avoid significant degradation in detection limits.

Marcel Dekker, Inc.
270 Madison Avenue, New York, New York 10016

2. Dust

TXRF is also effective in the analysis of dust samples. Dust can be removed from a conventional filter chemically (by dissolution) and physically (by ultrasonic disaggregation), and the mixture of dissolved and particulate material can be deposited on a reflector, together with an internal standard element for conventional analysis as above. Conversely, a more elegant procedure is to use a Plexiglas reflector as the collector plate in a cascade impactor sampling device. The Plexiglas must be coated with a thin layer of grease or oil (e.g., medical grade petroleum jelly) to ensure that the particulate material is not blown off nor is able to bounce off the collector plate. Detector limits down to the 0.1 ng level are expected in this application.

3. Plant and Vegetable Material

TXRF can also be used in the analysis of plant (and vegetable) material relevant to environmental investigations. A typical procedure would involve ashing or freeze-drying the sample and taking it into solution, using a nitric acid–pressure bomb digestion, for example. After adding an internal standard element, a suitable aliquot (e.g., 10 μL) can be pipetted onto a quartz reflector and analyzed by TXRF. Alternatively, it may be appropriate to undertake a chemical separation using chromatography techniques, whereby individual biologically active species can be isolated and analyzed by TXRF.

4. Soils and Sediments

In an interesting study of the heavy metal speciation in coastal sediments to assess environmental behavior, Battiston et al. (1993) undertook a five-stage selective extraction in order to determine the concentrations of elements of interest bound to, or associated with the following fractions: exchangeable, bound to carbonates, bound to iron and manganese hydroxides, bound to organic matter and residue (metals structurally bound in silicates), and determined the elements K, Ca, Ti, Mn, Fe, Ba, Rb, Cr, Cu, Sr, Zn, and Pb by TXRF using typical measuring times of 500 s. The procedure involved diluting a 100 μL solution of the extracted fraction to 10 mL, adding 20 μL of internal standard element solution (Co) and transferring 10 μL of the final solution onto a siliconized quartz sample carrier prior to vacuum drying. TXRF was considered to offer a convenient method for the determination of a large number of elements at high sensitivity. This method illustrates how, in principle, TXRF can be used to characterize the bioavailability of elements in both soil and sediment samples.

D. SYNCHROTRON RADIATION APPLICATIONS

As summarized in Sec. II.F, synchrotron radiation offers high intensity, low divergence, and a polarized excitation source that can be exploited in two ways. First, because of the polarized nature (and high intensity) of the source, significant suppression of the scattered background occurs in detected fluorescence spectra, so the technique is particularly suited to trace element determination in small sample masses. Secondly, synchrotron x-rays can readily be coupled to focusing optics to form an x-ray microprobe, capable of providing spatially resolved XRF analyses on a lateral scale of 1 to 15 μm. A further consideration of relevance to the direct analysis of biological material is that energy transfer to the sample during the x-ray excitation process is much smaller than competitive microbeam techniques, so that beam damage is correspondingly diminished. An overview of applications has been presented by Smith and Rivers (1995). The following paragraphs serve to illustrate the analytical capabilities of these two types of measurement.

1. The Bulk Analysis of Lake Sediment

An example of the use of synchrotron radiation XRF to determine trace elements in bulk samples of sediment core was presented by Trounova et al. (1996). Measurements were undertaken on the VEPP-3 synchrotron storage ring (Novosibirsk), and the polychromatic synchrotron radiation beam was diffracted off a pyrolytic graphite or Si(111) crystal, which served as a monochromator. In this way, the energy of the x-ray beam exciting the sample could be adjusted to values in the range 3 to 48 keV to permit selective (and optimized) excitation of the K lines of elements from K and Ca to Ba, La, Ce, and Nd. The sediment core sample was dried and 36 g aliquots were pressed into 10 mm diameter pellets in preparation for analysis. Using count times of 100 to 1000 s, detection limits in the range 1 to 2 $\mu g\, g^{-1}$ could be achieved for elements such as Rb, Sr, Y, Zr, Nb, Ba, La, Ce, and Nd. The aim of this work was to evaluate the homogeneity of the above elements with depth in the core for characterizing geological events.

2. Synchrotron X-Ray Microprobe

Similar advantages to those described above can also be achieved using a synchrotron for x-ray microprobe analysis. One simple way of forming an x-ray microprobe is to use a pinhole. More sophisticated methods can be used to focus the x-ray beam and take advantage of enhanced intensities that will then be obtained. Focusing devices normally make use

Marcel Dekker, Inc.
270 Madison Avenue, New York, New York 10016

of total reflection phenomena that occur when an x-ray beam is directed at a precisely shaped "mirror" substrate at an angle of incidence of a few milliradians (as in TXRF) or diffracted off a silicon crystal or multilayer device. In this way, the x-ray probe can be focused down to diameters of 1 to 20 μm. In the Kirkpatrick–Baez arrangement, two spherical "mirrors" are arranged to intercept the x-ray beam at grazing incidence in orthogonal configuration (Fig. 17). Alternatively, a single ellipsoidal mirror can be used as the focusing device, based on total reflection from a platinum-coated substrate or diffraction off a precisely curved silicon crystal. Each device has different excitation characteristics, particularly in the range of energies (bandwidth) transmitted to the sample.

Owing to radiation hazards, these microprobe devices must be mounted in an experimental "hutch" to shield operators from significant radiation doses. The sample must be observed remotely using a video camera system in conjunction with remote control of the movement of the sample holder. When used as an x-ray microprobe, the lateral footprint of the x-ray beam is controlled by the focusing optics. However, analysis depth is controlled by the critical penetration depth of the fluorescence x-ray of interest, which may, in the case of the standard thin section, be greater than the specimen thickness. These considerations allow the x-ray microprobe to be used, for example, in the analysis of fluid inclusions trapped beneath the surface of the sample, but careful consideration is needed when interpreting data from solid samples, taking into account the depth of the analyzed volume. The particular advantage in the analysis of biological samples

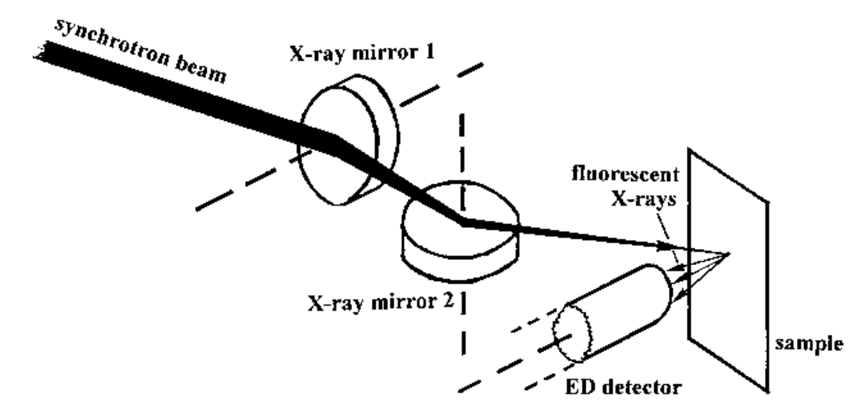


Figure 17 Synchrotron x-ray microprobe in which the x-ray microprobe is formed by reflection at grazing incidence off two spherical mirrors in the Kirkpatrick–Baez configuration. (Based on Smith and Rivers, 1995.)

Marcel Dekker, Inc.
270 Madison Avenue, New York, New York 10016

concerning low-energy transfer has already been mentioned. The synchrotron x-ray microprobe has also been used to analyze sediments, fly ash particulates, urban particulates, and aspects of the environmental chemistry of nuclear waste disposal. These and other applications are discussed by Smith and Rivers (1995).

VI. CONCLUSIONS

Although x-ray fluorescence analysis is an old and well-established technique, it continues to find widespread use in the analysis of soils and other environmental samples. One reason for the continuing popularity of the technique is the simple sample preparation, since materials are normally analyzed in the solid state. Another is the wide range of elements that can be determined to a uniformly high sensitivity. Perhaps one of the most significant drawbacks of the technique is that it is not possible to determine *directly* some of the environmentally important elements such as Cd, Hg, and Se. XRFS is also not usually the technique of choice for the analysis of liquids or solid samples that have to be taken into solution, although there are important environmental applications of total reflection XRF, where advantage can be taken of the very high sensitivity and multielement capability in the analysis of samples deposited on quartz, or Plexiglas, reflector plates.

Although XRFS is a very well established technique, new analytical capabilities continue to result from modern developments in materials and technology. Thus, although conventional WD-XRF instrumentation has a clear role in the modern environmental laboratory, new opportunities have arisen in the use of polarized excitation geometries (based on Barkla scatter) and portable instrumentation. In terms of the degree of sophistication, it is hard to beat synchrotron radiation application, especially the capabilities of the synchrotron x-ray microprobe. X-ray fluorescence is, therefore, a technique that has not only withstood the test of time but is also moving into new applications as advances in technology permit the capabilities of instrumentation to be extended.

REFERENCES

Ahmedali, S.T., ed. 1989. *X-Ray Fluorescence Analysis in the Geological Sciences: Advances in Methodology*. *Short Course*, Vol. 7, Geological Association of Canada.

Andermann, G. and Kemp, J.W. 1958. Scattered X-rays as internal standards in X-ray emission spectroscopy. *Anal. Chem.* 30:1306–1309.

Argyraki, A., Ramsey, M.H. and Potts, P.J. 1997. Evaluation of portable x-ray fluorescence instrumentation for *in situ* measurements of lead on contaminated land. Analyst 122:743–749.

Battiston, G.A., Gerbasi, R., Degetto, S. and Sbrignadello, G. 1993. Heavy metal speciation in coastal sediments using total-reflection X-ray fluorescence spectrometry. *Spectrochim. Acta* 48B:217–221.

Bennett, H. and Oliver, G.J. 1992. *XRF Analysis of Ceramics, Minerals and Allied Materials*. John Wiley, Chichester, England.

Bertin, E.P. 1975. *Principles and Practice of X-Ray Spectrometric Analysis*. (2d ed.). Plenum Press, New York.

Hill, S.J., Arowolo, T.A., Bulter, O.T., Cook, J.M., Cresser, M.S., Harrington, C. and Miles, D.L. 2003. Atomic Spectrometry Update. Envirnomental Analysis. *J. Anal. Spectrom.* 18:170–202.

Chappell, B.W. 1991. Trace element analysis of rocks by X-ray spectrometry. *Adv. X-Ray Anal.* 34:263–276.

Cohen, L.H. and Smith, D.K. 1989. Thin-specimen X-ray fluorescence analysis of major elements in silicate rocks. *Anal. Chem.* 61:1837–1840.

Criss, J.W. and Birks, L.S. 1968. Calculation methods for fluorescent X-ray spectrometry. *Anal. Chem.* 40:1080–1086.

De Jongh, W.K. 1973. X-ray fluorescence analysis applying theoretical matrix corrections. Stainless steels. *X-ray Spectrom.* 2:151–158.

De Jongh, W.K. 1979. The atomic number $Z = 0$: loss and gain on ignition in XRF analysis treated by the JN-equation. *X-Ray Spectrom.* 8:52–56.

UK Government Department of the Environment, Food and Rural Affairs and the Environment Agency 2002. An overveiw of the development of soil guideline values and related research, CLR7.

Dost, A.A. 1996. Monitoring surface and airborne inorganic contamination in the workplace by a field portable X-ray fluorescence spectrometer. *Annals Occupat. Hyg.* 40:589–610.

Hallett, B.R. and Kyle, P.R. 1993. XRF and INAA determinations of major and trace elements in Geological Survey of Japan igneous and sedimentary rock standards. *Geostand. Newlett.* 17:127–133.

Haupt, O., Klaue, B., Schaefer, C. and Dannecker, W. 1995. Preparation of quartz fiber filter standards for X-ray fluorescence analysis of aerosol samples. *X-Ray Spectrom.* 24:267–275.

Heckel, J., Brumme, M., Weinert, A. and Irmer, K. 1991. Multielement trace analysis of rocks and soils by EDXRF using polarized radiation. *X-Ray Spectrom.* 20:287–292.

Hower, J. 1959. Matrix correction in the X-ray spectrographic trace element analysis of rocks and minerals. *Am. Min.* 44:19–32.

Jenkins, R. 1976. *An Introduction to X-Ray Spectrometry*. Heyden, London.

Jenkins, R., Manne, R., Robin, R. and Senemaud, C. 1991. Part VIII. Nomenclature system for X-ray spectrometry. *X-Ray Spectrom.* 20:149–155.

Jenkins, R., Gould, R.W. and Gedcke, D. 1995. *Quantitative X-Ray Spectrometry*. (2d ed.). Marcel Dekker, New York.

Klockenkämper, R. and von Bohlen, A. 1996. Elemental analysis of environmental samples by total reflection X-ray fluorescence: A review. *X-Ray Spectrom*. 25:156–162.

Lachance, G.R. and Claisse, F. 1995. *Quantitative X-Ray Fluorescence Analysis: Theory and Application*. John Wiley, Chichester, England.

Lachance, G.R. and Traill, R.J. 1966. A practical solution to the matrix problem in X-ray analysis. *Can. Spectrosc*. 11:(Part I)43–48; (Part II)63–71.

Lupton, D.F., Merker, J. and Schoelz, F. 1997. The correct use of platinum in the XRF laboratory. *X-Ray Spectrom*. 26:132–140.

Moseley, H.G.J. 1913. The high frequency spectra of the elements. *Phil. Mag*. 26:1024–1034.

Moseley, H.G.J. 1914. The high frequency spectra of the elements II. *Phil. Mag*. 27:703–714.

Potts, P.J. 1987. Chapters 8 and 9. In: *A Handbook of Silicate Rock Analysis*. Blackie, Glasgow, 226–325.

Potts, P.J. 1993. Laboratory methods of analysis. In: Riddle, C., ed. *Analysis of Geological Materials*. Marcel Dekker, New York.

Potts, P.J. and Webb, P.C. 1992. X-ray fluorescence spectrometry. *J. Geochem. Explor*. 44:251–296.

Potts, P.J., Webb, P.C. and Watson, J.W. 1984. Energy dispersive X-ray fluorescence analysis of silicate rocks for major and trace elements. *X-Ray Spectrom*. 13:2–15.

Potts, P.J., Tindle, A.G. and Webb, P.C. 1992. *Geochemical Reference Material Compositions*. Whittles/CRC Press, Caithness/Boca Raton.

Potts, P.J., Webb, P.C., Williams-Thorpe, O. and Kilworth, R. 1995. Analysis of silicate rocks using field-portable X-ray fluorescence instrumentation incorporating a mercury (II) iodide detector: a preliminary assessment of analytical performance. *Analyst* 120:1273–1278.

Potts, P.J., Webb, P.C. and Williams-Thorpe, O. 1997. Investigation of a correction procedure for surface irregularity effects based on scatter peak intensities in the field analysis of geological and archaeological rock samples by portable X-ray fluorescence spectrometry. *J. Anal. Atomic Spectrom*. 12:769–776.

Potts, P.J., Ellis, A.T., Kregsamer, P., Marshall, J., Streli, C., West, M. and Wobrauschek, P. 2002. X-ray fluorescence spectrometry. *J. Anal. Atomic Spectrom*. 17:1439–1455.

Reynolds, R.C. 1963. Matrix corrections in trace element analysis by X-ray fluorescence: estimation of the mass absorption coefficient by Compton scattering. *Am. Min*. 48:1133–1143.

Reynolds, R.C. 1967. Estimation of mass absorption coefficients by Compton scattering: improvements and extensions of the method. *Am. Min*. 52: 1493–1502.

Rousseau, R.M. 1984a. Fundamental algorithm between concentration and intensity in XRF analysis. 1. Theory. *X-Ray Spectrom*. 13:115–120.

Rousseau, R.M. 1984b. Fundamental algorithm between concentration and intensity in XRF analysis. 2. Practical contribution. *X-Ray Spectrom*. 13: 121–125.

Schwenke, H. and Knoth, J. 1993. Total reflection XRF. Chapter 9. In: Van Grieken, R.E. and Markowicz, A.A., eds. *Handbook of X-Ray Spectrometry*. Marcel Dekker, New York, p. 459.
Sherman, J. 1955. The theoretical derivation of fluorescent X-ray intensities from mixtures. *Spectrochim. Acta* 7:283–306.
Sherman, J. 1958. The theoretical derivation of the composition of mixable specimens from fluorescent X-ray intensities. *Adv. X-Ray Anal.* 1: 231–251.
Shiraiwa, T. and Fujino, N. 1966. Theoretical calculation of fluorescent X-ray intensities in fluorescent X-ray spectrochemical analysis. *Japanese J. Appl. Phys.* 5:886–899.
Shiraiwa, T. and Fujino, N. 1974. Theoretical correction procedures for X-ray fluorescence analysis. *X-ray Spectrom.* 3:64–73.
Smith, J.V. and Rivers, M.L. 1995. Synchrotron X-ray microanalysis. In: Potts, P.J., Bowles, J.F.W., Reed, S.J.B. and Cave, M.R. eds. *Microprobe Techniques in the Earth Sciences*. Chapman and Hall, London, pp. 163–233.
Szaloki, I., Török, S.B., Injuk, J. and Van Grieken, R.E. 2002. X-ray spectrometry. *Anal. Chem.* 74:2895–2917.
Tertian, R. and Claisse, F. 1982. *Principles of Quantitative X-Ray Fluorescence Analysis*. Heyden, London.
Traill, R.J. and Lachance, G.R. 1965. A new approach to X-ray spectrochemical analysis. *Geological Survey of Canada Professional Paper* 64–87.
Trounova, V.A., Bobrov, V.A. Zolotarev, K.V. and Pampura, V.D. 1996. Synchrotron radiation X-Ray fluorescence study of the compositional homogeneity of a sediment core from Lake Baikal. *X-ray Spectrom.* 25:55–59.
Van Grieken, R.E. and Markowicz, A.A., eds. 1993. *Handbook of X-Ray Spectrometry*. Marcel Dekker, New York.
Watson, J.S. 1996. Fast, simple method of powder pellet preparation for X-ray fluorescence analysis. *X-Ray Spectrom.* 25:173–174.
Willis, J.P. 1989. Compton scatter and matrix correction for trace element analysis of geological materials. In: Ahmedali, S.T., ed. *X-Ray Fluorescence Analysis in the Geological Sciences: Advances in Methodology*. *Short Course*, *Vol. 7*. Geological Association of Canada.
Willis, J.P. 1991. Mass absorption coefficient determination using Compton scattered tube radiation: applications, limitations and pitfalls. *Adv. X-Ray Anal.* 34:243–261.
Wilson, P., Cooke, M., Cawley, J., Giles, L. and West, M. 1995. Comparison of the determination of copper, nickel and zinc in contaminated soil by X-ray fluorescence spectrometry and inductively coupled plasma spectrometry. *X-Ray Spectrom.* 24:103–108.
Winick, H., ed. 1994. *Synchrotron Radiation Sources—A Primer*. World Scientific, Singapore.

Marcel Dekker, Inc.
270 Madison Avenue, New York, New York 10016

8

Measurement of Radioisotopes and Ionizing Radiation

Olivia J. Marsden and Francis R. Livens
The University of Manchester, Manchester, England

I. INTRODUCTION

Approximately 1700 different isotopes are known, of which around 275 are stable. The remainder are radioactive; that is, their nuclear configurations are unstable and can change to more stable forms by nuclear transformations that are collectively known as radioactive decay. These radioactive decay processes are accompanied by the emission of particles and/or photons from the nucleus. Isotopes (or *nuclides*) are distinguished by the number of protons and neutrons (collectively known as nucleons) they contain and are commonly designated using mass number (A: number of protons + neutrons) and atomic number (Z: number of protons). For example, $^{14}_{6}C$ is an isotope of carbon in which the nucleus contains 14 nucleons, of which six are protons. The proton number defines the chemical identity of the atom, since the proton charge must be balanced by the appropriate number of electrons, but it also duplicates the information provided by the chemical symbol and, in practice, is often omitted, hence ^{14}C. Differences in the neutron number may control the stability, or otherwise, of a nucleus but have only subtle effects on chemistry, although these can be exploited in studies of stable isotope fractionation in natural systems, for example $^{2}H/^{1}H$, $^{13}C/^{12}C$, $^{15}N/^{14}N$, $^{17}O/^{16}O$, $^{34}S/^{32}S$ (see Chap. 9).

Only a minority of the unstable isotopes are formed in nature. Most are man-made, and the majority of these are available only in such small amounts, or are so short-lived or both, that they are unlikely to be

Marcel Dekker, Inc.
270 Madison Avenue, New York, New York 10016

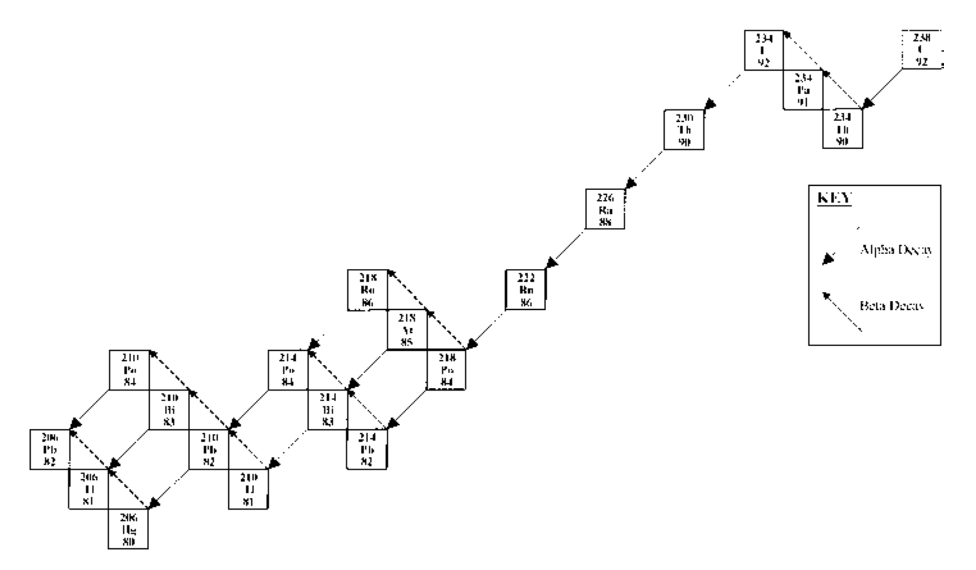


Figure 1 Isotopes produced by the decay of ^{238}U.

encountered in the environment or to be of any use as radiotracers. The naturally occurring radioisotopes fall into three groups:

1. Primordial isotopes that have existed since the formation of the Earth about 4.5×10^9 years ago. These have half-lives (see later) comparable to the age of the Earth, that is, in the range 10^8 to 10^{12} yr. Examples include ^{235}U ($t_{1/2}$ 7.5×10^8 yr) and ^{138}La ($t_{1/2}$ 1.35×10^{11} yr).
2. Short-lived isotopes formed by the decay of long-lived parents. These have widely varying half-lives, ranging from 3×10^{-7} s (^{212}Po) to 2.4×10^5 yr (^{234}Pa) and are constantly being formed by decay of the parent isotope and removed by their own decay. In many cases, these isotopes form part of long decay series, in which multiple transformations occur before a stable nucleus is reached. An example is the decay of ^{238}U through a sequence of 14 α- and β-decay steps to the stable isotope ^{206}Pb (Fig. 1).
3. Short-lived isotopes formed constantly by nuclear reactions in the atmosphere and transported to the Earth's surface by atmospheric mixing and wet and dry deposition. Examples include ^{3}H ($t_{1/2}$ 12.3 yr), ^{7}Be ($t_{1/2}$ 53.4 d), and ^{14}C ($t_{1/2}$ 5736 yr).

The exploitation of nuclear reactions in nuclear weapons and nuclear power, and the use of radioisotopes in industrial and medical applications, has led to the global dispersion of radioisotopes. Some of these are also formed to a significant extent in nature (for example, ^{3}H and ^{14}C) but many are not (examples include ^{239}Pu, ^{237}Np, ^{137}Cs, ^{125}I, ^{129}I, ^{35}S).

II. THEORY OF RADIOACTIVITY

A. Nuclear Stability

The phenomenon of radioactivity originates in the instability of some nuclear configurations. Very simply, for a nucleus to remain intact, the Coulomb repulsion arising from the interaction of the protons must be less than the "strong" attractive force between all nucleons. Thus the forces arising from the presence of protons in the nucleus have both attractive and repulsive components, whereas those arising from the presence of neutrons are predominantly attractive. The balance between attractive and repulsive forces controls nuclear stability and is dependent on the neutron/proton ratio in the nucleus. In the lightest nuclei, up to about $A = 40$, a neutron/proton ratio of about 1.0 is adequate for stability, but beyond this point, the Coulomb repulsion for each extra proton rises faster than the attractive force for each extra neutron, and so the neutron/proton ratio needed for stability increases progressively up to a value of about 1.5 in ^{209}Bi, the heaviest stable nucleus. Nuclei with an unstable nuclear configuration (i.e., with an imbalance of protons or neutrons) can move toward stability by changing the neutron/proton ratio.

The most common route toward stability is the transformation of a neutron into a proton (for a neutron-rich nucleus) or of a proton into a neutron (for a proton-rich nucleus). There are three ways in which this can occur and these are collectively known as beta decay processes. In the neutron-rich nuclei, the reaction:

$$^1_0\mathrm{n} \rightarrow {}^1_1\mathrm{p}^+ + {}^{\;\,0}_{-1}\mathrm{e}^-$$

occurs, with the electron (negatron) being ejected from the nucleus. Note that, in this reaction, A remains the same, while Z increases by 1, so that, in general, in this type of decay,

$$^A_Z\mathrm{M} \rightarrow {}_{Z+1}^{\;\;\;A}\mathrm{N} + {}^{\;\,0}_{-1}\mathrm{e}^-$$

A specific example is that of ^{90}Sr:

$$^{90}_{38}\mathrm{Sr} \rightarrow {}^{90}_{39}\mathrm{Y} + {}^{\;\,0}_{-1}\mathrm{e}^-$$

In proton-rich nuclei, the reverse reaction may occur:

$$^1_1\mathrm{p}^+ \rightarrow {}^1_0\mathrm{n} + {}^0_1\mathrm{e}^+$$

The positively charged particle (positron) emitted in this case is identical to an electron in all respects except its charge, which is equal in magnitude to that of the electron but positive in sign.

In general, in positron emission,

$$^{A}_{Z}\mathrm{M} \rightarrow {}^{A}_{Z-1}\mathrm{N} + {}^{0}_{1}\mathrm{e}^{+}$$

An example of this type of decay is that of ^{11}C:

$$^{11}_{6}\mathrm{C} \rightarrow {}^{11}_{5}\mathrm{B} + {}^{0}_{1}\mathrm{e}^{+}$$

The negatron and positron are sometimes denoted β^{-} and β^{+} respectively. An alternative way of converting a proton into a neutron is for orbital electron capture to occur:

$$^{1}_{1}\mathrm{p}^{+} + {}^{0}_{-1}\mathrm{e}^{-} \rightarrow {}^{1}_{0}\mathrm{n}$$

No particles are emitted in this reaction. Since the captured electron originates in one of the inner orbitals, usually the K shell, electron capture is often referred to as K capture. An example of this decay type is

$$^{182}_{77}\mathrm{Ir} + {}^{0}_{-1}e^{-} \rightarrow {}^{182}_{76}\mathrm{Os}$$

In the heaviest nuclei, alternative decay modes may be observed. Alpha decay is characteristic of neutron-rich nuclei with $A > 209$ and of a small number of lanthanide isotopes. In this decay mode, a helium nucleus (or α-particle) is ejected from the parent nucleus:

$$^{A}_{Z}\mathrm{M} \rightarrow {}^{A-4}_{Z-2}\mathrm{N} + {}^{4}_{2}\mathrm{He}^{2+}$$

An example is the decay of ^{239}Pu:

$$^{239}_{94}\mathrm{Pu} \rightarrow {}^{235}_{92}\mathrm{U} + {}^{4}_{2}\mathrm{He}^{2+}$$

Spontaneous fission is an alternative decay mode found in some of the heaviest known isotopes. Many of these decay by both α-emission and spontaneous fission to varying degrees (e.g., ^{252}Cf: 96.9% by α, 3.1% by spontaneous fission).

Marcel Dekker, Inc.
270 Madison Avenue, New York, New York 10016

B. Gamma Ray Emission

Both α- and β-decay processes may proceed via one or more excited states of the product nucleus, although transitions directly to the product ground state do occur and indeed are the dominant transitions in a number of important isotopes (e.g., ^{3}H, ^{14}C, ^{32}P, ^{35}S, ^{90}Sr, ^{241}Pu). Where the first decay product is an excited state, this can de-excite to the ground state by a number of mechanisms. The most important of these is the emission of one or more photons of electromagnetic radiation, which are known as γ-rays. These photons are characterized by high energies (typically 40 to 2000 keV), and the energy with which they are emitted is that separating the nuclear states between which the γ-transition has occurred. In most cases, the transition from excited to ground state occurs unmeasurably fast and is effectively coincident with the accompanying α- or β-decay event. However, in some cases, the excited states have measurable lifetimes, in which case they are known as "nuclear isomers" or "metastable states." One of the best known of these is ^{110m}Ag ($t_{1/2}$ 249.9 d), which was released in significant quantities during the Chernobyl reactor accident.

It is important to recognize that, because there may be a variety of routes from parent ground state to product ground state, the decay of a particular isotope may be accompanied by the emission of photons with a number of different energies and also that not all decay events lead to the emission of a γ-photon of a particular energy (or indeed any γ-photons at all). The proportion of decays that lead to a particular γ-transition is known as the "abundance" and is usually expressed as a percentage. Thus the α-decay of ^{241}Am proceeds directly to the ^{237}Np ground state in 65% of cases and via an excited state at 59.5 keV in the remaining 35%. De-excitation takes place in one step, so ^{241}Am is described as an α-emitter giving a 59.5 keV γ-ray with 35% abundance.

C. Decay Energies

Since all radioactive decay events arise as an unstable nucleus moves toward a more stable (i.e., lower energy) state, the energy difference between the initial and final states has to be dissipated during the decay process. Both initial and final nuclear states are of well defined energies, and it is easy to calculate the total expected decay energy. Where the product nucleus is formed in a nuclear excited state, which subsequently de-excites to the ground state (see above), the decay energy corresponds to the gap between initial and excited product states.

In α-decay processes, the energy associated with the transition from parent to product states is almost all dissipated as kinetic energy associated

with the α-particle. The product nucleus has some recoil energy, but conservation of momentum and the usually much larger mass of the product nucleus leave the α-particle with the majority of the kinetic energy. For example,

$$^{238}_{92}\mathrm{U} \rightarrow \, ^{234}_{90}\mathrm{Th} + \, ^{4}_{2}\mathrm{He}^{2+}$$

Since momentum before decay is approximately 0, momentum after decay is approximately 0 as well. Thus

$$M_{\mathrm{d}} v_{\mathrm{d}} = M_{\alpha} v_{\alpha} \tag{1}$$

where d and α denote daughter and α, respectively and

$$\frac{v_{\alpha}}{v_{\mathrm{d}}} = \frac{M_{\mathrm{d}}}{M_{\alpha}} = \frac{234}{4} = 58.5 \tag{2}$$

The ratio of the kinetic energies $E_{\mathrm{d}}/E_{\alpha}$ is thus

$$\frac{234 \times (1)^2}{4 \times (58.5)^2} = 0.017$$

In other words, the α-particle carries away 98% of the decay energy as its kinetic energy.

When they were first discovered, β-decay processes were difficult to interpret in this way since the particles are emitted with a range of energies from effectively zero up to a maximum value characteristic of a particular isotope (E_{max}). It was difficult to reconcile the emission of particles with a spectrum of energies with their supposed origin in transitions between well-defined, quantized energy levels. When the existence of the neutrino was proposed in 1927, this paradox was resolved, although the neutrino was not detected experimentally until 1953. The neutrino is a particle with zero rest mass, which is also formed during a positron or negatron emission and which carries away a variable proportion of the total decay energy. Thus the decay energy is the sum of neutrino and β-particle energies. Where the β-particle energy is zero, all the decay energy is removed by the neutrino, and conversely when the β-particle energy is equal to E_{max} the neutrino energy is zero.

D. Quantitative Treatment of Radioactive Phenomena

For any given isotope, the rate of radioactive decay (the activity, denoted A) is proportional only to the number of atoms present in the source, denoted N. Thus if one compares the α-count rate from a 1 ng source of ^{241}Am with that from a 2 ng source under identical conditions, the first count rate will be half the second. The activity is related to the number of atoms present by the decay constant, λ, which has units of time^{-1} i.e.

$$A = N\lambda \tag{3}$$

The SI unit of activity is the Becquerel (Bq), which is equal to 1 disintegration per second. Thus a 1 ng source of ^{241}Am, which has a decay constant of 1.600×10^{-3} yr^{-1} ($= 5.07 \times 10^{-11}$ s^{-1}), will have an activity of

$$\frac{10^{-9}}{241} \times 6.022 \times 10^{23} \times 5.07 \times 10^{-11} = 126\,\text{Bq}$$

Since the activity depends only on the number of atoms present and the decay constant characteristic of that isotope, repeated measurement of a radioactive source's activity will show a decrease in count rate with time, since the decay process is removing atoms, and the fewer the atoms present, the lower the activity. The activity follows first-order kinetics and can be described by a simple exponential function:

$$A_t = A_0 e^{-\lambda t} \tag{4}$$

where A_t = activity at time t, A_0 = initial activity, and t = time elapsed, or more usefully,

$$\ln A_t = \ln A_0 - \lambda t \tag{5}$$

Clearly, since A is proportional to N, $N_t = N_0 e^{-\lambda t}$. After 1000 years, the activity of our 1 ng of ^{241}Am will therefore have fallen from its initial value of 126 Bq to 25 Bq.

We can also characterize a radioactive isotope by the time required for half of the atoms originally present to decay (or for a source's initial activity to fall to 50% of the initial value). This time is known as the half-life and is denoted $t_{1/2}$. It is straightforward to demonstrate the relationship between

Marcel Dekker, Inc.
270 Madison Avenue, New York, New York 10016

λ and $t_{1/2}$. After one half-life has elapsed, a source's activity will have fallen from A_0 to $A_0/2$, thus

$$\frac{A_0}{2} = A_0 e^{-\lambda t_{1/2}} \tag{6}$$

so

$$t_{1/2} = \frac{\ln 2}{\lambda} = \frac{0.693}{\lambda} \tag{7}$$

and for our ^{241}Am example, $t_{1/2} = 433$ years.

E. Radioactive Decay Series

The simplest example of a radioactive decay is a one-step transformation of a radioactive parent into a stable product nucleus, for example ^{14}C:

$$^{14}_{6}\mathrm{C} \rightarrow \ ^{14}_{7}\mathrm{N} + \beta^-$$

However, in many cases. e.g., ^{238}U, ^{235}U, ^{232}Th, there are multiple decays before a stable product nucleus is reached. The decay scheme of ^{238}U has been illustrated in Fig. 1 as an example. In this, and in the corresponding schemes of ^{235}U and ^{232}Th, the decay of the long-lived parent isotope generates shorter-lived isotopes. These short-lived isotopes may be radiologically significant (e.g., ^{220}Rn and ^{222}Rn), or they may be exploitable as tracers (e.g., ^{210}Pb, ^{234}U, ^{234}Pa) in natural systems.

The number of atoms of any of these short-lived isotopes which is formed depends on the balance between the production rate (i.e., the decay of the parent) and the removal rate (i.e., the decay of the product). The mathematical relationships between the activities of different members of the natural decay series were first derived by Bateman (1910) and are discussed in Choppin et al. (1995). Three cases can be identified, depending on the half-lives of the parent and product isotopes.

The most important in the environmental context, and the only one discussed here, is that where a long-lived parent decays to a short-lived product ("secular equilibrium"). If we isolate an isotopically pure sample of the parent isotope, its decay starts to form the product isotope immediately. Initially, the production rate ($= N_{\mathrm{parent}}\lambda_{\mathrm{parent}}$) is greater than the removal rate ($= N_{\mathrm{product}}\lambda_{\mathrm{product}}$), so that the product isotope activity increases with time. Eventually, the situation is reached where production is balanced by

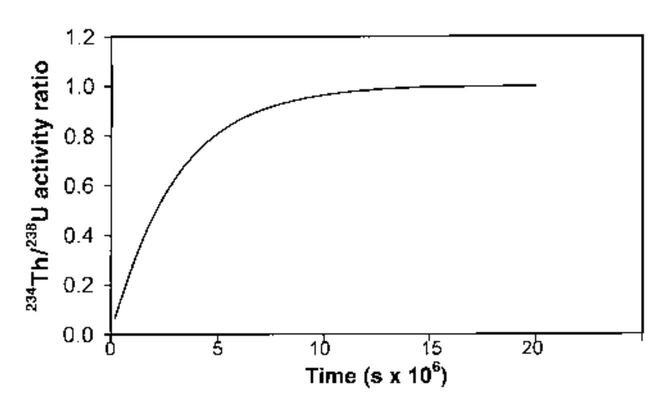


Figure 2 Ingrowth of ^{234}Th in ^{238}U to reach secular equilibrium.

removal, at which point the product isotope activity is said to be in a "steady state" or "secular equilibrium". An example is provided by the production of ^{234}Th ($t_{1/2}$ 24.1 days) from the α-decay of ^{238}U. The change in the ^{234}Th activity with time in an initially isotopically pure source of ^{238}U is illustrated in Fig. 2.

III. MEASUREMENT OF RADIOACTIVITY

A. Interaction of Radiation with Matter

The particles and photons emitted during radioactive decay processes and nuclear reactions are, in general, highly energetic, with energies in the range keV to MeV. These are much greater than the energies typically associated with chemical reactions, where only a few eV are needed to make or break a chemical bond. As a result, the particles and photons are capable of breaking large numbers of chemical bonds or generating a large number of atoms in excited states during their passage through matter, often forming ions and/or free radical species. These processes allow ionizing radiations to be detected very efficiently.

The rate of dissipation of energy (linear energy transfer or LET) is an indicator of the efficiency with which a particle or photon loses its kinetic energy during passage through a medium. Different particles and photons have very different LET values; for example, the LET for α-particles in air is of the order of 1 MeV cm^{-1}, while that for γ-photons of moderate energy (about 500 keV) in air is around 1 keV cm^{-1}. These very different characteristics lead to the use of different types of detectors to measure the different types of radiation even though the vast majority of detectors

measure the ionization or excitation induced by passage of a particle or photon.

B. Nucleonics

The majority of radiation detectors rely on the interaction of the radiation with the detector medium, which may be a suitable solid, liquid, or gas, and the generation of a measurable electrical signal. This may be generated indirectly, for example through the stimulation of light (visible or UV) emissions, which are converted to electrical impulses, or it may be stimulated directly. Most measurement systems also include amplifiers to boost the often small output from the detectors; analog-to-digital converters (ADCs) to convert the amplifier outputs into digital signals; and data acquisition devices. These may be multichannel analyzers (MCAs, also known as pulse height analyzers, PHAs), where appropriate, which display the output data as a histogram of channel number on the x-axis (proportional to photon or particle energy) against number of counts (proportional to emission intensity), or they may be simpler scalers that just measure the total number of signals. A key parameter in the measurement of detector performance is the energy resolution, that is, the sharpness of the signals generated, which is usually expressed in terms of the full width at half maximum (FWHM), although full width at tenth maximum values are sometimes quoted as well. The other parameter of general importance is the detection efficiency, that is, the probability of a particle or photon being detected. Other parameters can also be defined, for example peak : Compton intensity ratios in γ-spectroscopy, or figures of merit in liquid scintillation counting.

The use of MCAs allows the accumulation of energy-resolved spectra, which is particularly useful in α- and γ-spectroscopies and in some types of β-counting. Accurate timing is, obviously, essential in measuring count rates, and much modern instrumentation is based around personal computers, which are readily adapted to data acquisition and can run the computer programs needed to collect and analyze what can sometimes be complex data.

C. Detectors

It is probably best to describe each counting technique in turn, since many are adaptable to the measurement of more than one radiation type. Table 1 contains a summary of the techniques that can be used to measure different radiations either in the field or in environmental samples.

Marcel Dekker, Inc.
270 Madison Avenue, New York, New York 10016

Table 1 Summary of Principal Radiation Types and Detection Methods

	Radiation type		
Detector type	Alpha	Beta	Gamma
Gas counters	possible but unusual	common	possible, esp. portable Geiger detectors
Surface barrier and related detectors	common	possible	
Ge(Li), HPGe, Si(Li) semiconductors, NaI(Tl) scintillators			common
Plastic or ZnS(Ag) scintillators	in portable monitors	common	common
Liquid scintillation counters	possible, esp. using PERALS	common	

1. Gas-Filled Counters

Gas-filled counters detect the ionization of a gas contained within the detector and are best used for quantitative measurement of β-particles, although portable instruments can be used to measure combined β,γ-radiation fields. Such detectors have relatively limited use in quantitative γ-ray measurement, since they have small volumes, and the probability of complete deposition of γ-photon energy in the sensitive volume of the detector is relatively low. The gas-filled counters are among the simplest detection devices and have now been used for over 80 years, The Geiger–Müller and proportional counters are technically very similar, consisting of a gas-filled tube with a central axial anode. A potential difference is maintained between the anode and a cathode, and the detector can operate in either ‘‘proportional’’ or ‘‘Geiger–Müller’’ mode, depending on the applied voltage. The ionizing radiations can enter the tube through a thin mica window on the end of the tube or through a thin glass side wall of the tube, although both attenuate the particle or photon energies. Low-energy (<200 keV) β-particles can be measured using windowless gas-flow detectors, in which the fill gas flows through and is constantly replenished.

At relatively low applied voltages (200 to 600 V), the incident radiation ionizes the detector fill gas and the electrons formed are collected at the central anode. The number of electrons released is directly proportional to the energy dissipated in the detector, so the charge collected at the anode is proportional to the β-particle energy, hence the term ‘‘proportional’’

counting. Data from proportional counters are usually collected using some form of PHA equipment in order to resolve the different emission energies.

At higher applied voltages (800 to 1000 V), the electrons released in the primary ionization of the fill gas are accelerated so rapidly by the applied potential that they are capable of inducing secondary ionizations, which in turn cause further ionizations and so on. This leads to a signal of the same size, more or less regardless of the energy of the incident particle or photon. The large size of the signal means that the ancillary signal processing equipment need only be very simple, and the loss of proportionality to particle energy means that there is no need for energy resolution. This makes the G–M tube ideal for use in portable monitoring equipment and in measuring the activity of chemically separated β-emitters.

2. Scintillation Counters

Scintillation devices are among the oldest established radiation detectors and were used in much of the pioneering radioactivity research in the early 20th century. Different scintillators have been developed for the efficient measurement of all the different radiation types.

Liquid scintillation counting (LSC) was developed in the 1950s as a technique for measuring β-particles, particularly the low-energy emissions from isotopes such as ^{3}H or ^{14}C. In LSC, the radioisotope is intimately mixed with a solution containing one or more scintillants, compounds that can be efficiently promoted into an excited state by energy transfer from a β-particle. On de-excitation, the excited molecules emit light in the visible/near-UV region, which can be detected by a photomultiplier tube. The wavelength of the light emissions from those molecules which are most efficiently excited by β-particles does not match the most sensitive spectral region for detection using a PM tube. Modern scintillants are therefore "cocktails" containing a "primary" scintillant, which is an efficient absorber of β-particle energy, and one or more "wavelength shifters" or "secondary" scintillants, which reabsorb the light from the primary scintillants and re-emit at a wavelength better suited to the PM tubes. The scintillants are usually complex organic compounds containing extensive delocalized aromatic structures, e.g., 2,5-diphenyloxazole (PPO), used as a primary scintillant, and 1,4-bis-[2-(5-phenyloxazolyl)]-benzene (POPOP), used as a secondary scintillant. The early scintillants were soluble only in nonpolar organic solvents such as benzene and dioxan, which severely limited their use with aqueous solutions. Much effort has been devoted to the development of scintillation cocktails that can accommodate significant quantities of aqueous material, often as an emulsion, and it is now possible to dissolve or disperse up to 50 % by volume of aqueous solution into some

modern scintillants. Even so, great care has to be taken to avoid phase separation, and there are severe restrictions on the pH of the samples and on the salt loading that can be tolerated. Precipitates can be dispersed in gel scintillants for counting (e.g., Anon., 1989).

In practice, liquid scintillation measurements are made by dissolving or dispersing the sample in around 15 mL of scintillant in a polythene or glass vial. The liquid scintillation counter transfers the vial into a light-tight counting chamber, and the light emissions are counted by two PM tubes 180° apart in coincidence mode (in other words, only signals detected by both PM tubes simultaneously are treated as real; those detected only by one, for example stray light, are rejected). Instrument background can be further reduced by heavy shielding of the counting chamber and/or by pulse shape analysis which allows signals from different sources to be distinguished.

There are a number of potential interferences in liquid scintillation. The most important is ''quenching'', which arises from a number of sources, but commonly from absorption of the light photons within a colored sample (color quench) or else from interference with the energy transfer from β-particle to scintillant (chemical quench). There are several techniques available to correct for quench, and it is essential that adequate corrections are made if reliable results are to be obtained. Not all these techniques are straightforward and, while most modern counters can be programmed to carry out automatic quench corrections, it is important to ensure that the corrections they perform are satisfactory. Quench correction is probably the most difficult aspect of liquid scintillation counting, whereas the measurement of background and of counting efficiency is relatively straightforward.

The energy of an emitted β-particle is rapidly, and often quantitatively, transferred to the scintillator. Thus the number of excited states produced, and the intensity of the light emissions stimulated, are proportional to β-particle energy. Early scintillation counters had relatively simple energy-resolving equipment, consisting of one or more variable ''discriminators,'' which defined the lower level below which signals were rejected, and ''windows,'' within which signals were counted. These instruments provided sufficient energy resolution to allow simultaneous analysis of, for example, ^{3}H (E_{max} 18.6 keV) and ^{14}C (E_{max} 156 keV). More modern electronics and PHAs allow more sophisticated data acquisition and display, although the analysis of isotope mixtures will always be difficult owing to the β-particles' continuous energy distributions (Fig. 3).

Cerenkov counting is a variation on basic LSC. It relies on the emission of light (Cerenkov radiation) in the visible/UV region of the spectrum when a particle passes through a medium with a velocity greater than that of light in that medium. The two great attractions of Cerenkov radiation are its automatic discrimination against low-energy β-particles

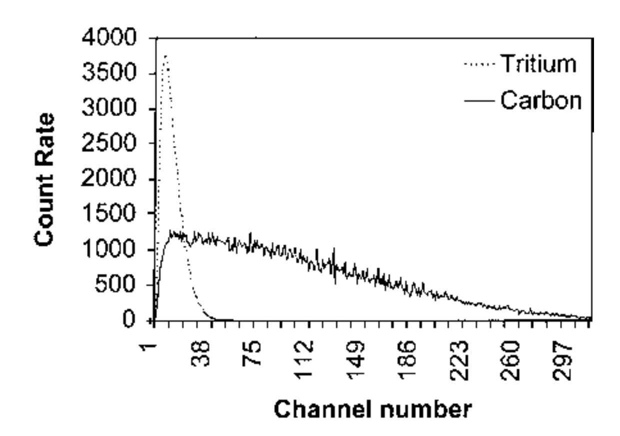


Figure 3 LSC spectra of ^{3}H and ^{14}C.

(the minimum energy needed to stimulate Cerenkov radiation in aqueous solution is about 500 keV) and the avoidance of any scintillators, thus allowing direct counting of aqueous solutions in a conventional LSC instrument. The wavelength of Cerenkov light (blue and near-UV) is such that the signals appear in the same spectral regions as scintillations stimulated by very-low-energy β-emitters such as ^{3}H. Although the absence of scintillators means that chemical quench is not a problem, color quench can be. Efficiency calibration and background subtraction are carried out exactly as in normal LSC. Among the isotopes measured by Cerenkov counting are ^{32}P in radiotracer experiments (e.g., Harrison et al., 1991) and ^{90}Y (decay product of ^{90}Sr) in environmental samples (e.g., Zhu et al., 1990; Scarpitta et al., 1999; Vaca et al., 1999).

Historically, α-particles were measured using solid scintillators [ZnS(Ag) screens], which functioned in the same way as those used for β-particle measurement. However, given the limited range and penetrating ability of α-particles, α-scintillators need only to be arranged as very thin films of scintillator, coupled to a photomultiplier. Such detectors are still in use today, primarily in simple monitors since they have no energy-resolving capability but a high sensitivity.

In the last 10–15 years, much effort has been devoted to the development of liquid scintillation counting for α-particles, since the high LET of an α-particle leads to very efficient transfer of energy to the scintillant. Instruments that can discriminate between α- and β-particles are now commercially available. These use pulse shape discrimination (Pates et al., 1993, 1998) to distinguish between the particle types, and good energy resolution is now achievable. Alpha scintillation counting is particularly attractive where the separation chemistry results in the isolation

of the element of interest in an organic solvent, since many of these can be readily incorporated into scintillants. Counting of aqueous solutions is a little more difficult, since these often need to be acidic to prevent hydrolysis, and many scintillants have only a limited capacity for such solutions.

Photon/Electron Rejecting Alpha Counting by Liquid Scintillation (PERALS®) is a more recent development in α-scintillation. Since much of the complexity in commercial LSC arises from the need to reduce backgrounds in β-measurement, a spectrometer designed specifically for α-scintillation can be made relatively simple. The PERALS spectrometer fits in a standard NIM crate and incorporates signal discrimination to reject pulses arising from β-decay events and passage of γ-photons. Some applications are discussed by Cadieux (1990) and Cadieux et al. (1994). Coupled with a conventional MCA, it is capable of providing high detection efficiency (100%) with energy resolution that is adequate for many purposes, although peaks that are close in energy (e.g., ^{241}Am and ^{243}Am at 5.5 and 5.35 MeV, respectively) are not always cleanly resolved (Dacheux and Aupiais, 1997, 1998).

Scintillation counting can also be used to measure γ-photons. Since these have low LET, the scintillator needs to be dense in order to maximize the probability of interaction, and liquid scintillation counting is therefore not really practical. The most commonly used solid scintillator is NaI(TI), which is available as very large single crystals (up to 30 cm diameter). Other materials such as CsI(Tl) are more efficient, much more expensive, and used occasionally. The main advantage of γ-scintillation counting is the high detection efficiency that can be achieved, and its main disadvantage is the poor energy resolution (about 50 keV FWHM at 660 keV), which can lead to uninterpretably complex spectra from mixed isotopic sources. The poor energy resolution arises from the amount of energy needed to generate a scintillation event. This is about 350 eV, compared with around 3.5 eV needed to create an electron/hole pair in a semiconductor (see below).

Gamma spectroscopy, whether using scintillation or semiconductor detectors, is not as simple as it perhaps seems. Although the penetrating ability of γ-photons means that it is possible to measure solid samples without much or any pretreatment and, almost always, without lengthy chemical separations, the accuracy of the final results is greatly affected by the care that is taken in calibrating the detector. It is necessary to establish two different relationships: one to relate position in the spectrum to γ-photon energy (which is diagnostic of the presence of a particular isotope) and one to establish the efficiency of photon detection as a function of energy.

In practice, since NaI(Tl) detectors are largely restricted to the measurement of single isotopes or simple mixtures, calibration is best

achieved by using a standard containing a known activity of the isotope of interest. Since the way the sample is presented to the detector (the "geometry") and the nature of the sample matrix (the capacity for self-absorption) can have a very significant effect on counting efficiency, the simplest form of calibration standard is a blank of the appropriate matrix material spiked with a known activity of the isotope(s) of interest. It is then possible to calculate detection efficiency directly for the relevant combination of isotope, matrix, and geometry.

3. Semiconductor Detectors

The semiconductors used for general γ-ray spectroscopy are large-volume single crystals, usually of germanium. Ge of the purity needed was not readily available initially, so early detectors were Li-drifted, that is, Li^+ ions were diffused into the crystal to eliminate the effects of impurities in the Ge. These are known as Ge(Li) crystals and need to be maintained permanently at liquid nitrogen temperatures, both to prevent the Li from becoming mobile in the lattice and aggregating and also to reduce thermal noise. Lower energy photons, in the x-ray region, are better detected with lower atomic mass materials, and Si(Li) detectors are used for this purpose. In the last 10 to 20 years, "hyperpure" Ge has become available and has supplanted Li-drifted semiconductors to a significant extent. So-called HPGe detectors can be made much larger than Ge(Li) crystals could, so that much higher relative efficiencies [$> 150\%$ relative to 7.5×7.5 cm NaI(Tl)] are possible. These detectors can be stored at room temperature, although they must still be operated at liquid nitrogen temperatures. Different detector configurations ("reverse electrode" and "planar") are also available and provide improved low-energy performance. Both scintillators and semiconductors are available in "well type" configurations, in which the sample tube is inserted into a narrow well in the center of the detector, surrounding the sample with sensitive material. This maximizes counting efficiency, but at the cost of severely restricting sample size. Large samples of the order of 1.0 liter in volume can be counted with reasonable efficiency in a recessed Marinelli beaker that surrounds the sensitive region of the detector.

All semiconductor detectors work on the same principle. Within the electronic structure of the crystal, there exists an occupied "valence band" of electronic states and, about 3.5 eV higher in energy, there is an empty "conduction band." When a γ-photon interacts with the detector crystal, the dissipation of its energy causes promotion of electrons from valence to conduction bands, creating vacancies ("holes") in the valence band. Under the influence of the applied voltage, the electrons in the conduction band and the holes in the valence band migrate to electrodes attached to the

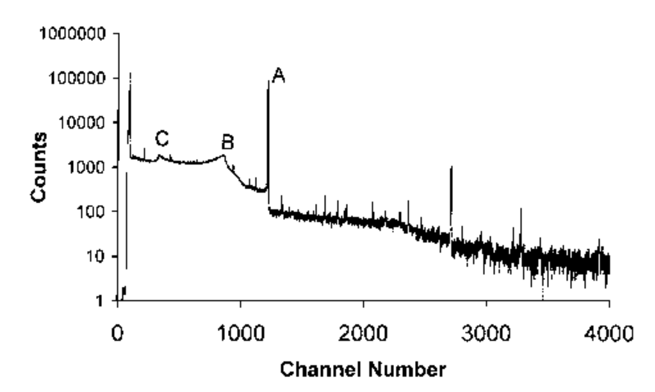


Figure 4 Gamma spectrum of a sediment sample, obtained with a semiconductor detector.

crystal. The magnitude of the charge collected at the electrodes is proportional to the number of electron/hole pairs created, which in turn is proportional to the energy dissipated in the detector crystal by the γ-photon. Conventional signal processing and pulse height analysis equipment allow the collection of data as an energy-resolved spectrum.

Gamma spectra contain a number of characteristic features, some of which are visible in Fig. 4, a spectrum obtained from a sediment sample contaminated with artificial radionuclides from a fuel reprocessing plant. In Fig. 4, A is the full energy photopeak, the signal arising from the dissipation of all the photon energy in the sensitive volume of the detector. B is the Compton edge. Many photons can pass through the detector without dissipating all their energy in the sensitive volume. Some of these remove an electron from an atom in the detector (Compton scattering), reducing the photon energy by an amount equal to the electron binding energy. If the photon then dissipates some or all of its remaining energy in the detector, its energy will be measured as the reduced value. The Compton edge thus arises from photons that have undergone a Compton scattering interaction and then dissipated all their remaining energy in the detector. Feature C is due to photons that have suffered partial energy loss through interaction with other materials before interaction with the detector (backscattering).

Other spectral features may also be observed. If a photon has a total energy greater than 1022 keV, a process known as pair production can occur, in which the photon's energy is converted into a positron/electron pair. The mass equivalent of 1022 keV is 2 electron masses. If one electron is lost from the detector, then the resulting signal will appear at 511 keV below the full energy peak. Similarly, double escape may also occur.

Marcel Dekker, Inc.
270 Madison Avenue, New York, New York 10016

The peak due to this will appear at 1022 keV below the full energy peak and arises from the escape of both the positron and the electron formed by pair production from the detector.

Annihilation radiation may also be observed. This signal always arises at 511 keV and is particularly prominent in the spectra of β^+-emitters. It results from the interaction of the positron with an electron, which causes annihilation (the inverse of pair production) and the production of two photons, each with 511 keV energy. Since these photons do not arise from a specific isotope, it is very difficult to use the 511 keV peak in analysis.

The calibration of semiconductor γ-detectors is relatively complex, since they are so often used for the identification and measurement of a very wide range of isotopes, not all of which are available for the preparation of calibration standards. These detectors are usually calibrated using a mixture of γ-emitters, present in known activities and covering the energy range from about 50 to 2000 keV. Typically, such mixed standards will give spectra containing about a dozen peaks, and both the energy and the efficiency calibrations can be performed using these materials. While the energy calibration should be linear, detection efficiency varies with energy in a complex fashion (Fig. 5). As with NaI(T1) detectors, geometry and matrix effects are of critical importance. Most commercial γ-spectroscopy systems include software for the calculation of calibration equations from mixed isotopic standards. It should be noted that error in efficiency calibration is a major source of error in γ-spectroscopy, since actual counting efficiencies are low (often 1% or less for large-volume samples), so small errors in calculated efficiencies lead to large errors in the final results. The calibration of semiconductor detectors at low energies (< 50 keV) can be quite difficult, and single isotopes or simple isotope mixtures are often used. Photons above around 2000 keV are rarely encountered in environmental measurements.

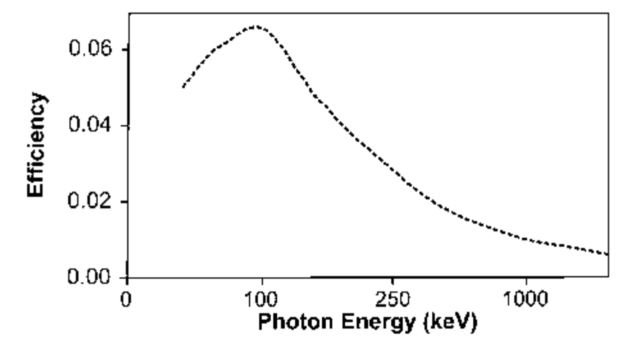


Figure 5 Variation of detector efficiency with energy, for a semiconductor detector.

Some radioisotopes, such as ^{60}Co or ^{134}Cs, are characterized by the emission of two photons in rapid succession ($< 10^{-14}$ s apart). These may not be separated in time by the detection system, which will therefore detect them as one photon, with an energy equal to the sum of their individual energies. This is known as ''coincidence summing'' and leads to loss of counts from the full energy photopeak and the appearance of a ''sum peak'' at a position equivalent to the sum of the two photon energies. Analysis of such a spectrum using a standard efficiency equation will give a misleadingly low result, and the only way to obtain an accurate analysis in such cases is to use a calibration standard prepared from the isotope of interest. The probability of coincidence losses is dependent on the counting geometry.

Background reduction is also critical in γ-spectrometry. Signals from a large number of naturally occurring radioisotopes are readily detected with an unshielded detector, but these can be reduced greatly in intensity with suitable shielding. This usually consists of a thick outer layer of Pb (10 cm thickness is common), lined with Cd and Cu sheet. The purpose of the liners is to absorb the x-rays excited from the material making up the outer layers, and the use of materials of decreasing atomic weight (i.e., with x-ray absorption edges shifting to lower and lower energies) maximizes absorption.

In extreme cases, ''active'' shielding may be used, in which a semiconductor detector is entirely surrounded by a second [usually NaI(T1)] detector and the circuitry is arranged so that pulses generated simultaneously by both detectors are rejected. This reduces background since such pulses can only be generated by a photon entering the counters from outside (i.e., a genuine background signal), or by a photon being emitted from the counting source and dissipating only a fraction of its energy in the semiconductor, in which case it will not contribute to the full energy photopeak. Active shielding is very effective at reducing background for isotopes that emit single photons, but the emission of photons in coincidence will lead to the rejection of genuine signals (Branford et al., 1998). In spite of heavy and/or active shielding, γ-detectors still have very significant backgrounds, especially at medium and low energies, so it is essential that a careful background correction be made.

The majority of quantitative low-level measurements of α-emitters is made using α-spectroscopy. In this technique, an α-sensitive semiconductor detector is used. The detector is a thin Si wafer several hundred mm^2 in area, which has been either coated or implanted with Au to create a thin (typically 100 μm depth for α-detection) sensitive layer across the detector area. The α-emitting isotope(s) are presented to the detector as a suitable thin counting source (Wyllie and Lowenthal, 1984); it is usually prepared by electrodeposition (Talvitie, 1972; Hallstadius, 1984), although direct

evaporation (Anon., 1989) or microprecipitation (Sill and Williams, 1981; Kaye et al., 1995; Luskus,1998) can also be used. In order to prevent energy loss and peak broadening by scattering from gas molecules, detector and counting source are mounted in an evacuated chamber. The interaction of the α-particles with the detector generates electron/hole pairs in exactly the same way as described above for γ-photon detection, and a well-resolved spectrum can be obtained. Typical resolution for an α-detector is 20 keV FWHM, which in practice means that it is adequate to resolve the α-energies of most α-emitters that might be encountered in environmental samples, although $^{208}Po/^{210}Po$ and $^{241}Am/^{243}Am$ can be difficult, particularly with imperfect sources. The major problem is separation of the signals from ^{239}Pu and ^{240}Pu: these isotopes' α-emissions are so close in energy (5.157 and 5.160 MeV, respectively) that they generally cannot be resolved cleanly (but see Amondry and Burger, 1984), and alternative nonradiometric methods are used (Sec. IV). In low-level counting, resolution is often sacrificed for counting efficiency, since the best resolution is often only achieved at large source–detector separations, which lead to low efficiency.

IV. NONRADIOMETRIC MEASUREMENT

In some circumstances, radiometric measurement is not the best technique for the measurement of a particular isotope. In many cases, this is because the isotope is long-lived, so its specific activity (activity per unit mass) is low, and other techniques are potentially more sensitive than radiation counting. For the measurement of actinides, the point at which α-spectrometry becomes less sensitive than inductively coupled plasma-mass spectrometry (ICP-MS) is a half-life of around 25,000 years (McMahon, 1992) although developments in ICP-MS are now making it more competitive at shorter half-lives. The major isotopes for which mass spectrometric measurement may be preferred are ^{232}Th, ^{235}U, ^{238}U, ^{237}Np, ^{239}Pu, ^{240}Pu, and ^{99}Tc. These may be present in environmental samples at mass concentrations above 1 $ng\,g^{-1}$, which can correspond to an activity concentration as low as 10–20 $\mu Bq\,g^{-1}$. For the longest-lived isotopes, ICP-atomic emission spectrometry or spectrophotometric measurement may be adequate, although clearly these techniques cannot provide information on isotopic composition.

The use of mass spectrometry does allow additional information to be obtained, most notably $^{239}Pu/^{240}Pu$ ratios. As indicated above, these cannot easily be determined radiometrically, although a combined x-ray and α-counting technique has been used (Komura et al., 1984), whereas they are routinely obtainable by ICP-MS analysis. They have also been

determined by thermal ionization mass spectrometry (McCarthy and Nicholls, 1990), and this latter technique has also been used by several other groups to measure long-lived isotopes (Landrum et al., 1969; Efurd et al., 1986; Taylor et al., 1998; Goodall and Lythgoe, 1999). In terms of ultimate sensitivity, counting techniques are usually better than ICP-MS. This is particularly so for α-spectrometry, which has a near-zero background so that very long acquisition times (weeks to months) are possible and very low activities, of the order of 10 μBq, can be determined (Harvey et al., 1993).

In specialized applications where very small numbers of atoms (10^6 to 10^9) of isotopes with moderate to long half-lives are to be analyzed, accelerator mass spectrometry (AMS) can be used (Rucklidge, 1995). Such situations can arise if there is a very limited amount of sample available, which is often the case with ^{14}C dating, or if concentrations are very low, for example in measurement of ^{36}Cl, or both. AMS has a detection limit of the order of 10^6 atoms, depending on the instrumentation used, and is widely used for ^{14}C (Donahue, 1995) or ^{36}Cl (Beasley et al., 1997) measurement. More recently, the potential of AMS for the measurement of artificial radionuclides has been demonstrated for ^{99}Tc (McAninch et al., 1998), ^{129}I (Schmidt et al., 1998; Lopez-Gutierrez et al., 1999), ^{237}Np (Fifield et al. 1997), and Pu isotopes (Fifield et al., 1996). Resonance ionization mass spectrometry (RIMS) is a highly sensitive isotope-selective technique that has found some application in environmental analysis (e.g., Zimmer et al., 1994; Erdmann et al., 1997).

Although one of the great attractions of nonradiometric measurements, particularly ICP-MS, is the possibility of avoiding lengthy sample preconcentration and cleanup procedures, in practice this is rarely the case. The large samples often used lead to high dissolved solid concentrations in solution and to serious matrix effects, so cleanup for ICP-MS analysis is often as demanding as for radiometric measurement (Hursthouse et al., 1992; Butterworth et al., 1995). Thorough decontamination is also essential to avoid possible isobaric interferences in ICP-MS. Possible examples include ^{99}Ru (12.7% abundance), which will coincide with ^{99}Tc and $^{238}UH^+$, which will coincide with ^{239}Pu. Only in the simplest analyses (e.g., U in some waters, U or Th in soil or sediment) is it really possible to analyze a sample solution or extract directly.

An older-established technique that has not been surpassed is the use of neutron activation analysis (NAA). This is applicable to a wide range of major, trace, and ultratrace elements, including a number of long-lived radioisotopes (Salbu and Steinnes, 1992). It is based on the principle that, following the capture of a neutron in a small nuclear reactor, a stable or long-lived unstable isotope can be converted into a relatively short-lived

radioactive one. Since the activation process has produced a neutron-rich product nucleus, decay generally occurs by negatron emission and is often accompanied by one or more γ-ray photons. Thus if the γ-ray spectrum of the irradiated sample is analyzed and a number of parameters (e.g., neutron flux, irradiation time, capture cross section, counting efficiency, counting time) are known, it is possible to calculate the concentration of the target element in the sample.

Since NAA depends on totally different principles from other measurement techniques, the range of "good" and "bad" elements is very different from that normally encountered. Elements may be difficult or impossible to analyze if reaction cross sections are low (e.g., ^{9}Be), if the capture reaction produces a stable or long-lived product [e.g., neutron irradiation of the naturally occurring radioactive isotope ^{144}Nd ($t_{1/2}$ 2.1×10^{15} yr) forms the stable ^{145}Nd], if the capture reaction produces a short-lived product [e.g., ^{7}Li (92.5% natural abundance) activates to ^{8}Li ($t_{1/2}$ 0.844 s)], or if an alternative nuclear reaction causes interference. NAA could be used to analyze elements that do not form β,γ-emitting products (e.g., P, Si, S), but only where the product isotope is chemically separated and β-counted; this is rarely done, since alternative methods exist for these elements.

NAA is really useful when the capture cross section is high, a β,γ-emitting product of suitable half-life is formed free of interfering side reactions, and its γ-spectrum is easily measured. For such elements, the sensitivity of NAA was unmatched until the development of ICP-MS, and there are a number of NAA methods for long-lived radionuclides, principally ^{129}I (Muramatsu and Yoshida, 1995; Parry et al., 1995), ^{232}Th and ^{238}U (Edgington, 1967; Fakhi et al., 1988), and ^{237}Np (Ruf and Friedrich, 1978; Byrne, 1986; May and Pinte, 1986). For the metal ions, NAA has largely been supplanted by ICP-MS, but it remains very attractive for the measurement of ^{129}I ($t_{1/2}$ 1.57×10^{7} years, E_{max} β 150 keV). The low specific activity and low β-particle energy make ^{129}I very difficult to determine at environmental concentrations by radiometric methods.

A technique that can be used to obtain information about the physical form of radioisotopes, particularly α-emitters, in soils and sediments, is solid state nuclear track detection (SSNTD). This is most useful for the identification of particulate material of relatively high specific activity and can be used to locate such material for further detailed analysis (Hamilton, 1981, 1985). At its simplest, the technique involves putting the soil sample into close contact with a sensitive plastic [CR39 polycarbonate (Hamilton and Clifton, 1981) is commonly used]. Alpha particles escaping from the sample cause localized damage in the plastic, which can be etched to enlarge the particle tracks until they are visible under the microscope. SSNTD

has little capacity to resolve particle energies, although efforts have been made to relate track dimensions and geometries to energies (Bondarenko *et al.*, 1996). However, by combining α-track and fission track analysis (a similar procedure, but the samples are neutron-irradiated in a reactor to stimulate fission reactions; the energetic fission product nuclei produce extensive tracks in the detector), it is possible to identify specifically those particles containing fissile isotopes (Bersina et al., 1995). Other detector media can similarly be used to locate particles containing β- and β,γ-emitting isotopes (Kushin et al., 1993).

V. RADIOCHEMICAL SEPARATIONS

The principles on which radiochemical separations are based are relatively straightforward and long established. All are based on the transfer of the radionuclide(s) of interest from one phase to another, leaving behind part or all of the potentially interfering elements. Such phase transfers can be from solution to solid, solid to gas, or solution to gas. There are a huge number of separations published, and useful sources include the US DOE Environmental Measurements Laboratory (EML) Manual (Chieco et al., 1992), the Royal Society of Chemistry International Conferences on Environmental Radiochemical Analysis (e.g., RSC, 1999), the report "Sampling and Measurement of Radionuclides in the Environment" (Anon, 1989), and analytical methods journals. In the remainder of this section, the principles underlying radiochemical separations are discussed and a number of typical separations are outlined.

Given that the purpose of radiochemical separations is to isolate very small amounts of radioisotope, generally in very high purity, often from large samples, it is unsurprising that radiochemical separations are frequently complex. In these circumstances, it is almost impossible to guarantee quantitative recovery of the radioisotope of interest, so losses during separation have to be corrected (Harvey and Lovett, 1984). This can be achieved by using a radioisotopic yield monitor (an isotope not present in the sample of which a known amount is added before separation begins, such as ^{85}Sr in ^{90}Sr analysis, ^{239}Np in ^{237}Np analysis, ^{236}Pu or ^{242}Pu in Pu analysis, ^{243}Am in ^{241}Am ana1ysis) or a stable element (e.g., stable S in ^{35}S analysis, stable Sr in ^{90}Sr analysis, stable Re in ^{99}Tc analysis). The activity of radioisotopic yield monitor recovered is an index of the efficiency of chemical recovery. Stable element yield monitors can be measured by straightforward analytical techniques following separation.

Phase separation can be achieved in a variety of ways. Volatilization is the most obvious and can be achieved by, for example, combustion of

samples to separate ^{14}C as CO_2 from involatile matrix components, by dissolution or extraction of solid samples and concentration of isotopes of Ru or Tc by distillation (Dutton and Ibbett, 1973), or by roasting of solid samples to volatilize ^{210}Po, followed by condensation and trapping on glass wool (Eakins and Morrison, 1978).

Liquid–liquid extraction using two immiscible solvents is commonly used, either to eliminate excessive quantities of matrix elements (e.g., di-isopropyl ether extraction of Fe from soil extract prior to transuranic element separation) or to extract the radioisotopes of interest from complex solutions. Typical examples are the extraction of Am isotopes from 10 *M* nitric acid solutions with dibutyl diethyl carbamoyl phosphonate (Butler and Hall, 1970) and extraction of a range of actinides from solutions of animal tissues and other samples using amines (Singh and Wrenn, 1981; Singh et al., 1984; Singh, 1987). A useful variation on solvent extraction is extraction chromatography, in which the reagent is adsorbed onto an inert solid support, which is packed into a column the extraction is carried out by simply passing the sample solution through the column (e.g., Martin and Pope, 1982; Jia et al., 1998). The element of interest is concentrated onto the column packing; further cleanup can be achieved by passing other reagents through the column, and the purified radioisotope fraction can then be eluted. Until relatively recently, extraction chromatography reagents were not widely available commercially, but a range of highly selective immobilized extractants manufactured by EIChroM (http://www.eichrom.com) is now available, and these have proved very useful in replacing or simplifying difficult, lengthy, and complex ion exchange and solvent extraction procedures, for example in the separation of ^{90}Sr (Clark, 1995), ^{99}Tc (Butterworth et al., 1995), and ^{241}Am (Bunzl et al., 1995). Although, in many cases, the use of these reagents provides huge advantages in time, cost, and reliability over earlier methods, chemical interferences can still occur; in the authors' experience, these reagents are best used to replace particularly difficult steps in an existing procedure, rather than as substitutes for multistage separations.

Ion exchange is also widely used in separations chemistry. In this, the charge on the ions in solution is manipulated by changing oxidation state and concentration of the complexing ion (usually Cl^- or NO_3^- for actinides) in order to generate species with positive or negative charges. These solutions are passed through a column packed with an appropriate ion exchange resin, and the species of the appropriate charge are scavenged from solution. For example, in 8 to 9 *M* HNO_3 Pu(IV) forms anionic complexes (Veirs et al., 1994), whereas Fe(III) does not. Thus passage through an anion exchange column allows the concentration of Pu onto the resin and its separation from Fe. The Pu can then be eluted from the column

by reduction with I^- in HCl to give Pu(III), which forms neutral and cationic species. Both anion and cation exchange resins have been very extensively used in low level separations.

Coprecipitation is a technique by which ultratrace quantities of a species, which is not present in sufficient concentration to exceed the solubility product of a solid compound, may nevertheless be removed from solution by precipitation. These procedures depend on the precipitation of an appropriate host solid phase, which is chemically sufficiently similar to that which would be formed by the trace species. The trace element is incorporated in the host precipitate and scavenged from solution. Coprecipitations find use in analytical separations [e.g., $BiPO_4$ coprecipitation of Pu and Am (Mathew et al., 1981); NdF_3 coprecipitation of actinides (Hindman, 1986)] and are a particularly attractive means of concentrating very low radionuclide concentrations from water samples [e.g., U isotopes in freshwater (Morris et al., 1994), Pu isotopes in seawater (Eroglu et al., 1998)].

A. Examples

The purpose of these examples is not to provide a detailed description of the steps needed in the separation and analysis of the chosen isotopes but rather to illustrate the way in which the individual steps in radiochemical separations are used both to eliminate potential interferences and to convert the radioisotope(s) into a suitable form for final measurement.

1. Separation of Sr Radioisotopes from a Calcareous Matrix and Analysis by Cerenkov and Liquid Scintillation Counting (Clark, 1995)

The bulk of the organic matter is first destroyed by dry ashing at 600°C and the residue dissolved in 8 *M* HNO_3. Then 10 mg of stable Sr are added as a carrier and residual organic matter is removed by repeated treatment with H_2O_2 and 8 *M* HNO_3. Once all organic matter has been eliminated, the residual sample is dissolved in 8 *M* HNO_3 and passed through a Sr. Spec extraction chromatography column. This consists of 4,4′(5′)-bis-*t*-butylcyclohexano-18-crown-6, a highly selective complexant for Sr^{2+}, immobilized on an inert support. The column is washed with 12 column volumes of 8 *M* HNO_3, which removes Ca and all other metals. Strontium is then eluted from the column with 5 column volumes of 0.05 *M* HNO_3. The samples are Cerenkov counted immediately to measure ^{89}Sr (the β-particle energy of ^{90}Sr is too low to stimulate Cerenkov emission, and by counting immediately, interference from the ingrowth of ^{90}Y is avoided). After Cerenkov counting, the sample is evaporated to dryness and the mass of $Sr(NO_3)_2$ determined by

weighing to give a measure of Sr recovery. The residue is then redissolved in dilute HNO_3, mixed with scintillation cocktail, and counted. Two separate energy regions are measured, 20 to 500 keV, in which the ^{90}Sr decays are measured, and 500 to 1500 keV, in which ^{89}Sr decays are measured.

2. Separation of ^{237}Np and α-Emitting Isotopes of Pu and Analysis by ICP-MS and α-Spectrometry (Morris and Livens, 1996)

The sample is dry-ashed to destroy organic matter and then leached with mineral acids. As with Sr above, if the actinides have been exposed to high temperatures they may be present as ceramic oxides or incorporated in silicates, in which case total dissolution will be necessary. At the dissolution stage, ^{239}Np (a β-emitter with a 2.3 day half-life, chemically separated from ^{243}Am in which it is formed by α-decay) and ^{242}Pu are added as yield monitors. The solution is made up to a standard volume and γ-counted to determine the initial ^{239}Np activity.

Nitric acid is eliminated from the solution and the HCl concentration adjusted to 9 *M*. Hydriodic acid is added to control Np valency and Np separated from the solution by anion exchange. The presence of I^- maintains Np in the tetravalent state, in which it forms anionic chloro-complexes, whereas Pu is reduced to the trivalent state, in which it forms cationic species and passes through the column. The effluent from the anion exchange column is retained for Pu analysis and other contaminants, principally Fe, are eluted from the anion exchange column with 8 *M* HNO_3 and 12 *M* HCl, before Np is eluted with dilute HCl. The solution composition is changed to dilute HNO_3 and the volume adjusted for γ-counting to determine Np recovery. After yield determination, the solution is analyzed by ICP-MS to determine ^{237}Np concentrations.

The Pu fraction is evaporated to dryness and dissolved in 8 *M* HNO_3, and the Pu valence is adjusted to IV with $NaNO_2$. The solution is passed through an anion exchange column, and the Am that is also present in the Pu fraction passes through. The remaining contaminants are eluted with 12 *M* HCl, and the Pu is eluted with HI/HCl. The Pu fraction is evaporated to dryness and dissolved in an electrolyte solution, and the Pu is electrodeposited onto a planchet for α-spectrometry. The ^{242}Pu yield monitor can be measured at the same time as the other α-emitting Pu isotopes.

VI. QUALITY CONTROL AND METHOD VALIDATION

The problems of quality control and method validation are more acute in environmental radiochemical analysis than in most analytical chemistry

Marcel Dekker, Inc.
270 Madison Avenue, New York, New York 10016

(Christmas, 1984). The combination of ultratrace mass concentrations (10^{-12} g g^{-1} or lower), the need for complex multistage chemical separations in many determinations, and the use of very sophisticated instrumentation lead to particular difficulties. Nevertheless, the same principles apply as in any other type of analysis, and there is the same need to quantify the accuracy and precision of the methods used (Harvey and Young, 1988; Haase et al., 1993, 1996).

As in most cases, accuracy is best demonstrated by measuring as unknowns samples for which the radionuclide concentrations are actually well established. Ideally, these materials should have been validated independently, and a range of such samples is available from the IAEA Marine Environmental Laboratory (Monaco; http://www.iaea.org/monaco) and the National Institute of Standards and Technology (Gaithersburg, USA; http://www.physics.nist.gov). These cover a range of the more common matrices and radioisotopes (e.g., Inn et al., 1996). However, there is frequently a mismatch between the concentrations found in a laboratory's typical samples and those in the reference materials, or between the materials available and the sample matrices to be analyzed, so that a method's performance in the analysis of a reference material may not be entirely representative of performance in routine use. This may be due to matrix effects that arise only in the analysis of samples or reference materials, or to differences in the chemical form of the radioisotopes. For example, isotopes present in oxide particles that have been exposed to high temperatures will not behave in the same way as those derived from effluents (Fridkin et al., 1992; Oughton et al., 1993).

The certification procedure for environmental radioactivity reference materials is also more problematic. In some cases, the certified value is arrived at from the results obtained by a small number of reputable laboratories, while in others, the material is freely circulated and the certified value is based on all the results remaining after rejection of outlying values that fail statistical tests. A potential problem in both these approaches is that the values obtained in the certification process are often obtained using very similar chemical separations, with yield tracers from the same sources and using similar instrumentation. While this is often the only way any results can be obtained at all, the use of a greater range of separations chemistries, yield monitors, and measuring instrumentation would give more confidence in the certified values. Probably the most satisfactory approach is to spike the appropriate matrix materials with known radioisotope activities and homogenize them thoroughly. This has usually been done for liquid samples such as milk or water, although soil samples have been prepared in the same way (e.g., Sill and Hindman, 1974). Even this is not ideal, since there is always the question of homogeneity of solid

samples, and the chemical form of the spike in these materials may not be a good match for real samples.

The routine use of reference materials is also very expensive. The low concentrations in reference materials and the large samples used in analysis mean that, in many cases, no more than a couple of determinations can be made on a reference sample costing upwards of $100. Moreover, most laboratories process environmental samples in small batches (4–10 would be typical) at high cost, so the inclusion of a reference material with each batch of samples would consume 10–25 % of the analytical effort and represent a very substantial cost. The use of in-house reference materials significantly reduces the material cost but still represents a major analytical effort.

Laboratory intercomparisons (e.g., Harvey and Young, 1988; Cooper et al., 1992; Haase et al., 1993, 1996) are also valuable in method validation, although in many cases the range of laboratories analyzing materials that are directly comparable may be small. They again suffer from the problem that only a limited range of techniques can be used; and if there is poor agreement between laboratories, it can be difficult to know which result is wrong. These exercises are also potentially time-consuming and expensive. It is also useful to have some information regarding the reliability of software, particularly that used in quantitative spectral analysis (Decker and Sanderson, 1992).

Similarly, blank analyses are problematic, particularly in the case of artificial radioisotopes. They again can represent a major analytical effort, and it is not always easy to interpret the meaning of a "positive" blank determination. In many trace element analyses, the blank is unlikely to be zero, and it is assumed that it arises principally from contamination of the reagents, in which case the blank value can be subtracted from the sample data. In the case of most artificial radioisotopes, however, the reagent blank value is effectively zero (e.g., there is unlikely to be significant Pu in laboratory reagents), so a significant blank value represents cross-contamination from glassware or samples and cannot simply be compensated by subtraction. It more usually demonstrates a need for improved laboratory housekeeping (Harvey et al., 1987).

A. Sources of Radionuclide Standards

The supply of reliable radioisotope standard solutions has improved greatly in the last 10 years or so, and the range of high-purity certified solutions of useful isotopes has increased considerably. A number of suppliers now exist that supply materials that are useful as standards. The principal suppliers in the U.K. are Amersham, CIS(UK), the National Physical Laboratory, and New England Nuclear. Nevertheless, there are a significant number of

isotopes that are not readily available in satisfactory chemical and isotopic purity, with a certified activity and at reasonable cost. Examples include ^{95}Tc, ^{235}Np, ^{244}Pu, and ^{243}Am, all of which would be very useful both as yield monitors and in multiple labeling experiments.

B. Restrictions on Experimental Design and Replication

The expense and complexity of radiochemical analyses mean that sample analysis is not something to be undertaken lightly. The true cost of each analysis in time, consumables, and capital equipment is considerable and can often exceed several hundred dollars. Moreover, many laboratories do not have the staff or equipment to process more than a few hundred samples per year even for "routine" analytes. These limitations can impose severe restrictions on sampling and analytical programs, and it is essential that those designing experimental programs should liaise effectively with the analysts to prevent the sampling program becoming prohibitively expensive or time-consuming. Similarly, those funding such programs should appreciate that high-quality analysis is technically demanding, time-consuming, and expensive.

VII. EXAMPLES OF APPLICATIONS

Two selected examples of the application of radioanalytical techniques to soils are discussed here. The first is a retrospective attempt to estimate the inventories released in two major releases associated with the Soviet nuclear weapons program, the Kyshtym accident in 1957 and the aerial dispersion of contaminated material from Lake Karachay in 1967 (Aarkrog et al., 1997). The starting point is a series of measurements of radioisotope activities in grass, litter, and soil, expressed as Bq m^{-2}. Other sources of radionuclides include global fallout and releases from the 1986 Chernobyl reactor accident. The global fallout contribution of ^{90}Sr was determined by measurement at a site uncontaminated by the Kyshtym or Karachay releases and the global fallout ^{137}Cs estimated using the known ^{90}Sr/^{137}Cs ratio in fallout. This baseline was then subtracted from the ^{90}Sr and ^{137}Cs data. The Chernobyl ^{137}Cs contribution was estimated from the ^{134}Cs value (^{134}Cs is not produced directly in fission and is therefore only found in highly irradiated materials, such as the Chernobyl reactor fuel, and not in the lightly irradiated U used for producing weapons grade ^{239}Pu) and was also subtracted from the Cs data. After making these corrections, it was possible to set up and solve a series of simultaneous equations to quantify

the relative contributions of the Kyshtym and Lake Karachay events to the total soil inventory at each sample site.

The next stage was to determine the unknown ratios $^{239,240}Pu/^{90}Sr$ and $^{239,240}Pu/^{137}Cs$ in the Karachay and Kyshtym components by identifying sites affected only by one event and, using this information, to estimate the total activities of ^{90}Sr, ^{137}Cs, and $^{239,240}Pu$ released. While the results of this study were in general agreement with previous work, the estimated ^{137}Cs release from Lake Karachay was almost an order of magnitude higher than the previous estimates of 1.6×10^{13} Bq. Each of the two releases was estimated to contain about 10^{12} Bq $^{239,240}Pu$.

In the second example (Bunzl et al., 1995), a sequential extraction procedure has been used to evaluate changes in the speciation of $^{239,240}Pu$ and ^{241}Am, originating from global fallout, as a function of depth in a soil profile. Due to the very low activity concentrations present, particularly in the case of ^{241}Am, samples of up to 500 g dry weight were used. The nature of the extracts from the sequential extraction procedure necessitated changes in the sample pretreatment procedures, so that all the activity was solubilized, and potential interferences were eliminated.

The results showed that the exchangeable fraction of ^{241}Am was consistently higher than that of $^{239,240}Pu$, and there was also generally more ^{241}Am held in the oxide fraction. The organically bound fraction of the two elements was very similar, while there was more Pu in the residual fraction. Although the results of the leaching experiments might be interpreted as indicating that ^{241}Am should have a greater mobility than $^{239,240}Pu$, no difference in overall mobility was observed; both elements displayed a very similar distribution down the soil profile.

VIII. SUMMARY

The measurement of radioisotopes in environmental samples is necessary, both to measure the potential radiological impacts of natural and artificial radionuclides in the environment and also as a result of the widespread application of radioisotopes in tracer experiments. A wide range of analytical techniques may be employed, depending on the activity and/or mass concentrations of the isotope(s) present, and their chemical and radioactive decay properties. In many cases, the low levels of radioisotope present in environmental samples make the analyses particularly demanding, and complex chemical separations may need to be employed before measurement is possible. Such methods are notoriously time-consuming and expensive. Quality control and validation of radiochemical separations and radiosotope measurements, by both radiometric and nonradiometric means,

Marcel Dekker, Inc.
270 Madison Avenue, New York, New York 10016

are difficult owing to the restricted range of reference materials available, the limited number of laboratories with the ability to make measurements, the nonavailability of a number of isotopic yield monitors, and the constraints imposed by the time and cost of analysis. Time and cost may also restrict the extent of sampling programs and limit replication in analytical work.

REFERENCES

Aarkrog, A., Dahlgaard, H., Nielsen, S. P., Trapeznikov, A. V., Molchanova, I. V., Pozolotina, V. N., Karavaeva, E. N., Yushkov, P. I. and Polikarpov, G. G. 1997. Radioactive inventories from the Kyshtym and Karachay accidents: estimates based on soil samples collected in the south Urals (1990–1995). *Sci. Total Environ.* 201:137–154.

Amondry, F. and Burger, P. 1984. Determination of $^{239}Pu/^{240}Pu$ ratio by high resolution α-spectrometry. *Nucl. Inst. Meth. Phys. Res.* 223:360–367.

Anon. 1989. *Sampling and Measurement of Radionuclides in the Environment*. Her Majesty's Stationery Office, London.

Bateman, H. 1910. Solution of a system of differential equations occurring in the theory of radio active transformations. *Proc. Cambridge Phil. Soc.* 15:423–435.

Beasley, T. M., Cooper, L. W., Grebmeier, J. M., Kilius, L. R. and Synal, H. A. 1997. ^{36}Cl and ^{129}I in the Yenisei, Kolyma and Mackenzie rivers. *Environ. Sci. Technol.* 31:1834–1836.

Bondarenko, O. A., Salmon, P. L., Henshaw, D. L., Fews, A. P. and Ross, A. N. 1996. Alpha particle spectroscopy with TASTRAK (CR-39 type) plastic and its application to the measurement of hot particles. *Nucl. Inst. Meth. Phys. Res. A* 369:582–587.

Bersina, I. G., Brandt, R., Vater, P., Hinke, K. and Schutze, M. 1995. Fission-track autoradiography as a means to investigate plants for their contamination with natural and technogenic uranium. *Radiation Measurements* 24:277–282.

Branford, D., Mourne, R. W. and Fowler, D. 1998. Spatial variations of wet deposition rates in an extended region of complex topography deduced from measurements of ^{210}Pb soil inventories. *J. Environ. Radioactivity* 41:111–125.

Bunzl, K., Flessa, H., Kracke, W. and Schimmack, W. 1995. Association of fallout $^{239,240}Pu$ and ^{241}Am with various soil components in successive layers of a grassland soil. *Environ. Sci. Technol.* 29:2513–2518.

Butler, F. E. and Hall, R. M. 1970. Determination of actinides in biological samples with a bidentate organophosphorus extractant. *Anal. Chem.* 42:1073–1076.

Butterworth, J. C., Makinson, P. R. and Livens, F. R. 1995. Development of a technique for the determination of ^{99}Tc in soils and sediments. *Sci. Total Environ.* 173/174:293–300.

Byrne, A. R. 1986. The determination of ^{237}Np in Cumbrian (UK) sediments by neutron activation analysis: preliminary results. *J. Environ. Radioactivity* 4:133–144.

Cadieux, J. R. 1990. Evaluation of a photon-electron rejecting alpha liquid scintillation (PERALS) spectrometer for the measurement of alpha emitting radionuclides. *Nucl. Inst. Meth. Phys. Res. A* 299:119–122.

Cadieux, J. R., Clark, S., Fjeld, R. A., Reboul, S. and Sowder, A. 1994. Measurement of actinides in environmental samples by photon electron rejecting alpha liquid scintillation. *Nucl. Inst. Meth. Phys. Res. A* 353:534–538.

Chieco, N. A., Bogen, D. C. and Knutson, E. O., eds. 1992. *EML Procedures Manual. 27th ed.* HASL-300. US DOE Environmental Measurements Laboratory, New York.

Choppin, G. R., Rydberg, J. and Liljenzin, J. O. 1995. *Radiochemistry and Nuclear Chemistry. 2d ed.* Butterworth-Heinemann, Oxford.

Christmas, P. 1984. Traceability in radionuclide metrology. *Nucl. Inst. Meth. Phys. Res. B* 223:427–434.

Clark, S. B. 1995. Separation and determination of isotopes of strontium in calcium carbonate matrices of biological origin. *J. Radioanal. Nucl. Chem.* 194:297–302.

Cooper, E. L., Valkovic, V., Strachnov, V., Dekner, R. and Danesi, P. R. 1992. Intercalibration study of laboratories involved in assessing the environmental consequences of the Chernobyl accident. *J. Environ. Radioactivity* 17:129–145.

Dacheux, N. and Aupiais, J. 1997. Determination of uranium, thorium, plutonium, americium and curium ultratraces by photon-electron rejecting alpha liquid scintillation. *Anal. Chem.* 69:2275–2282.

Dacheux, N. and Aupiais, J. 1998. Determination of low concentrations of americium and curium by photon/electron rejecting alpha liquid scintillation. *Anal. Chim. Acta* 363:279–294.

Decker, K. M. and Sanderson, C. G. 1992. A reevaluation of commercial IBM PC software for the analysis of low level environmental gamma ray spectra. *Appl. Radiation Isotopes* 43:323–337.

Donahue, D. J., 1995. Radiocarbon analysis by accelerator mass spectrometry *Int. J. Mass Spec. Ion Processes* 143:235–245.

Dutton, J. W. R. and Ibbett, R. D. 1973. The determination of technetium-99 in marine biological samples. *CEGB Symposium Paper* AED CONF 73-085 020.

Eakins, J. D. and Morrison, R. T. 1978. A new procedure for the determination of lead-210 in lake and marine sediments. *Int. J. Appl. Radiation Isotopes* 29:531–536.

Edgington, D. N. 1967. The estimation of Th and U at the sub-microgram level in bone by neutron activation. *Int. J. Pure Appl. Isotopes* 18:11–18.

Efurd, D. W., Drake, J., Roensch, F. R., Cappis, J. H. and Perrin, R. E. 1986. *Quantification of Neptunium by Isotope Dilution Mass Spectrometry*. Los Alamos Natl. Lab. Rep. LA-10701-MS. Los Alamos, New Mexico.

Erdmann, N., Herrmann, G., Huber, G., Kohler, S., Kratz, J. V., Mansel, A., Nunnemann, M., Passler, G., Trautmann, N., Turchin, A. and Waldek, A. 1997. Resonance ionisation mass spectroscopy for trace determination of plutonium in environmental samples. *Fresenius J. Anal. Chem.* 359:378–381.

Eroglu, A. E., McLeod, C. W., Leonard, K. S. and McCubbin, D. 1998. Determination of plutonium in seawater using coprecipitation and inductively

coupled plasma mass spectrometry with ultrasonic nebulisation. *Spectrochim. Acta B* 53:1221–1233.

Fakhi, S., Paulus, J. M. and Bouhlassa, S. 1988. Neutron activation analysis of U via ^{239}Np. *J. Radioanal. Nucl. Chem.* 121:99–107.

Fifield, L. K., Cresswell, R. G., di Tada, M. L., Ophel, T. R., Day, J. P., Clacher, A. P., King, S. J. and Priest, N. D. 1996. Accelerator mass spectrometry of plutonium isotopes. *Nucl. Inst. Meth. Phys. Res. B* 117:293–303.

Fifield, L. K., Clacher, A. P., Morris, K., King, S. J., Cresswell, R. G., Day, J. P. and Livens, F. R. 1997. Accelerator mass spectrometry of the planetary elements, *Nucl. Inst. Meth. Phys. Res. B* 123:400–404.

Fridkin, A. M., Ryzhinskii, M. B., Stepanov, A. V., Dubasov, Y. V., Statsevich, V. P. and Gavrish, Y. I. 1992. Evaluation of the plutonium content in soils of the Chernobyl NPP region by means of an interlaboratory experiment. *Sov. Radichem.* 34:599–606.

Goodall, P. and Lythgoe, C. 1999. Rapid separation of uranium and plutonium by extraction chromatography for determination by thermal ionisation mass spectrometry. *Analyst* 124:263–269.

Haase, G., Wiechen, A. and Tait, D. 1993. Results of the 1993 interlaboratory comparison on the determination of gamma nuclides and ^{90}Sr in grass powder. *Kieler Milchwirtschaftliche Forschungsberichte* 45:273–291.

Haase, G., Tait, D. and Wiechen, A. 1996. Results of the 1993 interlaboratory comparison on the determination of gamma nuclides, ^{90}Sr, ^{238}Pu and ^{239}Pu in soil in 1995/96. *Kieler Milchwirtschaftliche Forschungsberichte* 48:209–239.

Hallstadius, L. 1984. A method for the electrodeposition of the actinides. *Nucl. Inst. Meth. Phys. Res* 223:266–267.

Hamilton, E. I. 1981. Alpha particle radioactivity of hot particles from the Esk estuary. *Nature* 290:690–693.

Hamilton, E. I. 1985. The disposal of radioactive wastes into the marine envornment—the presence of hot particles containing Pu and Am in the source term. *Min. Mag.* 49:177–194.

Hamilton, E. I. and R. J. Clifton, 1981. CR-39, a new alpha particle sensitive polymeric detector applied to investigations of environmental radioactivity *Int. J. Appl. Radiation Isotopes* 32:313–324.

Harrison, A. F., Taylor, K. Hatton, J. C., Dighton, J. and Howard, D. M., 1991. The potential of a root bioassay for determining P-deficiency in high altitude grassland. *J. Appl. Ecol.* 28:277–289.

Harvey, B. R. and Lovett, M. B., 1984. The use of yield tracers in the determination of alpha emitting actinides in the marine environment. *Nucl. Inst. Meth. Phys. Res. A* 223:224–234.

Harvey, B. R. and Young, A. K., 1988. Determination of natural radionuclides in a coastal marine sediment—an analysts' intercomparison exercise. *Sci. Total Environ.* 69:13–28.

Harvey, B. R., Lovett, M. B. and Boggis, S. 1987. Some experiences in controlling contamination of environmental materials during sampling and processing for low level actinide analysis. *J. Radioanal. Nucl. Chem.* 115:357–368.

Harvey, B. R., Lovett, M. B. and Blowers, P. 1993. Quantifying the alpha spectrometric analysis of plutonium and americium nuclides down to the 10 μBq level. *Appl. Radiation Isotopes* 44:957–966.
Hindman, F. D. 1986. Actinide separations for α-spectrometry using neodymium fluoride coprecipitation. *Anal. Chem.* 58:1238–1241.
Hursthouse, A. S., Baxter, M. S., McKay, K. and Livens, F. R. 1992. Evaluation of methods for the assay of neptunium and other long-lived actinides in environmental materials. *J. Radioanal. Nucl. Chem.* 157:281–294.
Inn, K. G. W., Lin, Z. V., Liggett, W. S., Schima, F. F., Krey, P., Feiner, M., Liu, C. K., Holloway, R., Harvey, J., Larsen, I. L., Beasley, T., Huh, C. A., McCurdy, D., Germain, P., Yamamoto, M., Handl, J., Popplewell, D. S., Woods, M. J., Jerome, S., Bates, T. H., Holmes, A., Harvey, B. R., Odell, K. J., Warren, B. B. and Young, P. 1996. Low level radioactivity ocean sediment standard reference material. *Appl. Radiation Isotopes* 47:967–970.
Jia, G. G., Testa, C., Desideri, D., Guerra, F. and Roselli, C. 1998. Sequential separation and determination of plutonium, americium-241 and strontium-90 in soils and sediments. *J. Radioanal. Nucl. Chem.* 230:21–27.
Kaye, J. H., Strebin, R. S. and Orr, R. D. 1995. Rapid, quantitative analysis of americium, curium and plutonium isotopes in Hanford samples using extraction chromatography and precipitation plating. *J. Radianal. Nucl. Chem.* 194:191–196.
Komura, K., Sakanoue, M. and Yamamoto, M. 1984. Determination of ^{239}Pu/^{240}Pu ratio in environmental samples based on the measurement of the L X-/alpha-ray ratio. *Health Phys.* 46:1213–1219.
Kushin, V. V., Lyskov, V. N., Sagitova, L. I. and Samoukov, A. V. 1993. Application of solid state track detectors for measurements of the characteristics of hot particles from the vicinity of the Chernobyl NPP. *Nucl. Tracks Radiation Meas.* 21:405–409.
Landrum, J. H., Lindner, M. and Jones, N. 1969. A mass spectrometric method for the determination of sub-nanogram quantities of ^{237}Np. *Anal. Chem.* 41:840–842.
Lopez-Gutierrez, J. M., Garcia-Leon, M., Schnabel, C., Schmidt, A., Michel, R., Synal, H. A. and Suter, M. 1999. Determination of ^{129}I in atmospheric samples by accelerator mass spectrometry. *Appl. Radiation Isotopes* 51:315–322.
Luskus, C. A, 1998. Electroplating versus microprecipitation of the actinides in alpha spectrometric analysis. *J. Radioanal. Nucl. Chem.* 234:287–292.
Martin, D. B. and Pope, D. G. 1982. Separation of tervalent lanthanides from actinides by extraction chromatography. *Anal. Chem.* 54:2552–2556.
Mathew, E., Matkar, V. M. and Pillai, K. C. 1981. Determination of plutonium, americium and curium in environmental materials. *J. Radioanal. Chem.* 62:267–278.
May, S. and Pinte, G. 1986. Neutron activation determination of ^{237}N$_P$ in irradiated experimental fuels and in waste solutions and distribution studies in sea water and submarine flora and fauna of disposal areas. In: *Modern Trends in Activation Analysis*. Risø National Laboratory, Copenhagen, pp. 1343–1350.

McAninch, J. E., Marchetti, A. A., Bergquist, B. A., Stoyer, N. J., Nimz, G. J., Caffee, M. W., Finkel, R. C., Moody, K. J., Sideras-Haddad, E., Buchholz, B. A., Esser, B. K. and Proctor, I. D. 1998. Detection of ^{99}Tc by accelerator mass spectrometry: preliminary investigations. *J. Radioanal. Nucl. Chem.* 234:125–129.

McCarthy, W. and Nicholls, T. M. 1990. Mass spectrometric analysis of plutonium in soils near Sellafield. *J. Environ. Radioactivity* 12:1–12.

McMahon, A. W. 1992. An intercomparison of non-radiometric methods for the measurement of low levels of radionuclides. *Appl. Radiation Isotopes* 43:289–303.

Morris, K. and Livens, F. R. 1996. The distribution of transuranic elements in sediment profiles from an intertidal area in West Cumbria UK. *Radiochim. Acta* 74:195–198.

Morris, H. W., Livens, F. R., Hilton, J. and Nolan, L. 1994. Determination of ^{234}Th/^{238}U disequilibrium in freshwater systems. *Analyst* 119:2403–2406.

Muramatsu, Y. and Yoshida, S. 1995. Determination of ^{127}I and ^{129}I in environmental samples by neutron activation analysis (NAA) and inductively coupled plasma mass spectrometry (ICP-MS). *J. Radioanal. Nucl. Chem.* 197:149–159.

Oughton, D. H., Salbu, B., Brand, T. L., Day, J. P. and Aarkrog, A. 1993. Under-determination of ^{90}Sr in soils containing particles of irradiated uranium oxide fuel. *Analyst* 118:1101–1105.

Parry, S. J., Bennett, B. A., Benzing, R., Lally, A. E., Birch, C. P. and Fulker, M. J. 1995. The determination of I-129 in milk and vegetation using neutron activation analysis. *Sci. Total Environ.* 173:351–360.

Pates, J. M., Cook, G. T., MacKenzie, A. B. and Pass, C. J. 1998. Implication of beta energy and quench level for alpha/beta liquid scintillation spectrometry calibration. *Analyst* 123:2201–2207.

Pates, J. M., Cook, G. T., MacKenzie, A. B. and Thomson, J. 1993. The development of an alpha-beta separation liquid scintillation cocktail for aqueous samples. *J. Radioanal. Nucl. Chem.* 172:341–348.

RSC (Royal Society of Chemistry). 1999. *Environmental Radiochemical Analysis: A Collection of Papers Presented at the Eighth Symposium on Environmental Radiochemical Analysis, Blackpool, 23–26 September 1998*. Royal Society of Chemistry, Cambridge, England.

Rucklidge, J. 1995. Accelerator mass spectrometry in environmental geoscience—a review. *Analyst* 120:1283–1290.

Ruf, H. and Friedrich, M. 1978. Neutron activation analytical determination of small amounts of ^{237}Np in solutions containing U, Pu and fission products. *Nucl. Technol.* 37:79–83.

Salbu, B. and Steinnes, E. 1992. Applications of nuclear analytical techniques in environmental research—plenary lecture. *Analyst* 117:243–249.

Scarpitta, S., Odin-McCabe, J., Gaschott, R., Meier, A. and Klug, E. 1999. Comparison of four ^{90}Sr groundwater analytical methods. *Health Phys.* 76:644–656.

Schmidt, A., Schnabel, C., Handl, J. Jakob, D., Michel, R., Synal, H. A., Lopez, J. M. and Suter, M. 1998. On the analysis of iodine-129 and iodine-127 in environmental materials by accelerator mass spectrometry and ion chromatography. *Sci. Total. Environ.* 223:131–156.

Sill, C. W. and Hindman, F. D. 1974. Preparation and testing of standard soils containing known quantities of radionuclides. *Anal. Chem.* 46:113–118.

Sill, C. W. and Williams, R. L. 1981. Preparation of actinides for alpha spectrometry without electrodeposition. *Anal. Chem.* 53:412–415.

Singh, N. P. 1987. Amines as extracting agents for the quantitative determination of actinides in biological samples. *J. Radioanal. Nucl. Chem.* 115:203–210.

Singh, N. P. and Wrenn, M. E. 1981. Tracers and methods for determining thorium and uranium in biological samples. In: *Proceedings of Snowbird Actinide Workshop*, *October 15–17*, *1979*. R. D. Press, Salt Lake City, UT, pp. 53–68.

Singh, N. P., Zimmerman, C. J., Lewis, L. L. and Wrenn, M. E. 1984. Quantitative determination of environmental levels of U, Th and Pu in bone by solvent extraction and alpha spectrometry. *Nucl. Inst. Meth. Phys. Res.* 223:558–562.

Talvitie, N. A. 1972. Electrodeposition of actinides for alpha spectrometric determination. *Anal. Chem.* 44:280–283.

Taylor, R. N., Croudace, I. W., Warwick, P. E. and Dee, S. J. 1998. Precise and rapid determination of $^{238}U/^{235}U$ and uranium concentration in soil samples using thermal ionisation mass spectrometry. *Chem. Geol.* 144:73–80.

Vaca, F., Manjon, G. and Garcia-Leon, M. 1999. Sr-90 in an alkaline pulp mill located in the south of Spain. *J. Environ. Radioactivity* 46:327–344.

Veirs, D. K., Smith, C. A., Berg, J. M., Zwick, B. D., Marsh, S. F., Allen, P. and Conradson, S. D. 1994. Characterization of the nitrate complexes of Pu(IV) using absorption spectroscopy, N-15 NMR and EXAFS. *J. Alloys Compounds* 213:328–332.

Wyllie, H. A. and Lowenthal, G. C. 1984. Ultra-thin radioactive sources. *Int. J. Appl. Radiation Isotopes* 35:257–258.

Zhu, S., Ghods, A., Veselsky, J. C., Mirna, A. and Schelenz, R. 1990. Interference of ^{91}Y with the rapid determination of ^{90}Sr originating from the Chernobyl fallout debris. *Radiochim. Acta* 51:195–198.

Zimmer, K., Stenner, J., Kluge, H. J., Lantzsch, J., Monz, L., Otten, E. W., Passler, G., Schwalbach, G., Schwarz, M., Stevens, H., Wendt. K., Hermann, G., Niess, S., Trautmann, N., Walter, K. and Bushaw, B. A. 1994. Determination of ^{90}Sr in environmental samples with resonance ionisation spectroscopy in collinear geometry. *Appl. Phys. B—Laser and Optics* 59:117–121.

9

Stable Isotope Analysis and Applications

Charles M. Scrimgeour
The Scottish Crop Research Institute, Dundee, Scotland

David Robinson
The University of Aberdeen, Aberdeen, Scotland

1. INTRODUCTION

The biologically important light elements are hydrogen, carbon, nitrogen, oxygen, and sulfur. Each has at least two stable isotopes, and the most abundant isotope in a pair is the lighter: $^{2}H/^{1}H$ (i.e., D/H), $^{13}C/^{12}C$, $^{15}N/^{14}N$, $^{18}O/^{16}O$, and $^{34}S/^{32}S$. Variations in isotope abundances can reveal and quantify processes in which these elements are involved. Such processes include photosynthesis, respiration, evaporation, organic matter turnover, and C, N, and S metabolism. Stable isotopes can also be used in activities as diverse as monitoring pollution events, tracking animals' food sources, reconstructing past climates, identifying plants' water sources, and untangling biochemical pathways.

Valuable general references include Fritz and Fontes (1980), Vose (1980), O'Leary (1981, 1988, 1993), Hoefs (1987), Raven (1987), Rundel et al. (1989), Coleman and Fry (1991), Griffiths (1991, 1998), Krouse and Grinenko (1991), Robinson and Smith (1991), Handley and Raven (1992), O'Leary et al. (1992), Ehleringer et al. (1993), Engel and Macko (1993), Knowles and Blackburn (1993), Lajtha and Michener (1994), Boutton and Yamasaki (1996), Handley and Scrimgeour (1997), Kendall and McDonnell (1998), Bingham et al. (2000), Mook (2001), Robinson (2001), and Dawson et al. (2002). The Internet is being used increasingly as a source

Marcel Dekker, Inc.
270 Madison Avenue, New York, New York 10016

of the latest stable isotope information. The ISOGEOCHEM website at *http://geology.uvm.edu/isogeochem.html* is a good place to start; Kendall and Campbell (1998) list others.

Many of the approaches described in these references rely on isotopes being used as *tracers*. An isotopically distinct, but chemically indistinguishable, material, the tracer, is introduced into an experimental system, and isotope abundances are later measured in particular compartments of that system. Sometimes the tracer is a naturally occurring substance that happens to be isotopically distinct from others in the system. Increasingly, however, use is being made of *isotope fractionations*. These can report on the operation of chemical and physical processes that change the natural isotopic abundances of substrates and products involved in those processes. The tracer and fractionation approaches are conceptually distinct and capable of addressing different research questions (Table 1).

Each approach demands its own theory and protocols, but both require similar instrumentation. Most of this chapter (Secs. III and IV) describes current instrumentation and analytical techniques used for stable isotope analysis. It relies heavily on our experience of automated, continuous-flow mass spectrometers to analyze the isotopic contents of soil, plant, and animal samples. Examples of tracer and fractionation applications are discussed in Sec.V. Section VI is, finally, a brief preview of future developments. We begin, however, with an overview of terminology.

II. TERMINOLOGY

A. Isotope Ratio

Mass spectrometers (see Sec. III) measure the *ratio* (R) of heavy to light isotopes:

$$R = \frac{n_{\mathrm{H}}}{n_{\mathrm{L}}} \tag{1}$$

where n_{H} and n_{L} are the *numbers* of atoms containing heavy and light isotopes, respectively. For example, if five out of every 100 N atoms in an N sample are ^{15}N and the rest ^{14}N, the sample's $^{15}N/^{14}N$ ratio is $5/95 = 0.0526$.

Isotope ratios are usually converted into more convenient quantities. For tracer work, atom percentages are suitable; for natural abundances, δ values are more appropriate.

Table 1 Tracer and Fractionation Approaches Compared

	Tracer approach		
	Labeled tracers	Natural tracers	Fractionation approach
Isotope abundance range	Much greater than natural abundance range	Within natural abundance range	Within natural abundance range
Extent of perturbation to system	Large	Small or zero	Zero
Cost of tracer	Potentially huge	Zero	Zero
Sensitivity of detection	Excellent	Poor to good	Poor to excellent
Appropriate duration of study	< 1 h to 1 yr	Unsuitable for short-term (< 1 h) studies	< 1 h to $> 3.8 \times 10^9$ yr (Schidlowski, 1988)
Appropriate scale of investigation	Usually pot or small plot, but for lightly enriched tracers, small catchment studies are feasible (Nadelhoffer and Fry, 1994)	Pot to landscape	Molecular to global
Conditions required	Isotopic composition of tracer greater than natural range. Steady-state labeling achieved within sinks (Deléens et al., 1994)	Reliable and distinct differences in isotopic composition of all potential source pools	Reliable measurements of isotopic compositions of all potential source pools

continued

Table 1 Continued

	Tracer approach		
	Labeled tracers	Natural tracers	Fractionation approach
Information required	Isotopic composition of tracer before addition to system; system components before addition; system components after addition. Amount of tracer added	Isotopic composition of all potential tracer sources; of system containing no tracer; of components of system containing tracer. Fluxes among pools if more than two sources are involved	Isotopic composition of all important pools. Amounts of element in each pool. Fractionation factors for candidate processes
Interpretive model	Mixing	Mixing	Fractionation and mixing
Information obtained	Amounts and rates of mixing of tracer in nontracer pools	Amounts and (possibly) rates of mixing of tracer in nontracer pools	Quantitative identification of likely processes causing fractionations

B. Atom Percentage

The abundance of the heavier isotope in an isotope pair as the fraction of the total amount of the element is the *atom fraction* or, more usually, *atom percentage* (A):

$$A = 100\frac{n_H}{n_H + n_L} = 100\frac{R}{R+1} \tag{2}$$

In the example for ^{15}N given above, A is $[5/(5+95)] \times 100 = 5$ atom %. The *mass* percentage (A_m) of ^{15}N in this sample is not, however, 5%. It is calculated by multiplying n for each isotope by its atomic mass, m, so that

$$A_m = 100\frac{m_H n_H}{m_H n_H + m_L n_L} \tag{3}$$

where m_L and m_H are the masses of the light and heavy isotopes, respectively. For our N sample, m_L and m_H are 14 and 15, respectively, and A_m is 5.338%.

A and A_m are related by

$$A_m = 100\frac{m_H A}{100 m_L + A(m_H - m_L)} \tag{4}$$

Using Eq. (2) rather than Eq. (3), as often happens in practice, slightly underestimates the true mass fraction.

The amount (X^*) of an element in a sample that is derived form a tracer is given by

$$X^* = \frac{X(A_{sample} - A_{background})[m_L(100 - A_{tracer}) + m_H A_{tracer}]}{(A_{tracer} - A_{background})[m_L(100 - A_{sample}) + m_H A_{sample}]} \tag{5}$$

where X is the total amount of the element in the sample, A_{sample} is the sample's atom % (Eq. 2), A_{tracer} is the atom % of the tracer originally added, and $A_{background}$ is the background atom % in the system before the tracer was added.

For a given isotope pair, Eq. 5 is simplified considerably by substituting the appropriate values for m_L and m_H. Let us suppose that our N sample for which $A_{sample} = 5$ atom % is from an experiment to which a tracer containing 7.5 atom % ^{15}N had been added (A_{tracer}), and assume that the background ^{15}N abundance in the system ($A_{background}$) is 0.3663 atom % (*cf.* Table 2; see Sec. V.A.1). If the sample contains a total of

Marcel Dekker, Inc.
270 Madison Avenue, New York, New York 10016

Table 2 Heavy : Light Isotope Ratios ($R_{standard}$) and Atom % Values (A) in the International Standards Used for the Analysis of D/H, $^{13}C/^{12}C$, $^{15}N/^{14}N$, $^{18}O/^{16}O$, and $^{34}S/^{32}S$. By Definition, the δ Value of Each is 0‰

Isotope pair	Standard material	$R_{standard}$	A
D/H	Vienna Standard mean Ocean Water (V-SMOW)	0.00015576	0.01557
$^{18}O/^{16}O$	Vienna Standard mean Ocean Water (V-SMOW)	0.00200520	0.20012
$^{18}O/^{16}O$	Vienna PeeDee Belemnite (V-PDB)	0.0020671	0.20628
$^{13}C/^{12}C$	Vienna PeeDee Belemnite (V-PDB)	0.0112372	1.11123
$^{15}N/^{14}N$	Atmospheric N_2	0.0036765	0.3663
$^{34}S/^{32}S$	Canyon Diablo Troilite	0.0450045	4.30663

100 g N (X), then the amount of N in the sample that is derived from the tracer (X^*) is 65.1 μg.

The term *atom percent enrichment* or *atom percent excess* (*APE*) is used frequently. This is simply the difference in atom % between a sample and background. In Eq. (5), the terms ($A_{sample} - A_{background}$) and ($A_{tracer} - A_{background}$) are *APE* values.

C. δ Notation

The natural abundances of D, ^{13}C, ^{15}N, ^{18}O, and ^{34}S range from only 0.01 to ~4 atom % (Fig. 1). Close to natural abundance, it is more convenient to express the isotope ratio of a sample as the relative difference from that of a standard; this is the *δ notation*. δ values are expressed in parts per thousand or 'per mille' (‰). The δ value of a sample, δ_{sample}, is given by

$$\delta_{sample} = 1000 \frac{R_{sample} - R_{standard}}{R_{standard}} \tag{6}$$

where R_{sample} and $R_{standard}$ are the isotope ratios of sample and standard, respectively [Eq. (1)]. Values of $R_{standard}$ are listed in Table 2, with the corresponding atom % values. In practice, working standards are calibrated against these primary standards using materials supplied by the international Atomic Energy Agency (Vienna), the Los Alamos National Laboratory (U.S.A.), and other agencies. By definition [Eq. (6)], each standard in Table 2 has a δ value of 0‰.

Samples with negative δ values are "depleted" in the heavier isotope relative to the standard; those that are positive are "enriched" (see Kendall and Caldwell, 1998). For example, if a sample has a $^{13}C/^{12}C$ ratio of 0.0111372, this differs by only 0.0001 from the standard (Table 2). This is

Marcel Dekker, Inc.
270 Madison Avenue, New York, New York 10016

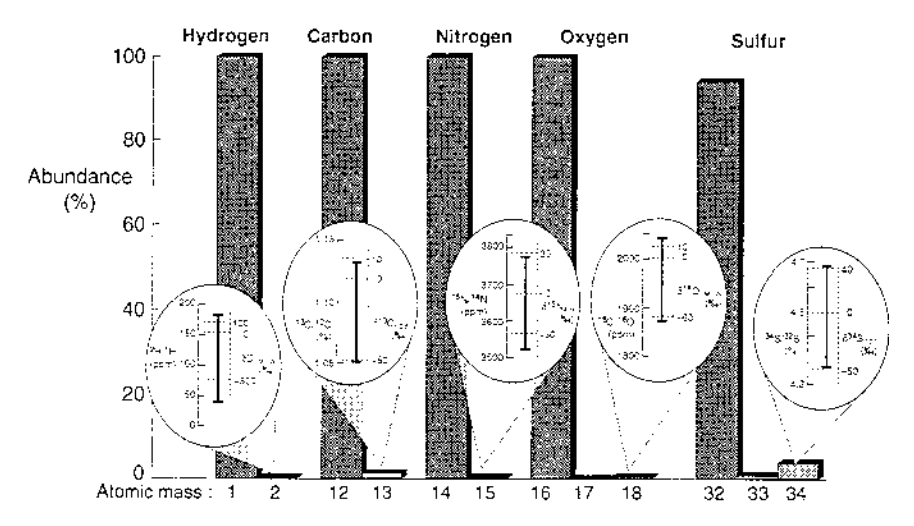


Figure 1 Natural abundances of $^2H/^1H$, $^{13}C/^{12}C$, $^{15}N/^{14}N$, $^{18}O/^{16}O$, and $^{34}S/^{32}S$. The insets show the range of natural variation in isotope ratio and the δ values (‰) to which these correspond.

equivalent to $\delta^{13}C = -8.9‰$ in the sample, i.e., it is ^{13}C-depleted compared with the standard.

For a particular isotope pair, δ and A are related by

$$\delta = 1000\left[\frac{A}{R_{\text{standard}}(100 - A)} - 1\right] \tag{7}$$

where R_{standard} is the value in Table 2 appropriate for the isotope pair.

D. Fractionation and Discrimination

D, ^{13}C, ^{15}N, ^{18}O, and ^{34}S occur naturally in varying amounts in different materials. These variations reflect isotopic fractionations of the heavier and lighter isotopes in a pair. Fractionations occur because more energy is needed to break or form chemical bonds involving the heavier isotope of a pair (Atkins, 1998, p. 833).

For a reaction occurring over an infinitesimal time interval, a *fractionation factor*, α, can be defined. This is the isotope ratio of the substrate divided by that of the product for that time interval:

$$\alpha = \frac{R_{\text{substrate}}}{R_{\text{product}}} \tag{8}$$

When $\alpha > 1$, the heavier isotope accumulates in the substrate as a reaction proceeds; when $\alpha < 1$, it accumulates in the product. If $\alpha = 1$, $R_{substrate} = R_{product}$ and there is no fractionation. (Note that some authors define α as $R_{product}/R_{substrate}$: e.g., Mariotti et al., 1981). An expression that translates α values onto a ‰ scale for direct comparison with α values is

$$\varepsilon = 1000(\alpha - 1) \tag{9}$$

where ε is the instantaneous *isotopic enrichment factor*; see Mariotti et al. (1981).

α and ε values are not strictly constants, but depend on temperature, the identities of the reactants (including any enzymes that mediate the reaction), and bond energies (Atkins, 1998, p. 833). This is true whether the fractionation occurs during a unidirectional kinetic reaction (e.g., $NH_4^+ + OH^- \rightarrow NH_3 + H_2O$) or in a system at equilibrium (e.g., $NH_4^+ + OH^- \leftrightarrow NH_3 + H_2O$). In each of these examples, the NH_4^+ becomes more ^{15}N-enriched than the NH_3. For a given reaction under defined, closed conditions, however, α is effectively constant irrespective of substrate availability and may be characteristic of the reaction. α values for some biologically important reactions are tabulated in Friedman and O'Neill (1977), Leary et al. (1992), Handley and Raven (1992), O'Leary (1993), Nordt et al. (1996), Wada and Ueda (1996), and Handley et al. (1999). Most of these indicate the magnitudes of fractionations when substrate availability is not limiting and other conditions are favorable. They do not necessarily indicate the fractionations that occur in vivo and which are often smaller than those in vitro.

As a reaction proceeds, the δ values of substrates and products change in a predictable way, as described by Rayleigh equations (Mariotti et al. 1981; Hoefs, 1987). The δ value of the substrate (δ_S) depends on its initial δ value (δ_0), on ε (Eq. 9), and the fraction (ϕ) of the substrate that has been consumed in the reaction:

$$\delta_S = \delta_0 - \varepsilon \ln(1 - \phi) \tag{10}$$

The δ value of the instantaneous product (δ_{Pi}) is approximated as

$$\delta_{Pi} \approx \delta_S - \varepsilon \tag{11}$$

The product created in any particular time-step mixes with that from earlier time-steps. The resulting δ value of the accumulated product ($\bar{\delta}_P$) is given by

$$\bar{\delta}_P = \delta_0 + \frac{\varepsilon(1 - \phi)[\ln(1 - \phi)]}{\phi} \tag{12}$$

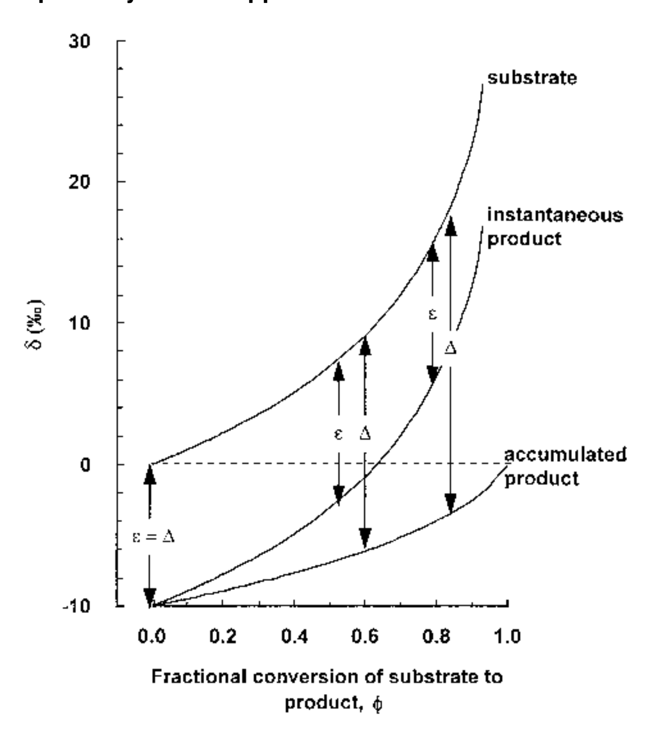


Figure 2 Changes in δ values of substrate and product in a closed system as a function of the fraction (ϕ) of substrate consumed in a reaction. The initial δ of the substrate in this example is 0‰. The δ values of substrate, instantaneous product, and accumulated product are calculated using Eqs. (10–12). ε is the instantaneous isotope fractionation factior [Eq. (9)], which is constant and, in this example, $=10$‰. Discrimination (Δ; Eq. (14)] is not constant but approximates to the difference between the δ values of substrate and accumulated product. Only when $\phi \sim 0$ does $\Delta = \varepsilon$.

Figure 2 illustrates how δ_S, δ_{Pi} and $\bar{\delta}_P$ vary with ϕ. Equations 10–12 apply strictly to a unidirectional single-step reaction in a closed system. In such a reaction, the final product has the same isotopic composition as the initial substrate, i.e., as ϕ tends to 1, $\bar{\delta}_P$ tends to δ_0. Equations 10–12 can, however, also be applied to natural systems comprising multiple open reactions, especially if one fractionating process dominates (O'Leary, 1988; Sec. V.C.3). Open reactions involve the addition of new substrate and/or the removal of accumulated product, and are never "completed" Isotopic differences between substrates and products persist (although the differences are not necessarily constant). Such differences are termed isotope

discriminations (symbolized as Δ). If substrate availability is effectively unlimited (i.e., if $\phi \sim 0$: see Fig. 2), then

$$\Delta \approx \varepsilon \tag{13}$$

Combining Eqs. 6, 8, 9, and 13 gives (O'Leary, 1981)

$$\Delta = \frac{\delta_{\text{substrate}} - \delta_{\text{product}}}{1 + (\delta_{\text{product}}/1000)} \approx \delta_{\text{substrate}} - \delta_{\text{product}} \tag{14}$$

A positive discrimination indicates that the heavier isotope accumulates in the substrate ($\delta_{\text{substrate}} > \delta_{\text{product}}$); a negative discrimination indicates the opposite.

The most extensive biological use of Δ has been to compare discriminations against ^{13}C during photosynthesis by C_3 plants (Sec. V.C.2). Unfortunately, other systems are not so amenable. For example, it is not yet possible to calculate Δ for N assimilation by plants growing in soil. This is because the availability and $\delta^{15}N$ values of putative substrates [e.g., NO_3^-, NH_4^+, dissolved organic-N (DON)] at the assimilatory site(s) or metabolic branch points (O'Leary, 1981) where $^{15}N/^{14}N$ fractionations may occur cannot be assumed or measured reliably by current methods (Sec. V.C.3).

E. Isotope Mass Balances and Mixing Models

One of the most useful and frequently encountered isotope equations is the isotope mass balance. The relates the δ value of a composite sample to those of its components, each weighted by its mass. If a sample has two components of mass X and Y with δ values δ_X and δ_Y, respectively, then δ value of the composite sample ($\bar{\delta}$) is

$$\bar{\delta} = \frac{X\delta_X + Y\delta_Y}{X + Y} \tag{15}$$

If it has more than two components, Eq. (15) is modified accordingly. Depending on the available information, Eq. (15) can be solved to estimate an unknown δ value or mass.

For example, suppose one wished to enrich 1 kg of C_3 plant material with ^{13}C so that its $\delta^{13}C$ value was about 500‰. How much ^{13}C-enriched CO_2 containing 5 atom % ^{13}C would be needed? 1 kg (fresh weight) of plant material would contain about 40 g C (X) with a $\delta^{13}C$ value (δ_Y) of about -27‰. 5 atom % ^{13}C is equivalent to a $\delta^{13}C$ value (δ_Y) of 3684‰ [Eq. (7)].

Marcel Dekker, Inc.
270 Madison Avenue, New York, New York 10016

By setting $\bar{\delta}$ to 500‰, Eq. (15) can be solved for Y, which, in this example, is 6.6 g C, or about 0.5 mol. The plants should, therefore, be exposed to about 1 mol of ^{13}C-enriched CO_2 to allow for inefficient C assimilation, leakages from the chamber enclosing the plants, and other losses during exposure. This is a rough calculation, but it is sufficient to estimate the likely amounts (and costs) of an isotope that will be required.

If absolute masses of each component are not known, but their fractional contributions are, Eq. (15) becomes, for a two-component mixture,

$$\bar{\delta} = x\delta_X + (1 - x)\delta_Y \tag{16}$$

where x is the fraction derived from component X. Solving Eq. (16) for x gives

$$x = \frac{\bar{\delta} - \delta_Y}{\delta_X - \delta_Y} \tag{17}$$

Equation (17) can be used in many stable isotope applications (e.g., Sec. V.B.1) to calculate the fraction of one source present in a mixture of two (and only two) isotopically distinct sources. The precision with which this can be done increases with the isotopic difference between the two sources (δ_X and δ_Y)—the "end members" of the mixing model. Variations in end member δ values caused by fractionations or imprecise measurement reduce the precision of x. Equation (17) can also be used with atom % values substituting for δ, if appropriate.

III. ISOTOPE RATIO MASS SPECTROMETRY

A. General Principles of Mass Spectrometry

Measuring natural abundance isotope ratios or low tracer enrichments of the biologically important light elements is a challenge. The natural range in abundance of the heavier isotope in a pair varies from twofold for D to $< 10\%$ for ^{15}N, ^{13}C, and ^{18}O (Fig. 1). Kinetic or equilibrium fractionations or mixing of isotopically distinct sources (Sec. II.D) may change net isotope abundance by only a small fraction of the natural range. The analytical problem is to measure changes as small as one part per thousand or less in a ratio of 1/10000, as is the case for D/H. At the other extreme, S, with $\sim 4\%$ as ^{34}S, is less of a challenge in this respect but is more difficult to handle chemically.

Marcel Dekker, Inc.
270 Madison Avenue, New York, New York 10016

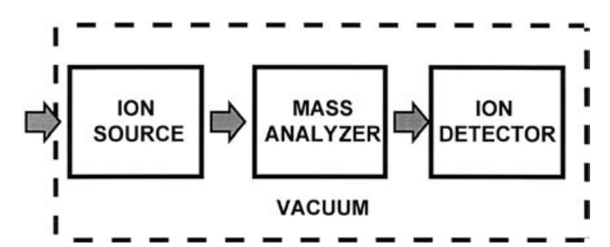


Figure 3 Schematic diagram of the essential components of any mass spectrometer.

Certain spectroscopic techniques such as nuclear magnetic resonance and infrared spectroscopy can detect and measure the abundance of stable isotopes. However, only mass spectrometry is capable of measuring natural isotopic variations in H, C, N, O, and S with a large sample throughput and high precision, and at a modest cost. All of these are now essential requirements in most analytical laboratories that serve environmental research. Even with a mass spectrometer, the problem is not easily solved, and specially designed *isotope ratio mass spectrometers (IRMS)* have been developed for this purpose over the past 50 years.

All mass spectrometers contain three essential components: an ion source, a mass analyzer, and an ion detector (Fig. 3). These perform the following basic functions in any mass spectrometer. The sample is first introduced to the *ion source*, where the substance is converted into positive or negative ions. These ions are focused into a beam that then enters the *mass analyzer*. There, ions of different *mass/charge* (*m/z*) *ratio* are separated either in time or in space before entering the *ion detector*. This produces an output signal proportional to the abundance of each *m/z* species separated by the mass analyzer. The output is generally referred to as the mass spectrum. The ion source, mass analyzer, and detector are contained in a high vacuum system to minimize dispersion of the ion beam by collisions with air molecules. Here we are concerned with IRMS. Before describing the two basic types (dual-inlet and continuous-flow), we consider some general principles that underlie the operation of each.

B. Isotope Ratio Mass Spectrometry

1. General Principles

The measurement of ion beam intensities with sufficient precision to determine isotope natural abundances requires purpose-built IRMS. The basic IRMS design has changed little since it was first developed. Only

major developments in materials, electronics, and data handling distinguish modern automated IRMS from their predecessors.

An IRMS for low atomic weight elements can analyze only low molecular weight "fixed gases," irrespective of the nature of the original sample. H_2 is used for D/H measurement, N_2 for $^{15}N/^{14}N$, CO_2 for both $^{13}C/^{12}C$ and $^{18}O/^{16}O$, and SO_2 or SF_6 for $^{34}S/^{32}S$. The gas is admitted to the mass spectrometer from a reservoir through a fine capillary. This gives a steady supply of gas to the ion source and avoids diffusive fractionation of the isotopes in the inlet. In the source, the gas is ionized by an electron beam produced from a hot filament of rhenium or thoriated tungsten. The ion stream is accelerated through 3–5 kV before entering a magnetic sector mass analyzer. The ion beam passes through a magnetic field at 90° to its direction of travel. This causes the beam to bend. Ions of different m/z leave the source with equal velocity, but the heaviest have most momentum and are deflected less easily by the magnetic field. Once separated in this way, ions of different m/z are focused into different ion beams at the end of the mass analyzer or "flight tube" (Fig. 4).

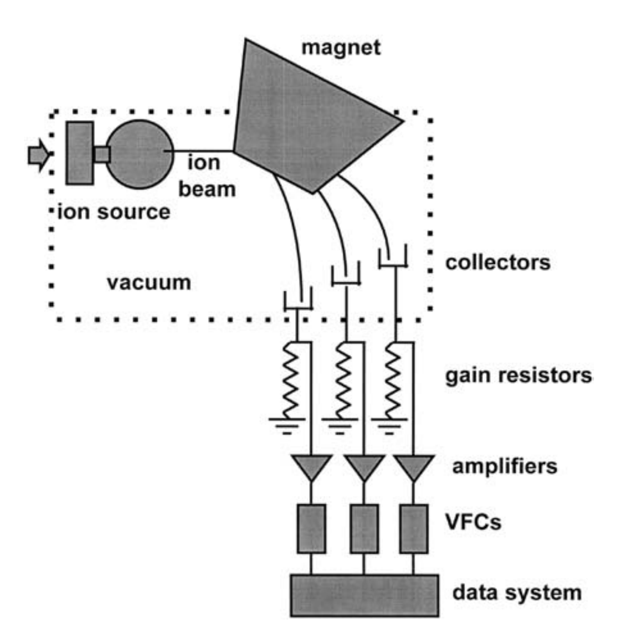


Figure 4 Schematic diagram of a triple-collector IRMS designed for low molecular weight gases. The parallel arrangement of collectors, gain resistors, and voltage-to-frequency converters (VFC) allows simultaneous measurement of the isotopomer ion currents.

The geometry of the source and flight tube gives low resolution of the ion beams, each beam having a constant intensity over a significant portion of its peak width. These "flat-topped" ion beams are each detected by separate Faraday cup collectors. Separate collectors are required to cope with the large intensity range (up to 1 : 10,000) between the most and the least abundant ion beams, and allow the isotopomer ion currents to be measured simultaneously. The ion beams are focused by adjusting the accelerating voltage and/or the magnetic field strength so that the middle of the flat top of each beam enters a Faraday cup. In this way, small drifts in the focusing parameters do not alter the measured intensity ratio between the ion beams, as would be the case if the beams had sharp peaks.

The cups are connected to ground through a large resistance, completing the circuit from the source. The ion current flowing through the resistor creates a voltage that is the output from the mass spectrometer. The voltage is fed into a computer-based data system via an impedance-matching amplifier (Fig. 4). The ion current through an IRMS is $\sim 10^{-8}$ A for the most intense beam and 10^{-11} A or less for the other beams. To produce a useful output voltage for the data system (a range of 1–10 V), resistors of 10^8 to 10^{12} Ω are required for the most and least intense beams, respectively.

By using a higher resistor for the less abundant ion beams, the output entering the data system can be brought into the same voltage range for each beam. The respective ion beam intensities are then measured by integrating the output voltages over a time period using parallel voltage frequency converters (VFCs) and counter circuits. An important design feature is that the gain resistors and amplifiers must be very stable and produce a minimum of spontaneous noise, thereby minimizing drift during sequential measuring periods.

2. Handling IRMS Output

Although an IRMS measures isotope ratios for a particular fixed gas (H_2, N_2, CO_2, or SO_2: Sec. II.A), the information usually required is the isotope ratio of a particular element. Further processing of the IRMS output is required to derive this information. The need to apply corrections to the measured isotope ratios is not a major drawback of the method compared with the significant advantages of analyzing stable and readily prepared gases. Providing the corrections are fully understood and carefully used, precise and accurate results can be obtained by applying a standardized measurement method to a few gases derived from a wide variety of samples. In modern IRMS, these "ion corrections" are normally carried out

Marcel Dekker, Inc.
270 Madison Avenue, New York, New York 10016

automatically by the instrument software, and it should be remembered that assumptions may be involved in the calculations.

CO_2. When analyzing CO_2, we measure the isotope ratios for $m/z =$ 45/44 and 46/44. These correspond to the significant isotopomers of CO_2^+. We wish to know either $^{13}C/^{12}C$ or $^{18}O/^{16}O$ but must allow for the presence of ^{17}O. More information is required to calculate the desired ratios than is available (only two measured isotope ratios for three independent isotope ratios). Only by assuming that ^{17}O abundance covaries with the ^{18}O abundance can $^{13}C/^{12}C$ and $^{18}O/^{16}O$ abundances be estimated from the experimental measurement (Mook and Grootes, 1973). This correction may be invalid for certain samples, e.g., when even small amounts of enriched O isotopes are present.

H_2. Different corrections are required for H_2 analysis, where the measured isotope ratio at $m/z = 3/2$ is a combination of the required D/H ratio and the H_3^+/H_2^+ ratio. H_3^+ is unavoidably formed in the ion source and has the same mass as dihydrogen containing ^2H and ^1H. Careful source design can minimize the amount of H_3^+ formed, but prior calibration of the IRMS is required to correct for this interfering signal.

N_2. With N_2, no ion correction is required at natural abundance, but correction for residual air in the IRMS may be required. With ^{15}N-enriched samples, the possibility of $^{15}N_2$ ($m/z = 30$) being formed must be allowed for. Corrections may be applied above a threshold ^{15}N enrichment of ~ 5 atom%.

SO_2. Correction for the contribution of ^{18}O to the $m/z = 66/64$ ratio is required. This is usually done by assuming a fixed value for $^{18}O/^{16}O$ (Eriksen, 1996). With SF_6 no correction is required.

C. Dual-Inlet IRMS

Despite all the above adaptations to cope with large differences in ion currents and to achieve stability, it is not possible to make absolute measurements of isotope ratios sufficiently accurate for natural abundance studies. Differential measurements against a defined standard are used to achieve this and to minimize the effect of instability during measurement. Differential measurement compares the isotope ratio of a *reference gas* with that of the sample, each measured under the same conditions and within a short time period of each other. The conventional way of arranging this is to use a dual-inlet (DI) system.

Gas is held in separate reference and sample reservoirs. From these, gas flows through matched capillaries to a system of crossover valves. These

Marcel Dekker, Inc.
270 Madison Avenue, New York, New York 10016

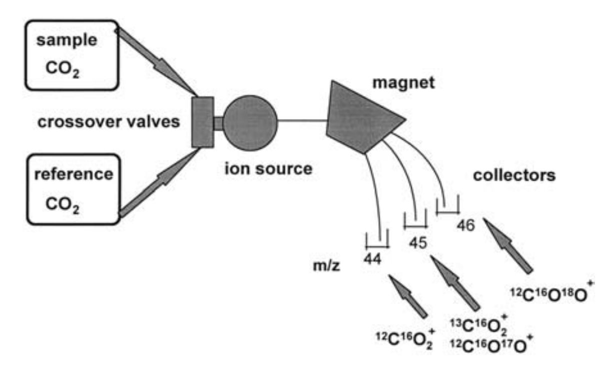


Figure 5 Schematic diagram of a DI-IRMS, measuring *m/z* 45/44 and 46/45 ratios for CO_2. CO_2 from the sample and reference reservoirs are measured alternately after adjusting the reservoir volumes to give the same major beam ion current.

valves allow the gases to enter alternately the IRMS or a waste vacuum line (Fig. 5). The crossover valves are designed to perturb the gas flow as little as possible during the switchover, and to avoid mixing of sample and reference gases. The pressure in each reservoir can be adjusted and matched by altering reservoir volumes using bellows. This ensures that the reference and sample gases are measured at the same ion current. Such a degree of controlled matching is possible only with gaseous samples.

Using a DI, the reference and sample signals are each integrated for 10–20 s following a settling period of 5–15 s after each changeover. This is repeated for several (3–10) cycles and the data averaged over each cycle and over the set. In this way, drifts in the detector system can be compensated for as far as possible and aberrant measurements caused by transient noise or spikes rejected.

The measurement process, valve operation, and data collection are now usually computer-controlled. However, sample introduction may often be manual, and the IRMS may provide information only on isotope ratios and not on elemental amounts. Sample conversion may be on- or off-line. DI-IRMS are still widely used, despite now being replaced in many laboratories by more convenient continuous-flow IRMS (Sec. III.D). DI-IRMS remain the most usual instruments for measuring D/H, but recent developments in continuous-flow approaches (Prosser and Scrimgeour, 1995; Begley and Scrimgeour, 1997) will change this in the future.

D. Continuous-Flow IRMS

The development of solid-state electronics provides electronic stability over many minutes. This, and improved vacuum pumping, has led to the

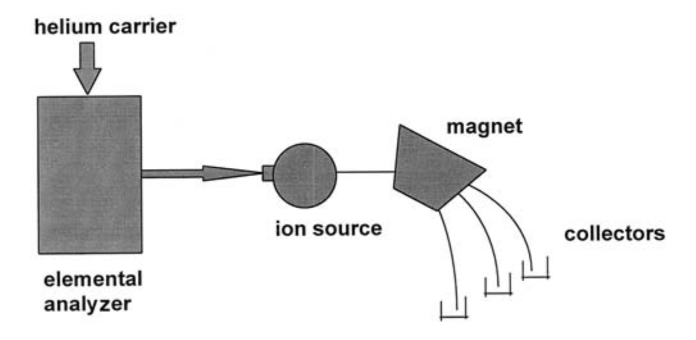


Figure 6 Schematic diagram of a CF-IRMS, consisting of an elemental analyzer and gas IRMS. After each solid sample is dropped into the elemental analyzer, pulses of purified analyte gas (e.g., N_2 or CO_2) are carried by the continuous flow of He into the IRMS.

development of an alternative sample inlet system known as a *continuous-flow* (CF) inlet. Here, pulses of gas are introduced to the source in a steady flow of He carrier. Up to ten samples can be analyzed between pulses of reference gas (Fig. 6). The CF inlet is considerably simpler (and cheaper) than the DI and suited to more rapid analyses. The precision of modern CF-IRMS can approach that of many DI-IRMS in routine use.

CF-IRMS systems are designed to be integrated with a sample preparation device to produce regular pulses of analyte gas. The original and most common sample preparation device is a Dumas combustion elemental analyzer or ANCA (automated C and N analyzer: see also Chap. 6), the combination often being called an ANCA-MS (Sec. IV.A). Other sample preparation systems for gas analysis and trace gas concentration are available for integrated CF-IRMS systems.

The ultimate exploitation of CF-IRMS is in systems that first separate individual compounds from a mixture by GC and then convert them to an IRMS-compatible gas. This technique has already acquired an unfortunate variety of names and acronyms: compound-specific isotope analysis, stable isotope ratio monitoring–GC/MS, GC-combustion IRMS; or just GC-IRMS. This is still a specialized area, but it will undoubtedly lead to a much more detailed understanding of C and N metabolism in biological systems.

E. Sample Preparation for IRMS

Sample preparation is a nontrivial part of isotope analysis and may require as much time and care as the final IRMS measurement. All samples—animal,

Marcel Dekker, Inc.
270 Madison Avenue, New York, New York 10016

vegetable, or mineral—must be converted into a gas suitable for isotope analysis by IRMS. Each gas must be pure to enable sample and reference matching and to avoid interfering reactions in the ion source. For example, a trace of CO_2 in N_2 will produce some CO^+ in the ion source. CO^+ has $m/z = 28$, the same as for N_2. It is equally important that the isotope ratio of the prepared gas truly reflects that of the original sample. This means that sample conversion must be complete to avoid isotope fractionation or that an equilibrium is set up under identical conditions for all samples.

It is often possible to integrate and automate sample preparation systems with an IRMS, and this has great practical advantages. Automated systems can operate unattended overnight, making efficient use of instrument time, and can produce better sample-to-sample and batch-to-batch reproducibility than the most patient and careful operator. An important example of such an integrated system is the ANCA-MS (Sec. IV.A).

Even with automation, considerable labor may be needed to provide samples. Approximately the same amount of material must be analyzed for each sample. This requires careful dispensing of liquid samples or weighing of solids. Solid samples must also be finely ground before analysis to ensure representative subsampling. For example, the amount of plant material required for an elemental analyzer is ~ 1 mg oven-dry weight. These subsamples must be weighed accurately into a tinfoil cup. The time-consuming steps of grinding and weighing have been a characteristic of all elemental analyzer use for many years and are largely unavoidable.

Most studies of natural abundance variations in C and N have used bulk samples, with little or no chemical separation of the components of the sample. Detailed understanding of the mechanisms controlling the isotopic composition of the material will increasingly require such separation. The methods used will vary with the compounds being studied, but the fundamental requirement is for those that are quick and efficient. Complete separation of a compound from its matrix ensures that no isotope fractionation will occur (although the risks of fractionation decrease as the molecular weight increases).

IV. CF-IRMS IN PRACTICE

We turn now to the CF-IRMS analysis of particular isotopes in different sample types. The procedures that we describe have evolved from our experience of analyzing both solid and gas samples at the SCRI laboratory. Slight modifications to accommodate different instruments and applications are to be expected.

A. ANCA-MS for Carbon and Nitrogen

The CF inlet is particularly suited (and indeed was developed) for use with an elemental analyzer. Elemental analyzers oxidize samples of organic material to give a mixture of N_2 and CO_2. In an ANCA-MS, this mixture is carried by the He carrier into a gas chromatograph (GC). There the gases are separated and emerge as two peaks that can be fed sequentially into the IRMS (Fig. 7).

1. Principle of Operation

Samples containing suitable amounts of N and/or C are contained in tinfoil cups and loaded into a rotating disk autosampler. This may consist of one or more wheels with a capacity for up to 150 samples plus the necessary standards. During operation, a cup is dropped from the wheel into the combustion tube containing chromium trioxide at 1000°C as a pulse of O_2 is injected. Flash combustion of the tin raises the local temperature to around 1700°C, ensuring complete combustion of the sample. The He flow sweeps

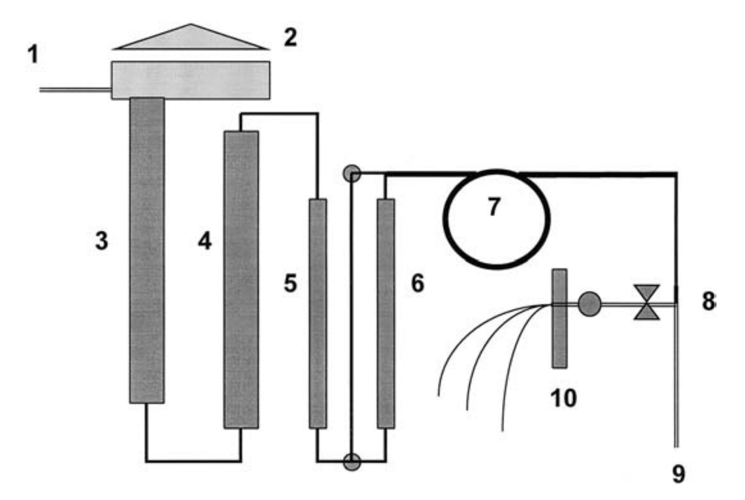


Figure 7 Typical layout of an ANCA-MS system. (1) Continuous flow of He into the elemental analyzer and autosampler. (2) Autosampler holding solid samples in tinfoil cups. (3) Combustion tube containing chromium trioxide at 1000°C. (4) Reduction tube containing copper at 600°C. (5) Water trap containing magnesium perchlorate. (6) Optional CO_2 trap containing Carbosorb. (7) Gas chromatograph to separate N_2 and CO_2. (8) Open split where a small portion of the He flow enters the IRMS through a crimped capillary. (9) Open capillary vent for remainder of He. (10) IRMS. Helium flows continuously from (1) to (9).

the combustion products first through a copper reduction furnace at 600°C where N oxides are reduced to N_2 and then through magnesium perchlorate at room temperature to remove water. Optionally, the gases may be passed through a Carbosorb trap to remove CO_2. The gases are then separated on a GC column, to give fully resolved peaks of N_2 and CO_2 in the He carrier flow.

Only a fraction of the effluent enters the IRMS, to keep the analyzer pressure at $\sim 10^{-6}$ mbar. This is achieved with a narrow crimped capillary and three-way valve or concentric capillaries—sometimes referred to as an open split. The bulk of the effluent passes to atmosphere, through a long capillary to minimize back-diffusion of atmospheric gases.

After combustion, but before the sample gas reaches the mass spectrometer, the background signals are measured. As the gas pulse enters the IRMS, the appropriate mass signals are integrated, *m*/*z* 28, 29, and 30 for N_2 and 44, 45, and 46 for CO_2 (Fig. 8). Following the peak, the background is again measured, and the mean background subtracted from the integrated areas. Blank values, obtained when no sample is introduced, are also subtracted from the peak areas; this is particularly important when traces of N in the O_2 pulse interfere with the N produced by combustion.

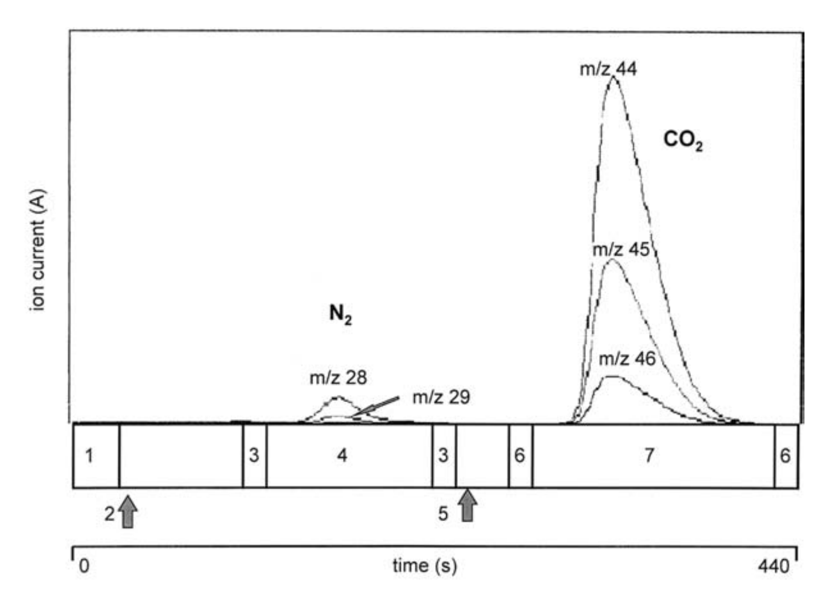


Figure 8 ANCA MS trace showing the timing of a sample analysis. (1) O_2 pulse. (2) Sample drops. (3) N_2 zero. (4) Measure N_2. (5) Switch source to CO_2. (6) CO_2 zero. (7) Measure CO_2.

Calibration is made against reference material introduced before and after batches of (usually ten) samples.

A run of samples is set up after a daily check procedure. This consists of a background scan to check that there are no interfering signals or air leaks, and peak centering to ensure stable ratio measurement. The water and CO_2 traps are checked and replaced if necessary. The ash collection tube in the combustion furnace is checked and replaced if a bright red glow is not visible. After venting the O_2 supply for 30 s to remove any air, three blanks are run with no samples in the autosampler. This allows correction for the inevitable small N_2 signal from the O_2 pulse. The C blank should be negligible.

The sample identifiers and weights are entered into the sample table of the data system. Samples and standards are put in the autosampler wheel in the same order as in the sample table. The analysis sequence starts with two or three working standards used as dummies, followed by a working standard, and then ten samples, and then a pair of working standards. The first working standard (sometimes referred to as a check standard) is used for quality control and the second as a standard. The check standard can also be substituted for the standard if there is a problem such as an electrical spike while the standard is being measured. The pattern of ten samples and pairs of working standards is continued until the set is complete. A practical limit to the number of samples in a run is set by the analysis time and the capacity of the autosampler. When the number of samples is more than the autosampler can hold, the run can be started some hours before the end of the working day. The remaining samples are added to the autosampler once sufficient spaces are free. In addition to the check standards, further quality control standards may be included at the end or during the run.

Once the analysis is complete, the data can be replayed rapidly to check the traces for spikes or other anomalies. Any suspect samples are noted, and if need be, changes to timing windows or selected standards are made and the data reprocessed. The final report gives the signal size, elemental composition (based on that of the working standards), and isotopic composition (in δ or atom %) for each sample. The data are available as hard copy or as data files. These can be imported into a spreadsheet for more convenient data reduction.

2. ANCA-MS of Biological Samples

CF-IRMS measurements of $\delta^{13}C$ and $\delta^{13}N$ using an ANCA-MS are now the method of choice for many applications requiring bulk isotopic data on plant, animal, and other ecological samples. ANCA-MS can also be used

for individual chemical species, providing they can be isolated in sufficient amount and purity (and preferably routinely). ANCA-MS offers high throughput and a precision that is adequate for most purposes. Indeed, with newer instruments, the precision for $\delta^{13}C$, in particular, is almost as good as can be achieved by on- or off-line sample conversion and a DI system. Unlike manual methods, the rapid analysis makes replication of samples practical, and realistic estimates of both analytical precision and biological variation can be made.

The SCRI laboratory processes up to 25,000 samples per year, using two ANCA-MS systems (Tracermass + Roboprep and 20-20 + ANCA-SL, both from PDZ Europa Ltd., Crewe, U.K.). The philosophy used to carry this out is discussed below, followed by some practical examples of analytical methods and supporting techniques. This approach achieves satisfactory results for a range of plant, soil, and animal tissue samples, using only a few standard robust analytical methods. Two guiding principles in all these analyses are (1) the amount of analyte element is kept within ~20% of that in the working standards, and (2) the standards reflect the chemical composition of the samples.

The precision that can be achieved depends on the kind of sample being analyzed and on how this analysis is done. Some samples containing little of the analyte element will be unsuitable for ANCA-MS analysis.

All isotope ratio measurements are more or less subject to sample size effects. These have many causes, of which ion-source behavior may be regarded as the most significant, but background signals, electronic offsets, and amplifier linearity may all contribute. Further, IRMS operate successfully only over a small range of sample size. Large ion currents saturate the detectors, while small ones result in excessive noise. The design and operation of DI systems aims to minimize these problems by keeping sample and reference signals both equal and constant from one measurement to the next.

Sample conversion may also introduce variable background contamination, which becomes more serious as samples get smaller. Since ANCA-MS combines sample conversion and measurement, the causes of sample size effects are less easy to establish than with a DI system. It is generally easier to maintain a constant amount of analyte in the samples than to eliminate or even minimize sample-size-dependent shifts in measured isotope ratio. Where a range of sample sizes is unavoidable, a set of calibration standards can be run with the samples and a suitable correction made. These standards consist of different amounts of a material of the same known isotope ratio. The small increase in the number of analyses that this causes should not be a problem with CF systems. Such additional calibration samples would be a considerable burden with manual measurements.

We use analytical methods designed for approximately equal amounts of analyte (N, C), not of sample. This is achieved from knowing the typical composition of the sample ($\sim$40% C in plant dry matter, $\sim$10% N and 50% C in proteins and animal samples). Alternatively, a preliminary analysis of the sample is done using the ANCA-MS for elemental composition only. Only samples of similar type are run together.

The working standards used are matched to the sample composition. For plant samples either flour or, more conveniently, a synthetic mixture of $\sim$2% N and 40% C can be used. For animal samples, an amino acid such as leucine is suitable. The sample size is chosen to give a large enough signal for good precision, and for most purposes this is $\sim$100 μg of analyte element. Samples too large for the autosampler or which cause unnecessary ash buildup in the combustion tube are avoided.

Most ANCA-MS can switch elements during a run and operate in a dual-isotope mode, and $\delta^{15}N$ and $\delta^{13}C$ can be measured from the same sample. This can produce good results for both isotopes when there is a sufficiently low C/N ratio, as in protein or animal samples. As the C/N ratio increases, it is increasingly difficult to get good $\delta^{15}N$ data from the sample. This is probably due to increased CO_2 entering the MS and being incompletely pumped away before the next N_2 peak is measured.

For most plant samples, we determine $\delta^{13}C$ and $\delta^{15}N$ as follows. First, in the dual-isotope mode and using 1 mg dry subsamples (Table 3), we determine % C, $\delta^{13}C$, and % N. Then, in single-isotope mode, in which the CO_2 is trapped before it enters the IRMS, a second subsample is analyzed for $\delta^{15}N$. The subsample's weight is determined by its % N such that we have a constant amount of N in each sample, usually 100 μg.

When measuring light tracer enrichments (i.e., above 100‰), there are less stringent requirements for precision, and the constraints on the amount of analyte can be relaxed. ^{13}C and ^{15}N can be measured together on 1 mg dry plant samples (containing 20 to 50 μg N). This reduces the amount of ash formed, as well as the potential for memory effects between samples. Natural abundance and enriched samples should not be run together as there is the possibility of memory affecting the precision. It is probably wise to replace the combustion tube if natural abundance samples are to be run after many enriched samples.

In summary, it is desirable

- To use a few standard methods
- To use a constant amount of analyte element
- To match standards to samples in both amount and composition
- To only use the dual isotope mode when the C/N ratio is low ($\sim<5$)

Table 3 Specific Methods for $\delta^{13}C$ and $\delta^{15}N$ Determination. The Precisions are Realistic Estimates of What can be Achieved Routinely Over an Extended Period. For Plant and Soil $\delta^{15}N$, the Precision Deteriorates as Sample % N Falls

Type of analysis	Analysis mode	Sample size	Working standards	Precision (1σ) (‰)	
				$\delta^{13}C$	$\delta^{15}N$
Dual isotope C and N: amino acids/protein/animal material containing ~5–10% N	Dual isotope, CO_2 trap not used	~1 mg dry wt has sufficient N and C for quantitation and isotope analysis in the dual isotope mode	1 mg leucine	$< 0.1^A$	$< 0.2^A$
Dual isotope C and % N: plant material, soils containing ~2% N	Dual isotope, CO_2 trap not used	~1 mg dry wt plant and ~10 mg dry wt soil has sufficient N and C for quantitation and sufficient C for isotope analysis in the dual isotope mode. N isotope values should be ignored	1 mg 1:4 leucine: citric acid mixture (2% N)	$< 0.1^A$ 0.6^B	$< 0.6^A$ $> 1.0^B$
Single isotope N: plant material containing ~2% N	Single isotope (N_2), CO_2 trap used	Calculated weight containing 100 μg N, obtained from % N from dual isotope analysis (above) if required	5 mg 1:4 leucine: citric acid mixture (2% N)	—	$< 0.4^A$ $\sim 0.6^B$
Small sample mode N: soils containing < 1% N	Single isotope (N_2) small sample, CO_2 trap used	Calculated weight containing 25 μg N, obtained from dual isotope analysis (above) if required	1 mg 1:4 leucine: citric acid mixture (2% N).	—	$1–2^B$

A: Precisions obtained with the Europa 20-20 system; B: Precisions obtained with the Europa Tracermass system.

Other instruments will have different strengths and options, such as adjusting the proportion of sample entering the IRMS between elements. However, to optimize any analysis, foreknowledge of the sample composition and choosing a suitable sample size remain important.

It is also important to maintain a constant and comfortable laboratory temperature to achieve satisfactory and consistent performance. The cost of air conditioning is modest compared with that of CF-IRMS instruments and is quickly repaid in reliability of both instruments and results.

The analytical methods that we use for particular types of samples, along with the appropriate standards and realistically achievable precision, are summarized in Table 3.

3. Quality Control: Assessing Precision and Accuracy of ANCA-MS Data

The check standards included at regular intervals throughout an analytical run indicate the precision of the data produced and how this compares from run to run. Since these standards are of similar composition to the samples, matrix effects in the sample conversion are unlikely to produce great differences in precision between samples and check standards. We calculate the mean and standard deviation of the check standards for each run and plot those on quality control charts for each analytical protocol. These charts provide a check on the day-to-day performance of the whole ANCA-MS system and a realistic estimate of the quality of the data being produced. When the precision is significantly poorer than on previous runs, some remedial action (checking the water/CO_2 traps, replacing the ash collection tube, etc.) is indicated. The quality control charts also show the extent to which running enriched samples alters the precision of the results and any memory effects on subsequent runs.

Further quality control standards can be included in the run, and we routinely use a bulk supply of flour for this purpose, particularly for plant samples. Two flour standards are included at the end of each run and the results again recorded on quality control charts. Since these standards are weighed out (rather than freeze-dried like the working standards), they also provide a check on the accuracy of the elemental composition.

The accuracy of the isotopic results depends on the calibration of the working standards. Herein lies a problem that is becoming increasingly common. The reference materials for isotopic analysis come in a limited number of chemical forms, and some (e.g., metal carbonates) may not be suitable for ANCA-MS. Others may have a chemical composition so different from the samples and working standards as to raise doubts about their direct comparability. This is not really a new problem but was less obvious when sample conversion and DI-IRMS were two separate steps.

The range of available reference materials is increasing in recognition of this problem, and some secondary standards suitable for ANCA-MS are now available commercially, e.g., "Europa Flour".

The precision with which working standards are calibrated is limited by the precision of the analytical method used for the comparison. In practice, limited accuracy and precision in the calibration of working standards may not be a serious problem. A small offset in a self-contained set of samples will not affect the interpretation of the results. Biological variation among samples is likely to be greater than any imprecision in calibration. Only when data are to be compared directly with those from other studies does the calibration of the measuring scale have to be rigorously addressed. Nevertheless, regular interlaboratory comparisons of working standards are strongly recommended. These give a realistic estimate of the differences between laboratories and, perhaps more importantly, a degree of confidence in the results within each laboratory.

B. Sample Preparation for ANCA-MS

Whatever form a sample takes, it must eventually be contained in a small tinfoil cup suitable for the elemental analyzer. This usually means getting the bulk sample into a form from which a representative subsample can be accurately weighed directly into the cup. Some samples suitable for ANCA-MS are dry solids capable of being ground to a homogeneous fine powder. These include plant material, soils, invertebrates, compounded fertilizers, isolated protein, and other biological samples. Or they are discrete solids of suitable analyte content such as some individual invertebrates and seeds. Soluble materials (amino acids, fertilizers, soil extracts) are best prepared, and are easier to transfer into the tin cups, as solutions from which small aliquots are freeze-dried. This is particularly true when N-rich fertilizers are analyzed, as gram amounts can be dissolved giving a homogeneous solution from which a suitable subsample can be taken.

1. Solids

Whole lots or representative samples of dry solid samples are ball milled to the consistency of fine flour. Ball mills with stainless steel cups and balls are suitable and can mill 0.05–2 g dry weight, depending on the material. The power and duration of milling also depend on the sample material. Soil should first be sieved through a 2 mm sieve to remove stones.

Some samples, particularly those with a high fat content, produce a paste rather than a powder when ball-milled. These are better ground while frozen in liquid N_2, either manually in a mortar and pestle or in a freezer

mill designed for the purpose. Fibrous or woody samples may also benefit from being ground in a freezer mill.

2. Solutions

Freeze-drying is a convenient way to prepare large batches of working standards as well as samples in solution. Aqueous solutions for freeze-drying directly into tin cups should contain the required amount of analyte (e.g., 100 μg N) in 50–100 μL of solution. We freeze dry batches of samples in aluminum blocks 76 × 76 × 20 mm with 64 holes, each 5 mm diameter, 14 mm deep. Suitably sized tin cups (6 × 4 mm for 50 μL and 8 or 12 × 5 mm for 100 μL) are set in the holes, and samples are subsequently identified by their position in the block. The block is set in a polystyrene tray and cooled with liquid N_2 for 2 min. The appropriate volumes of solutions are then dispensed using a displacement pipette and freeze rapidly in the cups. A fresh pipette tip is used for each solution. Freeze drying of these samples takes 3–4 hours, but is routinely continued overnight.

Ammonium solutions should be acidic and those of nitrate alkaline to ensure there is no fractionating loss of volatile NH_3 or HNO_3. This does not appear to be as big a problem when freeze-drying as when heating to dryness. However, enriched and natural abundance samples should not be freeze-dried together, as contamination can occur if, e.g., volatile NH_3 is trapped by more acidic samples.

C. CF-IRMS of Sulfur

The successful coupling of an elemental analyzer to an IRMS for measuring $^{34}S/^{32}S$ ratios was first reported by Pichlmayer and Blochberger (1988) and Haystead (1991). However, it was somewhat later that this technique was reassessed and widely used (Giesemann et al., 1994). Even then, it has been more commonly applied to mineral S prepared from biological samples than to intact plant or animal samples.

We have successfully used CF-IRMS for S in plant samples with as little as 0.1% S (Monaghan et al., 1999) and in a range of terrestrial and marine animals with ~0.5% S (Neilson, 1999). Most soil samples we have examined contained too little S for direct analysis by CF-IRMS and would still require the extraction of relatively large samples before analysis (e.g., Krouse et al., 1996).

1. Instrumentation

The general principles and methods described above for C and N isotopes apply to S isotope analysis by CF-IRMS. The conditions for satisfactory

conversion of samples to SO_2 are rather different, however, and require the elemental analyzer to be set up specifically for S analysis. SO_2 has a reputation as a "sticky" gas in DI-IRMS systems, being prone to adsorption on the metal surfaces of the inlet system, leading to memory effects. DI-IRMS systems are, for this reason, often operated with heated inlet systems when handling SO_2. Our experience is that most of the problems in analyzing S stem from sample conversion in the elemental analyzer, and *once dry*, SO_2 is easily handled in a conventional CF-IRMS system. Most biological samples produce at least a hundred times more water and CO_2 than SO_2, and these have to be completely removed before the SO_2 enters the IRMS.

The essential features of the system are as follows (Fig. 9):

1. Combined oxidation and reduction tube, with tungstic oxide (WO_3) as the oxidant and copper at the bottom of the tube to convert any SO_3 to SO_2. We have found tungstic oxide on zirconia quite satisfactory,

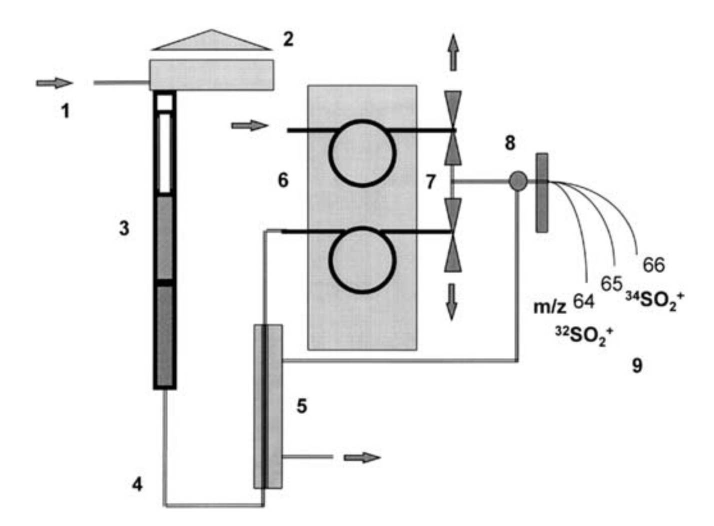


Figure 9 Layout of CF-IRMS system for ^{34}S measurement. (1) Continuous flow of He into the elemental analyzer and (2) autosampler. (3) Combustion/reduction tube at 1000°C (top section: removable ash tube; middle section: packed with tungstic oxide on zirconia; bottom section: packed with copper wires. (4) PTFE connections and tubing to (5) the Nafion™ drying trap, purged with the waste He flow from the open split. (6) Dual column GC oven at 35°C with Porapak QS column in use. (7) Gas-switching valves to direct the standby flow from the other column to the open split, except when SO_2 is eluting from the Porapak QS column. (8) Open split. (9) IRMS, Arrows show He flow into and out of the system. Valves (7) are operated to maintain flow past the open split throughout the analysis.

and it is cheaper than pure tungstic oxide. Tungstic oxide on alumina was less successful, possibly owing to the large amount of absorbed water initially present.

2. Removable ash tube. Severe tailing of the SO_2 peak occurs if too much ash is present and only half the ash acceptable for C and N analysis can be tolerated. The removable quartz liner allows the ash to be easily and completely removed. This is done after each completed run of ~ 100 samples, before significant tailing occurs.

3. PTFE couplings and tubing between the combustion tube and the drying stage. If water is present, it is important that the combustion products do not contact metal surfaces.

4. Nafion^{TM} drying tube. This is a sulfonated PTFE membrane with a high affinity with water, but impervious to other gases. The tube is 300 mm long and 0.5 mm in internal diameter, housed within an outer tube flushed with dry He, which removes the water taken up by the Nafion^{TM}. As water is produced only as a short pulse after each sample is combusted, the waste He flow from the IRMS open split can be used for purging. Although it is probably unnecessary, we have retained a small magnesium perchlorate trap after the Nafion^{TM}. Magnesium perchlorate alone is unsatisfactory as, once a little water has been trapped, variable and tailing SO_2 peaks are observed.

5. GC column suited to SO_2 analysis. The column packings used for complete separation of N_2 and CO_2 are not suitable for SO_2. Porapak QS achieves a good separation of N_2+CO_2 from SO_2 (the SO_2 eluting later). For biological samples where a large amount of CO_2 is produced, complete separation of the SO_2 is essential and the column may have to be operated near to room temperature to achieve this. When an instrument is to be used for both S and C or N analysis, an oven with the two different GC columns, selectable with software-switchable valves, is desirable.

6. Sample gas switching. When samples produce CO_2, it is highly desirable that this does not enter the IRMS before the small SO_2 pulse. This is achieved by switching the GC eluent to the IRMS only when the SO_2 is eluting, and directing the standby flow from the other column to the IRMS at all other times. The necessary valve switching can be incorporated into the analysis timings in the control software.

2. Samples

Complete and consistent sample conversion is aided by adding vanadium pentoxide (V_2O_5) to the samples (twice the sample weight), although this is not required for all samples (e.g., ammonium sulfate and some sulfide minerals).

Marcel Dekker, Inc.
270 Madison Avenue, New York, New York 10016

Biological samples are prepared as for C and N analysis, apart from the addition of V_2O_5. The choice of sample size is a compromise between signal size and efficient combustion without too much ash being formed. 10 mg samples are the maximum used (with an additional 20 mg V_2O_5), but samples below 5 mg are preferred. Where there is sufficient S (~0.5% S) the samples are weighed out to contain 25 μg S, otherwise (down to 0.1% S), 10 μg S is used. Samples much below 0.1% S are unsuitable for direct analysis.

3. Working Standards

Pairs of ammonium sulfate working standards are run after each 10 samples. These are freeze-dried from solution in tin cups, in amounts to match the S content of the samples. Ammonium sulfate alone is used rather than the sample-like matrix we use for C and N analysis, as small tin cups can be used without V_2O_5, minimizing ash formation. Any differences in peak shapes between samples and standards indicate problems with ash buildup or exhaustion of the combustion tube. The working standard solution is calibrated against the silver sulfide standards S1 and S2 from IAEA, Vienna.

4. Precision

The precision (1σ) of our $\delta^{34}S$ measurements depends on the amount of analyte in the sample. The precision for samples of S-rich minerals containing ~200 μg S is ~0.2‰, while plant and invertebrate samples with 25 μg S reliably give 0.4‰ or better. The precision for samples with only 10 μg S is somewhat poorer, 1‰, but this is still quite adequate for many source mixing and natural tracer studies where the natural range of $\delta^{34}S$ is considerably greater than the uncertainty in the measurements (Sec. V.B.5).

D. CF-IRMS of CO_2 for ^{13}C and ^{18}O Measurement

Automated gas sampling systems are available for most CF-IRMS systems (Fig. 10). These were originally developed for analyzing CO_2 in human breath samples for ^{13}C, for clinical diagnosis, hence the acronym ABCA (automated breath carbon analyzer). Samples are contained in 10–20 mL glass tubes whose tops incorporate a septum. The screw-topped Exetainer tubes are now generally preferred to the plug-topped Vacutainer tubes, as the former are more robust, are readily fitted with new tops, and are less prone to contamination.

The ABCA-MS design is similar to the ANCA systems described above, with a gas autosampler in place of the combustion and reduction

Marcel Dekker, Inc.
270 Madison Avenue, New York, New York 10016

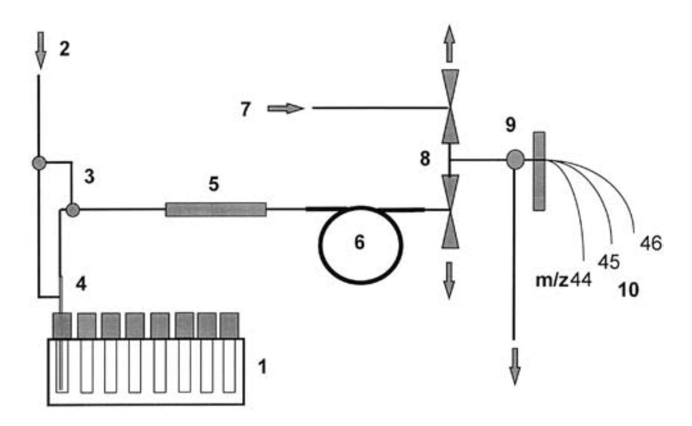


Figure 10 Typical layout of an ABCA system for gas analysis. (1) Autosampler rack with Exetainer sample tubes. (2) Continuous flow of He into the autosampler. (3) Valves to allow needle flushing before injection and to bypass the needle when not in a sample tube. (4) Concentric double sampling needle allowing He into the sample tube and He plus sample out. (5) Magnesium perchlorate water trap. (6) GC column to separate CO_2 from other air gases. (7) Bypass He flow. (8) Gas-switching valves to direct the bypass flow to the open split except when the CO_2 is eluting from the GC column. (9) Open split. (10) IRMS. The arrows show He flow into and out of the system. Valves (8) are operated to maintain a flow past the open split throughout the analysis.

tubes. The Exetainer tubes are loaded into the autosampler. The contents of each is flushed with He through a drying trap plus GC column to separate the CO_2 from water, N_2, and O_2 before IRMS measurement. A switchable bypass flow of He is directed to the open split except when the CO_2 peak is eluting from the GC. This prevents large pulses of N_2 and O_2 from breath or atmospheric samples entering the ion source.

These systems have several applications in environmental studies, particularly in measuring CO_2 in soil atmospheres or the ^{18}O of water samples following equilibration with CO_2. Direct equilibration of soil and plant samples with CO_2 (Scrimgeour, 1995) provides an attractive alternative to exhaustive water extraction. If used in conjunction with an ABCA system, this approach is ideal for processing the large sample sets typical of environmental research. With a little ingenuity, they may also be adapted to measure other gases such as N_2O, N_2, and O_2, or be interfaced with pre-concentration units as one solution to trace gas analysis. The comments below reflect out experience with a Europa Roboprep G+ linked to a Tracermass IRMS.

1. Samples and Sampling

As ABCAs were developed for analysis of ~ 10 mL breath samples with $\sim 3\%$ CO_2, the optimum sample size is 100–500 μL CO_2. In common with other isotope analyses, the careful matching of sample and standard size is important for maintaining accuracy and precision. In some cases this is readily achieved, e.g., when equilibrating CO_2 with water, where constant and known amounts of CO_2 can be added and sampled. Where variable amounts of CO_2 are expected (e.g., from soil atmospheres), it is best to analyze these for CO_2 first and then take samples containing the required amount of CO_2 for isotopic analysis.

New Exetainer tubes come already evacuated, and gas can be injected directly into them. Septa can be used several times, and the tubes re-evacuated through a fine needle for about 30 s. Replacement caps with septa are available. Gas samples can often be handled in disposable syringes fitted with a two-way tap. When sampling through a septum from a closed tube, the syringe is drawn out beyond the required volume and the tap closed. The plunger is pushed in till the pressure is a little above atmospheric pressure before opening the tap and reducing the volume to the required amount. Note: *Always point the syringe needle away from you* (*and anyone else*) *while compressing the gas with the tap closed.*

2. Standards

As with other CF-IRMS systems, pairs of standards are run after every six to ten samples. Either pure CO_2, or more conveniently 5% CO_2 in air or N_2, is used for the working standards. An appropriate volume is injected into evacuated Exetainer tubes as described above. Each new cylinder of standard gas must be calibrated, usually by comparison with the previous batch or against that of another laboratory. Where high accuracy of calibration is required, CO_2 generated from IAEA or NBS standards under standard conditions may be used. For measuring ^{18}O in water, V-SMOW and SLAP (or laboratory standards calibrated against them) are equilibrated and measured along with the samples and the measured values normalized to the nominal values of the standards.

3. Sample Size Dependence

It is not always possible to get sufficient or constant amounts of CO_2 for analysis, e.g., from soil atmospheres. It may be easier to accept the variable sample size and correct for any sample size effects. This is done by analyzing differently sized samples of the working standard, over the range of expected sample size. It is best to keep the working standards the usual size (say 200 μL

Marcel Dekker, Inc.
270 Madison Avenue, New York, New York 10016

CO_2) so that they can be measured with good precision. Inevitably, precision will deteriorate, but it will remain acceptable for many purposes, down to $\sim 20\,\mu L$ CO_2. The measured values for the differently sized standards will show an approximately linear drift. A linear calibration of the offset against sample size is then used to correct the samples. The slope of this calibration curve depends somewhat on the IRMS tuning, amplifier zero setting, etc. A set of calibration standards should be included with each run. We normally use two each of 100 and $50\,\mu L$ CO_2 along with the $200\,\mu L$ CO_2 working standards to produce the calibration curve (Van Vuuren et al., 2000). Where the CO_2 concentration is very low, there may be no alternative to cryogenic trapping or using a preconcentration unit (Broadmeadow et al., 1992).

V. APPLICATIONS

Here we discuss briefly some examples of stable isotope applications, summarized in Table 4. These are chosen to illustrate the range of such applications and are far from being an exhaustive selection.

A. Labeled Tracers

1. D/H: Hydraulic Lift by Deep Roots

Deep-rooted dryland shrubs such as *Artemisia tridentata* draw water from many meters below the soil surface and transport it to shallow roots and above-ground structures. At night, some water flows out of the shrubs' shallower roots into the topsoil if the soil water potential falls below that of the plant. This process is called hydraulic lift (Richards and Caldwell, 1987). The possibility of hydraulic lift suggested that shallow-rooted grasses growing next to shrubs might be able to access that water.

This suggestion was proved conclusively by Caldwell and Richards (1988) using D-labeling. They excavated deep trenches next to *Artemisia* shrubs. At the bottom of each trench they placed a single intact root (which could have belonged only to *Artemisia*) into a vial of D_2O for 37 h. During the next 3 d, D was measured in water extracted from stems of the labeled *Artemisia* plants and from neighboring *Agropyron desertorum* tussocks. Not surprisingly, a large D increase ($\sim 1000‰$) was seen in *Artemisia*. About 24 h later, a smaller ($\sim 150‰$) D increase was seen in *Agropyron*, a pattern consistent with hydraulic lift.

2. $^{13}C/^{12}C$: The Fate of C in Plants and Soil Microbes

Rates of C incorporation into various plant parts and organic molecules can be measured by growing plants in atmospheres containing ^{13}C-enriched or

Table 4 Examples of Different Applications of Stable Isotope Approaches

Isotope pair	Tracer approach		
	Labeled tracers	Natural tracers	Fractionation approach
D/H	Measuring nocturnal hydraulic lift by deep-rooted vegetation (Caldwell and Richards, 1989)	Identifying water sources (rain- vs. groundwater) for trees (White et al., 1985; Dawson, 1993)	Analyzing water fluxes and energy balance of field crops (Bariac et al., 1989) (^{18}O also used)
$^{13}C/^{12}C$	Tracing recently assimilated CO_2 in whole plants (Schnyder, 1992; Deléens et al., 1994)	Estimating C transfers among various organic matter pools in soil (Balesdent and Mariotti, 1996), trees and fungi (Högberg et al., 1999)	Analyzing gas exchange of C_3 plants in terms of physical and biochemical processes (Farquhar et al., 1982; Vogel, 1993) Reconstructing prehistoric climate and vegetation distributions (Street-Perrott et al., 1997) and carbonate pedogenesis (Nordt et al., 1996)
$^{15}N/^{14}N$	Recovery of N fertilizer by crops (Powlson et al., 1986; Powlson and Barraclough, 1993)	Identifying NH_3 use by vegetation (Erskine et al., 1998)	Detecting denitrification using $\delta^{15}N$ values of residual NO_3^- (Mariotti et al., 1988)
$^{18}O/^{16}O$	Quantifying water and C turnover in animal metabolism (Nagy, 1983) (D also used)	Identifying origins of soil NO_3^- (Wassenaar, 1995)(^{15}N also used)	Analyzing processes (e.g., photosynthesis, respiration) that influence gas exchange between vegetation and the atmosphere (Farquhar et al., 1993; Yakir and Wang, 1996)
$^{34}S/^{32}S$	Tracing recently assimilated S in whole plants (Monaghan et al. 1999)	Simulating effects of atmospheric S deposition on soils (Preitzel et al., 1994; Krouse et al., 1996). Identifying trophic relations in aquatic food webs (Peterson et al., 1985; Van Dover et al., 1992) (^{13}C and ^{15}N also used)	Reconstructing the evolution of the S cycle from geological specimens and biological processes (Canfield and Teske, 1996; Habicht and Canfield, 1996)

depleted CO_2 (Schnyder, 1992). Inorganic or organic ^{13}C-labeled compounds are commercially available, as is ^{13}C-labeled CO_2. In the U.K., CO_2 supplied in pressurized cylinders is usually derived from fossil fuel combustion, with $\delta^{13}C \sim -30$ to $-40‰$, different significantly from that of ambient CO_2 ($\delta^{13}C \sim -8‰$). CO_2 with a specified $\delta^{13}C$ can be obtained by mixing ^{13}C-enriched CO_2 with ambient CO_2 using mixing pumps and mass flow controllers (Deléens et al., 1994).

^{13}C pulse labeling of plants requires source CO_2 very ^{13}C-enriched for it to be detected in plant C. Longer, steady-state labeling, however, can be effective using CO_2 only lightly ^{13}C-enriched. For example, Deléens et al. (1994) grew 45-d-old maize plants (initial $\delta^{13}C \sim -12‰$) for 8 d in an atmosphere containing CO_2 with $\delta^{13}C = +162‰$. This produced plants with $\delta^{13}C$ ranging from $-6‰$ (in roots) to $+44‰$ (in stems), between those of the end members ($-12‰$ and $+162‰$), just as a two-source mixing model [Eq. (16)] would predict. The different labeling patterns indicated the relative rates at which newly assimilated C was allocated to various tissues.

The specificity of soil microbial metabolism can be studied by incubating a microbial mixture with a ^{13}C-labeled substrate. Isolation of ^{13}C-DNA from the microbes indicates assimilation of the ^{13}C substrate and the identities of the microbes confirmed by gene probing and sequence analysis. Radajewski et al. (2000) discovered that methanol-utilizing soil microbes (i.e., those that assimilated ^{13}C into their DNA from ^{13}C-methanol) comprised two phylogenetically distinct bacterial groups, information that could not have been obtained from simply measuring methanol consumption.

3. $^{15}N/^{14}N$: The Recovery of Soil N by Plants

One of the most widespread applications of any stable isotope technique has been the use of ^{15}N-enriched fertilizer to estimate how much fertilizer N is captured by crops. Powlson and Barraclough (1993) described the practicalities of introducing ^{15}N-labeled fertilizers into agricultural soil, as did Watkins and Barraclough (1993) for ^{15}N-labeled crop residues.

Powlson et al. (1986) measured the N balance in a long-term winter wheat experiment. In spring they applied N fertilizer containing 2 to 4 atom % ^{15}N at various rates to the soil in 2×2 m microplots contained within a large-scale field experiment. This was done using a custom-built device to ensure uniform spreading of the ^{15}N label. The fate of fertilizer N was calculated from measurements of crop and soil ^{15}N enrichments. When compared with the total N contents of crop and soil and with N uptake by unfertilized crops, these enrichments allowed atmospheric N inputs to, and net N losses from, the system to be estimated.

More sophisticated ^{15}N techniques allow N fluxes through various soil and microbial pools to be derived (Powlson and Barraclough, 1993; Hart and Myrold, 1996; Mary et al., 1998). These rely on initially labeling either soil NH_4^+ or NO_3^- pools by adding small amounts of $^{15}NH_4^+$ or $^{15}NO_3^-$ containing ~ 99 atom % ^{15}N to minimize changes in pool size. Changes in the ^{15}N enrichment of N pools measured on several occasions after labeling reflect the rates at which N entered or left the initially labeled pool(s). From that information, a dynamic picture of N cycling, including gaseous losses by, e.g., denitrification, can be constructed.

^{15}N-enriched inorganic and organic compounds are readily available for these purposes. For N_2-fixation studies, ^{15}N-enriched N_2 is also available, or it can be generated from ^{15}N-labeled ammonium salts by oxidation with alkaline hypobromite (Warembourg, 1993). ^{15}N-depleted material (A ~0.01 atom %) is also available and may be relatively inexpensive compared with ^{15}N-enriched compounds. Formulating compounds with specific ^{15}N enrichments (or depletions) is usually done in solution. The final ^{15}N enrichment of a mixture should be verified by analyzing subsamples, as should that of the medium into which it is being introduced. The $\delta^{15}N$ of soil (Yoneyama, 1996) can differ appreciably from that in atmospheric N_2 ($\delta^{15}N = 0‰$, $A = 0.3663$ atom %: Mariotti, 1981; Table 2). For light ^{15}N-enrichment experiments it may be unsafe to assume that background $A = 0.3663$ atom % when applying Eq. (5), and actual background ^{15}N abundances should be measured and used.

4. $^{18}O/^{16}O$: Animal Energetics

Another popular stable isotope technique (Nagy, 1983; Speakman, 1997) uses doubly labeled water (usually $DH^{18}O$) to measure the metabolic turnover of H and O (and, because of ^{18}O equilibrium between CO_2 and H_2O, also of C). A small amount of $DH^{18}O$ is injected into the bloodstream of a free-living animal, and blood samples are taken at intervals thereafter. Whereas D is subsequently lost from the animal only in water, ^{18}O is lost in water and in respired CO_2. By measuring the δD and $\delta^{18}O$ of blood fluid, a detailed picture can be constructed of an animal's use of water and its energy expenditure in its natural environment.

5. $^{34}S/^{32}S$: S Accumulation and Redistribution in Wheat

There are few good examples of the use of ^{34}S-labeled tracers in soil and environmental science because supplies of ^{34}S-labeled tracers are practically nonexistent. Only ^{34}S-enriched elemental S, H_2S, and CS_2 are readily available, and all are expensive. This is unsatisfactory because, compared

Marcel Dekker, Inc.
270 Madison Avenue, New York, New York 10016

with the short-lived radioisotope ^{35}S, ^{34}S has considerable attraction as a tracer in field experiments.

Natural ^{34}S tracing (Sec. V.B.5) is probably the only practical option for most applications, but Monaghan et al. (1999) managed to find $CaSO_4$ sources that differed in $\delta^{34}S$ by 9.6‰. This was sufficient to trace the uptake and redistribution of S supplied to hydroponically grown wheat at different growth stages (cf. Sec. V.A.2).

B. Natural Tracers

1. D/H: Identifying Plants' Water Sources

1f δD and $\delta^{18}O$ in groundwater differ from those of recent rainfall, the two water sources can be distinguished. Then the extent to which vegetation can access the two sources can be estimated using a two-source mixing model [Eq. (16)]. This technique can be used only where clear isotopic differences in δD or $\delta^{18}O$ exist between precipitation and groundwater, and this can be discovered only by direct measurement. Hoefs (1987), Dawson (1993), and Ingraham (1998) discuss possible reasons for such differences.

One of the best examples of this application is the work of White et al. (1985). Immediately after a rainstorm, the δD of xylem sap collected from *Pinus strobus* (white pine) trees growing in New York State matched that of the rainwater ($\delta D \sim -20‰$). On subsequent rain-free days, the xylem δD became progressively more negative. After six days, it matched that of groundwater at that site ($\delta D \sim -60‰$). This indicated that *P. strobus* absorbed mainly rainwater when it was available, via its surface roots. As rainwater was consumed, a mixture of rain- and groundwater was absorbed, the former by surface roots and the latter by deep roots. These sources become mixed within the plant. With time, the contribution of rainwater to the mixture became smaller, until only groundwater was available for uptake via deep roots. The fraction of the trees' water derived from the rainwater can be calculated using a two-source mixing model [Eq. (17)], with $\bar{\delta}$, δ_y, and δ_x as the δD values of xylem sap, groundwater and rainwater, respectively.

2. $^{13}C/^{12}C$: Incorporation of New Organic Matter into Soil

The $\sim 15‰$ difference in $\delta^{13}C$ between C_3 and C_4 plants means that C from one source can be traced as it is incorporated into a pool consisting of C derived from the other. For example, suppose that a C_4 crop such as maize is grown in soil on which only C_3 species have previously been grown. Then the incorporation of C_4-derived C in the soil can be followed by measuring the ^{13}C abundance of soil CO_2 or organic matter. Its rate of incorporation

Marcel Dekker, Inc.
270 Madison Avenue, New York, New York 10016

can be estimated by making sequential measurements at the same site, or by finding sites where the C_4 crop has been grown for different lengths of time. Again, a model based on Eq. (17) is used to estimate the fraction of total C derived from the recent inputs. Balesdent and Mariotti (1996) review this technique and discuss its limits of resolution.

Similar logic applies wherever there is a robust difference in $\delta^{13}C$ between C pools. Högberg et al. (1999) made use of the $\delta^{13}C$ differences (~2 to 4‰) that they found between forest trees and associated fungi, and among fungal and tree species. They estimated that ectomycorrhiza-forming fungi that associated "promiscuously" with many tree species obtained 57 to 100% of their C from dominant conifers. Those trees, it was suggested, could "subsidise" the C costs of the mycorrhizal symbiosis in smaller understorey trees to which those fungi could also be connected. As with many such studies, the $\delta^{13}C$ values provided circumstantial evidence that was consistent with a certain process, rather than definitive evidence for it. Nevertheless, Högberg et al.'s study shows how such evidence can be used to develop ideas and generate testable hypotheses.

3. $^{15}N/^{14}N$: Atmospheric N Use by Vegetation

There are few good examples of the use of $\delta^{15}N$ as a tracer of environmental N sources. This is because the $\delta^{15}N$ values of many common N sources (e.g., NO_3^-, NH_4^+) are usually unknown (and so cannot be used as tracers) and often cannot be measured reliably (Sec. V.C.3). When they can be measured reliably, their ranges often overlap.

An exception is the work of Erskine et al. (1998) who exploited the exotic $\delta^{15}N$ value of NH_3 derived from penguin guano on Macquarie Island in the subantarctic to demonstrate its incorporation into plant N pools. The $\delta^{15}N$ of guano-derived NH_3 was ~ -10‰. The guano-N itself was more ^{15}N-enriched: $\delta^{15}N \sim +13$‰. This provided a wide working range in $\delta^{15}N$ between two putative plant N sources: NH_3 volatilized from guano and the various forms of soluble N in guano [the precise $\delta^{15}N$ value(s) of which were unknown]. Vegetation growing in the penguin colony had a mean leaf $\delta^{15}N \sim +5$‰. Those plants probably had access to relatively ^{15}N-enriched soluble N. Plants downwind of the colony had leaf $\delta^{15}N \sim -5$‰. They had probably intercepted significant amounts of ^{15}N-depleted NH_3 volatilized from the guano and deposited onto them from the atmosphere.

That it required the annual production of almost 4 million kg of excrement on a subantarctic island distant from industrial N sources to produce N sources with genuinely distinct, unambiguous $\delta^{15}N$ values indicates that using $\delta^{15}N$ as a reliable tracer is a rare luxury. Even the previously accepted use of $\delta^{15}N$ to trace N_2 fixation (Shearer and Kohl,

1993) is now regarded by some (e.g., Handley and Scrimgeour, 1997), but not all (e.g., Boddey et al., 2000), as potentially inaccurate in many field settings. The technique can work well if appropriate precautions are taken and cross-checks are made. These are too numerous to list here, but Pate and Unkovitch (1999) and Unkovitch et al. (2000) set the standards that have to be met. Kendall (1998) discusses some of the general problems in tracing N sources in the environment.

4. $^{18}O/^{16}O$: The Origin of NO_3^- in Groundwater

The use of δD and $\delta^{18}O$ to trace water sources was described in Sec. V.B.1. $\delta^{18}O$ may also be used to trace NO_3^-. Measuring ^{18}O in NO_3^- requires that the NO_3^- be converted to CO_2 for analysis by IRMS. The standard method involves heating the sample with mercuric cyanide—not a procedure for routine use. Wassenaar (1995) described the best application of this technique so far. Using $\delta^{15}N$ and $\delta^{18}O$ measurements of NO_3^- in British Columbian groundwaters, he showed that the NO_3^- probably originated from the nitrification of poultry manure. The isotopic data were not consistent with those of NO_3^- in precipitation or fertilizers.

There are many potential uses for this technique, but its routine application will demand preparative chemistry that is more user-friendly. Direct pyrolysis of NO_3^- samples is one possibility for future development.

5. $^{34}S/^{32}S$: Pollutants and Food Webs

Because of the limited availability of ^{34}S-enriched compounds (Sec. V.A.5), greater reliance has been placed on natural $\delta^{34}S$ tracers. Natural S pools can differ by $\sim$10–15‰ (Giesemann et al., 1995; Krouse et al., 1996; Mitchell et al., 1998), depending on environment (see below), so there is some scope for doing natural ^{34}S tracer experiments.

Industrial SO_2 emissions may be ^{34}S-enriched compared with S in soils and plants. If so, SO_2 depositions downwind from a polluting source may be detected by the enrichment of ^{34}S in topsoil compared with its abundance in deeper layers (Krouse et al., 1996).

$\delta^{34}S$ has been used, often with $\delta^{13}C$ and $\delta^{15}N$, to trace animals' food sources, especially in aquatic systems. For example, Peterson et al. (1985) showed that mussels in an estuary were probably feeding on a mixture of plankton and detritus from the C_4 salt marsh grass *Spartina*. There was no evidence that the mussels had fed on detritus from upland plants washed into the estuary. This conclusion was possible because a putative food source (*Spartina*) had ^{13}C values different from those of the plankton, and because significant ^{34}S differences existed among ecosystem components. The latter occurred because the plankton's main S source (seawater SO_4^{2-})

Marcel Dekker, Inc.
270 Madison Avenue, New York, New York 10016

had a constant $\delta^{34}S$ of +21‰ and plankton $\delta^{34}S$ approximated this value. In contrast, *Spartina* probably used a mixture of S sources: seawater SO_4^{2-} and sediment sulfides. Sulfides in sediments tend to be depleted in ^{34}S compared with SO_4^{2-}. Certain bacteria that use SO_4^{2-} as an electron acceptor in anaerobic respiration may discriminate strongly against ^{34}S during SO_4^{2-} reduction to sulfide. The result was that *Spartina* had a $\delta^{34}S$ value clearly different from that of the plankton.

Such clean isotopic separation among putative food sources is essential in such applications. For $\delta^{34}S$, this was achieved in the above example because the transiently hypoxic sediment promoted large $^{34}S/^{32}S$ fractionations. In the pollution-food web study by Van Dover et al. (1993), the $\delta^{34}S$ of sewage sludge reflected that of land vegetation from which it was derived, via humans and livestock, and differed from the $\delta^{34}S$ of plankton-derived organic matter. When these sources were mixed at an offshore sewage dumping site, the sewage-derived S could be traced into the benthic fauna.

$\delta^{34}S$ differences among ecosystem components may not exist in some environments. One example is in aerobic soils, where only small $^{34}S/^{32}S$ fractionations occur (e.g., during SO_4^{2-} transformation: Krouse et al., 1996). This restricts the usefulness of $\delta^{34}S$ as a natural tracer in soil trophic studies (Kirchmann et al., 1996; Neilson, 1999).

C. Fractionation Approaches

1. D/H: Crop Water Balances

Evaporative fractionations of D/H and $^{18}O/^{16}O$ increase δD and $\delta^{18}O$ in the water of transpiring leaves compared with soil water. Their magnitude depends on the conductance of H_2O vapor through the leaf–atmosphere boundary layer. That, in turn, varies with temperature, humidity, wind speed, and other interrelated factors. δD and $\delta^{18}O$ of leaf water could provide information about these factors and their impact on vegetation even where micro meteorological data are unavailable.

Bariac et al. (1989) attempted to do this for an alfalfa crop. They linked changes in leaf δD and $\delta^{18}O$ to the δ values of source water and to local climatic conditions. The latter were used as inputs to a simple physical model of D/H and $^{18}O/^{16}O$ fractionations. The model failed to predict completely the measured changes in leaf δ values. This, Bariac et al. concluded, indicated the presence of stored water in the crop. This is an example of how isotope fractionations can reveal the occurrence of a previously unsuspected phenomenon in a complex system of interacting processes.

2. $^{13}C/^{12}C$: Linking Plant CO_2 Uptake to H_2O Loss

Farquhar et al. (1982) developed the standard theory for $^{13}C/^{12}C$ fractionation during CO_2 assimilation by C_3 plants. It can be summarized by

$$\frac{P}{E} \approx \frac{c_{\mathrm{air}}}{1.6\nu}\left[1 - \frac{\Delta - a}{b - a}\right] \tag{18}$$

where P and E are, respectively, net rates of CO_2 assimilation and transpiration per unit leaf area (mol m^{-2}s^{-1}). c_{air} is the CO_2 concentration in ambient air (mol m^{-3}). ν is the pressure difference between leaf and air (mol m^{-3}). Δ is given by Eq. (14), or which $\delta_{\mathrm{substrate}}$ and $\delta_{\mathrm{product}}$ are, respectively, the $\delta^{13}C$ of ambient CO_2 and of leaf C. a is the $^{13}C/^{12}C$ fractionation during CO_2 diffusion into the leaf ($= +4.4‰$); b is that during CO_2 assimilation by Rubisco ($\sim +30‰$). The factor 1.6 is the ratio of the diffusivities of H_2O vapor and CO_2 in air.

Equation (18) enables plants' ^{13}C values (which are easy to measure: Sec. IV.A) to be explained in terms of a few physiological processes and environmental factors that are difficult to measure continuously. It is simple, transparent, based on established biophysical principles, and testable (Farquhar et al., 1982; Vogel, 1993). Substrate availability (atmospheric $[CO_2]$) and $\delta_{\mathrm{substrate}}$ are assumed constant, so the only measurements required in practice are of plant $\delta^{13}C$. These can reveal the extent to which gas exchange is limited by CO_2 diffusion to carboxylation sites in the leaf or by carboxylation itself, because $^{13}C/^{12}C$ discriminations for both processes are known.

Δ in Eq. (18) has been used extensively as a surrogate for the ratio P/E, called instantaneous water use efficiency (Ehleringer et al., 1993, p. 5). This quantity has obvious agricultural and ecological importance. Δ values integrate effects of short-term fluctuations in gas exchange. However, the indiscriminate use of Δ as an indicator of "water use efficiency," especially in comparisons among ecologically diverse species growing in different environments, is unjustified. Plant $\delta^{13}C$ also depends on factors other than those shown in Eq. (18). These include the loss of C as root exudates and respired CO_2 and $^{13}C/^{12}C$ fractionations during metabolism. Leaf $\delta^{13}C$, for example, is the weighted average of the $\delta^{13}C$ values of all the leaf's C-containing molecules. Leaves with different proportions of carbohydrates, lipids, and proteins will have different $\delta^{13}C$ values for reasons unrelated to the factors in Eq. (18).

Equation (18) is limited to C_3 species. Its extension to other photoautotrophs (C_4 plants and algae) has been less successful. The physiological characteristics of such plants are less amenable to simple

MARCEL DEKKER, INC.
270 Madison Avenue, New York, New York 10016

description such as Eq. (18). The same applies to the heterotrophic assimilation of C by microbes such as fungi and bacteria, primary decomposers of soil organic matter.

Measurements of $\delta^{13}C$ in atmospheric CO_2 now have a major role in suggesting causes of the atmospheric CO_2 increase that has occurred since the mid-19th century. $^{13}C/^{12}C$ (and $^{18}O/^{16}O$: Sec. V.C.4) fractionations associated with photosynthesis and respiration are valuable in explaining year-to-year variations in atmospheric CO_2 concentration. $\delta^{13}C$ measurements can provide durable records of the $^{13}C/^{12}C$ fractionating processes that occurred in fossils and other ancient materials (Schidlowski, 1988). This property is used to reconstruct prehistoric climates and vegetation distributions (Street-Perrott et al., 1997) and carbonate pedogenesis (Nordt et al., 1996). $\delta^{13}C$ (and $\delta^{18}O$) values of CO_2 trapped in ice cores are unique isotopic footprints of climate changes that have occurred over millennia, but which provide decadal resolution of climatic events (Wahlen, 1994). Such information is providing the historical perspective to assess the stability (or otherwise) of present-day climates and their resilience (or otherwise) to sudden or gradual perturbations.

3. $^{15}N/^{14}N$: Detecting Denitrification

Mariotti et al. (1988) pioneered the use of ^{15}N to detect specific N cycle processes. They wished to know if NO_3^- in an aquifer was being denitrified or was mixing with NO_3^- flowing into the aquifer from elsewhere. In a near-closed system, NO_3^- being denitrified becomes enriched in ^{15}N relative to its initial $\delta^{15}N$ (cf. Fig. 2). A superficially similar change occurs if two NO_3^- sources with different $\delta^{15}N$ values mix. Mariotti et al. distinguished these alternatives using the observed relation between $\delta^{15}N$ and the reciprocal of NO_3^- concentration. In a mixing process, this relation is linear with positive slope. In a fractionating process whose kinetics approximate those of a Rayleigh system (Fig. 2), the relation is curvilinear, with a steadily decreasing slope. Mariotti et al. found evidence for only the latter relation, suggesting that denitrification, not mixing, had occurred.

There is, however, a major technical problem to be overcome before the full potential of $^{15}N/^{14}N$ fractionation approaches can be realized in environmental science. The problem is in isolating pure *N* pools (e.g., NO_3^-, NH_4^+, and DON) from complex matrices (e.g., soils, sediments, and cells) without causing $^{15}N/^{14}N$ fractionations, and in sufficient quantity for reliable ^{15}N determination. Unless we know the $\delta^{15}N$ values of these N forms, it is difficult to interpret whole-plant $\delta^{15}N$, for example, in terms of source $\delta^{15}N$ vs. subsequent $^{15}N/^{14}N$ fractionations. Standard methods exist to measure the concentrations of specific N forms (Knowles and

Blackburn, 1993), but not their $\delta^{15}N$ values. Robinson (2001) discusses the problem in detail and suggests possible solutions.

4. $^{18}O/^{16}O$: Scaling-Up Gas Exchange

Much effort is being devoted to understanding how the composition of the Earth's atmosphere depends on processes such as photosynthesis, respiration, and denitrification. A major problem is that these processes are measured most accurately at small scales: in single leaves or soil cores, for example. Can such measurements be informative at global scales?

Yakir and Wang (1996) combined $\delta^{18}O$ and $\delta^{13}C$ measurements in atmospheric CO_2 with micrometeorological data to estimate photosynthesis respiration at field scales. From these data, the net C flux between land and air was estimated. Simultaneously, net evapotranspiration rates were estimated from measurements of $\delta^{18}O$ in H_2O vapor. At even larger scales, Farquhar et al. (1993) deduced that CO_2/H_2O exchange between atmosphere and vegetation could explain why the $\delta^{18}O$ in atmospheric CO_2 varies latitudinally and seasonally.

$\delta^{18}O$ has also been used extensively (with $\delta^{15}N$) to infer major global sources of and sinks for N_2O, one of the most radiatively active atmospheric gases. The isotopic data do not match known rates and pathways of N_2O production and destruction (Kim and Craig, 1993; Rahn and Wahlen, 1997). This provides strong circumstantial evidence that our understanding of a key part of atmospheric N_2O chemistry is incomplete.

The challenge is now to develop these approaches to assess how changes in vegetation cover, climate, and human activities directly influence the atmosphere and hence global climate itself. Identifying potential feedbacks (e.g., Robinson and Conroy, 1999) and their likely scale will be a major task.

5. $^{34}S/^{32}S$: Reconstructing the S Cycle

In pure cultures, sulfides produced by SO_4^{2-}-reducing bacteria are depleted in ^{34}S by an average of 18‰ (Canfield and Teske, 1996; Habicht and Canfield, 1996). In contrast, the mean ^{34}S depletion in marine sedimentary sulfides is 51‰. This discrepancy confirms that $^{34}S/^{32}S$ fractionation during SO_4^{2-} reduction alone cannot explain the origin of marine sulfides. The "extra" fractionations in the sediments may have been caused by nonphotosynthetic SO_4^{2-}-*oxidizing* bacteria. These evolved during the late Proterozoic (0.64 to 1.05×10^9 years ago) when atmospheric O_2 accumulated probably to within 20% of its present concentration. $\delta^{34}S$ analysis of modern and ancient S pools combined with the molecular systematics of SO_4^{2-}-oxidizing organisms allowed the evolution of the Earth's S cycle to be

Marcel Dekker, Inc.
270 Madison Avenue, New York, New York 10016

reconstructed. Processes in the contemporary S cycle are also now being revealed from $\delta^{34}S$ measurements (e.g., Raven and Scrimgeour, 1997).

VI. CURRENT AND FUTURE DEVELOPMENTS

Section IV dealt in detail with the CF-IRMS analysis of whole plant, invertebrate, soil, and water samples for a range of stable isotopes. Such analyses are likely to remain the basis of many tracer and fractionation applications. However, it is increasingly likely that more detailed information will be needed, particularly for fractionation studies. We need to know about isotope abundances in individual chemical species, and even about particular atomic positions within different molecules. Another area of growing interest is trace components (particularly gases) for which normal sampling methods are not sufficiently sensitive.

Greater attention will be devoted in future to sample collection, isolation, and preparation for natural isotopic abundance determinations in specific compounds. Correspondingly less emphasis will be given to the IRMS aspects. Compound-specific and trace gas analyses are less amenable to the use of a few standard methods, as both sample matrix and analyte dictate what can be used satisfactorily. Specific methods continue to be developed for particular problems. Compound-specific methods are (and will remain) more time-consuming, and they demand rigorous validation to ensure that reliable results are obtained. This is as true for methods using off-line compound isolation for ANCA-MS as it is for on-line separation by GC-IRMS.

An example of the kind of development we are likely to see in the coming years is that reported by Johnston et al. (1999). They devised a method specifically to isolate NO_3^- from waters (including soil extracts) for ^{15}N determination. NO_3^- is converted to 1-phenylazo-2-naphthol (Sudan-1), and the product is concentrated by reverse-phase chromatography before CF-IRMS. The reaction dilutes NO_3^--N in the sample with reagent-derived N, and there is systematic $^{15}N/^{14}N$ fractionation during the reaction. These effects are allowed for by preparing and analyzing NO_3^- standards in each batch of samples. Using this method, surface water samples containing 50 μg NO_3^--N have been analyzed for ^{15}N with a precision of 0.2‰ with no interference from other forms of N in samples or reagents. This method also works with 1 *M* KCl soil extracts, requiring only one additional step to remove the bulk of the DON (Handley et al., 2001). This promises to solve some of the problems detailed in Sec. V.C.3. A similar approach has very recently been reported for NH_4^+ (Johnston et al., 2003). More work is now needed to provide comparable methods for the various forms of DON.

The satisfactory development of these and similar methods for other stable isotopes will undoubtedly stimulate and expand future applications of stable isotopes in soil and environmental sciences.

ACKNOWLEDGMENTS

The Scottish Crop Research Institute receives grant-in-aid from the Scottish Executive Environment and Rural Affairs Department.

REFERENCES

Atkins, P.W. 1998. *Physical Chemistry*. 6th ed. Oxford University Press, Oxford.

Balesdent, J., and Mariotti, A. 1996. Measurement of soil organic matter turnover using ^{13}C natural abundance. In *Mass Spectrometry of Soils* (Boutton, T.W., and Yamasaki, S., eds.) Marcel Dekker, New York, pp. 83–111.

Bariac, T., Rambal, S., Jusserand, C., and Berger, A. 1989. Evaluating water fluxes of field-grown alfalfa from diurnal observations of natural isotope concentrations, energy budget and ecophysiological parameters. *Agric. For. Meteorol.* 48:263–283.

Begley, I.S., and Scrimgeour, C.M. 1997. High-precision δ^2H and $\delta^{18}O$ measurement for water and volatile organic compounds by continuous-flow pyrolysis isotope ratio mass spectrometry. *Anal. Chem.* 69:1530–1535.

Bingham, I.J., Glass, A.D.M., Kronzucker, H.J., Robinson, D., and Scrimgeour, C.M. 2000. Isotope techniques. In *Root Research: a Handbook of Methods* (Smit, A.L., Bengough, G., Engels, C., van Noordwijk, M., Pellerin, S., and van de Geijn, S.C. eds.) Springer, Heidelberg, pp. 366–402.

Boddey, R.M., Peoples, M.B., Palmer, B., and Dart, P.J. 2000. Use of the ^{15}N natural abundance technique to quantify biological nitrogen fixation by woody perennials. *Nutr. Cycl. Agroecosys.* 57:235–270.

Boutton, T.W., and Yamasaki, S., eds. 1996. *Mass Spectrometry of Soils*. Marcel Dekker, New York.

Broadmeadow, M.S.J., Griffiths, H., Maxwell, C., and Borland, A.M. 1992. The carbon isotope ratio of plant organic material reflects temporal and spatial variations in CO_2 within tropical forest formations. *Oecologia* 89:435–441.

Caldwell, M.M., and Richards, J.H. 1989. Hydraulic lift—water efflux from upper roots improve effectiveness of water uptake by deep roots. *Oecologia* 79:1–5.

Canfield, D.E., and Teske, A. 1996. Late Proterozoic rise in atmospheric oxygen concentration inferred from phylogenetic and sulphur-isotope studies. *Nature* 382:127–132.

Coleman, D.C., and Fry, B., eds. 1991. *Carbon Isotope Techniques*. Academic Press, San Diego, CA.

Dawson, T.E. 1993. Water sources of plants as determined from xylem-water isotopic composition: perspectives on plant competition, distribution, and

water relations. In *Stable Isotopes and Plant Carbon-Water Relations* (Ehleringer, J.R., Hall, A.E., and Farquhar, G.D., eds.). Academic Press, San Diego, CA, pp. 465–496.

Dawson, T.E., Mambelli, S., Plamboeck, A.H., Templer, P.H., and Tu, K.P. 2002. State isotopes in plant ecology. *Ann. Rev. Ecol. Syst.* 33:507–559.

Deléens, E., Cliquet, J.-B., and Prioul, J.-L. 1994. Use of ^{13}C and ^{15}N plant label near natural abundance for monitoring carbon and nitrogen partitioning. *Aust. J. Plant Physiol.* 21:133–146.

Ehleringer, J.R., Hall, A.E., and Farquhar, G.D., eds. 1993. *Stable Isotopes and Plant Carbon—Water Relations*. Academic Press, San Diego, CA.

Engel, M.H., and Macko, S.A., eds. 1993. *Organic Geochemistry. Principles and Applications*. Plenum Press, New York.

Eriksen, J. 1996. Measuring natural abundance of stable S-isotope in soil by isotope ratio mass spectrometry. *Comm. Soil Sci. Plant Anal.* 27:1251–1264.

Farquhar, G.D., Lloyd, J., Taylor, J.A., Flanagan, L.B., Syvertsen, J.P., Hubick, K.T., Wong, S.-C., and Ehleringer, J.R. 1993. Vegetation effects on the isotope composition of oxygen in atmospheric CO_2. *Nature* 363:439–443.

Farquhar, G.D., O'Leary, M.H., and Berry, J.A. 1982. On the relationship between carbon isotope discrimination and the intercellular carbon dioxide concentration in leaves. *Aust. J-Plant Physiol.* 9:121–137.

Friedman, I., and O'Neill, J.R. 1977. Compilation of stable isotope fractionation factors of geochemical interest. In *Data of Geochemistry. 6th ed.* (Fleischer, M., ed.). United States Government Printing Office, Washington, pp. KK1–KK12.

Fritz, P., and Fontes, J.C., eds. 1980. *Handbook of Environmental Isotope Geochemistry Vol. 1, The Terrestrial Environment, A*. Elsevier Scientific, Amsterdam.

Giesemann, A., Jager, H.J., Norman, A.L., Krouse, H.P., and Brand, W.A. 1994. On-line sulfur-isotope determination using an elemental analyzer coupled to a mass-spectrometer. *Anal. Chem.* 66:2816–2819.

Giesemann, A., Weigel, H.J., and Jäger, H.-J. 1995. Stable S-isotope analysis as a tool to assess Sulphur turnover in agro-ecosystems. *Z. Pflanzenenähr. Bodenk*, 158:97–99.

Griffiths, H. 1991. Applications of stable isotope technology in physiological ecology. *Funct. Ecol.* 5:254–269.

Griffiths, H., ed. 1998. *Stable Isotopes and the Integration of Biological, Ecological and Geochemical Processes*. BIOS Scientific, Oxford.

Habicht, K.S., and Canfield, D.E. 1996. Sulphur isotope fractionation in modern microbial mats and the evolution of the sulphur cycle. *Nature* 382:342–343.

Handley, L.L., Johnston, A.M., Hallett, P.D., Scrimgeour, C.M. and Wheatley, R.E. 2001. Development of $\delta^{15}N$ stratification of NO_3^- in soil profiles. *Rapid Comm. Mass Spec.* 15:1274–1278.

Handley, L.L., and Raven, J.A. 1992. The use of natural abundance of nitrogen isotopes in plant physiology. *Plant Cell Environ.* 15:965–985.

Handley, L.L., and Scrimgeour, C.M. 1997. Terrestrial plant ecology and ^{15}N natural abudance: the present limits to interpretation for uncultivated systems with original data from a Scottish old field. *Adv. Ecol. Res.* 27:133–212.

Handley, L.L., Austin, A.T., Robinson, D., Scrimgeour, C.M., Heaton, T.H.E., Raven, J.A., Schmidt, S., and Stewart, G.R. 1999. The ^{15}N-natural abundance ($\delta^{15}N$) of ecosystem samples reflects measures of water availability. *Aust. J. Plant Physiol.* 26:185–199.

Hart, S.C., and Myrold, D.D. 1996. ^{15}N tracer studies of soil nitrogen transformations. In *Mass Spectrometry of Soils* (Boutton, T.W. and Yamasaki, S., eds.). Marcel Dekker, New York, pp. 225–245.

Haystead, A. 1991. Measuring natural abundance variations in sulphur isotopes by Dumas elemental analysis-mass spectrometry. In *Stable Isotopes in Plant Nutrition, Soil Fertility and Environmental Studies*. International Atomic Energy Agency, Vienna, pp. 37–48.

Hoefs, J. 1987. *Stable Isotope Geochemistry*. 3d ed. Springer, Berlin.

Högberg, P., Plamboeck, A.H., Taylor, A.F.S., and Fransson, P.M.A. 1999. Natural ^{13}C abundance reveals trophic status of fungi and host-origin of carbon in mycorrhizal fungi in mixed forests. *Proc. Natl. Acad. Sci. USA* 96: 8534–8539.

Ingraham, N.L. 1998. Isotopic variations in precipitation. In *Isotope Tracers in Catchment Hydrology* (Kendall, C., and McDonnell, J.J., eds.). Elsevier, Amsterdam, pp. 87–118.

Johnston, A.M., Scrimgeour, C.M., Henry, M.O., and Handley, L.L. 1999. Isolation of NO_3^--N as 1-phenylazo-2-naphthol (Sudan-1) for measurement of $\delta^{15}N$. *Rapid Comm*un. *Mass Spec*. 13:1531–1534.

Johnston, A.M., Scrimgeour, C.M., Kennedy, H.A., and Handley, L.L. 2003. Isolation of NH_4^+-N as 1-sulfonato-iso-indole for measurement of NH_4^+ $\delta^{15}N$. *Rapid Commun. Mass Spec*. 17:1099–1106.

Kendall, C. 1998. Tracing nitrogen sources and cycling in catchments. In *Isotope Tracers in Catchment Hydrology* (Kendall, C., and McDonnell, J.J. eds.). Elsevier, Amsterdam, pp. 519–576.

Kendall, C., and Caldwell, E.A. 1998. Fundamentals of isotope geochemistry. In *Isotope Tracers in Catchment Hydrology* (Kendall, C., and McDonnell, J.J., eds.). Elsevier, Amsterdam, pp. 51–86.

Kendall, C., and McDonnell, J.J., eds. 1998. *Isotope Tracers in Catchment Hydrology*. Elsevier, Amsterdam.

Kim, K.-R., and Craig, H. 1993. Nitrogen-15 and oxygen-18 characteristics of nitrous oxide: a global perspective. *Science* 262:1855–1857.

Kirchmann, H., Pichlmayer, F., and Gerzabek, M.H. 1996. Sulfur balances and sulfur-34 abundance in a long-term fertilizer experiment. *Soil Sci. Soc. Am. J.* 60:174–178.

Knowles, R., and Blackburn, T.H., eds. 1993. *Nitrogen Isotope Techniques*. Academic Press, San Diego, CA.

Krouse, H.R., and Grinenko, V.A., eds. 1991. *Stable Isotopes: Natural and Anthropogenic Sulphur in the Environment*. *Scope 42*. John Wiley, New York.

Krouse, H.R., Mayer, B., and Schoenau, J.J. 1996. Applications of stable isotope techniques to soil sulfur cycling. In *Mass Spectrometry of Soils* (Boutton, T.W., and Yamasaki, S., eds.). Marcel Dekker, New York, pp. 247–284.

Lajtha, K., and Michener, R.H., eds. 1994. *Stable Isotopes in Ecology and Environmental Science*. Blackwell Scientific, Oxford.

Mariotti, A., Germon, J.C., Hubert, P., Kaiser, P., Letolle, R., Tardieux, A., and Tardieux, P. 1981. Experimental determination of nitrogen kinetic isotope fractionation: some principles: illustration for the denitrification and nitrification processes. *Plant Soil* 62:413–430.

Mariotti, A., Landreau, A., and Simon, B. 1988. ^{15}N isotope biogeochemistry and natural denitrification process in groundwater: application to the chalk aquifer of northern France. *Geochim. Cosmochim. Acta* 52:1869–1878.

Mary, B., Recous, S., and Robin, D. 1998. A model for calculating nitrogen fluxes in soil using ^{15}N tracing. *Soil Biol. Biochem.* 30:1963–1979.

Mitchell, M.J., Krouse, H.R., Mayer, B., Stam, A.C., and Zhang, Y. 1998. Use of stable isotopes in evaluating sulfur biogeochemistry of forest ecosystems. In *Isotope Tracers in Catchment Hydrology* (Kendall, C., and McDonnell, J.J., eds.). Elsevier, Amsterdam, pp. 489–518.

Monaghan, J.M., Scrimgeour, C.M., Stein, W.M., Zhao, J.J., and Evans, E.J. 1999. Sulphur accumulation and redistribution in wheat (*Triticum aestivum*): a study using stable sulphur isotope ratios as a tracer system. *Plant Cell Environ.* 22:831–839.

Mook, W.G., ed. 2001.*Environmental Isotopes in the Hydrological Cycle:Principles and Applications*. Online at http://www.iaea.org/programmes/ripc/ih/volumes/volumes.htm.

Mook, W.G., and Grootes, P.M. 1973. The measuring procedure and corrections for the high-precision mass-spectrometric analysis of isotopic abundance ratios, especially referring to carbon, oxygen and nitrogen. *Int. J. Mass Spectrom. Ion Physics* 12:273–298.

Mulvaney, R.L., and Khan, S.A. 1999. Use of diffusion to determine inorganic nitrogen in a complex organic matrix. *Soil Sci. Soc. Am. J.* 63:240–246.

Nadelhoffer, K.J., and Fry, B. 1994. Nitrogen isotope studies in forest ecosystems. In *Stable Isotopes in Ecology and Environmental Science* (Lajtha, K., and Michener, R.H., eds.). Blackwell Scientific, Oxford, pp. 22–44.

Nagy, K.A. 1983. *The Doubly-Labeled Water Method*: A Guide to Its Use. UCLS Publication No. 12-1417, Los Angeles.

Neilson, R. 1999. Trophic inter-relationships between soil invertebrates and plants investigated using stable isotope natural abundances. Ph.D. thesis, University of Dundee, U.K.

Nordt, L.C., Wilding, L.P., Hallmark, C.T., and Jacob, J.S. 1996. Stable carbon isotope compositions of pedogenic carbonates and their use in studying pedogenesis. In *Mass Spectrometry of Soils* (Boutton, T.W., and Yamasaki, S., eds.). Marcel Dekker, New York, pp. 133–154.

O'Leary, M.H. 1981. Carbon isotope fractionation in plants. *Phytochem.* 20:553–568.

O'Leary, M.H. 1988. Carbon isotopes in photosynthesis. *BioScience* 38:328–336.

O'Leary, M.H. 1993. Biochemical basis of carbon isotope fractionation. In *Stable Isotopes and Plant Carbon-Water Relations* (Ehleringer, J.R., Hall, A.E., and Farquhar, G.D., eds.). Academic Press, San Diego, CA, pp. 19–28.

O'Leary, M.H., Madhavan, S., and Paneth, P. 1992. Physical and chemical basis of carbon isotope fractionation in plants. *Plant Cell Environ.* 15: 1099–1104.
Pate, J.S. and Unkovitch, M.J. 1999. Measuring symbiotic nitrogen fixation: case studies of natural and agricultural ecosystems in a Western Australian setting. In *Physiological Plant Ecology* (Press M.C., Scholes, J.D., and Barker, M.G., eds.). Blackwell Science, Oxford, pp. 153–173.
Peterson, B.J., Howarth, R.W., and Garritt, R.H. 1985. Multiple stable isotopes used to trace the flow of organic matter in estuarine food webs. *Science* 227:1361–1363.
Pichlmayer, F., and Blochberger, K. 1988. Isotopic abundance analysis of carbon, nitrogen and sulfur with a combined elemental analyser-mass spectrometer system. *Fresenius Z. Anal. Chem.* 331:196–201.
Powlson, D.S., and Barraclough, D. 1993. Mineralization and assimilation in soil-plant systems. In *Nitrogen Isotope Techniques* (Knowles, R., and Blackburn, T.H., eds.). Academic Press, San Diego, CA, pp. 209–242.
Powlson, D.S., Pruden, G., Johnston, A.E., and Jenkinson, D.S. 1986. The nitrogen cycle in the Broadbalk wheat experiment: recovery and losses of ^{15}N-labelled fertilizer applied in spring and inputs of nitrogen from the atmosphere. *J. Agric. Sci. Camb.* 107:591–609.
Preitzel, J., Mayer, B., Krouse, H.R., Rehfuess, K.E., and Fritz, P. 1994. Transformation of simulated wet sulfate deposition in forest soils assessed by a core experiment using stable sulfur isotopes. *Water Air Soil Pollut.* 79:243.
Prosser, S.J. and Scrimgeour, C.M. 1995. High-precision determination of ^{2}H/^{1}H in H_2 and H_2O by continuous-flow isotope ratio mass spectrometry. *Anal. Chem.* 67:1992–1997.
Radajewski, S., Ineson, P., Parekh, N.R., and Murrell, J.C. 2000. Stable-isotope probing as a tool in microbial ecology. *Nature* 403:646–649.
Rahn, T., and Wahlen, M. 1997. Stable isotope enrichment in stratospheric nitrous oxide. *Science* 278:1776–1778.
Raven, J.A. 1987. The application of mass spectrometry to biochemical and physiological studies. In *The Biochemistry of Plants, Vol. 13, Methodology* (D.D. Davies, ed.). Academic Press, London, pp. 127–180.
Raven, J.A., and Scrimgeour, C.M. 1997. The influence of anoxia on plants of saline habitats with special reference to the sulphur cycle. *Ann. Bot.* 79 (Suppl. A): 79–86.
Richards, J.H. and Caldwell, M.M. 1987. Hydraulic lift: substantial nocturnal water transport between soil layers by *Artemisia tridentata* roots. *Oecologia* 73:486–489.
Robinson, D. 2001. δ^{15}N as an integrator of the nitrogen cycle. *Trends Ecol. Evol.* 16:153–162.
Robinson, D., and Conroy, J.P. 1999. A possible plant-mediated feedback between elevated CO_2, denitrification and the enhanced greenhouse effect. *Soil Biol. Biochem.* 31:43–53.

Robinson, D., and Smith, K.A. 1991. Analysis of nitrogen isotope ratios by mass spectrometry. In *Soil Analysis. Modern Instrumental Techniques* 2d ed. (Smith, K.A., ed.). Marcel Dekker, New York, pp. 465–503.

Rundel, P.W., Ehleringer, J.R., and Nagy, K.A., eds. 1980. *Stable Isotopes in Ecological Research*. Springer, Berlin.

Schidlowski, M. 1988. A 3,800-million-year isotopic record of life from carbon in sedimentary rocks. *Nature* 333:313–318.

Schnyder, H. 1992. Long-term steady-state labelling of wheat plants by use of natural $^{13}CO_2/^{12}CO_2$ mixtures in an open, rapidly turned-over system. *Planta* 187:128–135.

Scrimgeour, C.M. 1995. Measurement of plant and soil water isotope composition by direct equilibration methods. *J. Hydrol.* 172:261–274.

Shearer, G., and Kohl, D.H. 1993. Natural abundance of ^{15}N: fractional contribution of two sources to a common sink and use of isotope discrimination. In *Nitrogen Isotope Techniques* (Knowles, R., and Blackburn, T.H., eds.). Academic Press, San Diego, CA, pp. 89–125.

Sørensen, P., and Jensen, E.S. 1991. Sequential diffusion of ammonium and nitrate from soil extracts to a polytetrafluoroethylene trap for ^{15}N determination. *Anal. Chim. Acta* 252:201–203.

Speakman, J.R. 1997. *Doubly-Labelled Water. Theory and Practice*. Kluwer Academic, Dordrecht.

Stark, J.M., and Hart, S.C. 1996. Diffusion technique for preparing salt solutions, Kjeldahl digests, and persulfate digests for nitrogen-15 analysis. *Soil Sci. Soc. Am. J.* 60:1846–1855.

Street-Perrott, F.A., Huang, Y., Perrott, R.A., Eglinton, G., Barker, P., Ben Khelifa, L., Harkness, D.D., and Olago, D.O. 1997. Impact of lower atmospheric carbon dioxide on tropical mountain ecosystems. *Science* 278:1422–1426.

Unkovich, M.J., Pate, J.S., Lefroy, E.C., Arthur, D.J. 2000. Nitrogen isotope fractionation in the fodder tree legume tagasaste (*Chamaecytisus proliferus*) and assessment of N_2 fixation inputs in deep sandy soils of Western Australia. *Aust. J. Plant Physiol.* 27:921–929.

Van Dover, C.L., Grassle, J.F., Fry, B., Garritt, R.H., and Starczak, V.R. 1992. Stable isotope evidence for entry of sewage-derived organic material into a deep-sea food web. *Nature* 360:153–156.

Van Vuuren, M.M.I., Robinson, D., Scrimgeour, C.M., Raven, J.A., Fitter, A.H. 2000. Decomposition of ^{13}C-labelled wheat root systems following growth at different CO_2 concentrations. *Soil Biol. Biochem.* 32:403–413.

Vogel, J.C. 1993. Variability of carbon isotope fractionation during photosynthesis. In *Stable Isotopes and Plant Carbon-Water Relations* (Ehleringer, J.R., Hall, A.E., and Farquhar, G.D., eds.). Academic Press, San Diego, CA, pp. 29–46.

Vose, P.B. 1980. *Introduction to Nuclear Techniques in Agronomy and Plant Biology*. Pergamon Press, Oxford.

Wada, E., and Ueda, S. 1996. Carbon, nitrogen, and oxygen isotope ratios of CH_4 and N_2O in soil ecosystems. In *Mass Spectrometry of Soils* (Boutton, T.W., and Yamasaki, S., eds.). Marcel Dekker, New York, pp. 177–204.

Wahlen, M. 1994. Carbon dioxide, carbon monoxide and methane in the atmosphere: abundance and isotopic composition. In *Stable Isotopes in Ecology and Environmental Science* (Lajtha, K., and Michener, R.H., eds.). Blackwell Scientific, Oxford, pp. 93–113.
Warembourg, F.R. 1993. Nitrogen fixation in soil and plant systems. In *Nitrogen Isotope Techniques* (Knowles, R., and Blackburn, T.H., eds.). Academic Press, San Diego, CA, pp. 127–156.
Wassenaar, L.I. 1995. Evaluation of the origin and fate of nitrate in the Abbotsford Aquifer using the isotopes of ^{15}N and ^{18}O in NO_3^-. *Appl. Geochem.* 10:391–405.
Watkins, N.K., and Barraclough, D. 1996. Gross rates of N mineralization associated with the decomposition of plant residues. *Soil Biol. Biochem.* 28:169–175.
White, J.W.C., Cook, E.R., Lawrence, J.R., and Broecker, W.S. 1985. The D/H ratios of sap in trees: implications for water sources and tree ring D/H ratios. *Geochem. Cosmochim. Acta* 49:237–246.
Yakir, D., and Wang, X.-F. 1996. Fluxes of CO_2 and water between terrestrial vegetation and the atmosphere estimated from isotope measurements. *Nature* 380:515–517.
Yoneyama, T. 1996. Characterization of natural ^{15}N abundance of soils. In *Mass Spectrometry of Soils* (Boutton, T.W. and Yamasaki, S., eds.). Marcel Dekker, New York, pp. 205–223.

Marcel Dekker, Inc.
270 Madison Avenue, New York, New York 10016

MARCEL DEKKER, INC.
270 Madison Avenue, New York, New York 10016

10

Measurement of Trace Gases, I: Gas Analysis, Chamber Methods, and Related Procedures

Keith A. Smith and Franz Conen
The University of Edinburgh, Edinburgh, Scotland

I. INTRODUCTION

The exchange of gases between the biosphere and the atmosphere has had a profound effect on the development of the Earth environment. Globally, vegetation (principally forests) releases and absorbs about 60 billion tonnes of carbon dioxide, CO_2, annually and it is the perturbation of this exchange by additional anthropogenic emissions of about a tenth of this quantity that is the principal contribution to global warming—the "greenhouse effect." Emissions of methane from natural wetlands, rice fields, and landfills, and of nitrous oxide from fertilized agricultural soils and the soils of tropical rainforests, add to global warming. A further contribution comes from tropospheric ozone, produced by reactions involving volatile organic compounds from natural vegetation, and NO_x, which comes variously from combustion sources and from soils. Soil surfaces can, on the other hand, act as sinks for many pollutant gases in the atmosphere, through both physicochemical sorption and microbial oxidation. Improved methods of measurement of the fluxes of these gases have become of major environmental importance, both to determine flux levels and in order to improve understanding of the processes involved, to aid the prediction of future trends.

This chapter covers the principles of current instrumental techniques for the determination of trace gases, and the experimental procedures used

Marcel Dekker, Inc.
270 Madison Avenue, New York, New York 10016

to make flux measurements in the field on a small scale: from 0.1 m^2 of land surface to 10–100 m^2. Examples of recent applications are included. Chapter 11 contains complementary information on micrometeorological methods for the determination of fluxes at larger scales. Throughout, the commonly used concentration units ppm and ppb will be used for convenience, instead of the more rigorous notation in volumetric units ($\mu L\,L^{-1}$ and $nL\,L^{-1}$), or partial pressure units (1 ppm $\cong$ 0.1 Pa and 1 ppb $\cong 10^{-4}$ Pa) unless the context dictates otherwise.

II. GAS CHROMATOGRAPHY

Gas chromatography, GC, is the principal analytical method used for the measurement of trace gases in soil air and in the atmosphere above the soil. In particular, it has provided most of the data on the fluxes of the greenhouse gases methane and nitrous oxide and is also used in some studies for measuring carbon dioxide released by soil respiration.

A. Principles

A brief outline of the principles involved in gas chromatography (GC) is given below, but for a more comprehensive discussion, the reader is referred to books solely devoted to this subject, e.g., Bruner (1993) and Braithwaite and Smith (1995). The subject (though more related to the analysis of nongaseous substances) is also covered in Chap. 12.

Chromatography is essentially the separation of the components of a mixture resulting from differences in their partition between a stationary phase with a large active surface area and a moving phase that flows over the stationary phase. Depending on the state of the moving phase, a distinction is made between liquid and gas chromatography. Separations that would be very difficult to achieve by any other means are possible by chromatographic methods, because even small differences between the components in their partition between the phases are multiplied many times during their passage through the chromatographic system.

GC may be conveniently classified into two types: gas–liquid and gas–solid chromatography. In the former, the stationary phase is an involatile liquid coated either on an inert support material in a packed column, or on the internal wall of an open tubular (capillary) column. In the latter type, the column is packed with an adsorbent of small particle size, or the inner surface of a capillary column is coated with a thin adsorbent layer. For separations of gaseous mixtures, solid adsorbents (see below) have been used more widely than liquid stationary phases.

At constant temperature, pressure, and carrier gas velocity, the rate at which a component travels along the column is related to the partition coefficient K:

$$K = \frac{C_s}{C_g} \tag{1}$$

where C_s and C_g are the concentrations in the stationary and gaseous phases, respectively, The more strongly bound components stay for a longer time in the stationary phase and thus travel along the column more slowly than the more weakly bound components. The zone occupied by a component broadens as it moves along, due to the diffusion of molecules in the gaseous phase.

The separation of the components in a sample depends on the relative values of the partition coefficients. The closer the values are to each other, the longer is the column required to give an adequate separation. Reducing the temperature has the effect of increasing the separation. In practice, the variables that are most commonly exploited to achieve satisfactory separations are

1. The material used as stationary phase
2. The length and diameter of the column
3. The column temperature
4. The flow rate of the moving phase (the carrier gas)

The essential parts of all gas chromatographs consist of

1. A carrier gas system, generally in the form of a cylinder supply at pressures up to 20 MPa (200 bar), with a two-stage regulator to reduce the pressure and a flow-rate regulating valve
2. A device for introduction of the sample into the carrier gas stream
3. A column to separate the components of the sample
4. A detector to indicate the elution of each component and produce a response proportional to the quantity of the component present
5. A recording system to provide a permanent record of the detector response

The column and detector (and sometimes the injection port) are normally enclosed in separate thermostats (“ovens”) that can be controlled individually. This is because the optimum column temperature for achieving a desired separation is usually different from the optimum detector temperature.

B. Commercial Instruments

A wide range of gas chromatographs (GCs) is available from manufacturers in several countries (Table 1). For many applications the choice of instrument is not critical, because the substances to be measured are easily within the detection capabilities of any current instrument; where this is so, the cost of the instrument and the availability of after-sales service are more important. Modern GCs usually have the capacity for at least two columns and two detectors (of the same or different types) and also have digital control of all important functions: inlet, oven, and detector temperatures, carrier gas flow rates, detector output settings, etc. If it is desired to add, say, another detector to the original configuration, the necessary electronic control/amplifier circuitry is now usually added as a plug-in board, whereas in earlier generations of GCs it would generally have been housed in a separate unit and linked by cable to the main system. The modern systems have many advantages but do make it more difficult for the user to assemble hybrid systems of units from different manufacturers. For information on the latest developments, manufacturers' literature and websites should be consulted. The web site addresses of some of the major suppliers are given in Table 1.

C. Systems for Gas Analysis

1. Columns and Packings

Porous Polymer Beads. Solid adsorbents such as porous polymer beads, marketed under such names as Porapak and HayeSep, are commonly used for separations of permanent gases. These materials are available in different grades that vary in their retention characteristics for particular substances. Porapak Q and its equivalents have been used widely for separating CH_4, CO_2, and/or N_2O from nitrogen and oxygen in air samples. Columns 1–2 m in length, 1/8–1/4″ (3.2–6.4 mm) in diameter, packed with these materials, give satisfactory separations of these gases at modest temperatures in the range 30–70°C.

Nongraphitized Carbon Molecular Sieve. These materials offer an alternative to porous polymer beads for separating permanent gases. Separations of air (oxygen plus nitrogen), carbon monoxide, methane, CO_2, and/or C_2 hydrocarbons can be readily achieved with a 2 m × 1/8″ packed column of carbon molecular sieve, depending on the column temperature (Fig. 1).

Table 1 Some Manufacturers of Gas Chromatographs

Manufacturer	Address	Website	Comments
Agilent	395 Page Mill Rd, PO Box 10395, Palo Alto, CA 94303, USA	www.agilent.com	Formerly Hewlett-Packard
Buck Scientific	58 Fort Point St, East Norwalk, CT 06855, USA	www.bucksci.com	Small transportable instruments suitable for field use
CE Instruments	Strada Rivoltana, 20090 Rodano, Milan, Italy	www.ceinstruments.it	Formerly Carlo Erba/Fisons. Now part of Thermoquest
GOW-MAC Instruments	277 Brodhead Rd, Bethlehem, PA 18017-8600, USA	www.gow-mac.com	
PerkinElmer Instruments	710 Bridgeport Ave., Shelton, CT 06484-4794, USA	www.perkinelmer.com	
Shimadzu Scientific Instruments	1 Noshinokyo Kuwabarocho, Kyoto 604-8511, Japan and	www.shimadzu.co.jp	
	7102 Riverwood Dr. Columbia, MD 21046, USA	www.shimadzu.com	
SRI Instruments	3882 Del Amo Blvd., Ste 601, Torrance, CA 90503, USA	www.srigc.com	Range includes small transportable instruments suitable for field use
Unicam Chromatography	Viking Way, Bar Hill Cambridge, CB3 8EL, UK	www.unicam.co.uk	Formerly Pye-Unicam. Now part of Onix Process Analysis
Varian Instruments	2700 Mitchell Dr., Walnut Creek, CA 94598, USA	www.varianinc.com	

Marcel Dekker, Inc.
270 Madison Avenue, New York, New York 10016

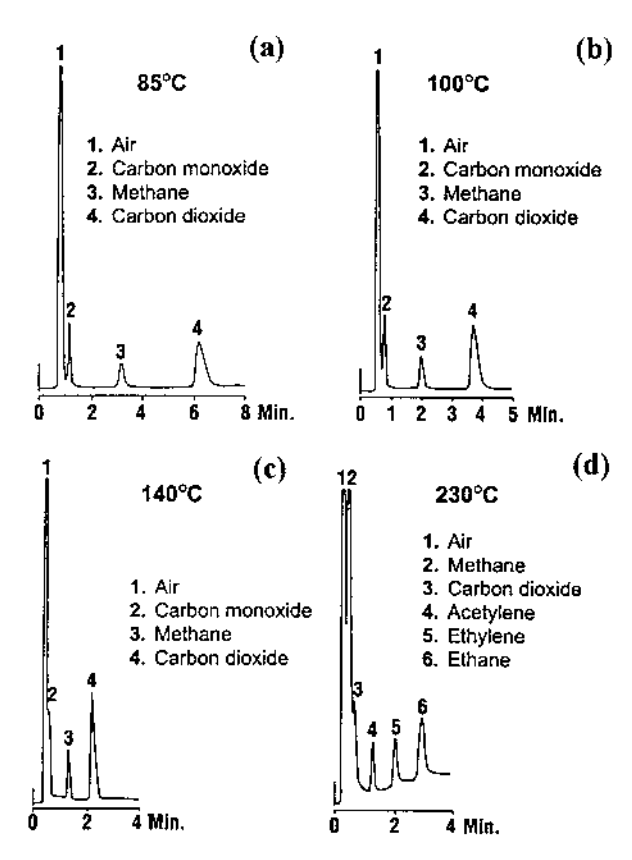


Figure 1 Effect of temperature on separation of permanent gases on Carbosphere carbon molecular sieve. (Reproduced by permission of Alltech Associated Inc., Deerfield, IL, USA.)

Capillary Columns and Open Tubular Columns. Complex mixtures of volatile organic compounds (VOCs), emitted to the atmosphere from vegetation, are analyzed using long capillary or open tubular columns. Examples are a Megabore Carbowax 20 M column, 60 m long, with a film thickness of 1.2 μm, and a 50 × 0.22 mm BP1 column, with a film thickness of 0.12 μm (Kesselmeier et al., 1996) (see Sec. IV below).

2. Procedures for Key Gases

Methane, CH_4. Methane is determined with a flame ionization detector, which responds to combustible compounds (in effect, organic compounds) and, to some extent, to oxygen, but which is insensitive to the

presence of inorganic gases and water vapor. Methane must, therefore, be separated satisfactorily from oxygen and other organic compounds, and this can be done readily on Porapak Q and similar materials. The limit of detection for this gas is of the order of 1 ppb, so there is no problem of determining concentrations at ambient level (1.7 ppm) and above. In some studies, in fact, dilution of samples becomes necessary to avoid nonlinear detector response (see below).

Nitrous Oxide, N_2O. This gas is determined normally with a selective electron capture detector (ECD: see below), operated at high temperature (340–390°C). The ECD responds primarily to gases with a high affinity for electrons, e.g., oxygen, water vapor, and halogenated compounds. Thus effective separation of N_2O from such gases is very important. This is achieved easily on Porapak Q or HayeSep Q. Analysis times can be reduced by using backflushing techniques to remove the more slowly eluted substances such as water vapor (e.g., Arah et al., 1994). ECDs also have some sensitivity for CO_2, and separation from the latter gas can also be achieved on the same column packings, if the temperature is low enough. Alternatively, the sample can be passed through a precolumn of soda lime to remove the CO_2 before it enters the analytical column.

Carbon Dioxide, CO_2. If this gas is to be determined by GC rather than with an IRGA, the most common procedure is separation from oxygen/nitrogen on Porapak Q and detection with a thermal conductivity detector (TCD). Aternatively an ECD can be used, operated at a lower temperature (ca. 270°C) than is commonly employed for N_2O; however, if the relative concentrations of CO_2 and N_2O are in a suitable range, these two gases can be determined simultaneously by this procedure (Thomson et al., 1997).

Isoprene and Monoterpenes. These are the most important VOCs. They play an important part in atmospheric chemistry by, for example, contributing to tropospheric ozone production (through photochemical reactions involving NO_x). Separation requires the use of a capillary or open tubular column (see above). Temperature programming, in which the column oven increases in temperature at a predetermined rate during the analysis, is also employed, to speed up the elution of the more involatile components of the mixture. Detection of VOCs is normally by FID, but the mass spectrometer has become an increasingly attractive alternative, because of its high sensitivity and its capability for distinguishing between compounds with similar retention times by their fragmentation patterns (Parrish and Fehsenfeld, 2000).

Simultaneous Measurement of Two or More Gases. The separation and quantification of a family of related compounds, such as the VOC separation discussed in the previous paragraph, may require a long column and take many minutes for a single analysis, but it normally only requires one column and one detector. Sometimes, however, there is a need to determine simultaneously in the same sample different gases that require different columns and/or different detectors. Some earlier multicolumn and multidetector systems for this purpose were described in the previous edition (Smith and Arah, 1991), and more recent examples are given in Sec. IV below.

3. Calibration

The concentration of the target gas in a sample is conveniently determined by comparisons of peak height (or peak area) with those obtained with gas standards of known concentration, having first established the relationship between peak height (or area) and detector response. Most modern detector/amplifier systems have a linear response over a concentration range covering several orders of magnitude. If the response becomes nonlinear but is not saturated, the system can still be used, provided several standards of different concentrations are analyzed in order to construct a response curve. The alternative is to make dilutions, e.g., with air or nitrogen, before sample injection. Better reproducibility of results is usually obtained with a sampling valve than by direct injection with a syringe.

4. Automation

When large numbers of samples have to be analyzed, a degree of automation can greatly reduce operator time. Commercial headspace samplers are available that consist of a conveyor/sample changer system carrying 10–50 glass vials sealed with serum caps, and an automatically operated gas syringe. The syringe needle punctures the cap of each vial in turn, a gas sample is withdrawn, the syringe moves to a position above the GC injection port, and the sample is injected through the septum. The main problem is expense—a headspace sampler commonly costs more than the GC to which it is attached.

Automated systems for the injection of gas samples collected in the field in Tedlar bags, syringes, or other containers are not commercially available. Either the samples have to be transferred to evacuated vials, and thence to a headspace sampler, or a "do-it-yourself" automatic injection system has to be constructed. In one such system used by our group, the loop of a motor-driven gas sampling valve is evacuated by a pump and then coupled, by the operation of a rotary switching valve, to each of a series of

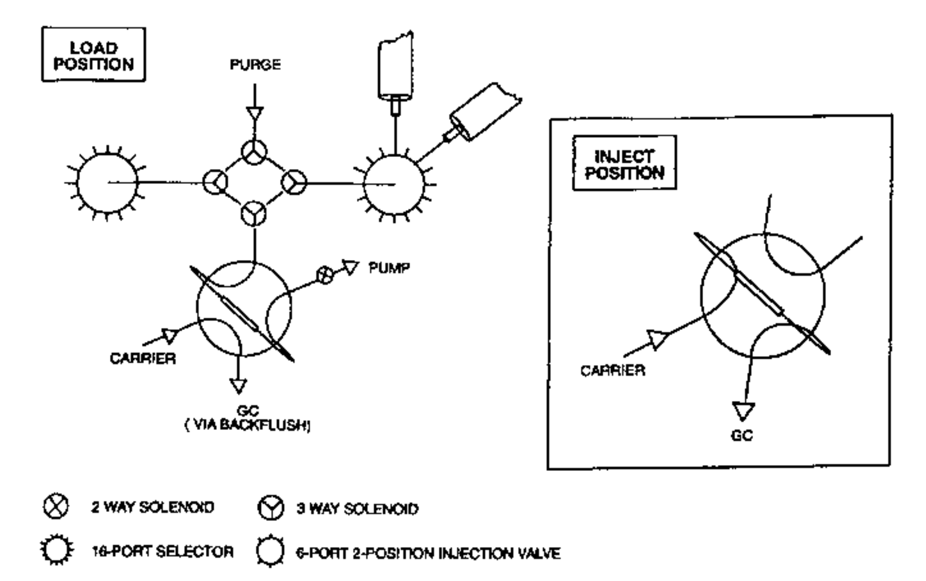


Figure 2 Schematic diagram of automatic GC injection system for gaseous samples. (From Arah et al., 1994.)

sample containers (syringes, bags, or even small incubation vessels) in turn. Each container is connected to the valve via luer-lock fittings. The gas in the sample vessel expands into the loop, the contents of which are then injected (Fig. 2).

Data acquisition and processing is nowadays almost always performed electronically. The chromatographic data are recorded either with a digital integrator or via a computer interface, using specialized software. Statistical evaluation of replicate analyses can take place, and results can be stored for subsequent retrieval, without the manual transfer of data at any stage. This has the benefit of eliminating errors, as well as saving operator time.

III. NONDISPERSIVE INFRARED GAS ANALYSIS

A. Principles

Gaseous compounds such as CO_2, N_2O, CH_4, and H_2O vapor absorb electromagnetic radiation in the infrared (IR) part of the spectrum, due to the particular vibrational/rotational energies of their interatomic bonds. This is, of course, the characteristic that makes these compounds greenhouse gases and thus the focus of much environmental research, but it also provides the basis for sensitive methods of analysis. The main

Marcel Dekker, Inc.
270 Madison Avenue, New York, New York 10016

constituents of the atmosphere, N_2 and O_2, being symmetrical diatomic molecules, do not absorb in the IR region; thus analyzers based on IR absorption can be used to determine trace concentrations of CO_2, N_2O, CH_4, and H_2O vapor in air without interference from N_2 or O_2. These instruments contain three main components: an infrared source, a gas cell through which the radiation passes, and an IR detector. Absorption of IR radiation at any particular wavelength takes place according to the Beer–Lambert law:

$$I = I_0 e^{-kcd} \tag{2}$$

where I and I_0 are the intensities of the transmitted and incident radiation, respectively, k is the molar extinction coefficient for the particular wavelength, c is the concentration of the absorbing gas, and d is the path length through the cell.

Infrared gas analyzers (IRGAs) fall into two main categories: dispersive (DIR) and nondispersive (NDIR). In the former, an IR beam from a source filament passes through a monochromator, and radiation of a selected wavelength that is strongly absorbed by the target gas passes through a gas cell and then to a detector. By changing the wavelength passing through the cell, other gases may be targeted, and if a scanning system is used, an absorption spectrum will be obtained. However, for study of, for example, CO_2 fluxes during photosynthesis or respiration, a simpler approach, NDIR analysis, is generally used. Here there is no attempt to select particular wavelengths. Instead, the broad band of radiation from the source is employed, and the total absorption of all the lines in the 4.26 μm major absorption band of CO_2 is measured (Long and Hällgren, 1993).

B. Commercial Instruments

Current IRGA system include

The range of instruments made by LI-COR (Lincoln, Nebraska, USA), such as the LI-6252 CO_2 Analyzer and the LI-6262 CO_2/H_2O Analyzer

The Rosemount Analytical (Orrville, Ohio, USA) BINOS series of instruments

The PP Systems Inc. (Haverhill, Mass., USA) CIRAS-2 portable photosynthesis system

The ADC Bioscientific Ltd. (Hoddesdon, Herts., UK) Mini-IRGA

These analyzers are compact and portable and can be used in the field under battery power, as well as in the laboratory on a mains AC power

supply. The most sensitive instruments, such as the LI-5262, are capable of determining a change of < 1 ppm of CO_2 against a background ambient concentration of about 360 ppm. For dedicated CO_2 analysis, an optical filter only allows radiation within the 4.26 μm band to pass, thus preventing interference from other IR-absorbing gases, particularly water vapor.

Gas concentration is measured by detecting the difference in IR absorption in two parallel optical cells (Fig. 3). The system can be operated in two different ways. In *absolute* mode, the reference cell contains CO_2-free air and the sample cell contains an air sample with unknown CO_2 concentration; in *differential* mode, the reference cell contains a known concentration of CO_2. Infrared radiation is alternately transmitted through each cell, via a chopping shutter, and the resulting detector output V is proportional to the difference between the signals generated by the detector when it sees the sample cell (ν_s) and when it sees the reference cell (ν_r):

$$V = k(\nu_r - \nu_s) \tag{3}$$

The reference output ν_r is kept constant, and thus

$$V = K\left(1 - \frac{\nu_s}{\nu_r}\right) \tag{4}$$

where $K = k\nu_r$.

The constant K then scales the infrared absorption, represented by $1 - (\nu_s/\nu_r)$ in Eq. (4), to analyzer output V (Eckles et al., 1993). The relationships between ν_s/ν_r and gas concentration, and concentration and V, respectively, are shown in Fig. 4.

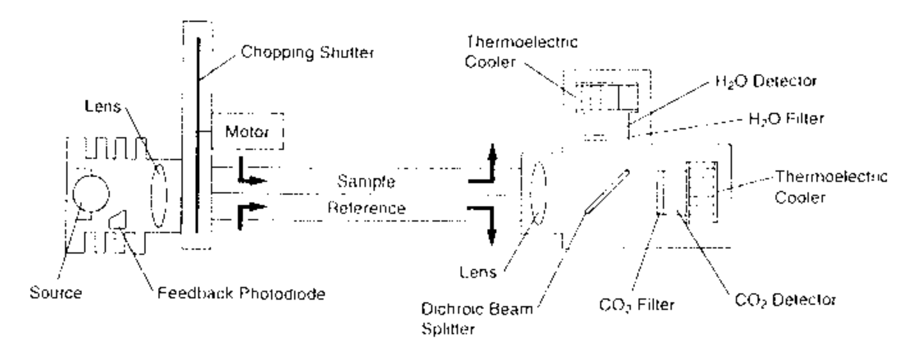


Figure 3 Schematic diagram of infrared absorption gas analyzer (IRGA). This version (LI-COR 6262) has two detectors, for measurement of both CO_2 and water vapor. (Courtesy of LI-COR Corp., Lincoln, NB, USA.)

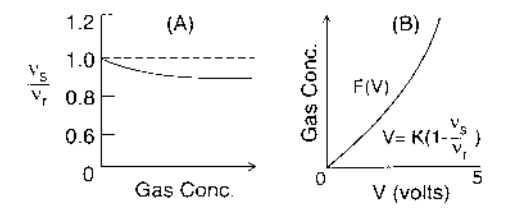


Figure 4 Relationships between (A) signal ratio (IRGA cell/reference cell) and CO_2 concentration, and (B) CO_2 concentration and IRGA output voltage. (Courtesy of LI-COR Corp., Lincoln, NB, USA.)

Infrared Source. This is a vacuum-sealed long-life filament, heated to a temperature between 1000 and 1250 K, that emits radiation over a wide range of wavelengths. Typically, the filament temperature is monitored by a light-sensing diode that is part of a feedback circuit that controls the power input to the source, thus maintaining a constant output and ensuring a stable radiation source (Eckles et al., 1993).

Optical Cells. The cells are small (12 mL in the LI-COR series instruments) and gold-plated to enhance IR reflection. The radiation is collimated by CaF_2 lenses and focused on the detector. Air from the sample source (e.g., a photosynthesis or soil respiration chamber, see Sec. III below) is pumped through the sample cell, while a CO_2 standard of known concentration flows through the reference cell.

Detectors. In the LI-6252 and 6262 instruments, the detectors are temperature-controlled solid-state devices, made of lead selenide, cooled to $-5°C$ by a thermoelectric Peltier cooler. The LI-6252 analyzer has a single detector for CO_2, while the LI-6262 analyzer (Fig. 3) incorporates a beam splitter and two detectors, one for CO_2 and the other for H_2O. The filter for the H_2O detector is centered at 2.59 μm.

C. Practical Considerations

1. Calibration

Instruments vary considerably in the frequency with which they require calibration, and it is advisable initially to recalibrate daily. If no significant change in settings is found, then a longer interval may be employed (Long and Hällgren, 1993). Calibration gas mixtures may be purchased from commercial sources, or prepared using either gas mixing pumps or high-precision mass flow controllers. In the field, a gas syringe may be used to mix a small quantity of pure CO_2 with CO_2-free air.

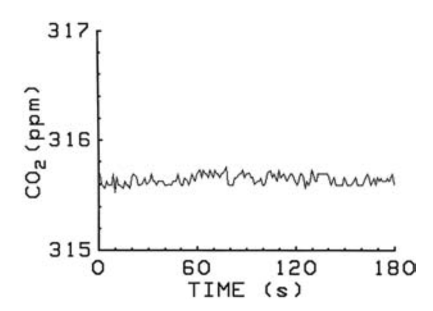


Figure 5 CO_2 concentration readout from an IRGA logged at 1 s intervals (Courtesy of LI-COR Corp., Lincoln, NB, USA.)

2. Response and Averaging Time

Response times of NDIR analyzers are very rapid, typically 1–15 s. They measure concentrations in a flowing gas stream, in contrast with GC systems, which analyze discrete small samples, and in normal operation the signal is averaged over a period of 1–30 s; the noise decreases as this period lengthens. Figure 5 shows the output of an IRGA (LI-6250) logged at 1 s intervals.

IV. OTHER METHODS

A. Photoacoustic Infrared Spectrometry

In photoacoustic spectroscopy, the gas to be measured is irradiated by infrared radiation of a preselected wavelength, in an optical cell. Some of the radiation is absorbed, which results in heating and therefore expansion and a rise in pressure. Interrupting the infrared beam by a chopper causes the pressure alternately to increase and decrease, and an acoustic signal is generated, which is detected by two microphones. This principle is the basis of the 1300 series of trace gas analyzers (TGAs) produced by Innova Airtech Instruments (Ballerup, Denmark). The TGAs (shown schematically in Fig. 6) are fitted with up to five optical filters, each of which is suitable for a different trace gas, and one for water vapor. The filters are mounted in a carousel and used in turn to determine the concentrations of the different gases. Gas samples are pumped from up to 12 flux chambers in turn, via automatic switching valves, and each measurement of all the target gases can be completed in about 2 min (Ambus and Robertson, 1998). The analyzers are portable and can be used in the field, but they require 110 or 220–240 V electric power from the mains or an AC generator.

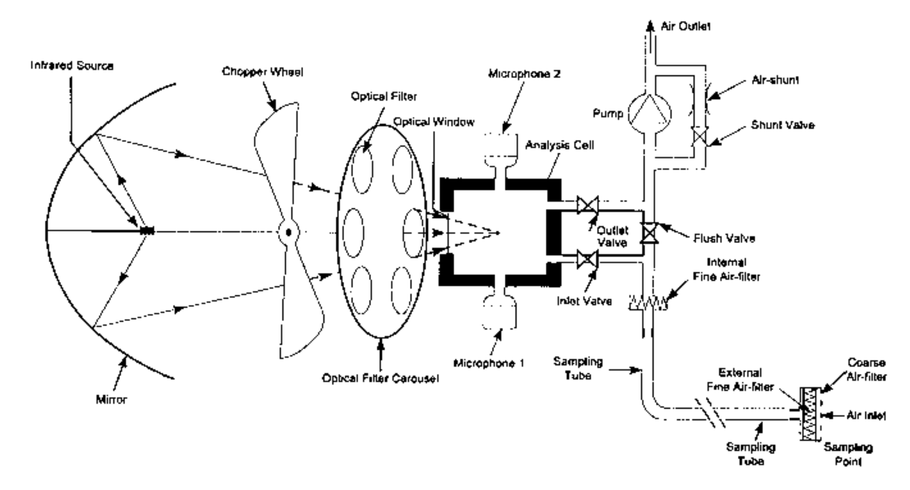


Figure 6 Schematic diagram of Innova Model 1312 photoacoustic infrared spectrometry system used for trace gas analysis. (Courtesy of Innova Airtech Instruments A/S, Ballerup, Denmark.)

The system corrects for interference from water vapor, which affects the determination of most gases, and also for other interferences such as CO_2 during the measurement of N_2O. The limit of detection for N_2O is 30 ppb (one-tenth of ambient) and for methane 0.1 ppm (about 6% of ambient), using 5 s integration times. The response is linear over a wide range of concentrations. Longer times up to 50 s may be used, which will improve accuracy. Ambus and Robertson (1998) compared the results obtained for N_2O and CO_2 chamber concentrations with those obtained by electron-capture GC and NDIR methods, respectively. The agreement was good (Fig. 7).

B. Fourier-Transform Infrared (FTIR) and Tunable Diode Laser (TDL) Absorption Spectrometry

1. FTIR Systems

FTIR spectrometers are complex and expensive compared with NDIR devices. However, they are capable of analyzing a wide range of gases, such as CO_2, N_2O, CH_4, CO, and NH_3, with great sensitivity. The basis of commercial FTIR spectrometers is a Michelson interferometer, in which a collimated beam from an IR source is split and then recombined after introducing a slowly varying path length difference in one beam. Fourier transformation of the resulting time-dependent pattern in the recombined

Marcel Dekker, Inc.
270 Madison Avenue, New York, New York 10016

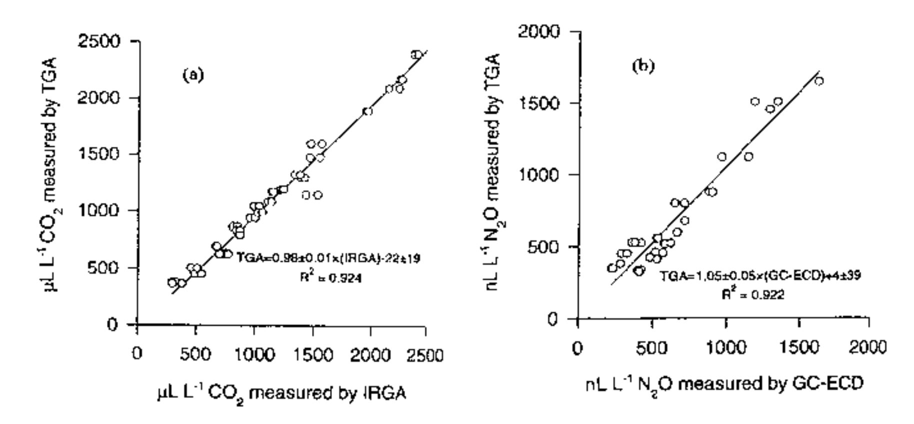


Figure 7 Relationships between (A) CO_2 concentrations measured by photoacoustic trace gas analyzer (TGA) and by IRGA, and (B) N_2O concentrations measured by TGA and by ECD-GC. (Reproduced from Ambus and Robertson, 1998, by permission of the Soil Science Society of America.)

beam provides the spectrum of the input beam and the absorption by any sample inserted in the beam (Griffith and Galle, 2000). For analysis of trace gases, air is drawn continuously from the sampling point through Teflon tubing and then into two 25-L optical cells (White cells). Each part of the split IR beam is reflected backwards and forwards 70 times through one of the White cells, to achieve a long absorption path length (70 m), for maximum sensitivity and then, after recombination, is focused on an InSb or MCT detector (Griffith and Galle, 2000). The spectra are analyzed by a specialized computer program that employs a library of reference spectra (Griffith, 1996).

The FTIR system has been used both in micrometeorological flux measurements by the flux gradient method (see Chap. 11) and in combination with large or ‘‘mega’’ chambers (Galle et al., 1994; see Sec. V.C below).

2. Tunable Diode Laser (TDL) Systems

TDL absorption spectroscopy combines very high sensitivity, comparable with that of FTIR analyzers, with fast response and great selectivity. The tunable diode laser source is usually a crystal of a lead salt semiconductor of the general formula $Pb_{1-x}Sn_xSe$ (Werle, 1999). It is mounted together with a small heater on a copper bar in a liquid nitrogen–filled dewar. Precise control of a current through the heater can adjust the laser temperature by a minute fraction of a degree, and this produces fine adjustment—tuning—of

the emission wavelength of the laser (in the near-infrared). A particular laser diode may only be used for one gas, though two may be possible if suitable IR absorption lines are close enough and the system can be tuned from one equivalent emission wavelength to the other. Available commercial systems include the Campbell TGAI00 (Campbell Scientific, Logan, Utah, U.S.A.), which uses only a single pass of the radiation through a 1.5 m absorption cell, and the Aerodyne (Billerica, Mass., U.S.A) models, which employ much longer path lengths, achieved by multiple reflections through the cell.

Like the FTIR, TDL analyzers can be used in micrometeorological applications (see next chapter) and are fast enough to be used for eddy covariance as well as in the flux gradient mode; however, because of their sensitivity they are also very useful for determining very small changes from normal ambient concentrations in discrete gas samples (usually a few liters in size collected in Tedlar bags), which are pumped through the optical cell of the analyzer. Such samples may be taken from chambers, or collected from the atmosphere, e.g., during aircraft flights to determine average emissions over a wide area (Beswick et al., 1998). More local trace gas accumulation, e.g., under a nocturnal inversion layer, may be measured directly by raising the inlet end of a sampling tube to the desired height with a balloon, and pumping the air directly through the optical cell (Beswick et al., 1998).

C. Chemiluminescence Analyzers

The chemiluminescence technique is now well established as a reliable way of determining nitric oxide, NO, and nitrogen dioxide, NO_2, in atmospheric samples (Parrish and Fehsenfeld, 2000). The technique for NO is based on the chemical reaction with added ozone, and the detection of the chemiluminescence from the excited NO_2 reaction product by a photomultiplier (Fontjin et al., 1970; Ridley and Howlett, 1974). Commercially available chemiluminescence analyzers also routinely measure NO_2. For NO determination, the sample airstream is switched directly by a solenoid valve to the reaction chamber, whereas for NO_2 determination the stream passes first through a catalytic converter (molybdenum oxide) where the NO_2 is reduced to NO ("NO_x mode" in Fig. 8). This mode will give an output equivalent to the sum of the NO and NO_2 concentrations, and analyzers such as the Thermo Environmental (Franklin, Mass., U.S.A.) Model 42C automatically cycle between the NO and NO_x modes and calculate the NO, NO_2, and NO_x concentrations. The system is extremely sensitive: the limit of detection for NO, using a 60 s averaging time, is 0.4 ppb.

To measure soil emissions of NO, air is passed at between 50 and 150 L min^{-1} through a charcoal filter, to remove any ozone, then through a

Marcel Dekker, Inc.
270 Madison Avenue, New York, New York 10016

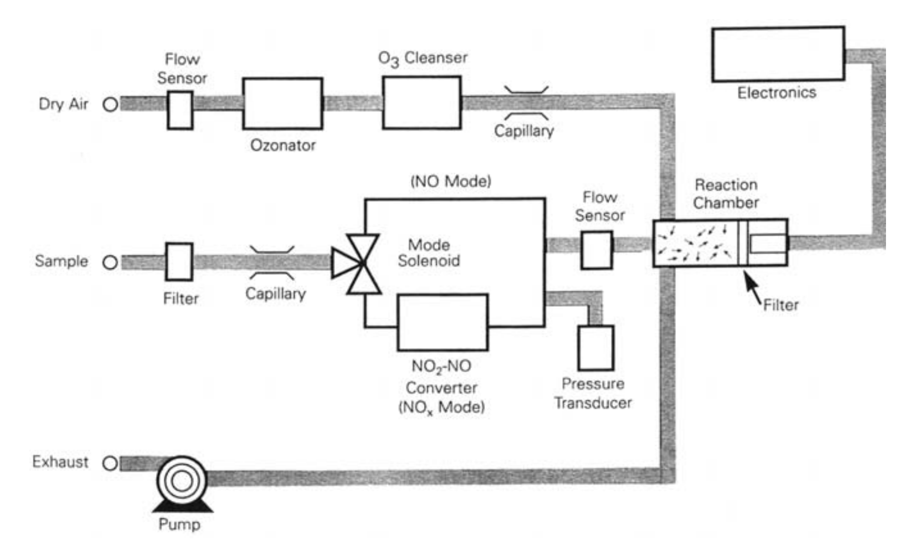


Figure 8 Schematic diagram of chemiluminescence analyzer (Thermo Environmental Model 42C) used for measurement of NO and NO_2. (Courtesy of Thermo Environmental Instruments Inc., Franklin, MA, USA.)

chamber covering the soil (see Sec. V below) and finally through the chemiluminescence analyzer (e.g., Skiba et al., 1992). This procedure is necessary to prevent reaction between the NO and ozone in the flux chamber.

D. Automated Denuder Systems

Ammonia, released from land surfaces following the application of organic manures or urea fertilizer, or emitted from livestock housing or manure stores, is a major pollutant and can contribute greatly to N deposition on sensitive ecosystems (Wyers et al., 1993). The method of choice to determine the atmospheric concentration of ammonia is the denuder tube. Ferm (1979) devised diffusion denuder tubes in which gaseous ammonia in an airstream passing through the tubes diffused to an acid-coated surface where it was trapped, while ammonium in solution in water droplets or in the form of aerosol particles passed straight through. Several automated denuder systems have been described (e.g., Keuken et al., 1989; Langford et al., 1989; Wyers et al., 1993). In the sensitive system developed by Wyers et al. (1993), ambient air is pumped at 30 $L\,min^{-1}$ through an annular denuder rotating at 30 $rev.\,min^{-1}$. The ammonia is collected in 3.6 mM $NaHSO_4$

Marcel Dekker, Inc.
270 Madison Avenue, New York, New York 10016

solution covering the walls of the annular space in the denuder. Two peristaltic pumps continuously pump the solution in and out, in the opposite direction to the airflow. The solution leaving the denuder is mixed with 0.5 *M* NaOH to release the ammonia, part of which passes through a semipermeable membrane into deionized water and is determined conductometrically. The limit of detection in air is 6 ng $NH_3\,m^{-3}$.

The system can be employed in micrometeorological flux gradient systems for field-scale flux measurement (see Chap. 11), as well as in atmospheric monitoring stations.

V. CHAMBERS, SOIL PROBES, AND GAS SAMPLING

The most commonly used methods for measuring the exchange of trace gases such as CH_4, N_2O, and NO between soils and the atmosphere have involved enclosure, or *chamber*, methods. Much of the current investigation of total CO_2 exchange between terrestrial ecosystems and the atmosphere is conducted on a landscape scale by micrometeorological techniques (see Chap. 11); however, here too there is a need for chambers, to determine individual fluxes such as soil or leaf respiration rates, or the rate of photosynthesis, that contribute to the overall CO_2 flux.

Chamber methods involve what is basically a very simple technique: an inverted box of known dimensions is placed over the soil surface (or water surface, in wetlands and rice paddies), and the change in concentration with time of a gas emanating from the soil (or being absorbed by the soil from the air in the box) is measured by one of the instrumental techniques discussed in the preceding sections. This section describes various versions of the technique and discusses the advantages and disadvantages that they offer.

A. Closed Chambers

Methods involving closed chambers are the simplest variant of this approach to gas flux measurement. In essence, a container of known dimensions is sealed over the soil surface (or water surface for studies in wetlands, rice paddies, lakes, and rivers), for periods usually of the order of 20–60 min. When operated in the static mode, gas samples are taken from the chamber at intervals during the closure period (or only at the end—see below) and analyzed off-line for the target gas: most commonly CH_4, N_2O, or CO_2. A variety of types of static chamber is shown in Fig. 9.

Figure 9a shows an example of a simple shallow box-shaped chamber, sealed into the soil to a depth of 5 cm or so, and remaining in place for an

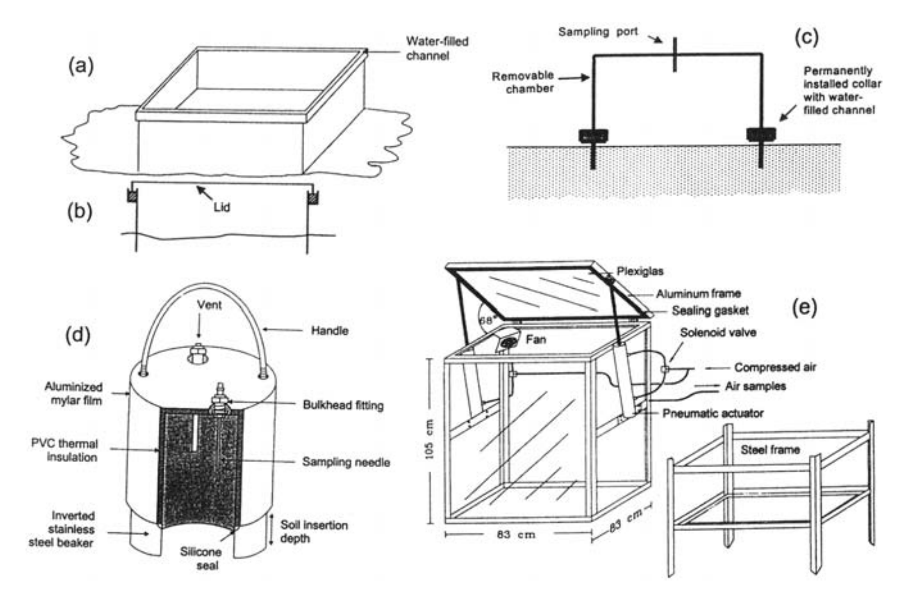


Figure 9 Various designs of closed static chamber: (a), (b) Square sheet-metal chamber with water-sealed lid. (After IAEA, 1992.) (c) Removable chamber on permanent soil collar. (d) Removable metal chamber with vent. (From Hutchinson and Mosier, 1981, by permission of the Soil Science Society of America.) (e) Transparent acrylic chamber with mixing fan and pneumatic actuators for opening and closing the lid, on steel mounting frame, used in rice paddy. (From Butterbach-Bahl, 1993, by permission of Wissenshafts-Verlag Dr. Wigbert Maraun Frankfurt/M, Germany.)

extended period. When a flux measurement is to be made, a lid is placed on the box, fitting into a water-filled channel that makes an effective gas seal (Fig. 9b).

Figure 9c shows another common variant, in which a "collar" or chamber base (which may be circular, square, or rectangular) remains permanently installed in the ground and protrudes only a few cm above the surface. The chamber is sealed to the collar when a measurement is to be made, and then removed. This approach has advantages when it is necessary to avoid shading of growing plants between measurements, and readily allows chambers of different height to be used on the same bases.

Figure 9d shows a movable chamber made from a metal beaker that can be easily inserted into a new sampling point prior to making the measurement.

Figure 9e shows a more elaborate system, appropriate for use in measuring methane emissions from rice fields or natural wetlands.

Pneumatic actuators are used to open and close the lid of a transparent plastic box, which encloses the plants as well as an area of the water surface. An electric fan is used to mix the air within the chamber during closure.

Some other designs can be found in the companion volume to this one (Smith and Mullins, 2000), and in IAEA (1992).

Closed chambers may also be operated in the dynamic mode, in which the air in the chamber is circulated through a gas analyzer (e.g., an IRGA) (Fig. 10), and the increase in concentration with time is determined. In the procedure described by Longdoz et al. (2000), before making a measurement, the airstream is diverted through a soda lime scrubber to deplete the chamber CO_2 concentration, and then the air concentration is measured about every 3 s from 15 ppm below to 15 ppm above atmospheric concentration. The soil efflux is deduced from the slope of the linear increase in concentration with time.

Rochette et al. (1992) reported that soil CO_2 fluxes obtained with dynamic closed chambers were consistently higher than those obtained with static chambers incorporating NaOH traps for the CO_2. Norman et al. (1997) came to a similar conclusion, when they compared two dynamic closed chamber/IRGA systems and two closed static systems combined with GC analysis. However, the different methods were strongly correlated. The size of the discrepancy between methods depends on soil conditions, and results obtained by both methods for a given site can be compared provided intercalibration exercises are carried out under the conditions prevailing at that site.

A dynamic chamber system has been developed for measuring CO_2 exchange by tree branches in situ. Between measurements, the ventilation fan blows air through the chamber (or "branch bag") at a high rate

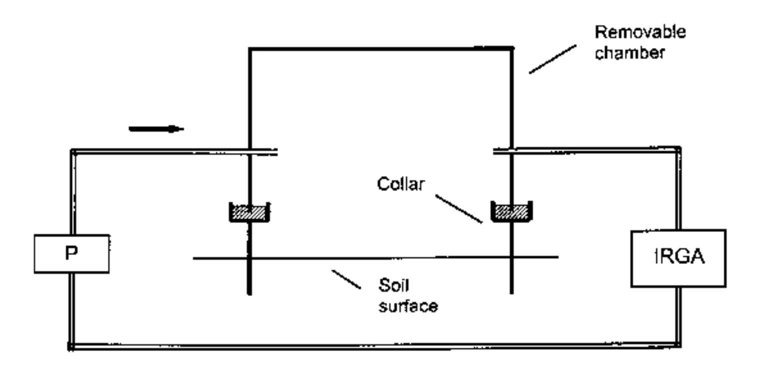
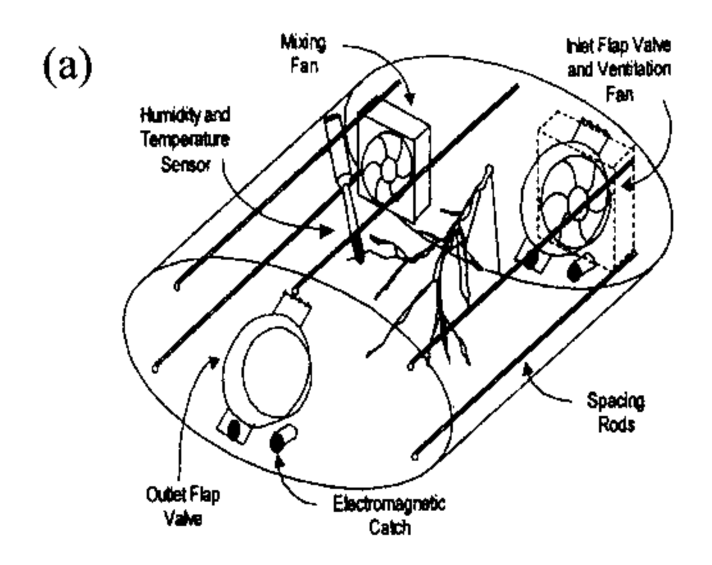


Figure 10 Schematic diagram of system for soil CO_2 flux measurement, using a closed dynamic chamber and IRGA.

Marcel Dekker, Inc.
270 Madison Avenue, New York, New York 10016

(40 L min^{-1}), and air is circulated between the bag and a box containing an IRGA at 5 L min^{-1}. Then at measurement time the bag is closed off by flap valves (Fig. 11a) and a fraction of the circulating air (0.2 L min^{-1}) is diverted through the IRGA (Fig. 11b).



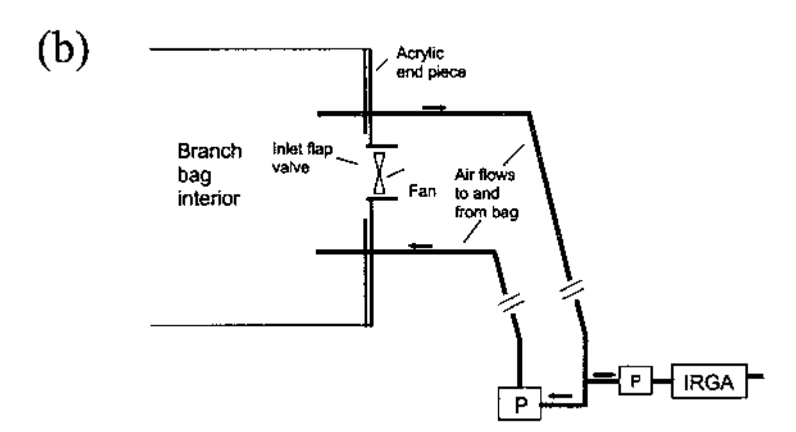


Figure 11 Dynamic chamber ("branch bag") system for measuring CO_2 exchange by tree branches in situ. (a) Branch bag with ventilation and mixing fans and flap valves. (From Rayment and Jarvis, 1999, by permission of NRC Research Press, Canada.) (b) Gas circulation system between branch bag and IRGA located near ground level.

Advantages and Disadvantages of Closed Chambers. The advantages are that they are capable of measuring very small fluxes, the source of the flux is well defined, the method can be applied in conventional experimental designs involving replicated field plots, and most of the chamber designs are cheap and easily fabricated in a laboratory workshop. The main disadvantage is the potential to influence the magnitude of the flux that is to be measured; covering the surface with a chamber, and circulating or not circulating the air within it, can affect gas transport between soils and the atmosphere. Evidence for this is provided by the comparison between dynamic and static systems discussed above. Pressure changes can accelerate gas exchange by inducing some mass flow close to the surface in very coarse and porous media (Kimball and Lemon, 1971). This is prevented when a sealed chamber is used; an improved design with a vent tube (Fig. 9d), which transfers these pressure fluctuations to the inside of the chamber, was introduced by Hutchinson and Mosier (1981). However, wind passing over this vent tube can cause a continued depressurization of the chamber (Venturi effect), leading to a continuous mass flow of soil gas into the chamber (Conen and Smith, 1998). This can result in much larger measurement errors than could be expected from the exclusion of pressure fluctuations.

A chamber can also induce a rise in temperature inside it, increasing the rate of production or consumption of the target gas. Using insulated and/or reflective materials can help to minimize this effect (e.g., Matthias et al., 1980). Keeping closure times to a minimum also helps. Closed chambers also affect gas concentration profiles within the soil. The accumulation of gas inside the chamber is accompanied by gas accumulation within the soil profile below the chamber. Thus the air-filled pore space below the chamber may be regarded as an extension of the chamber volume. This can be corrected for (Conen and Smith, 2000) or, more practically, minimized by increasing the chamber height, especially on soils with a large air-filled porosity.

1. Sampling

Gas sampling usually involves withdrawing a few mL of air from the chamber headspace through a septum or a sampling port fitted into the chamber top or wall at known times after closure. Gas-tight syringes, evacuated vials, Vacutainers or metal tubes, or Tedlar (polyvinyl fluoride) gas sample bags may be used as sample containers. The samples are then analyzed (usually by GC methods) off-line in the laboratory. Acceptable sample storage times depend on the containers used. Samples in syringes should preferably be analyzed within a few hours of collection, whereas

those in glass or metal containers or Tedlar bags are much more durable—there is normally negligible gas exchange with the outside atmosphere over a few days, as long as the container is at or above atmospheric pressure (e.g. Priemé and Christensen, 1999). Where containers are closed with rubber seals, there is always the possibility that the particular material used can absorb (or even be a source of) the trace gas of interest, and it is desirable to test any new batch of seals for such characteristics before use.

Photoacoustic infrared analyzers may be used in the field with an array of closed chambers. Air samples from each chamber in turn are pumped through the measurement cell of the analyzer, through up to 50 m of small-bore tubing, then back into the chamber, to avoid pressure changes that might induce mass flow of the soil gas into the chamber (Ambus and Robertson, 1998; de Klein et al., 1999).

2. Flux Calculation

Where there is a net efflux of the target gas from the soil to the atmosphere, there is usually a linear increase in gas concentration with time, within the chamber. Flux is calculated from the rate of change in concentration, the chamber volume and area, the molecular weight of the gas, and the gas density as a function of air pressure and temperature:

$$F = \frac{\Delta C}{\Delta t} \cdot \frac{v}{A} \cdot \frac{M}{V} \cdot \frac{P}{P_0} \cdot \frac{273}{T} \tag{5}$$

where ΔC is the change in concentration in time interval Δt, v and A are the chamber volume and area, respectively, M is the molecular weight of the gas, V is the volume occupied by 1 mol of the gas at STP (0.024 m^3, or 22.4 L), P is the barometric pressure (mbar), P_0 is the standard pressure (1013 mbar), and T is the ambient temperature (K). v/A can be replaced by the average chamber height, h, and at or near sea level the pressure factor can usually be ignored; thus the equation simplifies to

$$F \approx \frac{\Delta C}{\Delta t} . \frac{h.M}{V} \cdot \frac{273}{T} \tag{5a}$$

If, on the other hand, there is a net sink for the gas in the soil, then the concentration within the chamber may be expected to decrease exponentially (first-order reaction kinetics):

$$C_t = C_0 \cdot e^{-\alpha t} \tag{6}$$

where C_0 and C_t are the concentrations at the time of closure and at time t, respectively, and α is the rate constant. To determine the rate of uptake of atmospheric methane, the chamber is closed, a sample of the air inside is taken immediately, and then further samples are taken at intervals over a period of typical1y 30–90 min. The best fit of Eq. (6) to the data is obtained [see the example in Fig. 12] and to calculate the flux, $\Delta C/\Delta t$ in Eq. (5a) is replaced by $\alpha \cdot C_0$:

$$F \approx \alpha \cdot C_0 \cdot \frac{h \cdot M}{V} \cdot \frac{273}{T} \tag{7}$$

B. Open Chambers

Open chambers, in spite of their name, provide a cover over an area of soil surface, but the essential feature distinguishing them from closed systems is that they have a continuous flow through the chamber of outside air, which then passes to the gas analyzer (Fig. 13). The difference in concentration of the target gas between that in the incoming and that in the outgoing air is measured. Flux is then a function of this concentration difference, the flow rate, the chamber area, and the gas density. Open chambers are thus well suited to analytical systems that are designed to measure concentration in a flowing gas stream, and are used in conjunction with IR analyzers, mainly for CO_2 flux measurements but also for N_2O (as shown in Fig. 13), and with chemiluminescence analyzers for NO determination.

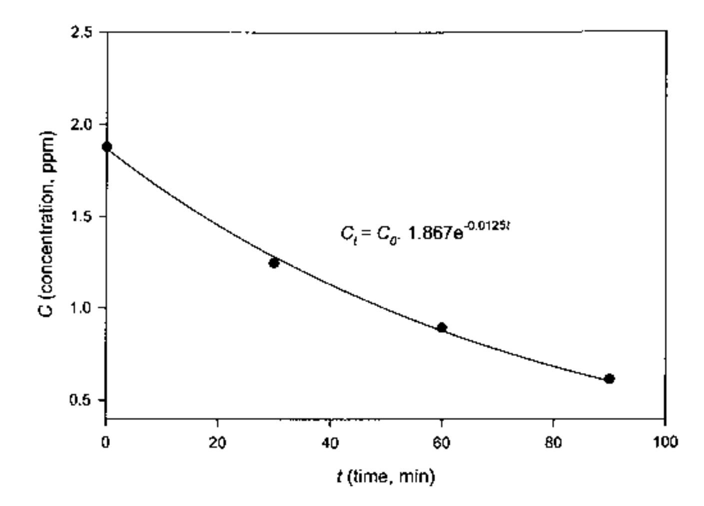


Figure 12 Typical exponential decrease in CH_4 concentration with time, in chamber located on aerobic soil acting as sink for atmospheric CH_4.

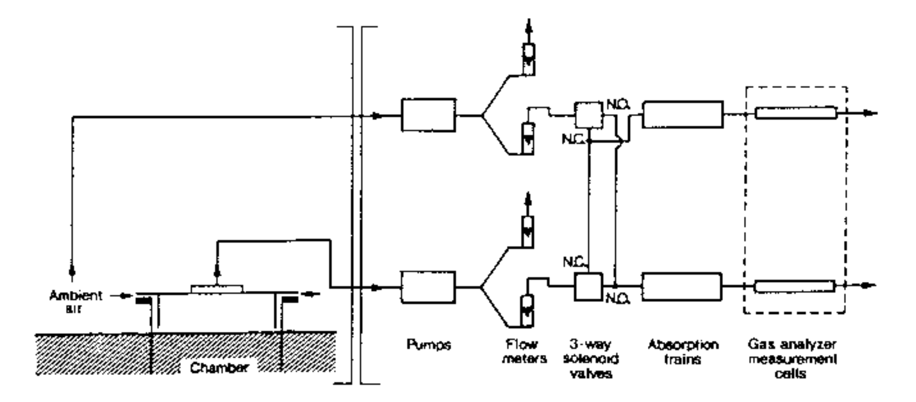


Figure 13 Schematic diagram of open (dynamic) chamber system. (From Denmead, 1979, by permission of the Soil Science Society of America.)

Open systems have an inherent problem caused by pressure differences between the outside atmosphere and the inside of the chamber. A certain pressure difference is necessary to maintain an airflow through the chamber, but this also results in either mass flow of air out of the soil into the chamber, or mass flow of atmospheric air into the soil. The first process leads to an overestimation, the second to an underestimation, of real flux. This effect can be considerable. For example, as a result of the inside pressure exceeding outside pressure by only 0.5 Pa, measured CO_2 flux can be reduced by 70% (Lund et al., 1999).

The mass flow of soil gas across the surface area covered by a circular chamber is described by Darcy's law (Kirkham, 1946):

$$Q_s = \frac{\Delta p \cdot K_s \cdot \pi \cdot r_s^2}{\eta \cdot \Delta L_s} \tag{8}$$

where Q_s is the rate of soil gas flow into the chamber, Δp is the pressure difference between outside and inside the chamber, K_s is soil air permeability, r_s is the radius of the chamber, η is the viscosity of air, and ΔL_s is the path length of the soil gas flow.

Pressure difference and the resistance of the inlet or outlet tube of the chamber control the flow of atmospheric air through the chamber. Poiseuille's law describes laminar flow through a pipe:

$$Q_A = \frac{\Delta p \cdot \pi \cdot r_A^4}{8 \cdot \eta \cdot L_A} \tag{9}$$

where Q_A is the flow rate of atmospheric air into the chamber, r_A is the radius of the outlet tube (if air is pushed into the chamber) or inlet tube (if air is sucked into the chamber), and L_A is the length of the respective tube.

Combining Eqs. (8) and (9) to describe the proportion of undesired gas flow through the soil profile in relation to gas flow through the inlet and outlet tubes of the chamber, we obtain

$$\frac{Q_s}{Q_A} = \frac{K_s \cdot r_s^2 \cdot 8 \cdot L_A}{\Delta L_s \cdot r_A^4} \qquad (10)$$

Thus open dynamic chambers can be optimized by decreasing chamber radius, r_s, and the length of inlet and outlet tubes, L_A. Inserting the chamber deeper into the soil and thereby increasing the path length of soil gas flow (L_s) can make further improvement. The largest effect can be expected from an increase of the radius of inlet or outlet tube, r_A. An upper limit to the tube diameter is set at the point where diffusion out of the inlet tube is faster than mass flow into the chamber. All these measures become more important as the soil air permeability, K_s, increases. Features of chamber design to minimize pressure differences include the use of an adjustable annular space rather than a pipe, for the air inlet (Fang and Moncrieff, 1998).

Comparison of Results with Closed and Open Systems. Longdoz et al. (2000) compared the results of soil CO_2 efflux measurements with dynamic closed chamber and open chamber systems. There was a very high correlation between them ($r^2 = 0.99$), but with the former giving results 12% higher than the latter. This confirmed the findings of Norman et al. (1997). As discussed above in relation to static vs. dynamic closed chambers, results obtained with the different methods can be related and combined in ecosystem studies, provided intercalibration takes place under the relevant site conditions.

C. Very Large (“Mega”) Chambers

A major problem with both closed and open conventional chambers is that they cover a very small area of soil surface. Even the chambers used in rice paddies, which have tended to be larger than average, are normally 80 cm by 80 cm (0.64 m^2; Marik et al., 2001), or less, while sizes down to 0.032 m^2 (20 cm diameter circular chambers; Mosier et al., 1991) are common. Therefore the measurements made with such chambers are subject to what is often very great spatial variability (Smith et al., 1995). One way of reducing this variability involves the construction of a very large (or “mega”)

Marcel Dekker, Inc.
270 Madison Avenue, New York, New York 10016

chamber, e.g., 25 m by 2 m (Galle et al., 1994; Smith et al., 1994), which increases the surface area covered by two to three orders of magnitude compared with conventional devices. Such a chamber can be cheaply constructed from heavy-gauge polythene sheet (as used for damp-proofing in the construction industry) stretched over a series of hoops to form a hemicylindrical tunnel, and weighted down against the soil surface with soil or sandbags (Smith et al., 1994).

Such large chambers can either have long-path FTIR or other infrared analyzers mounted inside them (Galle et al., 1994; Smith et al., 1994), or air from the chamber can be pumped to a trailer nearby (L. Klemedtsson and P. Weslien. unpub.), where it is analyzed by FTIR in a White cell (Griffith and Galle, 2000).

D. Automation of Chamber Operation and Sampling

Automated flux chambers, coupled with automated gas sampling, make possible much more intensive measurements than can be readily carried out by manual methods and are particularly valuable for investigating temporal variations, e.g., diurnal cycling, in gas fluxes.

Closed Chamber Systems. Several designs of automated systems have been published (e.g., Brumme and Beese 1992; Silvola et al., 1992; Butterbach-Bahl et al., 1997a,b; Ambus and Robertson, 1998; Scott et al., 1999; Crill et al., 2000). All these systems have been developed within the institutes concerned, as no equipment of this type is available commercially. In most versions, the flux chambers are connected by sampling tubes to an automated switching valve/GC system mounted in a hut or trailer at the experimental site, and supplied with mains power. A variant on this is the mobile laboratory of Ineson et al. (1998), which can be moved from site to site, with power provided by a generator.

The system used in our institute (Smith and Dobbie, 2001) allows field sampling where mains power is unavailable, being powered by two 12 V batteries. Gas analysis takes place in the laboratory. The chambers (Fig. 14) are 70×70 cm in area and made of galvanized steel. Closure and reopening is achieved by a 24 V DC actuator. Each chamber is combined with a sampler/control unit and shares the same battery power. Gas samples are pumped from the chamber into one of 24 sample loops, made from 1/8″ copper tubing and attached to rotary valves (Fig. 15). The valve/loop assembly forms a removable "carousel." After a loop is filled, the valve is turned to the next position, isolating the sample. When sufficient samples have been taken (e.g., after a week of sampling at a frequency of three times per day), the carousel is replaced by an identical one, to allow sampling to

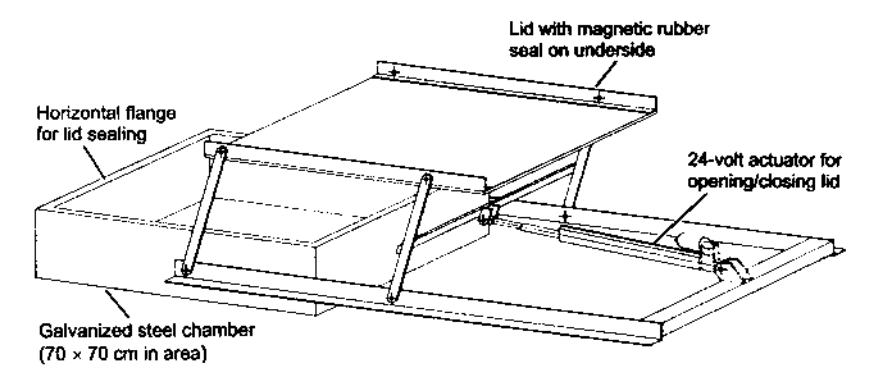
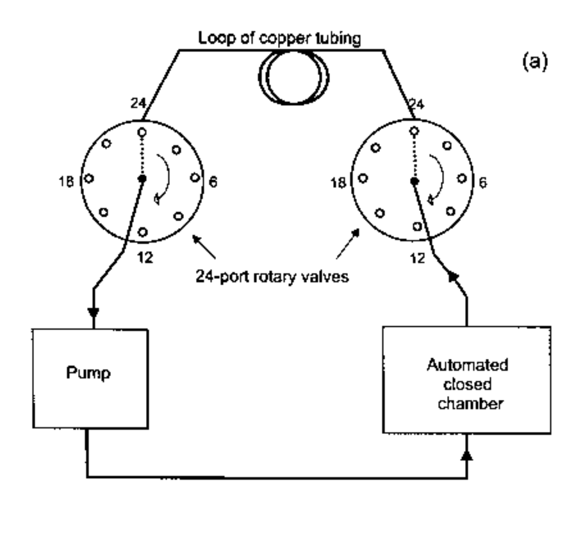


Figure 14 Automatic closed chamber, with battery-powered actuator for chamber closure. (From Smith and Dobbie, 2001.)



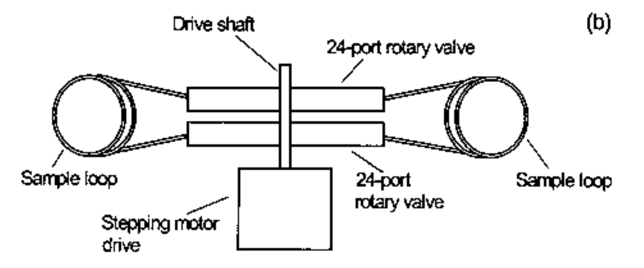


Figure 15 Schematic diagram of automatic gas sampler, used in conjunction with chamber shown in Fig. 14. (From Smith and Dobbie 2001.)

continue. Meanwhile, each filled loop in turn is automatically connected to a GC for gas analysis (Arah et al., 1994).

Open Chamber System. Several workers have constructed measurement systems that switch automatically between multiple open chambers. One such system is available commercially, through Icom-Scottech (Kelso, Scotland). This system measures CO_2 efflux from up to eight open chambers, designed to minimize the pressure difference between the chamber interior and the atmosphere, as described by Rayment and Jarvis (1997). Each chamber is equipped with a pneumatically actuated lid and is only closed for the duration of the measurement.

E. Soil Atmosphere Sampling

Various types of investigation require sampling of the soil atmosphere. This can be, for example, in the context of studying soil conditions for root growth (Strojny et al., 1998), trace gas flux between soil and atmosphere (Gut et al., 1999), soil gas diffusivity (Dörr and Münnich, 1990; Lehmann et al., 2000), or for identifying the depth and the rate at which a gas species is produced or consumed in the soil (Neftel et al., 2000).

A variety of sampling devices can be used, depending on the requirements of the investigation. If a large number of locations has to be sampled and permanent installation of sampling probes is not necessary or practical, instantaneous samples can be obtained with devices of the type shown in Fig. 16. These consist essentially of a tube with an opening at the lower end and a sampling port at the upper end. The tube can be directly driven into the soil until the opening at the lower end reaches the desired sampling depth, but care has to be taken not to plug sample inlet and tube with soil. Locating the opening at the side of the tube (Fig. 16a) helps to avoid this problem. Alternatively, an open-ended tube can be used, if a solid rod is inserted into it during installation so that it protrudes slightly from the open end. When the rod is withdrawn it leaves a small cavity from where the soil air sample is drawn. In a further variation, a loose-fitting rod with an enlarged diameter at the lower end can be pushed slightly further into the soil after tube installation, to open a gap between the tube and the rod-end through which air can be withdrawn (Fig. 16b).

Several issues need to be considered when taking instantaneous samples. The cross section of soil exposed to the sampling inlet may be very small, and resistance to airflow may be large. Care must therefore be taken to avoid gaps between the tube and the soil, otherwise the path of least resistance could be along the outer wall of the sampling tube, and much of the sample will consist of above-ground air. While a small sample volume is

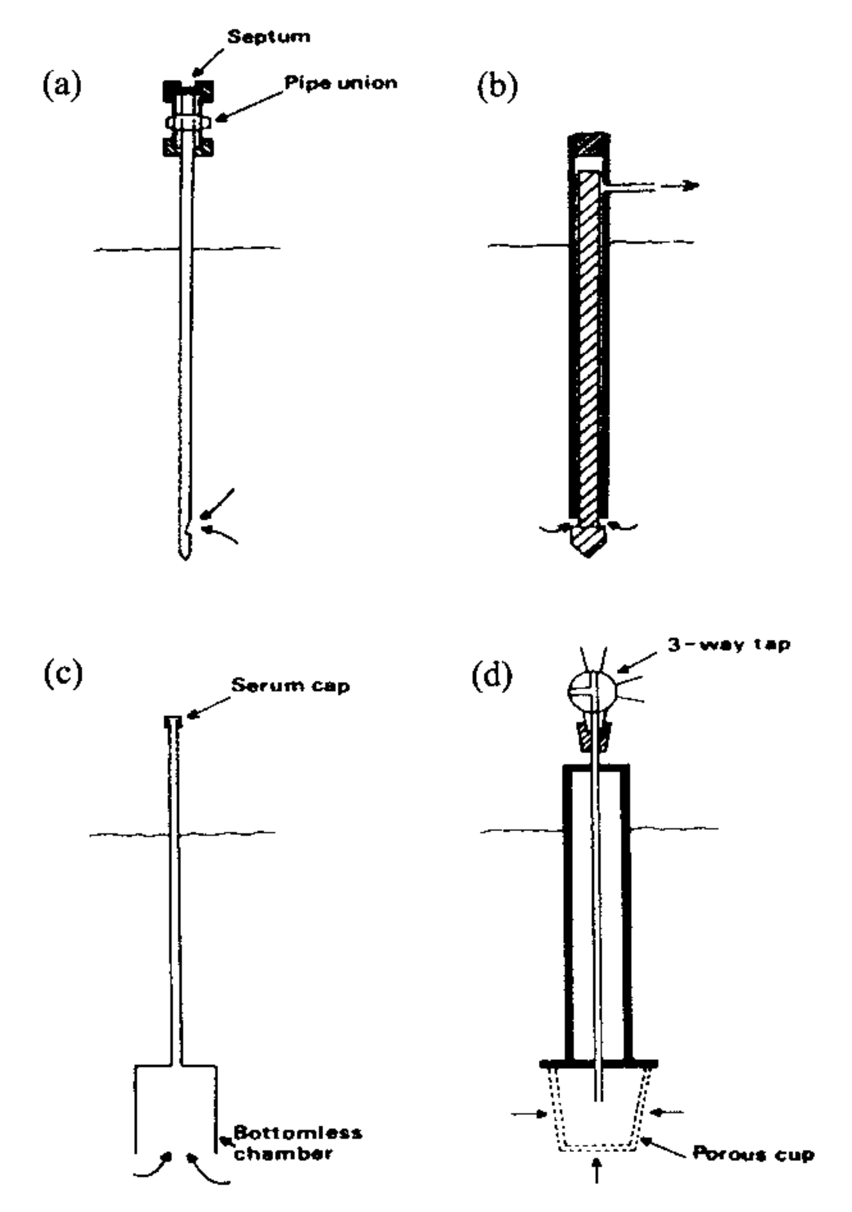


Figure 16 Devices used for sampling the soil atmosphere: (a), (b), probes for instantaneous sampling; (c), (d), probes with diffusion well, installed for longer periods.

desirable from the point of view of minimizing unpredictable soil airflow and related uncertainty about the exact depth from where the sample air is coming from, the withdrawn volume has to be large enough to flush the dead space of the sampling tube. Minimizing internal tube diameter is therefore desirable. Depending on sampling equipment and procedure, results can vary widely. In an intercomparison of soil gas radon measurements, the standard deviation for ^{222}Rn concentrations as measured by 11 groups at 0.4–0.5 m depth was larger than the mean of all values (Hutter and Knutson, 1998).

For repeated sampling of the same location and for integrating over a longer time and a larger cross-sectional area, permanent sampling devices can be installed. These generally differ from the sampling tubes described above in that they have a larger cavity at the lower end (Fig. 16c,d) that acts as a diffusion well, which comes into equilibrium with the neighboring soil pore space. Such probes are normally inserted into an auger hole slightly larger than the maximum diameter and are then backfilled with soil or bentonite. Kammann et al. (2001) have described a sampler made from a flat coil of silicone tubing of 10 mm internal diameter, inserted into a horizontal slot made in the vertical wall of a soil pit, which is then backfilled. This system has the advantage that it only allows the entry of gas, and not water, when the water table is high. It takes about 7 h for CO_2, N_2O, and CH_4 to come to equilibrium with the concentration outside the sampler.

All the above types of sampling preclude continuous sampling, which would create a continuous mass flow of air in the soil, and result in a distortion of the natural gas concentration profile around the sampling inlet. A technique described by Gut et al. (1998) and Neftel et al. (2000) overcomes this problem. An air-permeable hydrophobic polypropylene tube (Accurel® PP V8/2) is inserted into the soil, and air is circulated between it and a nondestructive gas analyzer (Fig. 17). Another advantage of this permanently installed device is the relatively large area over which it is integrated.

VI. APPLICATIONS

The chamber and soil atmosphere sampling methods described in Sec. V, together with the methods used for trace gas analysis described in Secs. II–IV, have been widely used to measure fluxes of greenhouse gases and ozone precursors between soils (or vegetation) and the atmosphere. A wide range of ecosystems has been investigated, including agricultural land, natural and plantation forests, natural grassland and moorland, tundra, and wetlands. Landfills, which constitute a significant source of methane, have also been

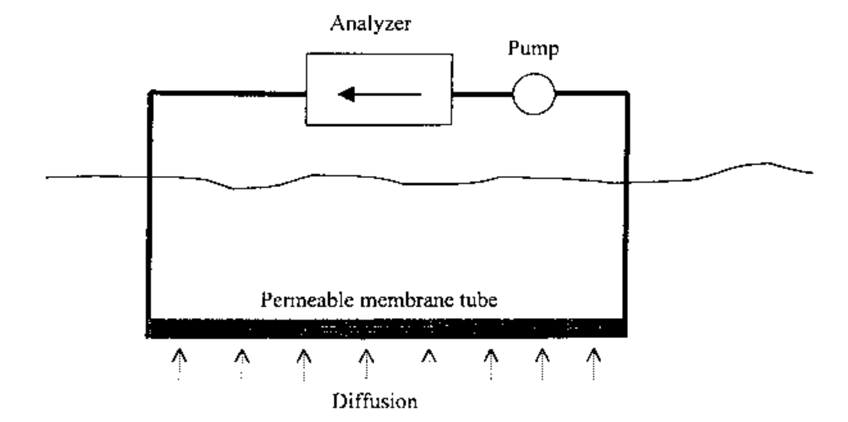


Figure 17 System using gas-permeable plastic tube inserted into the soil, with gas circulation through an analyser on the surface. (After Gut et al., 1998, and Neftel et al., 2000.)

studied by the same methods. This section provides some illustrative examples of such applications, including the equipment combinations employed, and the type of data that can be obtained.

A. CO_2 from Soil Respiration

Forest Soils. Uchida et al. (1997) used closed static chambers 27 cm in diameter and 12 cm high to measure soil respiration rates in a mixed forest in Japan. They sampled the chamber atmosphere every 5 min with plastic syringes, and determined the CO_2 concentrations in a GC fitted with a thermal conductivity detector. No significant differences were found between the measurements made in this way and those based on a ^{222}Rn tracer method, in which the soil atmosphere was sampled at different depths (via sampling probes), the CO_2 and ^{222}Rn concentration profiles were determined, and the ^{222}Rn emission rate was also measured, using a closed chamber and an alpha counter. Davidson and Trumbore (1995) used a vented dynamic chamber system and the ^{222}Rn tracer method in deep forest and pasture soils in the eastern Amazon, and concluded that 20–30% of the CO_2 emission from the soil surface resulted from root respiration and decay below 1 m depth. Davidson et al. (1998) used similar vented dynamic chambers to investigate the effects of temperature and soil water content on CO_2 flux from the soil of a temperate hardwood forest. They circulated the chamber air through a battery-powered LICOR IRGA for 5 min, logging

the CO_2 concentrations at 12 s intervals. The results showed a mean CO_2 efflux of 7.2 Mg ha^{-1}, with high Q_{10} values (mean 3.9).

Bowden et al. (2000) used closed static chambers and a syringe sampling procedure in a deciduous forest in Pennsylvania, U.S.A., together with a GC with a Porapak Q column and an ECD at 275°C, to determine simultaneously CO_2 and N_2O. This GC procedure has also been used by Christensen (1983), Thomson et al. (1997), and Brumme (1995), who combined it with an automated closed chamber system to investigate CO_2 emission due to soil respiration in a beech forest. Three chambers were installed in each of four plots and were sampled 0, 30, and 60 min after closure. Each chamber was closed four times per day. The results showed an exponential increase in CO_2 flux with temperature, with a Q_{10} value of 2.3. Rayment and Jarvis (1997) applied an open chamber/IRGA system to the determination of soil CO_2 flux in the international BOREAS study site in a black spruce forest in Saskatchewan, Canada. The system was operated continuously for 3 months and yielded results indicating a substantial spatial variability in efflux over distances of only a few m; the Q_{10} values for soil respiration showed a skewed distribution, with a mode of 2 to 2.25.

Agricultural Soils. Closed dynamic chambers together with an IRGA have been used to determine soil CO_2 fluxes from conventional and no-tillage cropping systems in Ontario, Canada (Fortin et al., 1996). A major part of the difference of $75\,g\,C\,m^{-1}\,y^{-1}$ ($750\,kg\,C\,ha^{-1}\,y^{-1}$) between the tillage treatments was attributed to differences in soil temperature. Similar methods used on Finnish agricultural soils showed that the rate of CO_2 release from cropped fields in this northern environment was comparable with that determined in similar circumstances in warm-temperate and temperate climates (Koizumi et al., 1999).

Rochette et al. (2000) investigated the effect on CO_2 efflux of 19 consecutive years of pig slurry application to a loam soil in Quebec, Canada. They used a 60 by 60 cm acrylic chamber in the dynamic closed mode, together with an LI-6200 IRGA, and found that half the total emission following an application occurred in the first week and decreased exponentially with time. The second phase was linear and much slower and was attributed to the decomposition of more recalcitrant material.

B. Methane Emissions

Natural Wetlands. The bulk of the published data on CH_4 emissions from natural wetlands have been obtained by closed chamber methods in conjunction with FID gas chromatography. A typical example is the study by Moore et al. (1994) of emissions from 39 sites along a transect through

the Hudson Bay wetlands in Ontario, Canada. Locations varied from hummock and hollows in raised bogs to deep pools, with the water tables ranging from 30 cm below the peat surface to 1 m above. The closed static chamber method was used. Chambers were made from 18 L polycarbonate bottles, from which the bottoms had been removed, with a basal area of 0.053 m^2. They were covered with aluminum foil to reduce heating, and inserted into the peat or floated within styrofoam collars in the larger pools. The neck of each bottle was closed with a rubber stopper containing a glass tube and rubber septum, through which gas samples could be taken with a 10 mL syringe. The seasonal fluxes ranged from 0.3 to 16.6 g CH_4 m^{-2}, with a highly significant relation between the flux and the mean position of the water table over the whole range of sites. Where the fluxes could be compared with tower- and aircraft-based [-δ-] estimates, the agreement was satisfactory, although earlier work by two of the authors (Moore and Roulet, 1991) had indicated that static chambers gave flux values 20% lower than dynamic ones.

Frolking and Crill (1994) investigated climatic controls on CH_4 emission from a New England fen with closed static chambers. They employed much larger chambers (150 L volume, and approx. 0.4 m^2 in area) than those of Moore et al. (1994) described in the previous paragraph. The chambers were made from aluminum and placed in water-filled channels in previously installed aluminum collars inserted 8 cm into the peat. 60 ml gas samples were taken with plastic syringes at 4 min intervals over 20 min and analyzed by FID-GC. Fluxes were more strongly correlated with temperature than with water table and ranged from 21.4 mg $CH_4\,m^{-2}\,d^{-1}$ in February to 639 mg $CH_4\,m^{-2}\,d^{-1}$ in July.

Flooded Forest Land. Flooding large areas of tropical forest behind hydroelectric dams creates a potent source of CH_4. Galy-Lacaux et al. (1997) used floating stainless steel closed chambers 0.25 m^2 in area to measure the CH_4 outgassing from the surface of one lake formed in this way (in French Guyana), as well as determining the bubble flux rate and the vertical CH_4 profile in the water. A linear relation was found between CH_4 concentration in the surface water layer and the flux into the chamber, and the maximum emission rate from the flooded area was estimated at 800 t CH_4 d^{-1}.

Rice Paddies. Chambers used in rice paddies are generally constructed of transparent acrylic or polycarbonate plastic, made high enough to enclose the plants and allow photosynthesis to proceed while the chamber remains in place. Several different sizes have been used, typically ranging from 30 × 30 × 100 cm high (Nouchi et al., 1994) to the 83 × 83 × 105 cm dimensions used by Butterbach-Bahl et al. (1997b) (Fig. 9e). The chambers

are normally fitted with a small electric fan to provide rapid mixing of the air inside. Chamber operation, gas sampling, and GC analysis have been fully automated in several studies (e.g. Schütz et al., 1989; Bronson et al., 1997a,b; Marik et al., 2002), thus providing a more or less continuous record of CH_4 emissions during the growing season.

Nouchi et al. (1994) measured fluxes in Japan by taking five successive 0.3 L air samples from their chambers at 5 min intervals, pumping the air into Tedlar (polyvinyl fluoride) bags, for GC analysis. They found a very large effect of rice straw incorporation on CH_4 emission, with a total seasonal emission of only 3.2 g CH_4 m^{-2} in the absence of straw, compared with 49.7 g CH_4 m^{-2} with rice straw and a microbiological amendment. Butterbach-Bahl et al. (1997b) investigated the impact of the rice cultivar grown on CH_4 emissions in Italy. They combined their chambers with the automated sampling and analysis system described by Schütz et al. (1989). In two consecutive years, fields planted with the cultivar Lido showed emissions 24–31% lower than those from fields planted with the cultivar Roma.

Bronson et al. (1997a,b) managed to combine measurements of both CH_4 and N_2O emissions from a rice paddy soil in the Philippines during the fallow period, using an automated chamber/GC system. CH_4 emissions were only detected immediately after rice harvest and 1–2 weeks after the establishment of the permanent flood for the following rice crops. N_2O fluxes were highest after rainfalls exceeding 20 mm and after the establishment of the flooding at the end of the fallow period.

Landfills. A very detailed mapping of the surface emissions of CH_4 from large landfills in the Moscow region of Russia was carried out by Nozhevnikova et al. (1993). They used 1 liter "accumulative vessels" (i.e., static chambers) and FID-GC analysis on a silica column, and measured emission rates from zero up to 1400 $mg\,m^{-2}\,h^{-1}$, two to three orders of magnitude higher than from natural systems. Trégourès et al. (1999) carried out a comparison of different methods for measuring CH_4 flux from a landfill. They obtained satisfactory agreement between closed static chambers, closed dynamic chambers, and an SF_6 tracer method.

C. Methane Oxidation in Soils

A detailed compilation of published measurements of the rates of oxidation of atmospheric CH_4 in soils (Smith et al., 2000) showed that virtually all the data were obtained by using manually operated closed static chambers together with FID-GC analysis. CH_4 oxidation rates varied over two orders of magnitude, with similar distributions in different climatic zones. Land use

Marcel Dekker, Inc.
270 Madison Avenue, New York, New York 10016

has been shown to have a significant impact on the rate of oxidation, with a general decrease being observed in agricultural land, compared with adjacent natural forest (Dobbie et al., 1996) or grassland (Mosier et al., 1997) on the same soil type. Castro et al. (1995) showed that the oxidation rate decreased from 0.1 to 0 mg CH_4 m^{-2} h^{-1} as the soil water-filled pore space increased from 60 to 100%, because of the increasing barrier to gas diffusion. Brumme and Borken (1999) demonstrated that in a temperate forest, leaf litter type affected gas diffusivity and therefore the rate of CH_4 oxidation: broad beech leaves reduced the rate more than spruce needles.

Following earlier claims that from 10 to 90% of the CH_4 produced in rice paddies was oxidized in the rhizosphere, Krüger et al. (2001) used a novel gaseous oxidation inhibitor, difluoromethane, in a new attempt to quantify this process. They injected the inhibitor into their closed chambers to obtain a concentration of 1% and took gas samples every 30 min over 2 h. They found that about 40% of the CH_4 produced was oxidized at the start of the season, but this proportion fell to zero by the end of the season.

D. N_2O and NO Emissions

N_2O from Agricultural Soils. As with CH_4 emissions, a very high proportion of all N_2O flux data has been obtained with closed static chambers, with ECD-GC analysis. Studies have shown that soils are major sources of N_2O emissions to the atmosphere, and high fluxes are correlated with rapid N cycling (providing NH_4^+ and NO_3^- substrates) and high soil water content and temperatures. A typical study in a temperate agricultural environment is that of Velthof et al. (1997), who found that 5–14% of the N applied to a poorly drained sandy soil in a wet spring was emitted as N_2O. Smith and Dobbie (2001) compared the cumulative N_2O fluxes obtained with replicated closed static chambers operated manually at intervals of 3–7 days, with the fluxes determined every 8 h with the automatic chamber/sampler system shown in Figs. 14 and 15 above. The automatic sampling identified short-term peaks in emissions not observed with the manual sampling, but the cumulative flux values obtained with the more intensive system were only slightly greater, and not significantly different from the "manual" values.

The effects of tillage on N_2O emissions from arable land have been investigated, with very different results in different environments. Thus Ball et al. (1999), using automated chamber/sampler systems, found that in imperfectly drained soils in Scotland much higher N_2O fluxes occurred under spring barley in a no-till system than in a conventionally plowed treatment. In contrast, in a U.S. Midwest soil, Robertson et al. (2000) found

only a very small and statistically nonsignificant increase in a maize–soyabean–wheat rotation under no-till conditions.

Measurements with gas sampling probes showed N_2O concentrations in the soil profile reaching a maximum of about 300 ppm at 50 cm depth under fertilized spring barley (Ball et al., 1999). The air-permeable tube system of Gut et al. (1998) and Neftel et al. (2000) described in Sec. V.E has been used to study the variations with time and depth of N_2O concentrations in a mown grassland soil in Switzerland. The highest concentrations found in the topsoil occurred when precipitation followed fertilization with mineral N (Schmidt et al., 2001). The highest concentrations of N_2O in the subsoil were found when the water content fell below 92% of saturation after a wet period, and less complete reduction to N_2 took place.

N_2O from Forest Soils. Butterbach-Bahl et al. (1997a) measured N_2O fluxes from forest soils in Germany receiving substantial inputs of N from atmospheric deposition. They used a fully automated flux chamber/analysis system, and found mean flux rates between 6 and 53 μg N_2O-N m^{-2} h^{-1} in three pine forest ecosystems, and 8–102 μg N_2O-N m^{-2} h^{-1} in a beech stand. Weitz et al. (1998) measured the emissions of N_2O from soils following the clearing and burning of tropical forest, in Costa Rica. Average emissions from forest soils were 15 μg N_2O-N m^{-2} h^{-1}, which increased to 27 μg N_2O-N m^{-2} h^{-1} after clearing, and gave short-term peaks averaging 123 μg N_2O-N m^{-2} h^{-1} after burning.

NO Emissions. Veldkamp and Keller (1997) investigated the NO (and N_2O) emissions from the soil of a banana plantation in Costa Rica. They used 25 cm diameter closed dynamic chambers on previously installed soil collars, and a Scintrex LMA-3 chemiluminescence detector. 5.1–5.7% of the fertilizer N applied to the soil was emitted as NO, compared with 1.3–2.9% as N_2O (determined with vented closed static chambers mounted on the same collars). In the studies by Butterbach-Bahl et al. (1997a) and Weitz et al. (1998) mentioned in the previous paragraph, NO was also measured, by chemiluminescence methods. Butterbach-Bahl et al. found that NO fluxes generally exceeded those of N_2O, except in the beech stand, while Weitz et al. found that the NO fluxes varied between one-third and three times those of N_2O.

E. VOC Emissions

A typical example of a study of VOC emissions from woody vegetation is the study of Kesselmeier et al. (1996) of the emissions of isoprene and monoterpenes from the Mediterranean oak, *Quercus ilex* L. This species was found to emit mainly monoterpenes, with only very small emissions of

Marcel Dekker, Inc.
270 Madison Avenue, New York, New York 10016

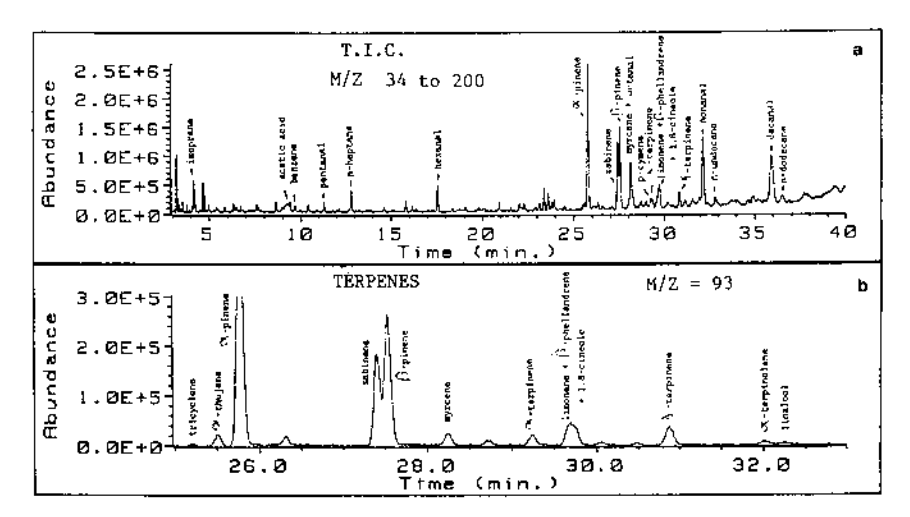


Figure 18 VOC emissions from the Mediterranean oak, analyzed by capillary column GC and a quadrupole mass spectrometer. (Reprinted from Kesselmeier et al., 1996, with permission from Elsevier Science.)

isoprene. This contrasted with results reported for other oak species, which were mainly isoprene emitters. Dynamic cuvettes (chambers) enclosing whole branches were used. Air from the cuvettes was pumped through a Teflon tube to an adsorbent trap, from which the volatile compounds were desorbed at 230°C and passed into a GC capillary column. A quadrupole mass spectrometer was used as detector. The results demonstrated that α- and β-pinene and sabinene were the main monoterpenes present (Fig. 18).

REFERENCES

Ambus. P. and G.P. Robertson. 1998. Automated near-continuous measurement of carbon dioxide and nitrous oxide fluxes from soil. *Soil Sci. Soc. Am. J.* 62:394–400.

Arah, J.R.M., I.J. Crichton, K.A. Smith, H. Clayton, and U. Skiba. 1994. Automated gas chromatographic analysis system for micrometeorological measurements of trace gas fluxes. *J. Geophys. Res.* 99:16593–16598.

Ball, B.C., A. Scott, and J.P. Parker. 1999. Field N_2O, CO_2 and CH_4 fluxes in relation to tillage, compaction and soil quality in Scotland. *Soil Till. Res.* 53:29–39.

Beswick, K.M., T.W. Simpson, D. Fowler et al. (1998). Methane emission on large scales. *Atmos. Environ.* 32:3283–3291.

Bowden, R.D., G. Rullo, G.R. Stevens, and P.A. Steudler. 2000. Soil fluxes of carbon dioxide, nitrous oxide, and methane at a productive temperate deciduous forest. *J. Environ. Qual.* 29:268–276.

Braithwaite, A. and F.J. Smith. 1995. *Chromatographic Methods*. Kluwer, Dordrecht, The Netherlands.
Bronson, K.F., H.U. Neue, U. Singh, and E.B. Abao, Jr. 1997a. Automated measurements of methane and nitrous oxide flux in a flooded rice soil: I. Residue, nitrogen, and water management. *Soil Sci. Soc. Am. J.* 61: 981–987.
Bronson, K.F., U. Singh, H.U. Neue, and E.B. Abao, Jr. 1997b. Automated measurements of methane and nitrous oxide flux in a flooded rice soil: II. Fallow period emissions. *Soil Sci. Soc. Am. J.* 61:988–993.
Brumme, R. 1995. Mechanisms for carbon and nutrient release and retention in beech forest gaps, 3. Environmental regulation of soil respiration and nitrous oxide emissions along a microclimatic gradient. *Plant Soil* 168/169:593–600.
Brumme, R. and F. Beese. 1992. Effects of liming and nitrogen fertilization on emission of CO_2 and N_2O from a temperate forest. *J. Geophys. Res.* 97:12,851–12,858.
Brumme, R. and W. Borken. 1999. Site variation in methane oxidation as affected by atmospheric deposition and type of temperate forest ecosystem. *Glob. Biogeochem. Cycl.* 13:493–501.
Bruner, F. 1993. *Gas Chromatographic Environmental Analysis*. Wiley-VCH, Weinheim, Germany.
Butterbach-Bahl, K. 1993. Mechanismen der Produktion und Emission von Methan in Reisfeldern. Doctoral thesis, Technical Univ., Munich. Wissenschafts-Verlag Dr. Wigbert Maraun Frankfurt/M, Germany.
Butterbach-Bahl, K., R. Gasche, L. Breuer, and H. Papen. 1997a. Fluxes of NO and N_2O from temperate forest soils: impact of forest type, N deposition and of liming on the NO and N_2O emissions. *Nutr. Cycl. Agroecosys.* 48:79–90.
Butterbach-Bahl, K., H. Papen, and H. Rennenberg. 1997b. Impact of gas transport through rice cultivars on methane emission from rice paddy fields. *Plant Cell Environ.* 20:1175–1183.
Castro, M.S., P.A. Steudler, J.M. Melillo, J.D. Aber, and R.D. Bowden. 1995. Factors controlling atmospheric methane consumption by temperate forest soils. *Glob. Biogeochem. Cycl.* 9:1–10.
Christensen, S. 1983. Nitrous oxide emission from the soil surface: continuous measurement by gas chromatography. *Soil Biol. Biochem.* 15:531–536.
Conen, F. and K.A. Smith. 1998. A re-examination of closed flux chamber methods for the measurement of trace gas emissions from soils to the atmosphere. *Eur. J. Soil Sci.* 49:701–707.
Conen, F. and K.A. Smith. 2000. An explanation of linear increases in gas concentration under closed chambers used to measure gas exchange between soil and the atmosphere. *Eur. J. Soil Sci.* 51:111–117.
Crill, P.M., M. Keller, A. Weitz, B. Grauel, and E. Veldkamp. 2000. Intensive field measurements of nitrous oxide emissions from a tropical agricultural soil. *Glob. Biogeochem. Cycl.* 14:85–95.
Davidson, E.A. and S.E. Trumbore. 1995. Gas diffusivity and production of CO_2 in deep soils of the eastern Amazon. *Tellus* 47B:550–565.

Davidson, E.A., E. Belk, and R.D. Boone. 1998. Soil water content and temperature as independent or confounded factors controlling soil respiration in a temperate mixed hardwood forest. *Glob. Change Biol.* 4:217–227.

De Klein, C.A.M., I.P. McTaggart, K.A. Smith, R.J. Stevens, R. Harrison, and R.J. Laughlin. 1999. Measurements of N_2O emissions from grassland soil using photo-acoustic infra-red spectroscopy, long-path infra-red spectroscopy, gas chromatography and continuous-flow isotope-ratio mass spectrometry. *Commun. Soil Sci. Plant Anal.* 30:1463–1477.

Denmead, O.T. 1979. Chamber system for measuring nitrous oxide emission from soils in the field. *Soil Sci. Soc. Am. J.* 43:89–95.

Dobbie, K.E., K.A. Smith, A. Priemé, C. Christensen, A. Degorska, and P. Orlanski. 1996. Effect of land use on the rate of methane uptake by surface soils in northern Europe. *Atmos. Environ.* 30:1005–1011.

Dörr, H. and K.O. Münnich. 1990. ^{222}Rn flux and soil air concentration profiles in West Germany. Soil ^{222}Rn as tracer for gas transport in the unsaturated soil zone. *Tellus* 42B:20–28.

Dufrêne, E., J.-Y. Pontailler, and B. Saugier. 1993. A branch bag technique for simultaneous CO_2 enrichment and assimilation measurements on beech (*Fagus sylvatica* L.), *Plant Cell Environ.* 16:1131–1138.

Eckles, R.D., J.M. Welles and K. Petersen. 1993. CO_2 and CO_2/H_2O infrared gas analysers. *Measurements and Control*, No. 510, Oct. 1993.

Fang, C. and J.B. Moncrieff. 1996. An improved dynamic chamber technique for measuring CO_2 efflux from the surface of soil. *Funct. Ecol.* 10:297–305.

Fang, C. and J.B. Moncrieff. 1998. An open-top chamber for measuring soil respiration and the influence of pressure difference on CO_2 efflux measurement. *Funct. Ecol.* 12:319–325.

Ferm, M. 1979. Method for determination of atmospheric ammonia. *Atmos. Environ.* 13:1385–1391.

Fontjin, A., A.J. Sabadell, and R.J. Ronco. 1970. Homogeneous chemiluminescence measurement of nitric oxide with ozone. *Anal. Chem.* 42:575–579.

Fortin, M.C., P. Rochette, and E. Pattey. 1996. Soil carbon dioxide fluxes from conventional and no-tillage small-grain cropping systems. *Soil Sci. Soc. Am. J.* 60:1541–1547.

Frolking, S. and P. Crill. 1994. Climate controls on temporal variability of methane flux from a poor fen in southeastern New Hampshire: measurement and modeling. *Glob. Biogeochem. Cycl.* 8:385–397.

Galle, B., L. Klemedtsson, and D.W.T. Griffith. 1994. Application of a Fourier transform IR system for measurements of N_2O fluxes using micrometeorological methods, an ultra-large chamber system, and conventional field chambers. *J. Geophys. Res.* 99:16,575–16,583.

Galy-Lacaux, C., R. Delmas, C. Jambert et al., 1997. Gaseous emission and oxygen consumption in hydroelectric dams: a case study in French Guyana. *Glob. Biogeochem. Cycl.* 11:471–483.

Griffith, D.W.T. 1996. Synthetic calibration and quantitative analysis of gas phase infrared spectra. *Appl. Spectrosc.* 50:59–70.

Griffith, D.W.T. and B. Galle. 2000. Flux measurements of NH_3, N_2O and CO_2 using dual beam FTIR spectroscopy and the flux-gradient technique. *Atmos. Environ.* 34:1087–1098.
Gut, A., A. Blatter, M. Fahrni, B.E. Lehmann, A. Neftel, and T. Staffelbach. 1998. A new membrane tube technique (METT) for continuous gas measurements in soil. *Plant Soil* 198:79–87.
Gut, A., A. Neftel, T. Staffelbach, M. Riedo, and B.E. Lehmann. 1999. Nitric oxide flux from soil during the growing season of wheat by continuous measurement of the NO soil-atmosphere concentration gradient: a process study. *Plant Soil* 216:165–180.
Hutchinson, G.L. and A.R. Mosier, 1981. Improved soil cover method for field measurements of nitrous oxide fluxes. *Soil Sci. Soc. Am. J.* 45:311–316.
Hutter, A.R. and E.O. Knutson, 1998. An international intercomparison of soil gas radon and radon exhalation measurements. *Health Phys.* 74: 108–114.
Ineson, P., P.A. Coward, D.G. Benham, and S.M.C. Robertson. 1998. Coniferous forests as ‘‘secondary agricultural’’ sources of nitrous oxide. *Atmos. Environ.* 32:3321–3330.
International Atomic Energy Agency (IAEA). 1992. *Manual on Measurement of Methane and Nitrous Oxide Emissions from Agriculture*. IAEA-TECDOC-674, IAEA, Vienna.
Kammann, C., L. Grühage, and H.-J. Jäger. 2001. A new sampling technique to monitor concentrations of CH_4, N_2O and CO_2 in air at well-defined depths in soils with varied water potential. *Eur. J. Soil Sci.* 52:297–303.
Kesselmeier, J., L. Schäfer, P. Ciccioli et al. 1996. Emission of monoterpenes and isoprene from a Mediterranean oak species *Quercus ilex* L. measured within the BEMA (Biogenic Emissions in the Mediterranean Area) project. *Atmos. Environ.* 30:1841–1850.
Keuken, M.P., A. Wayers-Ypelaan, J.J. Mols, R.P. Otjes, and J. Slanina. 1989. The determination of ammonia in ambient air by an automated thermodenuder system. *Atmos. Environ.* 23:2177–2185.
Kimball, B.A. and E.R. Lemon. 1971. Air turbulence effects upon soil gas exchange. *Soil. Sci. Soc. Am. Proc.* 35:16–21.
Kirkham, D. 1946. Field method for determination of air permeability of soil in its undisturbed state. *Soil Sci. Soc. Am. Proc.* 11:93–99.
Koizumi, H., M. Kontturi, S. Mariko, T. Nakadai, Y. Bekku, and T. Mela. 1999. Soil respiration in three soil types in agricultural ecosystems in Finland. *Acta Agric. Scand.* 49B:65–74.
Krüger, M., P. Frenzel, and R. Conrad. 2001. Microbial processes influencing methane emission from rice fields. *Glob. Change Biol.* 7:49–63.
Langford, A.O., P.D. Goldan, and F.C. Fehsenfeld. 1989. A molybdenum oxide annular denuder system for gas-phase ambient ammonia measurements. *J. Atmos. Chem.* 8:359–376.
Lehmann B.E., M. Lehmann, A. Neftel, and S.V. Tarakanov. 2000. Radon-222 monitoring of soil diffusivity. *Geophys. Res. Lett.* 27:3917–3920.

Long, S.P. and J.-E. Hällgren. 1993. Measurement of CO_2 assimilation by plants in the field and the laboratory. In: *Photosynthesis and Production in a Changing Environment* (D.O. Hall et al., eds.), Chapman and Hall, London, pp. 129–167.

Longdoz, B., M. Yernaux, and M. Aubinet. 2000. Soil efflux measurements in a mixed forest: impact of chamber disturbances, spatial variability and seasonal evolution. *Glob. Change Biol.* 6:907–917.

Lund, C.P., W.J. Riley, L.L. Pierce, and C.B. Field. 1999. The effects of chamber pressurization on soil-surface CO_2 flux and the implications for NEE measurements under elevated CO_2. *Glob. Change Biol.* 5:269–281.

Marik, T., H. Fischer, F. Conen, and K.A. Smith. 2002. Seasonal variations in stable isotope ratios in methane from rice fields. *Glob. Biogeochem. Cycl.* 16:41-1–41-11.

Matthias, A.D., A.M. Blackmer, and J.M. Bremner. 1980. A simple chamber technique for field measurement of emissions of nitrous oxide from soils. *J. Environ. Qual.* 9:251–256.

Moore, T.R. and N. Roulet. 1991. A comparison of dynamic and static chambers for methane emission measurements from subarctic fens. *Atmos.-Ocean* 29: 102–109.

Moore, T.R., A. Heyes, and N. Roulet. 1994. Methane emissions from wetlands, southern Hudson Bay lowland. *J. Geophys. Res.* 99:1455–1467.

Mosier, A.R., D.S. Schimel, D. Valentine, K.F. Bronson, and W.J. Parton. 1991. Methane and nitrous oxide fluxes in native, fertilized, and cultivated grasslands. *Nature* 350:330–332.

Mosier, A.R., J.A. Delgado, V.L. Cochran, D.W. Valentine, and W.J. Parton. 1997. Impact of agriculture on soil consumption of atmospheric CH_4 and a comparison of CH_4 and N_2O flux in subarctic, temperate and tropical grasslands. *Nutr. Cycl. Agroecosys.* 49:71–83.

Neftel, A., A. Blatter, M. Schmid, Lehmann, and S.V. Tarakonov. 2000. An experimental determination of the scale length of N_2O in the soil of a grassland. *J. Geophys. Res.* 105:12,095–12,103.

Norman, J.M., C.J. Kucharik, S.T. Gower et al. 1997. A comparison of six methods for measuring soil-surface carbon dioxide fluxes. *J. Geophys. Res.* 102:28,771–28,777.

Nouchi, I., T. Hosono, K. Aoki, and K. Minami. 1994. Seasonal variation in methane flux from rice paddies associated with methane concentration in soil water; rice biomass and temperature, and its modelling. *Plant Soil* 161: 195–208.

Nozhevnikova, A., A.B. Lifshitz, V.S. Lebedev, and G.A. Zavarzin. 1993. Emission of methane into the atmosphere from landfills in the former USSR. *Chemosphere* 26:401–417.

Parrish, D.D. and F.C. Fehsenfeld. 2000. Methods for gas-phase measurements of ozone, ozone precursors and aerosol precursors. *Atmos. Environ.* 34:1921–1957.

Priemé, A. and S. Christensen. 1999. Methane uptake by a selection of soils in Ghana with different land use. *J. Geophys. Res.* 104:23,617–23,622.

Rayment M.B. and P.G. Jarvis. 1997. An improved open chamber system for measuring soil CO_2 effluxes in the field. *J. Geophys. Res.* 102:28,779–28,784.

Rayment, M.B. and P.G. Jarvis. 1999. Seasonal gas exchange of black spruce using an automatic branch bag system. *Can. J. For. Res.* 29:528–1538.

Ridley, B.A. and L.C. Howlett. 1974. An instrument for nitric oxide measurements in the stratosphere. *Rev. Sci. Instrum.* 45:742–746.

Robertson, G.P., E.A. Paul, and R.R. Harwood. 2000. Greenhouse gases in intensive agriculture: contributions of individual gases to the radiative forcing of the atmosphere. *Science* 289:1921–1925.

Rochette, P., D.A. Angers, and D. Côté. 2000. Soil carbon and nitrogen dynamics following application of pig slurry for the 19th consecutive year: I. Carbon dioxide fluxes and microbial biomass carbon. *Soil Sci. Soc. Am. J.* 64:1389–1395.

Rochette, P., E.G. Gregorich and R.L. Desjardins. 1992. Comparison of static and dynamic closed chambers for measurement of soil respiration under field conditions. *Can. J. Soil Sci.* 72:605–609.

Schmid, M., A. Neftel, M. Riedo and J. Fuhrer. 2001. Process-based modelling of nitrous oxide emissions from different nitrogen sources in mown gassland. *Nutr. Cycl. Agroecosys* 60:177–187.

Schütz, H., A. Holzapfel-Pschorn, R. Conrad, H. Renneberg, and W. Seiler. 1989. A 3-year continuous record on the influence of daytime, season and fertilizer treatment on methane emission rates from an Italian rice paddy. *J. Geophys. Res.* 94:16,405–16,416.

Scott, A., I. Crichton, and B.C. Ball. 1999. Long-term monitoring of soil gas fluxes with closed chambers using automated and manual systems. *J. Environ. Qual.* 28:1637–1643.

Silvola, J., P. Martikainen, and H. Nykänen. 1992. A mobile automatic gas chromatograph system to measure CO_2, CH_4 and N_2O fluxes from soil in the field. *Suo* 43:263–266.

Skiba, U., K.J. Hargreaves, K.A. Smith, and D. Fowler. 1992. Fluxes of nitric and nitrous oxides from agricultural soils in a cool temperate climate. *Atmos. Environ.* 26A:2477–2488.

Smith, K.A. and J.R.M. Arah. 1991. Gas chromatographic analysis of the soil atmosphere. In: *Soil Analysis.* 2d ed. (Smith, K.A., ed.). Marcel Dekker, New York, pp. 505–546.

Smith, K.A. and K.E. Dobbie. 2001. The impact of sampling frequency and sampling times on chamber-based measurements of N_2O emissions from fertilized soils. *Glob. Change Biol.* 7: 933–945.

Smith, K.A. and C.E. Mullins, eds. 2000. *Soil and Environmental Analysis: Physical Methods.* 2d ed. Marcel Dekker, New York.

Smith, K.A., A. Scott, L. Klemedtsson, and B. Galle. 1994. Use of a long-path infrared monitor for measurement of nitrous oxide flux from soil. *J. Geophys. Res.* 99:16,585–16,592.

Smith, K.A., H. Clayton, I.P. McTaggart, P.E. Thomson, J.R.M. Arah, and A. Scott. 1995. The measurement of nitrous oxide emissions from soil by using chambers. *Phil. Trans. Roy. Soc. London Ser. A* 351:327–338.

Smith, K.A., K.E. Dobbie, B.C. Ball et al. 2000. Oxidation of atmospheric methane in Northern European soils, comparison with other ecosystems, and uncertainties in the global terrestrial sink. *Glob. Change Biol.* 6: 791–803.

Strojny, Z., P.V. Nelson, and D.H. Willits. 1998. Pot soil air composition in conditions of high soil moisture and its influence on chrysanthemum growth. *Sci. Hortic.* 73:125–136.

Thomson, P.E., J.P. Parker, J.R.M. Arah, H. Clayton, and K.A. Smith. 1997. Automated soil monolith/flux chamber system for the study of trace gas fluxes. *Soil Sci. Soc. Am. J.* 61:1323–1330.

Trégourès, A., A. Beneito, P. Berne et al. 1999. Comparison of seven methods for measuring methane flux at a municipal solid waste landfill site. *Waste Man. Res.* 17:453–458.

Uchida, M., Y. Nojiri, N. Saigusa, and T. Oikawa. 1997. Calibration of CO_2 flux from forest soil using ^{222}Rn calibrated method. *Agric. For. Meteorol.* 87: 301–311.

Veldkamp. E. and M. Keller. 1997. Nitrogen oxide emissions from a banana plantation in the humid tropics. *J. Geophys. Res.* 102:15,889–15,898.

Velthof, G.L., O. Oenema, R. Postma, and M.L. Van Beusichem. 1997. Effects of type and amount of applied nitrogen fertilizer on nitrous oxide fluxes from intensively managed grassland. *Nutr. Cycl. Agroecosys.* 46:257–267.

Weitz, A.M., E. Veldkamp. M. Keller, J. Neff, and P.M. Crill. 1998. Nitrous oxide, nitric oxide, and methane fluxes from soils following clearing and burning of tropical secondary forest. *J. Geophys. Res.* 103:28,047–28,058.

Werle, P. 1999. Laseroptical sensors for in-situ gas analysis. *Recent Res. Dev. Opt. Eng.* 2:1–17.

Wyers, G.P., R.P. Otjes, and J. Slanina. 1993. A continuous-flow denuder for the measurement of ambient concentrations and surface-exchange fluxes of ammonia. *Atmos. Environ.* 27A:2085–2090.

11

Measurement of Trace Gases, II: Micrometeorological Methods at the Plot-to-Landscape Scale

John B. Moncrieff
The University of Edinburgh, Edinburgh, Scotland

I. INTRODUCTION

The range of environmental concerns that face us and the realization that the issues are complex have produced a situation in which scientists from a number of disciplines increasingly find themselves collaborating to investigate some issue of soil–vegetation–atmosphere exchange. This chapter discusses the methods that can be used at the scale of the agricultural landscape. The methods belong to the general field of micrometeorology in that they have time and space scales that are on the order of tens of minutes and a few km^2 respectively. The space scale is influenced both by the length scales of atmospheric turbulence, which are a result of mechanical (surface friction) effects, and by thermal effects which influence atmospheric stability. The reporting time scale for surface fluxes of about 30 min is related to the need to make observations over a suitably long period, so that the majority of the spectra of flux-carrying eddies are sampled, yet not so long that natural diurnal variabilities in scalar concentrations, or forcing functions such as solar radiation, are included.

One important difference between micrometeorological methods and other techniques to measure surface fluxes is that they are nondestructive in that they only sample the air as it advects past the sensor; they also are noncontact in that we merely sample passively as the air passes our instrumentation—they cannot alter the microclimate as chamber methods,

Marcel Dekker, Inc.
270 Madison Avenue, New York, New York 10016

for instance, could do (see Chap. 10). Traditionally, micrometeorologists have sought to establish their measuring systems on landscapes that are as flat as possible and with homogeneous surface cover as far as possible upwind. The earliest micrometeorological experiments were made over surfaces such as extensive wheat fields or prairie grass. Measurements were made generally in good weather, partly to protect the type of instrumentation then available. In the past decade, instrumentation has developed to the extent that routine flux measurements are possible in all weather and for long periods of time. There has been a proliferation of routine flux stations across the globe (although irregularly distributed in space), and this has inevitably led to many of the stations being in nonideal terrain, e.g., on the gentle slopes of hills. The challenge for micrometeorology in the next decade or so is to develop the theoretical issues that such an expansion of sites brings.

Micrometeorological methods can be used to scale up to observations made by aircraft or interpolated from remote sensing platforms. They can also be used to check observations made on much smaller scales, e.g., chambers on leaves or soil. To that extent they are an integral part of the observation strategy that is being used to solve many of the current environmental problems facing us. It is the scaling issues that bring micrometeorologists and other observational and modeling scientists together.

II. THEORY AND SCALES OF OBSERVATION

A. Where the Observations Are Made

All micrometeorological measurements are made within the atmospheric boundary layer (ABL, Fig. 1), defined by Lenschow (1995) as "the lower part of the atmosphere that interacts with the biosphere and is closely coupled to the surface by turbulent exchange processes." The depth of the ABL depends on the degree of mechanical (caused by surface friction) and buoyant mixing (thermals rising from the warmed surface), and its depth can also be dictated by synoptic scale motions such as anticyclonic subsidence. The ABL is sometimes also called a convective boundary layer (CBL) when it is several kilometers deep as a result of the development of thermals rising during the day. At night, the ABL may be perhaps only a few tens of meters deep. The top of the ABL represents a fairly sharp boundary between the turbulent, chaotic motions of the ABL and the smoother, streamlined flow of the free atmosphere above. The rate of change in vertical profiles of temperature, water vapor, and carbon dioxide is highest near the active surface, in a region typically about one-tenth the

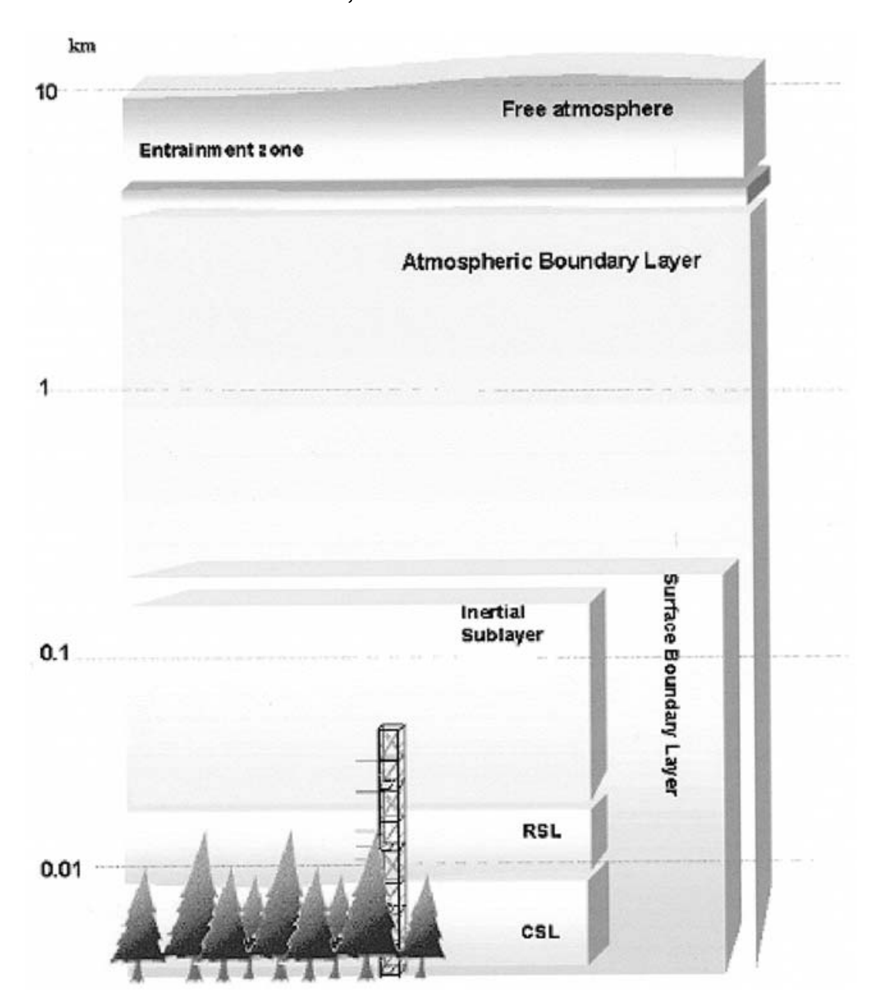


Figure 1 The atmospheric boundary layer and its sublayers.

depth of the ABL that is called the surface boundary layer (SBL). It is in this region that most conventional micrometeorological measurements are made The SBL can further be divided into two sublayers: inertial and roughness (Raupach and Thom, 1981). In the inertial sublayer, wind profiles in neutral stability conditions are logarithmic with height, and well-established scaling schemes apply (Kaimal and Finnegan, 1994). Fluxes are considered constant with height (or at least within 10% of their surface values). Close to surface vegetation lies an interfacial layer in which turbulence is enhanced over

that in the inertial sublayer above by wake turbulence or thermal effects. The depth of this so-called roughness sublayer has been variously estimated to be three times the height of the vegetation (Kaimal and Finnegan, 1994) or sometimes three times the spacing between the vegetation elements (Raupach and Legg, 1984). The implication of the enhanced diffusivities in the roughness layer is that micrometeorological methods that rely on establishing eddy diffusivities are difficult to apply in this layer. By going beyond the roughness sublayer, however, concentration gradients can become small and difficult to measure over rough vegetation, and this poses further problems.

The top of the surface layer is not physically as well defined as the top of the ABL. Although most tower-based flux measurements are made within the surface boundary layer, the evolving structure of the ABL over a day does present opportunities for other measurements using aircraft, tether-sondes, and ABL budget methods (Raupach et al., 1992).

B. Flux Footprint

Fluxes measured by micrometeorological sensors are effectively the integration of fluxes from a variety of sources and sinks in the landscape for a distance of several hundred meters upwind from the measuring point. The height at which the measurements are chosen to be made must be determined both by consideration of the frequency response of the instrumentation and also by the "fetch" or extent of the upwind area from which the signal comes. Eddies become progressively larger with height up to the depth of the planetary boundary layer, typically 1 km by day, and this means that instrumentation with a slower response can be used successfully at heights well above the vegetation. As the surface is approached, however, the spectrum of turbulence includes a larger proportion of smaller eddies that actively exchange mass and momentum between the surface and the atmosphere. Instrumentation used in the eddy covariance method must therefore be capable of sampling high frequency eddies, typically up to 10 Hz. In principle one could use an eddy covariance system (see Sec. III.C) well above the canopy in order to avoid the problem of frequency response of analyzers. However, as we move up in height the area of flux integration becomes larger and the requirements of surface homogeneity become more and more stringent. In fact if the instruments are placed too high above the surface it is possible that they could extend above the boundary layer representative of the nearby vegetation and be measuring some component of fluxes from a different type of vegetation further upwind. A convenient rule of thumb suggests a fetch : height ratio of about 100 : 1; thus a fetch of 500 m would

allow instruments to be placed up to a height of about 5 m above the surface. The fetch:height ratio depends on atmospheric stability and surface roughness insofar as they influence the degree of mixing of internal boundary layers as they are advected over different types of surface (Mulhearn, 1977; Gash, 1986; Grelle and Lindroth, 1996). The footprint or source region defines the relative importance of sources upwind that contribute to the measured flux. This area can be regarded as contributing most of the flux measured, and its areal extent and position can be calculated from a knowledge of surface roughness, atmospheric stability, and wind speed and direction (e.g., Schuepp et al., 1990, Schmid and Oke, 1990). The approach is based on the same theory as underlies dispersion modeling of pollutants using the Gaussian plume approach. Such models can be used to calculate the relative contribution to the vertical flux at any measurement height coming from a point upwind. Figure 2 is an example of the distribution of the relative contribution to the vertical flux as a

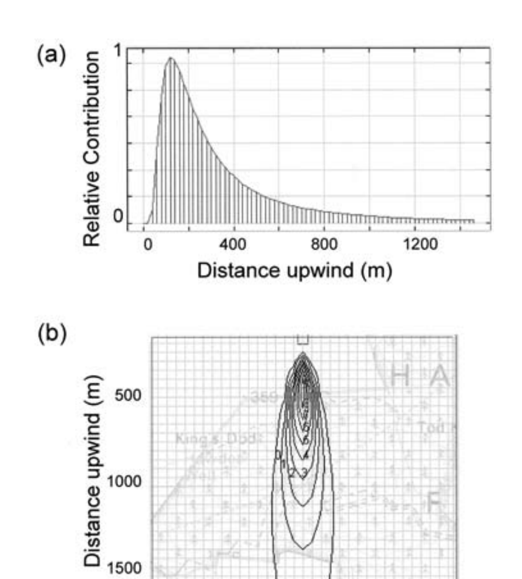


Figure 2 A "flux footprint" showing the relative contribution to the total measured flux contributed by sources at various distances upwind from the measuring point. (The simulation is available at http://www.ierm.ed.ac.uk/jbm/java/jflux/jf2.htm.)

function of height of measurement. The data are normalized so that the flux at the distance of maximum source contribution appears as a peak in this representation. In this simulation, the peak source distribution is within about 50 m of the measurement point. The contribution from sources upwind decreases exponentially with distance from the tower. Calculation of the cumulative fraction shows that even at a distance of about 1500 m from the tower, only about 95% of the measured flux has been accounted for by sources within this distance or footprint. Both the peak and the cumulative fraction depend on measurement height and atmospheric stability. As the height of measurement increases, the peak of the flux footprint becomes more and more distant from the point of measurement. Similarly, the peak contribution moves closer to the point of measurement as the atmosphere becomes more unstable. With increasing stability, the peak contribution moves further from the point of measurement.

Many agricultural landscapes are characterized by relatively small-scale heterogeneity (small fields of a few hundred meters on a side) and thus any tower-based flux measuring system will "see" fluxes coming from different fields within the footprint. The flux footprint concept permits the integration of fluxes from such a landscape by permitting the calculation of the relative source strengths in the area upwind of the flux tower. Soegaard et al. (2003) examined the CO_2 fluxes over several very different agricultural surfaces (winter wheat, winter barley, spring barley, maize, and grass) in conjunction with a footprint modeling exercise. Good agreement was found between the surface flux measured on a tower where it could be expected to integrate across the different land-use types and the modeled fluxes (based on 3-D footprint and biophysical models). Such an approach is likely to be of increasing value in the real world where homogeneous extensive landscapes for micrometeorological research are really quite rare.

C. Measurements of Net Ecosystem Exchange

Fluxes of gases measured by micrometeorological methods above the canopy are the net fluxes from the whole system. If the gases of interest are carbon dioxide and water vapor then the net fluxes are measures of the net ecosystem exchange of carbon (NEE) or total evaporation (ET), respectively, from the canopy, its elements and the ground surface (Fig. 3). The upper system boundary (USB) marks the level through which the vegetation exchanges carbon and water with the atmosphere. Direct micrometeorological methods such as eddy covariance operate at this level. Below the

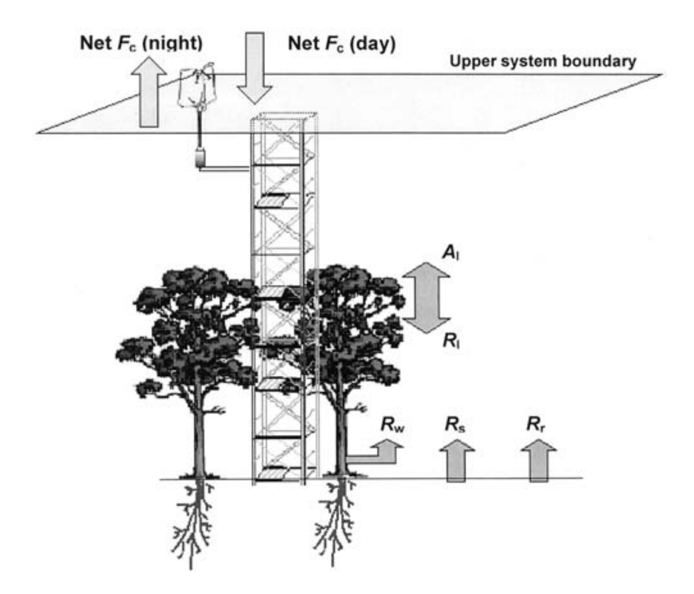


Figure 3 Fluxes above and within the canopy.

USB, A_l and R_l are the net assimilatory and respiratory exchanges by the leaves. The subscripts w, s, and r refer to respiratory fluxes from wood, soil, and roots, respectively. Instrumentation placed above the upper system boundary (USB) measures the net exchange of material passing through that arbitrary level and of itself cannot distinguish the pathways by which that flux arrived at the sensor. Thus, the NEE is the measured flux (F_c) above the USB, plus the component that represents storage of carbon between the point of observation and the ground, i.e., $F_c + \Delta S$. (It is assumed that there are no advective fluxes in this representation; this assumption will be examined later.) Profiles of carbon dioxide concentration within the canopy, and up to the height at which the flux measurements are made, are used to measure changes in storage of carbon.

NEE is the net sum of a number of component processes that take place within the stand. These include the gains of carbon in photosynthesis by the foliage of the trees, understorey, and mosses, and the losses from respiration by the above-ground foliage and wood as well as the below-ground roots, mycorrhizas, and heterotrophic microorganisms (the so-called "soil respiration"). Of these the major components are the gains by photosynthesis and the losses through soil respiration.

III. PRINCIPLES

The transport of gases, heat, and pollutants in the atmosphere is produced by the eddying motion of the atmosphere as air parcels are displaced from one level to another. Micrometeorological methods used to quantify this turbulent exchange can either sample the air as it flows past a sampling point for its vertical windspeed and direction and its gas concentration directly (the *eddy covariance* or *eddy accumulation* methods), or they can be based on quantifying the rate of diffusion down concentration gradients (the *aerodynamic* and *Bowen ratio* methods). The direct method of eddy covariance involves sampling at one height only but with relatively sophisticated sensors and logging equipment. The methods based on measuring gradients require measurements at two or more heights but use simpler sensors. The disadvantage of the gradient techniques is, however, that a number of empirical functions are required to account for thermal stratification of the atmosphere; additionally, the gradients in atmospheric properties become very small above vegetation canopies, and the aerodynamic technique in particular cannot be used inside plant canopies. All three techniques, when used above vegetation, require that steady-state conditions exist, i.e., that atmospheric conditions are not changing rapidly over the sampling period; they also all require extensive upwind areas of the vegetation, i.e., these methods cannot be used on isolated plots or small fields. If these conditions are met, it is assumed that the flux measured just above the vegetation is equal to that at the ground or plant surfaces and fluxes are constant with height up to a level dependent on the extent of upwind surface homogeneity and atmospheric mixing.

The question of which method to use depends not only on the available resources but also crucially on the surface type over which the measurements are to be made (Moncrieff et al., 2000). For example, over very rough surfaces in an aerodynamic sense such as forests, gradients of scalars are small, and their measurement places extreme emphasis on the precision of sensors. Under these conditions, gradient techniques are problematic. On the other hand, as turbulence is enhanced over forests, the eddy covariance technique is made easier as the size of the fluctuations in vertical windspeed and other atmospheric properties is increased. Measurements over smooth surfaces such as water or ice are difficult using any of the techniques mentioned. Increasingly, eddy covariance-based systems are being integrated into global observing networks both to monitor carbon and water exchange on the global scale and to validate remotely sensed products such as fraction photosynthetically active radiation (FPAR) and normalized difference vegetation index (NDVI) both of which can be used to estimate

leaf area index, which in turn can be used to model NEE (Running et al., 1998).

A. Aerodynamic Gradient Method

The vertical exchange of atmospheric entities such as momentum, temperature, water vapor, and CO_2 by turbulent transport is driven by and is proportional to their vertical concentration gradients. We can describe the transport process in a flux-gradient form which defines the constant of proportionality K known as an eddy diffusivity. In generic form, the flux density (F_x, the amount of that entity transported vertically through unit area in unit time) of any scalar (X) is

$$F_x = -K_x \frac{dX}{dz}$$

The eddy diffusivities for scalars such as temperature, water vapor, and CO_2 have been the subject of much experimentation over several decades, as their relative magnitudes depend on both surface and atmospheric features. In practice, the diffusivities are related to the eddy diffusivity for momentum, which can be established from profiles of wind speed. Wind profiles are used to calculate the friction velocity, a measure of the degree of atmospheric mixing (Thom, 1975) and from which we find

$$K_x = ku^*(z - d)$$

where k is von Karman's constant (0.40), u^* is the friction velocity (m s^{-1}), z is height of measurement (m), and d is zero-plane displacement (m).

The gradients of the scalar in question need to be precisely determined, and obtaining accurate gradients over rough vegetation can be difficult because of the substantial degree of atmospheric mixing over such canopies (McNeil and Shuttleworth, 1975). One of the concerns about the aerodynamic technique is that a number of empirical corrections are required to account for changes in atmospheric stability (which influences the shape of wind profiles). A number of semiempirical formulae have been extensively investigated and are well accepted (e.g., Webb, 1970; Paulson, 1970). The aerodynamic technique has been used extensively in the past to obtain fluxes of sensible and latent heat over forests (e.g., Thom, 1975; Lindroth, 1984) and extended to other trace gas species over different surface types (e.g., Fowler and Unsworth, 1979; Sutton et al., 1993). It is not possible to use the aerodynamic technique in the roughness sublayer or

within the canopy as the variation in sources and sinks for heat, water vapor, and carbon dioxide invalidates the underlying assumptions in the method (Raupach and Legg, 1984).

B. Energy Balance/Bowen Ratio Method

The energy balance at the surface is

$$R_n - G - S = H + LE$$

where R_n is net radiation absorbed by the vegetation, G is soil heat flux, and S is heat stored in the vegetation. The ratio of sensible (H) to latent heat (LE) flux is known as the Bowen ratio (β), and by writing the fluxes in their flux-gradient form, an equation can be found that permits either flux to be found from measurements of the gradient of temperature (T) and humidity (e), irrespective of atmospheric stability:

$$\beta = \frac{1}{\gamma} \frac{dT}{de}$$

where γ is the psychrometric constant (Monteith and Unsworth, 1990). Once β has been obtained, substituting for LE and H we find

$$H = \frac{R_n - G - S}{1 + \beta^{-1}}$$

and

$$LE = \frac{R_n - G - S}{1 + \beta}$$

This method can also be used to measure fluxes of other gases or pollutants by writing a more generalized form of the flux-gradient equation by combining H and LE as before to yield

$$R_n - G - S = K\rho c_p \frac{dT_e}{dz}$$

where K is an eddy diffusivity assumed equal for all entities (other than momentum) and T_e is the equivalent temperature ($T + e/\gamma$) (Monteith and

Marcel Dekker, Inc.
270 Madison Avenue, New York, New York 10016

Unsworth, 1990). If all pollutants and gases share this value of *K*, then the flux density for any scalar, as determined by the energy balance method, can be written as

$$F_x = (R_n - G - S)\frac{dx}{dT_e}$$

The gradient for any gas *x* can be found by plotting the concentration of *x* in air against T_e at the same height for a number of measurement levels. The available energy ($R_n - G - S$) can be found using net radiometers, and soil heat flux plates, and from profiles of temperature within the canopy.

The technique is reliable in most conditions, but when the available energy becomes small, e.g., at night, or the gradients are small, as over rough vegetation, then large errors can occur. Also the method involves measuring *G* and *S*, which poses problems. In low-windspeed conditions, where the aerodynamic method fails because of the stalling of anemometers, the Bowen ratio method works well. The Bowen ratio method can also be used in the roughness sublayer because it only requires the assumption of equality between the eddy diffusivities for sensible heat and water vapor, i.e., there is no need for stability factors invoking similarity with K_M as are needed with the aerodynamic method (Lenschow, 1995).

C. Eddy Covariance

The eddy covariance technique measures the flux of a scalar (heat, mass) or momentum at a point centered on instruments placed at some height above the surface. The principal instruments are (a) a fast gas analyzer, with a response time < 0.1 s, and (b) a sonic anemometer capable of measuring the three-dimensional components of the wind and with a similar time resolution to the gas analyzer. For these measurements to be identical to the flux at the underlying surface, the instruments must be located in the internal boundary layer where the flux is constant with height. Figure 4 shows a typical time series of the turbulent signals of vertical wind speed and CO_2 measured over a forest. We can split any of the turbulent signals into a mean and δ fluctuating part, in the form of a Reynold's decomposition. Thus, for vertical wind speed, the instantaneous value (*w*) is a function of both the long-term mean value ($\overline{w}$) and the instantaneous difference (w′) between that value and $\overline{w}$, i.e., $w = \overline{w} + w'$. We can write the signal for the scalar density in the same format, $\rho_c = \overline{\rho_c} + \rho'_c$. The vertical transfer

Marcel Dekker, Inc.
270 Madison Avenue, New York, New York 10016

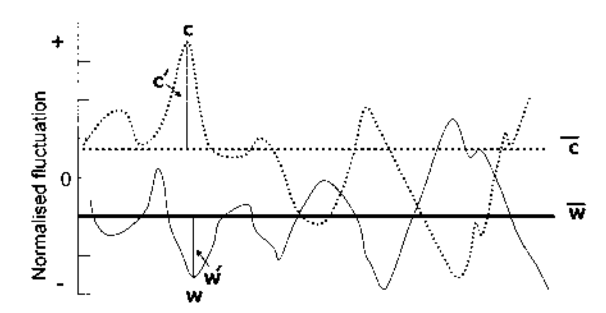


Figure 4 A schematic of the eddy covariance method. The turbulent signals of the instantaneous concentration of a scalar, *c* and the instantaneous vertical wind speed, *w* are shown. Mean values of these quantities over a time period, typically 10–30 min, are indicated by an overbar. Fluctuations from the mean are indicated by a prime.

of the scalar is simply the product of the two fluctuating terms w' and ρ_c' averaged over a suitable interval of time (usually 10–30 min).

$$F_c = \overline{w'\rho_c'} + \text{corrections}$$

where F_c is the eddy flux of a scalar such as carbon dioxide. There are many papers that discuss the "correction" terms in detail, so we will not be concerned with such detail here. Good detailed reviews of eddy covariance appear in Aubinet et al. (2000) and Baldocchi (2003).

Eddy covariance instrumentation is usually placed at some distance above the source of trace gas so the storage of that gas below the instruments must be considered. This is particularly important during stable atmospheric conditions, usually at night, when turbulent mixing is light or nonexistent; gas effluxing from the soil below a canopy, for instance, may be stored in the canopy below the instruments. The contribution to the total flux from storage is

$$F - \int_0^z \frac{\partial \bar{s}}{\partial t}\, \partial z$$

This term represents the change in storage of scalar s in the air mass between the surface and the height z. Baldocchi et al. (1988) showed that these errors are generally small during the day but can be significant at dusk, overnight, and at dawn, when turbulent mixing is low; this is particularly relevant to flux measurements over forests and less of a problem over agricultural sites. The equation for eddy flux above shows that we must have instruments

that can sample vertical wind speeds and scalar concentrations and be able either to perform real-time analysis, in which means are subtracted from raw data to yield the fluctuating components from which cross products are formed, or to store all the raw data for later processing in the laboratory. Figure 5 shows the components of a typical eddy covariance system. A sonic anemometer above the canopy measures the turbulent fluxes of horizontal and vertical wind speeds. Air is sucked down an inlet tube near the sonic head to a fast-responding infrared gas analyzer at the base of the tower. The expanded schematic shows the gas path within the gas analyzer. A mass flow controller and pressure transducer can be used to maintain a constant rate of flow down the sample tube (and hence constant lag of gas sample between the sonic head and the optical bench of the IRGA). Gas concentrations in the sample cell are measured relative to a reference cell in which the air has been dried and scrubbed of carbon dioxide and water vapour.

The size of the storage correction can be small or negligible during the day, but in tall vegetation such as forests, it can be substantial at night. A correction term for nonzero mean velocity or convergence arises at even seemingly ideal field sites for micrometeorology. Atmospheric subsidence is common in highly convective conditions and in synoptic-scale subsidence; local circulations such as lake breezes (Sun et al., 1998) and katabatic drainage even on slopes as little as 1 : 1000 can induce a nonzero mean vertical velocity, as drainage flow on a slope is compensated for by a descending motion. According to Lee (1998), a mean vertical velocity of 3 $cm\,s^{-1}$ could be generated on a slope of only 1°. The implications for long-term flux measurement over a forest site of a trace gas such as CO_2 are important. Lee (1998) showed that the mass flow mechanism may contribute as much as 12 $\mu mol\,m^{-2}\,s^{-1}$ with a mean vertical velocity of only 0.5 $cm\,s^{-1}$. He also gives the example of a typical flux site with a slope of 1°, which induced a mean vertical velocity at night of 1 $cm\,s^{-1}$, sufficient to induce a mass flux that was twice the size of the measured eddy flux. As Lindroth et al. (1998) point out, for their long-term flux site in an old-growth spruce plantation in Sweden, a 1 $\mu mol\,m^{-2}\,s^{-1}$ bias averaged over 12 h per day for 365 days would be equivalent to 200 $g\,C\,m^{-2}\,y^{-1}$ and large enough to change the sign of the net carbon flux over this period. Since the size of the correction term is proportional to height, the problem is not so large over short canopies such as cereals.

The instruments used in the eddy covariance method are now sufficiently robust, reliable, and waterproof that they can be used to measure surface fluxes for extended periods of time. Figure 6 shows CO_2 fluxes for five years from 1997 at a forest in the Highlands of Scotland. Photosynthesis dominates over respiration (the heavy black line represents 0 flux) during the summer months, but even in the winter there are periods

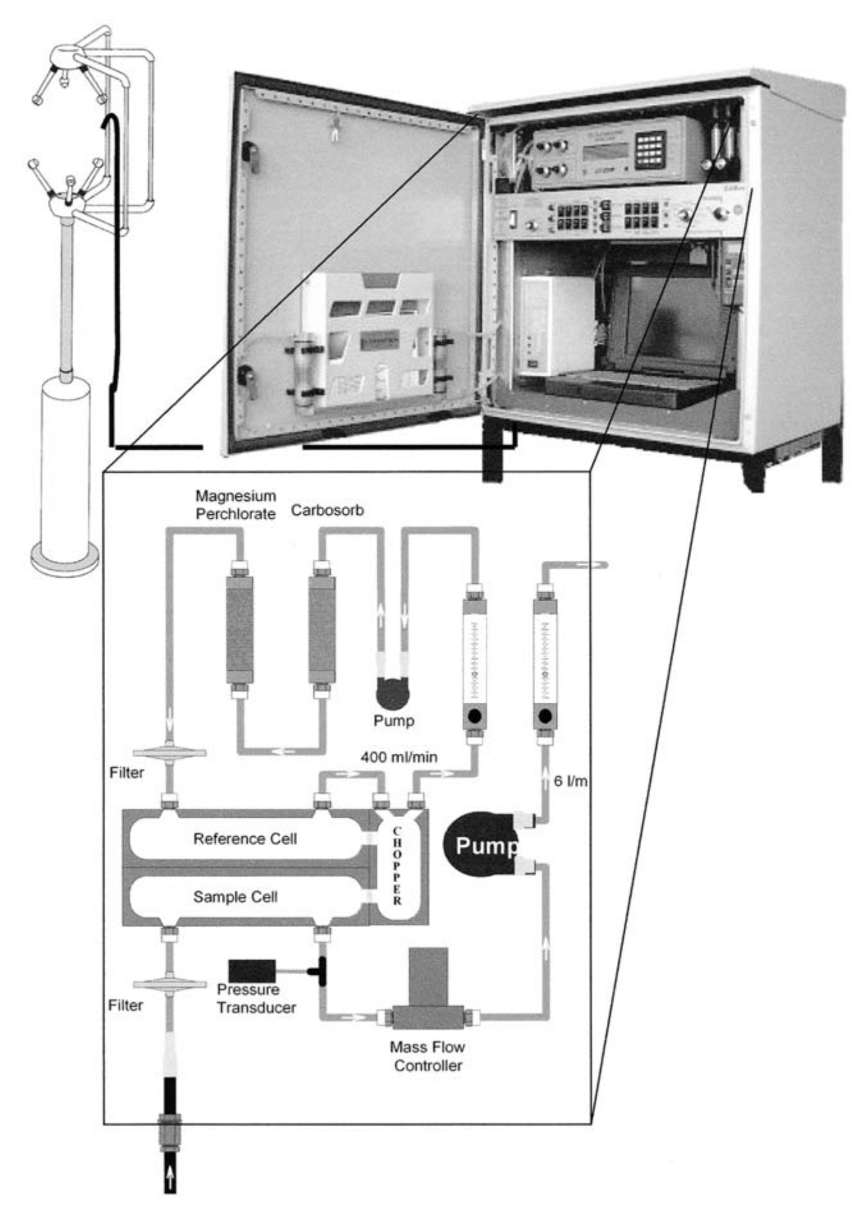


Figure 5 A schematic of a typical eddy covariance system.

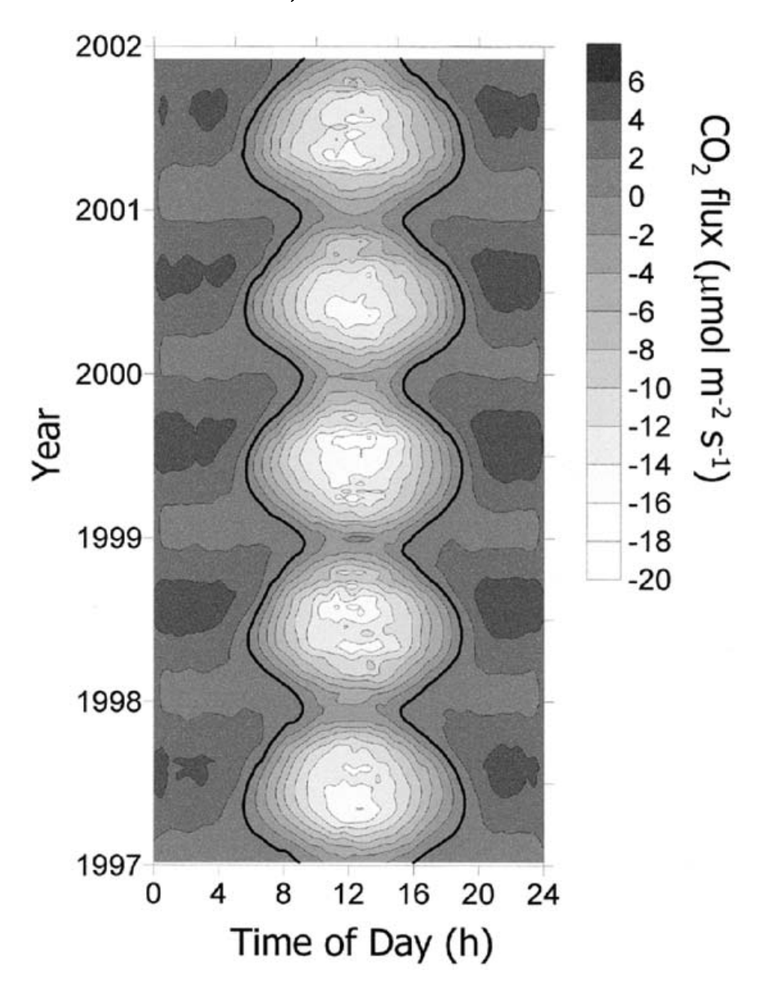


Figure 6 CO_2 flux from Griffin Forest, Scotland, 1997–2001.

during the day when C is being fixed by the canopy. Data such as shown in Fig. 6 can be used to estimate the total C sequestered by forests over long periods of time (in this instance, typical rates of sequestration averaged over the five years are about 6.5 t C ha^{-1} yr^{-1}). The accuracy of such long-term results is difficult to judge, at least for trace gases, since there is no other check against which to compare the measurements. One accepted method is to check whether the other instruments usually deployed as part of the same micrometeorological experiment achieve energy balance, i.e., whether the sum of available energy [net radiation (R_n) minus heat taken up by the soil

Marcel Dekker, Inc.
270 Madison Avenue, New York, New York 10016

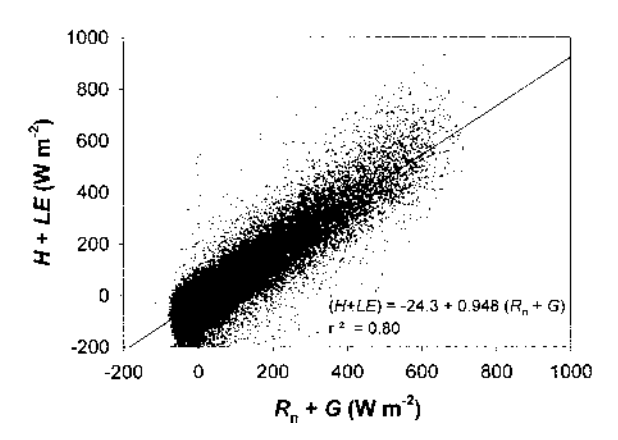


Figure 7 Energy balance closure at Griffin Forest, Scotland, 1997–2001.

(G)] balances the losses of energy through sensible (H) and latent heating (LE) of the air). Figure 7 shows results from the same forest as shown in Fig. 6 and for the same period, but for energy balance closure. The data show that about 95% of the energy was accounted for by the instruments and analysis used to obtain H and LE (also by eddy covariance), thus suggesting that the CO_2 flux data should have been calculated to a similar level of accuracy (Moncrieff et al., 1996).

D. Relaxed Eddy Accumulation

Relaxed eddy accumulation (REA), also known as conditional sampling, is a conceptually simple micrometeorological technique in which air is sampled into one of two sampling reservoirs (or sampling lines for on-line analysis), according to whether an up- or a down-draught of air is measured simultaneously by a sonic anemometer. After a suitable interval of time, say 30–60 min, the net vertical flux of the trace gas species of interest is proportional to the difference in gas concentration between the sampling reservoirs. The method is attractive, as it can be used for trace gases or pollutants for which no suitable fast-response sensor is available and hence the alternative technique of eddy covariance is unsuitable (e.g., Majewski et al., 1993). The requirement for a fast sensor to measure vertical wind speed remains, but there is considerable relaxation in the speed requirement for the chemical analyzer. A further advantage is that by accumulating gas into reservoirs, the difference in concentration between the samples is enhanced, and it is then possible to use high-precision gas analyses in the laboratory to determine the differences (Businger and Delaney, 1990).

Marcel Dekker, Inc.
270 Madison Avenue, New York, New York 10016

Early studies using eddy accumulation sampled air at a rate proportional to the magnitude of the vertical wind speed, but this was technically difficult to achieve with the required accuracy (Desjardins, 1977). Hicks and McMillen (1984) suggested, almost as an aside, that the simpler method of sampling air at a constant rate into either bag might work, and with fewer practical difficulties. One bag will then contain air collected in updraughts and the concentration of CO_2, say, will be c^+; the downdraught bag will have a CO_2 concentration of c^-. The idea was taken up by Businger and Oncley (1990) who wrote the flux (F_c) for a gas with concentration c, as

$$F_c = \beta\sigma_w(c^+ - c^-)$$

where β is an empirical coefficient usually determined by experiment, σ_w is the standard deviation of the vertical windspeed, and $(c^+ - c^-)$ is the gas concentration difference between the two sampling bags at the end of the sampling period. As Businger and Oncley pointed out, the measurement of $(c^+ - c^-)$ is a direct difference of concentration not weighted by the magnitude of vertical wind speed in the original method. Thus in this variant of the method they *relax* the conditions for the original eddy accumulation and the method is based simply on sampling air into different reservoirs on the condition of either upward or downward moving air. The technique is known equally as conditional sampling or relaxed eddy accumulation (CS/REA). Figure 8 shows a schematic of a typical conditional sampling system in which fluxes of CH_4 were routinely monitored on-line. In this representation, the system is set up to measure simultaneous fluxes of methane and nitrous oxide. The vertical wind speed is measured by a sonic anemometer (center left of the diagram) and, dependent on whether an updraught or a downdraught has been measured, the appropriate sample valve is opened and air is sucked into a reservoir or passed into a gas analyzer. Further details of the systems shown here can be found in Beverland et al., 1996. (The tunable diode laser in Fig. 8 is operating as part of a ducted eddy covariance system.) In general, the CS/REA method has been well validated over the past few years, although for fluxes of CO_2 and water vapor, eddy covariance remains the more appropriate choice (Pattey et al., 1992; Oncley et al., 1993). Conditional sampling has a role in measuring fluxes of biogenic compounds and other trace gases for which suitable eddy covariance sensors either do not exist, e.g., nonmethane hydrocarbons (Moncrieff et al., 1998; Christensen, 2000) and herbicides (Pattey et al., 1995) or are very expensive and complex, e.g., for N_2O and CH_4 by tunable diode lasers (see Sec. IV.D). The use of the semiempirical

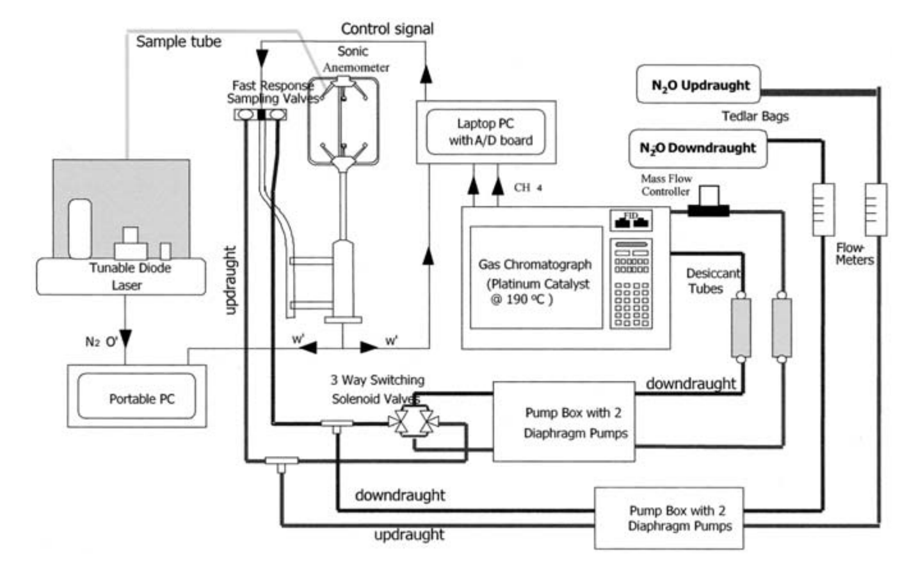


Figure 8 A schematic of a conditional sampling system.

beta factor worried some researchers, but it has since been put on a much sounder footing by its interpretation with the statistics of turbulence (Milne et al., 1999; Baker, 2000).

E. Hyperbolic REA

An interesting development of the REA technique has been made by Bowling et al. (1999b), in which the usual vertical wind speed threshold used to open and close the sampling valves is increased, effectively permitting the system to collect only the strongest updraughts and downdraughts that contribute to the flux. The threshold is defined as a ‘‘hyperbolic hole’’ (*H*) and can be written as

$$H = \left| \frac{w'}{\sigma_w} \frac{c'}{\sigma_c} \right|$$

where w' and c' are the turbulent fluctuations of vertical wind speed and CO_2 concentration, respectively, and σ_w and σ_c are the standard deviations of vertical wind speed and CO_2 concentration, respectively. A hole size is

Marcel Dekker, Inc.
270 Madison Avenue, New York, New York 10016

decided upon before sampling begins, and the sampling valves are only energized when

$$\left|\frac{w'}{\sigma_w}\frac{c'}{\sigma_c}\right| > H.$$

The advantage of this method is that differences in scalar concentration are maximized, thus increasing the likelihood of achieving a resolvable difference between the up- and the down-sampling reservoirs. It is necessary to obtain information on the scalar independently of the REA method, e.g., c' (or a similar scalar with similar probability distribution) could be obtained by simultaneous measurements by eddy covariance. Wichura et al. (2000) have shown how to use hyperbolic REA to measure fluxes of the stable isotope ^{13}C over a spruce forest.

F. Mass Balance Method

The mass balance method is well named, since it involves accounting for the mass of material leaving a well-defined volume through any of its sides. Material emitted at the surface, for example CH_4 by ruminant animals within the volume, will be carried by the turbulent wind outwith the volume; in the mass balance method, the wind speed is measured at the same heights as the concentration of the gas species of interest, since the net horizontal flux density of a gas, q, is the time mean of the product of the instantaneous wind speed, u, and gas density ρ_g (Denmead et al., 1998), i.e., $q = \overline{u\rho_g}$. Figure 9 shows an open enclosure that could be used to measure the gaseous emission from sheep. The "fence" enclosing the plot is made from sample tube; air can be drawn from any or all of the sides to gas analyzers. The difference between the upwind and the downwind concentrations of the relevant trace gas will show the extent by which the trace gas concentration has been enriched by addition from the animals.

The mean emission rate ($\overline{F}$) of gas from the volume is:

$$\overline{F} = X\int_0^z [\overline{U}_z(\langle\overline{\rho}_{g4,z}\rangle - \langle\overline{\rho}_{g2,z}\rangle) + \overline{V}_z(\langle\overline{\rho}_{g3,z}\rangle - \langle\overline{\rho}_{g1,z}\rangle)]\,dz$$

X is horizontal distance, z is height; the boundaries of the volume are 1–4 with boundaries 1 and 2 being upwind, 3 and 4 downwind; U is the vector wind normal to horizontal boundaries 2 and 4; V is the vector wind normal to boundaries 1 and 3. Time averages are indicated by an overbar, and thus $\bar{\rho}_{g4,z}$ is for example, the gas density at height z on boundary 4. This equation

Marcel Dekker, Inc.
270 Madison Avenue, New York, New York 10016

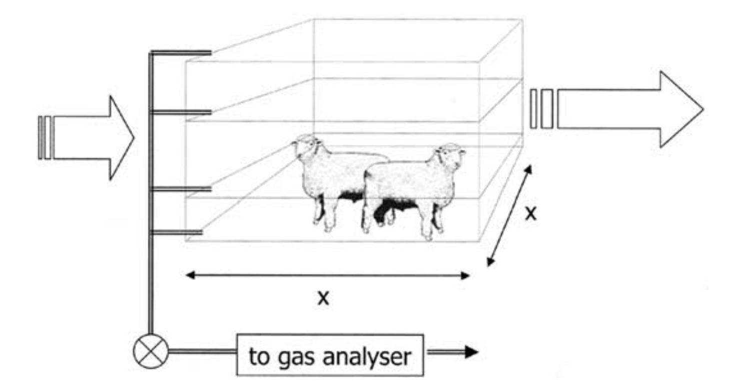


Figure 9 The mass balance method in a configuration that could be used to measure gaseous exchange from ruminant animals. The "box" as shown is made from sample lines, with each of the four sides being composed of a number of sample lines arranged vertically. Inlets are arranged at various points along each side of the box and at each of the different heights.

is integrated numerically (Denmead et al., 1998). The advantage of the mass balance approach is that it can be used on small patches or plots and does not disturb the emission process. The disadvantages are that several gas analyzers may be required, and these analyzers need to have a high precision to measure the small differences in concentration across the boundaries of the volume. Denmead et al. (1998) also noted that the temporal variation can be high even in apparently steady flux conditions; and that in light winds when the wind direction can also be variable, uncertainties arise. In a later paper, Denmead et al. (2000) tested the mass balance method on fluxes of N_2O from grazed pasture and found that, even with the inherent limitations of the technique, it gave more reliable measurements over a short experimental study than conventional micrometeorological methods.

G. Boundary Layer Budget Methods

1. Convective Boundary Layer (CBL)

Eddy covariance sensors can be adapted for flight on-board aircraft and flown through the ABL at heights of 100 m and more. When such measurements are made in conjunction with tower-based flux estimates, much of the difference in flux estimates comes down to differences in flux footprint, as seen by the different systems (Desjardins et al., 1992). Aircraft-based techniques remain expensive to buy and maintain, and operate for

Marcel Dekker, Inc.
270 Madison Avenue, New York, New York 10016

only limited periods at a time. A more practical alternative is required that can be used by many research groups. One method currently being tested is a mass budget of the CBL, developed by Raupach et al. (1992). Under commonly encountered daytime conditions, a CBL is present over the surface of the earth. At the top of this layer is a temperature inversion, which effectively separates the air that has been influenced by the surface from the overlying air of the free atmosphere. Over the course of a day, the CBL grows from tens of meters in the early morning to a height of 1 to 3 km in the late afternoon, entraining air from the free atmosphere as it rises. As the photosynthetic rate increases with irradiance, the CO_2 concentration in the CBL is reduced below that in the free atmosphere above.

In principle, the CBL can be treated as a huge cuvette, in which the surface fluxes can be inferred from measured changes in CO_2 concentration and CBL height over time. The method is based on the conservation-of-mass equation for CO_2 in the *well-mixed* CBL, which can be written in integral form as

$$F_c = \frac{(\rho_2 h_2 + \rho W_t([t_2 - t_1])(C_t - C_{m2}) - \rho_2 h(C_t - C_{m1})}{t_2 - t_1}$$

where F_c is the flux of CO_2 integrated between time t_1 and t_2, ρ is air density averaged over the CBL, h is the height of the CBL, W_t is the vertical velocity above the CBL, and C_m and C_t are the CO_2 concentrations in the mixed layer of the CBL and the free troposphere above, respectively. The above equation yields cumulative surface fluxes representing the area traversed by a column of air in the course of a day, and so it may extend a few hundred kilometers upwind and cover an area of 1000 to 10,000 km^2 (Raupach et al., 1992).

The budget method requires an estimate of the CO_2 concentrations of the air that is entrained as the CBL grows over the day. Tropospheric values (C_t) may be estimated from oceanic sites. Also, if there is a significant residual layer in the morning, the concentration in this layer can be measured with tethered balloon-borne instruments. The budget method has been tested in a number of field experiments so far (Munley and Hipps, 1991; Denmead et al., 1996; Levy et al., 1998), generally with encouraging results.

Again, as with aircraft platforms, the flux obtained by this boundary-layer budget approach is unlikely to be exactly the same as that obtained by tower-based systems, because of the different source areas for the two fluxes. The height of the CBL can be monitored by a radiosonde system or modeled according to best practice. Vertical velocity (W_t) can also be obtained from

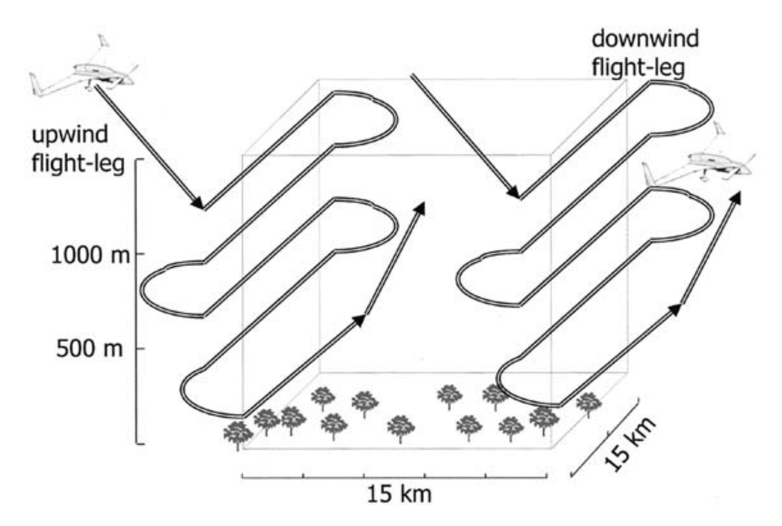


Figure 10 Mass balance obtained at a large scale by sampling by aircraft.

radiosonde data if it is assumed that horizontal divergence is constant with height or from operational analysis from major weather forecasting bureaux. Profiles of CO_2 concentration can be obtained either from balloon-borne systems or from tall towers. The method is sensitive to the value for C_t and this is best obtained with an aircraft-borne system.

An alternate method treats the atmosphere as a large mixing volume and measures the profiles of gas concentration (up to the height of the mixed layer) moving in and out of this large volume (Fig. 10). This requires aircraft sampling and hence is expensive and noncontinuous and can only be used in appropriate conditions. Nonetheless, it has been used to produce inventories of greenhouse gases on a regional scale for Kyoto inventory purposes (e.g., Gallagher et al., 1994). This top-down approach has been used to estimate methane fluxes from agriculture in New Zealand that agree well with per-animal emission factors obtained from a bottom-up approach (Wratt et al., 2001).

2. Nocturnal Boundary Layer Budgets

On a smaller scale, and with fewer resources required than in the CBL method, the budget of trace gases can be measured in the air layer trapped below a nocturnal inversion. The surface flux of a gas (F_c) such as methane or CO_2 in this method is obtained by measuring the time rate of change of

Marcel Dekker, Inc.
270 Madison Avenue, New York, New York 10016

concentration C, at several heights, up to the top of the nocturnal inversion, Z_i (Eugster and Siegrist, 2000):

$$F_c = \int_0^{z_i} \frac{\partial C}{\partial t} dz + A_c$$

where A_c is the height integrated horizontal flux divergence and should be negligible; t is time. Z_i can be determined as the height at which the gradient of potential temperature or gas concentration goes to zero. Pattey et al. (2002) deployed such a system over agricultural crops for several field seasons in Canada and obtained good agreement between this method and data from a concurrent study using eddy covariance. This is important given that obtaining believable fluxes by eddy covariance at night, when windspeeds can be low, can be difficult. In Pattey et al.'s study, some two-thirds of the summer nights of the campaign were classified as calm; in any one night, about the same proportion of 30-min periods were also classified as calm. Using the NBL budget method as an alternative to the procedure whereby eddy covariance data is replaced by empirical relationships based on soil respiration and temperature when the wind is light, is to be welcomed. Kelliher et al. (2002) used the nocturnal budget method to determine fluxes of nitrous oxide from grazed pasture in New Zealand.

IV. INSTRUMENTATION

A. Sonic Anemometer

A typical ultrasonic anemometer used in eddy covariance systems is a three-axis design, manufactured by Gill Instruments (Fig. 11, Solent A1012R3, Gill Instruments, Lymington, U.K.). The instrument is fully waterproof, consumes < 300 mA at 12 V D.C., and can operate at windspeeds up to 60 m s^{-1}. The time-of-flight principle is employed to produce u, v, w, and the speed of sound (which is used to calculate the virtual temperature). A pair of transducers acts alternately as receiver/transmitter of ultrasound. Let t_1 be the time taken for a sound pulse to be sent in one direction along transducer axis 1, and be received, and t_2 the time taken in the opposite direction.

$$t_1 = \frac{d}{c_s + v_1}$$

Marcel Dekker, Inc.
270 Madison Avenue, New York, New York 10016

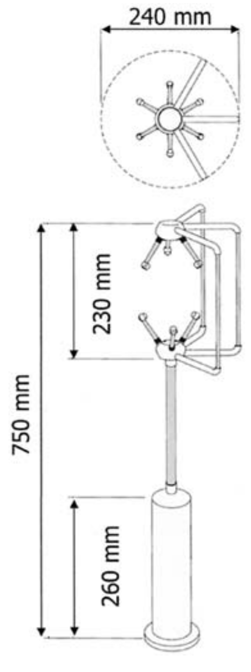


Figure 11 A sonic anemometer. (Model A1012R3, Gill Instruments, Lymington, Southampton, U.K.)

and

$$t_2 = \frac{d}{c_s - v_1}$$

where v_1 is the wind speed along axis 1, c_s is the speed of sound in still air; d is the distance between the transducers. By subtraction of the two sampling times

$$v_1 = \frac{1/t_1 - 1/t_2}{2}.$$

This is repeated for the other two pairs of transducers (subscripts 2 and 3) arranged nonorthogonally to yield the three nonorthogonal components of the wind, i.e., v_1, v_2 and v_3. A vector transformation converts these nonorthogonal wind speeds into the orthogonal components u, v, and w, where u and v are the horizontal components of the wind speed and

w is the vertical wind speed. Sets of these alternate transmissions are made between each pair of transducers at a rate of 100 Hz, producing an accuracy of 1 $cm\,s^{-1}$ in horizontal and vertical components and the speed of sound. The virtual temperature is also obtained from the transit time of the ultrasonic pulses (Kaimal and Businger, 1963; Kaimal and Gaynor, 1991) using the relation

$$c_s^2 = 403 T_{air}\left(1 + 0.32\,\frac{e}{p}\right)$$

where T_{air} is absolute air temperature, e is the vapor pressure of water in air, and p is the absolute atmospheric pressure. A sonic temperature (T_s) is defined as

$$T_s = \frac{c_s^2}{403} = T_{air}\left(1 + 0.32\,\frac{e}{p}\right)$$

According to Stull (1988), the sonic temperature is close to the virtual or potential temperature (θ), and true temperature can be obtained if there are simultaneous measurements of humidity and atmospheric pressure:

$$\theta = T_{air}\left(1 + 0.38\,\frac{e}{p}\right)$$

Using the sonic virtual temperature for the calculation of sensible heat flux will be adequate under most conditions. At high wind speeds there are additional errors due to wind speed and momentum stress that need to be considered (Schotanus et al., 1983). Some sonic anemometers have built in analog-to-digital converters, and so signals from auxiliary instruments such as gas analyzers can be digitized along with the turbulence data and sent to a logger for analysis. This has the advantage not only of reducing costs but also of improving the synchronization of the signals that are required in eddy covariance.

B. Infrared Gas Analyzer

A common gas analyzer used in eddy covariance is the LI-COR 7000 model (LI-COR, Lincoln, NB, Fig. 12), which measures CO_2 and H_2O in air with a quoted cutoff frequency of 5 Hz. This is a differential nondispersive infrared gas analyzer with solid-state detectors. Crucially for eddy covariance work, flow rates as high as 10 $L\,min^{-1}$ can be maintained in the optical cell, thus

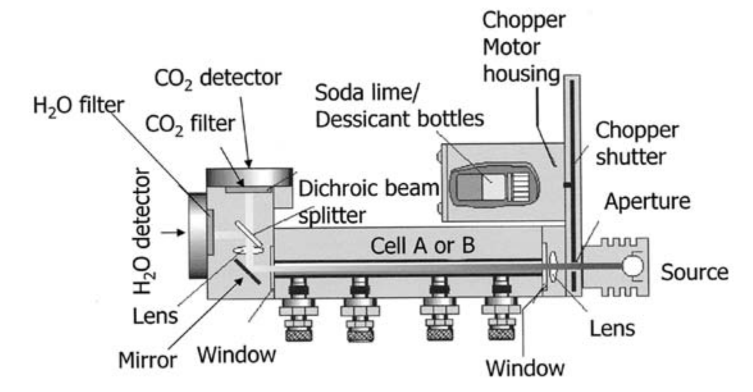


Figure 12 An infrared gas analyzer in the ‘‘closed-path’’ mode. (Model Li-7000, LI-COR, Lincoln, NB.)

ensuring a rapid response to turbulent eddies carrying carbon dioxide and water vapor. Output from the RS232 port can be up to 20 Hz. Software on the IRGA can be used to correct CO_2 measurements for water vapor dilution and band-broadening effects. Changes in barometric pressure affect the analyzer span, but this can be corrected for in software by continuous measurement of the pressure in the atmosphere and the sample tube of the analyzer. Changes in instrument temperature affect zero drift. Power consumption of this IRGA is 15–40 W at 12 V DC dependent on temperature and pump configuration. IRGA systems are also described in Chap. 10.

The type of analyzer described in the previous paragraph is operated in the closed-path mode, in which air is brought to the optical bench via a tube whose entrance is close to the sampling volume of the sonic anemometer. This arrangement works well in all weather conditions, albeit at the expense of some loss of resolution of high-frequency components of the signal as the sampled air passes down the tube and through the complex ‘‘plumbing’’ that precedes entry into the analyzer; such practical problems are well known and can be easily accounted for, however (Moncrieff et al., 1997). It is also possible to operate an infrared gas analyzer in the open-path mode (Fig. 13), where the path between the detector and the source is exposed only to the atmosphere. Such an arrangement is clearly simpler to operate and avoids the pumps and plumbing of the closed-path systems. An open-path analyzer such as the LI-7500 can also measure fluctuations in atmospheric CO_2 and water vapor concentrations at frequencies up to 20 Hz and this particular model consumes only about 10 W. One problem with such open-path sensors is that raindrops on the lenses and falling through the path can cause their performance to deteriorate, and it is not usual to find such gas analyzers at long-term sites which have frequent

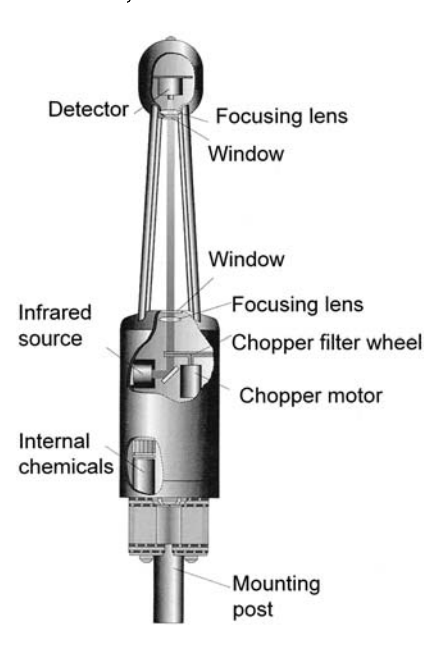


Figure 13 An infrared gas analyzer in the "open-path" mode. (Model Li-7500, LI-COR, Lincoln, NB.)

rainfall. In the wetter parts of the U.K., for instance, the closed-path gas analyzer would give a more continuous record of flux.

Figure 5 depicts the air circuit part of a typical closed-path eddy covariance system, with air being drawn through the analyzer by a pump at the end of the sampling line (Moncrieff et al., 1997). The material of the sample tube (Dekabon) does not interact with CO_2 or water vapor. Tube diameter affects flow rate, pressure drop, and the energy required to draw air through the system. More importantly, the internal diameter of the tubing can be chosen to ensure either turbulent or laminar flow (Leuning and Moncrieff, 1990). The mass flow controller maintains the flow rate in the tube within a small range and thus ensures that the time of travel for any air sample remains nearly constant.

C. Fourier Transform Infrared (FTIR) Spectroscopy

The principle of infrared spectroscopy to identify the concentration of trace gases (see Chap. 10) has been extended with the now routine calculation of the absorption spectra by Fourier transforms of the interference pattern

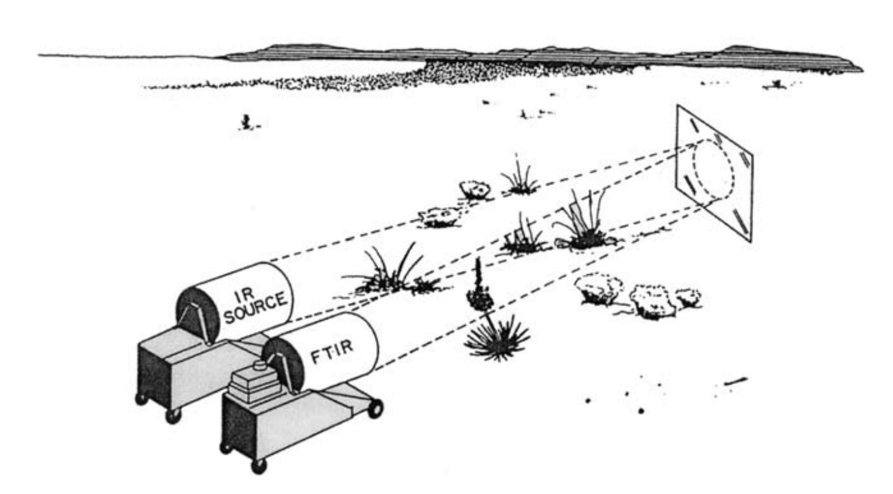


Figure 14 A schematic of a Fourier-transform infrared (FTIR) spectrometer in the field.

generated in an instrument. By setting a source of infrared energy at some distance from a receiver, the path-averaged concentration of various trace gases can be obtained. FTIR instruments can therefore be used to make measurements in the scale gap between those for which chambers and eddy covariance methods, respectively, are suitable.

FTIR has been used in two different modes to obtain fluxes over long path lengths. FTIR can simultaneously measure concentrations of CO_2, N_2O, CH_4, CO, and H_2O (Galle et al., 1994). One method will set the FTIR source to focus on a remote target, several tens of meters from the source. The infrared beam will be reflected back to the detector (Fig. 14, Gosz et al., 1988). Kelliher et al. (2002) used FTIR in the nocturnal boundary layer to measure simultaneous fluxes of CO_2 and N_2O from grazed pasture. Their path length was 97 m, and they estimated a precision of 1% for averages obtained over 3 min. Since FTIR will give *concentration* when *flux* is required, they used simultaneous CO_2 soil efflux measurements together with the ratio of CO_2 to N_2O concentration to obtain the flux of N_2O.

FTIR is also used with the aerodynamic gradient method to obtain fluxes. Griffith et al. (2002) developed a system that was fully automated, and they report a precision of 0.1 to 0.2% over a period of several weeks. They sampled air at a number of heights above the ground to 22 m over a lucerne pasture and used their FTIR spectrometer as a high precision analyzer, achieving a measurement precision (defined as the standard deviation of repeated measurements) of 0.71 ppmv for CO_2, 0.19 ppbv for

Marcel Dekker, Inc.
270 Madison Avenue, New York, New York 10016

N_2O, and 1.6 ppbv for CH_4. Griffith and Galle (2000) also report using the flux-gradient technique with a FTIR spectrometer to obtain fluxes of NH_3 over a young wheat crop.

D. Tunable Diode Lasers (TDL)

TDLs also use infrared absorption spectroscopy (as in FTIR) but scan the output wavelength of a tuned diode laser over a single isolated absorption line of the target gas (Zahniser et al., 1995). Some TDLs can measure trace gases that have absorption lines in the 1–11 μm range, e.g., nitrous oxide (Wienhold et al., 1994; Laville et al., 1999), methane (Simpson et al., 1995), ammonia (Leuning et al., 2000) and others (Wagner-Riddle et al., 1996). The TDLs are typically field-portable but require the diode laser to be cooled to temperatures approaching 80 K and hence require cryocooling by liquid nitrogen (Fig. 15). They can be used in eddy covariance work, as they have typical sampling rates of 10 Hz, but they have also been deployed in gradient studies via control switches to sample air from different heights. The measurement specifications of one of these instruments, the TGA100 (Campbell Scientific, Logan, Utah) illustrate their performance. They are as follows:

Sample rate: 10 Hz
Averaging period: 0.1 s
Frequency response (@ 4 L/s flow rate): 1.6 Hz
Noise (0.01 to 5 Hz bandwidth: 1.5 ppbv (N_2O), 7 ppbv (CH_4), 2 ppbv (NH_3)
Gradient resolution (30 min averaging time): 0.03 ppbv (N_2O), 0.15 ppbv (CH_4), 0.06 ppbv (NH_3)
(*Source*: http://www.campbellsci.com/tga.html)

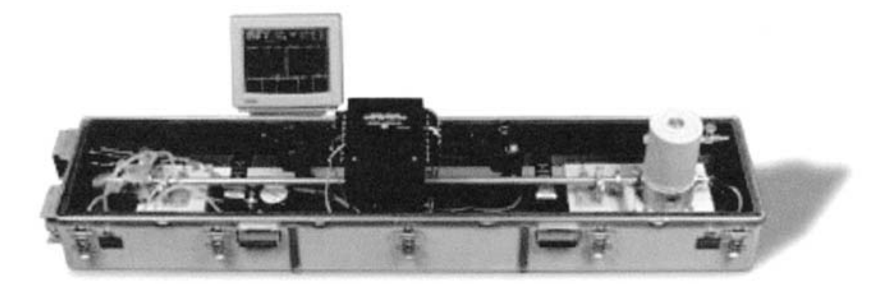


Figure 15 A tunable diode laser, TDL. (Model TGA, Campbell Scientific Inc., Logan, UT.)

E. Scintillometers

Scintillometers have been used to study the fundamental properties of atmospheric turbulence in the lower boundary layer. Scintillometers use a transmitter-receiver pair operating at optical or radio wavelengths to sense the change in radiation caused by refractive scattering of turbulent eddies in the scintillometer path. Fluctuations in the observed intensity are related to changes in refractive index along the path of the scintillometer and changes in refractive index can be related to changes in temperature, water vapor or momentum along the path. By careful choice of wavelength, and with an analysis rooted in classical turbulence theory, scintillometers can measure fluxes of sensible and latent heat and momentum. This latter point is relevant in the context of this book, given that classical turbulence theory was derived for homogeneous surfaces yet most agricultural landscapes are usually quite heterogeneous over the scales of interest (up to several km in horizontal extent). De Bruin (2002) introduces recent experimental evidence that scintillometers may be used in most real-world situations (e.g., Meijninger et al., 2002). One promising avenue for scintillometers is for them to be deployed in complex terrain where conventional surface-layer micrometeorological methods such as eddy covariance cannot be applied, since the theory they are based on is violated. Scintillometers can be set up on either side of a valley, for instance, to measure turbulent properties (and possibly fluxes) in the valley (Poggio et al., 2000).

V. CONCLUSIONS

There is often great spatial and temporal variability in emissions of gases such as N_2O and CH_4 from such environments as agricultural fields, forests, and wetlands. Methods to quantify the fluxes of these gases (which can integrate over the landscape at the plot-to-landscape scales), can be used to complement the more intensive chamber measurements that often accompany them in the field. Some micrometeorological methods have been in use for a few decades, and their potential and their difficulties are well known. Methods such as gradient, energy balance, and eddy covariance have been widely applied to many of the biogenic trace gases of interest. The need to confirm or create emission factors for anthropogenic sources of these gases from agriculture, for example, has prompted the development of some novel micrometeorological methods such as mass balance and nocturnal budget methods (Denmead et al., 2000). Developments in theory combined with advances in high-precision gas analysis employing Fourier transform

infrared spectroscopy (FTIR) or tunable diode lasers (TDL) have further advanced our measurement capability. One final point is also apparent: the community of agricultural meteorologists, soil scientists, ecologists, and boundary-layer meteorologists realize that no one method or instrument is suitable for all purposes. Micrometeorological methods are but one part of a toolkit of methods that should be used and checked against other techniques and constrained against appropriate biophysical models of the landscape.

VI. GLOSSARY OF TECHNICAL TERMS

Atmospheric stability: A measure of the atmosphere's capacity to enhance or quash the vertical movement of air parcels. The atmosphere can be unstable, neutral or stable. During a summer's day for example, warm air rising (by free convection) will tend to enhance the vertical movement of air parcels and the atmosphere is said to be unstable. At night, free convection will be eliminated and in the absence of strong winds (so-called forced convection), vertical movement of air parcels will be considerably reduced; this will be a stable atmosphere. During a cloudy day or whenever the wind speed is strong, a neutral stability regime will exist.

Cuvette: Usually a small clear plastic enclosure that can be attached to the ground and which may enclose whole plants. Whole leaves or branches can be enclosed in appropriately sized cuvettes. Used in gas exchange studies to determine the physiological response of vegetation to environmental changes in air temperature, irradiance, vapor pressure deficit, etc.

Eddy diffusivity: A measure of the rate of exchange of material in the atmosphere by turbulent (or overturning) eddies. Has units of $m^2\,s^{-1}$ and is several orders of magnitude greater than molecular diffusivity, for example.

Eddy: A convenient term to describe a discrete parcel of air that is rotating above the surface of the Earth and carried along by the mean wind.

Fetch: Similar to footprint although generally restricted to one dimension only, i.e., the horizontal extent of the homogeneous vegetation upwind of the tower.

Flux Density: The rate of transfer of unit substance across unit area. In energy units for the transfer of sensible and latent heat ($J\,m^{-2}\,s^{-1}$), and mass units for a gas such as CO_2 ($\mu mol\,m^{-2}\,s^{-1}$).

Marcel Dekker, Inc.
270 Madison Avenue, New York, New York 10016

Footprint: The area upwind of a flux tower that contributes to the measured flux. Typically a footprint can be several hundred meters to a few km in horizontal extent and a few tens of meters to hundreds of meters wide at its widest point. Can be thought of as a ‘‘field of view’’ of a turbulent flux measurement.

Friction velocity: A measure of the rate at which momentum is brought down to the earth’s surface by the action of turbulent eddies.

Gaussian plume: The concentration of a gas in a plume after it is released from, say, a chimney, along a cross-section either in the horizontal or vertical dimension, has a normal or gaussian distribution. This distribution can be well described mathematically and the spread of the plume can be predicted according to how atmospheric stability and turbulence stretch and diffuse the plume as it travels away from the source.

Katabatic drainage: Drainage of cold air downhill, usually at night.

Mass balance: A method in which an account is kept of all material entering and leaving the sides of a hypothetical ‘‘box’’ placed above ground. The scale of the box can range from the patch to the region (with aircraft sampling the sides of the hypothetical box).

Momentum: Traditionally this quantity is mass $\times$ velocity; in this context, fluxes of momentum from the atmosphere to the ground are caused by the drag of the ground slowing down the air layers closest to it. Momentum is abstracted from the air and it is this process that also brings about the exchange of trace gases.

Psychrometer constant: A term relating dry- and wet-bulb thermometers (psychrometers) and used in the calculation of evaporation and vapor pressure. Different for psychrometers in a Stevenson screen and fully-aspirated psychrometers. (Meteorological units of mbar $^\circ C^{-1}$.)

Radiosonde: An instrumentation package to measure Temperature, Pressure and Humidity in Earth’s atmosphere—the so-called three state variables of our atmosphere. A radiosonde is suspended below a meteorological balloon and released from the surface; they can typically reach altitudes of 20–25 km and signals are received by telemetry at ground stations. In practice there are several thousand radiosonde stations around the globe, simultaneously releasing radiosondes at predetermined times throughout the day.

Reynold’s decomposition (or averaging): The expansion of terms in the equations of fluid motion into their mean and fluctuating parts.

Scalar: As opposed to a vector quantity, a scalar has magnitude but no direction. Air temperature, water vapor and CO_2 are scalars, whereas velocity is a vector.

Storage: As discussed in this chapter, this is the build-up of CO_2 below an eddy covariance sensor in the canopy layer. CO_2 efflux from the soil may not escape the canopy at night since vertical mixing will be reduced in the stable atmosphere; CO_2 may accumulate between the soil and the top of the canopy and may not pass the flux instrumentation. Measurements of the CO_2 concentration can be made at several heights within this layer to determine the storage of CO_2. The storage term can then be added to the measured flux to obtain the true CO_2 exchange. Storage is less of a problem during the day when eddies can penetrate into the canopy, thus ensuring mixing with the air above the canopy. Storage can be substantial in deep, dense canopies such as in tropical forests.

Synoptic scale subsidence: The general descent of air in high-pressure systems (anticyclones) at the rate of a few $cm\,s^{-1}$. This type of subsidence and its associated adiabatic heating of the air can lead to the formation of inversions in the atmosphere. Since inversions can act as a "lid" to vertical motion, this type of subsidence can give rise to poor air quality at the ground surface.

Von Karman's constant: A constant used in the logarithmic wind profile equation in the surface layer (= 0.4).

Zero-plane displacement: An estimate of the height in the vegetation canopy at which the wind speed profile is assumed to decrease to zero. Typically, the zero-plane displacement is about two-thirds of the height of the vegetation. It is usually given the symbol "*d*" and was first introduced as a mathematical "trick" to permit the use of simple log-linear wind profile analysis to be attempted over tall vegetation.

REFERENCES

Aubinet M.A. Grelle, A. Ibrom, U. Rannik, J. Moncrieff, T. Foken, A.S. Kowalski, P.H. Martin, P. Berbigier, C. Bernhofer et al. 2000. Estimates of annual net carbon and water exchange of forests: the EUROFLUX methodology. *Adv. Ecol. Res.* 30:113–75.

Baker, J.M. 2000. Conditional sampling revisited. *Agric. For. Meteorol.* 104:59–65.

Baldocchi, D.D., B.B. Hicks, and T.P. Meyers. 1988. Measuring biosphere–atmosphere exchanges of biologically related gases with micrometeorological methods. *Ecology* 69:1331–1340.

Baldocchi, D.D. 2003. Assessing ecosystem carbon balance: problems and prospects of the eddy covariance technique. *Glob. Change Biol.* 9:479–492.

Beverland, I.J., D. Ónéill, S.L. Scott, J.B. Moncrieff. 1996. Design, construction and operation of flux measurement systems using the conditional sampling system. *Atmos. Environ.* 30:3209–3220.

Bowling, D.R., A.C. Delany, A.A. Turnipseed, D.D. Baldocchi, and R.K. Monson. 1999. Modification of the relaxed eddy accumulation technique to maximize measured scalar mixing ratio differences in updrafts and downdrafts. *J. Geophys. Res.* 104:9121–9133.

Businger, J.A. and A.C. Delaney. 1990. Chemical sensor resolution required for measuring surface fluxes by three common micrometeorological techniques. *J. Atmos. Chem.* 10:399–410.

Businger, J.A. and S.P. Oncley. 1990. Flux measurement with conditional sampling. *J. Atmos. Ocean. Technol.* 7:349–352.

Christensen, C.S., P. Hummelshøj, N.O. Jensen, B. Larsen, C. Lohse, K. Pilegaard and H. Skov. 2000. Determination of the terpene flux from orange species and Norway spruce by relaxed eddy accumulation. *Atmos. Environ.* 34:3057–3067.

Coe, H. and M.W. Gallagher. 1992. Measurements of dry deposition of NO_2 to a Dutch heathland using the eddy correlation technique. *Q. J. Roy. Meteorol. Soc.* 118:767–786.

De Bruin, H.A.R. 2002. Renaissance in scintillometry. *Bound.-Lay. Meteorol.* 105:1–4.

Denmead, O.T., M.R. Raupach, F.X. Dunin, H.A. Cleugh, and R.L. Leuning. 1996. Boundary layer budgets for regional estimates of scalar fluxes. *Glob. Change Biol.* 2:255–264.

Denmead, O.T., L.A. Harper, J.R. Freney, D.W.T. Griffith, R. Leuning, R.R. Sharpe. 1998. A mass balance method for non-intrusive measurements of surface-air trace gas exchange. *Atmos. Environ.* 32:3679–3688.

Denmead, O.T., R. Leuning, I. Jamie and D.W.T. Griffith. 2000. Nitrous oxide emissions from grazed pastures: measurements at different scales. *Chemosphere – Glob. Change Sci.* 2:301–312.

Desjardins, R.L. 1977. Description and evaluation of a sensible heat flux detector. *Bound.-Lay. Meteorol.* 11:147–154.

Desjardins, R.L., R.L. Hart, J.I. MacPherson, P.H. Schuepp, and S.B. Verma. 1992. Aircraft- and tower-based fluxes of carbon dioxide, latent, and sensible heat. *J. Geophys. Res.* 97:18477–18485.

Eugster, W. and F. Siegrist. 2000. The influence of nocturnal CO_2 advection on CO_2 flux measurements. *Basic Appl. Ecol.* 1:177–188.

Finn, D., B. Lamb, M.Y. Leclerc and T.W. Horst. 1996. Experimental evaluation of analytical and lagrangian surface-layer flux footprint models. *Bound.-Lay. Meteorol.* 80:283–308.

Fowler, D. and M.H. Unsworth. 1979. Turbulent transfer of sulphur dioxide to a wheat crop. *Q. J. Roy. Meteorol. Soc.* 105:767–783.

Gallagher, M.W., T.W. Choularton, K.N. Bower, I.M. Stromberg, K.M. Beswick, D. Fowler, and K.J. Hargreaves. 1994. Measurements of methane fluxes on

the landscape scale from a wetland area in North Scotland. *Atmos. Environ.* 28:2421–2430.
Gash, J.H.C. 1986. A note on estimating the effect of limited fetch on micrometeorological evaporation measurements. *Bound.-Lay. Meteorol.* 35:409–414.
Galle, B., L. Klemedtsson, and D.W.T. Griffith. 1994. Application of a fourier-transform IR system for measurements of N_2O fluxes using micrometeorological methods, an ultralarge chamber system, and conventional field chambers. *J Geophys. Res.* 99:16575–16583.
Gosz, J.R., C.N. Dahm, and P.G. Risser. 1988. Long-path FTIR measurement of atmospheric trace gas concentrations. *Ecology* 69:1326–1330.
Grelle, A. and A. Lindroth. 1996. Eddy-correlation system for long-term monitoring of fluxes of heat, water vapor and CO_2. *Glob. Change Biol.* 2:297–307.
Griffith, D.W.T. and B. Galle. 2000. Flux measurements of NH_3, N_2O and CO_2 using dual beam FTIR spectroscopy and the flux-gradient technique. *Atmos. Environ.* 34:1087–1098.
Griffith, D.W.T., R. Leuning, O.T. Denmead, and I.M. Jamie. 2002. Air-land exchanges of CO_2, CH_4 and N_2O measured by FTIR spectrometry and micrometeorological techniques. *Atmos. Environ.* 35:1833–1842.
Guenther, A.B. and A.J. Hills. 1998. Eddy covariance measurement of isoprene fluxes. *J. Geophys. Res.* 103:13145–13152.
Hicks, B.B. and R.T. McMillen. 1984. A simulation of the eddy accumulation method for measuring pollutant fluxes. *J. Clin. Appl. Meteorol.* 23:637–643.
Kaimal, J.C. and J.A.A. Businger. 1963. A continuous wave sonic anemometer-thermometer. *J. Appl. Meteorol.* 2:156–164.
Kaimal, J.C. and J.E. Gaynor. 1991. Another look at sonic thermometry. *Bound.-Lay. Meteorol.* 56:401–410.
Kaimal, J.C., J.C. Wyngaard, Y. Izumi, and O.R. Cote. 1972. Spectral characteristics of surface-layer turbulence. *Q. J. Roy. Meteorol. Soc.* 98:563–589.
Kaimal, J.C., and J.J. Finnegan. 1994. *Atmospheric Boundary Layer Flows, Their Structure and Measurement*. Oxford University Press, Oxford.
Kelliher, F.M., A.R. Reisinger, R.J. Martin, M.J. Harvey, S.J. Price, and R.R. Sherlock. 2002. Measuring nitrous oxide emission rate from grazed pasture using Fourier-transform infrared spectroscopy in the nocturnal boundary layer. *Agric. For. Meteorol.* 111:29–38.
Laville, P., C. Jambert, P. Cellier, and R. Delmas. 1999. Nitrous oxide fluxes from a fertilised maize crop using micrometeorological and chamber methods. *Agric. For. Meteorol.* 96:19–38.
Lee, X. 1998. On micrometeorological observations of surface-air exchange over tall vegetation. *Agric. For. Meteorol.* 91:39–49.
Lenschow, D.H. 1995. Micrometeorological techniques for measuring biosphere-atmosphere trace gas exchange. In: Matson, P.A. and R.C. Harriss, eds., *Biogenic Trace Gases: Measuring Emissions from Soil and Water. Methods In Ecology Series*. Blackwell Science, Cambridge, pp. 126–163.

Leuning, R.L. and J.B. Moncrieff. 1990. Eddy covariance CO_2 flux measurements using open- and closed-path CO_2 analyzers: corrections for analyzer water vapor sensitivity and damping of fluctuations in air sampling tubes. *Bound.-Lay. Meteorol.* 53:63–76.

Leuning, R., S.K. Baker, I.M. Jamie, C.H. Hsu, L. Klein, O.T. Denmead, and D.W.T. Griffith. 1999. Methane emission from free-ranging sheep: a comparison of two measurement methods. *Atmos. Environ.* 33:1357–1365.

Levy, P.E., A. Grelle, A. Lindroth, M. Molder, P.G. Jarvis, B. Kruijt, and J.B. Moncrieff. 1999. Regional-scale CO_2 fluxes over central Sweden by a boundary layer budget method. *Agric. For. Meteorol.*, 98–99:169–180.

Lindroth, A. 1984. Gradient distribution and flux profile relations above a rough forest. *Q. J. Roy. Meteorol. Soc.* 110:553–563.

Lindroth, A., A. Grelle, and A. Moran. 1998. Long term measurements of boreal forest carbon balance reveal large temperature sensitivity. *Glob. Change Biol.* 4:443–450.

Majewski, M.S.; R.L. Desjardins, P. Rochette, E. Pattey, J.N. Seiber, and D.E.A. Glotfelty. 1993. A field comparison of an eddy accumulation and an aerodynamic-gradient system for measuring pesticide volatilization fluxes. *J. Environ. Sci. Tech.* 27:121–128.

Meijninger, W.M.L., O.K. Hartogensis, W. Kohsiek, J.C.B. Hoedjes, R.M. Zuurbier, and H.A.R. De Bruin. 2002. Determination of area-averaged sensible heat fluxes with a large aperture scintillometer over a heterogeneous surface – Flevoland field experiment. *Bound.-Lay. Meteorol.* 105:37–62.

McNeil, D. and W.J. Shuttleworth. 1975. Comparative measurements of the energy fluxes above a pine forest. *Bound.-Lay. Meteorol.* 9:297–313.

Milne, R., I.J. Beverland, K. Hargreaves, and J.B. Moncrieff. 1999. Variation of the beta coefficient in the relaxed accumulation method. *Bound.-Lay. Meteorol.* 93:211–225.

Miranda, A., P.G. Jarvis, and J. Grace. 1984. Transpiration and evaporation from heather moorland. *Bound.-Lay. Meteorol.* 28:227–243.

Moncrieff, J.B., I.J. Beverland, D.H. Ónéill, and F.D. Cropley. 1998. Controls on trace gas exchange observed by a conditional sampling method. *Atmos. Environ.* 32:3265–3274.

Moncrieff, J.B., Y. Malhi, and R.L. Leuning. 1996. The propagation of errors in long-term measurements of land-atmosphere fluxes of carbon and water. *Glob. Change Biol.* 2:231–254.

Moncrieff, J.B., J.M. Massheder, H. DeBruin, J. Elbers, T. Friborg, B. Huesunkveld, P. Kabat, S.L. Scott, H. Soegaard, and A. Verhoef. 1997. A system to measure surface fluxes of momentum, sensible heat, water vapor and carbon dioxide. *J. Hydrol.* 188–189:589–611.

Moncrieff, J.B., P.G. Jarvis, and R. Valentini. 2000. Canopy fluxes. In: Sala, O.E., R.B. Jackson, H.A. Mooney, and R.W. Howarth (eds.), *Methods in Ecosystem Science*. Springer, Berlin, pp. 161–180.

Monteith, J.L. and M.H. Unsworth. 1990. *Principles of Environmental Physics*. 2nd edn. Arnold, London.
Mulhearn, P.J. 1977. Relations between surface fluxes and mean profiles of velocity, temperature and concentration, downwind of a change in surface roughness. *Q. J. Roy. Meteorol. Soc.* 103:785–802.
Munley, W.G. and L.E. Hipps. 1991. Estimation of regional evaporation for a tallgrass prairie from measurements of properties of the atmospheric boundary layer. *Water Resources Res.* 27:225–230.
Oncley, S.P., A.C. Delaney, and T.W. Horst. 1993. Verification of flux measurements using relaxed eddy accumulation. *Atmos. Environ.* 27:2417–2426.
Pattey, E., R.L. Desjardins, F. Boudreau, and P. Rochette. 1992. Impact of density fluctuations on flux measurements of trace gases: implications for the relaxed eddy accumulation technique. *Bound.-Lay. Meteorol.* 59:195–203.
Pattey, E., A.J. Cessan, R.L. Desjardins, L.A. Kerr, P. Rochette, G. St-Amour, T. Zhu, and K. Headrick. 1995. Herbicides volatilization measured by the relaxed eddy accumulation technique using two trapping media. *Agric. For. Meteorol.* 76:201–220.
Pattey, E., I.B. Strachan, R.L. Desjardins, and J. Massheder. 2002. Measuring nighttime CO_2 flux over terrestrial ecosystems using eddy covariance and nocturnal boundary layer methods. *Agric. For. Meteorol.* 113:145–158.
Paulson, C.A. 1970. The mathematical representation of wind speed and temperature profiles in the unstable atmospheric surface layer. *J. Appl. Meteorol.* 9:857–861.
Poggio, L., M. Furger, A.S.H. Prévôt, W.K. Graber, and E.L. Andreas. 2000. Scintillometer wind measurements over complex terrain. *J. Atmos. Oceanic Technol.* 17:17–26.
Raupach, M.R., O.T. Denmead, and F.X. Dunin. 1992. Challenges in linking atmospheric CO_2 concentrations to fluxes at local and regional scales. *Aus. J. Bot.* 40:697–716.
Raupach, M.R. and B.J. Legg. 1984. The uses and limitations of flux-gradient relationships in micrometeorology. *Agric. Water Man.* 8:119–131.
Raupach, M.R. and A.S. Thom. 1981. Turbulence in and above canopies. *Ann. Rev. Fluid Mech.* 13:97–129.
Running, S.W., D. Baldocchi, W. Cohen, S.T. Gower, D. Turner, P. Bakwin, and K. Hibbard. 1999. A global terrestrial monitoring network scaling tower fluxes with ecosystem modelling and EOS satellite data. *Rem. Sens. Environ.* 70:108–127.
Schmid, H.P. and T.R. Oke. 1990. A model to estimate the source area contributing to turbulent exchange in the surface layer over patchy terrain. *Q. J. Roy. Meteorol. Soc.* 116:965–988.
Schotanus, P., F.T.M. Nieuwstadt, and H.A.R. de Bruin. 1983. Temperature measurements with a sonic anemometer and its application to heat and moisture fluxes. *Bound-Lay Meteorol.* 26:81–93.
Schuepp, P.H., M.Y. Leclerc, J.I. MacPherson, and R.L. Desjardins. 1990. Footprint prediction of scalar fluxes from analytical solutions of the diffusion equation. *Bound.-Lay. Meteorol.* 50:355–376.

Simpson, I.J. et al. 1995. Tunable diode laser measurements of methane fluxes from an irrigated rice paddy field in the Philippines. *J. Geophys. Res.* 100:7238–7290.

Soegaard, H., N.O. Jensen, E. Boegh, C.B. Hasager, K. Schelde, and A. Thomsen. 2003. Carbon dioxide exchange over agricultural landscape using eddy correlation and footprint modelling. *Agric. For. Meteorol.* 114:153–173.

Stull, R.B. 1988. *An Introduction to Boundary Layer Meteorology*. Kluwer Academic Publishers Dordrecht, The Netherlands.

Sun, J., R. Desjardins, L. Mahrt, and J.I. MacPherson. 1998. Transport of carbon dioxide, water vapor and ozone by turbulence and local circulations. *J. Geophys. Res.* 103:25873–25885.

Sutton, M.A., D. Fowler, and J.B. Moncrieff. 1993. The exchange of atmospheric ammonia with vegetated surfaces. I: Unfertilized vegetation. *Q. J. Roy. Meteorol. Soc.* 119:1023–1045.

Thom, A.S. 1975. Momentum, mass and heat exchange. In: Monteith J.L. (ed.), *Vegetation and the Atmosphere*. Academic Press, Chichester, pp. 57–109.

Wagner-Riddle, C. et al. 1996. Micrometeorological measurements of trace gas fluxes from agricultural fields and natural ecosystems. *Infrared Phys. Technol.* 37:51–58.

Webb, E.K. 1970. Profile relationships: the log-linear range and extension to strong stability. *Q. J. Roy. Meteorol. Soc.* 96:67–90.

Webb, E.K., G.I. Pearman, and R.L. Leuning. 1980. Correction of flux measurements for density effects due to heat and water vapor transfer. *Q. J. Roy. Meteorol. Soc.* 106:85–100.

Wichura, B., N. Buchmann, and T. Foken. 2000. Fluxes of the stable isotope ^{13}C above a spruce forest measured by hyperbolic relaxed eddy accumulation method. American Meteorological Society. *14th Symposium on Boundary Layers and Turbulence*. pp. 559–562, 7–11 August 2000. Aspen, CO.

Wienhold, F.G., H. Frahm, and G.W. Harris. 1994. Measurements of N_2O fluxes from fertilised grassland using a fast response tunable diode laser spectrometer. *J. Geophys. Res.* 99:16557–16567.

Wratt, D.S., N.R. Gimson, G.W. Brailsford, K.R. Lassey, A.M. Bromley, and M.J. Bell. 2001. Estimating regional methane emissions from agriculture using aircraft measurements of concentration profiles. *Atmos. Environ.* 35:497–508.

Zahniser, M.S., D.D. Nelson, J.B. McManus, and P.L. Kebabian. 1995. Measurement of trace gas fluxes using tunable diode laser spectroscopy. *Phil. Trans. Roy. Soc. Lond.* A351:371–382.

12

Analysis of Organic Pollutants in Environmental Samples

Julian J. C. Dawson, Helena Maciel, and Graeme I. Paton
The University of Aberdeen, Aberdeen, Scotland

Kirk T. Semple
Lancaster University, Lancaster, England

I. INTRODUCTION

The identification and quantification of organic pollutants in environmental matrices have improved significantly over the past two decades. Fundamentally, the determination of organic contaminants requires selective solvent extraction of the determinant(s) from the matrix followed by quantifiable analysis using specialized instrumentation. Often the researcher needs to identify a target compound and/or its metabolites, thus focusing the choice of technique to suit the particular matrix and determinant(s). Significant advances in instrument automation and reliability, precision of flow control, detector development, and competitive instrument pricing have greatly increased the number and range of laboratories capable of fulfilling reliable and routine organic pollutant analysis.

This chapter describes the main steps required in analysis of key organic pollutants in environmental samples, concentrating on soil analysis to provide illustrative examples, as soil is one of the more challenging matrices. Citations are made to references that provide specific information about instrumentation and the underpinning principles and scientific rationale. Several widely used methods are described and discussed in detail to exemplify the considerations needed for techniques.

Marcel Dekker, Inc.
270 Madison Avenue, New York, New York 10016

A. Why Quantify and Identify Organic Contaminants?

The presence of organic pollutants in the environment is ubiquitous. From the high arctic to the tropics (Jones and de Voogt, 1999), recalcitrant and volatile pollutants are detectable in all environmental spheres. Soils and sediments are major sinks for organic pollutants and can retain the highest concentrations of released pollutants (Northcott and Jones, 2000). Drinking water contaminated with biocides from runoff into surface waters or by the leaching of agrochemicals through soil to aquifers is widely acknowledged (Stackelberg et al., 2001). Researchers and regulators need sensitive and routine techniques to identify and quantify these contaminants. Scientists also need to be able to study samples for signs of degradation and the occurrence of metabolites and cocontaminants that may indicate the relative damage or indeed remediation in soil or sediment systems.

II. OVERVIEW OF ORGANIC ANALYSIS

Once a representative sample has been obtained, there are three further stages that underpin organic analysis: (1) the preparatory (drying) and extraction stage, (2) the cleanup stage(s) and (3) the determination stage. Some determinations may only be performed after derivatization, when the determinant needs to be chemically altered to improve analytical resolution. Organotin determination, for example, requires extensive derivatization because the determinants are not sufficiently volatile for direct gas chromatographic analysis (Abalos et al., 1997). Each of these stages will be dealt with separately, and using illustrative examples, the selection criteria for certain approaches will be justified.

A. Sample Preparation and Analysis

The type of drying technique carried out is determined by the nature of the determinant(s) and the matrices. It is usually inappropriate to dry a soil or sediment in an oven as may be done for inorganic analysis, as this may cause a substantial loss of the determinants. Instead, a sulfate salt is often used to remove the water (Hess et al., 1995; Guerin, 1999). After drying, the organic determinant present must be brought into an appropriate organic solvent prior to quantification by gas chromatography (GC) or high-pressure liquid chromatography (HPLC). Determinants in water samples can be extracted using sequential volumes of organic solvent, which are then passed through the sulfate salt to remove residual water (Meharg et al., 1999). The extraction technique also enables the sensitivity of the analysis to be

Marcel Dekker, Inc.
270 Madison Avenue, New York, New York 10016

manipulated through sample concentration. Depending upon the nature of the sample and the target determinant, an appropriate technique can be selected.

1. Liquid/Liquid Phase Extraction

When a solvent is immiscible with water and the target determinant is more soluble in the solvent than in water, then this is an ideal technique. The partitioning coefficient of the determinant material is equal to the ratio of its concentration in the solvent divided by that in water. The partitioning coefficient is independent of the volume ratio of solvent : water but constant at any given temperature; thus increasing the amount of solvent increases the amount of determinant extracted. Repeated extractions with the same solvent will also increase the efficiency of determinant extraction. Extraction efficiency can be further improved by heating of the sample-extraction mixture (Dean and Xiong, 2000).

2. Soxhlet Extraction

This is a commonly used technique for quantifying total concentrations of semivolatile and nonvolatile hydrophobic contaminants. A diagram of the main components of the Soxhlet apparatus is shown in Fig. 1. The soil or

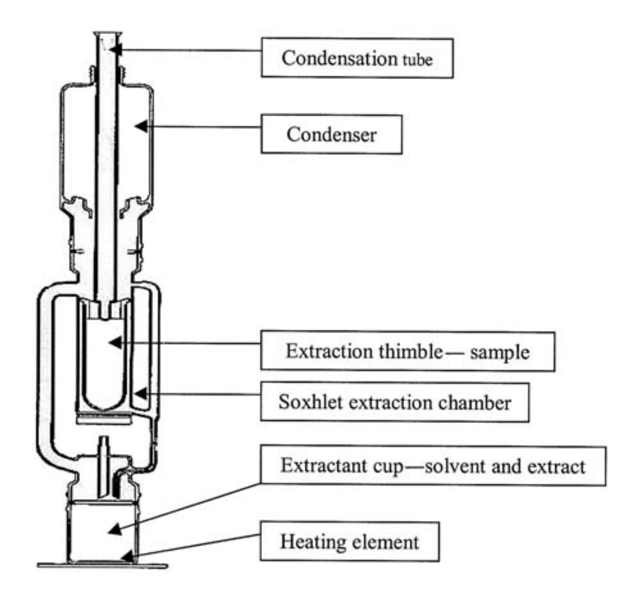


Figure 1 Soxhlet apparatus for solvent extraction of organic pollutants from soils and sediments.

sediment sample is placed in a porous extraction thimble. Below this thimble is a cup containing the solvent, which is heated and passed through distillation and condensation stages, ensuring that there is a rigorous mixing of the solvent with the sample. Although the procedure is slow, it is a harsh but effective technique. This method continuously re-extracts the sample with the same quantity of solvent: the solvent is refluxed in a Soxhlet apparatus, condenses, and trickles down through the sample back to the bottom of the apparatus, where the determinant collects. This method is used for nonvolatile and semivolatile organics, and it will not collect any compounds with a boiling point lower than, or close to, that of the solvent used. The solvent is typically a mixture of a nonpolar compound such as dichloromethane (DCM) with about 10% of a water-miscible polar solvent such as methanol or acetone added.

3. Supercritical Fluid Extraction (SFE)

A supercritical fluid (SCF) is a substance held above its critical temperature and pressure. SCFs have many advantages over liquid solvents for use in extraction of environmental samples (Camel, 2001). Their physical properties include low viscosity, high diffusion coefficients, low toxicity, low flammability, and negligible surface tension. These allow SCFs to penetrate an environmental matrix very quickly, allowing rapid extractions compared to those with conventional solvents. A further advantage is that SFE systems can be interfaced directly with a chromatography column, thus minimizing sample preparation. Supercritical carbon dioxide, possibly modified by the addition of methanol or acetone, is the most common solvent used in environmental analysis; however, a SCF with a dipole moment may be more effective (Alonso et al., 1998). Hawthorne et al. (1992) found that supercritical $CHClF_2$ (Freon-22) was more effective than CO_2 for the extraction of PAHs and PCBs from soils, consistently extracting 2–10 times more determinant. SFE with $CHClF_2$ was also fast: 30–45 minutes were required to extract comparable amounts to that obtained by 18 hours ultrasonication in DCM, or 32 hours Soxhlet extraction in hexane/methanol and hexane/acetone mixtures. SCF techniques are not routinely used in soil analysis because they are quite expensive to set up and to run routinely. However, they may be more widely used in future, particularly if they are shown to be applicable to a range of determinants that are not routinely tested for at present.

4. Thermal Desorption

This method is used in conjunction with a gas chromatograph (GC) and is suitable for volatile and semivolatile hydrocarbons. The solid sample is

warmed to approximately 85°C in an enclosed system to desorb and volatilize the hydrocarbons, which are then purged, trapped, and subsequently transferred onto the column. Volatile organic compounds, such as benzene, toluene, ethylbenzene, xylene (BTEX), methyl tertiary butyl ether (MtBE), and naphthalene from liquid environmental samples, e.g., fresh and marine waters, soil extracts, and wastewater, can also be extracted by purging of the sample using an inert gas and trapping the extracted determinants. The contents of the trap are then injected directly onto the column of the GC. Although slow and costly to set up, the method is the most reliable one for quantifying relatively water-soluble determinants.

5. Solid/Liquid Phase Extraction

This technique is also known as solid phase extraction (SPE). The process is simple and fast and may prove cost-effective for some users. A measured volume of the sample is passed through a cartridge tube with a suitable solid material, which sorbs the target determinant. The determinant is then eluted from the cartridge using an appropriate solvent. Semiautomated SPE systems use vacuum pumps to speed up the solvent flow, enabling elution to take place much more quickly. SPE is also extensively used as a cleanup technique to remove material that may damage a chromatography column or slow down the chromatographic procedure. Most of the large chromatographic suppliers sell SPE systems. The selection of the packing material is based upon the polarity of the contaminants to be determined. Nonpolar hydrophobic adsorbents retain the nonpolar determinants and allow polar substances to pass through the column, whereas hydrophilic adsorbents adsorb the polar components, allowing the nonpolar materials to pass through.

6. Other Methods

Ultrasonication. An ultrasonic probe may be used to agitate soil or sediment samples in a solvent such as DCM. It is used for non- and semivolatile organics at various concentrations (Guerin, 1999).

Accelerated Solvent Extraction (ASE). This uses traditional solvent mixtures as for Soxhlet extraction, but the sample is held at increased temperature and pressure, thus reducing extraction time and solvent volume required (Fisher et al., 1997; Hubert et al., 2001).

Microwave-Assisted Solvent Extraction (MSE). This method is similar in function to ASE in that it enables reduced extraction times and solvent volumes compared to traditional techniques. The equipment is quite

costly to purchase, and the technique is not widely reviewed in publications; hence comparative evaluation may prove to be problematic.

B. Cleanup Techniques

Sample cleanup of organic extracts is used to prolong the life of the instrument column, injector, and detector. A purified sample will also produce clearer peaks with improved resolution that will prove easier to quantify. Sample purification tends to be based on one of the following principles: (1) partitioning between immiscible solvents; (2) adsorption chromatography; (3) gel permeation chromatography; (4) chemical destruction of interfering substances; or (5) distillation.

The simplest of the above is the acid/base partitioning, in which a solvent extract is shaken with dilute alkali that enables acidic organics to partition into the aqueous layer while the basic and neutral fractions remain in the organic solvent. The aqueous layer can then be acidified and extracted using DCM so that the organic layer will now contain the acid fraction. This technique is widely used in cleanup procedures for determining phenols and associated herbicides from soils and sediments (Patnaik, 1997).

Cleanup columns, either as premanufactured SPE systems or as laboratory-produced columns, are the most common routine technique for cleanup. For example, highly porous and granular aluminum oxide (alumina) can be used and is readily available in acidic, neutral, or basic forms (Polese et al., 1996). Target determinants can be differentiated by chemical polarity. After the column is packed with the granular material it is covered in anhydrous sodium sulfate and the sample is placed on the column. By using the appropriate solvent, this enables the determinants to be separated from impurities that are present. Basic alumina is used in purification of steroids, alcohols, and pigments (Cho et al., 1997); the neutral form is used for esters and ketones (Polese and Ribeiro, 1998), while the acidic form separates strong acids and acidic pigments. Alumina is also ideal for the cleanup of hydrocarbons (Cho et al., 1997; Shen and Jaffe, 2000).

Amorphous silica gel is suitable for the removal of interfering compounds of differing polarities (Shamsipur et al., 2000). Activated silica gel is heated for several hours at 150°C prior to use and is also well suited for the cleanup of hydrocarbons (Miege et al., 1999). Deactivated silica gel has significantly more water present and is used to separate plasticizers, lipids, esters, and some organometallic compounds (Shamsipur et al., 2000). If used appropriately, high specificity for target herbicides can be achieved. In addition, the selection of different solvents (Supelco, 2001) can be used to manipulate adsorbent activity of the SPE system.

Table 1 Suggested Cleanup Techniques for a Number of Common Contaminant Groups

Determinant	Cleanup technique
Nitrosamines	Gel permeation, alumina, Florisil
Organochlorines	Gel permeation, Florisil
Organophosphates	Gel permeation, Florisil
Petroleum	Alumina, acid–base
Phenols	Gel permeation, acid–base, silica gel
PAHs	Gel permeation, alumina, silica gel

Source: Patnaik, 1997.

Florisil is a form of magnesium silicate with acidic properties. A packed column of Florisil is used the same way as silica and alumina columns. The material is ideal for the separation of aliphatic compounds from aromatics (Abdallah, 1994) and is used for a wide range of pesticides (Smeds and Saukko, 2001) and halogenated hydrocarbons (Schenck and Donoghue, 2000).

Gel permeation is able to differentiate material on the basis of pore size using hydrophobic gels (Knothe, 2001). As with SPE, this system is capable of performing to a high level of specificity, though equipment and consumable costs will reflect this.

In some solid environmental samples, the presence of specific materials may impose analytical problems. For example, sulfur may reduce the resolution of chromatograms. Sulfur has a solubility that is similar to a range of organochlorine and organophosphate pesticides and cannot be resolved using Florisil (Patnaik, 1997). Commonly, copper turnings are shaken with the sample to remove sulfur from the solvent extract (Schulz et al., 1989). Mercury or tetrabutyl ammonium sulfite (Duinker et al., 1991) are also used. Table 1 describes the materials typically chosen for cleanup procedures of selected contaminants extracted from soils and sediments.

C. Methods of Determination

Chromatography is a simple concept in that analyte components become separated as they either move in the mobile phase or become sorbed in another phase. The characteristics of the sorption phases determine the extent to which analyte components become separated. The resolution can be manipulated by using appropriate columns in consideration of the determinants sought. The major factors to ensure high quality chromatography are (1) purity of the mobile phase, (2) a reliable flow rate, (3) an

appropriate column, and (4) a suitably sensitive detector. Regardless of the type of chromatography, these rules must be adhered to. The most commonly used chromatographic techniques in environmental analysis are GC and HPLC, and these methods will be described briefly and then considered in more detail, using representative case studies, later in this chapter.

For routine analysis it is important to consider the value of an autosampler. Current microrobotic technology provides high precision and reproducibility. In many instruments, sample vials can undergo heating and mixing (with slight modifications to the sampler), thus enabling some automated derivatization. Automated dilution systems where available, are also very useful, as the system is capable of operating with small volumes. The automated injection system resolves problems associated with manual techniques, which may cause excessive and variable peak broadening on the column. Most significantly, the autosampler allows hundreds of samples to be systematically analyzed. This is ideal, because of the long retention times associated with some determinations.

1. Gas Chromatography

Traditionally this has been called gas–liquid chromatography because samples being carried through a column undergo partition between a gas phase (mobile) and a sorbed liquid phase (stationary). For the purpose of this chapter, only capillary GC will be considered, but further details on packed columns can be found in Bruno (2000), and in Chap. 10.

The main components of a GC are

The Injector. After sample preparation and cleanup, the sample is ready for injection. Most GC analysis will be carried out using split or splitless injection. This means that the sample is injected into a chamber where, under heating, it expands and then moves in the gas flow onto the column. The selection of the solvent used for injection is therefore very important, as different solvents have different expansion characteristics. In the case of split injection, a proportion of the sample is discarded, as it may overload the column and detector and cause a reduction in resolution. Common split ratios are between 15 : 1 and 40 : 1, and thus a large proportion of the sample is discarded. Splitless analysis, on the other hand, enables expansion of the solvent vapor within a glass liner, but the entire sample is presented to the column. On-column injection is required for trace analysis and has no pre-expansion stage for the sample. The injector systems are usually tailor-made to suit the style of analysis.

Gas Flow Selection and Rate. Many laboratories using gas chromatography do not have access to high-purity gases and thus have to use

supplies containing small amounts of impurities, e.g., oxygen, moisture, and carbon compounds. In such circumstances, filters should be used to remove these impurities, to avoid damaging the column and affecting the response of the detector. A carrier gas ensures steady flow of sample through the column while often an additional "make-up" gas is required for the detector. Any new GC will have highly sensitive electronic or manual gas controls, which can be altered according to column-specific requirements.

The Capillary Column. The nature of the column will determine the success or failure of the separation. Users should be aware of the range of columns on the market and the relative merits of inexpensive and expensive purchases. The selection of a column is governed by what is referred to as the "theoretical plates per meter" concept. This parameter describes the chromatographic performance of a column. There is a wide range of texts that consider the principles that underpin this parameter, and for more information, Marr and Cresser (1983) is a good source. All the major capillary column suppliers have catalogs either available in paper format or from the internet. These should be consulted prior to purchase, as they will enable the most appropriate column to be selected. The columns are composed of fused silica, and a narrow-bore inside diameter (i.d.) (usually 0.20, 0.25, or 0.32 mm) will provide the best separation for closely eluting components and isomers. In general, the smaller the i.d., the greater is the level of resolution that can be achieved. Conversely, to avoid sample overload for analytes in high concentrations, a larger i.d. may be more appropriate. The characteristics of some typical columns are shown in Table 2.

The Oven Control. The column will have been selected to favor the particular determinant(s) and analytes. However, it is possible to alter the analysis most effectively by the manipulation of temperature. For determinants to be separated, they are differentially partitioned between the mobile and stationary phases: the proportion in the gas phase depends

Table 2 Examples of Some Available Columns and Their Characteristics

Column type	Temperature	Polarity
Dimethyl silicone oil	0–350°C	Very low
Phenyl methyl silicone oil	0–350°C	Low
Phenyl cyanopropyl methyl silicone	0–275°C	Medium
Carbowax 1540	0–200°C	High

on temperature. When analyzing a broad suite of hydrocarbons, for example, it is not possible to select a column that is capable of discriminating between all determinants. The most volatile fraction will move rapidly along the column, while the larger molecules will trail significantly behind. To speed up this process, the oven can be adjusted to produce a temperature "ramp" during which the column temperature changes across a predetermined regime. This simply means that as the analysis is progressing, the oven temperature is progressively raised, which means that the sample begins to reach "vapor pressure" and elutes more readily through the column. Without the use of this ramp, retention time would rise significantly if the temperature were set too low, whereas if the temperature were initially set too high, all the determinants would elute together.

The Detector. Thermal conductivity detectors (TCDs) and flame ionization detectors (FIDs) are the most commonly used types. Because of its lack of specificity, the TCD is more appropriate for gas analysis (see Chap. 10), and it will not be considered in more detail here. The FID, however, is an excellent detector for a wide range of determinants because it responds to the presence of organic carbon compounds (but not to CO, CO_2, or CS_2). In the FID, the passage of the organic compounds through a hydrogen-rich flame results in the creation of ions and a corresponding electrical response. The FID is sensitive at the $mg\,L^{-1}$ level to a plethora of compounds (Marr and Cresser, 1983). It is also a very forgiving detector, as it has a linear response to concentration over seven orders of magnitude and is resistant to overload and damage. Flame photometric detectors (FPDs) can be used to measure determinants containing specific groups, including organic S, P, and Sn compounds (Singh et al., 1996). The FPD has a range of filters to suit the optical emission characteristics of the target determinants. The halogen-specific detector or the electron capture detector (ECD) is an essential detector for the measurement of trace levels of organochlorine compounds (Schulz et al., 1989).

The most significant detector used for routine analysis now is the mass spectrometer. This is an excellent tool for identifying a range of unknown determinants in the target matrix. Over the last decade the application of this detector in water, soil, and sediment analysis has grown enormously, and as a consequence the cost has dropped. After separation of components in an appropriate column, the eluted fractions are subjected to electron impact or chemical ionization. The fragmented and molecular ions are resolved from characteristic mass spectra and determinants identified from their distinctive primary and secondary ions. Quantification is achieved by peak height, representing the total ion count, at each specific mass : charge

ratio. Although widely used, there is no specific example in this chapter, but examples can be found in the literature (De la Guardia and Garrigues, 1998; Eriksson et al., 1998; Ragunathan et al., 1999; Choudhary et al., 2000). The mass spectrometer detector requires a high vacuum, while the gas chromatograph requires a gas flow. Hence GC-MS coupling is achieved by combining a low flow rate with the use of a fast pumping low-density carrier gas, usually helium. The capillary GC can produce sharp peaks, which enables a rapid scan with the mass spectrometer, and it is generally acknowledged that a mass spectrometer detector is as sensitive as a flame ionization detector. With the application of a mass spectrometer detector, a library of stored spectra makes it possible to identify unknown determinants.

Chromatographic Analysis and Quantification. Modern GCs are computer-controlled, and the resultant chromatograms are generally managed and analyzed by an appropriate software system. An older GC is usually managed manually and the results calculated from an integrator output. As with all other methods, calibration curves for the target determinant(s) must be prepared from at least four standards. Calibration can be performed with external or internal standards, though it is most common to use an internal standard method. This involves the addition of equal volumes of an internal standard to each of the calibration standards and the sample extracts, to ensure reproducibility of detector response. Further details about standardization and quantification can be found in Harvey (2000).

Routine GC analysis for soil and/or sediment samples involves carrying out confirmatory calibration checks prior to sample analysis to verify consistency of response. Variations in the gas flow, in the presence of impurities, in the consistency of injection, and in oven temperatures may cause substantial variations in the response. It is also worth noting that the length and "plumbing" of the column will have an impact on the retention characteristics, so analytical setup time can be substantial for complex determinants.

2. High Performance Liquid Chromatography

In this instrument, liquid/sorbed-phase chromatography is the principle of separation. The analyte is carried in a liquid that is supported (adsorbed) on an inert solid. The separation efficiency of a column can be expressed in terms of the theoretical plates in the column, which are defined by the physical structure of the column and the type of packing (Harvey, 2000). A sample is placed at the start of the column, and sample constituents are

flushed through the column by the carrier solvent(s). The component parts of the instrument are

The pump, which may be binary or quaternary. In the case of a binary pump, two-solvent mixtures can be regulated. A real-time pressure feedback and control system automatically provides solvent compressibility compensation for accurate and precise flow, regardless of solvent composition. Consistent gradients and precise retention times are provided by proven control algorithms and high-speed proportioning valves.

The solvent vacuum degaser is commonly next in line to the pump on a modern instrument. This component ensures optimal performance of the HPLC pump system. The removal of the gases from the solvents allows more stable baselines, improved gradient shape, and high temporal reproducibility. Dissolved gases account for most of the common problems encountered in routine analyses, such as bubble formation, pump cavitation, detector noise, baseline drift, and loss of gradient precision. This solvent degaser ensures the optimum performance of the HPLC system by thoroughly removing these dissolved gases from the mobile phase. All wetted materials in the degaser are chemically and biologically inert. This ensures maximum corrosion resistance and compatibility with sensitive biomolecules.

The column is ideally maintained in a temperature-controlled incubator. The column is selected according to the specific application. A useful ''general column'' is a C18 reverse phase column, which is composed of bonded silica. The applications for this include a wide range of nonionic polar compounds and aromatics.

The detector that is most commonly used is a multiwavelength UV/visible type. The detector has a flowcell into which column-partitioned fractions of the determinant are passed. Time-programmable functions enable optimization of separations or exchange. The detector must be able to respond to particularly small volumes of determinants separated by the column. Accordingly, rapid response is required. Photometric detectors provide the necessary sensitivity, and often the limitation may prove to be the subsequent integrator. The main photometric detector is usually composed of a dual-lamp design, ensuring sensitivity across the entire UV/visible spectrum. A modern system will have high-speed scan mechanisms capable of achieving a slewing speed of 30,000 nm s^{-1} and positional precision accuracy of less than 0.01 nm (Agilent, 2001). This scanning ability means that detection can be achieved at the peak of the absorption spectrum, offering a combination of selectivity and sensitivity. The cell volume should not be greater than one tenth of the volume containing the determinant yielding the smallest peak likely to be encountered, and it should be designed so that any bubbles can be rapidly cleared; this is often achieved by using a restriction block downstream

(Agilent, 2001). Refractive index detectors are also available but have fewer applications for environmental samples, as they have notoriously unstable baselines. The most significant developments at the moment are taking place in LC- mass spectrometric detectors. This type of detector is commercially available from a range of manufacturers and has been widely used in the pharmaceutical and biochemical industries. Over the next decade it is likely to have a significant effect on soil and sediment analysis, as GC-MS has had over the past decade. Applications to soil analysis that have been published include, for example, the determination of organometal speciation and recalcitrant compounds (Dass, 1999; Mondello et al., 1999).

Integration. Automation of chromatographic operation is complemented by automation of peak integration. Originally, when chromatograms were recorded on chart paper, researchers would cut out the peaks and weigh them to quantify the determinants. Now the PC achieves high-resolution determination of peak areas with user-friendly software. It can calculate the retention times and recognise peaks as required. It also enables computerization of all of the data collation, which can be extensive. Chromatographic analysis features include use of wavelength ratios, baseline subtractions, and mathematical manipulations, including first and second derivatives.

III. APPLICATIONS: CASE STUDIES

A. Determination of Total Petroleum Hydrocarbons (TPHs) in Soil Using FID-GC

1. Method of Extraction and Analysis

Typically, this technique is used for comparative evaluation either in a spatial or a temporal context. There is a need therefore to be able to put through a large number of samples and to have a relatively rapid extraction technique that has been developed and optimized specifically for TPHs. Approximately 10 g soil (wet weight) is weighed accurately (± 0.01 g) and ground over anhydrous Na_2SO_4 using a mortar and pestle, until the soil/Na_2SO_4 mixture is fluid. The sample is transferred to a 250 mL conical flask equipped with a PTFE-lined screw cap, and 1 mL of internal standard solution (see below) added. This mixture is then extracted by sonication in 50 mL of dichloromethane (DCM) (glass-distilled grade) for 10 minutes and filtered through Whatman No. 4 paper. The extraction is repeated with 25 mL of DCM, filtered through the same paper, and the two extracts combined. An aliquot of the extract (5 mL) can then be stored at $-20°C$ in a foil-capped vial for future use; the remainder, for analysis, can be

Marcel Dekker, Inc.
270 Madison Avenue, New York, New York 10016

evaporated under nitrogen at 40°C to a volume of 1 mL. The extract is then cleaned by liquid chromatography using 2 g of octadecyl-bonded silica (60 Å, < 200 μm) conditioned with 10 mL of DCM. The sample is then loaded onto the column and eluted with 2 × 10 mL of DCM. The eluate can then be concentrated further as necessary by evaporation under a stream of nitrogen at 40°C.

TPHs are measured by FID-GC. Extract (1 μL) is injected using an autosampler onto a GC equipped with a Phenomenex ZB-1 (100% polydimethylsiloxane) capillary column (30 m × 0.32 mm i.d. × 0.5 μm), split injector, and flame ionization detector. GC conditions are as follows: column gas flow (N_2): 1 mL min^{-1}; split flow: 20 mL min^{-1}. Injector temperature is varied to suit the associated hydrocarbon composition: 200°C (kerosene); 250°C (diesel and motor oil). The detector temperature is held at 250°C for kerosene, 320°C for diesel and 350°C for motor oil. As previously discussed, to cope with analyzing this complex matrix, a temperature ramp is used: the temperature is held initially at 80°C for 2 minutes, then increased at 10°C min^{-1} to 250°C (for kerosene), 320°C (for diesel), and 350°C (for motor oil), after which it is held for a further 10 minutes at the final temperature.

The internal standard (IS) is a chemically related compound of known concentration, but not present in the environmental samples, used to test extraction and chromatographic performance as well as the reproducibility of the techniques. Ideally, an IS should be added at both the extraction and analysis stages. Squalene is used as the IS for diesel, while pristane is used as an IS for kerosene and motor oil (pristane elutes after the kerosene envelope [the mixture of components constituting kerosene] and before the motor oil envelope). The IS can be dissolved in DCM and stored in a UV-proof bottle with a PTFE-lined screw cap. Routinely R_F (response factor) values are calculated over a range of 5 concentrations, and nonlinear regressions are fitted of R_F against concentration. Quantification includes some unresolved complex mixtures (UCMs) as well as resolved peaks. A typical resulting chromatogram is shown in Fig. 2.

2. Critical Evaluation of the Technique

Estimation of TPHs is the most commonly performed quantification for petroleum contamination and typically is used to set regulatory levels and cleanup targets. There are two techniques for measuring TPHs. First, infrared spectroscopy can be used to measure the absorption at 2930 cm^{-1} (corresponding to the methylene C-H stretching frequency (Lambert et al., 2001). This has the disadvantage of poor sensitivity to aromatic compounds. It is also necessary to use a solvent with no C-H bonds, e.g., a

Marcel Dekker, Inc.
270 Madison Avenue, New York, New York 10016

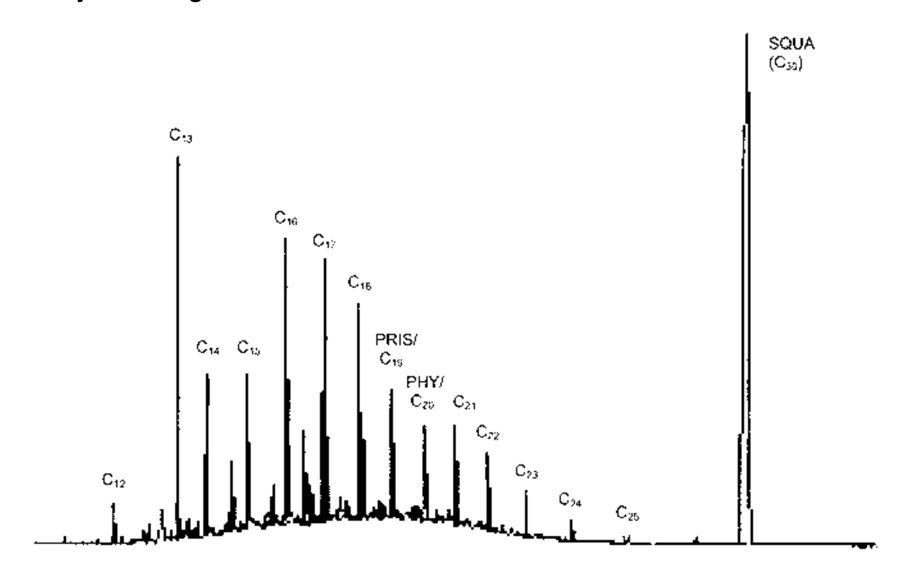


Figure 2 A typical chromatogram of diesel oil extracted from sandy soil. TPH can be calculated by adding each of the component fractions identified. PRIS: pristane; PHY: phytane; SQUA: squalene.

perhalogenated freon compound, which is very expensive. Alternatively, FID-GC can be used. The entire signal is integrated to provide a measure of TPH, or TPH can be measured for specific classes of compounds after preliminary liquid chromatography (LC) fractionation (e.g., alkanes, aromatics). As described, TPH determination by IR is insensitive to aromatics, making it unsuitable for heavy oils, or for oils that have undergone extensive weathering. Measuring TPHs by FID-GC also has drawbacks, as it is necessary to calibrate the analysis on a standard sample of oil. Often it is difficult to obtain a pristine oil sample to enable a standard calibration curve to be made. Instrumental limitation also plays a part: FID-GC can produce overrecoveries caused by memory effects in the column; of significantly greater concern is the fact that after several weeks of weathering (degeneration and decay of the oil sample) in the environment, GC traces may collapse to UCMs. Finally, TPH determination is an inherently limited technique, as it produces only a single numerical measurement of contamination. However, this makes it a popular choice for regulators, who prefer a straightforward and easily measured standard (Schreier et al., 1999).

Whittaker et al. (1995, 1996) discussed the possible use of compound-specific isotope ratio-MS for assessing oil contamination and concluded that a major drawback is that the detailed effects of degradation on isotope

Marcel Dekker, Inc.
270 Madison Avenue, New York, New York 10016

ratios of individual compounds are not well characterized. It is thought that $\delta^{13}C$ increases for saturates, decreases for asphaltenes, and remains largely unchanged for aromatics, once the hydrocarbons are in soils. Physical effects, such as migration through soil, could also alter isotope ratios.

B. Determination of Readily Extractable Chlorophenols and Total Chlorophenols in Soil Using HPLC

1. Readily Extractable Chlorophenols

In this study, 2,4-dichlorophenol (2,4-DCP), 2,4,6-trichlorophenol (2,4,6-TCP), pentachlorophenol (PCP), and 2,4-dibromophenol (2,4-DBP) are the target determinants, and 2,4-dibromophenol is used as an internal standard. Soil samples are sieved through a 2 mm sieve and stored at 4°C. A 5 g soil subsample (based on dry soil) is weighed and extracted with water or a mixture of methanol and water with a ratio of 1 : 1. The soil extract is cleaned up by SPE in order to cleanup the sample and preconcentrate the chlorophenols. 100 mg Bond Elut C18 (1 mL capacity) is used as absorbent material for trapping chlorophenols. The SPE column is conditioned with 1 mL of methanol, and the sample preparation is performed on the SPE manifold (suction pump and sample manifold). The aqueous soil extract sample is passed through the column at 1 mL min^{-1} or less. Sample volume affects the breakthrough volume, and this is determined both by column capacity and the efficiency of extraction. After this the column is washed using 1 mL of doubly deionized water. The chlorophenols are then eluted from the column using 1 mL methanol and collected into HPLC-compatible vials for determination. Darkened (amber) vials are routinely used to avoid photodegradation of samples.

2. Total Chlorophenols in Soil

Soil (10 g) is sieved to 2 mm and placed in a cellulose Soxhlet extraction thimble. A portion of 10 g of anhydrous sodium sulfate is added to the thimble. The water content of the soil determines the actual amount of sodium sulfate required. The thimble is placed in a Soxhlet unit with a few boiling chips and refluxed as required, usually overnight, with 500 mL of hexane. The use of a Büchi extraction system has streamlined the whole extraction procedure, and it is now possible to carry out a rigorous Soxhlet extraction in about 4 hours instead of overnight (Ehlers et al., 1999). After extraction, the sample is transferred to a rotary evaporator flask, and the solvent is evaporated until 5 mL of the sample remains. Using a long-necked Pasteur pipette, the sample is transferred to a 10 mL volumetric flask. The sample is then passed through a PTFE filter to remove particulate matter.

3. Determination of Chlorophenols

The extracts can be analyzed by liquid chromatography. The analytical column, supplied by Thomson Scientific, Aberdeen, Scotland, is an ODS-IK5-2509 (15 cm × 4.6 mm i.d.), packed with ODS2-Inertpak, with a particle diameter of 5 µm. The mobile phase is 70% acetonitrile and 30% 0.1% acetic acid in HPLC-grade water at 1 mL min^{-1}. The detector is set at 230 nm. The optimization of the HPLC system is carried out as follows:

1. Pass the mobile phase through the column at 1 mL min^{-1} for at least 30 minutes to equilibrate it.
2. Inject pure methanol (at least 5 injections) to check the background level or noise of signal.
3. Inject individual standards in triplicate to check retention times.
4. Create a calibration graph.
5. Run the calibration first and then run samples, using sample queuing.

4. Critical Evaluation of Technique

The efficiency of SPE using Bond Elut C18 (1 mL) can be described in terms of percentage recovery. The results for the readily extracted chlorophenols can be summarized as 2,4-DCP 95.5%, 2,4-DBP 86.8%, 2,4,6-TCP 83.7%, and PCP 85.8% recovery. As can be seen from Fig. 3, the SPE is most effective when there is methanol (up to 20% for DCP and TCP) present in

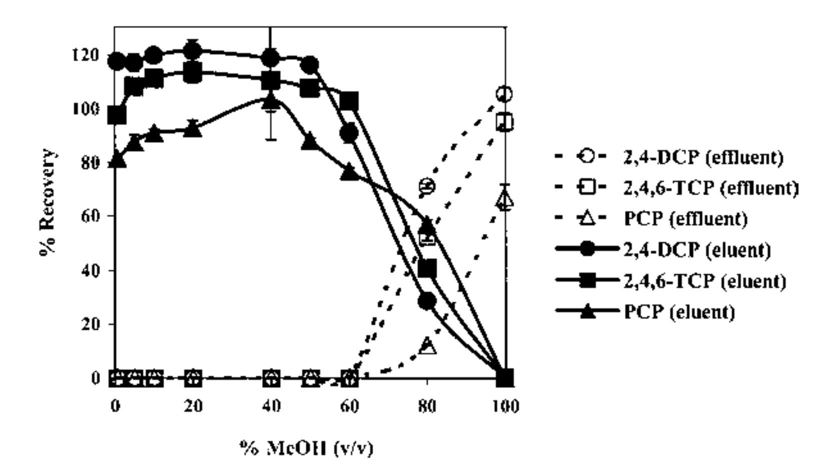


Figure 3 Effect of percentage of methanol in aqueous phase on the recovery of chlorophenols extracted by SPE.

the extraction phase. The SPE enables the LC to produce a clean well-distinguished peak.

The extractions are highly dependent upon the amount of water present in the soil sample. In the case of hexane, as it is nonpolar and immiscible in water, it is ineffective at high water contents. Conversely, in a very dry soil, the highly halogenated compounds become irreversibly bound. McGrath and Singleton (1997) reported that for PCP, optimal extraction could be achieved at 10–30% moisture content for an arable soil at pH 7.5, but for an organic soil at pH 4, moisture contents of between 40 and 70% were more favorable.

The reason that hexane can be used for a total extractable chlorophenol determination is that the solvent extracts far less interfering soil carbon, thus reducing the cleanup requirements. However, this does mean that it is not applicable to all soils, and users may have to use a more polar, water-miscible extractant, such as acetone, methanol, or an appropriate mixed extractant. When the sample is dissolved in hexane, the mobile phase may be enhanced if methanol replaces acetonitrile.

One of the major problems of using soil extracts in HPLC is the chance of column damage as a consequence of particulate and other organic extractable material being deposited on the column. A guard column or a filtration unit can prevent this damage and improve peak resolution and consistency. It is important either way to allow the column to settle for a considerable period of time before analysis, as the presence of a complex soil organic matter fraction can disrupt each of the component parts of the HPLC. To verify the performance, it is also wise to run standard samples regularly during analysis.

C. Analysis of Polychlorinated Biphenyls in Soils and Sediments, Using Soxhlet Extraction and ECD-GC

Polychlorinated biphenyls (PCBs) and organochlorines are present in all environment samples. Unlike chlorophenols, PCB concentrations tend to be low and a trace analysis technique is required. The most suitable and sensitive method is gas chromatography with an electron capture detector (ECD).

1. Method

Soil samples that have been collected should be stored cold or frozen. Samples are then air dried in a fume hood before analysis. It is advisable first to determine the approximate concentration of PCBs present. For this a 1 g aliquot of soil is shaken with 10 mL of acetone and then shaken twice in

succession with mixtures of 1 mL acetone and 9 mL hexane. The samples are then cleaned and analyzed by ECD-GC. By determining the approximate amount in this way, the weight of soil that should be used for Soxhlet extraction for the main determination can be assessed.

For the Soxhlet extraction, an appropriate amount of soil is weighed into a cellulose extraction thimble and spiked with 2,4,6-trichlorobenzene. The extraction is carried out for 24 hours with 100 mL of a 1 : 1 acetone : hexane mixture. The volume of the extractant is reduced by rotary evaporation and the remainder shaken with acid-rinsed copper powder to remove sulfur. The sample is then placed in a separating funnel and back extracted with saline water to remove the acetone. The remaining hexane is then mixed with 4 mL of concentrated sulfuric acid. The acid is then removed and the sample rinsed with saline water. Anhydrous sodium sulfate is then used to remove any remaining water from the sample, which is then passed through a column composed of Florosil and acid-rinsed copper powder. At this stage, an internal standard such as *p*-chlorobiphenyl or tetrachloro-*m*-xylene can be added to the sample.

2. Analysis

The instrument used is a GC equipped with an ECD and a selective column. The columns used are either a CP-Sil5 CB fused silica WCOT or a Phenomenex ZB-5 (5% phenyl polysiloxane) capillary column (60 m $\times$ 0.32 mm i.d. $\times$ 0.25 μm). Helium is used as the carrier gas and nitrogen as the makeup gas. A 2 μL sample is introduced using split injection (10 : 1) at 220°C. The oven programme is held at 130°C for 1 min, ramped at 3°C min^{-1} to 300°C and held at this temperature for 5 minutes. Quantification of the PCB congeners (209 theoretical PCB molecules that differ in the 1 to 10 position of chlorine atoms) is carried out by using the internal standard technique. A typical chromatogram is shown for 56 PCB congeners in Fig. 4. The use of an effective data management system is paramount for resolving the peaks.

3. Critical Analysis of Technique

This method is tried and tested and has been shown to be very effective. The problem is that there are many steps that require, in some cases, the use of specialized equipment. Dealing with trace levels of determinants means that cleanup techniques and concentration techniques have to be scrutinized carefully.

It is likely that the Soxhlet stage will determine the effectiveness of extraction; laboratories that are intending to complete a great deal of this type of analysis are required to calibrate the performance. This method also

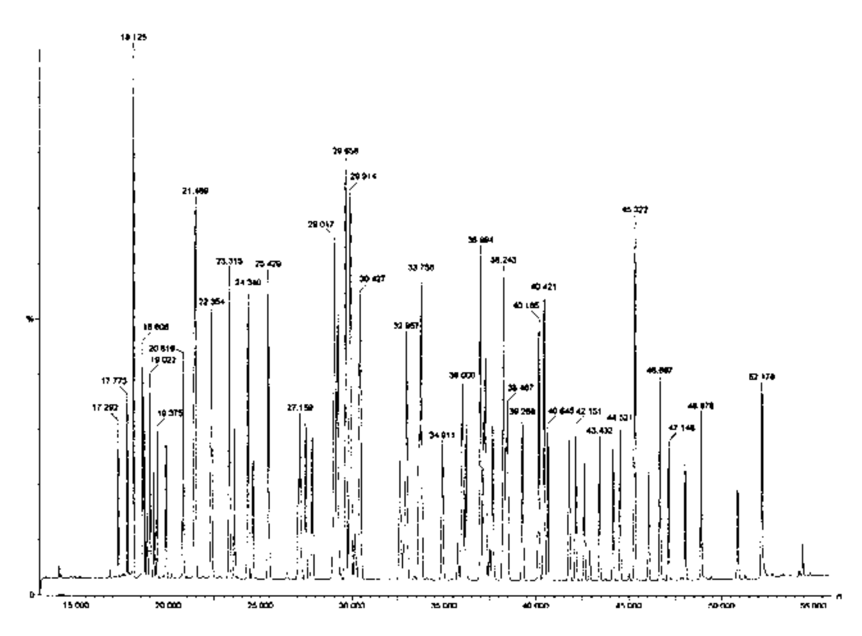


Figure 4 Chromatogram showing 56 resolved PCB congeners.

requires rotary evaporation for solvent reduction though some laboratories use Kuderna-Danish apparatus for concentrating materials dissolved in volatile solvents. This apparatus comes in various sizes and consists of a flask, a Snyder column containing glass, pear-drop shaped balls, and a graduated receiving vessel. It is difficult to estimate the effect of this alternative, and often the more common rotary evaporation apparatus is easier to use and maintain.

The biggest variations in the methodology are found in the actual chromatography (Schulz et al., 1989). Some users prefer the use of on-column injection, but this is often difficult to justify, as column damage is more likely when the sample is injected on-column. To resolve this problem, some users fit a short precolumn to guide the injection effectively into the column and to reduce the problems associated with overload. In a quality control environment, this is a commendable approach to trace analysis, but in some laboratories it is not feasible. An alternative is the use of a split injector, which will reduce the sensitivity of the system but will prolong the life of both the column and the detector. The main objective in the methodology is to attempt to differentiate as many congeners as possible using a strict protocol for preparation and analysis. For some analyses (most notably the USEPA Method 8081), the objective is to simplify the chromatogram and to use a few specific indicator peaks to estimate the

PCB load. For environmental policy purposes this approach may be adequate, but for studies of degradation this level of detail may not suffice. Although there is an increasing number of studies using GC-MS analysis for PCBs (Font et al., 1996), most users still feel that peak resolution and identification is best achieved using ECD-GC.

D. Determination of Volatile Organic Contaminants (VOCs) Using Purge and Trap Injection (PTI) and FID-GC

Water-soluble volatile organic contaminants are difficult to extract from their aqueous phase. The partitioning of the pollutant is such that seven or eight hexane extraction procedures may be required to remove a sizable fraction from the water phase. The analysis of these compounds is best performed using a technique that avoids a chemical extraction. A ‘‘purge and trap’’ is ideal for the analysis of monoaromatics, chlorinated monoaromatics, and other light hydrocarbon fractions. As the compounds are volatile a great amount of care must be taken in sampling, to avoid losses.

1. Purge and Trap Methodology

The PTI technique is used in conjunction with a GC equipped with an FID (Fig. 5). A water sample is purged with helium and then trapped in a liquid nitrogen cooling system where the condenser separates the water from the target determinants. The water is discarded. After purging is complete, the sample is forced into the heating rod, where a very rapid rise in temperature makes possible an on-column injection of the VOCs, and standard chromatographic analysis. For soil analysis, instead of using a water extract, a soil sample can be placed in a glass liner and purged directly on the instrument.

The PTI-FID-GC system requires H_2 (fuel gas), air (combustion/oxidizing gas), N_2 (makeup/preflush/backflush gas) and He (purging/carrier gas). The PTI has a number of parameters that need to be set and optimized before a sample can be injected. These are

- The length of one cycle
- The temperature of the injector rod, which is the heated interface between the PTI and the column
- The backflush rate through the condenser
- The temperature of the cold trap during precooling and desorption
- The time in which the system cools down the cold trap to the set temperature
- The temperature of the desorption oven during preflush

Marcel Dekker, Inc.
270 Madison Avenue, New York, New York 10016

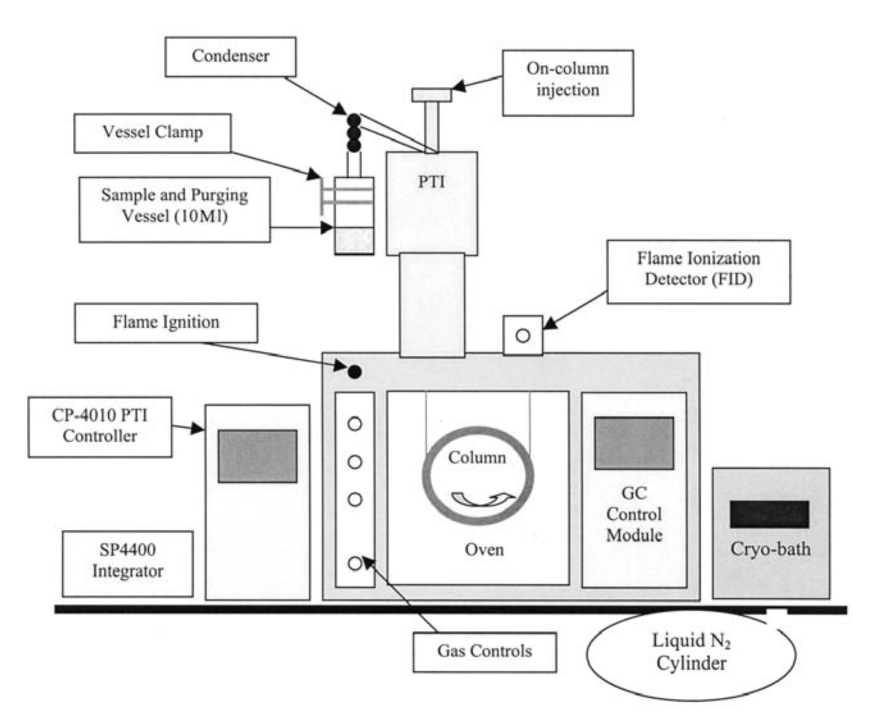


Figure 5 The PTI FID-GC instrument system.

The time for the preflush mode that removes the water from the system
The use (or not) of split flow during purging
The temperature in the desorption oven during the purge mode
The time for the desorption mode
The temperature of the cold trap during injection
The temperature and time for the backflush mode

It is possible to set the flow rates for the different modes described above without having to carry out a run. On most instruments, the flow of each mode needs to be measured with a flow meter via the outlets on the main instrument block. The gas flows for the carrier and FID are measured at the outlet to the FID, usually when the detector is cool. Once the parameters have been optimized, the next stage is to reduce the temperature of the cryobath down to -10°C and also activate the flow of liquid N_2 from the cylinder. The standard protocols used for the detection of BTEX and MtBE by PTI FID-GC are shown in Table 3.

Table 3 PTI Settings for the Determination of Volatile Organic Contaminants

Operation	Settings		
	Temp (°C)	Time (min)	Flow rate ($mL\,min^{-1}$)
Trap precooling	−100	2	
Preflushing	200	1	10
Purging	250	11	15
Injection	250	1	
Backflushing	275	10	10
Total cycle time		25	

#carrier is He at $10\,mL\,min^{-1}$; heating rod temperature setting at 290°C.

The GC column used is a DB-MtBE, (30 m, 0.45 mm i.d.) from J&W Scientific (Folsom, CA, USA). The GC oven program is as follows: isothermal operation at 45°C for 12 min, then increasing to 190°C at $20°C\,min^{-1}$, and finally holding at 190°C for 5 min.

2. Critical Analysis of Technique

The purge and trap procedure is used much more widely in the US than it is in Europe, where there is a general preference for headspace analysis (Seto, 1994). In headspace sampling, the sample is placed in a closed vial with an overlying headspace. After allowing time for volatile determinants to equilibrate between sample and overlying air, a portion of the vapor phase is sampled by syringe and directly injected into a GC (Harvey, 2000).

There are significant differences in the results obtained by the two methods, and each offers strengths and weaknesses in applications. Mineral soils are adequately measured using headspace analysis at 95°C, but those with high organic matter content give poor reproducibility. One of the greatest criticisms levelled at PTI is that it is prone to the introduction of errors. The reasons for this are that

The instrumental system is complex and has many valves that may be inadequately sealed. Minimizing instrumental errors is essential in trace analysis.

Because of the requirement for active purging, any gaseous impurities will have a substantial effect on the sample analysis. The nature of the determinants and Henry's law constant determines the purging rate.

Desorption of the trapped sample is dependent upon the flow rate and the temperature. The objective of an instantaneous release (hence minimum chromatographic band broadening) can only be realized if the setup procedure is fully optimized.

Highly concentrated determinants are prone to carryover, affecting subsequent samples; so the user must be able to estimate the level of dilution required.

Miermans et al. (2000) favored the complementary use of PTI FID-GC and PTI GC-MS, as the MS makes it possible to detect unknowns. They noted that there is a limited range of materials readily detectable by PTI.

Purge and trap is acknowledged as a mature and widely characterized technique, but the instruments are undergoing major modifications due to user applications and competitive marketing. It is one of the few solventless extraction techniques, making it applicable in sensitive working environments and also, in terms of analysis, reflects realistic environmental matrices.

IV. CONCLUSIONS

Over the last few years, chemical analysis for organic contaminants in environmental samples has become significantly more accessible to a wider range of users. The cost of chromatography has dropped, and instead of requiring highly specialized chromatographers, the introduction of automation and effective software has made this "black art" more accessible. Just as the number of papers on determination of heavy metals boomed in the 1980s, we are now seeing this repeated for organic contaminants.

Techniques are best developed and modified from existing protocols to suit the apparatus and instruments of each laboratory and to answer the specific question posed. When a technique is adopted, the user must be able to evaluate critically the shortcomings of the method and the steps needed to resolve them. Above all, the level of sophistication required in these analyses must never be compromised by poor field sampling. Ideally the laboratory scientist and the field scientist should actively communicate prior to sampling to avoid problems arising.

Chemical analysis of these organic pollutants is restricted less by the access to instrumentation than by the time constraints of producing clean preconcentrated samples. There is no doubt that over the next few years the cost of GC-MS and LC-MS will drop as the robustness of the apparatus to environmental samples and extracts increases. As regulators and

practitioners enforce and respond to guidelines regarding organic contaminants, there is an ever-growing need to develop these technologies for use by the wider scientific community.

ACKNOWLEDGMENTS

The authors wish to thank Rebekka Artz for use of the diesel extract chromatogram in Fig. 2 and Tinnakorn Tiensing for reproduction of Fig. 3.

REFERENCES

Abalos, M., J.M. Bayona, R. Compano, M. Granados, C. Leal, and M.D. Prat. 1997. Analytical procedures for the determination of organotin compounds in sediment and biota: a critical review. *J. Chromatogr. A* 788:1–49.

Abdallah, A.M.A. 1994. Isolation of petroleum and chlorinated hydrocarbons from the same extract. *Toxicol. Environ. Chem.* 44:129–135.

Agilent. 2001. *Agilent Technologies*. http://www.chem.agilent.com.

Alonso, M.C., D. Puig, I. Silgoner, M. Graserbauer, and D. Barcelo. 1998. Determination of priority phenolic compounds in soil samples by various extraction methods followed by liquid chromatography atmospheric pressure chemical ionization mass spectrometry. *J. Chromatogr. A* 823:231–239.

Bruno, T.J. 2000. A review of capillary and packed column gas chromatographs. *Separ. Purif. Meth.* 29:27–61.

Camel, V. 2001. Recent extraction techniques for solid matrices—supercritical fluid extraction, pressurized fluid extraction and microwave-assisted extraction: their potential and pitfalls. *Analyst* 126:1182–1193.

Cho, B.H., H. Chino, H. Tsuji, T. Kunito, H. Makishima, H. Uchida, S. Matsumoto, and Oyaizu, H. 1997. Analysis of oil components and hydrocarbon-utilizing microorganisms during laboratory-scale bioremediation of oil-contaminated soil of Kuwait. *Chemosphere* 35:1613–1621.

Choudhary, G., A. Apffel, H.F. Yin, and W. Hancock. 2000. Use of on-line mass spectrometric detection in capillary eletrochromatography. *J. Chromatogr. A* 887:85–101.

Dass, C. 1999. Recent developments and applications of high-performance chromatography electrospray ionization mass spectrometry. *Curr. Org. Chem.* 3(2):193–209.

Dean, J.R., and G.H. Xiong. 2000. Extraction of organic pollutants from environmental matrices: selection of extraction technique. *Trac-Trend Anal. Chem.* 19:553–564.

De la Guardia, M., and S. Garrigues. 1998. Strategies for the rapid characterization of metals and organic pollutants in solid wastes and contaminated soils by using mass spectrometry. *Trac-Trend Anal. Chem.* 17:263–272.

Duinker J.C., D.E. Schulz, and G Petrick. 1991. Analysis and interpretation of chlorobiphenyls—possibilities and problems. *Chemosphere* 23:1009–1028.

Ehlers, D., P. Schafer, H. Doliva, and J. Kirchhoff. 1999. Vanillin content and several ratios of components—influence of different extraction parameters of the analysis results. *Deut. Lebensm.-Rundsch.* 5:123–129.

Eriksson, M., A. Swartling, and G. Dalhammar. 1998. Biological degradation of diesel fuel in water and soil monitored with solid-phase micro-extraction and GC-MS. *Appl. Microbiol. Biotechnol.* 50:129–134.

Fisher, J.A., M.J. Scarlett, and A.D. Stott. 1997. Accelerated solvent extraction: an evaluation for screening of soils for selected US EPA semivolatile organic priority pollutants. *Environ. Sci. Technol.* 31:1120–1127.

Font, G., J. Manes, J.C. Molto, and Y. Pico. 1996. Current developments in the analysis of water pollution by polychlorinated biphenyls. *J. Chromatogr. A* 733:449–471.

Guerin, T.F. 1999. The extraction of aged polycyclic aromatic hydrocarbons (PAH) residues from a clay soil using sonication and a Soxhlet procedure: a comparative study. *J. Environ. Monit.* 1:63–67.

Harvey, D. 2000. Modern Analytical Chemistry. McGraw-Hill, Boston.

Hess, P., J. de Boer, W.P. Cofino, P.E.G. Leonards, and D.E. Wells. 1995. Critical review of the analysis of non- and mono-*ortho*-chlorobiphenyls. *J. Chromatogr. A* 703:417–465.

Hawthorne, S.B., J.J. Langfield, D.J. Miller, and M.D. Burford. 1992. Comparison of supercritical $CHClF_2$, N_2O, and CO_2 for the extraction of polychlorinated-biphenyls and polycyclic aromatic hydrocarbons. *Anal. Chem.* 64:1614–1622.

Hubert, A., K.D. Wenzel, and W. Engelwald. 2001. Accelerated solvent extraction—more efficient extraction of POPs and PAHs from real contaminated plant and soil samples. *Rev. Anal. Chem.* 20:101–144.

Jones, K.C., and P. De Voogt. 1999. Persistent organic pollutants (POPs): state of the science. *Environ. Pollut.* 100:209–221.

Knothe, G. 2001. Analytical methods used in the production and fuel quality assessment of biodiesel. *Trans. Am. Soc. Agric. Eng.* 44:193–200.

Lambert, P., M. Fingas, and M. Goldthorp. 2001. An evaluation of field total petroleum hydrocarbon (TPH) systems. *J. Hazard. Mater.* 83:65–81.

Marr, I.L., and M.S. Cresser. 1983. *Environmental Chemical Analysis*. Glasgow International Textbook Co., Glasgow.

McGrath, R., and I. Singleton. 1997. Analysis of pentachlorophenol in soils for use in bioremediation studies. In: *Bioremediation Protocols* (D. Sheehan, ed.). Methods in Biotechnology Series 2. Printer-Humara Press, Totowa, NJ, pp. 169–176.

Meharg, A.A., J. Wright, G.J.L. Leeks, P.D. Wass, and D. Osborn. 1999. Temporal and spatial patterns in γ-hexachlorocyclohexane concentrations in industrially contaminated rivers. *Environ. Sci. Technol.* 33:2001–2006.

Miermans, C.J.H., L.E. van der Velde, and P.C.M. Frintrop. 2000. Analysis of volatile organic compounds, using the purge and trap injector coupled to a gas chromatograph/ion-trap mass spectrometer: review of the results in Dutch

surface water of the Rhine, Meuse, Northern Delta Area and Westerscheldt, over the period 1992–1997. *Chemosphere* 40:39–48.

Miege, C., M. Bouzige, S. Nicol, J. Dugay, V. Pichon, and M.C. Hennion. 1999. Selective immunoclean-up followed by liquid or gas chromatography for the monitoring of polycyclic aromatic hydrocarbons in urban waste water and sewage sludges used for soil amendment. *J. Chromatogr. A* 859:29–39.

Mondello, L., P. Dugo, Dugo G, A.C. Lewis, and K.D. Bartle. 1999. High-performance liquid chromatography coupled on-line with high resolution gas chromatography—state of the art. *J. Chromatogr. A* 842:373–390.

Northcott, G.L., and K.C. Jones. 2000. Experimental approaches and analytical techniques for determining organic compound bound residues in soil and sediment. *Environ. Pollut.* 108:19–43.

Patnaik, P. 1997. *Handbook of Environmental Analysis: Chemical Pollutants in Air, Water, Soil, and Solid Wastes*. Lewis Publishers, CRC Press, New York.

Polese, L., E.V. Minelli, E.F.G. Jardim, and M.L. Ribeiro. 1996. Small scale method for the determination of selected organochlorine pesticides in soil. *Fresen. J. Anal. Chem.* 354:474–476.

Polese, L., and M.L. Ribeiro. 1998. Methods for determination of hexachlorobenzene and pentachlorophenol in soil samples. *Talanta* 46:915–920.

Raghunathan, N., K.A. Krock, C. Klawun, T.A. Sasaki, and C.L. Wilkins. 1999. Gas chromatography with spectroscopic detectors. *J. Chromatogr. A* 856:349–397.

Schenck, F.J., and D.J. Donoghue. 2000. Determination of organochlorine and organophosphorus pesticide residues in eggs using a solid phase extraction cleanup. *J. Agric. Food Chem.* 48:6412–6415.

Schreier, C.G., W.J. Walker, J. Burns, and R. Wilkenfeld. 1999. Total organic carbon as a screening method for petroleum hydrocarbons. *Chemosphere* 39:503–510.

Schulz, D.E., G. Petrick, and J.C. Duinker. 1989. Complete characterization of polychlorinated biphenyl congeners in commercial Aroclor and Clophen mixtures by multidimensional gas chromatography electron capture detection. *Environ. Sci. Technol.* 23:852–859.

Seto, Y. 1994. Determination of volatile substances in biological samples by headspace gas chromatography. *J. Chromatogr. A* 674:25–62.

Shamsipur, M., F. Raoufi, and H. Sharghi. 2000. Solid phase extraction and determination of lead in soil and water samples using octadecyl silica membrane disks modified by bis[1-hydroxy-9,10-anthraquinone-2-methyl]sulfide and flame atomic absorption spectrometry. *Talanta* 52:637–643.

Shen, L., and R. Jaffe. 2000. Interactions between dissolved petroleum hydrocarbons and pure and humic acid-coated mineral surfaces in artificial seawater. *Mar. Environ. Res.* 49:217–231.

Singh, H., B. Millier, and W.A. Aue. 1996. Time-integrated spectra from a flame photometric detector. *J. Chromatogr. A* 724:255–264.

Smeds, A., and P. Saukko. 2001. Identification and quantification of polychlorinated biphenyls and some endocrine disrupting pesticides in human adipose tissue from Finland. *Chemosphere* 44:1463–1471.

Stackelberg, P.E., L.J. Kauffman, M.A. Ayers, and A.L. Baehr. 2001. Frequently co-occurring pesticides and volatile organic compounds in public supply and monitoring wells, southern New Jersey, USA. *Environ. Toxicol. Chem.* 20:853–865.

Supelco. 2001. *Technical and Application Notes*. http://www.sigma-aldrich.com.

Whittaker, M., S.J.T. Pollard, and T.E. Fallick. 1995. Characterisation of refractory wastes at heavy oil-contaminated sites: review of conventional and novel analytical methods. *Environ. Technol.* 6:1009–1033.

Whittaker, M., S.J.T. Pollard, T.E. Fallick, and T. Preston. 1996. Characterisation of refractory wastes at hydrocarbon-contaminated sites. 2. Screening of reference oils by stable carbon isotope fingerprinting. *Environ. Pollut.* 94:195–203.

Index

Marcel Dekker, Inc.
270 Madison Avenue, New York, New York 10016

Marcel Dekker, Inc.
270 Madison Avenue, New York, New York 10016

Marcel Dekker, Inc.
270 Madison Avenue, New York, New York 10016

Marcel Dekker, Inc.
270 Madison Avenue, New York, New York 10016

Marcel Dekker, Inc.
270 Madison Avenue, New York, New York 10016

Marcel Dekker, Inc.
270 Madison Avenue, New York, New York 10016

MARCEL DEKKER, INC.
270 Madison Avenue, New York, New York 10016

Marcel Dekker, Inc.
270 Madison Avenue, New York, New York 10016

MARCEL DEKKER, INC.
270 Madison Avenue, New York, New York 10016

Marcel Dekker, Inc.
270 Madison Avenue, New York, New York 10016

Marcel Dekker, Inc.
270 Madison Avenue, New York, New York 10016